

THE UNIVERSITY OF HULL

DIAGENETIC MODELLING IN MIDDLE JURASSIC CLASTIC  
SEDIMENTS FROM THE RAVENSCAR GROUP, YORKSHIRE,  
AND THE BRENT GROUP, NORTHERN NORTH SEA.

being a Thesis submitted for the Degree of

Doctor of Philosophy

in the University of Hull

by

John Duncan Kantorowicz B.A. (Cantab.)

September 1982

TO CARMELA  
for typing it



# ABSTRACT

Diagenesis is the sum of those processes whereby an originally sedimentary assemblage attempts to reach and maintain an equilibrium with its environment. Numerous factors influence and affect the diagenesis of sedimentary clastic assemblages - fundamentally unstable when deposited but never reaching equilibrium with their environment. The interrelationship of these factors, however, precludes the identification of any single factor as wholly controlling the diagenesis of clastic sediments. The multifactorial nature of diagenesis is illustrated here by reference to the Middle Jurassic Dogger Formation and Ravenscar Group which outcrop on the North Yorkshire Moors and the Brent Group from Wells 3/3-1, -2, and -3 in the Ninian Field, and 210/15-2, also in the Northern North Sea.

The Ravenscar Group is interpreted as being deposited in a fluvio-deltaic complex. Here, attempted equilibration of non-marine sediments with their pore waters resulted in a variety of diagenetic modifications. These are interpreted as being influenced strongly by bacterial degradation of organic matter, which lowered pH and then reduced Eh. This reduction of pH caused feldspar dissolution and muscovite neomorphosis to kaolinites throughout. Similarly, in the texturally and mineralogically mature sandbodies, quartz overgrowths and vermiform kaolinites precipitated from oxygenated pore waters, whilst chlorite and overgrowths formed in anoxic pore waters. This resulted in complete reduction of porosity in, and cementation of, finer and texturally less mature overbank sands. Conversely, channel sands were cemented into rigid but porous quartzose frameworks. In addition, soil horizons of sphaerosiderite developed as standing water on the floodplains stagnated. Bacterial ferric iron reduction throughout the water table then raised the pH and extensive siderite cements were precipitated. During burial, calcium carbonate saturated formation waters migrated into the remaining porous sandbodies and

precipitated replacive ferroan calcite. In marine clastics, meanwhile, illite and potassium-feldspar overgrowths precipitated before in situ bacterial processes lowered pH here also. This resulted in dissolution of feldspars, muscovite neomorphism and precipitation of vermiform kandites. Subsequently, pH rose and ferroan calcite cementation occurred.

It is suggested that "aggressive fluids" migrated into the larger connected sandbodies during burial. They dissolved the carbonate cements and precipitated dense pockets of blocky kandites. These sediments were little affected during continued burial. However, their Recent weathering may have dissolved carbonates and feldspars as well as neomorphosing chlorite to vermiculite.

The reservoir rocks of the Ninian Field have formed from mature quartz-rich clastic sediments which accumulated in a transgressive sequence above Liassic mudrocks which was subsequently incised into by a fluvial system. Diagenetic modifications of the original sediments are similar to those of the Ravenscar Group, although neither chlorite nor soil horizons were observed in the wholly non-marine sediments. Porosity in marine sediments is occluded by extensive authigenic illite within a generally quartz framework. The effects of the fresh water table are also seen in the marine sediments over which the delta prograded. Then, during burial, ferroan calcite cementation and subsequent leaching and blocky kandite precipitation occurred here also. Hydrocarbon maturation and migration into the reservoir was preceded by alteration of pre-existing carbonates to ankerite, and minor illitisation of blocky kandites. However, the only effort which can be related to oil emplacement is the widespread pyritisation around the oil-water contact.

The sandstones from 210/15-2 are interpreted as formed from coarse clastic sediments which accumulated in a shallow-marine nearshore environment, possibly incised into by distributary channels. Initial marine connate water precipi-

tated potassium-feldspar overgrowths before bacterial processes lowered pH and caused widespread kandite formation. Subsequently, these sediments were affected by ferroan calcite cementation, then leaching and blocky kandite precipitation. Although oil has migrated into these sediments, no other effects were observed.

In addition to the factors which have been proposed previously as influencing diagenesis, I should like to propose that the climate of both the source area and of the depositional basin was of fundamental importance to diagenesis and many of the features observed in these rocks may be related to the original tropical climate. Moreover, as a result of the fundamental stability of the quartzose frameworks established during eogenesis, this climatic "fingerprint" may be recognised in all these sediments despite their subsequent diverse history.

## ACKNOWLEDGEMENTS

I should like to thank:

my supervisor Brian Waugh, for initiating this project and for his help, advice and guidance throughout its duration; my 'co-worker' Stuart Burley, for his constructive criticisms and support in all aspects of this research; and the other members of staff and research students at Hull University for their help and encouragement.

Mike Leeder and Steve Livera for their help in the field and in unravelling the sedimentological evolution of the Ravenscar Group.

B.Besly, R.H.Bate, B.Cooper, C.D.Curtis, J.A.D.Dickson, T.Elliott, J.Harris, J.E.Hemingway, A.R.Hurst, C.V.Jeans, E.F.McBride, M.J.Pearson, and A.H.Weir both for their advice and help with various aspects of this research.

I.G.S. Stable Isotopes Unit for use of their facilities at Grays Inn Road. I am also indebted to Max Coleman, Marge Cox and John Rouse for their help and encouragement with the complexities of stable isotope analysis and data interpretation.

Professor P.E.Baker of Nottingham University Geology Department for permission to use the luminoscope there; and Karl Ramseyer, of the Geologisches Institut, Bern, for examining and photographing numerous samples on his luminoscope and providing me with detailed notes and descriptions.

Professors House and Dunham for access to the facilities of the Geology Department at Hull University, without which this study would not have been completed; John Garner, for helping me to produce the plates in this thesis; Dick Middleton, for writing and translating into English the computer programmes used in support of this research; Tony Sinclair, for his help in operating the Scanning Electron Microscope; and Fred Wilkinson, for his assistance with the electron microprobe.

Phillips Petroleum (UK) and their partners for permission to examine and sample the core from Well 210/15-2; Chevron(UK) and their partners for permission to examine and sample cores from the Ninian Field.

Last but not least I should like to thank Mark Anderson and Andy Radford for making the 600 thin section without which this research would not have been possible.

This thesis was completed whilst in receipt of NERC Grant GTS/ 79/GS/39

CONTENTS

ABSTRACT	iii
ACKNOWLEDGEMENTS	vi
CONTENTS LIST	vii
CHAPTER ONE: AN INTRODUCTION TO THE DIAGENESIS OF CLASTIC SEDIMENTS	1
THESIS CONSTRUCTION	1
WHAT IS DIAGENESIS?	4
WHY DOES DIAGENESIS TAKE PLACE?	5
WHAT CONTROLS DIAGENESIS IN CLASTIC SEDIMENTS?	8
TERMINOLOGY AND METHODOLOGY	17
THE LIMITATIONS OF THIS THESIS	23
CHAPTER TWO: THE NORTH SEA BASIN, TECTONIC HISTORY AND MIDDLE JURASSIC SEDIMENTOLOGY: A REVIEW	25
THE NORTH SEA BASIN	25
THE EAST SHETLAND BASIN BRENT GROUP	28
SEDIMENTOLOGY OF MIDDLE JURASSIC STRATA IN THE CLEVELAND BASIN	31
THE BURIAL HISTORY OF MIDDLE JURASSIC SEDIMENTS IN THE NORTH SEA BASIN	40
CHAPTER THREE: DIAGENESIS OF CLASTIC SEDIMENTS FROM THE MIDDLE JURASSIC DOGGER FORMATION AND RAVENSCAR GROUP IN YORKSHIRE	45
PETROGRAPHY	45
Dogger Formation	45
Basal conglomerate	45
Shallow-marine sandstone	46
Beach sandstone, Whitby East Cliff	49
Interpretation	50

Saltwick Formation	52
Overbank sandstones	52
Channel sandstones	55
Interpretation	59
Millepore Bed	62
Interpretation	63
Yons Nab Beds	64
Interdistributary-bay and marsh-filling sequences	64
Tidal channel sandstone	67
Interpretation	68
Cloughton Formation: Gristhorpe Member	70
Channel sandstones	70
Overbank sandstones	71
Interpretation	75
Scarborough Formation	76
Tidal-sheet sand	76
The top of the Scarborough Formation	78
Beach sandstone (Sneaton Quarry)	78
Interpretation	79
Scalby Formation: Moor Grit	81
Moor Grit - South of Scarborough	83
Interpretation	84
Scalby Formation: Long Nab Member	86
Channel sandstone	86
Overbank sandstone	88
Interpretation	89
DISCUSSION	91
Eogenesis of marine sediments	95
Eogenesis of non-marine sediments	107
Ubiquitous mesogenetic changes	123

Telogenesis - Recent Weathering	129
CONCLUSIONS	130
CHAPTER FOUR: SEDIMENTOLOGY AND DIAGENESIS OF MIDDLE JURASSIC BRENT GROUP CORES FROM WELLS 3/3-1, 3/3-2, AND 3/3-3 NINIAN FIELD, EAST SHETLAND BASIN	133
SEDIMENTOLOGY	134
Core Description	134
Coarse-basal sandstone facies	134
Micaceous sandstone facies	135
Massive sandstone	136
Coarsening-upwards facies	137
Fining-upwards facies	138
3/3-3 sandbody	139
Interpretation	140
Coarse-basal sandstone facies	140
Micaceous sandstone facies	144
Massive sandstone	145
Coarsening-upwards facies	147
Fining-upwards facies	149
3/3-3 sandbody	150
3/3-1	151
Summary	151
Discussion	153
DIAGENESIS	155
Petrography	156
Beach sandstones	156
Foreshore sandstones	157
Foreshore to upper shoreface sandstones	159
Distributary channel sandstones	162

Interdistributary-bay filling sequences	163
Crevasse-splay sandstones	167
Channel sandstones	169
Interpretation	171
Eogenesis of marine sediments	171
Continued marine eogenesis or freshwater diagenesis?	173
Eogenesis of non-marine sediments	176
Mesogenesis of non-marine sediments	178
Ubiquitous mesogenetic changes	179
Cathodoluminescence observations	183
Summary	184
Discussion	185
CONCLUSIONS	196
 CHAPTER FIVE: SEDIMENTOLOGY AND DIAGENESIS OF THE MIDDLE JURASSIC	
BRENT GROUP CORE FROM WELL 210/15-2	198
SEDIMENTOLOGY	198
Core description	198
Micaceous facies	198
Fining-upwards facies (6876-6899')	199
Bioturbated micaceous sandstone facies	199
Coal-bearing facies	200
Fining-upwards facies (6780-6785')	200
Interpretation	201
Micaceous facies	201
Fining-upwards facies	203
Coal-bearing facies	204
Discussion	205
Summary	206
DIAGENESIS	207



Petrography	207
Interpretation	211
Discussion	216
CONCLUSIONS	222
 CHAPTER SIX: THE STABLE ISOTOPE INVESTIGATION OF AUTHIGENIC CARBONATES AND KANDITES FROM THE RAVENSCAR GROUP, YORKSHIRE AND THE BRENT GROUP, NINIAN FIELD, NORTHERN NORTH SEA	     223
METHODOLOGY	225
RESULTS	227
INTERPRETATION AND DISCUSSION	227
Ravenscar Group	227
Siderite spheruliths	227
Siderite nodules and concretions	230
Siderite cements	232
Calcite cements	232
Kandites	234
Brent Group	235
SUMMARY AND CONCLUSIONS	238
Ravenscar Group	238
Brent Group	239
 CHAPTER SEVEN: THE DIAGENESIS OF CLASTIC SEDIMENTS: CONTROLLING PROCESSES, PREDICTIVE MODELS AND GENERAL THESIS	     241
CONCLUSIONS	241
WHAT CONTROLS DIAGENESIS	242
Climate?	243
Inorganic effects	243
Organic effects	245

Depositional environment?	249
Sandbody texture and distribution	250
Pore-water chemistry	252
Sandbody geometry	253
Sediment composition?	254
Dissolution of sedimentary constituents	254
Nucleation on detrital grains	256
Framework stability	258
Burial?	260
Changing pore-water composition	261
Temperature and pressure	264
Hydrocarbons	264
GENERAL THESIS CONCLUSIONS	265
REFERENCES	268
APPENDICES	297

"I have long discovered that geologists never  
read each others works,  
and that the only object in writing a book is  
a proof of earnestness, and  
that you do not form your opinions without  
undergoing labour of  
some kind"

Charles Darwin.

## CHAPTER ONE: AN INTRODUCTION TO THE DIAGENESIS OF CLASTIC SEDIMENTS

This thesis reports the results of an investigation into the controls on diagenesis in clastic sediments from the Middle Jurassic Dogger Formation and Ravenscar Group in Yorkshire, and the Middle Jurassic Brent Group in the Northern North Sea. Its objectives are, firstly, to define and delineate where possible those diagenetic processes which may be directly related to the depositional environment, and, secondly, to distinguish quantitatively these processes from those operating subsequently.

### THESIS CONSTRUCTION

In this chapter I should like to outline the question to which this thesis is addressed, and the terminology used in discussing the concepts and data which I shall use in an attempt to answer this question. In the following sections I should like to propose a working definition of diagenesis, and review the controls on diagenesis proposed in recent publications. Having reviewed some of the more critical elements which have been proposed, I shall then address myself to the question "Can diagenetic controls be isolated, demonstrated, and distinguished quantitatively from each other?". Finally, I shall outline the choice of terminology employed in discussing and in answering the above question, and in recording the results of my research.

The most fundamental aspect of quantifying the depositional environment's control on diagenesis is a precise, and unequivocal, identification of the depositional environment and subenvironments of the rocks studied. The results of analysis of two Middle Jurassic fluvio-deltaic sequences are reported in this thesis, both with established sedimentological models interpreting their depositional environments. The Ravenscar Group in North Yorkshire has been studied by a succession of geologists during the past two hundred years, with

the most recent sedimentological interpretation incorporating research by a team from Leeds University, consisting of Drs Leeder, Nami and Livera. Chapter Two includes a review of sedimentological models for these strata, which outcrop on the North York Moors. This review concentrates specifically on the most recent research in an attempt to present a complete and integrated picture of the whole fluvio-deltaic complex.

The broad sedimentological evolution of the Brent Group is also reviewed from recent literature to illustrate the overall palaeogeographical development of the East Shetland Basin, from which the cores recorded in Chapters Four and Five were taken. The remainder of Chapter Two describes the influences on the origin and development of deltaic sedimentation in the Middle Jurassic in the North Sea Basin, and the factors affecting the burial history and changing pore-fluid compositions of both these sedimentary packets<sup>1</sup> up to the present day. Thus, Chapter Two outlines the broad tectonic controls on the origin and evolution of deltaic sedimentation in the Middle Jurassic, provides a detailed account of the Ravenscar Group, a more generalised account of the Brent Group, and discusses further gross tectonic controls on the burial history of both sequences.

In Chapters Three to Six original data, interpretations, and discussions are presented. Chapter Three records analyses of sandstones and mudrocks from a range of environments in the Ravenscar Group. These are summarised according to their depositional subenvironment and stratigraphical position in order to facilitate comparisons between subenvironments and to view the evolving fluvio-deltaic complex as a whole. Chapter Four reports original sedimentological logs, and detailed diagenetic investigations from Wells 3/3-1, -2, and -3,

---

<sup>1</sup> In general, a sedimentary packet is a possibly diachronous body of one lithology, such as sandstone, encased in relatively impermeable strata, such as mudrocks.

cored through the Brent Group of the Ninian Field in the East Shetland Basin. Although the Brent Group has been interpreted as a deltaic complex for some time (see Chapter Two), and the Ninian Field itself has been discussed in a recent paper (Albright et al, 1980), no precise details of its sedimentology are available. Thus, the cores studied are reported in detail as a prerequisite to the investigation of their diagenesis, which is summarised according to subenvironment within the delta. Chapter Five has a similar basis, reporting data from a cored Brent Group sequence in Well 210/15-2.

During basic investigation of these Ravenscar and Brent Group sediments, broadly comparable sequences of diagenetic events emerged. In an attempt to distinguish the origin of these minerals quantitatively, a suite of diagenetic clays and carbonates, as well as samples of siderite concretions observed during field work, was selected for stable isotope analysis. Although some of the results are integrated into earlier chapters, they are reported fully and discussed along with analytical procedures in Chapter Six.

Chapter Seven serves to integrate the conclusions reached in the preceding chapters, and to discuss the degree to which this thesis has established whether or not the depositional environment controls diagenesis. The Appendices contain analytical results as well as technical details to support the generalisations made in the text. Locality details for all the samples analysed are recorded in Appendix A. Technical details of analytical procedures are given in Appendix B, whilst the results of modal, microprobe and X-ray diffraction analyses from the Ravenscar Group are compiled in Appendices C, D, and E respectively. Results from the Brent Group cores are compiled in Appendix F for the Ninian Field, and Appendix G for 210/15-2 samples. Raw data collected during stable isotope analysis are listed in Appendix H.

## WHAT IS DIAGENESIS?

Unfortunately, despite the number of books and papers written on the subject within the past twenty years, there is no universally accepted definition of diagenesis. Throughout this thesis diagenesis will be considered in the loose sense of Blatt et al., (1972) as the sum of those processes by which an originally sedimentary assemblage attempts to reach an equilibrium with its environment. Diagenesis may be considered, therefore, to operate on a sediment from its initial deposition, throughout its lithification and burial, and until either metamorphism or subsequent uplift and erosion occurs. These processes include pedogenic activity and bioturbation; the precipitation of pore-filling and cementing minerals from solution and by the dissolution and reprecipitation of detrital components; the influence of bacterial organic degradation and hydrocarbon migration; the dissolution and reprecipitation of surviving detrital components, as well as initial pore-filling and cementing minerals, as the result of changes in pore-fluid composition; and the effects of increased temperature and pressure during burial. In addition to being variously defined in an absolute sense, diagenesis is also variously defined in a relative sense, that is, with respect to metamorphism. Heroux<sup>et al</sup> (1979) discuss the numerous indexes used in defining the boundary between diagenesis and metamorphism. Further consideration of this point is, however, beyond the scope of this thesis.

In order to establish whether or not diagenetic processes are controlled by the depositional environment, it is necessary to have some understanding of the physical and chemical conditions in a modern delta, and to be able to relate events in the rocks themselves to these conditions. Diagenetic events which can be explained in terms of equilibration of the original sediments and their depositional pore waters are eogenetic (Schmidt and McDonald, 1979a). Any such interpretation relies, therefore, on analogy to the present, as the

chemistry of the original depositional pore waters must be inferred. Defining diagenesis as above, eogenesis may now be defined as the sum of those processes by which sediments move towards an equilibrium with their depositional pore-fluids.

Mesogenesis is the regime in which diagenetic processes are unaffected by the influence of surface agents in the chemistry of the interstitial waters. This definition differs slightly from that proposed by Schmidt and McDonald (1979a) because "effective burial, under strata that seal the sandstone from a pre-dominant influence of surface agents in the chemistry of the interstitial water" is not the only mechanism whereby surface influences may become subordinate. Boles and Franks (1979b) discuss fluid flow from the Gulf Coast Tertiary, in which compaction expels formation waters upwards through sandbodies. These sandbodies are not necessarily effectively sealed, or buried.

Telogenesis, representing "the regime at or near the surface after effective burial", and including diagenetic modifications beneath unconformities, also requires redefinition because this fails to account for possible pore-fluid changes in shallow-marine sediments beneath progradational sequences. In this type of sequence, primary marine pore fluids could be succeeded by fresh water from the overlying alluvial system. Thus, eogenesis could be followed by exposure to a different regime at the surface, without effective burial. I propose, therefore, that telogenesis be redefined as resulting from the secondary introduction of surface waters.

#### WHY DOES DIAGENESIS TAKE PLACE?

Diagenesis is the sum of those processes by which originally sedimentary assemblages attempt to reach equilibrium with their environments. Diagenesis takes place because sedimentary clastic assemblages are fundamentally unstable



when deposited (Curtis, 1980), and immediately begin to react with their depositional pore waters. Such reactions may involve precipitation on stable and metastable components, neomorphosis of unstable into stable phases, and dissolution. All minerals formed at other than 25°C and atmospheric pressure are metastable or unstable under surface conditions. It is under these conditions that there is not normally sufficient free energy to promote neomorphism of high- into low-temperature polymorphs. Consequently, metastability is a function of pore-water chemistry. Those phases unstable in their pore waters will, therefore, either alter to stable phases, or dissolve. Alternatively, those phases which are stable in their depositional pore waters may act as nuclei for overgrowths or for precipitation from solution. In this sense, rounded detrital grains can be considered as anhedral crystals. They have, therefore, higher surface-free energy than euhedral crystals, and, given the opportunity, would become more stable and crystal-like if overgrowths precipitated on them.

The rates and products of dissolution or alteration of metastable phases are a function of pore-water chemistry. If a phase can neomorphose into another stable phase without dissolution and precipitation, it will do so. If, however, a phase is deposited in the stability field of another phase into which it cannot neomorphose, it must dissolve. This is the situation for micas and feldspars respectively in the field of kandite stability. In addition, the rate at which minerals react is a function of their structure and composition. At the earth's surface these reactions are essentially weathering processes (Curtis, 1976): the less stable the clastic assemblage, the faster it reacts. This is aptly demonstrated by Davies et al (1979), who estimate that volcani-clastic deposits in Guatemala are effectively cemented after 2000 years by the dissolution and reprecipitation of their relatively unstable constituents; and conversely, Milliken et al (1981) who describe unconsolidated Miocene sands buried to 3000 m in Texas.

As well as affecting reactions of clastic assemblages, pore waters may also effect direct precipitation. Where solutions are supersaturated with respect to phases which are not present in the sediment, these phases, after nucleation, will precipitate as discrete pore-filling or cementing crystals. If these solutions are merely saturated, precipitation will not take place, as they do not possess the free energy to promote crystal nucleation as distinct from crystal growth. If the respective detrital phases are present, however, they may act as nuclei for solutes and lead to the precipitation of, for example, overgrowths (Curtis, 1978; Berner, 1980, 1981).

This generalised scheme is, unfortunately, complicated by the reaction products of sediments interacting with pore waters. Dissolution and neomorphism, whilst forming stable phases, also release ions into solution and, therefore, affect pore-water composition. Moreover, bacterial degradation of organic matter removes oxygen, ferric oxides and sulphates from solution, whilst lowering and the raising pH, and also concomittantly lowering Eh. With burial, therefore, either as the result of in situ pore-fluid evolution, or after the introduction of formation waters, an assemblage moving towards an equilibrium with its initial environment may subsequently become unstable and effect further dissolution and precipitation reactions. As a consequence, the stability of the original sedimentary assemblage affects its diagenesis during burial. In relatively stable deposits, such as quartz arenites, quartz overgrowth cementation creates a rigid framework which may act as a conduit for later fluid movement, hence the rock contains labyrinths for the repeated precipitation and dissolution of authigenic minerals. Conversely, less stable and less coherent sediments break down to form assemblages which are relatively stable at the earth's surface but unstable during burial. Compare, for example, quartz arenites and volcanoclastic lithic arkoses after burial to 3000 m (Nagtegaal, 1978, 1980; Galloway, 1979): the latter are, effectively, greywackes.

## WHAT CONTROLS DIAGENESIS IN CLASTIC SEDIMENTS?

The increased interest in, and understanding of, clastic diagenesis during the last ten years has resulted from several factors. These are: the establishment of interpretative sedimentological models in the previous decade; technological advances involving the application of new and pre-existing quantitative analytical techniques to diagenetic problems; and the economic necessity of a complete understanding of hydrocarbon reservoir characteristics in order to exploit fully natural accumulations of fossil fuels.

During the past two decades one can trace the development of diagenesis in clastic sediments as a "science" from earlier papers, in which features were observed and recorded, through a period of interpretation leading to an understanding of these features, and involving the recognition of critical processes, reassessing previously documented fabrics and mineral phases, and finally to recent theories, models and predictive discourse. In these latest publications numerous attempts have been made to interpret diagenetic variations in terms of causes and controls. These range from the macroscale suggestion of plate tectonic controls on diagenesis (Dickinson and Suczek, 1979; Siever, 1979) to the microscale interpretation of a close association of haematite and siderite in tropical Carboniferous alluvium as the result of syndepositional variations in the position of the water table (Besly, 1980).

Although useful general principles may emerge from overviews of plate tectonic macrocontrol, I do not feel that our present understanding of microscale processes realistically allows the identification of plate tectonics as a control on sandstone diagenesis. However, those proposed controls which have been identified may be generalised into the following categories: depositional mineralogy, texture, and environment (including pore-water chemistry); changing

pore-fluid compositions, possibly during burial; burial itself, pressure and/or temperature, and time.

The complexity of isolating one single factor as a control on diagenetic processes is demonstrated by Hayes (1979). The possible interrelationship of factors he describes, which influence the format, deposition and diagenesis of a sediment is shown in Fig. 1.1. The question "Does depositional environment control diagenesis?" therefore requires some deliberation. Hence, one must also consider how any investigation can isolate and evaluate the depositional environment as a controlling influence on diagenesis.

Almon et al (1976) describe a marine and non-marine andesitic volcanoclastic sandstone complex showing a range of diagenetic modifications. Their data reveal the importance of the environment in influencing rather than controlling diagenesis. Non-marine sandstones contain authigenic corrensite, calcite and dolomite, whilst contemporaneous marine deposits contain montmorillonite and calcite. These two authigenic assemblages are similar in bulk chemistry, but consideration of Eh and pH controls of equilibrium thermodynamics demonstrates that the former is stable in fresh water, and the latter in sea water. However, depositional environment here is an influence, rather than the direct control, because surely a different unstable or even more stable suite of sedimentary components would not produce these same authigenic assemblages?

Alternatively, Walker et al (1978) detail the importance of depositional mineralogy, whilst again revealing the interaction of clastic sediments with environment. They describe the diagenetic modification of first cycle Cenozoic alluvial arkoses of varying ages, in which detrital mineralogical components break down in sequence, commencing with those of low stability, to the more stable components (Goldich, 1938). The primary detritus presumably was not

(and still is not) in equilibrium with circulating ground waters (Walker et al, 1978). Therefore, the in situ breakdown of unstable grains creating porosity, releasing mobile elements, and precipitating relatively stable authigenic phases, can be observed in time. Hence, the local control of one grain or mineral type on the consequent authigenic phases can be demonstrated.

The interaction of sedimentary components with primary pore fluids is also shown by Edwards (1978, 1979) in a study of Cretaceous fluvial sandstones from Spitsbergen. Edwards (1979) considers primary detrital mineralogy to control diagenesis. Quartz arenites are cemented with quartz overgrowths and calcite, feldspathic quartz arenites by quartz overgrowths, calcite and kaolinite, whilst in rocks containing basaltic rock fragments quartz overgrowths, chlorite and calcite occur. Finally, basalt rich sandstones (volcanic lith-arenites) contain authigenic smectites, calcite and zeolites. However, one might ask if the same authigenic phases would precipitate from these detrital assemblages in a different environment?

A more esoteric study by Stalder (1975) describes a quite unique control of source area runoff, and hence primary pore waters on diagenesis. In a sequence of Pliocene-Quaternary fluvial clastics from the Oman, an alternation of calcite and high-magnesium calcite with dolomite occurs. This variation is attributed to runoff from the source area. Thus, peridotite, gabbro, basalt and diabase from the Hawasina and Semail Formations contribute calcite, whilst high-magnesium calcite occurs with drainage from the peridotites in the Semail Formation only. The high magnesium concentration of the latter causes the precipitation of primary high-magnesium calcite, which is subsequently dolomitised in places by continued flushing of these porous clastics with further magnesium rich pore fluids.

Unique though this situation may be, it allows a little light to be cast on

the problem of distinguishing the control of the depositional environment, from the control of the interacting sediments. In the studies described above, neither depositional environment nor mineralogy can be isolated as the actual cause of the authigenic phases. Almon et al, (1976) demonstrate the control of choice between two assemblages. These assemblages, however, involve the interaction of sediments with primary interstitial pore fluids. Similarly, Walker et al (1978) emphasise the breakdown of unstable grains, and Edwards' (1978) authigenic suites are correlatable with a variation in detrital composition. Throughout these examples, the environment interacts with the sediment and, as well as precipitating authigenic phases directly from solution, also equilibrates with unstable components causing their breakdown and reprecipitation as stable authigenic phases. Consequently, the chemistry of the pore waters takes on a catalysing role in promoting the precipitation of phases stable under those particular geochemical Eh and pH conditions. However, an investigation of more stable, or even inert, detrital components should emphasise the role of the depositional environment as the, rather than a, direct control on diagenesis. Hence, for example, the occurrence of authigenic clays, carbonates or evaporites could be interpreted as a direct result of precipitation from primary pore fluids, and, therefore, reflect the geochemistry of the interstitial pore waters of the depositional environment.

The relationship between detrital mineralogy and depositional environment is further illustrated by Hawkins (1978) in a detailed study of Carboniferous sub-litharenites, feldspathic litharenites, and litharenites from the East Midland Bothamsall Oilfield. Hawkins (1978) demonstrates diagenetic variations which he relates, in different parts of the sequence, to the geochemistry of interstitial waters (mixed layer smectite-illite coatings on detrital grains in barrier bar sandstones, whilst clay rims are absent in non-marine facies); to sedimentary mineralogy (formation of kaolinite and illite by the selective in situ breakdown of some detrital feldspars); to

depositional texture (complete cementation by quartz overgrowths and carbonates of fine-grained sands, whilst coarser grained horizons have retained their porosity); and finally to the influence of hydrocarbons (oil-bearing sections contain only the first few of a series of diagenetic modifications more extensively developed elsewhere).

The discussion above is intended to demonstrate that the situation is far from simple, and that although several independent factors affect sediments after their deposition, the effects of these cannot be distinguished with any degree of clarity. During burial the situation is equally complex and the framework established during eogenesis is subjected to both physical and chemical stresses. Firstly, unless overpressuring<sup>1</sup> occurs, as sedimentary packets become buried, overburden pressures increase, and the framework formed at the surface is physically stressed. Response to physical pressure varies (Nagtegaal, 1978, 1980). Quartzose rocks, such as quartz arenites cemented with quartz overgrowths, are relatively resistant to pressure. By contrast, lithic arenites, dominated by polymineralic rock fragments or mudrock clasts, for example, containing clay rims and little effective cement, are liable to compact both by grain rearrangement and deformation of less rigid clasts. In general, harder, more resistant sediments and extensive early cements provide rigid frameworks, whilst softer, less resistant sediments and irregularly developed authigenic phases do not. The degree to which rocks are actually cemented prior to burial does not, however, have as profound an effect on their properties as previously believed: subsequent changes in pore-fluid chemistry may remove early cements, and recreate at depth a rock with reservoir characteristics similar to those of the initial assemblage (e.g. Stanton, 1977). Sediments

---

<sup>1</sup> Overpressuring: the effective sealing of pore fluids within a sedimentary sequence such that overburden pressures are dissipated by pore fluids, rather than framework constituents.

with little or no early cementation become compacted, and therefore the removal of cement does not create significant secondary porosity.

Several studies are relevant here in illustrating the changing nature of minerals and pore fluids with depth, although by virtue of the scale of events under consideration, extensive sequences and formations need to be considered, rather than the smaller scale bodies discussed above. The rates of these processes are related to larger scale influences: tectonically active zones, especially convergent plate margins, will impose high-temperature, low-pressure "diagenetic facies", whilst intracratonic basins with considerably lower heat flow will encounter higher pressure at a lower temperature during burial.

In a series of papers from the Gulf Coast of the United States, the relationship between conversion of smectites to illite, and burial temperatures has been demonstrated (Burst, 1959, 1969; Perry and Hower, 1970; Eberl and Hower, 1976; Hower et al, 1976). The significance of this is outlined by Boles (1981) and reviewed by Hower (1981). Over a range of temperatures from 70-200°C, smectite neomorphoses to illite, becoming progressively more ordered with depth, releasing cations and silica as structural layers are lost during the final transformation of ordered smectite to illite. Boles and Franks (1979a) illustrate the effects of this process, correlating a progressive increase of illite-layer percentage and ordering with depth in mudrocks, and the conversion of calcite to ankerite, and kaolinite to chlorite (reactions with cations released during smectite ordering) in adjacent sandstones. Boles and Franks (1979a) also relate progressive cementation of sandstones to the silica released during this process. Yeh and Savin (1977), in an isotopic study from this area, support the general conclusions of clay mineral ordering and silica release, although they propose that quartz precipitates in the mudrocks rather than in the sandstones. In a similar depth related study, Hutcheon et al (1980) describe the breakdown of an assemblage of dolomite and kaolinite which becomes



unstable at 220°C, and transforms to chlorite and calcite.

Research from the tectonically active west coast of the United States also serves to illustrate the concept of "diagenetic facies" during burial. However, in these sequences, the sediments are usually lithic arenites, and dominated by unstable volcanic rock fragments (Galloway, 1974, 1979; Burns and Ethridge, 1979). In the Eocene and Palaeocene Umpqua Formation of Oregon, Burns and Ethridge (1979) recognise a number of authigenic phases which are related to depositional texture or sedimentary mineralogy, with chlorite, calcite, and quartz overgrowths at less than 3000 m burial, and zeolites below 3000 m, apparently irrespective of the depositional environment, which is not stated. Galloway (1974, 1979) also demonstrates changes of assemblage that may occur with depth and increasing temperature. As Galloway (1974, 1979) does not describe the relationship between diagenesis and depositional environment, it is difficult to assess the degree to which depositional mineralogy, rather than environment, controls diagenesis. However, the widespread occurrence of the authigenic phases suggests that the environment does not significantly influence diagenesis here. Samples from shallow depths contain calcite and authigenic chlorite and montmorillonite, those at intermediate depths contain zeolites and a second generation of chlorite, whilst the most deeply buried samples contain laumontite, quartz, feldspar and a number of clays derived from recrystallization of pre-existing authigenic and detrital components. Of these phases only calcite appears to be related to the depositional environment, and may represent a palaeosol. Galloway (1974) relates progressive diagenetic modifications of these sediments to burial and increasing temperature, from a clean porous sandstone to a greywacke at depth.

The physical modifications outlined above are supplemented and probably dominated by changes in pore-fluid chemistry, which affect the equilibrium between solid assemblages and their environments, although basinal studies

can normally relate effects in one area with causes in another. Hence, mineralogical changes in response to pressure and temperature gradients in one part of a basin may cause pore fluid related chemical changes in another, as reported by Boles and Franks (1979a) and Irwin et al (1977).

Most basinal pore fluids (formation waters) are mildly alkaline, similar in composition to sea water, and contain concentrations of less common elements such as barium (White, 1965; Collins, 1975). Although marine sandstones will not, therefore, encounter significant changes in pore-fluid chemistry with depth, non-marine ones will. For example, phases precipitated from solution, or by equilibration of sediments with pore fluids following deposition in acidic ground waters, will be unstable in formation waters. The effect of changing pore fluids is illustrated in a series of papers from the Bureau of Economic Geology, Austin, Texas. Dutton (1977), Lindquist (1977), and Loucks et al (1977) describe deltaic sequences of a variety of ages in Texas. Apart from localised calcite deposits, interpreted as palaeosols (Loucks et al, 1977), diagenetic modifications begin with freshwater flushing of the sediments, precipitating quartz overgrowths and kaolinite. During burial the introduction of formation waters precipitates calcite, which replaces detrital components and the earlier formed authigenic phases.

However, not all basinal pore fluids are alkaline or saline and, under certain conditions, acidic solutions may be generated at depth. The principle cause of acid generation at depth is bacterial degradation of organic matter, releasing CO<sub>2</sub> into solution (Curtis, pers. comm. 1982). Organic matter passes through zones of aerobic, suboxic, and reducing processes (nitrate, iron and manganese oxide and sulphate reduction respectively) to bacterial methanogenic fermentation and decarboxylation on the path to thermal decarboxylation and hydrocarbon maturation (Irwin et al, 1977; Curtis, 1978, 1980). The importance of CO<sub>2</sub> generation in the subsurface is widely reported, and it is considered

to be most important in the creation of secondary porosity (Parker, 1974; McBride, 1977; Schmidt and McDonald, 1979a; Hutcheon et al, 1980). Irwin et al (1977) record progressive changes in carbon source during burial from the resulting carbonate phases accreted onto concretions. However, in the absence of suitable cations and alkaline solutions with which to equilibrate, these acidic fluids will cause dissolution rather than precipitation, at least initially. Curtis (pers. comm. 1982) describes such pore fluids as "aggressive" (Fig. 1.2) and points out that these solutions will dissolve carbonates, consequently increase in pH, and move towards an equilibrium with remaining phases. However, they will also move into the field of kandite stability. Hence alumina and silica, whether initially in solution, or derived from in situ feldspar dissolution (which would also occur at low pH and cause an increase in pH) will precipitate as kandites. It is significant, therefore, to note the correlation of secondary porosity development with kaolinite precipitation (Dutton, 1977; Lindquist, 1977; Loucks et al, 1977; Stanton, 1977; Land and Dutton, 1978).

In this thesis I should like to report analyses from two Middle Jurassic fluvio-deltaic sandstone sequences. They are both mature intracratonic sandstones, petrographically dominated by quartz arenites and subarkoses, their detrital mineralogy being therefore, relatively simple and stable. Both deltas contained a number of subenvironments, and comparison of these from within each delta, and between deltas, should help to demonstrate whether the depositional subenvironment played any significant role in diagenesis. Although these sedimentary packets have similar mineralogy, texture and depositional environment, and are, furthermore, of the same age, they have different burial histories. Thus if, for example, certain suites of early diagenetic events occur in both, but their later suites differ, these differences may be attributed to burial history, and changing pore-fluid compositions.

In view of the complexity of the interacting influences discussed above, possible isolation and evaluation of the absolute role of any one factor must be considered cautiously. Nonetheless, a review of the most recent literature reveals definite trends and variations in the diagenesis of clastic sediments. Specific research may help to elucidate and refine these patterns, and hence to understand their causal mechanisms.

The methodological basis for this research was, therefore, to sample sandstones from a range of known subenvironments within each sequence, to elucidate the nature, origin, and relative timing of all diagenetic events as far as possible, and to attempt to establish simple (geochemical-petrological) models for the diagenetic sequences observed in each subenvironment; and then to compare these models with each other in an attempt to explain differences and/or similarities between sequences of diagenetic events.

#### TERMINOLOGY AND METHODOLOGY

"There's glory for you! "  
"I don't know what you mean by 'glory'," Alice said.  
Humpty Dumpty smiled contemptuously. "Of course you don't -  
till I tell you. I meant 'there's a nice knock-down argument  
for you! ' "  
"But 'glory' doesn't mean 'a nice knock-down argument'," Alice objected.  
"When I use a word," Humpty Dumpty said in a rather scornful tone,  
"it means just what I choose it to mean - neither more nor less."

Lewis Carroll

Authigenesis, the formation of new minerals, is but one of many diagenetic processes. Unless specified otherwise, 'authigenesis' is used here in a loose sense, to include precipitation from solution and by alteration (neomorphism). In a stricter sense, one may restrict 'authigenesis' to precipitation, and describe neomorphism of a pre-existing phase as 'diagenetic'.

The terminology employed in all aspects of sample description follows standard

and widely used classification as far as possible. Schemes for textural maturity and mineralogical classification of sandstones are modified from those proposed by Folk (1968) and McBride (1963) respectively; mineralogical classification is summarised in Fig. 1.3. The terminology and classification used in the description and interpretation of porosity follows the schemes developed by Pittman (1979) and Schmidt and McDonald (1979b). Thus, observations are made in terms of intergranular (or enlarged intergranular), micro-, dissolution, and fracture porosity. The criteria developed by Schmidt and McDonald (1979b) are used in elucidating the nature of pore space, and interpreting either a primary or secondary origin for this porosity. Fine-grained sediments are uniformly categorised as mudrocks (Spears, 1980).

Blue-dye impregnated, and carbonate stained thin sections were made of all 600 sandstone samples collected. Petrographical descriptions concentrated on all aspects of the rock, and are summarised in Table 1.1. Modal analysis was performed on 35% of the thin sections to quantify visual estimates. Subsequently, a range of analytical techniques was applied to both selected and randomly chosen samples to supplement basic petrography, and elucidate features observed in thin section.

Scanning electron microscopy (SEM) was employed to enhance two-dimensional observations, and to elucidate the three-dimensional relationships between detrital and diagenetic phases, and porosity, in 45% of the sandstone samples. The chemistry of phases observed via SEM was confirmed by elemental energy dispersive analysis (EDS). Whole rock and clay fraction, X-ray diffraction analysis (XRD) was undertaken on 30% of the samples to identify structurally, confirm, and quantify the nature of clay minerals and other phases detected visually. Detrital and diagenetic components of selected samples were analysed with an electron microprobe to quantify chemical identifications from either visual or X-ray diffraction analysis. Authigenic phases as well as neomorphosed

detrital micas gave low totals, ranging from 40-90%. These low totals are not, however, entirely unexpected in view of the nature of authigenic clay mineral crystals and the loose, low density form of their pore-filling or pore-lining habits. Whilst SEM observation reveals many platelets to be up to 40  $\mu\text{m}$  in diameter, they are all fibrous or platey in form and usually less than 0.5  $\mu\text{m}$  thick. Thus, it is statistically likely that a 1  $\mu\text{m}$  beam, penetrating to a depth of approximately 3-4  $\mu\text{m}$  will 'analyse' a varying degree of epoxy resin, as well as the intended mineral. This is confirmed by the presence of anomalous S and Cl peaks with all clay mineral analyses, which correspond in proportion to those of control analyses of the resin.

Observation of selected samples under cathodoluminescence (CL) was undertaken to clarify sequences of diagenetic phases observed during the basic analyses outlined above. Stable isotope (SI) ratios were analysed in selected carbonate concretions and cements and clays to quantify the changing conditions during sequences of authigenic precipitation. Finally, mudrocks from all the localities at which sandstones were sampled were analysed by XRD. Details of all these techniques and compilations of the resulting data are contained in the appendices.

The habit, morphology and character of authigenic minerals vary greatly. During diagenesis minerals may nucleate on detrital grains of the same mineralogy as overgrowths, on grains of differing mineralogy and as discrete crystals. They may also form by the in situ alteration of pre-existing phases. Furthermore, the form and, indeed, the crystal habit, of an authigenic phase can vary both between samples and within the same sample. In this thesis the following terms will be used to describe authigenic minerals (they are illustrated in Fig. 1.4):

Overgrowth:        a precipitate of one mineral on a structurally similar, if not identical, host mineral. Overgrowths may or may not be

in optical continuity with the host, but some degree of crystallographic continuity is required. Although overgrowths necessarily line and fill pores, they shall not normally be described as such.

Pore lining: minerals lining, and/or growing into a pore space, and nucleated on or perhaps replacing the pore walls. Pore-lining phases may not be crystallographically related to their pore walls, which can be either earlier authigenic phases, or grains. Although a pore lining fills pore space, it will not be described as a pore filling.

Pore filling: discrete, or aggregates of discrete, crystal precipitates which fill pore spaces and are not structurally related to their pore walls. Precipitation of pore-filling phases may not require detrital seed crystals as nuclei, but may occur directly from solution.

Neomorphism: the in situ structural alteration of one phase to another involving the loss and/or addition of non-structural or mobile cations without dissolution and reprecipitation of the original phase.

Replacement: simply the precipitation of a new phase in the space previously occupied by a dissolved pre-existing phase. It is not always possible to determine whether these events occur simultaneously, along a thin-solution film between the two phases, or if they are separated in time.

Cement: authigenic phases may occur as overgrowths, inter- and intra-

granular pore linings and pore fillings, and neomorphosed or solution replacements. However, only those phases which are interpreted as contributing to the structural framework of the rock (i.e. binding or holding grains together) will be considered as cements. Thus, for example, a loose discrete pore-filling clay is not a cement, but poikilotopic calcite crystals and connected euhedral overgrowths in a quartz arenite are.

The following six groups (s.l.) of clay mineral species are identified in this thesis (details are given in Appendix B): chlorites (including chamosite), berthierine, kandites (including dickite and kaolinite), micas (including illite), smectites and vermiculites.

This differs from the AIPEA recommendations (Bailey, 1980) in one major respect, that is, the term kandite is preferred as the group name for the "kaolin" minerals. This preference is based on the confusion which may arise out of using the term "kaolinite" to define the group, and subgroup of "kaolin" minerals, as well as one of the species. Furthermore, use of the term "kaolins" in describing pseudo-hexagonal plates should not be allowed to become synonymous with identification of the mineral "kaolinite". This is because ~~all~~ the other species in this subgroup form pseudo-hexagonal plates as do certain varieties of authigenic chlorite (Wilson and Pittman, 1977). Furthermore, if the suggestions of Hanson et al (1981) are correct and dickite is the more stable polymorph of this group of minerals, a specific identification may be important if the conditions under which the various species form differs significantly.

The term "illite" (Grim et al, 1937) was proposed "for . . . clay size micaceous components in argillaceous rocks", but has since become the ~~synonym~~ for a



fibrous authigenic clay, sometimes shown to be potassium bearing (Wilson and Pittman, 1977; Hancock and Taylor, 1978; Odom et al, 1979). The exact position of this mineral is still, however, in doubt (Bailey, 1980), although it is included as a mica here. Furthermore, in addition to some cautionary rhetoric (Sellwood and Parker, 1978), recent work (Güven et al, 1980) has shown that illitic material may in fact contain a small percentage of randomly interstratified smectite. Güven et al, (1980) were unable to distinguish such clays from pure illite. Also, Burley (pers. comm. 1981), in analysing clay minerals similar in habit to those previously described as illite on a purely morphological basis, believes that a significant amount of smectite interstratification occurs. The degree to which modern usage has diverged from the original proposition is easily demonstrable. Illite is used as a term for authigenic material in sandstones as well as detrital mica in mudrocks, whilst illitic clays are often 30  $\mu\text{m}$  long, and not, therefore, "clay size". In view of these variations in definition and nomenclature, the terms illite and illitic are used throughout this study in a loose sense, unless otherwise stated to denote authigenic micaceous clay minerals containing  $\text{K}_2\text{O}$ ,  $\text{Al}_2\text{O}_3$ , and  $\text{Si}_2\text{O}$  with small quantities of  $\text{FeO}$  and  $\text{MgO}$ , and possibly interstratified with 0-10% smectite.

Semi-quantification of X-ray diffraction analysis of clay minerals follows the method outlined by Weir et al, (1975). This method involves the measurement of peak heights, rather than areas, as proposed by Jeans (1978), and ratioing of values after an adjustment for peak intensity. This method is preferred because the latter is affected by mineral crystallinity as well as quantity. Thus, any semi-quantitative comparison of clay minerals from different depths and areas within a basin, or even different basins, could express variations in crystallinity as well as quantity, and therefore be a less accurate guide in semi-quantification. This method should also allow comparison of trends documented in this thesis with recent work, particularly

that of the "Reading School" (Morris, 1979; Hurst, 1980; Watts, 1980; Rodd, pers. comm. 1981). However, in view of the numerous errors and inaccuracies introduced during sample preparation, running, and interpretation (Archer, 1970), the resulting "quantities" that ones estimates are likely to be up to 50% in error. Furthermore, comparisons of data collected by different workers, with different clay mineral suites, diffractometers, running conditions, etc, are likely to be of no more than qualitative value. However, despite these acknowledged problems, these results are internally consistent on a semi-quantitative level, and the resulting trends are comparable with similar studies.

#### THE LIMITATIONS OF THIS THESIS

"And each new problem would require a new crusade, and each new crusade would leave fresh problems for yet further crusades to solve and multiply in the same way."

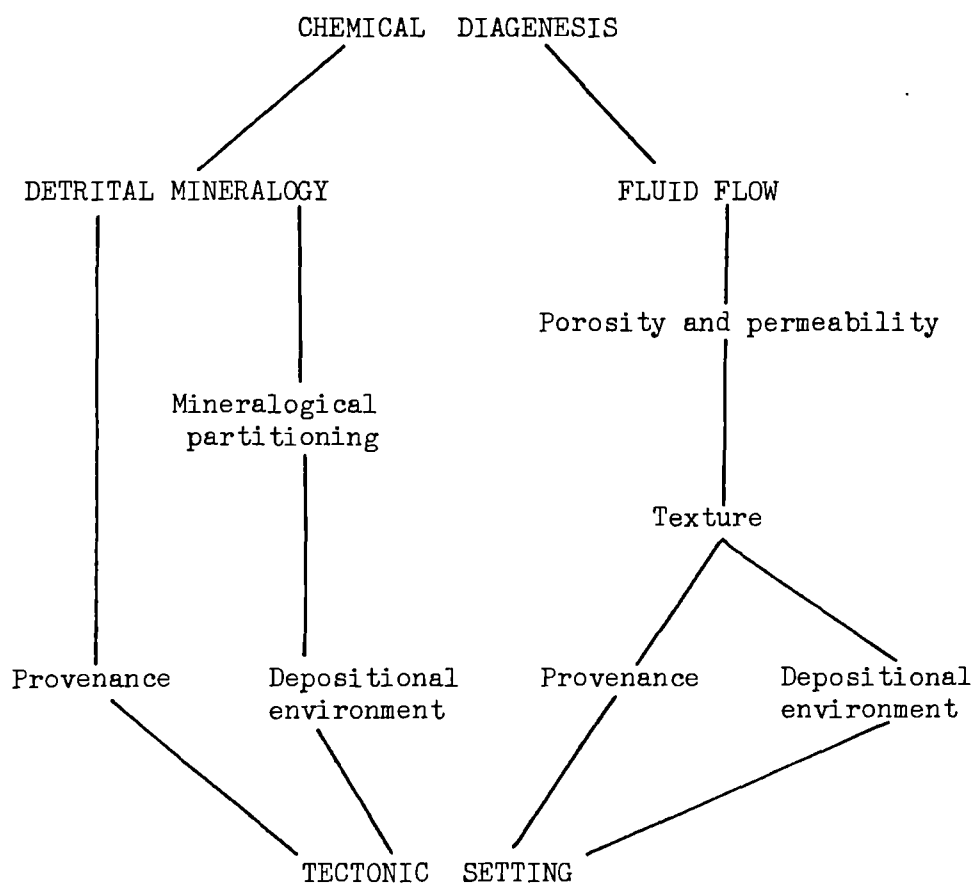
Julian Huxley

First and foremost, if either the gross regional, or local detailed sedimentological models used as the basis for this thesis are wrong, then the fundamental questions of diagenetic control must remain unanswered. Secondly, although some of the effects of weathering on outcrop samples have been identified, it is impossible, in the absence of fresh, subsurface samples, to evaluate the degree to which the samples from the North Yorkshire Moors studied in this thesis have been modified by Recent weathering. Thirdly, numerous problems arose during the planning, analysis and data recording reported in this thesis: both evaluation of the significance of these, and the degrees to which their solution was sought was necessarily subjective. In attempting to solve the problems set out in this thesis, an initially empirical and subsequently, hypothetico-deductive approach was followed. However, by the very nature of problem solving, one has to understand the

problems, and the language of the problems first, and the same or a similar language must be used in communicating the results of any investigation. This study has, therefore, suffered, and probably still suffers from the use of entrenched terminology and theory-laden observations: that is, objective description in this thesis may be hampered by constrictive use of geological and petrological terms which conjure up various differing ideas in the minds of the author and the reader.

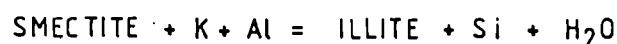
Fig. 1.1 Flow chart of the interrelationship of chemical diagenesis and prediagenetic conditions.

(after Hayes, 1979).

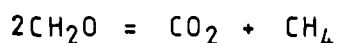


## FIG. 1.2 THE ORIGIN AND EVOLUTION OF 'AGGRESSIVE' PORE SOLUTIONS (Curtis,pers.comm.1982)

During burial of organic-rich mudrocks diagenetic processes continue:  
illitisation of smectites releases water

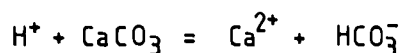


bacterial methanogenic fermentation liberates carbon dioxide

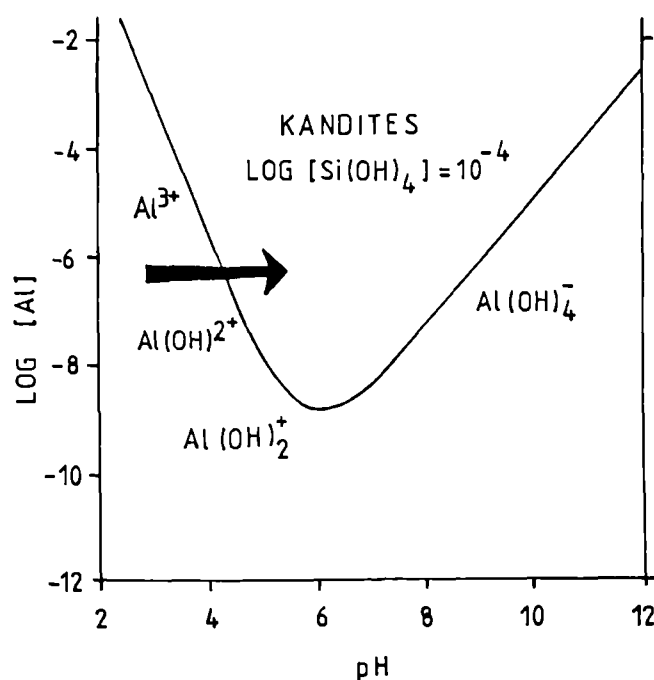
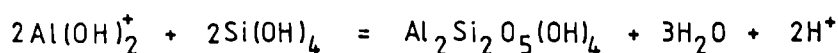


and so the resulting solutions are acidic. These solutions are also saturated with respect to silica and alumina: both released from the potassium source required for smectite illitisation (e.g. mica or feldspar).

During the generation of secondary porosity pH must rise



this raising of pH must cause supersaturation with respect to kandites (arrowed).



Consequently, whilst dissolving calcite, the pH of aggressive solutions rises, and kandites precipitate.

(after McBride, 1963)

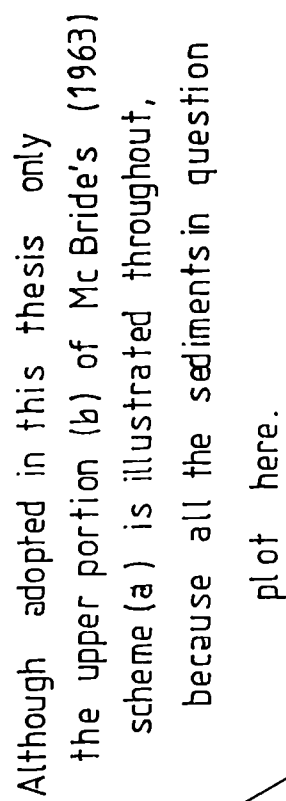


FIG. 1.4 AUTHIGENIC MINERALS: HABIT AND NOMENCLATURE

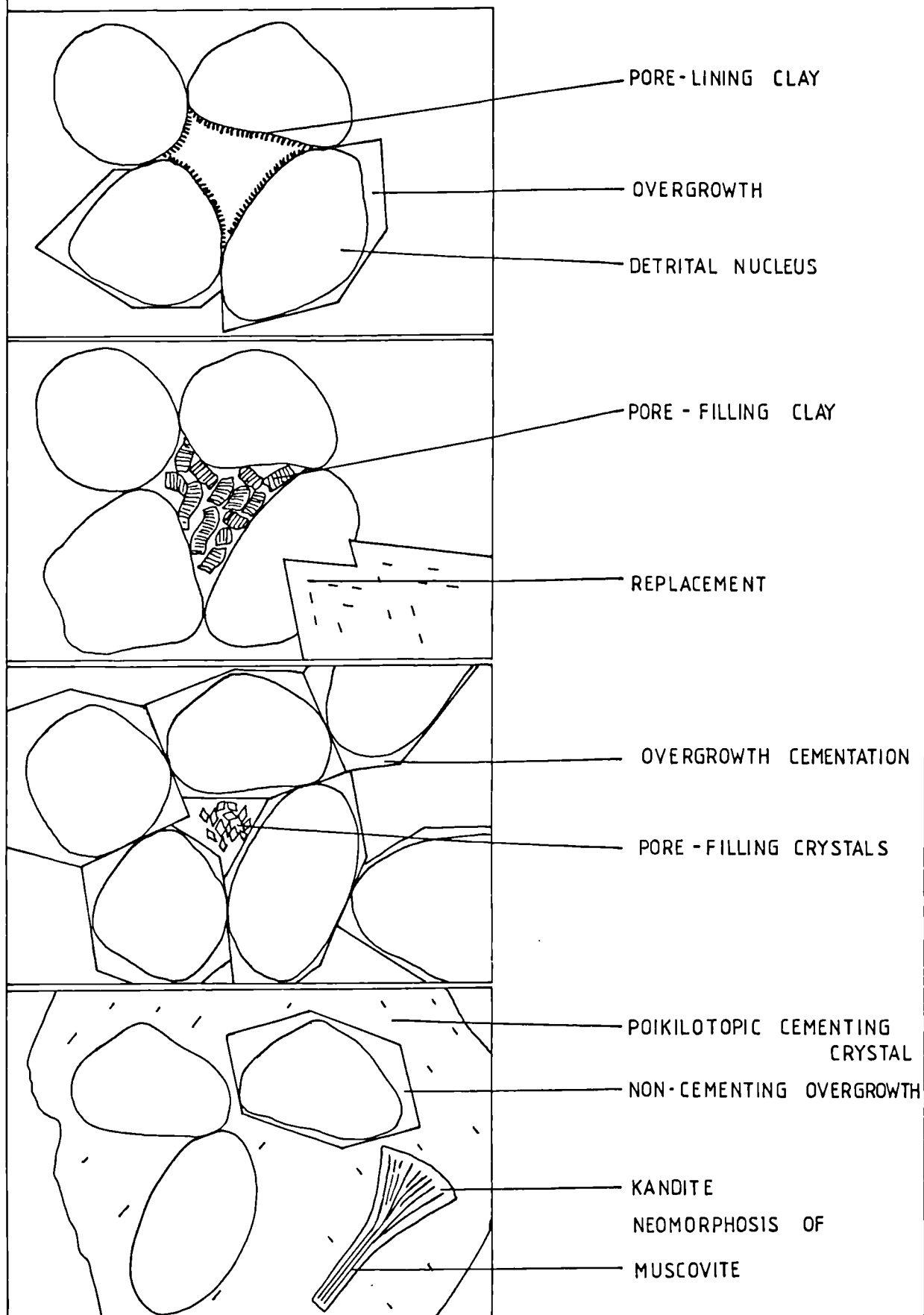


Table 1.1 Thin-section observation.

Sedimentary components.

Identification and semi-quantitative visual estimates of proportions.

Description of distribution and size fractionation.

Diagenesis.

Estimation of degrees of compaction and grain deformation.

Description of neomorphosed sedimentary phases.

Morphological identification and semi-quantification of authigenic phases.

Description of distribution and replacive, cementing, or pore-filling habits of authigenic phases.

Estimation of relative timing of solution and precipitation events, involving sedimentary and authigenic phases during diagenesis.

Porosity.

Semi-quantitative visual estimate and analysis of pore space.

Interpretative description of type and distribution of porosity including relative estimates of permeability.

Texture.

Estimates of average and range of grain sizes.

Degree of sphericity and sorting of predominant size fraction.

Packing, degree of compaction.

Clast, matrix, or cement supportive nature of framework.

Overall maturity.

Notes.

Comments emphasising features of individual rocks which are not dwelt on sufficiently within any one category above.



CHAPTER TWO: THE NORTH SEA BASIN, TECTONIC HISTORY AND MIDDLE JURASSIC  
SEDIMENTOLOGY: A REVIEW

This chapter reviews the tectonic history of the North Sea Basin in order to highlight the role of global tectonics in regional and local tectonics, and in sedimentology. In this chapter I intend demonstrating that the North Sea Basin formed and developed as an intracratonic basin, as a result of global tectonic events. Subsequently, during the Middle Jurassic, palaeogeographical facies distribution and evolution were controlled by both the tectonic framework of the area, and eustatic sea-level changes. Consequently, the sedimentological evolution of the North Sea Basin is the microscale result of macroscale influences. Moreover, I intend to demonstrate the complex interrelationship of subsequent events, relating subsidence and burial history of these sedimentary packets - Brent and Ravenscar Group - to global tectonics, eustatic sea-level change, and decaying heat flow beneath the North Sea.

THE NORTH SEA BASIN

The gross tectonic and sedimentological history of the North Sea Basin during the Middle Jurassic can be related to the Palaeozoic consolidation and eventual Mesozoic disintegration of Pangaea (Ziegler, 1981). Classic plate tectonic models of continental disintegration involve mantle upwelling and crustal thinning associated with lithospheric tension. At the triple foci of the resulting stresses, crustal doming, rift junctions, and basaltic volcanic activity are common. Subsequently, either two rift arms develop further into oceanic crust and the third arm fails, or all three fail, and the upwelling mantle cools and the region subsides. The graben systems of the North Sea Basin - Viking, Witch Ground, Central, etc. - (Fig. 2.1) are considered to be a complex of failed arms after the separation of Europe and North America (Burke, 1977).



The Hercynian orogeny led, in the Upper Palaeozoic, to the formation of a landmass in north-west Europe. Subsequently, as a result of regional stresses during the Triassic, and probably during the Permian also, trilete fault systems were widely emplaced in the North Sea Basin. However, these did not form active graben at this time. Later, during the early Mesozoic opening of the South, Central, and then North Atlantic Oceans, both Caledonian and Hercynian lines of weakness in the craton were reactivated. These modified the nascent graben system (Challinor and Outlaw, 1981). In addition, the broad tectonic pattern was locally modified by both episodic volcanic activity, which originated in the Permian (Woodhall and Knox, 1979), and mobilisation of Zechstein evaporites (Ziegler, 1981). Although most of the major tectonic structures were already present in the Triassic, the majority were inactive until crustal thinning and regional doming initiated graben development in the Jurassic.

Despite the difficulty of actually separating the causes and effects of events during the Jurassic, several broad generalisations may be made. During the Jurassic a general eustatic rise in sea level occurred (Vail et al, 1977; Hallam, 1978, 1981), the result perhaps of expansion of mid-ocean ridges (Hays and Pitman, 1973). However, local tectonic events in the North Sea Basin (the Cimmerian pulses) influenced sea level, causing local regression during the Middle Jurassic.

During the Liassic extensional tectonics activated and deepened the graben systems defined during the Triassic. Simultaneously, sea-level rose, and a gradual transgression resulted in the formation of a shallow-epeiric sea (Anderton et al, 1979). This sea was generally starved of sediment, and the resulting sequence is dominated by black organic-rich mudrocks and ironstones (Hallam, 1975; Morris, 1979). However, coarse clastics such as the Statfjord Formation, which occur locally, were probably derived from fault scarps:

synsedimentary faulting which may be related to early-Cimmerian pulses (Eynon, 1981). In addition, a dome developed at the junction of the Viking, Witch Ground, and Central Graben systems, the site of continued sporadic volcanic activity. This and other early Jurassic igneous activity in the North Sea Basin is typical of intracratonic rifts (Ziegler, 1981), and analogous to that of early Miocene extensional tectonics in the East African rift valley, a supposedly embryonic ocean forming system (Dixon et al, 1981).

Extensional tectonics in the Triassic and Lower Jurassic was related to the more distal South Atlantic opening, the end of the Lower Jurassic marking the onset of spreading in the Central Atlantic. Consequently, a further mid-Cimmerian pulse in the North Sea Basin reactivated positive structures such as the Shetland Platform and the Mid-North Sea High, and accentuated their dissection by rift systems such as the Viking and Central Graben. The resulting uplift and regression during the Middle Jurassic was centred on doming and subaerial basaltic volcanic activity in the Piper Field area. This resulted in a concentric arrangement of radiating conduits - the graben system - carrying erosion products away from the dome and their subsequent unconformable deposition (Eynon, 1981). Although much of the detritus was derived along the graben, local fault-scarp derivation was also important, especially in the half-graben of the Northern North Sea (Budding and Inglin, 1981; Hancock and Fisher, 1981; Ziegler, 1981). Consequently, the sediment starved shallow marine basins of the Lower Jurassic are unconformably overlain by a complex of coarser intracratonic shallow marine sheet sands and delta lobes. The Brent and Ravenscar Groups are two such lobes and their differences reflect the complex interrelationships of local and regional influences at this time. Facies distribution during the Middle Jurassic was controlled by continued sporadic bursts of rifting and regression throughout the basin, and terminated by a further Cimmerian pulse, subsidence, and the widespread Callovian transgression (Ziegler, 1981).

The North Sea Basin lay between 20° and 30°N during the Jurassic (Smith et al, 1973) and was, therefore, tropical.

#### THE EAST SHETLAND BASIN BRENT GROUP

Facies distribution of the Brent Group during the Middle Jurassic was controlled by three interacting influences. These were a slow eustatic sea-level rise, extensional rifting of the North Sea graben systems, and doming and volcanicity at the junction of the Moray, Central and Viking Graben. As sea level was not rising as fast as the doming, subaerial exposure and erosion took place. Lateral and vertical environmental changes in the Northern North Sea at this time reflect the northwards advance of a fluviially-dominated delta system into a shallow sea, but unconformably overlying the Lower Jurassic. Several things, however, hamper investigation of this deltaic progradation.

Firstly, recent workers have not fully accepted the five-fold lithostratigraphical division of the Brent Group proposed by Deegan and Scull (1977). Several factors contribute to this position. Only recently (Eynon, 1981) has any palaeontological basis been added to correlation within the Brent Group. Also, the formations identified by Deegan and Scull (1977) do not occur uniformly throughout the basin, being reduced or absent in places. Finally, as a delta progrades, different subenvironments occur contemporaneously. Thus at any one time marked lateral variations in lithology are likely to occur. As lithostratigraphy correlates possibly diachronous rock types, it is likely to correlate environmental changes, and hence fail when particular lithologies do not develop.

Secondly, palaeoenvironmental reconstructions are based on widely spaced cored intervals from productive hydrocarbon reservoirs (Fig. 2.2). These cores may be miles apart within individual reservoirs, and tens of miles from those

in the next reservoir. Moreover, as interpretations of any one sequence may differ between workers, and change as further information becomes available, the likelihood of reconstructing Middle Jurassic palaeogeography on the basis of the dozen detailed studies currently available in the literature is slight. However, some generalisations may be made on the basis of these studies and more general reviews of unpublished data.

The coarse-basal Broom Formation (Fig. 2.3A) overlies eroded Lower Jurassic sediments in the south of the basin. This sandstone, conglomeratic in places, thins northwards and away from fault scarps. It is, therefore, probably the result of subaerial or submarine erosion and reworking of such locally active structures. However, it is not present throughout the whole basin. It is missing, for example, from Wells 211/19-4 and 211/24-4 in the Murchison Field (Parry et al, 1981) and from the whole of the Thistle Field (Hallett, 1981). The Broom Formation is variably interpreted as a shallow shelf sheet sand (Eynon, 1981), and an offshore-sheet sand (Budding and Inglis, 1981). However, it appears to bear little resemblance or relation sedimentologically to the overlying Rannoch Formation.

The Rannoch Formation (Fig. 2.3B) is a micaceous sand in the south (Brent and Ninian) and fine silt and mudrock in the north (Murchison and Thistle). This northward fining reflects the progradation of the delta from the south. Thus, although the sediments in the Murchison area coarsen upwards, this occurs later in the north. This coarsening-upwards sequence is interpreted as a prodelta or delta-front sequence deposited in a shallow nearshore marine or possibly distal mouth-bar environment. The high sand:clay ratios reported reflect a fluvial influx of sand from the south (Budding and Inglis, 1981; Eynon, 1981).

The overlying Etive Formation (Fig. 2.3B) represents the prograding interface

between the marine and the fluvial system: it is variably interpreted throughout the basin. The Ninian succession is interpreted as a regressive sheet of coalescing mouth bars (Albright et al, 1980), capped with a distributary channel sand (Eynon, 1981). In the Statfjord Field, this formation coarsens upwards through mouth bars and delta-top sediments (Moiola and Jones, 1981). The Cormorant sequences are interpreted by Budding and Inglin (1981) as clean shoreface, barrier, beach and barrier-top sands with some incised channel deposits. The succession at Heather is similar (Gray and Barnes, 1981) whilst in the north the Murchison and Thistle successions are interpreted as recording the rapid advance of a fluvial system with distributary-mouth bars, coarsening upwards into a distributary system (Hallett, 1981; Simpson and Whitley, 1981).

The overlying "marine incursion event" reported by Eynon (1981) is not reported elsewhere and, therefore, cannot be used to refine the present lithostratigraphy, using biostratigraphical criteria.

The Ness Formation (Fig. 2.3C) which conformably overlies these coarsening upwards distributary, and interdistributary sequences, is wholly fluvial or non-marine with a variety of channel and crevasse-splay sandstones, floodplain mudrocks and lacustrine fillings, according to all the above authors except Parry et al (1981), who report palynological evidence for brackish and saline influences within these sediments. The Ness Formation is highly variable within the basin, but its non-marine or fluvial sequences all reflect the progradation of the distributary system into the basin from the south (Eynon, 1981), even though the massive sandstone interpreted as a major distributary channel is not always present.

The uppermost Tarbert Formation (Fig. 2.3D) is interpreted as recording a marine transgression over the delta plain (Brown and Deegan, 1981; Eynon, 1981)

although this is not recognised in all cored intervals (Albright et al, 1980; Simpson and Whitley, 1981). Furthermore, Eynon (1981) discusses the advances of the two Bathonian delta lobes prior to marine reworking at the end of the Middle Jurassic. This advance is not recognised or reported by other workers in the area.

In summary, although correlation of sequences across the East Shetland Basin is problematical, one may conclude that the Middle Jurassic Brent Group here records the northward progradation of a mostly fluviially dominated delta across a Lower Jurassic unconformity surface. Shallow marine fault-controlled conglomerates occur at the base, overlain by a coarsening upwards, prodelta, offshore, to nearshore sequence, capped by either distributary-mouth bars, or a barrier-bar system over which the fluvial delta top deposits prograded. Marine influences returned in the Upper Bathonian flooding the delta, and reworking the last deposits on the delta floodplain.

#### SEDIMENTOLOGY OF MIDDLE JURASSIC STRATA IN THE CLEVELAND BASIN

The purpose of this section is to review the sedimentological history of the Cleveland Basin during the Middle Jurassic. The resulting sequence has been a subject of debate for the past two hundred years. Indeed, a list of early workers on the subject reads like a Who's Who of British Geology, including Adam Smith (see Hemingway and Owen, 1975), Sedgwick (1826), Phillips (1829) and Murchison (1832). The Geological Survey undertook the first and only comprehensive mapping of the area towards the end of the last century, under the direction of Fox-Strangways. The nomenclature erected with the published maps introduced the term "Estuarine Series" and proffered the first interpretation of their depositional environment. However, Kendall and Wroot (1924) found a greater affinity between the Estuarine Series and the Coal Measures, than between the former and its lateral estuarine equivalents in

Lincolnshire. Subsequently, Black (1928, 1929, 1934), in a series of the earliest and classic sedimentological papers proposed a "Deltaic" origin. Both the continued and renewed interest in the Ravenscar Group probably owe more to the painstaking work of Hemingway, than to the recent discovery of hydrocarbon accumulations in analogous strata in the North Sea (Hemingway, 1974 and references therein).

Unless otherwise stated, the summary below is drawn from the following sources:  
Hemingway (1974)  
Knox (1969), Hemingway and Knox (1973),/Nami (1976a, 1976b), Nami and Leeder (1978), Leeder and Nami (1979), Hancock and Fisher (1981), Livera (1981), and Livera and Leeder (1981). The stratigraphical nomenclature used in this thesis is summarised in Table 2.1 incorporating the recent correlation of Eller Beck and Blowgill strata (Powell and Rathbone, in press), confirming Bate's (1967) suggestion. This scheme is preferred to that proposed by Cope et al, (1981).

Interpretation of the tectonic framework of the Cleveland Basin (Dingle, 1971) in the Middle Jurassic may be based on both palaeogeographical reconstructions and isopachyte maps of the area (Kent, 1980; Glennie and Boegner, 1981). This interpretation (Fig. 2.4) suggests that the hinterland and source area of the delta sediments was probably a combination of both a "Pennine" upland in the northwest and the Mid-North Sea High in the north and northeast, whilst to the south lay the Market Weighton area. Both the lateral thinning and impersistence of strata southwards from Yorkshire into Humberside (Gaunt et al, 1980) suggest that the Cleveland Basin was subsiding relative to the Market Weighton block on the line of the Howardian-Flamborough Fault Zone. The proposed extension of this fault zone into the Dowsing Fault (Kent, 1980) therefore suggests that the Cleveland Basin represents the landward end of a gently subsiding continuum with the Sole Pit Trough. The delta, however, does not extend far beyond the structural limits of the present basin, as marine sediments



of this age occur offshore in Well 42/29-1.

The timing and structural setting of the Middle Jurassic delta in Yorkshire was controlled by regional tectonics despite a global transgression. However, the sedimentological development of the delta was probably due to more local influences. In general, the deltaic sequence is made up of a coarsening-upwards marine or prodelta unit, and four non-marine sequences with three intercalated marine sequences. Careful interpretation of the nature of the boundaries between these units is critical to an understanding of the evolution of the delta. Although problems remain in interpreting the contact between the Scarborough and Scalby Formations, boundaries elsewhere suggest that the gross control on the sedimentary sequence recorded in Yorkshire was delta-distributary migration or abandonment against a background of gentle epeirogenic subsidence.

Fluvio-deltaic strata are restricted to the Bajocian and Bathonian Ravenscar Group. Nonetheless, Lower Jurassic and Aalenian (Dogger Formation) sequences in Yorkshire demonstrate aspects of the regressive evolution of the Cleveland Basin before and after the mid-Cimmerian pulse (Anderton et al, 1979).

Greensmith et al, (1980) report "prodelta sheet floods" from the Lower Jurassic Pliensbachian margaritatus Zone. Also, the Toarcian contains striatulum subzone shallow-marine sands in Rosedale, which coarsen upwards into the dumortieria levesquei Zone Blea Wyke Sands at Ravenscar.

The subsequent mid-Cimmerian pulse is reflected in an unconformity between the Lower and Middle Jurassic. Uplift and erosion at this time is demonstrated by both the gently folded nature of Lower Jurassic strata and the variable number of ammonite zones which are missing. The Dogger Formation overlies the falciferum subzone in the Brown Moor Borehole (SE 8126 6023) and, in the south, Hildoceras Zone at Whitby, and moorei subzone at Ravenscar. Furthermore, phosphatised pebbles of Lower Jurassic age occur throughout the Dogger Formation.

These pebbles enclose Toarcian ammonites and range down to recognisable clasts of Harpoceras falciferum Zone Jet Rock at Spy Hill (SE 749647). The base of the Dogger Formation is marked by a lag of these phosphatised pebbles and derived Whitbian concretions. The coarse enclosing sediments are intensively bioturbated by shallow-marine ichnofaunas. Although localised pockets of littoral limestones overlie this basal conglomerate in the northwest, the remainder of the Dogger is mostly comprised of clastics. To the southeast, bipolar herringbone cross lamination occurs in the basal unit, indicative of shallow-tidal activity and emergence. Furthermore, most of the subsequent lagoonal sedimentation in the southeast is intensively rooted, an additional indication of the degree of emergence in this area. To the northwest, the Dogger Formation coarsens upwards in bands running northeast to southwest, comprising a coastal barrier sequence and offshore black mudrocks. The early and persistent emergence of the area to the southeast suggests that a shoreline lay here, rather than to the northwest, where the uppermost Dogger sediments, offshore marine black mudrocks, are also rooted (Fig. 2.5A).

The transition from the Dogger to the Saltwick Formation probably represents fluvio-deltaic progradation. The Dogger Formation however, is a mostly shallow-marine complex of sandstones and mudrocks and does not, therefore, form a simply passive prodelta deposit beneath the delta advancing from the northeast. In addition to the reworked Liassic pebbles, much of the clastic material reflects marine reworking of the topmost Liassic.

This shallow-marine and littoral coarsening-upwards deposit is conformably overlain by the Saltwick Formation, an alluvial and delta-top sequence. Palynological data suggest that whilst the area to the east was wholly non-marine, and indeed contains a freshwater lake, brackish influence persisted for a time in the Saltwick Formation's westernmost outcrops (Hill, 1974).

The Saltwick Formation comprises up to 50 m of fluvial and alluvial sediments which are best exposed at Whitby and inland along the northern escarpment of the Moors. These non-marine strata are composed of fluvial channel sandstone deposits, incised into a sequence of lacustrine and alluvial mudrocks, levees and occasional crevasse-splay sandstones. This fluvial sequence was supplied with clastic material from the northeast by a number of straight and meandering rivers. These rivers, responsible for initiating and maintaining this alluvial progradation, incised into the underlying Dogger. However, the resulting channel sandstone deposits occur throughout the lower three-quarters of the Formation only. Contemporaneous fine-grained alluvial deposits on the floodplain at this time were well drained and plant colonised; several soil horizons, however, are preserved throughout the sequence (Retallack, pers. comm. to Leeder, 1980). However, whilst the upper few metres of the Saltwick Formation contains alluvial mudrocks, channel deposits are absent, suggesting that this alluvium was supplied by a fluvial or distributary channel system situated elsewhere in the delta. As a result of delta-lobe abandonment, the fluvial sequence stagnated, became marshy and eventually saline before subsiding beneath a shallow sea. No delta-front deposits are seen in the Saltwick Formation, suggesting that progradation and abandonment were rapid events. The thin succeeding shallow-marine Eller Beck Formation consists of a basal ironstone and coarsening-upwards sequence of sandstones which are rooted and overlain by a coal.

During marine incursion, the interaction of continued clastic input from the north with shallow-marine wave action produced a beach with repeated episodes of marsh colonisation in the north of the basin. Further south, contemporaneous deposition of shallow-marine sandstones, mudrocks and deeper water limestones - the Blowgill strata - occurred. As the active delta and clastic input increased, the northerly beach prograded southwards over the shallow-marine sands to generate this coarsening-upwards unit. A beach, rather than a complex of

barrier islands is inferred as the land/sea interface, because the latter would have resulted in the accumulation of lagoonal sediments, whereas the Eller Beck Formation sandstones are overlain by a coal and wholly alluvial-fluvial deposits.

The Sycharham Member is only poorly exposed throughout the basin, and the nature of its contact with the Lebberston Member is unknown. It consists of 25 m of fluvial and alluvial deposits, including a 1 km wide multiple channel sandbody at Hayburn Wyke. However, the sequence contains marine microfossils and may, therefore, have suffered sporadic marine incursions. The Lebberston Member transgressed over part of the basin from the south and southwest. It is composed of the lower calcareous Millepore Bed (Fig. 2.5B) and the upper, clastic, Yons Nab Beds. At its base the Millepore Bed is sometimes incised into the Sycharham Member.

There are marked differences between the sequences throughout the basin at this time. In the southwest, in the Hambleton Hills, oolites accumulated in relatively shallow-marine shoals. Conversely, on the coast, the Millepore Bed is a variable, high-energy deposit indicative of a shallow-marine near-shore environment. The sequences reflect the inferred advance of a storm beach from the north, over a shallow tidally influenced dune complex. Petrographically subarkoses, these sandstones contain shelly bioclastic debris and are intensively bioturbated. As there was little clastic input from the north, clear water prevailed, allowing carbonate coatings to form on grains. A normally calm offshore area is the probable source of storm derived influxes of oolites, which occur towards the top of the Millepore Bed. Intraformational conglomerates indicate that extremely rapid submarine lithification took place in this dune complex, and more generally throughout the Millepore Bed time, as interpreted from the karstic topography developed at the contact with the Yons Nab Beds at Osgodby Nab and Cloughton (Leeder,

pers. comm. 1981).

The Millepore Bed is overlain conformably by the clastic Yons Nab Beds. This sequence represents renewed deltaic activity and the return of detrital clastic supply from the north. The Yons Nab Beds are highly variable and consist of a suite of offshore mudrocks, coarsening upwards through shoreface and interdistributary-bay siltstones and sandstones, into tidal ridges and bars, separated by lagoonal fills and tidal marshes.

Although the Millepore-Yons Nab Beds sequence is conformable, there is an abrupt change from carbonate sedimentation in the former to the entirely clastic sediments of the latter. Delta-lobe or delta-distributary switching rather than any change of local marine geochemistry is a far more likely explanation for this change. The Yons Nab Beds (Fig. 2.5C) outcrop along the coast, but are poorly exposed inland. The sequence at Yons Nab itself coarsens upward from fully marine offshore mudstones and sandstones to a rooted and emergent contact with the fluvial Gristhorpe Member. This sequence may represent either the shoreface or a sheltered interdistributary bay; unfortunately, bioturbation has destroyed all the primary sedimentary structures, making any positive differentiation impossible. At Osgodby, 6 m of alternating bioturbated sandstone and siltstone occurs. These sandstones are internally erosive and probably represent a large migrating tidal-channel deposit. The sequence at Cloughton Wyke records a tidally influenced sheet sand protecting a lagoonal sequence and dissected by a tidal-rip channel. In general, the Yons Nab Beds record the north to south progradation of a tidal shoreface over the Millepore Bed. Outcrop paucity precludes the identification of erosive reworking of the latter. Sequences to the north suggest sheltered lagoonal filling or marsh buildup behind beach or tidal barriers.

The top of the Yons Nab Beds is plant colonised and overlain conformably

by the normally fluvial Gristhorpe Member. In places, lagoonal conditions and intense bioturbation persisted at the base of the Gristhorpe Member, but the upper half of the unit is wholly fluvial. Although the Gristhorpe Member is dominated by overbank or floodplain deposits, fluvial channels do exist, cutting down into the underlying Yons Nab Beds. At the top of the Gristhorpe Member, channel deposits, indicative of sluggish low-energy flow, dissect mudrock sequences with occasional marine influence. These sediments represent a coastal, rather than an alluvial plain.

The transition to the Scarborough Formation (Fig. 2.5D) is marked by an abrupt change from fluvial to tidal or fully marine mudrocks. Delta-distributary switching or abandonment is again suggested as the cause of this environmental change, possibly influenced by minor fault movements (Livera, 1981). A gradual transgression did not occur, as this would have caused considerable reworking of the underlying sediments. This rapid marine incursion extended across the eastern region of the basin. The depositional history of the Scarborough Formation is not fully understood, as there has not yet been a comprehensive study of these rocks as an entity and in relation to the basin as a whole. The lower units overlying the Gristhorpe Member are low-energy deposits, mudrocks passing upwards into a subtidal sheet which shallows northwards into an intertidal sandflat: the Blea Wyke Member. This sandbody is overlain by thin shallow marine, sandy limestones and mudrocks. These are in turn succeeded by the Crinoid Grit, a littoral deposit which, as the name implies, is coarse and fossiliferous. It is also bioturbated and thickens northwards, overstepping the Blea Wyke Member onto the Gristhorpe Member. This is overlain by further low-energy mudrocks containing ammonites (Parsons, 1977). The whole sequence terminates in a coarsening-upwards unit, interpreted as a wave-dominated shoreline, or beach deposit.

There is an abrupt break between the Scarborough Formation and the overlying

Scalby Formation, the nature of which is in doubt. The overlying Moor Grit Member is a coarse braided stream deposit, which in places appears to erode into the top of the Scarborough Formation. However, whether this boundary is truly erosive, or whether there is a substantial hiatus here, as suggested by Leeder and Nami (1979), is unclear, so the origin and significance of this transition also remains unclear. Moor Grit Member deposits outcrop throughout the Moors, usually forming a hard, coarse sheet of sandstone. This sandstone is interpreted as a braided river deposit in all localities except south of Scarborough, where it fines and the river is inferred to have become more sinuous. Further south, this river system became meandering, and the spectacular outcrop at Yons Nab is interpreted as a point-bar deposit. It is overlain by a complex meander-belt deposit, marking the transition from the incised Moor Grit to the low-alluvial plain occupied by the Long Nab Member. Although the meander belt is interpreted as fluvial, it is thoroughly bioturbated, including the presence of Ophiomorpha, contains water-escape structures, and a considerable amount of silt- and clay-size sediment, as well as occasional dinoflagellates, features previously interpreted as indicative of marine influence, but now in doubt (e.g. Stewart, 1978).

Although the presence of dinoflagellates would seem to imply a tidal, if not marine origin for all or part of these sediments, a moment's deliberation is necessary. The use of marine microfossils by Hancock and Fisher (1981) in revising sedimentological models should be viewed with caution. Firstly, within this and other deltas there is evidence of episodic reworking of the underlying sediments. The Saltwick, Gristhorpe and Scalby Formations are all incised into the underlying marine units. Consequently, the reworking of marine sediments along with their entrained microfossils is highly likely. The stability of microfossils during reworking and transportation is demonstrated by the Carboniferous spores identified in these strata (Windle, 1979). Secondly, the general model proposed by Livera and Leeder (1981) for this delta is

analogous to modern mangrove swamps with numerous tidal channels and inlets. Thus, the occasional, possibly seasonal or even more frequent, introduction of marine microfloras into alluvial sediments is quite feasible. Thirdly, as Livera (1981) points out, in a tidally influenced delta, the most likely period of overbank flooding is at high tide. Thus, crevassing and overbank flooding are likely to be coincident with the introduction of marine microfloras into the delta, and they will be consequently dispersed onto the floodplain (Fisher and Brown, 1972).

Above the meander belt the Long Nab Member is a sequence of floodplain mudrocks and sandstones, with occasional channel sandstones. The best exposures are again on the coast where several soil horizons and siderite concretionary horizons are developed.

The Scalby Formation is overlain by the wholly marine Callovian Cornbrash. The transition between the two appears to be a gradational transgression with no marked erosion surface (Leeder and Nami, 1979 and subsequent discussion).

#### THE BURIAL HISTORY OF MIDDLE JURASSIC SEDIMENTS IN THE NORTH SEA BASIN

The burial history of Middle Jurassic sediments in the North Sea Basin is influenced by both the opening of the North Atlantic Ocean and eustatic changes in sea level. Shallow marine and deltaic sedimentation was interrupted at the end of the Middle Jurassic by a mid-Cimmerian pulse. This pulse reactivated the rift system of the North Sea Basin, tilting and accentuating positive half-graben relief. Coincidentally, there was a further eustatic rise in sea level. Both may be related to global tectonics: the former is probably the result of the continuing attempts of the Viking Graben to dispatch the United Kingdom westwards; the latter perhaps resulted



from a change of spreading rate in a mid-oceanic ridge system.

During the Upper Jurassic, therefore, movement continued on active faults and sea-level rose. Consequently, the crests and tips of fault blocks formed in the Middle Jurassic were eroded. As the rift system at this time probably had considerable relief, its erosion may have been subaerial as well as submarine (cf. Surlyk, 1978). Nonetheless, the resulting boulder bed at the base of the Upper Jurassic was buried beneath argillaceous sediments accumulating under rapidly deepening water. Gentle subsidence and burial beneath marine sediments continued throughout the Upper Jurassic, although there was some fault movement resulting in a slight unconformity beneath the Kimmeridgian. The extensional tectonics of the Middle Jurassic were also prevalent at this time (Christie and Sclater, 1980).

The Upper Jurassic is separated from the Lower Cretaceous by a marked unconformity (Day et al, 1981). Although stresses were still extensional at this time, with high-heat flow throughout the basin (Cooper et al, 1975), the magnitude of this unconformity may reflect the initiation of a spreading axis in the Rockall Trough in addition to pre-existing stresses in the North Sea Basin (Glennie and Boegner, 1981). Furthermore, sea-level fell, creating a fault-block topography on a shallow-continental shelf (Brown and Deegan, 1981). Thus, at this time, there was further fault-block rotation, coincident uplift and a change from restricted marine sedimentation to highly erosive shallow-marine or non-marine environments. This erosion produced an unconformity which lowered the topography to the Middle Jurassic in Places (Hancock and Scholle, 1975). Extensional tectonics persisted in the North Sea Basin throughout the Lower Cretaceous, but the local and regional picture was radically altered at the boundary with the Upper Cretaceous.

Two events are significant at this time. Firstly, there was a major eustatic

rise in sea level, submerging the Lower Cretaceous continental shelf beneath deep water (Vail et al, 1977). Secondly, stresses in the region changed from extensional to compressional as the axis of spreading in the Atlantic Ocean switched from the Rockall Trough to the present ridge system (Christie and Sclater, 1980; Glennie and Boegner, 1981). These two may be directly related - a major increase in spreading rate caused by a changed spreading axis gradually displacing large volumes of water onto continental shelves.

Subsidence in the Northern North Sea continued throughout the Upper Cretaceous, Tertiary, and Quaternary up to the present day, burying Middle Jurassic strata beneath a 3 km thick cover of sediments. Subsidence rates throughout the Northern North Sea have decayed exponentially, in agreement with predictions from simple theoretical models for cooling attenuated lithosphere (Sleep, 1971; McKenzie, 1978; Sclater and Christie, 1980). Thus, as the axis of separation between Europe and America shifted westwards, extensional stresses in the North Sea ceased, and the mantle plume responsible for high-heat flow beneath the North Sea cooled and the lithosphere began to subside (Sclater and Christie, 1980; Wood, 1981). Palaeotemperature interpretations suggest that the Middle Jurassic sediments of the Northern North Sea hydrocarbon reservoirs are probably at their maximum depth of burial at present (Albright et al, 1980); the Ninian Field reservoir is presently at 100°C.

Although Jurassic sediments were slowly buried during the Lower Cretaceous, a time of high-heat flow in the North Sea, it is unlikely that either Kimmeridgian or Liassic organic-rich mudrocks matured at this time. However, following Cretaceous structural inversion, with deeper and more prolonged burial during the Tertiary, either or both of these sequences matured and generated hydrocarbons which migrated into their present reservoirs late in the Tertiary (Cooper et al, 1975; Barnard and Cooper, 1981).

The controlling influence of local events over global tectonics or eustasy is shown by a comparison between the East Shetland Basin and the Cleveland Basin in Yorkshire. Firstly, the Cleveland Basin has never been a half graben in the sense of the Northern Viking Graben system. Thus, assuming that the Scalby Formation is Bathonian, there is no tilting or unconformity beneath the Callovian. Secondly, although the unconformity between the Jurassic and Cretaceous is as marked in the Cleveland Basin, the Portlandian is absent, and Cretaceous strata rest on strata as old as the Lower Jurassic. The Lower Cretaceous here is composed of shallow-marine sediments on the Market Weighton Block and deeper-water mudrocks in the basin (Hemingway, 1974; Neale, 1974; Kent, 1980). Thirdly, inversion tectonics, which culminated in the mid-Cretaceous unconformity in Yorkshire, continued throughout the Cretaceous in the Sole Pit Trough, completely eroding the Lower Cretaceous sequence there (Glennie and Boegner, 1981). Finally, whilst the East Shetland Basin has subsided continuously since the mid-Cretaceous, the Cleveland Basin has undergone a second inversion to outcrop today (Kent, 1980), perhaps the result of Alpine tectonics during the closure of Tethys. The Lower Jurassic is overlain unconformably by the Quaternary in the Southern North Sea.

The Cleveland Basin was heated to 95°C during Upper Jurassic and Lower Cretaceous burial (Cooper, pers. comm. 1980). As this burial was probably to a depth of less than 1 km, heat flow at this time must, therefore, have been high. Following this, and structural inversion, burial during the Tertiary was deeper than in the Cretaceous, and for a longer period. However, regional heat flow had decreased by this time and Middle Jurassic rocks were heated to 95°C again but for longer on this occasion. Consequently, organic-rich Liassic mudrocks are marginally mature (Cooper, pers. comm. 1980). This is reflected in oil-filled ammonites in the Jet Rock of the Upper Liassic (Hemingway, 1974), bitumen impregnated horizons in the Dogger and coals in the Ravenscar Group (Livera, 1981). There is, however, no published evidence

to suggest that hydrocarbons did or did not migrate through the Ravenscar Group. The burial history of both the Ravenscar Group and the Brent Group in the Ninian Field is summarised in Fig. 2.6.

FIG. 2.1 THE TECTONIC FRAMEWORK OF THE NORTH SEA BASIN

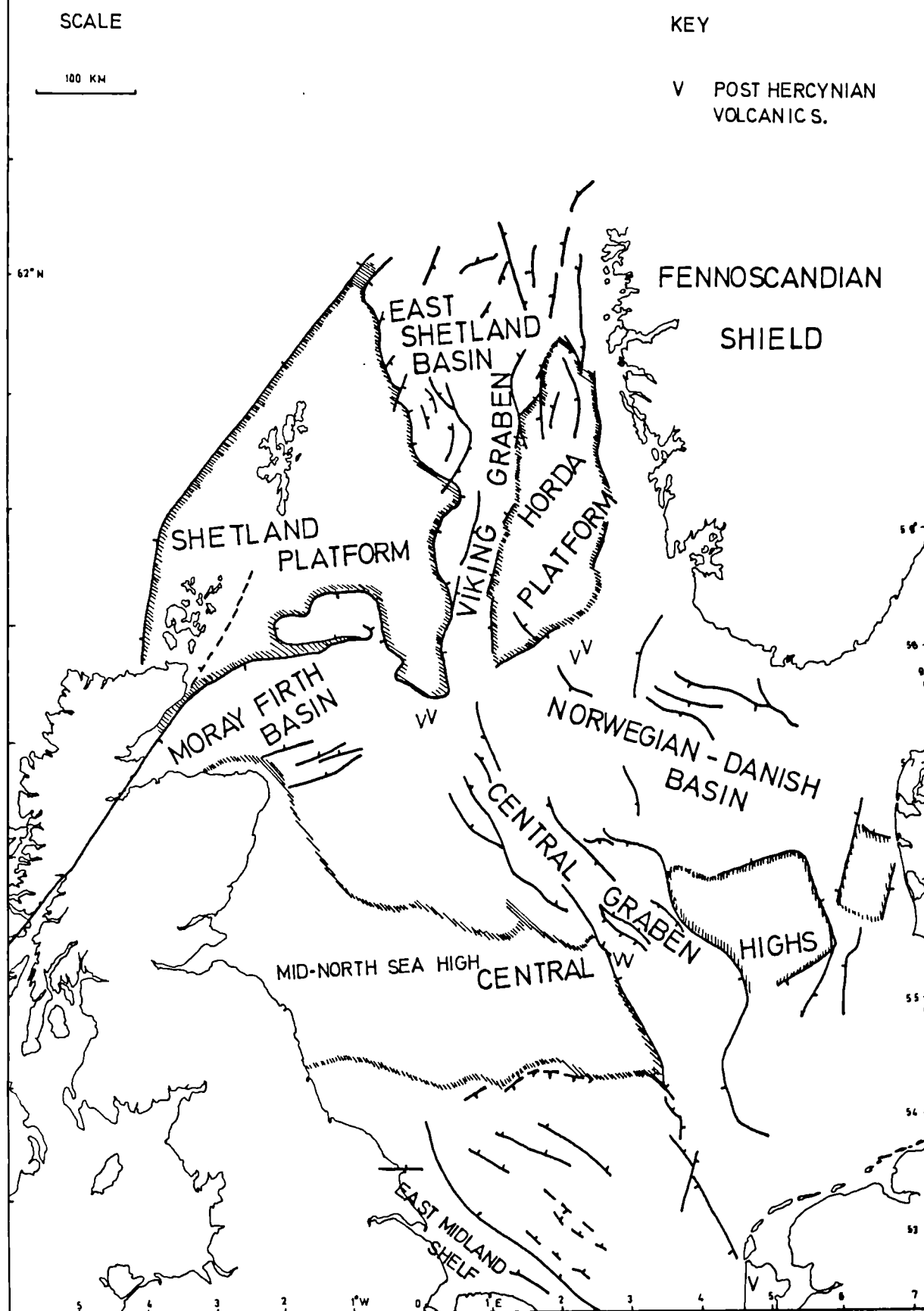


FIG. 2.2 THE EAST SHETLAND BASIN:  
STRUCTURE, AND HYDROCARBON  
RESERVOIRS

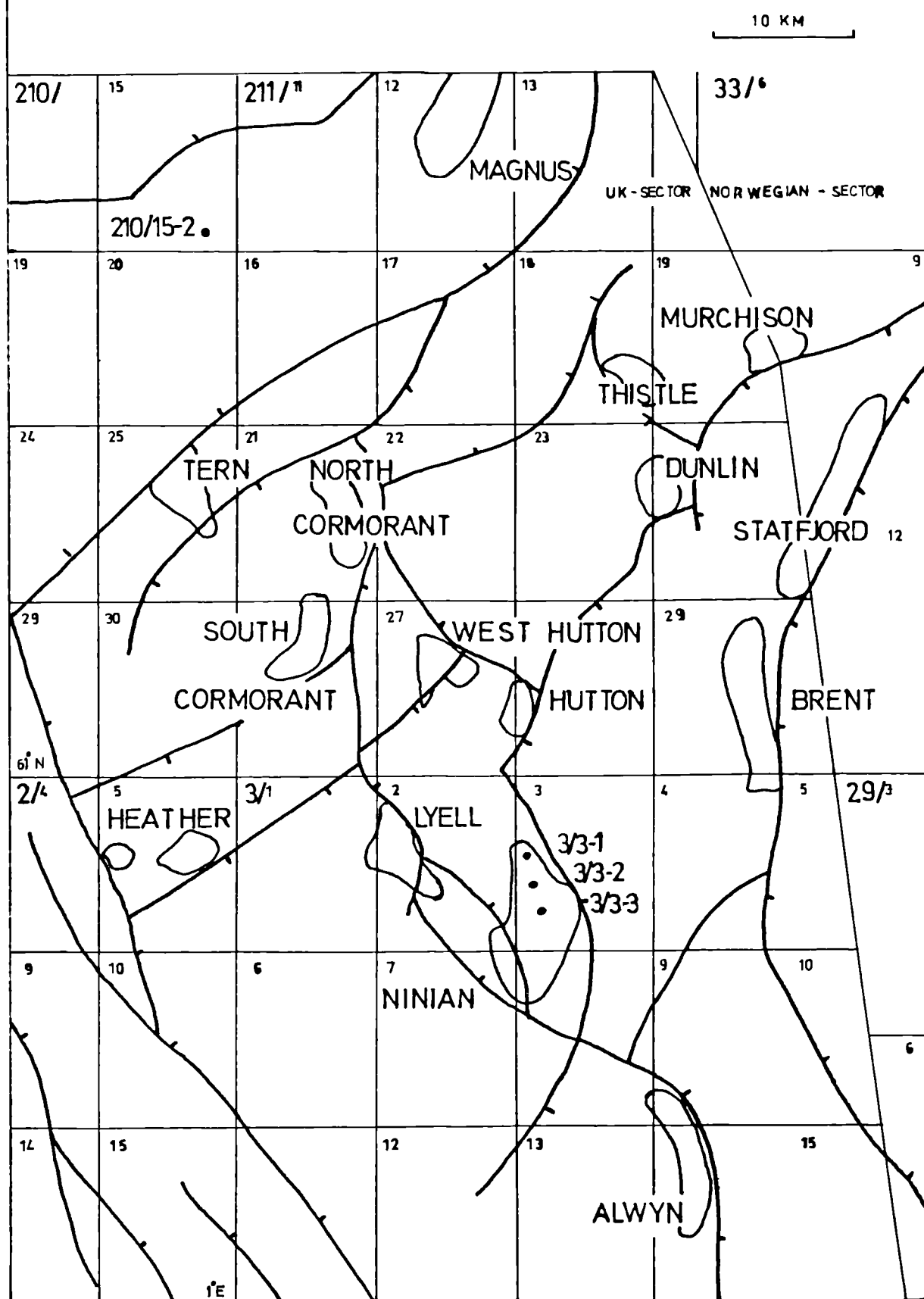


FIG. 2.3 THE EAST SHETLAND BASIN: BRENT GROUP FACIES EVOLUTION (a) BROOM FORMATION, (b) RANNOCH AND EIVE FORMATIONS, (c) NESS FORMATION, (d) TARBERT FORMATION (after Eynon, 1981).

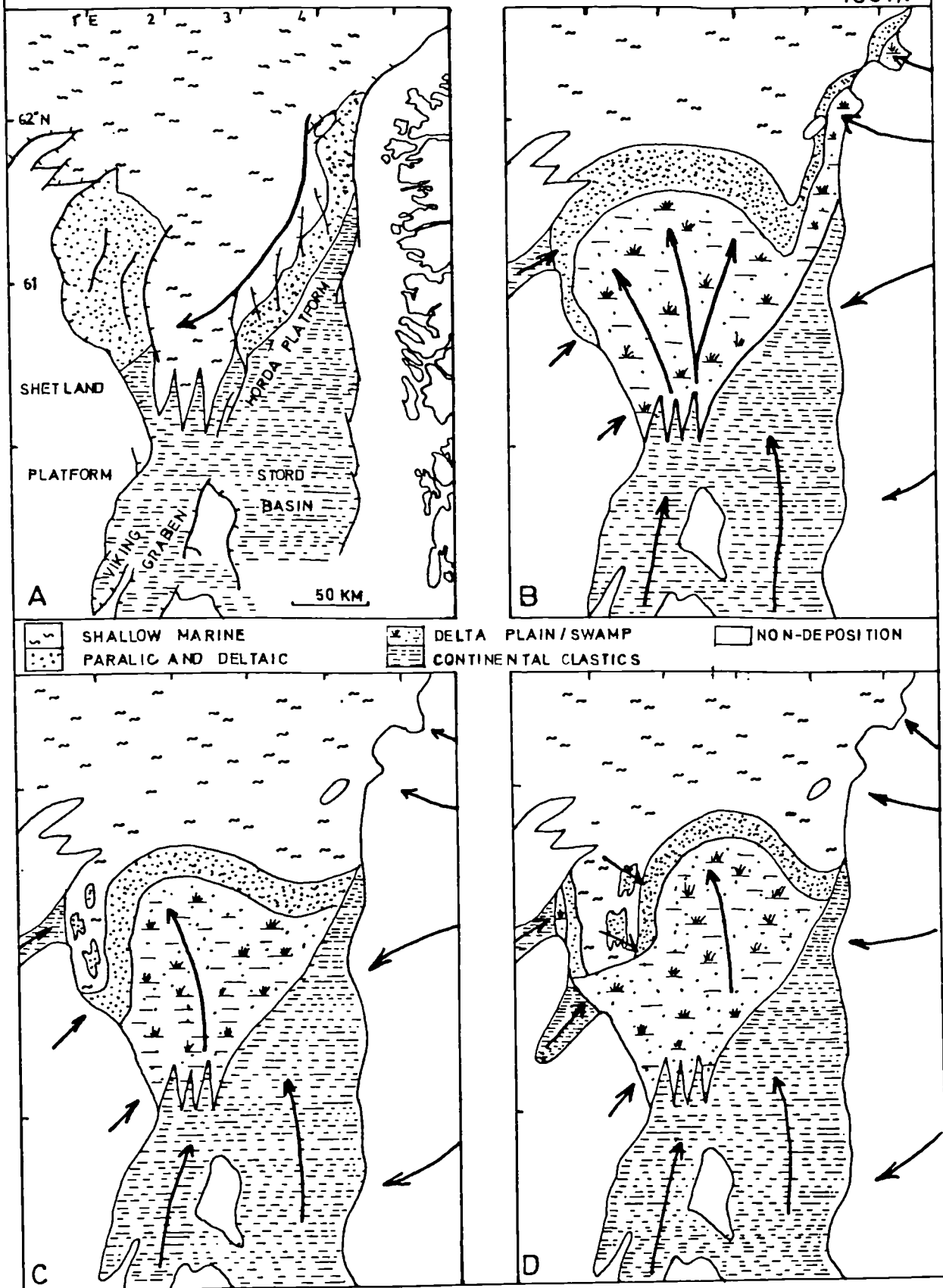


FIG. 2.4 STRUCTURAL GEOLOGY OF  
THE CLEVELAND BASIN,  
AND THE SOLE PIT TROUGH,  
(after Glennie and Boegner, 1981).

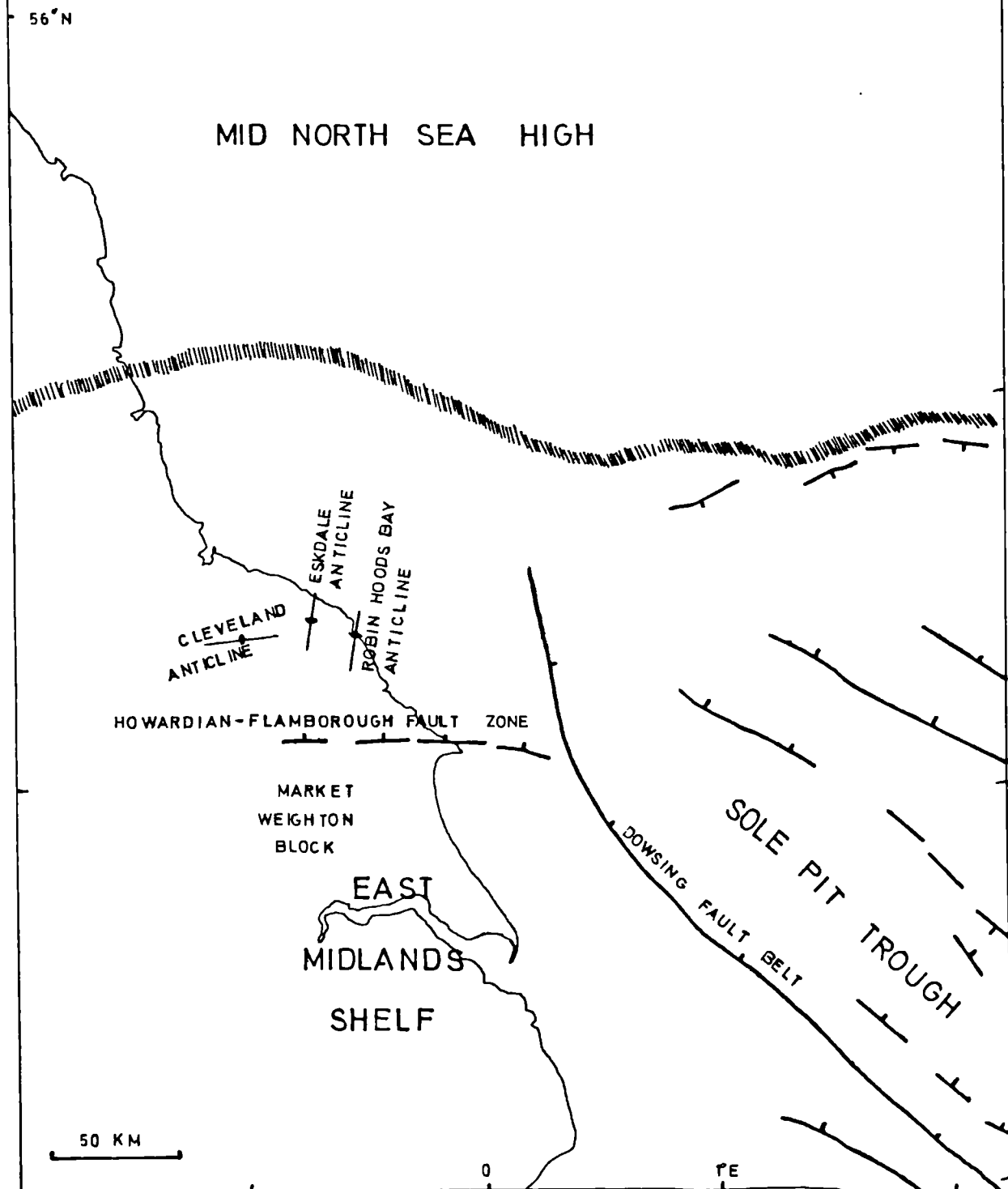
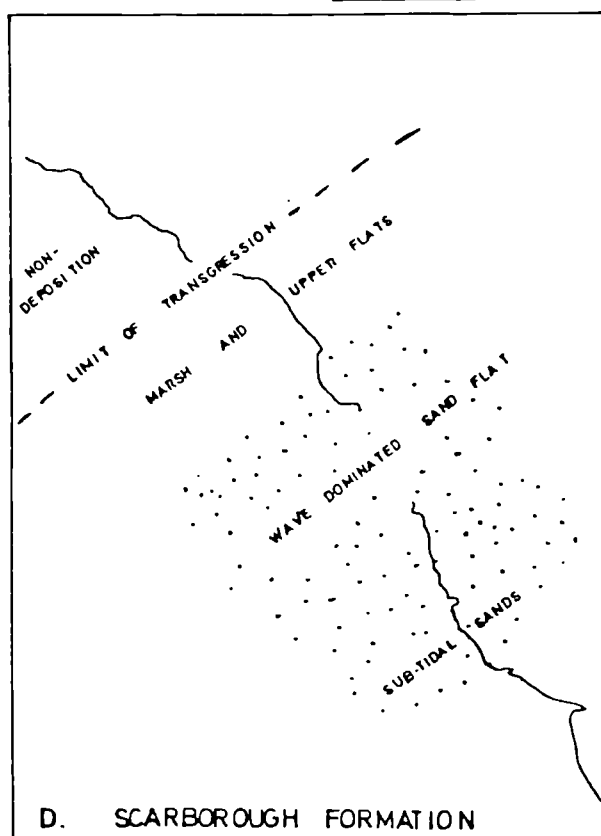
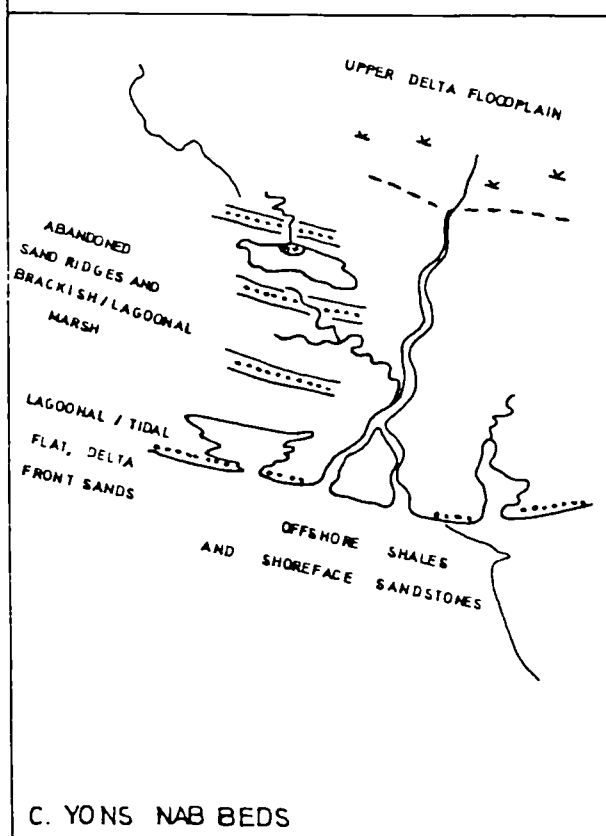
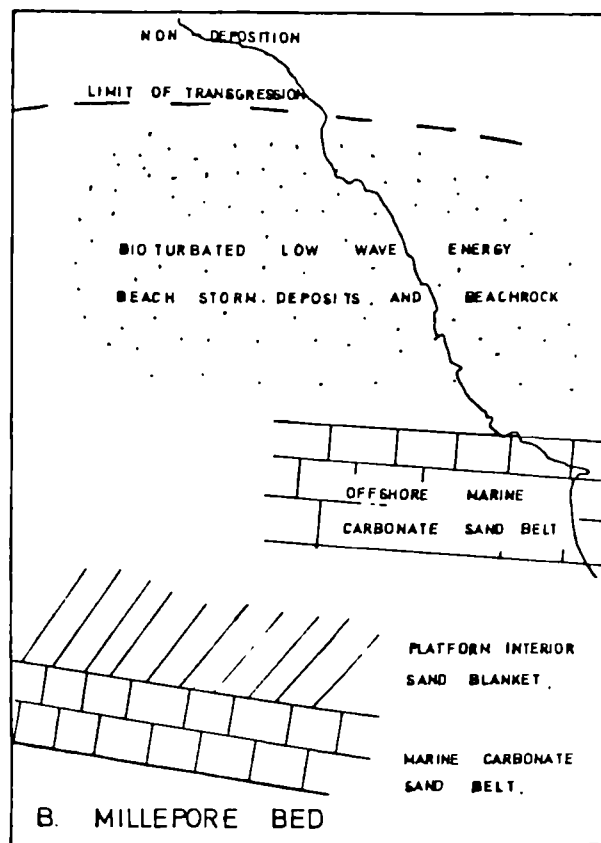
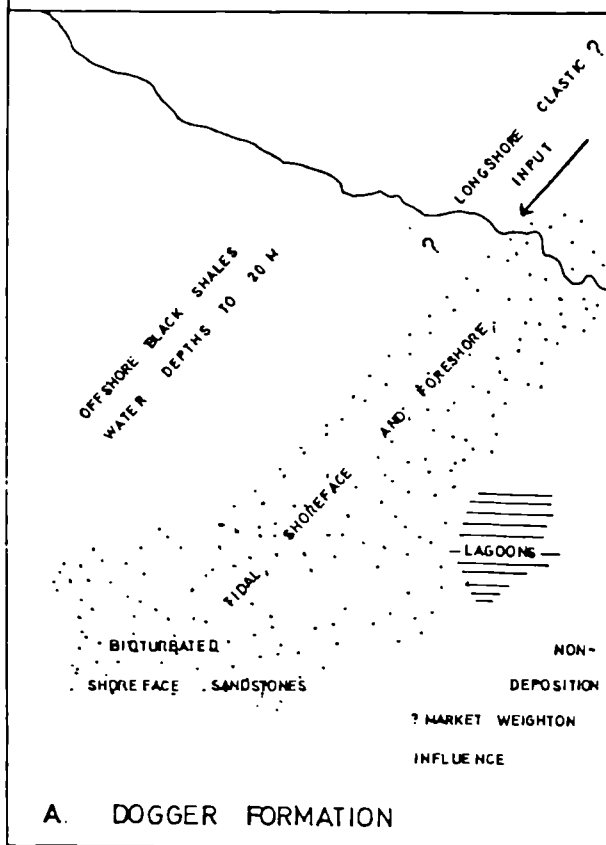




FIG. 2.5 THE CLEVELAND BASIN: MIDDLE JURASSIC SEDIMENTOLOGY, (after Livera, 1981).



10 KM

FIG. 2.6. THE BURIAL HISTORY OF THE MIDDLE JURASSIC BRENT AND RAVENSCAR GROUPS.

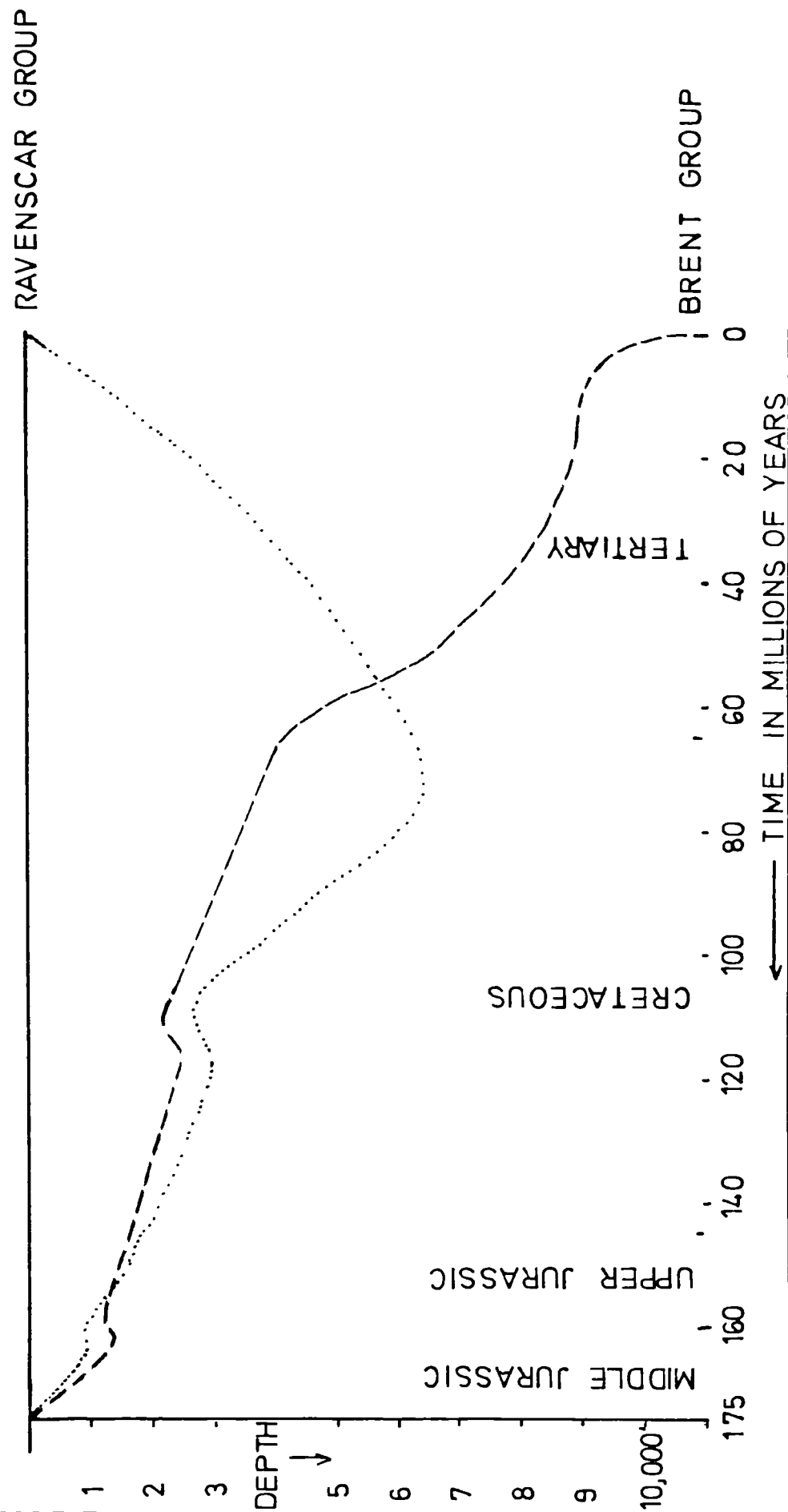


TABLE 2.1 The lithostratigraphical framework of the Middle Jurassic Ravenscar Group in Yorkshire

R	Scalby Formation	Long Nab Member	
A		Moor Grit Member	
V	Scarborough Formation		
E	Cloughton Formation	Gristhorpe Member	
N		Lebberston Member	Yons Nab Beds
S			Millepore Bed
G		Sycarham Member	
C	Eller Beck Formation		
R			
O	Saltwick Formation		
U			
P	Dogger Formation		

CHAPTER THREE:    DIAGENESIS OF CLASTIC SEDIMENTS FROM THE MIDDLE JURASSIC  
                    DOGGER FORMATION AND RAVENSCAR GROUP IN YORKSHIRE

"Although nature begins with the cause and ends with the experience,  
we must follow the opposite course, namely, begin with the  
experience, and by means of it investigate the cause."

Leonardo da Vinci

This chapter describes the detailed petrography and diagenesis of Middle Jurassic clastic sediments which outcrop on the North Yorkshire Moors. Descriptions are presented in stratigraphical units, and are subdivided on the basis of depositional facies, although the complete units are considered in the subsequent interpretations. The raw data on which the following descriptions are based are given in the appendices, and referred to in the text where directly relevant. Locality details and a location map are also given in Appendix A. Brief interpretations follow description of each stratigraphical unit, in order to highlight the differing origins of minerals from different environments. However, to avoid repetition, references and extended discourse in support of these interpretations are deferred to the subsequent discussion.

PETROGRAPHY

Dogger Formation

Basal conglomerate. This outcrops at several localities, and was sampled at Beck Hole, where it is incised into black Lower Jurassic mudrocks. The samples collected are all mature<sup>1</sup> litharenites, containing 20-30% simple and polycrystalline quartz, and 40-50% phosphatised mudrock and siltstone clasts, and concentric berthierine oololiths, the latter being fragmentary, or enclosed in

---

<sup>1</sup> maturity refers to textural maturity, not mineralogical maturity, throughout.

lithified clasts. These rocks also contain traces of shell fragments, plant debris, muscovite and biotite, and feldspars. Porosity is almost totally absent, with only occasional traces of grain dissolution and microporosity within clay rich areas. In these samples, three diagenetic modifications were observed: calcite and siderite cementation and replacement, and kandite pore filling. Siderite dominates all the samples and comprises 30-40% of each, whilst calcite and kandites are only present as traces.

Siderite is the most volumetrically significant authigenic phase, it fills all the pore space, and replaces both detrital grains and calcite, which is only seen in one or two isolated patches. Kandites only occur as a blocky pore filling or grain dissolution pore filling where siderite is absent. Kandites are not replaced or enclosed by either calcite or siderite.

XRD and SEM analysis suggest that both the concentric ooliths (Plate 3.1A) and probably the intergranular material are composed of berthierine, intimately intergrown with siderite in the latter (Plate 3.1E). Electron microprobe analysis (Fig. 3.1) indicates that stoichiometry varies from oolith to oolith, and within individual ooliths, however, traverses across single ooliths reveal no distinct trends of chemical variation.

Shallow-marine sandstones. These fine- to medium-grained sandstones were sampled from localities around the North Yorkshire Moors, including Rosedale and Upper Eskdale. They are petrographically variable, and are green, yellow and orange-brown at outcrop. The majority are subarkoses or quartz arenites, in which simple quartz grains predominate, comprising 30-70%, and averaging 60%, of the rock (Fig. 3.2A). A small percentage of polycrystalline quartz, orthoclase and albite also occurs. In addition, traces of whole and fragmented concentric berthierine ooliths occur. These rock fragments comprise no more than 1-2% of most samples, but in one, they comprise 20%. Finally, traces

of muscovite, biotite, rutile, tourmaline, zircon, matrix clay, chert, opaque minerals and plant debris occur in almost all the samples, whilst concentrations of shells are present in a few.

Diagenetic modifications in these sandstones are quite variable, the most quantitatively significant authigenic phases being vermiculite, quartz overgrowths, siderite and kandites, whilst there are also traces of illite, and feldspar overgrowths. Although they are poorly developed in the presence of matrix clay, authigenic phases comprise up to 60% of the rocks, but average around 25%.

Pore-lining vermiculite is normally only present as a trace, but in samples from the western side of Rosedale it comprises 10% of the rock. Individual plates of vermiculite are small, and usually less than 5  $\mu\text{m}$  in diameter. They constitute a pore lining often 5-10  $\mu\text{m}$  thick, which is only occasionally enclosed by later quartz or feldspar overgrowths. However, in samples where siderite is widely developed, only traces of vermiculite were observed, siderite in these samples replaces and engulfs the clay, (Plates 3.1D and 3.2A and B). It is likely that the mineral referred to throughout this chapter as vermiculite is, in fact, an irregularly interstratified chlorite-vermiculite mineral. The significance of this is elucidated in the discussion below and its problematical identification amplified in Appendix B.

Quartz overgrowths occur in the majority of samples, comprising 3-5%, although quantities range from a trace to 19% of the rock; the one tightly cemented sample is, however, an exception. They are normally uniformly distributed, occurring as a thin veneer of detrital quartz grains, occasionally filling intergranular porosity completely, but usually only partially reducing pore throats and pore spaces. Although some perfect, euhedral overgrowths are seen (Plate 3.1F), the majority appear corroded, either with small 'v' shaped

notches, or, on a larger scale, deep pits (Plates 3.1B and C). Quartz overgrowths are absent in samples with thick pore-lining vermiculite, or where a concentration of matrix clay occurs, and are often partially replaced by siderite. Cathodoluminescence examination reveals two episodes of quartz overgrowths in the sample examined from these sandstones. Quartz overgrowths are best developed in the most porous samples, in which clays and siderite are generally absent. Potassium-feldspar overgrowths, although considerably less abundant, appear to follow the same pattern of distribution and replacement as quartz overgrowths. Both orthoclase and albite grains are either fresh or partially dissolved, but neither are neomorphosed to, or replaced by, kandites.

Siderite dominates the authigenic phases in at least half of these samples. It occurs both as a pore-filling cement, and replacing quartz and feldspar grains and overgrowths. Siderite content varies from a trace to 53% of the rock, averaging 30% in those samples which it completely cements, both enclosing and replacing vermiculite and matrix clay. Irrespective of its concentration, siderite displays two habits: it occurs as spheruliths in those outcrops rooted from above and as both fresh and oxidised rhombs in all the others. Goethite occurs as a pseudomorph after siderite, occurring with a rhombic or sphaeroidal morphology (Plate 3.1G). However, in the majority of samples it occurs as an amorphous veneer.

Kandites are scattered throughout the samples as neomorphosed muscovite and loose vermiform pore fillings, both comprising traces of the rock. The most frequent kandite morphology is a dense, blocky pore filling of euhedral pseudo-hexagonal plates in enlarged and grain dissolution porosity. Vermiform kandites and neomorphosed muscovite are enclosed by siderite, whilst the blocky form is restricted to those samples in which siderite cementation is incomplete. Kandites vary from a trace to 10% of the whole rock.

The majority of samples are well cemented, their interstices are filled with overgrowths, siderite and kandites, and porosity comprises only 1-2% of the rock. In the remaining samples, an average of 5-10% irregularly shaped intergranular and grain dissolution porosity occurs.

Two additional samples were provided by Professor J. E. Hemingway from the Rosedale "magnetite", and from outcrop at Cold Moor. Both contain concentric berthierine oololiths, with iron oxide rims and cemented with both apatite and siderite. Chemical variations within these oololiths are similar to those observed elsewhere in the Dogger Formation (Fig. 3.1).

Beach sandstone, Whitby East Cliff. The buff yellow, or dull rust coloured, massive sandstone samples taken from this 50 cm thick outcrop are variable, ranging from mature to submature, medium-grained, quartz arenites and sub-arkoses. The most volumetrically significant authigenic phases are siderite and kandites, whilst occasionally enlarged intergranular porosity comprises 2-13% of the rocks. Four of the samples have sutured grain contacts, bent micas and crushed berthierine fragments, whilst the fifth has a loose framework of floating grains, in an extensive sphaerosiderite cement. This siderite encloses traces of pyrite, and replaces quartz.

The samples contain a predominance of simple and polycrystalline quartz (30-70%), fragments of berthierine oololiths, orthoclase and plagioclase (2-4%), and varying quantities of muscovite and micaceous matrix clay, rich in plant debris. Traces of opaque and heavy minerals occur, including rutile, zircon and tourmaline. In addition, rare phosphatised pebbles are found scattered throughout the samples.

Diagenetic modifications vary: one sample is completely cemented with replacive sphaerosiderite (Plate 3.1H), whilst others display differing quantities of



quartz overgrowths, kandites, siderite, calcite and pyrite.

Quartz overgrowths are found in all the samples as a thin veneer on detrital quartz grains, comprising some 5% of the rock, although they do not occur in the presence of abundant matrix clay. These overgrowths appear to be etched in places and replaced by siderite and calcite. Siderite is usually rhombic and constitutes on average 10% of the whole; it replaces quartz and feldspar grains and overgrowths, and is replaced, and enclosed, by non-ferroan calcite in one sample, which itself also replaces detrital and authigenic quartz and feldspar. Where these carbonate cements do not completely fill porosity, enlarged and intergranular, and grain dissolution pore spaces are partially filled with kandites. These are usually dense, tightly packed, "blocky" pore fillings of pseudo-hexagonal plates, which comprise some 5% of most samples. Neomorphism of muscovite to kandites also occurs, affecting both larger flakes and micaceous matrix clay; this, however, does not significantly contribute to the kandite total. Micaceous laminae are also associated with authigenic pyrite. Small, isolated pyrite crystals occur within matrix rich areas, whilst more extensive pyrite occurs, replacing plant debris. Feldspar grains display a range of diagenetic modifications: some are fresh, others are partially or wholly replaced by carbonates, whilst at least 50% are dissolved to varying degrees. In situ neomorphism of feldspar to either kandites, or illite, was not observed in these samples.

Interpretation. Diagenetic modifications to the Dogger Formation are extremely complicated. They reflect interstitial sea water, modifications to pore-fluid composition arising from anoxic bacterial processes, freshwater flushing, and aggressive fluids during burial. Illite, pyrite and berthierine probably began to form immediately following deposition; illite from interstitial sea water, either directly or by neomorphosis of detrital clays; pyrite subsequently, and under reducing conditions; and berthierine by

reduction of an intimate association of detrital alumina, silica (possibly in detrital kandites), and ferric hydroxides. Berthierine may also have formed within the oololiths during their formation, but prior to deposition, as well as after, which is the suggested origin for the matrix (see discussion below). Vermiculite is interpreted as a later neomorphic alteration product of chlorite, itself directly precipitated under reducing conditions rather than by in situ reaction of detrital components. Apatite, which locally cements berthierine oololiths, may reflect the relative undersaturation of interstitial sea water with respect to calcite; the non-depositional nature of the contact with the underlying Liassic, allowing accumulation of organic debris; and, bacterial degradation of organic matter releasing phosphates into solution.

Detrital feldspar is unstable in sea water and so began to dissolve immediately following its deposition. Potassium feldspar overgrowths occur here, however, and suggest that pore fluids rapidly equilibrated with feldspars rather than clays. Quartz overgrowths may also have begun to form at this time from evolving interstitial waters.

In the absence of ferroan calcite cementation (see Yons Nab Beds interpretation) the continued growth of quartz overgrowths, minor quantities of vermiform kandites, and neomorphosed muscovites which occur in places may be explained by subsequent flushing of these sediments with fresh oxygenated pore fluids, following burial and effective lithification. Whilst kandites may have formed from alumina and silica released into solution during feldspar dissolution, no in situ neomorphism of feldspars to kandites was observed.

Eogenetic, as well as mesogenetic, phases and detrital grains are replaced and enclosed by sphaero- and rhombic siderite. These are interpreted as soil horizons, and pore-filling cement respectively, formed under reducing conditions

during continued progradation of the Saltwick Formation floodplain above.

Non-ferroan calcite, which cements one sample, is inferred as precipitated from temporarily oxygenated pore fluids, following initially reducing conditions. The timing of siderite in each of the paragenetic sequences described above reflects the relative spatial and temporal proximity of the floodplain and its water table to these sediments.

Etch pits, corrosion and dissolution features on detrital and early formed authigenic phases suggest the dissolution of previously more extensive carbonate cements than those described above. Present intergranular porosity is, therefore, secondary cement dissolution porosity, and the scattered pockets of blocky kaolinites, which only fill the incompletely carbonates cemented samples, are secondary pore-filling clays. Furthermore, the second phase of quartz overgrowths observed during CL analysis probably formed at the same time as or after the blocky kaolinites within the secondary - pore system, and from the same aggressive solutions as the clay. Finally, oxidation of both forms of siderite to goethite is presumably a Recent weathering phenomenon.

#### Saltwick Formation

Overbank sandstones. Floodplain samples vary from occasional medium-grained sandstones, to clayey siltstones, although the majority are very fine sandstones or coarse siltstones. They are petrographically simple (50-70% simple quartz, 2-10% feldspars), the majority being subarkoses, and the remainder quartz arenites (Fig. 3.2C). Most are mature, but finer samples are occasionally immature, although the lack of matrix rich specimens is probably more a function of sampling than actual lithological variations. A small percentage of rock fragments occur throughout, these are fragments of berthierine oolites, feldspar-rich sandstone fragments, and rare mudrock clasts. Matrix clay content varies from a trace to 10% at most, and is usually micaceous, or illitic; it is invariably

heavily iron stained (Plate 3.2B). Coarser micas present include biotite and chlorite, but muscovite predominates. Feldspar is mostly orthoclase, with some plagioclase, which is mostly albite. Finally, traces of plant debris, rutile, tourmaline, zircon and opaque grains occur. Detrital material comprises up to 86% of the rock.

Porosity in these samples is generally low, consisting of small, irregularly distributed intergranular, and less significant grain dissolution pores; it ranges from 1-14%, but averages 5% or less of the rock. Although the majority is intergranular and isolated, its three-dimensional connectivity is slightly enhanced by the amount of intragranular feldspar dissolution. Deformed micas or feldspars were not observed in these samples.

Authigenic phases are predominantly quartz overgrowths, kandites and a variable amount of siderite, and they comprise from 10-50% of the whole rock. Overgrowths of potassium feldspar also occur on orthoclase grains, whilst minor authigenic phases include traces of illite, illitised kandites, vermiculite, kandite pseudomorphs after muscovite, pyrite and brookite. Although diagenetic modifications vary with lithology, the majority of the samples are tightly cemented with two or more authigenic phases, differences generally occur with grain size, and mica or matrix clay content.

Quartz overgrowths occur throughout all the samples on detrital quartz grains, comprising 1-3% of the rock where they occur as thin veneers, 5-7% as thicker veneers, and occasionally completely filling pore space. They are best developed in the coarser, matrix-free areas of samples. Indeed, in some graded or laminated sandstones, where centimetre thick laminae of fine sand occur separated by micaceous or clay rich laminae, overgrowths tightly cement the former, but are absent from the latter. Quartz overgrowths enclose traces of illitic clay and traces of vermiculite (Plates 3.2G and H). The latter

occurs as an authigenic pore lining at Hayburn Wyke and Ravenscar, on the coast. Although the majority of overgrowths are euhedral, some display steps on their terminal faces (Plate 3.2F). Unless they obliterate porosity completely, quartz overgrowths are normally enclosed, and sometimes replaced, by siderite. They are also corroded quite deeply, recognised by irregular pits intersecting crystal terminations (Plate 3.3A). In general, quartz overgrowths comprise up to 10% of the rock.

Kandites occur in three forms in these sandstones. The commonest are loose, open vermiform booklets and dense, blocky pore-fillings of euhedral pseudo-hexagonal plates. The former occur most frequently in micaceous laminae and occupy intergranular pore spaces only, and comprise from a trace to 3% of the rock. However, the latter, blocky kandites, occur in large, oversized and grain dissolution pores. They blanket quartz overgrowths and completely fill irregularly scattered pore spaces throughout the samples. These kandites are not replaced by carbonates, but are, however, sometimes illitised (Plate 3.2D), although this is not common. The third kandite habit seen is less common, in this case approximately 50% of the muscovite observed in thin section is neomorphosed to kandite, especially when concentrated in micaceous laminae. Neomorphism of feldspars to kandites was not observed, indeed the majority of feldspar grains are only altered by dissolution (Plate 3.2E). In total, kandites range from a trace to 10% of the rock.

Siderite is present in almost all the samples, usually as a replacive pore-filling which, when comprising 30-50% of the rock, fills almost all the pore space. It replaces detrital and authigenic quartz and feldspars, as well as the matrix clay. In almost all the samples, siderite is rhombic and occasionally pseudomorphed by goethite or limonite. In addition, it also encloses and replaces vermiculite, vermiform kandites, illite, muscovite pseudomorphed to kandites and pyrite.

In one sample from a thin crevasse-splay sandstone high in the Saltwick Formation, siderite occurs in two forms, namely, as small sphaerosiderite crystals, displacing the surrounding detrital grains, and a subsequent, replacive, rhombic-cementing phase. This sandstone is rooted and the overlying mudrock contains abundant plant debris. Small aggregated rhombic concretions occur elsewhere, concentrated along micaceous laminae with vermiform kandites and neomorphosed muscovite. The remaining authigenic phases comprise no more than a trace of the whole rock. Illitic clays and illite occur as a thin pore lining, and neomorphosing both authigenic kandites and detrital clay. Pyrite occurs, enclosed by siderite, and associated with plant debris, whilst scattered authigenic brookite was also observed.

Channel sandstones. There is little petrographical or diagenetic difference between the samples collected in two transects, one along the coast and the other through Eskdale, and along the northern escarpment of the Moors. At outcrop these sandstones vary from white to yellow, and buff to dark reddish brown.

Petrographically, all the samples are medium- to fine-grained, mature or supermature, quartz arenites or subarkoses (Fig. 3.2B). They comprise 50-70% simple quartz, 0-10% polycrystalline quartz, usually 0-2% fragments of berthierine oololiths (although up to 10% occur in the samples at Ravenscar), 2-10% feldspars (orthoclase, albite and microcline, with neither oligoclase nor more calcic phases), and traces of muscovite, rarer biotite, micaceous matrix clay, plant debris, opaque grains, heavy minerals such as tourmaline, rutile and zircon, and phosphatised mudrock clasts. The micas, plant debris and matrix clay are often concentrated in discrete laminae. Generally, detrital phases comprise 60-70% of the whole rock, dominated by quartz. Feldspar grains are often partially dissolved (Plate 3.4D), micas neomorphosed to kandites and sometimes crushed or broken, whilst berthierine fragments are

invariably deformed to some degree. However, whilst berthierine is usually, and mica occasionally, deformed, no deformation of dissolved feldspars or plant debris was observed.

Authigenic phases comprise from 10-35% of the whole rock. The most volumetrically significant are quartz overgrowths, kandites and siderite, with smaller, less frequent quantities of feldspar overgrowths, calcite, brookite, pyrite, illite, chlorite, vermiculite, goethite and anatase (representative EDS spectra of some of these phases are shown in Fig. 3.3).

Quartz overgrowths occur throughout the samples as a thin cementing veneer on simple detrital quartz grains, but they are poorly developed on polycrystalline quartz grains. They comprise from 2-10% of the rocks, averaging about 5%, reducing and closing pore throats (Plate 3.5C), and reducing intergranular pore space, without fully cementing any samples. They are present in all the samples, unless authigenic vermiculite, chlorite, illite or matrix clays are present. Overgrowths occasionally partially enclose authigenic pore-lining clays but are absent where thicker clay linings occur. In some samples quartz overgrowths enclose blocky pore-filling kandites (Plate 3.5A). Furthermore, in these, and some others where enclosure of kandites was not observed, euhedral overgrowth surfaces are stepped. Elsewhere, quartz overgrowths are occasionally replaced by siderite (Plate 3.3E), calcite, goethite, or where they line open pore spaces, corroded, showing the presence of either small notches or larger irregular areas (Plates 3.3B, F, G and H). Cathodoluminescence observation reveals quartz overgrowths which luminesce in two distinct colours, an inner bottle-green and an outer black zone. "Blobs" of goethite, isolated and coalescing into sheets, often occur on overgrowths; energy dispersive analysis shows them to be composed solely of iron (Plate 3.5E). Other more isolated "blobs", give iron and sulphur peaks, and are therefore possibly pyrite or pyrrhotite (Plate 3.5F).

Feldspar overgrowths are present in most samples, but comprise no more than a trace of the rock as a whole; they are not always in optical continuity with the host detrital feldspar grains. The majority of feldspar grains are partially dissolved (Plates 3.4 C and D), the remainder are fresh or replaced by siderite or calcite. In situ neomorphism to either kandites or illites was not observed.

Kandites occur in three forms: neomorphosed muscovite (Plate 3.4A and B, and Fig. 3.4); large, loosely pore-filling vermiform aggregates up to 40  $\mu\text{m}$  wide, but comprising several small plates across each aggregate (Plate 3.4 E and F); and dense, blocky pore-filling euhedral pseudo-hexagonal plates 10-15  $\mu\text{m}$  in diameter (Plate 3.4G and H). The former two are the least common, and of these the vermiform type is often associated with neomorphosed muscovite or micaceous laminae, whilst, in isolation, large vermiform aggregates only occur in intergranular porosity. Both these forms are sometimes enclosed by calcite or siderite, and they comprise no more than a trace of any sample. The blocky form is more common and occurs as an extensive, dense, coating, spread irregularly throughout samples, plugging pores and filling large composite spaces of enlarged intergranular and grain dissolution porosity. Blocky kandites comprise from 2-12% of the rocks. They do not occur in samples tightly and completely cemented with quartz overgrowths and carbonates, and are most abundant in the northeast and east around Whitby and in localities in Lower Eskdale. They are occasionally apparently enclosed by quartz overgrowths. Kandites are also occasionally altered to illite (Plate 3.5B). XRD of samples containing wholly blocky kandites identified dickite as the only phase present. Analysis of mixtures identified dickite and kaolinite.

Siderite comprises from a trace to 20% of some samples, but averages 5%. It only completely cements one of the samples examined and is usually present throughout the rock, rimming or filling pore space, and replacing both authigenic



and detrital quartz and detrital feldspar (Plate 3.3C and D). Siderite also encloses and replaces vermiform kandites, chlorite, vermiculite, micaceous detritus and plant debris. Siderite usually occurs as rhombs and is enclosed by ferroan calcite where the two occur together. Conversely, the rarer sphaerosiderite is only enclosed by non-ferroan, not ferroan calcite. Goethite often occurs pseudomorphing or neomorphosing rhombic siderite.

Calcite occurs in several samples, mostly from the Whitby area. It is normally ferroan, although one non-ferroan calcite cemented rock was sampled. This calcite is invariably blocky, enclosing vermiform kandites, neomorphosed muscovite, quartz and feldspar overgrowths, and siderite. Although it is usually absent or present as a trace only, calcite occasionally cements samples completely in which case it comprises 30% of the rock. In this case it commonly replaces detrital and authigenic quartz and feldspar. However, it does not enclose or replace blocky kandites

The remaining authigenic phases are only present as traces or small percentages of samples, and do not occur regularly throughout the area. Vermiculite and chlorite are present in several localities. A trace of chlorite occurs in one sample taken at Whitby, vermiculite at Hasty Bank, chlorite in Lower Eskdale, and both vermiculite and chlorite at Ravenscar. These clays occur as small discrete pore-lining plates 4-5  $\mu\text{m}$  in diameter which are occasionally aggregated into rosettes. Where thin or irregularly developed linings occur on quartz grains, they are enclosed by small or incipient quartz overgrowths, but where more extensive developments occur, quartz overgrowths are absent. These pore linings are present with blocky, but not vermiform kandites.

Authigenic illite occurs in a few samples, especially around Whitby. Although no discrete illite was observed, it neomorphoses detrital clays and authigenic kandites. The latter, however, is rarer compared with the former (Plates 3.5B and D)

These illitic coatings on grains are not enclosed by overgrowths. Authigenic brookite and anatase occur as traces: they are found in small pockets principally, often associated with laminae rich in detrital opaque and heavy minerals, many of which have been dissolved (Plates 3.5H, 3.6A and B). Authigenic pyrite occurs in one or two samples, associated with plant debris.

Porosity varies throughout from 6-20%, averaging 12% of the rock, although a few tightly carbonate cemented ones have none. In the most porous samples, it is mostly enlarged intergranular pore space, connected in two dimensions through narrow pore throats, whilst in the samples with more cement, porosity is lower and the percentage of isolated grain dissolution pore space higher. Furthermore, in samples with higher percentages of authigenic minerals, especially pore-filling clays, a greater percentage of microporosity occurs, further reducing the connectiveness of the pore space.

The mudrocks enclosing both the channel sandstones and intercalated floodplain deposits such as crevasse-splay sandstones are composed dominantly of kandites and micas, with traces of chlorites. Concentrations of siderite spheruliths occur in several horizons, and these mudrocks are often rooted

Interpretation. Diagenetic modifications which are common to both overbank and channel sandstones are interpreted as eogenetic, whilst those occupying solely channel sandstones are interpreted as mesogenetic, and interpreted to be a function of alluvial architecture.

Feldspars and micas are unstable in fresh water. This suggests that minor dissolution of feldspars, neomorphosis of muscovite to kandites, and resulting precipitation of vermiform kandites and quartz overgrowths are all most likely to have begun immediately following deposition. Consequently, precipitation of the latter may have been directly related to alumina and silica released

from dissolution and neomorphosis of the former, as well as that present in solution. Furthermore, the rapid dissolution of more abundant and finer aluminosilicates in the surrounding muds probably generated silica, which resulted in the tighter quartz overgrowth cementation, and more abundant vermiform kandites in floodplain sandstones. Brookite and pyrite are probably locally precipitated, the timing of which is uncertain: brookite precipitating following dissolution of a higher temperature polymorph of titanium oxide, probably rutile; and pyrite forming under reducing conditions, removing any sulphate ions from solution, and more especially, those derived locally from degradation of organic matter.

Feldspar overgrowths and localised traces of illite (including neomorphosed matrix clay) can be explained as forming after quartz overgrowths and kandites, with rising pH, from potassium released into solution by feldspar and muscovite dissolution, or as early phases in brackish water influenced environments. Formation of these phases ceased with the onset of widespread reducing conditions. Concentrations of sphaerosiderite crystals are interpreted as soil horizons, reflecting reducing conditions at the surface of the floodplain. Soil horizons occur both within mudrock sequences and in sandstones such as the crevasse splay sandstones at Whitby East Cliff. Where pore-lining chlorite and vermiculite occur enclosed within later incipient quartz overgrowths, reducing conditions are inferred during the earliest stages of diagenesis. Vermiculite and iron chlorite occur together or in isolation, but not with vermiform kandites. Vermiculite is interpreted as neomorphosed chlorite, whilst the latter formed from reduced iron reacting with alumina and silica in solution, either from ground water or from dissolution and neomorphosis of feldspars and muscovites, and perhaps derived berthierine oolites.

All the phases described above were enclosed and replaced by rhombic siderite cement, which formed from fresh water during more widespread reducing conditions.

The non-ferroan calcite is an exception and probably precipitated from inferred locally oxygenated pore fluids, following the initial reducing conditions in which the sphaerosiderite precipitated. Ferroan calcite, which cements a few channel sandstones, can be explained by precipitation from alkaline basinal pore fluids (formation waters) circulating during burial (mesogenesis), and not evolving interstitial water. Crevasse-splay sandstones already relatively tightly cemented with quartz overgrowths and siderite, were thus impermeable to these formation waters.

Dissolution features such as corrosion and etch pits, commonly observed in thin section, and during SEM examination of quartz overgrowths, suggest removal of a widespread replacive (carbonate) cement; porosity is therefore largely secondary. The distribution of this cement dissolution porosity and the blocky kandites which occur filling these large pores, and occasional grain dissolution pores, is a function of the depositional architecture of the original sequence. Thus, large and connected channel-filling sandstones, as well as nearby floodplain deposits, are relatively porous and contain significant quantities of blocky kandites. Conversely, smaller, more isolated sandstones, especially thin crevasse-splay and floodplain sandstones, are less porous and contain lesser quantities of kandites. The larger channel sandstones were, therefore, conduits for pore-fluid migration during burial, whilst smaller sand bodies, more tightly cemented during eogenesis, were relatively impermeable to these pore fluids. Kandites may have formed either directly from the acidic solutions which dissolved the carbonates, or by interaction of these solutions with detrital feldspars, or both. However, there is no evidence of in situ neomorphism of feldspar grains to kandites.

Dissolution of feldspars and reprecipitation of kandites liberates silica. Similarly, aggressive pore fluids saturated with alumina could also be saturated with silica, and so precipitation of kandites would release excess

silica. Therefore, the second episode of quartz overgrowth observed under luminescence is interpreted here as the phase enclosing blocky kandites, and probably formed from the same solutions.

Three diagenetic modifications postdate the final episode of cementation. These are: minor illitisation of kandites to illite, presumably from more alkaline formation waters; pyrite "blobs" on overgrowths, a local reduction product; and goethite, interpreted as Recent weathering of siderite.

#### Millepore Bed

These samples are petrographically and diagenetically variable. Those from Yons Nab and Osgodby Nab are pink-coloured, carbonate cemented oobiosparites, whilst the samples from Cloughton Wyke are reddish-brown subarkoses. There is no evidence to suggest that erosion took place beneath the Yons Nab Beds, therefore these sediments appear to represent lateral lithological variations at the top of the Millepore Bed.

The oobiosparites from Yons Nab contain bryozoans, gastropods, echinoid and shell fragments, quartz nucleated ooliths and rare quartz grains. They are tightly cemented with ferroan calcite. Interparticle pore space is lined with an isopachous calcite rim, irrespective of substrate, although crystals nucleated on ooliths tend to be larger. The remainder of interparticle pore space is completely filled with non-luminescent, sparry ferroan calcite cement (Plate 3.7A), which encloses traces of vermicular kandites (Plate 3.7B), and also fills fractures in rim cemented fossils and ooliths, and displaces loosely attached rims. The original intraparticle porosity within fossil fragments is, conversely, cemented with brightly luminescing zoned calcite cement (Plate 3.6C, D, E, F, G and H). Sutured contacts occur between ooliths occasionally.

Detrital and authigenic components comprise 65 and 35% of the rock respectively, some 95% of which is calcite. There is no porosity.

The samples from Osgodby Nab are similar, and, at outcrop, they display an increasing red coloration upwards to a nodular ferruginous crust. The lowermost ooliosparites are similar to those seen at Yons Nab. Oolith contacts are occasionally sutured, and the rocks are completely cemented with a thin, calcite meniscus, or rim, again thickly developed on some grains, and a pore-filling sparry ferroan calcite. Traces of vermiform kandites also occur in these samples, enclosed within the sparry calcite. One sample from the top of the sequence is a mature quartz arenite with a very thin veneer of quartz overgrowths on detrital quartz grains and an extensive poikilotopic ferroan calcite cement, which replaces authigenic and detrital quartz and feldspar. Quartz and calcite are replaced by siderite in the upper centimetres of the orientated thin section.

The samples from Cloughton Wyke are all mature subarkoses containing up to 20% ooliths and shells. The lowermost sample contains a calcite meniscus, and sparry ferroan calcite replacing the detrital components; all these phases are replaced by siderite, which now comprises half the rock. The uppermost beds are lithologically ironstones, due to complete replacement by siderite.

Interpretation. Diagenesis of these marine sediments is interpreted to reflect the interaction of evolving interstitial sea water and fresh water introduced during subsequent regression. Isopachous rim cemented intraformational conglomerates and intraparticle pore-filling non-ferroan calcite suggest rapid submarine (phreatic) lithification from interstitial oxygenated sea water. The rare vermiform kandites and quartz overgrowths which occur within interparticle pore spaces formed subsequently, as bacterial degradation of organic matter lowered pH. It is possible that these fluids also effected carbonate

dissolution, consequently forming the sutured contacts occasionally observed between grains.

Interparticle pore space is cemented with ferroan calcite suggesting precipitation from more alkaline but reduced pore fluids, generated during stages of anoxic degradation of organic matter, particularly iron reduction, which increases pH. The subsequent replacive siderite is a freshwater cement, formed by downward percolation and equilibration of the stagnant, anoxic water table above, in which the  $\text{Ca}^{2+}:\text{Fe}^{2+}$  ratio was relatively low, with these impermeable calcite cemented rocks during Yons Nab and Gristhorpe time.

The Millepore Bed samples studied contain no porosity, but extensively decalcified outcrops were observed at Yons Nab. This decalcification is interpreted as the result of acidic formation water introduction during burial. The reaction of the Millepore Bed and the surrounding sandstones to these fluids is distinctly different. In the former, the oolite consists of carbonate components and therefore wholesale dissolution occurs, whilst in the latter, the silici-clastic framework remains following dissolution of the carbonate cements.

#### Yons Nab Beds

Interdistributary-bay and marsh filling sequences. The sequence at Cloughton Wyke is interpreted as a beach deposit overlain by marsh deposits, periodically inundated with discrete crevasse-splay sands. The former is a mature quartz arenite, the latter are subarkoses deposited against a background of mica and kaolinite sedimentation (Fig. 3.5A).

The samples collected from the base of the beach deposits are cemented with a trace of smectitic clay and a veneer of quartz overgrowths on detrital

quartz grains, extensively replaced by siderite. Blocky pseudo-hexagonal kandite plates comprise 3% of the sample, and occur in large pores, lined with siderite, although they are not enclosed within the siderite. In the uppermost samples, detrital components are ringed with small carbonate crystals, which are enclosed within quartz overgrowths. Vermiform kandites and neomorphosed muscovite occur throughout the sample, and, together with the overgrowths, are enclosed by an extensive replacive siderite cement. There is no porosity in these samples.

In the overlying subarkoses, diagenetic modifications are diverse and widespread. The rocks are composed of discrete, fining upwards laminations, varying from fine sand to micas and matrix clay. In the coarser portions, authigenic phases are dominated by quartz overgrowths. These comprise up to 10% of the rock and form a tight cement, but are not developed where matrix or pore-filling, authigenic, illitic clay is present. When most extensively developed, overgrowths fill all the pore space, whilst where they only partially reduce intergranular pore space or pore throats, they are either replaced by siderite or are corroded.

Siderite is the most volumetrically significant authigenic phase in these sandstones. It comprises from 5-30% of the rocks and occurs as a pore-filling cement, replacing detrital and authigenic quartz and feldspar, as well as matrix clay. At outcrop, discrete horizons of complete siderite replacement occur. It is seen in thin section as both rhombic siderite and sphaerosiderite, and is occasionally pseudomorphed by goethite.

In the mica rich horizons, muscovite is altered to kandite and is associated with traces of vermiform kandites, whilst plant debris is often pyritised. These phases, which comprise a trace of each sample, are all enclosed by calcite. Kandites are most common with a blocky morphology of pseudo-hexagonal plates.



In this habit they comprise up to 5% of the rock. Blocky kandites only occur in enlarged or grain dissolution pore spaces in the coarser portions of the rocks. They do not occur in the samples or areas which are completely cemented with quartz overgrowths and siderite.

Pyrite and feldspar overgrowths are the least volumetrically significant authigenic phases present in these rocks, and at the most, they comprise only a trace in each. Porosity values are generally low, indeed most of the samples have no pore space; where present it is usually the result of grain dissolution or quartz corrosion and comprises up to 8% of the rock.

The sequence at Yons Nab coarsens upwards in 7 metres, from fossiliferous mudrocks to a rooted sandstone. The sandstones throughout the sequence are mostly mature subarkoses, comprising 50-60% quartz, up to 5% feldspars, up to 10% matrix clay, and traces of rock fragments, muscovite, plant debris, shelly fossils and heavy minerals (Fig. 3.5A). They are intercalated with mudrocks and silty mudrocks, composed of mica and kandites, but cemented with either ferroan calcite at the base, or siderite at the top.

Following deposition and bioturbation, chemical and mineralogical diagenetic modifications to these samples have occluded or filled all primary intergranular porosity. Ferroan calcite, siderite and, to a lesser extent, quartz overgrowths are the most volumetrically significant authigenic phases with traces of pyrite, kandites, illite and feldspar overgrowths. The major phases are dominated by ferroan calcite at the base of the sequence where it comprises at least 50% of some samples.

The samples at the base have thin quartz overgrowths on detrital quartz grains, and traces of pyrite (Plate 3.7C). They are completely cemented with ferroan calcite which fills pore space and replaces all the other detrital and

authigenic phases. Calcite was observed replacing quartz overgrowths. Where calcite was not observed during SEM examination (perhaps a function of sample preparation) quartz overgrowths were usually etched (Plate 3.7E, F, G and H). Where present, muscovite is neomorphosed to kandite, and one or two vermiform kandites were observed, which are also enclosed and replaced by calcite (Plate 3.7D).

The events described above persist towards the middle of the sequence. The calcite, however, is progressively replaced by siderite (plate 3.8B), which also replaces some of the remaining detrital components. Siderite concentration increases upwards and the sandstone at the top of the Yons Nab Beds is almost completely cemented and replaced by rhombic siderite.

Tidal channel sandstone. All the samples of this facies, collected from Osgodby Point, are yellow or buff, fine or fine-silty sandstones. They are all mature or supermature quartz arenites and subarkoses (Fig. 3.5A). The majority of the rocks contain 60-70% simple quartz grains, with up to 10% feldspars (mostly orthoclase and albite, with a trace of microcline), and traces of rutile, tourmaline, zircon, plant debris, opaques, muscovite and matrix clay. Diagenetic modifications are sparse, and the samples are all porous, porosity ranging from 10-30% and averaging around 17%. This consists almost entirely of enlarged intergranular pore space, with some intergranular feldspar grain dissolution contributing to the three-dimensional connectivity of the system.

Diagenetic phases are dominated by quartz overgrowths and kandites. There are also traces of brookite, chlorite, pyrite and feldspar overgrowths. These phases constitute 5-20% of all samples. Samples all contain a thin veneer of quartz overgrowths on detrital quartz grains, averaging 5-6% and ranging up to 8% of the rock. This veneer cements grains together and

reduces pore throats slightly, but does not completely fill any areas of porosity (Plate 3.8A). Frequently, it appears to be corroded. In one sample, thin, irregular pore-lining chlorite is enclosed within the overgrowths. Conversely, overgrowths are absent where matrix clay occurs. Feldspar overgrowths occur in all samples as a minor cementing constituent.

Kandites occur in three morphologies, as neomorphosed muscovite in all the samples as large open vermiform booklets within intergranular porosity in a few, and as a more blocky, dense, euhedral pore-filling of pseudo-hexagonal plates scattered irregularly throughout. In some samples, more predominant blocky kandites form up to 10% of the rock, whilst where they are absent, samples are relatively porous. Traces of siderite occur, replacing quartz overgrowths, and a trace of calcite was also observed. Pyrite occurs associated with a burrow filled with matrix clay, and brookite is present in those samples with the highest concentration of heavy minerals, particularly rutile.

Interpretation. The diverse diagenetic modifications displayed by these sediments are interpreted as reflecting complex mixing of sea water and fresh ground water in the range of environments in which they were deposited.

At Yons Nab, the Millepore Bed is succeeded by an interdistributary-bay filling sequence, capped by a nodular siderite horizon: an ironstone. Although deposited in open-marine to brackish-water conditions, initial diagenetic modifications produced vermiform kandites, partially dissolved feldspars, neomorphosed muscovite and quartz overgrowths, probably resulting from in situ bacterial degradation of organic matter, which lowered pH. This activity precluded precipitation of calcite from presumably undersaturated sea water. Subsequently, under inferred reducing conditions, pyrite precipitated, removing sulphate ions, and finally, as pH rose during iron reduction, ferroan calcite precipitated, effectively removing bicarbonate

ions from solution. The concentration of replacive siderite towards the interface with the overlying non-marine sediment suggests that it formed subsequently from fresh water percolating into, and equilibrating with, the crystalline ferroan calcite. This is analogous to the situation at Osgodby Nab below the Yons Nab Beds.

At Osgodby itself the formation of vermiform kandites and quartz overgrowths, feldspar dissolution and neomorphism of muscovite to kandites, suggests that acidic fresh water flushed through the sediments. However, local reducing conditions during these initial diagenetic reactions may be inferred from the occurrence of pore-lining iron chlorites and pyrite. Subsequently, chlorite inhibited the formation of quartz overgrowths, and the removal of sulphate ions into pyrite promoted the formation of siderite. Where oxygenated pore fluids persisted, feldspar overgrowths formed with increasing pH from the dissolution products of the reactions above. However, these phases are all either corroded and replaced or enclosed by freshwater siderite forming during continued reducing conditions, which eventually became ubiquitous.

At Cloughton Wyke the beach sediments contain smectitic clays and calcite, suggesting precipitation from interstitial sea water prior to the freshwater flushing and consequent decreasing pH, which was probably responsible for the quartz overgrowths, and vermiform kandites, as well as concomitant feldspar dissolution and muscovite neomorphosis. In samples from sequences at both Osgodby Nab and Cloughton Wyke irrespective of environment, cement dissolution features - etch pits, corrosion holes, etc - formed by dissolution of the carbonates described above. This secondary porosity occasionally contains blocky kandites, precipitated from either the aggressive dissolving pore fluids, or possibly interaction of these presumably acidic fluids with feldspar grains.

Cloughton Formation: Gristhorpe Member

Channel sands. These were sampled at Over Silton Forest, and on the coast. Samples taken are massive, yellow-brown, mature, medium-grained quartz arenites and subarkoses (Fig. 3.5B), containing concentrations of opaque and heavy minerals in discrete laminae. Petrographically, they comprise 60-70% simple quartz, up to 8% feldspar, 2-3% polycrystalline quartz and traces of plant debris, muscovite, berthierine, chert, shale clasts, rutile, tourmaline, zircon and opaque minerals, with patches of matrix clay. Opaque and heavy minerals comprise 5% of samples in which they occur as frequent discrete concentrations. Almost all the mica, feldspar and plant debris is undeformed.

Porosity in these sandstones is high, ranging from 10-30%, and averaging 20%. Enlarged intergranular pore space is the major component, although grain dissolution and intragranular (feldspar) dissolution add significantly to the total; floating grains are common. Authigenic phases comprise up to 17%, and average 12% of the rocks. They are dominated by quartz overgrowths (4-8%) and kaolinites (2-10%). There are also traces of feldspar overgrowths, siderite, goethite, pyrite and brookite. Diagenetically, the samples are almost identical, with variations in degrees rather than phases present. Quartz and feldspar overgrowths occur as a veneer on almost all their detrital counterparts; this veneer is usually thinly spread and reduces rather than fills any intergranular porosity. Overgrowths do not generally enclose any other phases, although they enclose a trace of vermiculite at Over Silton Forest. They are quite highly corroded in places, or replaced by siderite and goethite. Corrosion holes and replacing siderites have similar morphology. Small irregular steps were seen on the surface of some euhedral faces.

Most of the muscovite present is partially altered to kaolinites. Vermiform

kandites occur in the majority of samples, but blocky pseudo-hexagonal kandites are the dominant form, occurring in both enlarged intergranular and grain dissolution porosity.

In summary, the samples are generally porous, cemented with quartz overgrowths and loosely plugged with kandites.

Overbank Sandstones. Floodplain deposits from both Gristhorpe Member and from undifferentiated inland Cloughton Formation sequences were sampled at several localities, where they outcrop as white or buff-yellow sandstones. Despite the broad geographical range of these localities, the samples are uniformly mature and fine- to medium-grained. Furthermore, the majority outcrop as massive deposits. A few, however, contain discrete laminations, fining upwards from heavy minerals and medium-grained sand to fine sand, silt and mica, with occasional plant debris. Petrographically, all the samples are similar: they are either quartz arenites or subarkoses (Fig. 3.5B). Quartz is the major detrital component: simple quartz comprises 60-75% of the rock, whilst polycrystalline quartz up to 3% and feldspars (orthoclase and albite), also up to 3% are the only other consistently significant detrital phases. Micas, (biotite, chlorite, and muscovite), matrix clay, rock fragments (mudrocks and berthierine) and opaque or heavy minerals (including a predominance of rutile, tourmaline and zircon) each comprise from 0-4% of any sample, although they usually only comprise a trace or 1%. Plant debris is present as a trace throughout (Plate 3.9A).

Mica flakes are occasionally bent around or crushed between detrital quartz grains. However, neither widespread deformation of mica, nor any deformation of plant debris or dissolved feldspars was observed. The authigenic phases developed throughout these samples are similar, although they vary both in type and quantity with grain size and lithology. Authigenic phases comprise

20-30% of the rocks; they include pore-lining vermiculite and chlorite, kandites, quartz overgrowths, siderite, calcite, illite and feldspar overgrowths.

The samples from Yons Nab and Osgodby are similar: they are mature and medium grained, cemented with a veneer of quartz overgrowths on detrital quartz grains, comprising 4-5% of the rock, and contain traces of blocky kandites in enlarged pockets, or grain dissolution pore spaces. Quartz overgrowths are invariably corroded or replaced by a trace of goethite, and the pores they line are enlarged or oversized intergranular pore spaces. Porosity in these samples is high, ranging from 15-20% throughout. The intergranular porosity described above is augmented by large, irregularly distributed grain dissolution pore spaces. Where present, muscovite is neomorphosed to kandites. The remaining samples, comprising the majority of those collected, are either massive fine-grained sandstones, or fine upwards from medium sand to silt and clay, within 1-2 cm thick laminae. Within massive samples diagenetic modifications are relatively uniform, whilst in the laminated types they vary with both size and type of detrital components.

In the fine-grained, sheetflood, sandstones from Cloughton Wyke, samples contain patches of pore-lining chlorite rosettes, which comprise from a trace to 8% of the rock (Plate 3.9B). Inland, pore-lining vermiculite occurs, comprising up to 13% of the samples. These plates are usually small and occur in discrete clusters enclosed by quartz overgrowths (Plate 3.9C). Quartz overgrowths themselves occur throughout all the samples as a veneer on detrital quartz grains, comprising 6-20% of the rock. They were not observed where a thick concentration of matrix, neomorphosed matrix, or pore-lining authigenic clay occurs. Elsewhere, overgrowths tightly cement grains, often completely filling intergranular pore space. They are occasionally replaced by siderite or, more frequently, corroded, and comprise 10% of the

samples on average (Plate 3.9G).

Siderite varies from a trace to 10%, averaging 3% of the samples as a pore lining or pore filling, and replacing detrital and authigenic quartz. Patches of calcite were observed on one sample. Illite occurs irregularly throughout the samples as a neomorphic product from detrital matrix clay (Plates 3.8C and D), and from muscovite, as well as an alteration product of pore-filling blocky kandite. Illite usually comprises a trace of the samples. Kandites occur as large vermiform, loose pore fills in one (Plate 3.8G) and as dense blocky pore fills in all the samples. They comprise up to 3% of the rock and occur in grain dissolution/<sup>porosity</sup> or pore space rimmed with corroded quartz overgrowths. Gypsum was seen in several samples as a loose pore-filling cement (Plate 3.9H).

Porosity varies only slightly in these sandstones. In the predominant tightly packed and cemented samples it is often negligible, but may comprise 5-8% of the rock. In one or two less well cemented sandstones, however, values of up to 15% porosity occur. This is commonly isolated, enlarged intergranular or grain dissolution porosity, the majority of the two dimensionally connected intergranular pore space being occluded with overgrowths.

At Cloughton Wyke, Gristhorpe Member sediments are interpreted as tidally influenced, with a tidal bar and rip channel four metres from the base, overlain by marshy mudrocks etc, and the fluvial sheetflood sandstones discussed above. However, the diagenetic patterns observed are similar. Traces of chlorite occur as pore-lining rosettes (Plate 3.8E and F), enclosed by a thin veneer of quartz overgrowths. Elsewhere, overgrowths on detrital quartz grains are well developed, tightly interlocking and filling intergranular porosity. SEM examination reveals stepped euhedral faces on some overgrowths (Plate 3.9H). Siderite occurs, filling the remaining pore space and replacing authigenic clay. Where siderite is absent, overgrowths are often corroded



and the enclosed pores full of blocky kandites. Porosity is low, ranging from 2-5% of the rock. Halite occurs in all the coastal samples.

In the fining upwards laminations seen at localities inland, including Goathland and Darnholme Beck, diagenetic modifications vary with lithology. In the micaceous and matrix-rich horizons, clay and carbonate authigenesis dominates, whilst quartz overgrowths are most frequent in coarser, and in matrix poor areas. Sand sized fractions in these samples contain similar diagenetic assemblages to those described above from more massive sands.

Quartz overgrowths dominate these samples. In the majority of cases, overgrowths completely fill intergranular pore spaces (Plate 3.9D). In the remainder, unless inhibited by the presence of matrix or pore-lining clays, they are still quite thick and reduce pore space. Where pore-lining authigenic clays are present, overgrowths are restricted or absent, particularly where the clay rims are sufficiently thick to cover the whole grain surface within a pore. However, such clays are not common. Chlorites occur in three samples, whilst traces of illite occur in a few others. This illite neomorphoses detrital clay rims, or is wholly authigenic. When it is present, chlorite comprises 3-4% of the rock, as pore-lining rosettes of plates 5-6  $\mu\text{m}$  in diameter. Quartz overgrowths comprise on average 10% and up to 13% of the whole rock. They only rarely enclose authigenic detrital clays, and are themselves often corroded or replaced by traces of siderite. In several samples, SEM examination reveals steps on the euhedral faces.

Siderite is found throughout, but it usually comprises not more than 5% of the rock, filling pore spaces, unless precluded by overgrowths, and replacing matrix clay. Siderite cementation is commonest in micaceous areas where overgrowths are absent. It replace authigenic quartz, detrital feldspar and matrix clay, and is often pseudomorphed by goethite.

Kandites occur in three morphologies: loose, open vermiform aggregates in intergranular pore space, blocky pseudo-hexagonal plates, and as a pseudo-morph of muscovite. The latter habit is common in these samples, especially in micaceous laminae, where it is associated with vermiform kandites and the alteration of biotite to vermiculite. Vermiform aggregates comprise a trace of the 3-5% kandites that occur in these rocks. The remainder is a blocky pseudo-hexagonal form, scattered irregularly throughout the samples, filling pore spaces only partially filled with siderite, and large grain dissolution pores. They occur as dense pore-fillings of euhedral stacked booklets 10  $\mu$ m in diameter (Plate 3.9E and F). They are often tinted yellow with a fine veneer of goethite. A few, rare, pore fills are partially illitised.

Feldspar overgrowths occur commonly, yet as a trace, in each sample, whilst traces of pyrite were observed associated with plant debris. Although authigenic brookite also occurs in all samples, it is especially concentrated in heavy mineral rich laminae, and associated with dissolved rutile. Porosity in these samples is uniformly low, ranging from 1-5% of the rocks at the most. It comprises predominantly enlarged intergranular, or composite pore spaces of grain dissolution and intergranular pore space. All the sandbodies described above occur within a mudrock sequence composed of micas and kandites.

Interpretation. Diagenetic modifications in these sediments are qualitatively consistent, irrespective of environment. The general paragenetic sequence and diagenetic conditions are interpreted as analogous to those in the Saltwick Formation, although late-stage overgrowth-coating pyrite was not observed. Halite and gypsum have probably precipitated from Recent sea water.

### Scarborough Formation

Tidal-sheet sand. This sheet of tidal or subtidal silty sandstone, containing fine alternating white or grey sand and black micaceous laminations, occurs towards the base of the Scarborough Formation. It was sampled at Cloughton Wyke, Bloody Beck and Yons Nab. There are no noticeable differences in petrography or diagenesis between these localities.

Texturally, the samples are all mature, although being fine-sand or even silt sized, a small percentage of matrix clay or mica occurs in each. Petrographically, they are subarkoses or quartz arenites, simple quartz comprising 60-80% of the whole rock, with small percentages of feldspars (orthoclase and albite), muscovite, polycrystalline quartz, micaceous matrix clay, and heavy minerals such as rutile, tourmaline and zircon. Traces of plant debris are present (Fig. 3.5C). Authigenic phases are widely and variably developed in these sandstones, the most volumetrically significant are quartz overgrowths, calcite and siderite, although feldspar overgrowths, kaolinites, illites, pyrite, brookite and authigenic albite also occur.

Quartz overgrowths are the only evenly distributed authigenic phase. They comprise from 2-17% of the rock, are best developed as a thick cementing veneer on detrital quartz grains where illitic pore-lining or matrix clays are absent, and are conversely thin or absent where these clays are present (Plate 3.11F). The best developed overgrowths fill intergranular pore space completely, although elsewhere they are often corroded or replaced by carbonates.

Illite occurs as a pore lining in all the samples, usually as a thin coating on grains, and sometimes as a trace on detrital clay, enclosed by overgrowths (Plate 3.12A and B). The thickest neomorphic or authigenic developments are not enclosed by overgrowths. Pyrite occurs as a trace in several samples,

and best developed as large nodules enclosing quartz grains, but is most frequently observed as small framboids or individual cubes (Plate 3.11B). Where present, muscovite is neomorphosed by kandites, whilst detrital matrix clay is illitised. Detrital feldspars are either fresh, wholly or partially replaced by carbonates or partially dissolved. No in situ neomorphism of feldspars to kandites was observed.

Ferroan calcite is the most abundant, but also the most irregularly distributed authigenic phase. It was not observed in half the samples examined and varies from a trace to 33% in the others. In thin-section this carbonate was observed as both blocky and poikilotopic cement, replacing detrital and authigenic quartz and feldspar, whilst enclosing pyrite, neomorphosed muscovite and illite. Its temporal relationship with the scattered traces of corrosive or replacive rhombic siderite is not clear. Calcite was observed with the SEM in two morphologies, firstly as a sheet replacing quartz, and secondly as cones radiating from an amorphous carbonate core (Plate 3.11 C, D and E). In thin section edges of calcite crystals appear corroded.

Blocky kandites appear in most samples as a trace, usually within enlarged or grain dissolution porosity. The tightly carbonate cemented samples do not contain kandites. Authigenic feldspar occurs as overgrowths on albite and orthoclase grains, and as discrete crystals of albite (Plate 3.10E and 3.11A). Authigenic brookite was observed in one sample (Plate 3.10F).

Porosity varies, but is generally low, ranging from 0-10% at the most. The best developed porosity occurs in response to extensive grain dissolution, the remainder is enlarged intergranular porosity, often with a rim of siderite or goethite replacing the quartz pore walls. Microporosity is preserved within detrital matrix clay, and occurs within authigenic pore-filling illite. A slumped sand sheet occurs beneath this horizon. It is a tightly cemented

mature quartz arenite with traces of fibrous illite enclosed beneath a tight quartz overgrowth cement within which no porosity remains. The samples all contain halite (Plate 3.11 G and H). Mudrocks above and below this sandstone, and elsewhere in the sequence are composed of micas and kandites.

The top of the Scarborough Formation. Several of the samples were taken from horizons at the top of the Scarborough Formation, including two pieces of the iron encrusted limestone close to the top (the White Nab Ironstone Member), as well as siltstones and mudrocks from the thin beds above this. Siderite concretions occur in the Hundale Shales at the top of the Scarborough Formation, increasing in density towards the top.

The mudrocks and siltstones contain a high percentage of matrix clay. Diagenetic phases are rare, pyrite occurs widely (Plate 3.10 G and H), and replacement of whole samples by siderite is common. The limestone contains a number of shell fragments (bivalves and oysters included), cemented with ferroan calcite. Both the fossils and the calcite are widely replaced by rhombic siderite cement. There is no porosity in these rocks.

Beach sandstone (Sneaton Quarry). These fine-grained straw-coloured sandstones are all supermature subarkoses or quartz arenites (70-75 quartz and 2-5% feldspar). Other constituents comprise no more than 2% of the whole rock: these include matrix clay, muscovite, rutile, tourmaline, zircon and plant debris. Authigenic minerals comprise from 10-20% of the whole rock. They are: pore-lining vermiculite, quartz overgrowths, siderite and pore-filling blocky kandites.

Quartz overgrowths are the most volumetrically significant authigenic phase. They occur on detrital quartz grains as a thin cementing veneer, comprising 3-5% of the looser samples, and 10% of the tighter, finer ones. Overgrowths

are absent or only incipient in the presence of pore-lining vermiculite, which is itself spread irregularly throughout all the samples, varying from a trace to 7% of the whole rock (Plate 3.10A, B, C, and D). Elsewhere, overgrowths tightly cement pore spaces. They are corroded in all the samples, and replaced in most by traces of siderite.

Blocky kandites also occur as a trace or a low percentage in each sample. They fill oversized grain dissolution pore spaces with corroded overgrowths around the edge. In the tightly cemented samples, 5-8% porosity occurs, whilst in the coarser ones, which have a high proportion of grain dissolution and enlarged intergranular pore space, up to 15% porosity occurs.

Interpretation. Scarborough Formation sediments were deposited in a heterogeneous assemblage of environments, the variety of which is reflected in their diagenesis. In the tidal or subtidal sheet sand, the first phases formed, illite and potassium-feldspar overgrowths, suggest precipitation from interstitial sea water. Potassium ions in solution, as well as those liberated during neomorphism of muscovite to kandites, would promote the precipitation of these phases. Illitic clays either inhibit quartz overgrowths completely, or are partially enclosed by later overgrowths, also formed from primary pore fluids, but following potassium depletion of these pore fluids. Brookite presumably precipitated from locally dissolved detrital rutile.

Pyrite formation infers local, if not ubiquitous, sulphate reduction following aerobic bacterial depletion of oxygen, and reduction of iron. Pyrite and the phases above are enclosed and replaced by ferroan calcite. This cement probably formed from the same marine pore fluids as those above, but they are inferred to have been initially undersaturated with respect to calcite, and its formation delayed until precipitation became possible thermodynamically.

In the beach deposit at Sneaton Quarry, reduction of fresh - sulphate poor - pore waters rather than marine - sulphate rich - pore waters, is suggested by precipitation of iron chlorite (subsequently neomorphosed to vermiculite). This pore-lining clay is now enclosed by quartz overgrowths, interpreted as a freshwater cement, precipitated during continued flushing of the sediment with fresh water. Rhombic siderite fills pore space and replaces detrital and authigenic phases in the tidal sands, the beach sand, the Hundale Shales, and the White Nab Ironstone Member, which is nodular and iron encrusted in places. Furthermore, siderite concretions which occur towards the contact with the overlying Moor Grit are ellipsoidal and concentrated in specific horizons. Siderite is interpreted throughout these sediments as either a freshwater cement, filling remaining pore space, and replacing phases unstable at high pH and in reducing conditions with a low  $\text{Ca}^{2+} : \text{Fe}^{2+}$  ratio, or, as in the concretions, forming from bacterial degradation of organic matter, either during continued sulphate reduction and pyrite precipitation, or during methanogenic fermentation, or perhaps both. Their ellipsoidal shape is probably a function of horizontal permeability exceeding vertical permeability in these sediments.

Corrosion features, such as dissolution and etch pits, suggest dissolution of previously more extensive replacive carbonate cements. Consequently, blocky kaolinites, which only occur in porous samples not cemented with carbonates and filling this secondary porosity, may have formed from the aggressive dissolving pore fluids themselves or from the interaction of these pore fluids with feldspar grains.

Scalby Formation: Moor Grit Member

Thirty samples of the Moor Grit Member were collected from the outcrop at Hundale Point; these were taken in two vertical and one horizontal transect, across the massive, white exposure, some 12 metres thick and 50 metres long. Texturally, they are all supermature, ranging in grain size from medium sand at the top to coarse sand with a pebble lag at the base. Petrographically, of these samples, one is a subarkose, the other twenty-nine are quartz arenites (Fig. 3.6A). They comprise 60-80% simple quartz, 1-4% feldspar, 1-3% polycrystalline quartz, and traces of rock fragments, muscovite, matrix clay, plant debris and heavy minerals such as rutile, tourmaline and zircon.

The Moor Grit Member outcrops inland in a number of localities. It occurs as a thick, hard, white sandstone above the Scarborough Formation, and as the escarpment on areas of the Cleveland Hills, known locally as the "White Flint". The samples are all monotonous supermature, medium-grained sandstones, petrographically quartz arenites, and similar to those on the coast, except that the basal units are coarse sandstones and grits which contain up to 10% polycrystalline quartz.

Diagenetic modifications on the coast are restricted to quartz and feldspar overgrowths, blocky kandites, muscovites neomorphosed to kandites, corrosion of quartz, replacement of quartz by siderite, and suturing of quartz grains and overgrowths. There are no significant lateral or vertical variations in diagenesis. Authigenic phases are dominated by quartz overgrowths. These occur on all simple and some polycrystalline quartz grains throughout the samples. They usually occur as a thin veneer, reducing pore space and pore throats (Plate 3.12C), but when most thickly developed or in combination with sutured contacts, they completely fill intergranular pore space. Overgrowths average 10% and comprise up to 20% of the rock, and are corroded or replaced



by the trace of siderite present (Plate 3.12E, F, and G).

Cathodoluminescence occasionally reveals sutured grain contacts, and sutured overgrowths contacts. The former, in particular, were also observed in thin-section. There are no clay phases between grains along these sutured contacts, indeed, pore-lining chlorites were only observed in thin section in intergranular pore spaces unaffected by suturing. Cathodoluminescence also reveals the presence of two phases of quartz overgrowths. The remaining diagenetic features are not as widely or quantitatively significant as quartz overgrowths. Siderite and goethite are observed as a trace in most samples, replacing quartz overgrowths and feldspars. Plant debris is pyritised, muscovite neomorphosed to kandites, and blocky kandites scattered throughout the samples. These blocky kandites are extremely irregularly distributed; they occupy enlarged intergranular or grain dissolution pore spaces as large pockets, totally filling this porosity and blanketing quartz grains (Plates 3.13G and 3.12D, and 3.13H respectively). Kandites are present as a trace in all samples and comprise up to 3% of the whole rock in a few (Fig. 3.6C). Refined XRD analysis identified the blocky kandites as dickite.

In one sample, blocky kandites were observed adjacent to a quartz overgrowth with a stepped euhedral face (Plate 3.13E and F). Kandites are normally unaltered, occurring as euhedral pseudo-hexagonal plates, although in one sample illitised kandites were observed. Other authigenic phases present are orthoclase overgrowths, pyrite, anatase (Plate 3.14H), brookite and barytes, but they only occur as traces.

Inland, the Moor Grit Member was sampled at four localities, all of which display almost identical diagenetic modifications to those on the coast, apart from a variable quantity of pore-lining clay, (chlorite or vermiculite). At one locality, Danby Moor, these clays are absent, whilst at Bloody Beck

and Eller Beck Bridge, chlorite occurs, and, finally, samples from May Beck contain vermiculite. These pore linings are either thin traces, or thicker, well developed pockets. The thickest are not enclosed by quartz overgrowths, whilst thinner linings are covered either with incipient nucleations, or fully developed overgrowths (chlorite, Plate 3.13A, C, and D, and vermiculite, Plate 3.13B). These clays comprise up to 10% of the rock (Fig. 3.6C). The only significant variation between these samples and those on the coast is that overgrowths do not occur in the presence of thick pore-lining clays inland. Porosity comprises 2-25% and averages 12% of the rocks, being almost entirely enlarged intergranular porosity. Pore space appears to increase upwards through the Moor Grit Member.

Moor Grit - South of Scarborough. This Member changes in facies south of Scarborough and outcrops as a muddier white or yellow sandstone. The samples collected are mature and supermature quartz arenites with some subarkoses. Simple quartz predominates, comprising up to 70% of the rock, with 2-5% feldspar, patches of matrix clay and traces of plant debris, rutile, tourmaline and zircon. The majority of the samples are highly porous and are only cemented with quartz overgrowths. A few contain traces of carbonates also, whilst two are completely cemented, one with calcite and the other with siderite.

Quartz overgrowths are present as a thin veneer on detrital quartz grains in almost all the samples. They comprise up to 10% of the rocks, but average around 5%. They do not enclose any other diagenetic phases, and are replaced by siderite and calcite where the latter are present, and corroded where the carbonates are absent. Of the two completed cemented samples one contains rhombic siderite which replaces all detrital components, the other is completely cemented with poikilotopic ferroan calcite, which also replaces quartz and feldspar grains (Plate 3.14C). There is no evidence of overgrowths within

the former. Siderite also occurs as a veneer around a few pores in some samples, replacing quartz overgrowths. It is more concentrated around mica-ceous matrix clay rich pockets. Traces of calcite occur in two samples, whilst 5% of blocky ferroan calcite occurs in one, again replacing quartz grains and overgrowths. It is noteworthy that perfect euhedral faces are not replaced by calcite, although the sides and edges of poorly developed ones are.

The remaining diagenetic phases occur irregularly. Feldspar grains are invariably dissolved, but are not neomorphosed to kandites or illites. A patch of pyrite occurs as a nodule in one sample and a trace occurs in another. Finally, scattered blocky kandites occur in oversized pores, but comprise no more than 2% of any sample. These samples are dominated by their porosity. Most are loosely cemented, and a few contain numerous floating grains. The porosity is mostly enlarged intergranular with distinctly corroded quartz grains and overgrowths around the edges. Porosity values range from 15-35% and average 20%. Whilst field evidence suggests that the sideritic sample may be a concretion, the nature or origin of the calcitic one is not discernable.

Interpretation. Diagenesis in these sediments is interpreted as reflecting primarily eogenetic conditions, although subsequent mesogenetic influences occur widely.

Feldspars and micas are unstable in fresh water and will have begun to react immediately after deposition. However, widespread reducing conditions are inferred subsequently throughout these sediments. Vermiform kandites were not observed, but iron chlorite and vermiculite occur widely as localised pore-lining clays. Chlorite is interpreted as being subsequently neomorphosed to vermiculite. Chlorite itself probably formed in these reducing conditions

shortly after deposition from detrital iron hydroxides, and alumina and silica, either from solution or released during partial feldspar dissolution. In addition, pyrite occurs locally, often associated with plant debris, which suggests bacterial degradation of organic matter induced reduction and removal of sulphate ions from solution.

Quartz and feldspar overgrowths, where not inhibited by thickly developed pore-lining clays, may be explained by continued freshwater diagenesis of this massive porous sandbody. Authigenic quartz formed first, and authigenic feldspar subsequently, with increasing pH and probably from the potassium released during earlier dissolution. Anatase and brookite probably precipitated after the dissolution of detrital rutile. With the combination of inferred increasing pH, and reducing conditions siderite precipitated, as both a cement and concretions south of Scarborough. The succeeding ferroan calcite is, however, interpreted as formed from formation waters introduced into these sand bodies.

Corroded grains, etch pits, and dissolution features suggest dissolution of a more widespread carbonate cement. Porosity in these sandstones is therefore, secondary. Hence, the blocky kaolinites which occur filling enlarged or grain dissolution pore spaces are secondary pore-filling clays, precipitated either directly from the aggressive solutions responsible for carbonate dissolution or from reaction of these fluids with feldspar grains, but not in situ neomorphism. The stepped euhedral surfaces on quartz overgrowths enclosing these blocky kaolinites are probably the second phase of quartz overgrowths observed with CL.

Sutured contacts occur locally, between grains and overgrowths and have, therefore, formed after the overgrowths. Sutured contacts do not occur perpendicular to bedding, and therefore are not interpreted as "pressure

solution" effects, rather as a response to local geochemical variations. Finally, illitisation of blocky kandites, and local barytes crystal are mesogenetic phases, forming from concentrated solutions during burial.

Scalby Formation: Long Nab Member

Channel sandstones. White or yellow sandstones were sampled from two transects, one vertical and one horizontal, from meander-belt sandstones at the base of the Long Nab Member. They were also taken from all the channel sandstone outcrops on the coast between Hundale Point and Scalby Mills, as well as one disused quarry inland at Boltby.

These sandstones are all subarkoses or quartz arenites (Fig. 3.6B), the former predominating, and are mature and medium grained. Simple quartz grains comprise 60-70% of the rock, with up to 5% feldspar (albite and orthoclase), up to 4% polycrystalline quartz, traces of mica, opaque and heavy minerals, and plant debris; detrital matrix clay is usually absent or present as a trace, but comprises 10% of one sample. There are no significant variations in detrital mineralogy within the sequence, although there is a trend from quartz arenites in the meander belt to subarkoses and quartz arenites in the succeeding, isolated, channel sandbodies. Porosity values are uniformly moderate to high, ranging from 10-25% and averaging almost 20% of the rock. Pore spaces are usually large and well connected in two dimensions through wide pore throats, and are mostly enlarged intergranular or intragranular pores, with some grain dissolution porosity in addition; there is very little microporosity in these samples. The lowest values of perhaps 5% occur in the meander belt, where thick, tight quartz overgrowth cementation occurs. Generally, the three dimensional connectivity of this porosity is enhanced by feldspar grain dissolution (Plate 3.14B).

Authigenic phases comprise from 5-20% of the rocks, averaging around 10%. The most volumetrically significant are quartz overgrowths and siderite, with lesser quantities of kandites, illite, chlorite, feldspar overgrowths and pyrite. Quartz overgrowths occur throughout all the samples as a thin cementing veneer on detrital quartz grains. They comprise up to 10% of the rock, reducing and partially filling some pore space and pore throats (Plate 3.14E). In those rare areas of samples where detrital or authigenic illite and authigenic pore-lining chlorite occurs, overgrowths were not observed. Elsewhere, they do not enclose other authigenic phases. They are often corroded and replaced by siderite. SEM examination reveals stepped euhedral terminations on some authigenic quartz overgrowths. Cathodoluminescence examination reveals two phases of quartz overgrowths on some detrital grains, one bottle green, the other non-luminescent.

Siderite, often partly pseudomorphed by goethite, ranges from a trace to 8% of the rocks. It occurs as a pore filling and replacing detrital and authigenic quartz and feldspar, detrital matrix clay, micas and plant debris.

The remaining authigenic phases occur as traces or irregularly distributed throughout the samples. Orthoclase feldspar overgrowths were observed on some orthoclase grains, whilst authigenic pore-lining chlorite was observed in one sample, and pyritised plant debris in another. Illite makes up to 4% of the rock at the most, but is usually only present as a trace, or is absent entirely. It occurs in three forms, as a wholly authigenic pore filling and neomorphosing both detrital clay and authigenic kandites. Kandites themselves occur in two habits: as a neomorphic product from the breakdown of micas, and predominantly as discrete blocky pore fillings. These blocky pore fillings comprise up to 5% of the samples, they occur in both intergranular and enlarged intergranular porosity, as well as oversized grain dissolution pore spaces. Discrete smectite was detected in several samples

by XRD, but it was not observed either in thin section or with the SEM.

Overbank sediments. Crevasse-splay sandstones, which occur throughout the Moors, are white or yellow, mature and immature quartz arenites and subarkoses, in which matrix clay comprises from a trace to 15% of the rock (Fig. 3.6B). They are uniformly fine grained. Simple quartz is the predominant detrital phase, comprising 60% of the rocks, with feldspar up to 10% and traces of polycrystalline quartz, rutile, zircon, tourmaline, plant debris and muscovite. Micas, plant debris and matrix clay are often slightly bent or crushed between grains. Porosity is low in all the samples, ranging from a trace of microporosity within the matrix clay to 8% in the coarsest samples. There is, however, one exception, found at Cromer Point, in which grain dissolution and enlarged pore spaces are all lined with siderite or goethite. This sample contains 8% porosity.

Authigenic minerals comprise on average, up to 10% of the rock, principally quartz overgrowths, as thick veneers on detrital quartz grains, except where matrix clay, chlorite (Plate 3.14F) or vermiculite (Plate 3.14A) pore linings occur. Where matrix or authigenic clays are absent, overgrowths are more extensively developed, occasionally comprising up to 20% of the rock and completely filling pore space (Plate 3.14D). In the coarsest porous areas, overgrowths are sometimes corroded or replaced by siderite. Feldspar overgrowths occur on detrital feldspar grains, but are not volumetrically significant. A small amount of siderite is present in most samples, replacing matrix clay, feldspars and authigenic quartz. Kandites occur as loose vermiform pore fills, neomorphosed muscovites, and patchy, but rare blocky pore fillings of euhedral pseudo-hexagonal plates. They comprise 1-2% of each sample at the most. Whilst blocky kandites are ubiquitous, vermiform kandites do not occur with chlorite or vermiculite. Neomorphism of detrital clay to pore-lining illite is common. Pyrite occurs both within the dense

matrix clay fills, and associated with, or replacing plant debris.

Above two rooted crevasse-splay sandstones, between Crook Ness and Cromer Point, thick accumulations of discrete and coalesced spheruliths of sphaerosiderite occur. Both these horizons and the intervening shales contain siderite concretions. The spheruliths are composed of a ring of pyrite, around an amorphous siderite core, and enclosed by a single crystal of sphaerosiderite (Plates 3.1<sup>L</sup>4H, 6.1 and Fig. 3.7). However, analysis demonstrated heterogeneity within the spheruliths. Although siderite occurs throughout, it is not stoichiometrical. The pyritic zone contains an increased manganese concentration and decreased magnesium and calcium, whilst the outer zones become progressively enriched with respect to the latter. The concretions are generally ellipsoidal and, although bedding laminations may be traced through them, the surrounding mudrocks are compacted around both these concretions and nodules (Plate 6.2, Fig. 3.8). Siderite in the concretions encloses and replaces quartz grains and vermiform kandites. Cracks within the concretions contain pure white dickite. The mudrocks here, and elsewhere in the Long Nab Member, consist of micas and kandites.

Interpretation. Diagenetic differences between floodplain sediments and channel-filling sandstones are interpreted as reflecting the onset of reducing conditions at differing times in the two subenvironments. The majority of reactions are interpreted as eogenetic with mesogenetic events controlled by alluvial architecture and generally restricted to channel sandstones.

Pyrite, illite, vermiform kandites, and chlorite all occur in floodplain sediments, although, with the exception of pyrite, they are mutually exclusive. Vermiform kandites are associated with feldspar dissolution, quartz overgrowths, and neomorphosed micas, all of which suggest freshwater dissolution and widespread reprecipitation of alumina and silica. With increasing pH, the remaining



potassium ions may have been incorporated into authigenic and neomorphic illite and feldspar overgrowths. Alternatively, these sediments may have accumulated in a saline or brackish environment. Elsewhere, whilst freshwater dissolution occurred, reducing conditions are inferred from the presence of pore-lining chlorite, which subsequently inhibited overgrowths. Similarly, chlorite occurs in the sandbody overlain by the siderite soil at Crook Ness. Finally, the association of pyrite with plant debris suggests bacterial degradation of organic matter was primarily responsible for reduction of sulphate ions and iron, the latter present in excess and subsequently forming widespread siderite.

The dense sphaerosiderite horizons are interpreted as soil horizons, whilst siderite which also cements sandstones from both subenvironments is probably a freshwater cement. Furthermore, the concretions in the floodplain mudrocks at Crook Ness are interpreted as freshwater concretions. Microprobe analysis (Fig. 3.7) reveals the complexity of interstitial water's Eh, pH, and geochemistry at this time. From spherulith cores to edges, through the pyrite rings, analysis indicates iron remaining reasonably constant, manganese increasing significantly towards the edges. These trends suggest core formation in suboxic iron reducing conditions; pyrite ring and pyrite forming during sulphate reduction and, finally, rim formation during continued suboxic conditions.

The mudrocks are compacted around the edges of the concretions. However, equally spaced laminations may be traced through the concretions; hence there is no evidence of compaction during growth, only after growth. Alternatively, this suggests growth was virtually complete before significant burial. From their ellipsoidal shape it may be implied that even before compaction, horizontal permeability greatly exceeded vertical permeability, causing preferential horizontal growth. (Siderite soil spheruliths and concretions are discussed

in greater detail in Chapter Six).

Corrosion features, etch pits, and floating grains suggest dissolution of previously more extensive carbonate cements. Intergranular porosity is, therefore, secondary cement dissolution porosity. Furthermore, the pockets of blocky kandites in these pore spaces probably formed from the same aggressive solutions which caused dissolution of the replacive carbonates, or the interaction of these fluids with feldspar grains.

#### DISCUSSION

Diagenesis may be considered as the sum of those processes by which an originally sedimentary assemblage attempts to equilibrate with its environment. Although conclusions above suggest that this assemblage has been modified, one may interpret these data to show that most of its original solid components are still present, at least in part. Reconstruction of the assemblage suggests that the following phases were present: highly abundant and predominant  $\text{SiO}_2$ , much less abundant  $\text{Al}_2\text{O}_3$ , even smaller quantities of  $\text{K}_2\text{O}$  and  $\text{Na}_2\text{O}$ , and traces of  $\text{CaO}$  and  $\text{MgO}$ . Also, organic matter was present locally, both in channel-lag deposits and disseminated throughout fine-grained floodplain sediments. In addition, one may assume, by analogy to modern tropical weathering zones (e.g. Livingstone, 1963; Thomas, 1974), that interstitial waters were initially saturated with respect to quartz, alumina and amorphous iron hydroxides. These waters were neutral on the floodplain or alkaline and saturated with respect to calcium carbonate in brackish and open-marine environments (White, et al, 1963).

In the following discussion I should like to address myself to the question of how this assemblage has attempted to reach equilibrium with its environment. I shall present, therefore, models for changing pore-water composition during

the events described above. Although the majority of the reactions discussed below may proceed with oxidising or reducing conditions and will, therefore, continue regardless of Eh, they will be affected by others which, whilst effecting changes in Eh, also affect pH and pore-water composition.

Before discussing specific diagenetic reactions in detail, or establishing general models, I should like to consider briefly one of the problems posed by the volumes of authigenic phases in these strata. Bjørlykke (1979), Boles and Franks (1979b) and Land and Dutton (1979), have discussed the derivation of large quantities of authigenic quartz from pore fluids. Whilst the specific details of this discourse are not directly relevant to these strata, the general conclusion is that, assuming diffusion does not take place, it is not possible to derive significant quantities of authigenic quartz from pore waters, unless large volumes pass through the sediment. There are, however, two points which need to be considered. Firstly, a sediment need not, and indeed should not be considered as the finite record of any period of time. The geological column certainly does not contain enough sediment to record fully its duration. Consequently, one must consider that processes operate throughout a stratigraphical interval, not just within the depositional span of the resulting sedimentary sequence. Secondly, one must also consider reactions within sedimentary sequences between detrital components and pore fluids as possible sources of authigenic minerals, and finally, that they may move by diffusion rather than being transported in solution. Diffusion may be especially important before overburden begins physically to dewater muds.

The Ravenscar Group is some 250 m thick, but spans approximately 17 ammonite zones (Cope et al., 1980) and, following Hallam (1975), therefore, lasted approximately 17 million years. The average rate of sedimentation is thus 15 m per million years, an unacceptably slow rate, even allowing for possible

unconformities between the formations (Leeder and Nami, 1979), especially when some of the 5 m thick sandbodies within the sequence could have accumulated in a matter of hours (Leeder, pers. comm. 1980). Similarly, Leeder and Nami (1979) estimate that the Long Nab Member may have accumulated in 11,000 - 110,000 years, and the Moor Grit in 10 - 20,000 years at the most. Leeder and Nami assume 50% compaction of the floodplain sequence. Allowing for this underestimate, and assuming slowest rates of sedimentation from Holocene alluvium, 1 mm per year, with 90% compaction, floodplain accumulation would only have taken 500,000 years. Extrapolation of this to the other non-marine strata suggests the following maximum depositional spans:

Saltwick Formation	500,000 years
Sycarham Member	500,000 years
Gristhorpe Member	300,000 years

Even allowing for these gross overestimates, and considerably longer periods of marine sedimentation, the Ravenscar Group is significantly thinner than one would expect from 17 million years of sedimentation.

The point of this discussion is not to highlight the sedimentological problems of the area, but to suggest an alternative approach to sediment diagenesis. Whilst the actual sediments may not be recorded, evidence suggests that many erosive breaks, rather than non-depositional gaps occur. For example, Harris (1953) records eight truncated rootlet horizons in the Gristhorpe Member at Cloughton Wyke alone. Moreover, diagenetic interpretations suggest much of the floodplain was well drained at this time. Consequently, large connected and porous sandbodies would have been highly permeable in the sub-surface immediately following deposition (Beard and Weyl, 1973; Pryor, 1973). It seems logical to assume, therefore, that for some part of the 17 million years during which this fluvio-deltaic complex developed, substantial quantities

of fresh water, saturated with alumina, silica and iron hydroxides (Tardy, 1971), transporting soils, amorphous gels and clay micelles, probably coated with absorbed iron hydroxides (Greenland, 1975), and depositing organic matter and clastic sediments, passed onto, into, or through the sediment. The effect of this would be fourfold, but not recorded in the detrital sequence. Firstly, solute species would enhance and maintain pore-fluid saturation with respect to silica, alumina and iron hydroxides. Secondly, degradation of organic matter would generate bicarbonate rich solutions. Thirdly, clay particles and unstable aluminosilicates would dissolve or neomorphose, and supply further species to solution. Fourthly, the volumes of water involved would ensure removal of reaction products, and consequently perpetuate reactions propagated by the agents above. Thus, one need not deliberate on how the sediments preserved generated the volume of authigenic material, or the intense reactions inferred within the diagenetic regime at the surface.

The origin of the quantities of iron required throughout the Dogger Formation and the Ravenscar Group is problematical. Unfortunately, little progress has been made since Carroll (1958) originally discussed this general problem, and proposed transportation of iron into sediments by its absorption onto surfaces of clay micelles (e.g. Greenland, 1975). Iron may, alternatively, be carried into a basin as a colloidal suspension, complexed with humic acid (Picard and Felbeck, 1976), or other organic substances. However, all these possible sources of iron must lie outside this particular basin as there are no obvious products of degradation of iron enriched minerals in these sediments, (the contribution of neomorphosed muscovites is minimal).

When one considers the general climate at the time, a possible solution to this problem is revealed. Tropical weathering is often intense, leaching and effectively degrading unstable components of parent rocks to depths of tens or hundreds of feet (Feininger, 1971). The products of this weathering

may be considered either as relatively soluble and mobile, or as insoluble and immobile. The former group includes ionic species such as  $Mg^{2+}$ ,  $Ca^{2+}$ ,  $K^+$ ,  $Na^+$ , etc, whilst the latter includes lateritic soil forming phases such as silica, alumina and iron hydroxides. Consequently, tropical weathering enriches soils or surface sediments with respect to silica, alumina and iron hydroxides, variously forming kandites and gibbsite (Nicholas and Bildgen, 1979). Erosion, mobilising these amorphous or colloidal particles would result in their transportation into tropical lakes, or onto floodplains (e.g. Fitzpatrick, 1980; Gac and Tardy, 1980).

I propose to discuss, firstly, marine sediments and their diagenetic modifications; secondly, the effects of the fresh water table, or telogenesis, on these marine sediments; thirdly, diagenesis of non-marine sediments; and finally, ubiquitous changes during subsequent burial and Recent weathering.

#### Eogenesis of marine sediments

In this section I should like to discuss briefly diagenetic modifications to sediments from the Dogger Formation, and marine horizons in the Ravenscar Group. I should like to consider initially the carbonate sediments, then the more widespread clastics, and finally, concentrate on the slightly exotic sediments in the Dogger Formation.

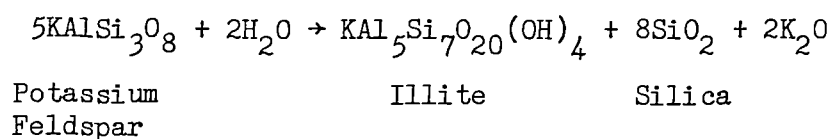
The solubility of calcium carbonate increases at a pH of less than 7.5 (Blatt, 1966). Sea water, conversely, has a pH of 8, and is generally saturated with respect to calcium carbonate (Bass Becking et al, 1960; Berner, 1971). However, the concentration of calcium carbonate in sea water reflects a fine balance between its removal by skeletal production in macroorganisms, and the productivity of microorganisms (Bathurst, 1975). Accumulation of carbonate sediments, therefore, occurs above the carbonate compensation depth where demand does not

exceed supply, and sediments are not dissolved either during or after deposition. Although carbonate sediments occur in the Millepore Bed and the Dogger and Scarborough Formations, only the former are cemented with eogenetic calcite. The absence of eogenetic carbonate cements from the latter formations presumably reflects relative undersaturation of sea water at those time.

This early, almost syndepositional, cementation of the Millepore Bed at Yons Nab and elsewhere, produced brightly luminescent intraparticle pore-filling calcite and a duller interparticle pore-lining or rim cementing calcite. Whilst the exact controls on luminescence of carbonate minerals is poorly understood (Pierson, 1981; Schofield, pers. comm. 1982), a broad generalisation may be made: although ratios rather than absolute concentration may be important (Fairchild, 1980), iron appears to inhibit or quench luminescence (siderite and ferroan calcite do not luminesce), whilst manganese may promote luminescence, iron concentration permitting (Pierson, 1981). The available data suggest that the poorly luminescent rim cement contains 7-9000 ppm  $\text{Fe}^{2+}$ , which is probably insufficient to inhibit luminescence completely (manganese concentration is below the detection limits here). Microprobe analysis failed to detect either  $\text{Fe}^{2+}$  or  $\text{Mn}^{2+}$  in the brightly luminescent intraparticle pore-filling calcite, and so is in accord with interpretation of calcite cementation from oxygenated pore waters shortly after deposition. Furthermore, the non-luminescent nature of the later ferroan calcite in these sediments, which contains 11-14000 ppm  $\text{Fe}^{2+}$ , is consistent with theoretical trends predicted in Pierson's (1981) dolomite study. Elsewhere, in the marine clastic sediments, with interstitial pore waters presumably only saturated or even undersaturated with respect to calcium carbonate, diagenesis reflected the interaction of different solid and amorphous sediments with pore fluids.

Sedimentary clastic assemblages are fundamentally unstable when deposited (Curtis, 1980). The initial diagenetic reactions of these marine sediments

reflect their mineralogy, alkaline interstitial waters, presumably saturated with respect to  $\text{Na}^+$ ,  $\text{K}^+$ ,  $\text{Ca}^{2+}$ ,  $\text{Cl}^-$ ,  $\text{HCO}_3^-$ ,  $\text{SO}_4^{2-}$ , and silica and carbonate ions liberated by bacterial degradation of organic matter. The initial diagenetic reactions of aluminosilicates deposited in open marine or brackish environments reflected this interaction of sediments and pore waters. When deposited, and during burial with interstitial waters of sea/<sup>water</sup>composition, feldspars and micas are unstable and will begin to react (dissolving or neomorphosing, respectively) to form illitic clays (Helgeson et al, 1969; Kastner and Siever, 1979). Such clay minerals are stable under these conditions (Siever and Woodford, 1973).



Consequently, illite probably formed as both a wholly authigenic phase, and neomorphosing detrital clays and micas (Harder, 1974). Subsequently, during burial, or in situ with low sedimentation rates, silica concentration probably rose,  $\text{K}^+$  concentration increased, and pH increased (Kastner and Siever, 1979). As a consequence, feldspar overgrowths became stable relative to illite, and with  $\text{K}^+$  concentration falling and silica concentration rising, quartz overgrowths formed (Fig. 3.9), even though pore-water composition may have been alkaline and similar to that of sea water (Mackenzie and Gees, 1971; Harder, 1974).

Whilst the diagenetic sequence discussed above may explain reactions involving oxygenated pore waters, all the succeeding modifications to the sediments required reducing conditions. As Curtis (1980, p. 192) points out,

"In environments close to the sediment-pore water interface, all soluble products of diagenetic reaction will be lost unless some very efficient fixation mechanism operates."

Conversely, oxygenated waters will diffuse into these pores from above and, as a consequence, aerobic bacterial processes, which began immediately following deposition, will continue, although the resulting bicarbonates will be lost.



During burial, however, and below the zone into which oxygenated waters diffuse, free oxygen is depleted rapidly and reducing conditions develop (Curtis, 1980). Diagenetic modifications to these marine clastic sediments also required acidic solutions. Both reducing conditions and a lowering of pH probably resulted from bacterial degradation of organic matter. Thus, following effective sealing from the surface, pore-water chemistry changed. The resulting modifications are, however, still eogenetic, because they result from equilibration of pore fluids and sediments, and do not involve the introduction of additional components.

Minor vermiform kandites, and muscovite neomorphosis in the Yons Nab Beds, for example, probably resulted from these changes where pH was lowered, whilst chlorite, pyrite and ferroan calcite cementation resulted from the onset of reducing conditions. Aerobic bacterial processes probably also caused the initial lowering of pH, and precipitation of kandites in the Millepore Bed at Yons Nab and Cloughton Wyke (Fig. 3.9). In addition, this initial lowering of pH may have resulted in carbonate dissolution at grain contacts, and consequently caused the suturing which predated extensive poikilotopic ferroan calcite cementation. Subsequently, anoxic processes, although liberating bicarbonates, probably raised pH whilst reducing iron oxides and sulphate ions. Consequently, minor siderite cementation took place where neomorphosing micas supplied iron. In addition, widespread pyrite marks the effective removal of original sea water sulphate ions. Finally, as iron reduction continued generating further bicarbonate, and pH rose, widespread ferroan calcite cementation occurred. Elsewhere, prior to calcite cementation, reducing conditions operated nearer to the surface, and diagenesis of aluminosilicates resulted in the formation of chlorite rather than either illite or kandites. Vermiculite also occurs in places but its inferred origin is by neomorphosis of chlorite rather than authigenic precipitation.

Some sediments remain completely cemented with ferroan calcite, and unaffected by fresh water from the overlying alluvial sequences. It is impossible in others, however, to distinguish between three possible diagenetic pathways. Firstly, ferroan calcite may have partially or completely cemented samples, but subsequently been removed by aggressive fluids. Secondly, samples may have been cemented with calcite, which was replaced or removed during fresh-water diagenesis. Thirdly, fresh water may have affected some sediments prior to calcite precipitation and consequently imposed similar diagenetic modifications on the overlying alluvial sequences.

The diagenetic modifications of almost all these marine Middle Jurassic sediments can be explained in terms of the models outlined above. Carbonate sediments were cemented with calcite, but subsequently affected by bacterial degradation of organic matter. Clastic sediments interacted with interstitial sea water to precipitate illite and potassium feldspar overgrowths, but they too were subsequently affected by bacterial processes.

These sediments reveal a number of controls on diagenesis. Their depositional mineralogy differs, and consequently the initial results of equilibration with their pore waters also differ. Both carbonates and clastics were subsequently affected by a lowering of pH and removal of free oxygen. However, in view of their differing mineralogy and the differing diagenetic modifications due to initial equilibration, their subsequent behaviour also differed slightly.

Finally, in this section, I should like to digress and consider specifically the diagenesis of parts of the Dogger Formation in which berthierine oolites occur. The origin of berthierine is somewhat problematical. In addition, the confusing use and misuse of nomenclature in the literature hampers the comparison of, and the comparison with, previous studies. This thesis follows Bailey (1980): berthierine is not a chlorite mineral, but an iron aluminium

silicate with a 1:1 layer structure and a  $7\text{\AA}$  basal spacing. On the other hand, chamosite, a distinctly different mineral, has a 2:1  $14\text{\AA}$  structure, and is the name recommended for iron-rich chlorites. The two, however, are often used synonymously, or alternatively, the older, established term "chamosite" is applied to anything green and oolitic shaped, often without XRD confirmation of its structure (see Brindley (1982) for discussion).

Interpretation of microprobe analysis indicates that all the iron in the oolites is ferrous. Thus, reducing conditions were required during their formation. However, oolitic structures suggest formation in agitated and, therefore, probably oxygenated environments (Bathurst, 1975). Bioturbation in these sediments, including the presence of Diplocraterion (Livera, 1981) is independent evidence for oxygenated conditions at the time. The paradox of berthierine oolites containing ferrous iron occurring in inferred oxygenated environments is amplified by Curtis and Spears (1968). In the following discussion I should like to consider a number of models for the formation of berthierine oolites. Firstly, direct in situ precipitation. Secondly, in situ formation of ferric oolites, and subsequent reduction to form berthierine. Thirdly, derivation of either ferric or ferrous oolites from elsewhere, the former subsequently being reduced. Fourthly, replacement of aragonitic oolites by iron-rich siliceous fluids.

The origin of oolitic ironstones has been a subject of debate since Sorby (1857, p. 460) wrote:

"The general conclusion that I therefore draw from these facts is that, at first the Cleveland Hill Ironstone was a kind of oolitic limestone, interstratified with ordinary clays, containing a large amount of the oxides of iron, and also organic matter, which by their mutual re-action gave rise to a solution of bicarbonate of iron - that this solution percolated through the limestone and, removing a large part of the carbonate of lime by solution, left in its place carbonate of iron; and not that the rock has formed as a simple deposit at the bottom of the sea."

Their origin has also been the subject of controversy in recent years:

James and van Houten (1979), Bradshaw et al, (1980), Hallam and Bradshaw (1979), and Kimberley (1979, 1980a, 1980b) present some of the opposing views. Dimroth (1977) and Kimberley (1979) reviewed the models proposed in the literature, and Kimberley himself proposed an "elaboration" of Sorby's model. He proposed that the ironstones were originally aragonitic ooliths, covered with deltaic mud, containing ferruginous minerals and iron hydroxides, and abundant organic matter; degradation of organic matter generated acidic solutions, which both leached aragonite from the underlying ooliths, and precipitated berthierine.

There is no evidence to support this model in these sediments. Intraformational conglomerates occur, and suggest that berthierine formed during and shortly after deposition, but not after progradation of "deltaic" muds above, and an effective change of environment. Furthermore, some ooliths are nucleated on fossil fragments: it is difficult to conceive a method whereby acidic iron aluminium silicate rich solutions would replace completely aragonite layers, but not the calcite clasts within. This problem was also the cause of Hallimonds' (1925) refutation of a replacive origin.

Berthierine cannot form in the presence of free oxygen (Curtis and Spears, 1968). Consequently, any proposals involving its direct formation as ooliths in presumably oxygenated waters should be rejected. In addition, proposals in which berthierine ooliths are reworked and deposited without further modification in these shallow marine environments should be rejected for similar reasons. I would, therefore, suggest that whilst the oolith structure was either derived or formed in situ, the constituents themselves only neomorphosed to berthierine subsequently. These constituents must have been dominated by iron oxides or hydroxides, alumina and silica (both possibly combined as a clay mineral), a typical lateritic weathering assemblage (Thomas, 1974).

Oololiths have been reported from three modern environments. Firstly, Porrenga (1965, 1967) describes chamositic oololiths forming by mineralisation of faecal pellets. Whilst reducing conditions may occur within these pellets, they are insulated from their oxygenated environment by a layer of goethite. Secondly, Lemoalle and Dupont, (1973) and Gac and Tardy (1980) describe goethite coated clay micelles transported into Lake Chad and forming ferruginous ooids. Thirdly, Nahon et al, (1980) describe ferruginous ooids not dissimilar to those described from Lake Chad and the Dogger Formation. Their ooids, however, are forming in situ as the result of lateritic weathering.

In spite of the fact that each of these examples is unique, ferruginous oololiths themselves only rarely occur within the geological record. It is perhaps significant that all three examples occur in the tropics. In addition, Odin and Matter (1981), reviewing the occurrence of Recent berthierine, report its concentration around the mouths of tropical rivers. Lateritic soils are widespread in the tropics (e.g. Fitzpatrick, 1980), whilst tropical weathering assemblages often comprise amorphous silica, gibbsite, kaolinite and iron hydroxides (e.g. Thomas, 1974). I would, therefore, propose that the berthierine oololiths in the Dogger Formation, and possibly those of the Eller Beck Formation described by Knox (1970), are either eroded lateritic soils, or formed in situ from kandite minerals, coated in iron hydroxides and, in both instances, reduced following deposition. This proposal does not preclude reduction in the cores of oololiths during their agitation. As Curtis and Spears (1968) pointed out, the principle problem with a model of this sort is that one would expect compositional differences within the resulting ironstones, because one would not expect homogeneity within the original assemblages. Fortunately, this is the case. Opal and kandites occur in the Cleveland Ore field oololiths (Dunham, 1960), kandites in those from Northampton (Taylor, 1949), and iron oxides coat the oololiths analysed here from Rosedale. Furthermore, the composition of berthierine varies within individual oololiths.

In effect, the identification of berthierine as the principal mineralogical component of these ooliths does little more than inflict current terminology on extensively studied rocks. In spite of Orcel et al (1949) resuscitating the term berthierine, Dunham (1960) retained the term "chamosite" as it was used then although he did point out that it has a  $7\text{\AA}$  basal spacing. However, it is not clear from his review whether any of the Yorkshire ironstones had actually been X-rayed at that time. Indeed, despite this, and the changing use of nomenclature, the term "chamosite" has persisted until recently (e.g. Hemingway, 1974).

In conclusion, irrespective of whether the original ooliths were allochthonous or autochthonous, berthierine is inferred to have formed by the in situ reaction of clays, probably kaolinite, and absorbed iron hydroxides. It is interesting to compare the inferred origin of berthierine and chlorite in these sediments: the former by in situ reaction, and the latter by direct authigenic precipitation. It is also interesting to note the occurrence of these ooliths at the base of the Dogger Formation and within the Scarborough and Eller Beck Formations. Nahon et al (1980), speculate that ironstones consisting of ooliths may serve as markers of previously exposed and weathered surfaces. Consequently, the ooliths here would record surfaces exposed prior to each transgression. Similarly, James and van Houten (1979, p. 132) conclude that their

"oolites accumulated in interdistributary embayments of a prograding delta during episodes of waning detrital input which followed successive distributary abandonments. (The ooliths) apparently formed directly from colloidal ferric oxide and silicate precursors."

Apatite and collophane are used here in a loose sense to describe structured and amorphous calcium phosphates. Collophane occurs replacing detrital mud clasts, and apatite as a pore-filling cement, although it is not immediately obvious whether it predates or post-dates the associated siderite. The

conditions under which phosphates form are restricted (Berner, 1974). They are as follows: low carbonate to phosphate ratio; low magnesium concentration and a moderate pH. Although sea water is the inferred depositional environment, it does not satisfy these conditions. In sea water, carbonates rather than apatite form from saturated solutions, whilst any magnesium which remains inhibits growth of apatite on the resulting aragonite or calcite crystals. Moreover, the generally low concentration of phosphorous in sea water precludes its direct precipitation. However, either during burial or in environments enriched in organic matter, apatite may form either authigenically or replacing carbonates. Its formation is not generally Eh dependent.

The concentration of phosphate deposits at the base of the Middle Jurassic in Yorkshire suggests that a unique environment existed at this time, possibly the result of erosion and reworking of fine-grained clastics rich in organic matter from the underlying Liassic. This suggestion may explain the enrichment of depositional pore waters with phosphates, hence direct mud replacement here rather than replacement of pre-existing carbonates. Consequently, the degradation of organic matter, releasing phosphates during burial, here and from the underlying Liassic, may have caused precipitation of apatite cements. It is interesting to note that pore-water composition throughout deposition of the Dogger Formation was undersaturated with respect to calcium carbonate, but when calcium concentration had increased, the phosphate to carbonate ratio precluded carbonate precipitation.

In conclusion, diagenesis in these marine sediments is variable, reflecting complex interrelationships between depositional mineralogy and interstitial-water chemistry, the effects of which are difficult to separate. In general, authigenic phases and diagenetic modifications reflect pore-water chemistry, but rates and timing of formation were controlled by depositional mineralogy. Thus, in the absence of a substrate or nucleus, ions in solution must have

been highly supersaturated before they precipitated. This is the case for calcite and pyrite in the clastic sediments, whilst calcite nucleates as a cement on carbonate sediments where they are present. These reactions also tended to reduce interstitial water salinity, and eventually lowered pH.

Authigenic quartz, illite and feldspar do not require such high supersaturation, they precipitated on detrital nuclei as overgrowths, under suitable Eh and pH conditions. However, these reactions were balanced in the evolving pore-water system by dissolution of detrital micas and feldspars. Also, the sandbodies in which these reactions occurred should not be considered as simply closed systems, similar ions could have been supplied into these more porous conduits at shallow depths by physical dewatering of the surrounding muds, containing compositionally similar reaction products.

All these sediments were subsequently affected by bacterial degradation of organic matter, which produced similar authigenic phases, but different diagenetic reactions in clastics and carbonates. Although the effects of the water table from the overlying fluvial system are minimal, two points need to be emphasised. Firstly, the diagenetic modifications of these sediments described above can be explained by a simple model involving attempted equilibration with their interstitial waters, continued bacterial degradation of organic matter, and pore waters expelled from the surrounding muds during the first few metres of burial. Secondly, whilst overgrowth formation may have continued in places after pore-fluid compositions changed, the majority of diagenetic reactions in these sediments were probably completed shortly after deposition. Whilst it is not possible to time any of these events absolutely, a burial scale of metres and tens of years rather than kilometres and millions of years is implied.

The influence of fresh water on these ferroan calcite cemented sediments



appears to have been minimal. Sideritic ironstones occur in each marine horizon in the Ravenscar Group, and in the Dogger Formation. However, SI analysis suggests that they formed from fresh water (see Chapter Six). In addition, petrographical evidence indicates that the siderite in these ironstones replaces ferroan calcite. Consequently, ferroan calcite cementation of these marine clastic sediments and occasional limestones must have been complete prior to the introduction of fresh water. The remaining diagenetic modifications of marine sediments are similar to those postdating ferroan calcite cementation of the non-marine clastics, and are assumed to have been ubiquitous.

In terms of definition, siderite precipitated from fresh water introduced from the fluvial sediments above is telogenetic. The other phases, however, are somewhat problematical. Eogenesis is the sum of those processes by which sediments move towards an equilibrium with their depositional pore waters. It is, therefore, relatively straightforward to describe phases precipitating from depositional pore fluids as eogenetic. These include calcite, for example, in the Millepore Bed. Similarly, potassium-feldspar overgrowths which follow illites are eogenetic, and resulted from movement of sediments and pore waters towards equilibrium. Subsequent phases, however, involved radical changes of Eh and pH. These are the result of bacterial processes operating on organic matter in the sediments. Are these phases, such as kandites or pyrite, eogenetic? Neither of these examples are likely to have precipitated directly from sea water. However, without changing its composition, one may affect the Eh and pH of sea water to effect precipitation of phases whilst equilibrating originally marine pore waters and sediments which contained organic matter. In this study, therefore, authigenic phases and diagenetic modifications which resulted from changes such as these will be considered as eogenetic. Eogenetic processes are, therefore, those which did not require the introduction of chemicals from outside the system. They

continued through changes of Eh and pH, resulting from equilibration of the sediments and their pore waters, but ceased when compositional changes occurred which cannot be explained as a result of these processes. These processes are summarised in Fig. 3.10.

#### Eogenesis of non-marine sediments

Before discussing diagenesis of non-marine sediments from the Ravenscar Group, it is perhaps necessary to mention that although the bulk of analytical work described above has concentrated on coarser clastics, finer grained sediments, mudrocks, comprise at least 70% of the sequence. Allowing for compaction during burial to some 20% or less of their original volume (Meade, 1966), muds, therefore, comprised at least 90% of the original volume of the preserved sediments (including porosity). One may assume that after mechanical compaction, involving grain rotation etc, during shallow burial, sandbodies retained 30% porosity. This porosity, which represents 2.5% or less of the original deposit has served as a conduit for water expelled from the enclosing muds, and all the fresh water entering the water table during the Middle Jurassic. These volumes of water are not large, and probably do not approach the quantities Bjørlykke (1979) suggests are required to cement sandstones. However, given quartz grains, for example, to act as nuclei for overgrowths precipitating from saturated solutions diffusion gradients would exist from silica sources in the muds. Moreover, the passage of water does not necessarily occur along this gradient at the same time. In addition, silica solubilities in natural ground waters, especially those associated with silicate rocks or sediments, often approach 100 ppm (Hem, 1970; Feth, et al, 1974), an order of magnitude more than Bjørlykke (1979) considers. This suggests that ground waters and in situ sources may contribute significantly to silica diagenesis following deposition.

I should like, also, to draw attention to the theoretical background to water table chemistry which influences much of the succeeding discussion. The relative temporal and spatial positioning of diagenetic reactions during shallow burial is controlled by sedimentation rate, and initial porewater composition, (although modifications occur with degradation of detrital components). Sequential reactions such as bacterial degradation of organic matter involving reduction of unstable amorphous material or interstitial solutes occur immediately following deposition (Curtis, 1977). These reactions occur in a profile from the surface downwards when reaction rates roughly equal sedimentary supply. Thus, reaction zones pass upwards through accumulating sediments, but remain a constant distance from the surface. However, where sedimentation rates are slow, reaction zones migrate progressively upwards, relative to the surface, as phases reduced in each zone become exhausted. Hence, in floodplains for example, with slow rates of sedimentation, an aerobic zone is maintained, into which oxygen diffuses. However, below this zone, nitrate and manganese oxide, iron oxide and hydroxide, and sulphate reduction will occur until finally, below a zone of effective oxygen diffusion, bacterial methanogenic fermentation takes place (Whelan, 1974; Whelan et al, 1975). Indeed, in certain circumstances, methane may be released to the atmosphere (Harris et al, 1982). These reactions will, of course, cease if organic matter becomes exhausted (Curtis, 1977; Coleman et al, 1979).

In the following discussion, I should like to propose a threefold division of the water table during initial diagenetic reactions in these clastic sediments following their deposition. This division is: firstly, stagnant anoxic swamp-like bodies of water on the floodplain; secondly, anoxic subsurface waters; and thirdly, oxygenated subsurface waters. These divisions reflected the interaction of two processes during diagenesis. Firstly, bacterial degradation of organic matter which caused the reduction of ferric iron, and eventually a build up of bicarbonates in solution. Secondly,

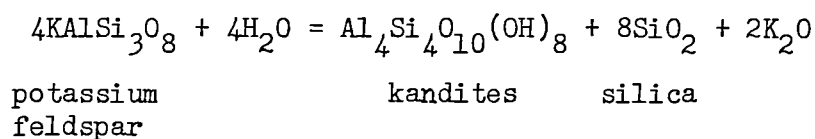
replenishment of the water table with oxygenated water, which perpetuated aerobic bacterial processes and generation of acidic solutions, but prevented the development of anoxic conditions. I should like to propose that in the stagnant anoxic waters bicarbonates built up and precipitated siderite soils, in the anoxic subsurface aluminosilicates broke down and reacted with ferrous iron to produce chlorite, whilst under oxygenated conditions kaolinites precipitated. The build up of bicarbonate ions in solution subsequently resulted in widespread siderite cementation irrespective of the original authigenic clays.

Well developed soil horizons are only rarely developed in the Ravenscar Group. Most mudrock sequences are rooted, but do not contain well developed profiles. These more monotonous grey mudrocks were presumably more effectively drained than those in which soils developed. Those soil horizons which do occur are composed of siderite spheruliths and reflect stagnation at the surface, as well as extremely slow sedimentation. Stable isotope analysis suggests that these spheruliths formed from a mixture of freshwater bicarbonate and bicarbonates released during reduction of iron hydroxides and sulphates (see Chapter Six). This build up of bicarbonates, released by generally later bacterial processes, presumably reflected relatively poor drainage at this time and migration of bacterial zones towards the surface. Moreover, sedimentation rate must have been relatively slow, to allow a build up of stagnant water saturated with bicarbonates, and to maintain these conditions until quite thick horizons had developed. In the Long Nab Member at Crook Ness, siderite concretions, precipitated from fresh water (see Chapter Six), enclose and replace the spheruliths, suggesting that drainage improved, and fresh water subsequently flushed through the sediments (Whelan and Roberts, 1973).

In the remainder of this section I should like to explain the possible

reason as to why more intensive quartz overgrowth cementation occurs in overbank sandstones than in channel sandstones, and the mutually exclusive distribution of authigenic kandites, chlorite and vermiculite throughout the sediments. All these phases are succeeded by siderite cementation, and occasional non-ferroan calcite, the final diagenetic modifications which can be related to the evolution of depositional pore waters and sediments.

Meteoric water is generally neutral (White et al., 1963), although fresh ground waters rapidly become acidic following bacterial degradation of organic matter (Curtis, 1977, 1978). Before considering the effect of this on coarser non-marine sediments in the Ravenscar Group, I should like to repeat the important premise: "sedimentary clastic assemblages are fundamentally unstable when deposited". Consequently, amorphous material rapidly dissolves and starts to react with solid components (Curtis, 1980), micas begin to neomorphose to kandites (Fanning and Keramides, 1977), and feldspars begin to dissolve, precipitating vermiform kandites elsewhere, and releasing silica (Curtis and Spears, 1971; Huang, 1977; Berner and Holdren, 1979). Also, these reactions would occur in, and continue through, the reduction zones described above (Fig. 3.11).



Moreover, it should be emphasised that the contribution made to diagenesis by amorphous material is most significant immediately following deposition, at the time of greatest disequilibrium, with its environment (cf. van Elsborg, 1978). Pore-fluid saturation with respect alumina may result from tropical weathering alone, but is certainly supplemented during diagenesis by the dissolution reactions described above. In addition, although feldspar dissolution is invoked here as one mechanism which may contribute to kandite precipitation, it is not the only mechanism, nor, in fact, is it necessary! Both Almon and Davies (1979) and Odom et al. (1979), consider kaolinite

precipitation to be unrelated to the presence of feldspars. Moreover, tropical ground waters are typically saturated with respect to kandites (e.g. White et al, 1963; Tardy, 1971). Consequently, given suitable conditions of positive Eh, low pH, and low salinity (Moore, 1968; Bucke and Mankin, 1971) kandites will precipitate. These conditions are generally satisfied by freshwater flushing, maintaining a low pH, removing reaction products and preventing reduction of ferric iron and consequently chlorite formation (Velde, 1977). Textural evidence here suggests that vermiform kandites predate quartz overgrowths in these sediments. However, their pore-filling habit did not inhibit subsequent overgrowth nucleation.

I should like to digress briefly and expand on the interpretation of kandite timing on the basis of occurrence and morphology (see Fig. 3.12). Vermiform kandites are often associated with neomorphosed detrital muscovite, and always occur within intergranular pore space. Also, they are occasionally enclosed by carbonates. Blocky kandites, conversely, are irregularly distributed in primary and secondary pores, and whereas vermiform kandites generally occur singly, blocky kandites fill pore spaces completely with numerous short small aggregates of thick pseudo-hexagonal plates. Furthermore, each blocky aggregate is one pseudo-hexagonal plate in diameter, whereas the larger vermiform aggregates are several thin plates in diameter, stacked and interlocked in a complex, but perfectly ordered sequence. Both types are inferred to have precipitated directly from solution. However, their two alternative morphologies suggests differing mechanisms. I should like to propose that vermiform aggregates have formed from saturated solutions, either on a pre-existing nucleus - for example, a neomorphosed muscovite - or on one or two authigenic crystals. Subsequently, slow growth of these crystals, probably by diffusion, would be promoted by relatively low supersaturation of the solution. Alternatively, supersaturated, or highly supersaturated, solutions in pore spaces without a crystalline nucleus

would precipitate numerous seed crystals, each of which would subsequently act as a nucleus for the growth of an aggregate of pseudo-hexagonal plates. This is the inferred mechanism of formation of blocky kandites. This proposal is similar to the diffusion and flux controlled processes proposed by Hurst and Irwin (1982). However, conclusions reached here do not support their general model, because both morphologies occur in non-marine sandstones, whereas Hurst and Irwin (1982) imply during much of their discussion that vermiform aggregates occur in non-marine sandstones before quartz overgrowths, and blocky aggregates in marine sandstones after overgrowths. Moreover, Hurst and Irwin (1982) proposed that blocky aggregates have grown more slowly than their vermiform counterparts, a suggestion not borne out by theoretical considerations of precipitation from supersaturated solution (Berner, 1980).

It is important to note that vermiform kandites comprise only a small percentage of the kandite total, and consequently, an even smaller percentage of the whole rock. The two alternative forms are not a function of timing, depth or facies, they reflect purely pore geometry, and degree of saturation. In addition to textural criteria for rejecting a fresh water flux hypothesis for the majority of kandite formation (cf. Bjørlykke et al, 1979), stable isotope interpretation does not support simple dissolution of feldspar grains by fresh water at the earth's surface (see Chapter Six).

Previous research (Hemingway and Brindley, 1952; Smithson and Brown, 1954, 1957) has identified either pure dickite or a mixture of dickite and kaolinite as the only clay minerals present in Middle Jurassic sandstones from Yorkshire. Although their respective locality details are sparse, the samples containing solely dickite appear to come from (channel) sandstones in the Saltwick Formation (Smithson and Brown, 1957). In this study, unoriented XRD analysis has also identified either dickite or a mixture of the two kandite minerals. Nevertheless, analysis of those samples containing only blocky kandites has identified only dickite. I should like to suggest tentatively, therefore,

that the vermiform kandites identified here are kaolinite, and the blocky ones dickite. I should also like to point out that the inferred authigenesis of these two minerals differs too, and perhaps also confirms the suggestions of Hanson et al (1981) that dickite is the more stable polymorph: its formation from supersaturated solutions here contrasting the metastable "pedogenic" kaolinite. The difficulty of finding supportive data for such a theory is exemplified by reference to Sommer, whose "dickite" (1975) mysteriously neomorphosed into "dickite and kaolinite" (1978).

Where oxygenated conditions were not perpetuated by renewed freshwater flushing, chlorite rather than kandites formed. Here, acidic solutions would also have existed, and caused aluminosilicate dissolution, releasing alumina and silica into solution. However, following depletion of free oxygen, ferric iron was reduced and anoxic pore waters developed (Curtis, 1977). Consequently, alumina and silica, either in solution as weathering products from the source area, or as the result of soil processes on the floodplain, reacted and equilibrated with ferrous iron now in solution to precipitate chlorite (chamosite s.s.). Where more extensive chlorite pore linings occur, quartz overgrowths were inhibited. Elsewhere, however, where detrital grain surfaces remained exposed, small incipient overgrowths developed. Chlorite formed before quartz overgrowths. Predictions on the basis of thermodynamic equilibria, however, suggest that quartz precipitation should precede chlorite in a closed system (Almon and Davies, 1979). Consequently, I would suggest that quartz precipitation was inhibited during chlorite authigenesis, or a more open system existed and silica concentrations only reached suitable levels after chlorite precipitation. Chlorite precipitation at or near the earth's surface is certainly not problematical (Velde, 1977). It is also reported by Rodd (pers. comm. 1981) who describes pedogenic chlorite with isopachous rims in inferred phreatic zones and meniscus rosettes in inferred vadose zones of the water table from a Torridonian Fan in Scotland.



As mudrocks in the Ravenscar Group consist almost entirely of unstable aluminosilicates and comprise a large percentage of the sequence, the consequences of the diagenetic reactions described above are of considerable significance on the floodplain. When deposited initially, these muds probably contained 80-90% pore space, filled with waters saturated with weathering products from throughout the drainage basin. Following deposition, these pore fluids would have been modified by their interaction with the sediments they surround. Consequently, reaction products such as silica build up in solution. The sandbodies which these muds enclose were comprised almost entirely of quartz. Furthermore, cathodoluminescence observations indicate that the majority of the detrital grains are rounded. Thus, when deposited, these grains would have behaved as imperfect crystals, ideal nuclei for silica precipitation and growth of the quartz lattice into perfect euhedral overgrowths. Sites for silica precipitation and sources of silica would, therefore, have existed immediately following deposition, and especially after diagenetic modifications of detrital aluminosilicates. However, the sources were probably, initially, mostly in the muds, and the sinks within the sandbodies. In these circumstances a diffusion gradient would exist from the former to the latter (Domenico, 1977). Consequently, diffusion may have been an important process following deposition and before physical dewatering began to expel entrained pore waters from the muds. Although physical dewatering itself would also move solutions in the same direction, its effectiveness would be reduced once waters had been expelled. The result of these processes is that diagenetic reaction products in the sandbodies mirror and reflect those in the adjacent mudrocks. The differences which occur, however, are a function of differing mineralogy and texture. Sandbodies contain greater percentages of quartz and significantly fewer unstable components. Quartz overgrowths may, therefore, precipitate here from saturated solutions, whereas supersaturation is required for nucleation in the adjacent mudrocks (Berner, 1980).

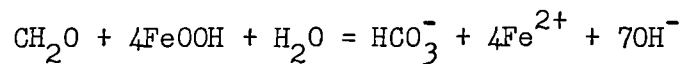
Similarly, differences in proportions of minerals within floodplain and channel sandstones reflect both their relative textural maturity and sandbody geometry. Diffusion and expulsion of silica from mud sequences led to thick quartz overgrowth cementation in crevasse-splay sandstones whilst channel sandstones which may, in fact, contain almost as much authigenic quartz are poorly cemented. This is partly a consequence of the poor sorting and finer grain size of the former, combined with lower primary porosity, and a considerably smaller free surface area on which to nucleate overgrowths. Channel deposits, however, are generally better sorted and, hence, presented a larger detrital quartz surface area to interstitial solutions, and so the resulting overgrowths are thinly distributed throughout the rock.

In addition, and perhaps more significantly, one should consider depositional sandbody geometry. Floodplain deposits, such as sheetflood, or crevasse-splay sands, occur generally as thin sheets. Channel sands, conversely, were deposited in long narrow tubes, with the exception of the meander-belt deposits which also have a sheet-like geometry. Consequently, the area of the interface between the sands and their enclosing muds differs, being considerably greater for sheets than channels (Fig. 13). Assuming that diffusion, for example, only operates for a finite distance, more mud should affect each unit volume of sand in the sheets than in the channels. Floodplain sandstones will, therefore, have been more intensely affected by diagenetic reactions in the enclosing muds.

The formation of quartz overgrowths during equilibration of depositional pore waters and sediments does not, therefore, present a problem, despite assertions elsewhere that quartz overgrowth cementation takes place above 60°C and after several kilometres of burial (e.g. Land and Dutton, 1978, 1979; Milliken et al., 1981); they have, after all, been observed in modern soils (Breese, 1960; Savin and Jackson, 1975; Taylor, 1978). In addition, Blatt (1979)

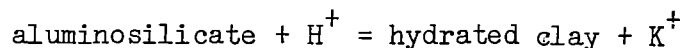
suggests that vertical rather than lateral movement of solutions through sandbodies is likely to result in extensive quartz cementation. Consequently, thick quartz overgrowth cementation is most likely to result from prolonged vertical connection to ground waters. These conclusions are borne out by this investigation, although even more localised controls such as depositional sandbody geometry are considered to be significant.

Following depletion of oxygen and generally acidic conditions, ferric iron reduction raised pH:



organic matter

This pH change is inferred to have caused a number of diagenetic modifications in these sediments. Traces of illite and potassium feldspar overgrowths occur throughout the sediments, the former in crevasse-splay sandstones especially. Whilst brackish influence may be invoked on the floodplain to explain illite formation in the absence of kaolinites or chlorite, it does not adequately explain potassium-feldspar overgrowths in sandstones which exhibit all the features of freshwater diagenesis described above. A possible explanation is that the potassium released during reactions under initially acidic conditions built up in solution to precipitate when pH increased. The initial diagenetic reactions described above involving feldspars and micas generally take the form



As well as initially lowering the pH of originally meteoric water by releasing bicarbonate ions, bacterial degradation of organic matter may have eventually raised the pH when iron oxides and sulphates were reduced. It is possible that at the resulting elevated pH, potassium in solution precipitated, either as overgrowths on feldspars, or as authigenic illite. These alternative potassium sinks would reflect relative concentrations of silica at the time, as well as the availability of detrital nuclei.

The onset of anoxic reducing conditions in sandbodies throughout the water table may be inferred at different stages of diagenesis from the type and distribution of ferrous minerals present. However, concentrations of sulphate ions are not generally found in fresh water (Berner, 1971). Consequently, where pyrite occurs, it probably records the introduction and rapid reduction of sulphate ions, either from elsewhere, such as during flooding at high tide, or perhaps locally from degraded organic matter. Indeed, pyrite is most frequently observed replacing plant debris. With the exception of the ring of pyrite within the siderite spheruliths, interpreted as the result of a flooding event, pyrite preceded siderite cementation. According to Froelich et al, (1979), iron reduction should precede sulphate, and so siderite ought to precede pyrite. However, iron carbonate is not stable in the presence of sulphate ions because pyrite formation is thermodynamically preferable to siderite formation (Berner, 1971). Consequently ferrous iron reduced sulphate ions and precipitated pyrite until the sulphate was effectively removed and siderite precipitation became possible.

Chlorite formation records inferred reducing conditions throughout diagenesis of some sediments, whilst in others oxygenated conditions persisted throughout kaolinite precipitation. Siderite cementation which followed both clays and quartz overgrowths in the sandbodies marks not only the onset of reducing conditions where it preceded kaolinites, but also the ubiquitous build up of bicarbonate ions in solution. Sideritic soil horizons are the exotic record of stagnating surface waters on the poorly drained floodplain.

This is the basis of the inferred threefold division of the water table during initial diagenetic reactions. In those areas of the floodplain nearest to the source of oxygenated waters, that is, the levees adjacent to the distributary systems, and in the sandbody conduits beneath, oxygenated pore waters persisted. Here, only aerobic bacterial processes operated, lowering

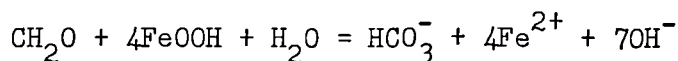
pH and precipitating kandites and quartz overgrowths. In more distal sandbodies, however, unaffected by replenished fresh water, bacterial processes continued and ferrous iron combined with aluminosilicates to precipitate chlorite. Chlorite is interpreted as wholly authigenic, rather than neomorphosing pre-existing kandites, because of its pore-lining habit as single plates, whereas vermiform kandites occur as a pore filling. On the surface of the floodplain, but also away from renewed oxygenated fresh water bacterial processes continued unabated until bicarbonate concentrations built up and siderite soils developed (see Fig. 3.14).

This threefold division incorporates portions of existing models for surface diagenesis. For example, Elliott(1968) described siderite soil spheruliths developed on Coal Measure floodplains, whilst levees adjacent to the distributaries were well drained and contained rhombic siderite. Similarly, the concept of fresh water flushing through crevasse-splay sandstones, cementing them with overgrowths and enriching the muds beneath with kandites, is analogous to the models discussed by Hemingway (1968) and Moore (1968) beneath coals, and Staub and Cohen (1977) beneath peat. It is also a wetter version of the tropical silcrete model proposed by Wopfner (1978) (Fig. 3.15).

Smithson (1942) culminated several decades of research in Yorkshire by reviewing the distribution and diagenesis of heavy minerals in the Middle Jurassic. He concluded that during diagenesis heavy minerals underwent a variety of processes including: dissolution of relatively unstable phases; dissolution and reprecipitation of high- as low-temperature polymorphs; and precipitation of overgrowths. As this study has not concentrated on heavy minerals specifically, comment on this previous work can only be made in passing. All the phenomena observed by Smithson (1942) have been observed in this study, that is, dissolution of heavy and opaque mineral grains, authigenesis of brookite and anatase, and occasional tourmaline overgrowths.

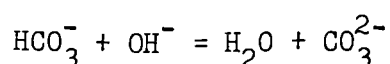
In spite of this, the interpretations made in this study do not agree with those made previously. Firstly, the absence of certain heavy minerals from the eastern half of the outcrop does not necessarily support a model for their preferential dissolution here. Secondly, these processes are inferred to operate immediately following deposition and during eogenesis, rather than during deep burial.

Siderite marks the onset of reducing conditions and the build up of bi-carbonate ions in solution throughout the water table. Although soil horizons record bacterial production of bicarbonates in a suboxic zone, the subsequent siderite cement formed from fresh water. Detailed interpretation of this siderite cementation, its timing and growth, is discussed in Chapter Six. Whilst the soil spheruliths may have precipitated at a pH as low as 5 (Fitzpatrick, 1980) widespread ferric iron reduction would have increased pH, and consequently allowed ubiquitous carbonate cementation from alkaline carbonate saturated solutions, for example:

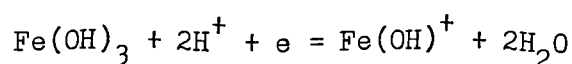


organic matter

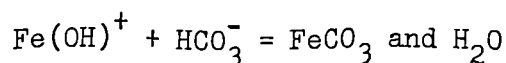
and



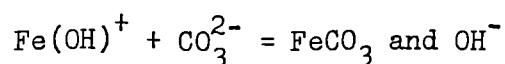
or



and



or



Siderite probably precipitated as a result of these equilibria where reducing conditions were maintained. In some sediments non-ferroan calcite encloses spheruliths suggesting that renewed freshwater precipitation is also supported

by stable isotope analysis.

Where the sediments were not effectively lithified by this stage, ferroan calcite cementation took place. It is difficult to establish whether or not this paragenetic sequence of siderite to ferroan calcite can be explained in terms of simple pore-fluid evolution, or whether a change of pore waters is required. Fresh water is not normally saturated with respect to calcium carbonate (Berner, 1971) and there is no reason to suggest that Jurassic fresh water was saturated either. Nonetheless, calcium occurs in fresh water today, and some was also present during the Jurassic: hence one finds calcium carbonate in bivalve shells such as Unio, for example (Hemingway, 1974), and comprising up to 30% of the invariably non-stoichiometrical siderite. Siderite itself precipitates from solutions in which the  $\text{Ca}^{2+}:\text{Fe}^{2+}$  ratio is less than 20:1. As iron is preferentially removed, this ratio is increased and calcite precipitation is subsequently favoured (Berner, 1971). It follows that if the original solutions contained enough calcium to precipitate the eventual calcite cement, pH must have been low prior to ferric iron reduction in order to prevent calcite precipitation before siderite. Although most of the inferred diagenetic reactions preceding carbonate precipitation require a low pH, and pH is only generally raised by ferric iron reduction itself, this is perhaps too tenuous an argument on which to base an inference of pore-water evolution. This diagenetic sequence, therefore, appears to require a marked change of pore-fluid composition and, consequently, passed from eogenetic to mesogenetic processes.

Stable isotope analysis was, therefore, undertaken to determine the possibility of a change in pore-water composition. The results (Chapter Six) do, in fact, confirm that this paragenetic sequence required a change of pore waters. Siderite is, therefore, the last major phase which can be explained by attempted equilibration of the sediments with their depositional pore waters, whilst

ferroan calcite is the first which cannot. Although the depositional pore waters of these non-marine sediments were oxygenated, the subsequent anoxic phases can be defined as eogenetic. The removal of oxygen was a consequence of bacterial processes operating on organic matter, and unrelated to the depositional environment. However, as confirmed by SI, fresh water continued to pass through the sediments and eventually precipitated siderite. Furthermore, this process was a consequence of equilibration of the sediments with their environment. Diagenetic reactions and authigenic phases culminating in non-ferroan calcite and rhombic siderite cementation are therefore interpreted as eogenetic, and related to the regime at the surface. These processes are summarised in Fig. 3.16.

Mesogenesis is the diagenetic realm which is not influenced by the regime at the surface. Ferroan calcite in these non-marine sediments is therefore mesogenetic, and precipitated from either basinal fluids, or formation waters. These waters circulated through the strata after their effective sealing from the regime at the surface. Although stable isotope analysis allows a quantitative interpretation of the change from eogenesis to mesogenesis, it does not allow a realistic estimate of the temperature or depth of burial at which the change takes place. However, the depths involved were certainly not great: Middle Jurassic sediments were not buried to more than 1.5 km before being structurally inverted during the Upper Jurassic and perhaps partially exposed in the Cretaceous.

Calcite remains in a few samples only. Moreover, complete cementation by either calcite or siderite also occurs in a few samples only. However, numerous features suggest that carbonate cementation was more widespread previously. In those samples where carbonate cements remain, detrital and earlier authigenic phases are frequently replaced. However, carbonate replacement is concentrated on certain selective points, those according to



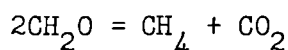
Hurst (1981) with the greatest free-surface energy (see Plate 3.14C). In those samples where carbonates are absent, their presence and subsequent removal is inferred, and porosity interpreted as secondary. Here quartz overgrowths display the same pitting and corrosion as seen where carbonates remain and replace them. These pits and notches are, therefore, interpreted here as being the result of subsequent removal of these replacive carbonates. This process of quartz replacement by carbonates presumably took place along a thin film, rather than by dissolution and subsequent carbonate infilling. The latter process would require a pH in excess of 9 above which wholesale dissolution would occur (Blatt, 1966). Thin-film dissolution operates selectively as a consequence of the solution-film chemistry; however its effects are controlled by the crystallography of the dissolving phase (Berner and Holdren, 1979). This replacement-dissolution process created small "v" shaped etch pits which subsequently coalesced into larger, irregular pits, eventually rendering the substrate crystal surface unrecognisable (see Plates 3.1B, 3.3B, C, D and G, for example).

Feldspar grains also suffered extensive replacement by carbonates. This replacement further complicated the possible diagenetic evolution of feldspar grains in these sediments, summarised in Fig. 3.17. Control on these processes is obscure, however. All the extant feldspars analysed, irrespective of the degree of grain dissolution or replacement, are stoichiometric potassium or sodium feldspars. Moreover, some grains of each phase are completely fresh, or fresh with overgrowths. They did not, therefore, all spontaneously begin to dissolve on deposition, to be reprecipitated as feldspar overgrowths (cf. Heald and Baker, 1977).

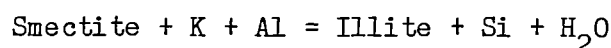
### Ubiquitous Mesogenetic Changes

Ferroan calcite cementation is mesogenetic in these non-marine sediments, but eogenetic in the marine sediments. However, all the subsequent events in the non-marine clastics may also be recognised in the marine ones, and they are, therefore, ubiquitous. These processes may be subdivided into the major event of secondary porosity creation and blocky kandite precipitation, and minor modifications in the remaining solid assemblage during the subsequent passage of formation waters.

Blocky kandites are interpreted here as filling secondary porosity, following the dissolution of extensive and replacive carbonate cements. The simplest model to explain all these processes involves the creation and action of aggressive fluids (Curtis, pers. comm. 1982). During burial, bacterial processes continued, liberating methane and carbon dioxide (Curtis, 1980):



Concomitantly, smectites slowly converted to illites with increasing temperature (Boles and Franks, 1979a). The basic reaction



according to Boles and Franks (1979a) liberates 24 moles of silica for each 1.57 moles of smectite. This reaction proceeds above 60-70°C when aluminous smectites are destroyed and illites created. It is significant that this reaction also requires potassium, probably derived from dissolution of either fine-grained feldspar or muscovite (Hower et al., 1976). Consequently, further alumina and silica are released. Whilst the former may be incorporated into the illite, the latter is released. As a result of these processes, "aggressive solutions" containing carbon dioxide, alumina and silica are created at depth. These solutions are termed "aggressive" because of their low pH and reactivity with respect to carbonate cements (Curtis, pers. comm. 1982).

The effect of such a fluid migrating from its source, an organic-rich mudrock, into a carbonate cemented sandstone would be profound. All the resulting features that one would expect are observed in the Ravenscar Group and so this explanation is preferred to alternatives such as structural inversion and the introduction of meteoric water (cf. Hancock and Taylor, 1978; Sommer, 1978). As this hypothetical solution migrated into the carbonate cemented sandbodies, it began to dissolve the cements. Consequently, as the two moved towards equilibrium, pH rose, and the solution entered the field of kandite (dickite?) stability. The result was extensive precipitation of seed crystals and subsequently the growth of dense blocky kandites from these supersaturated solutions. Removal of carbonates revealed quartz overgrowths with distinctive etchings where they had been replaced by the carbonates..

Etch or corrosion features similar to those observed here have been widely recorded in the past, although their interpretation has not always been consistent. Identical pits are observed here on grains and overgrowths from which carbonate cements have been artificially removed. Similar features have been recorded by Friedman et al, (1976) after an equivalent process - removal of calcite cements. They describe "v" shaped notches which coalesce into larger depressions and eventually form "spongy" surfaces. Whilst some of the features observed in this study are similar, others are not, especially those associated with siderite (e.g. Plate 3.3A to D). The dissolving phase should control the size, shape, and distribution of corrosion or dissolution features: they are a function of its crystallography (Berner, 1980). However, the dissolving phase in all these instances is quartz and any variations appear to be related to the replacing phases - carbonates.

The final feature I should like to discuss, and which I should like to relate to aggressive fluids, is the intergrowth texture of blocky kandites and

quartz seen in Plate 3.5A. Two alternative explanations of this texture are available. Either quartz enclosed pre-existing kandites, or kandites grew and replaced quartz. The latter explanation is preferred by Sommer (1978), and Ireland (pers. comm. 1980) and described as "etching" of quartz. However, CL analysis during this study revealed two phases of quartz overgrowth formation and, moreover, SEM examination revealed stepped euhedral overgrowth surfaces which may be evidence of different phases of overgrowth development. I suggest that, following kandite precipitation, excess silica remained in solution and precipitated locally as a second phase of quartz overgrowth, partially enclosing the kandites. In addition, as pore-filling kandites are widely reported in the literature, their formation would not appear to require or imply the need for a substrate on which to nucleate, or a further source of silica. After all, kandites occur in limestones (e.g. Dickson and Coleman, 1980). Furthermore, dissolution of a euhedral quartz overgrowth face requires energy. There would be little benefit in expending the free energy remaining in solution after precipitation of seed crystals on dissolution of quartz. Finally, although not allowing a precise estimate of its timing, SI analysis (Chapter Six) excludes the possibility of blocky kandite precipitation under surface conditions.

Mesogenetic processes, although unrelated to surface conditions or the depositional environment, were affected by the original depositional sandbody geometry, and consequently, the environment. The distribution of secondary porosity, carbonate dissolution features, and blocky kandites was, in general, facies controlled. Large, connected sandbodies such as the channel sandstone complex at Whitby, or the Moor Grit Member were porous and now contain significant quantities of blocky kandites. Smaller, isolated channel sandstones, or, more especially, crevasse-splay sandstones, were more tightly cemented, generally less porous and do not now contain appreciable quantities of blocky kandites. This is a result of the connectivity of these sandbodies, a function

of their original alluvial architecture (Leeder, 1978; Bridges and Leeder, 1979). The larger sandbodies served as conduits during burial but smaller and isolated sandbodies did not.

It is possible that the source of these fluids was extremely localised, that is, the enclosing mudrocks themselves. Alternatively, aggressive fluids may have migrated into these sands from mudrocks elsewhere within the hydrological system operating within this basin during burial.

Cooper (pers. comm. 1980) reports palaeoburial temperatures of no more than 90°C with a maximum around Rosedale. However, discrete smectites, which should not persist beyond 70°C (Boles and Franks, 1979a) occur in sandstones in the Long Nab Member. These smectites were only detected by XRD, and their relative timing is therefore unknown. As they cannot have formed, theoretically, before burial and heating to 90°C, it is logical to assume that they formed following the final structural inversion of the basin, perhaps from formation waters. Within the mudrock sequences, however, throughout the basin and irrespective of stratigraphical position, discrete smectite does not occur. These mudrocks consist of kandites and micas with up to 10% irregularly interstratified smectite, as well as occasional traces of chlorite.

In some samples no interstratified mica/smectite was detected. This, however, is not conclusive evidence that no interstratification occurs, since these samples may contain up to 10% interstratified smectite which would not be detected here (Reynolds, 1980). Furthermore, where a discrete interstratified clay including 20% smectite does occur, the 27Å superstructure characteristic of regular or ordered interstratification is only poorly developed, if at all. Unfortunately, a direct comparison of these data with previous work cannot be justified. Hower et al., (1976), Boles and Franks (1979a) and others have studied separate sequences of the same stratigraphical horizon

with different burial history, but only one such sequence has been studied here. Nevertheless, one general conclusion can be made. These data correspond to the inflexion point on graphs of depth versus percentage-illite layers from previous studies (Hower et al, 1976; Boles and Franks, 1979a; Pearson et al, in press) at which illite comprises 80% of the clay mineral. This point occurs in the transitional zone from a random interstratification to an ordered structure (Fig. 3.18). Therefore, between the onset of illitisation at about 60°C and maximum palaeoburial temperatures, illitisation of illite/smectite may have taken place (Boles and Franks, 1979a). I would suggest that this initial illitisation, the first stage of the two stage process - destruction of aluminous smectites - liberated the silica alumina and water involved in the aggressive fluids. The carbon dioxide source could also have been the enclosing muds, currently marginally mature (Cooper, pers. comm. 1980), or the underlying Liassic, which has generated oil (Hemingway, 1974).

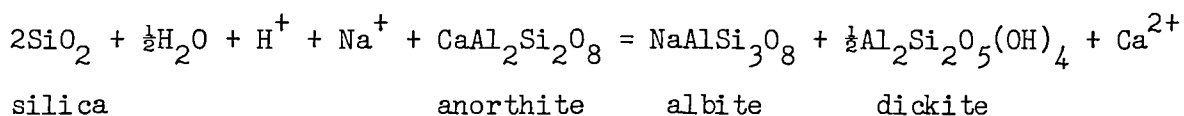
Hydrocarbon maturation also could have caused the localised and interesting, but quantitatively insignificant, iron sulphides which coat quartz overgrowths in places. Iron sulphide formation within hydrocarbon reservoirs results from either of two processes. These are the reaction of ferrous or ferric iron with H<sub>2</sub>S in gases, and reduction of sulphate ions by bacteria in water zones beneath anoxic oil-bearing sands, and their subsequent reaction with iron compounds (Evans et al, 1971). I am unaware of any alternative methods of generating sulphate and iron reducing conditions in diagenetically mature sediments at depth (see Chapter Four).

Other than outcrop weathering, the general timing and perhaps the origins of the remaining diagenetic modifications are obscure. Minor illitisation of both blocky and vermiform kandites occur. It is not clear whether this process involved neomorphism of kandites into illite, or whether illite merely nucleated on the kandites (see Plate 3.2D and 3.5B). As discussed by

Harder (1974), solutions capable of precipitating illite are saline, but not supersaturated with silica, and resemble sea water. As formation waters are often saline (White, 1965), illitisation could have taken place at any time during Tertiary burial. However, the possibility of precipitation from potassic solutions generated in situ, when aggressive solutions entered the sandbodies and perhaps dissolved feldspars, cannot be ruled out.

Barytes was observed as euhedral pore-filling crystals in one or two samples. It, presumably, also precipitated from formation waters during burial. Barytes saturated pore fluids are quite common in formation waters today (White, 1965; Sawkins, 1966; Collins, 1975), and may be directly related to hydrocarbon migration.

Although all the feldspars analysed in these sediments are either pure potassium or sodium end members, it is not clear whether this is due to the composition of the source area, or diagenetic processes. Or to rephrase the question, has albitisation of plagioclase feldspars taken place in these sediments? Neither EDS nor microprobe analysis detected any calcic plagioclase, irrespective of depositional environment. Albitisation is the process whereby calcic plagioclase reacts with saline formation waters and converts to albite, precipitating dickite and calcite (Boles, 1982):



According to Boles (1982), this process takes place in dilute solutions, under-saturated with respect to clays and at 110 to 120°C, although it can take place at lower temperatures in older rocks where different rate controlling processes operate (Boles, pers. comm. 1982). Whilst wholly authigenic sodium-feldspar overgrowths occur frequently here, they are not related to the same hypothetical process and may have formed at lower temperatures, but probably from formation waters during burial rather than during eogenesis. Despite

the purely sodic nature of the plagioclase here, albitisation has probably not taken place. The albite observed here does not contain the inclusions or wide pseudo-calcic lamellae that one finds as a result of albitisation (Boles, 1982). Moreover, these sediments contain no late stage calcite, replacing or intergrown with the sodiumfeldspar. This suggests that the original source was either plutonic or perhaps metamorphic but not volcanic (Boles, pers. comm. 1982).

#### Telogenesis - Recent Weathering

The vermiculite identified in marine and non-marine sediments in this study is an extremely iron-rich phase, containing on the basis of EDS, Si, Al, Fe and K. This mineral contains little or no sodium, magnesium, or calcium. Rather than invoking a further division of the water table during shallow subsurface diagenesis to explain vermiculite as a wholly authigenic precipitate here, I should like to suggest that it has formed by alteration of originally authigenic chlorite. This reaction may have taken place during burial involving potassium from formation waters. An alternative is that Recent weathering has effected this same process, an explanation which has been invoked to explain the occurrence of a similar potassium vermiculite elsewhere (Curtis, pers. comm. 1982). Either process would affect authigenic chlorite from both marine and non-marine sediments. The situation is further and unnecessarily confused if one attempts to explain vermiculite formation by differing mechanisms with respect to depositional environment. There is, however, neither overwhelming textural evidence, nor a theoretical basis for arguing any particular case convincingly, and so the origin of vermiculite in these sediments remains conjectural. Additional support for a weathering origin for this "vermiculite" may be found in recently weathered chlorites, neomorphosed to interstratified chlorite-vermiculite, whose behaviour during XRD analysis is similar to the vermiculite identified here (Nishiyama et al, 1978; see Appendix B).



Oxidation of siderite to goethite could have taken place at any time during burial, with the introduction of oxygenated pore fluids: it is not unknown in subsurface sediments (e.g. Hallett, 1981). However, it is assumed that siderite has been oxidised at outcrop during Recent weathering, as this would be the simplest explanation of the consistent combination of oxidised surface samples, with fresh siderite some 5-10 cm from the surface. In addition to oxidising siderite, Recent weathering may have been responsible for enhancing porosity, for example, further feldspar dissolution, or further carbonate dissolution, cannot be excluded.

### CONCLUSIONS

"How often have I said to you, that when you have eliminated the impossible, that whatever remains, however improbable, must be the truth?"

Sherlock Holmes  
(Sir Arthur Conan Doyle)

I should like to summarise briefly some of the more pertinent points brought out by the preceding discussion. "What controls diagenesis?" In general, although the results reported in this chapter may be interpreted to show diagenetic variations between environments, the environment itself cannot be isolated as a unique control on diagenesis.

Eogenetic modifications result from the attempted equilibration of depositional pore waters and detrital sediments. Here they were affected by the silica, alumina, and iron-rich pore waters; the subarkosic mineralogy of the sediments; the texture of sandbodies throughout the delta; the quantities of organic matter present in the sediments; and finally, the generally hot and wet climate which maintained a high water table.

On the floodplains, bacterial degradation of organic matter rapidly lowered

the pH of pore waters. As a result, amorphous silica and alumina, as well as detrital feldspar grains, began to dissolve. Additionally, muscovites neomorphosed to kandites. Where fresh water was continuously supplied to the sediments, Eh remained positive and vermiform kandites (kaolinite) precipitated. Elsewhere in the sediments, continued bacterial degradation of organic matter depleted oxygen and reduced ferric iron, as a result of which chlorite was formed. Similarly, stagnation on the surface led to the formation of siderite soils, as well as the growth of concretions in the muds below. Silica, both from solution and from the reactions proceeding in situ, then formed quartz overgrowths. Some of the least mature overbank sandstones were effectively cemented at this stage by silica released from the surrounding muds.

As bacterial processes continued ferric iron reduction raised pH and increased bicarbonate concentrations in solution. During this increase in pH, potassium precipitated locally in illite within immature sands, and in potassium-feldspar overgrowths. Subsequently, rhombic siderite cemented all the remaining porosity in overbank sandstones and most of the channels. Widespread ferroan calcite cementation took place later, but from formation waters introduced into the remaining porosity during burial.

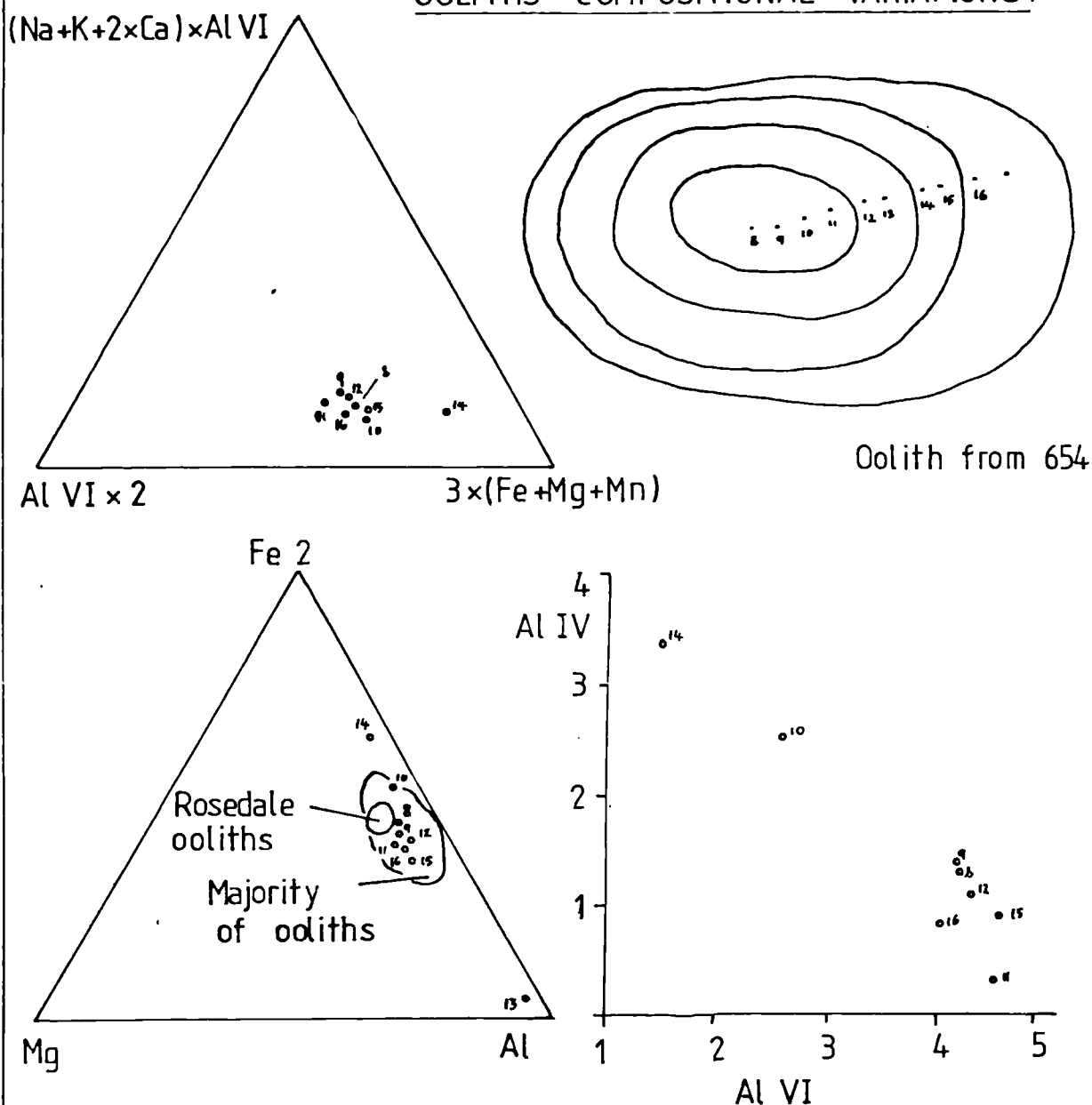
In the marine clastic sediments, the initial authigenic phases precipitated directly from interstitial waters. Thus, sandstones contain illite and are cemented with potassium-feldspar overgrowths. As bacterial degradation of organic matter commenced, the pH was then lowered and minor vermiform kandites, kandite neomorphism of muscovite and quartz overgrowths resulted. Finally, as bicarbonate concentration built up, ferroan calcite precipitated. In places this final eogenetic marine cement was replaced by siderite as the delta prograded above. I should like to emphasise this last point because freshwater siderite replacement of the last marine cement constrains formation

of all the earlier phases to a position at or near the earth's surface.

During burial the remaining diagenetic modifications of these sediments took place in the larger and connected sandbodies only. Aggressive fluids migrated into this sedimentary packet and both dissolved carbonate cements and precipitated blocky kaolinites in the resulting secondary porosity. Excess silica in solution at this time may have formed the second phase of quartz overgrowths observed in some samples.

Surface weathering has effected the most recent diagenetic modifications by oxidising siderite and pyrite, and possibly dissolving some carbonates and aluminosilicates. Recent weathering may also have neomorphosed chlorite to vermiculite or a mixed-layer chlorite /vermiculite.

FIG. 3.1 ELECTRON MICROPROBE ANALYSIS OF BERTHIERINE OOLITHS - COMPOSITIONAL VARIATIONS.

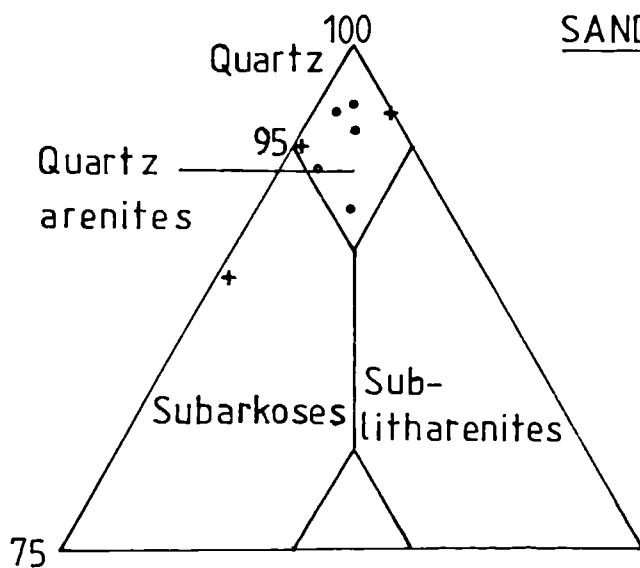


Data from appendix D

Sample	654	654	654	654	654	654	654	654	654
Code	665	665	665	665	665	665	665	665	665
Spot	8	9	10	11	12	13	14	15	16
SiO <sub>2</sub>	23.81	25.09	14.09	35.66	27.07	25.75	14.45	25.82	16.61
TiO <sub>2</sub>	n.d.	n.d.	0.21	n.d.	n.d.	0.20	n.d.	0.19	n.d.
Al <sub>2</sub> O <sub>3</sub>	16.48	17.39	11.28	19.23	18.55	17.34	12.51	16.90	9.47
FeO	21.00	22.40	20.15	21.93	22.27	17.34	36.53	17.75	10.37
MgO	2.13	2.18	1.24	2.57	2.46	1.61	1.47	1.98	1.16
MnO	n.d.	n.d.	3.12	n.d.	n.d.	n.d.	n.d.	n.d.	n.d.
CaO	0.48	0.45	0.62	0.35	0.48	0.23	0.40	0.33	2.50
Na <sub>2</sub> O	0.68	0.85	1.09	0.69	0.97	0.67	0.50	0.80	1.16
K <sub>2</sub> O	0.73	0.48	0.62	0.97	0.59	1.16	0.82	0.74	0.57
TOTAL	65.32	68.83	52.41	81.40	72.39	64.30	66.69	64.53	41.83

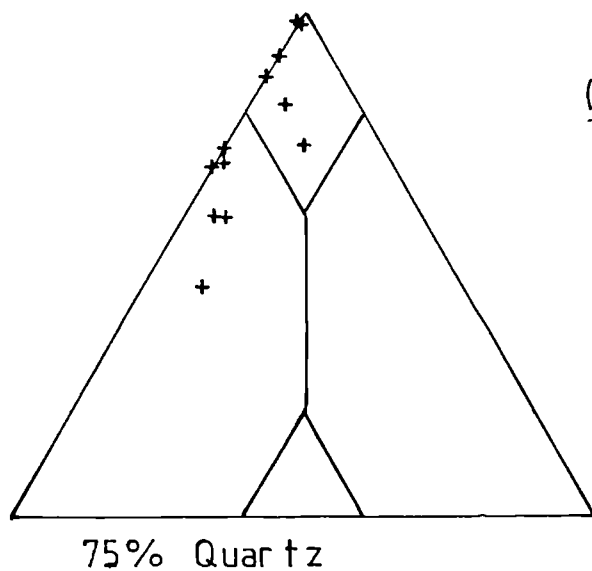
There are no uniform compositional variations across this, typical, berthierine oolith

FIG 3.2 FRAMEWORK MINERAL COMPOSITION AND SANDSTONE CLASSIFICATION



(a) Dogger Formation

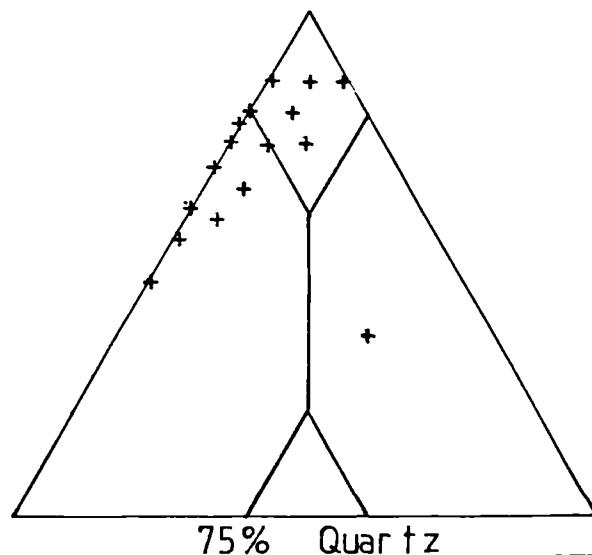
- + Beach sandstones
- Shallow marine sandstones.



(b) and (c)

Sandwick Formation

Channel sandstones



Overbank sandstones

FIG 3.3 REPRESENTATIVE EDS TRACES FROM THE SALTWICK FORMATION

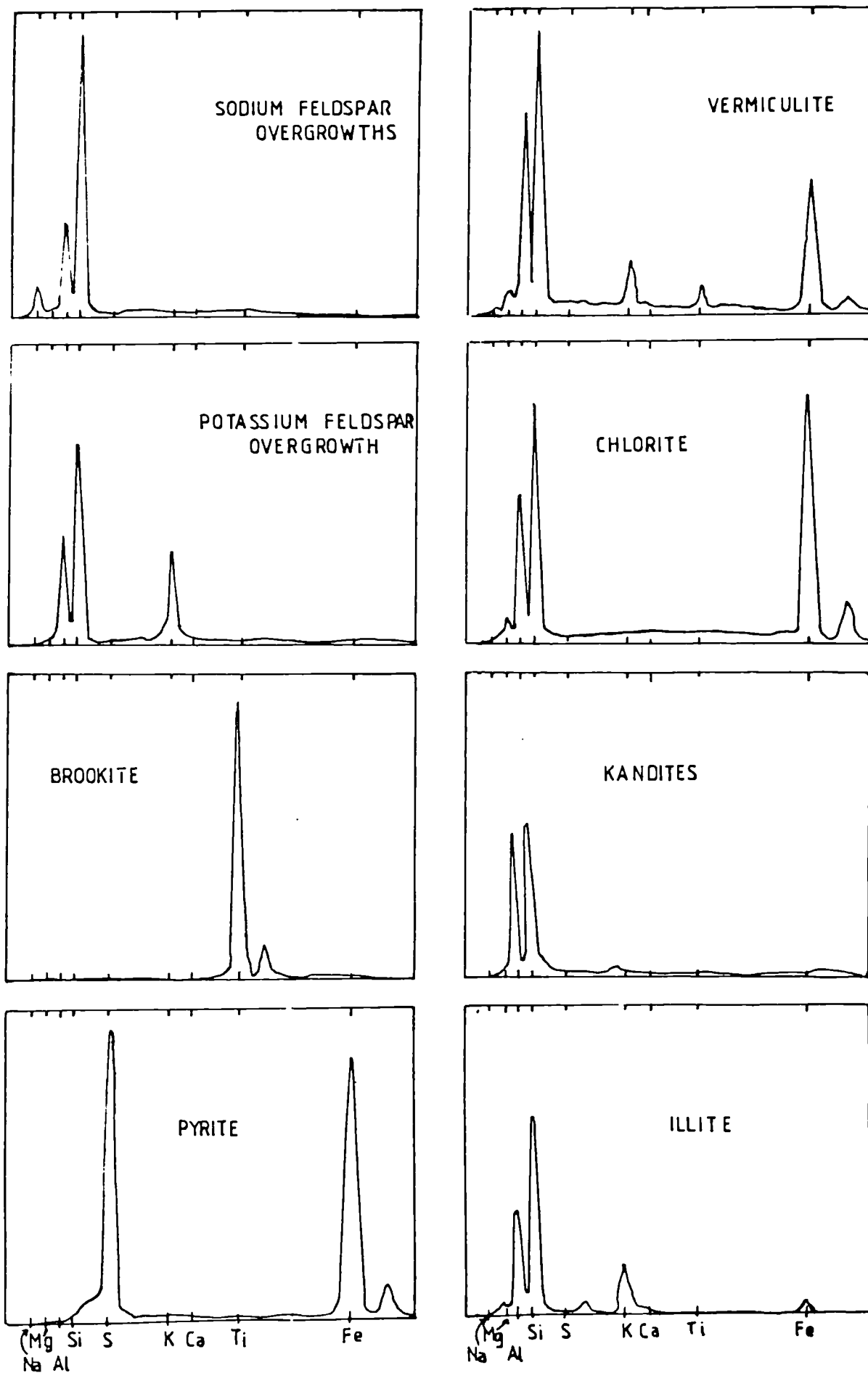
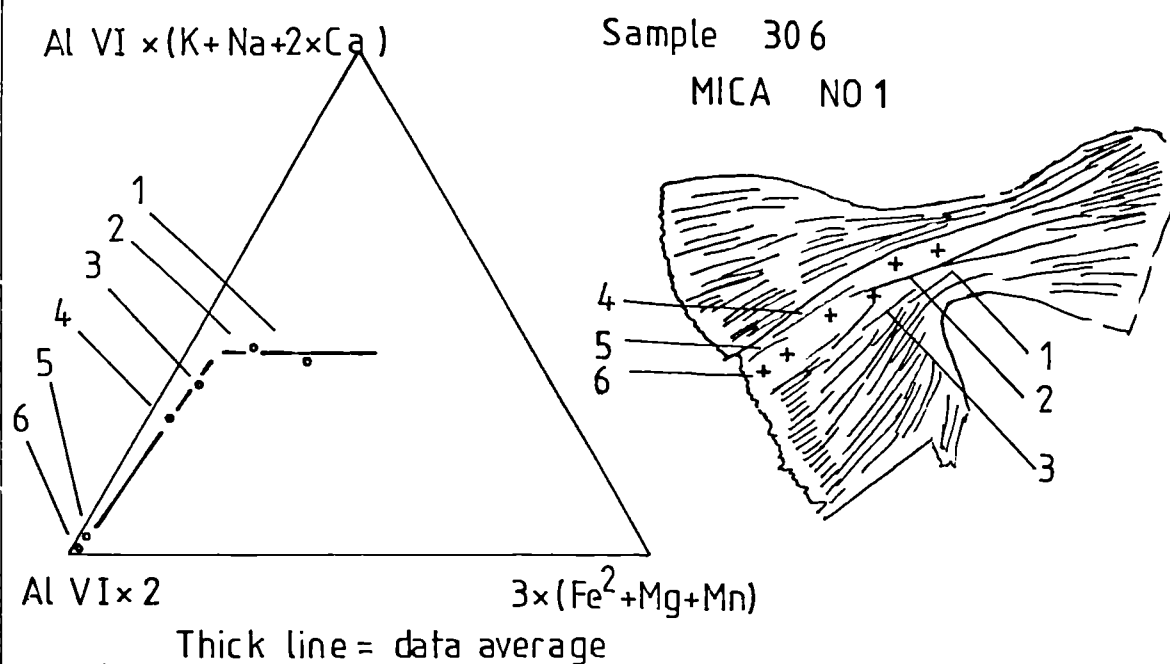


FIG. 3.4 NEOMORPHISM OF MICAS TO KANDITES

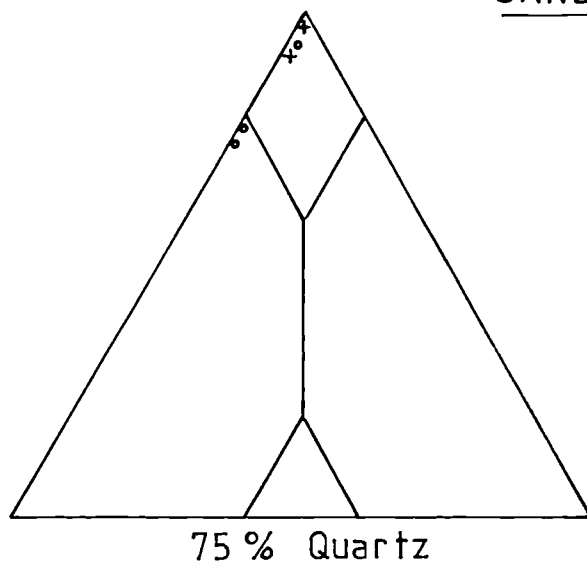


Sample	306	306	306	306	306	306
Code	N01	N01	N01	N01	N01	N01
Spot	1	2	3	4	5	6
SiO <sub>2</sub>	39.61	37.86	39.80	37.24	39.23	38.29
TiO <sub>2</sub>	0.32	0.28	0.36	n.d.	n.d.	n.d.
Al <sub>2</sub> O <sub>3</sub>	26.95	27.32	28.14	24.77	31.99	31.42
FeO	1.51	1.22	1.58	1.47	0.27	n.d.
MgO	1.13	0.79	0.98	0.88	n.d.	n.d.
MnO	n.d.	n.d.	n.d.	n.d.	n.d.	n.d.
CaO	n.d.	n.d.	n.d.	n.d.	n.d.	n.d.
Na <sub>2</sub> O	0.71	0.69	0.73	0.36	n.d.	n.d.
K <sub>2</sub> O	8.04	5.19	7.72	6.50	0.18	n.d.
TOTAL	78.27	73.35	79.33	71.23	71.67	69.71

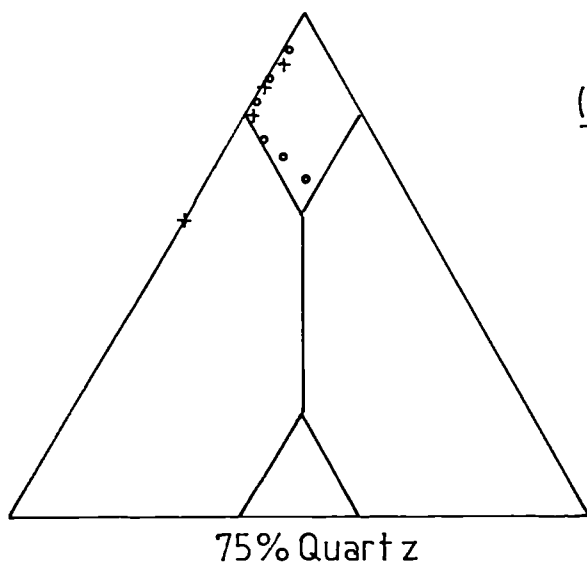
The data and recalculations upon which this figure is based are compiled in appendix D.

Compositional variations in neomorphosing muscovites show a two stage transformation. Firstly, ferromagnesian are released, and secondly, potassium is lost as the "mica" becomes a "kandite".

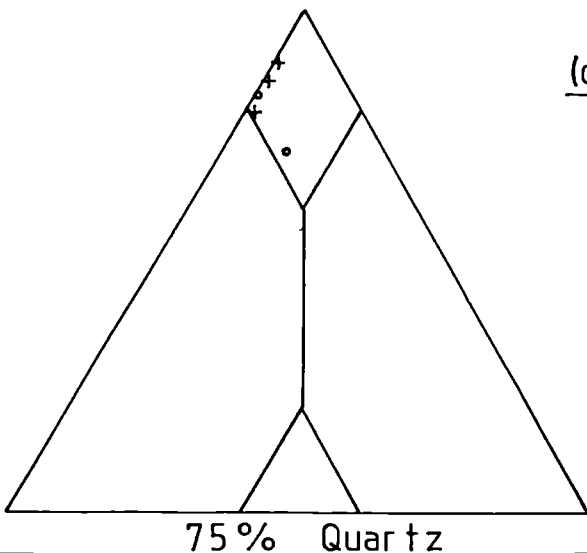
FIG 3.5 FRAMEWORK MINERAL COMPOSITION AND  
SANDSTONE CLASSIFICATION



- (a) Yons Nab Member
- + Tidal channel sandstone
  - Bay filling sandstones



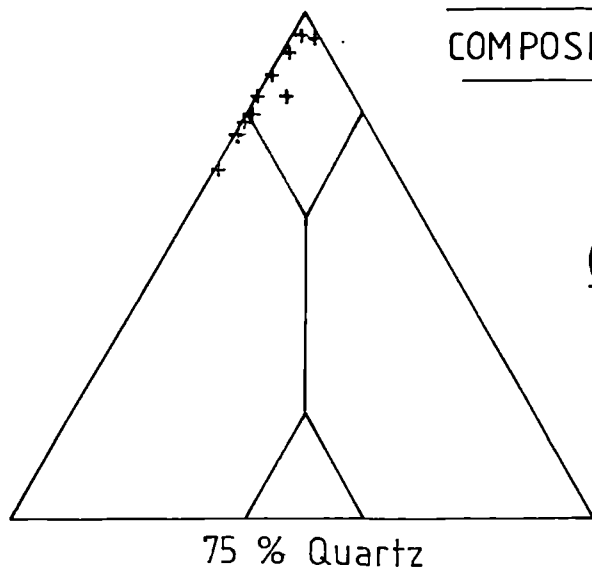
- (b) Gristhorpe Member
- Overbank sandstones
  - + Channel sandstones



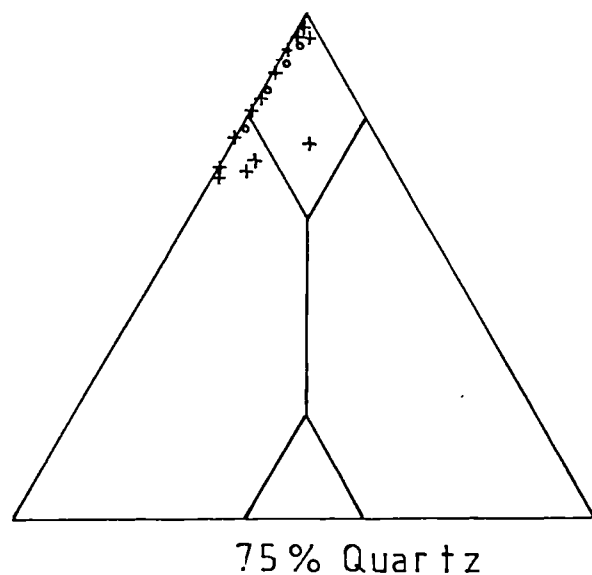
- (c) Scarborough Formation
- + Tidal sheet sandstone
  - Beach sandstone



FIG 3.6 FRAMEWORK MINERAL COMPOSITION, SANDSTONE CLASSIFICATION AND CLAY MINERAL COMPOSITION: SCALBY FORMATION



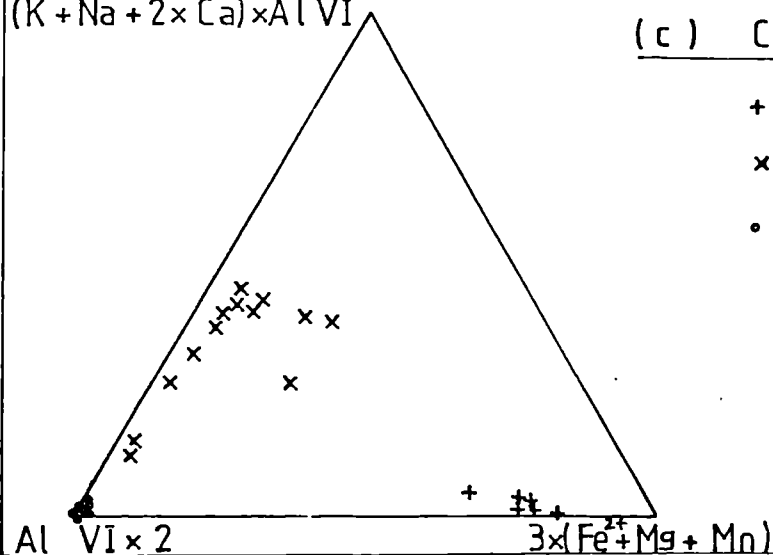
(a) Moor Grit Member



(b) Long Nab Member

- + Channel sandstones
- Overbank sandstones

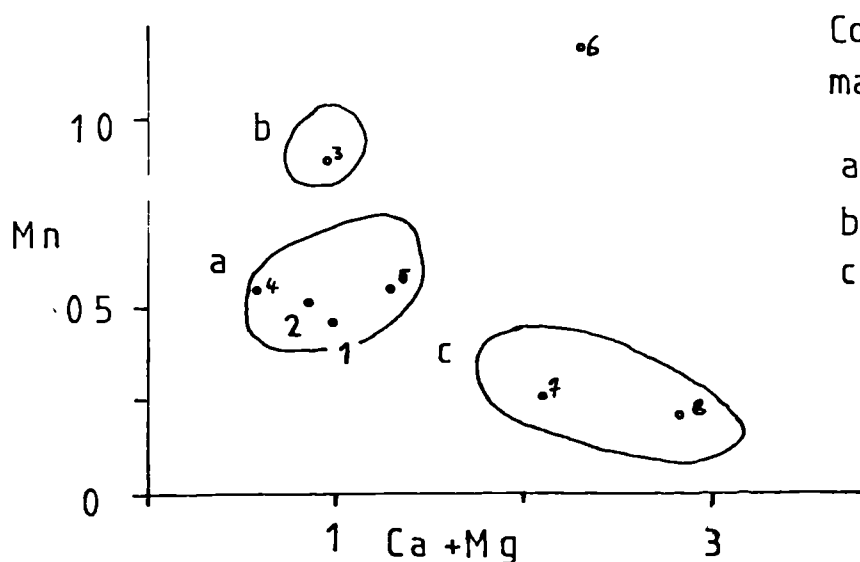
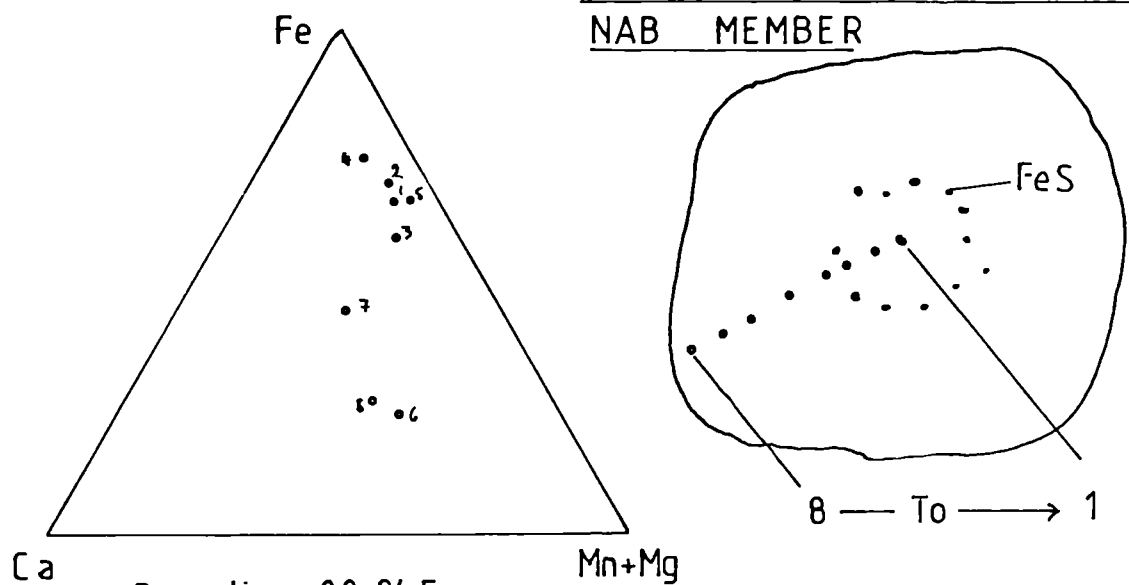
$(K + Na + 2 \times Ca) \times Al \ VI$



(c) Clay mineral composition

- + Chlorite
- x Neomorphosed micas
- Kandites

FIG 3.7 COMPOSITIONAL VARIATIONS IN SIDERITE  
SPHERULITHS FROM THE LONG  
NAB MEMBER



Composition of  
majority of analyses

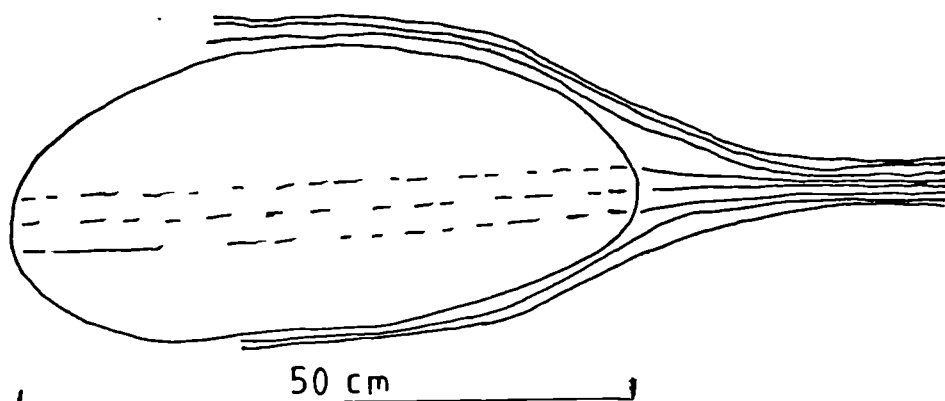
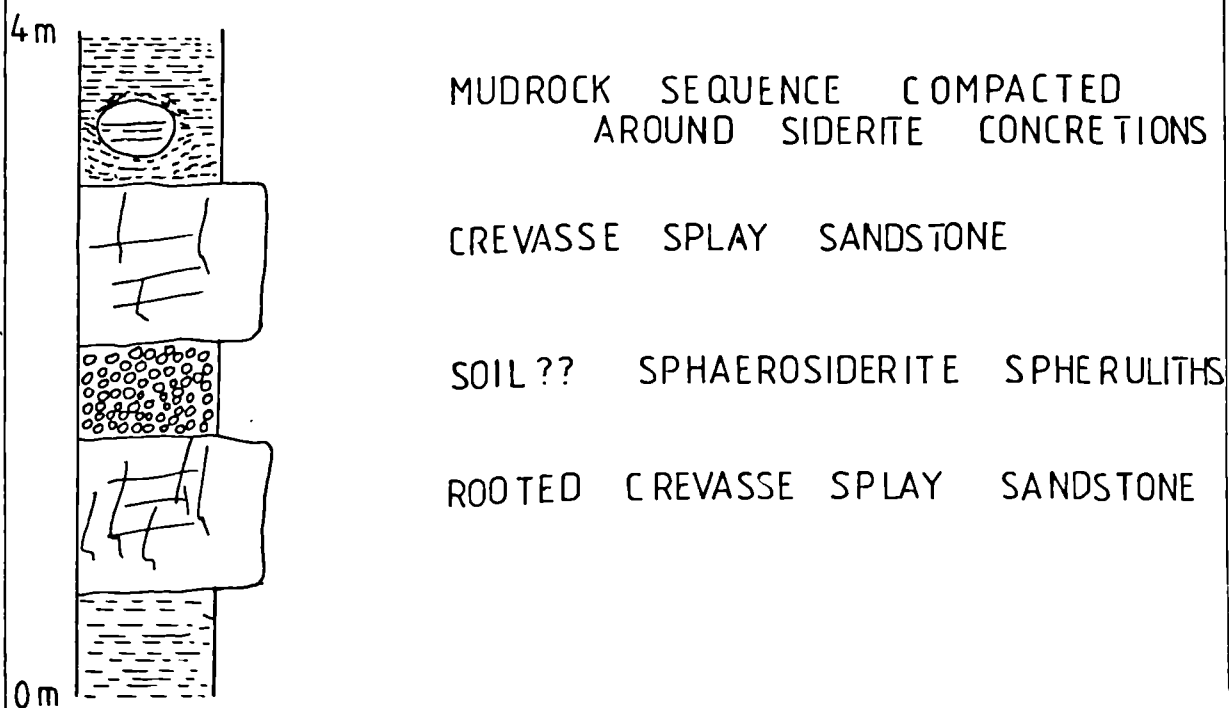
a inside pyrite  
b adjacent to "  
c outside "

Sample	A	A	A	A	A	A	A	A
Code	S	S	S	S	S	S	S	S
Spot	1	2	3	4	5	6	7	8
SiO <sub>2</sub>	0.22	0.32	1.61	0.44	0.23	0.97	0.69	0.67
TiO <sub>2</sub>	0.09	0.09	n.d.	n.d.	0.01	n.d.	0.22	n.d.
Al <sub>2</sub> O <sub>3</sub>	0.09	0.23	1.13	0.18	0.56	0.55	0.33	0.45
FeO	61.79	61.11	59.32	62.27	60.91	58.61	58.42	58.20
MgO	0.73	0.57	0.47	0.49	0.48	1.05	0.85	1.39
MnO	0.46	0.51	0.90	0.55	0.58	1.19	0.25	0.20
CaO	0.31	0.29	0.51	0.12	0.55	1.31	1.22	1.47
Na <sub>2</sub> O	0.09	0.15	0.25	0.01	0.30	0.46	0.26	0.13
K <sub>2</sub> O	n.d.	n.d.	0.23	0.01	n.d.	0.07	0.01	n.d.
TOTAL	63.78	63.27	64.42	64.07	63.62	64.21	62.29	62.51

Data from  
appendix D

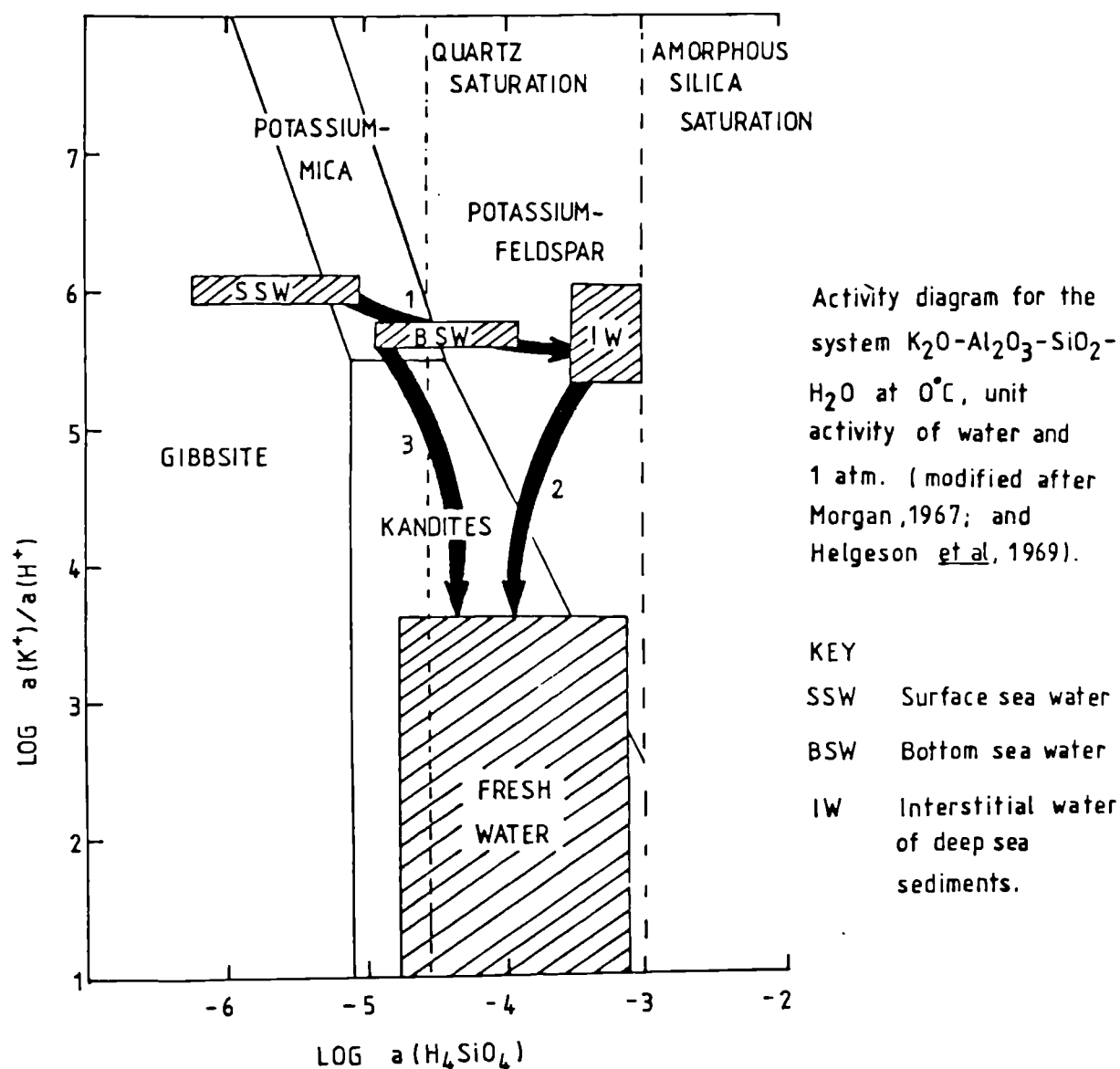
FIG 3.8

SCHEMATIC LOGGED SECTION THROUGH  
THE LONG NAB MEMBER SOUTH OF  
CROOK NESS, AND AN ILLUSTRATION OF  
CLAY LAMINAE COMPACTED AROUND A  
SIDERITE CONCRETION.



LAMINAE MAY BE TRACED ACROSS CONCRETIONS BUT  
THEY ARE COMPACTED AROUND AND OUTSIDE THE  
CONCRETIONS.

Fig. 3.9 Eogenesis of aluminosilicates in marine clastic sediments from the Ravenscar Group.



(1). Illite was stable in the initial pore waters (sea water), and so other phases dissolved whilst illite precipitated. Subsequently, silica saturation increased and potassium-feldspar overgrowths began to precipitate.

(2+3) Later, as bacterial processes lowered pH, both authigenic and detrital micas and feldspars became unstable with respect to kandites. Consequently, neomorphism and dissolution of these potassic phases occurred.

FIG. 3.10 Flow chart to summarise the diagenesis of marine sediments  
in the Ravenscar Group

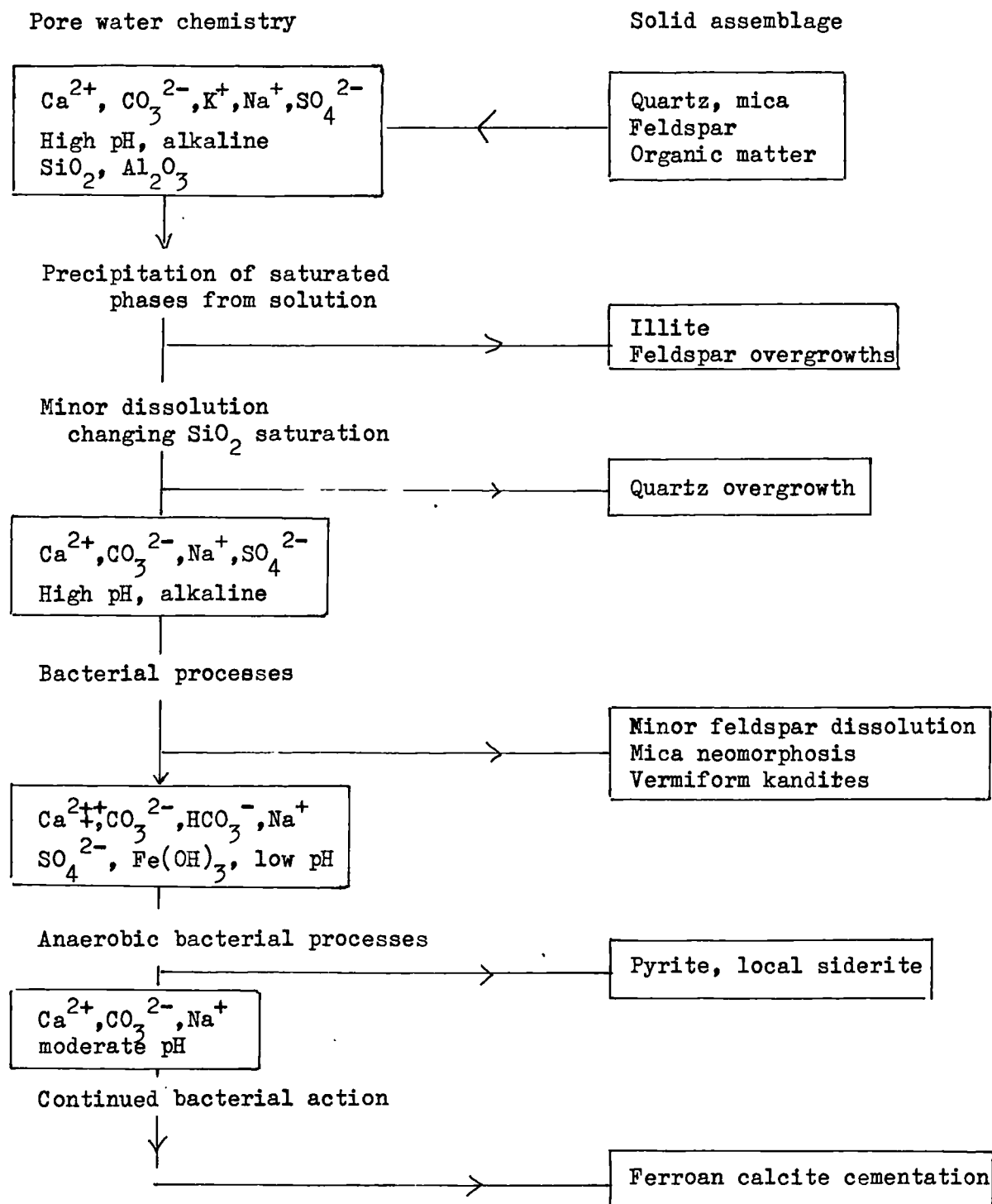
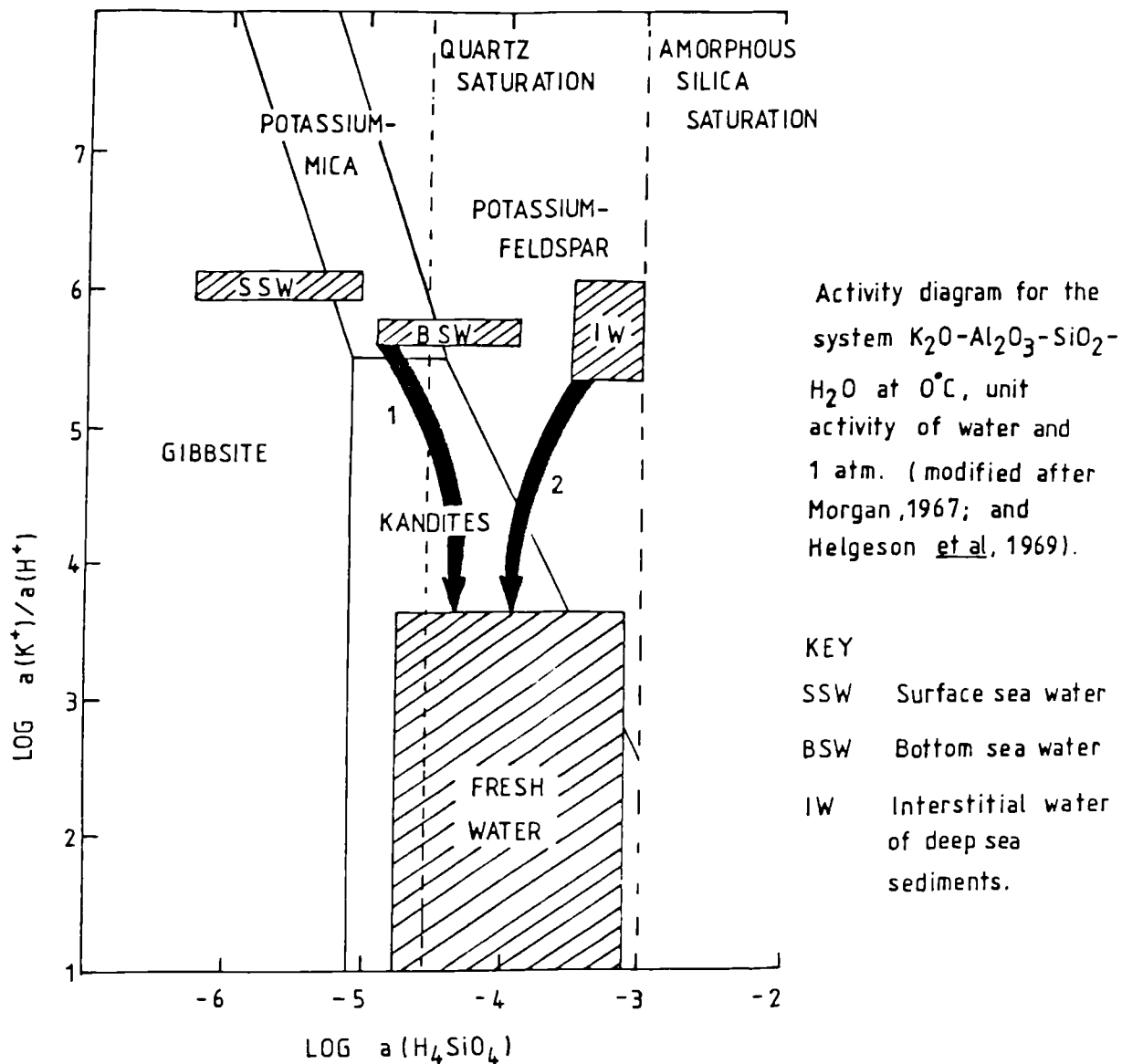
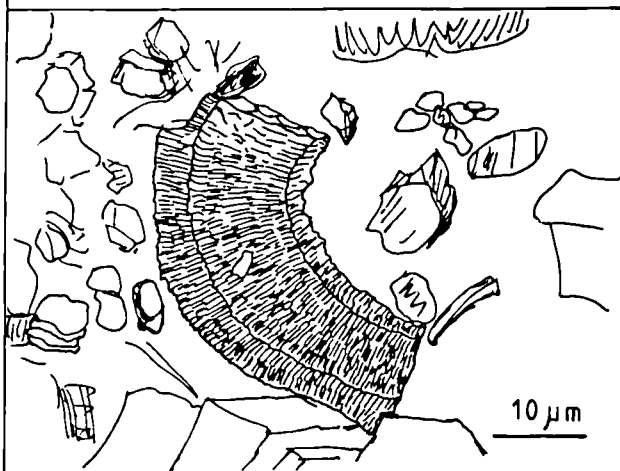


Fig.3.11 The formation of kandites during eogenesis  
of non-marine clastic sediments in the Ravenscar Group.



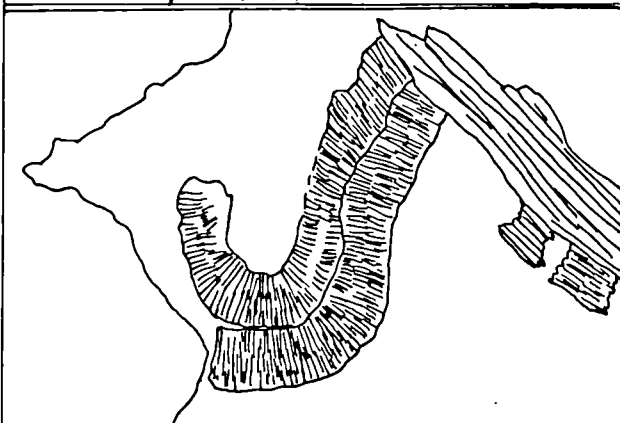
1. Micas or illitic clays, stable in more alkaline solutions, neomorphose to kandites.
2. Feldspars, also stable at a higher pH, dissolve as they attempt to reach equilibrium with fresh water.

FIG. 3.12 THE MORPHOLOGY AND OCCURRENCE OF KANDITES



(a) VERMIFORM (? KAOLINITE)

Large aggregates of stacked pseudo-hexagonal plates, each stack several plates in diameter. Only found in intergranular porosity, and often associated with muscovites. Enclosed by carbonate cements.



(PLATES 3.4 E, F.)

(b) BLOCKY (? DICKITE)

Short aggregates of thick pseudo-hexagonal plates, each aggregate one plate in diameter. Found throughout, especially in enlarged intergranular porosity. Not enclosed by carbonate cements.



(PLATES 3.12 D, 3.4 H)

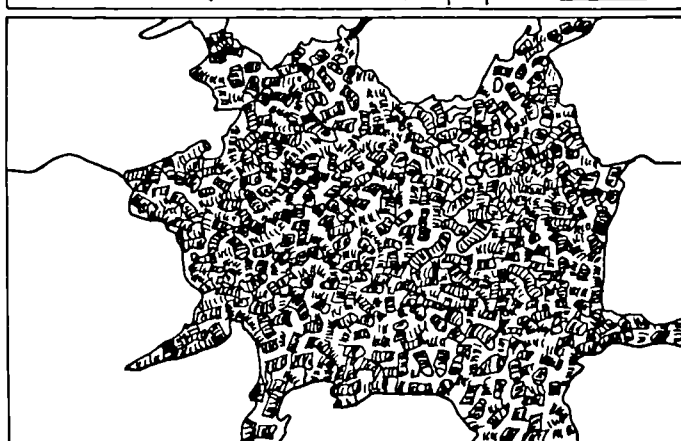
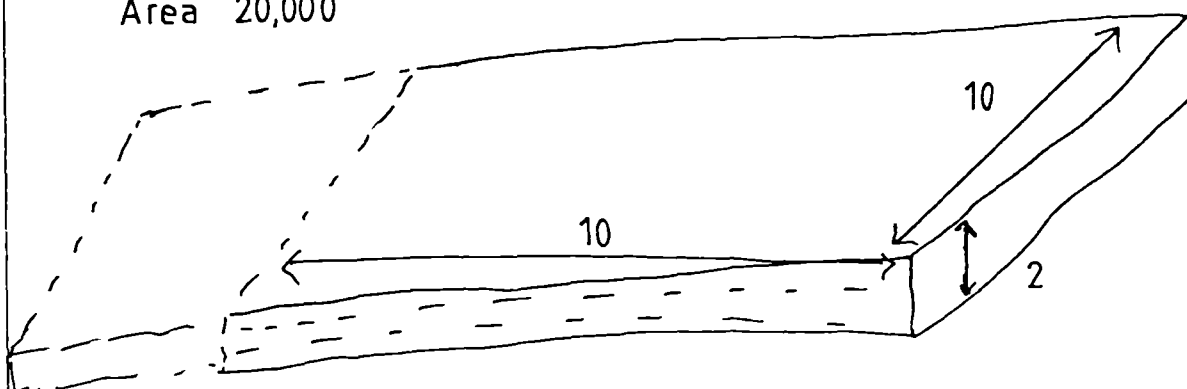


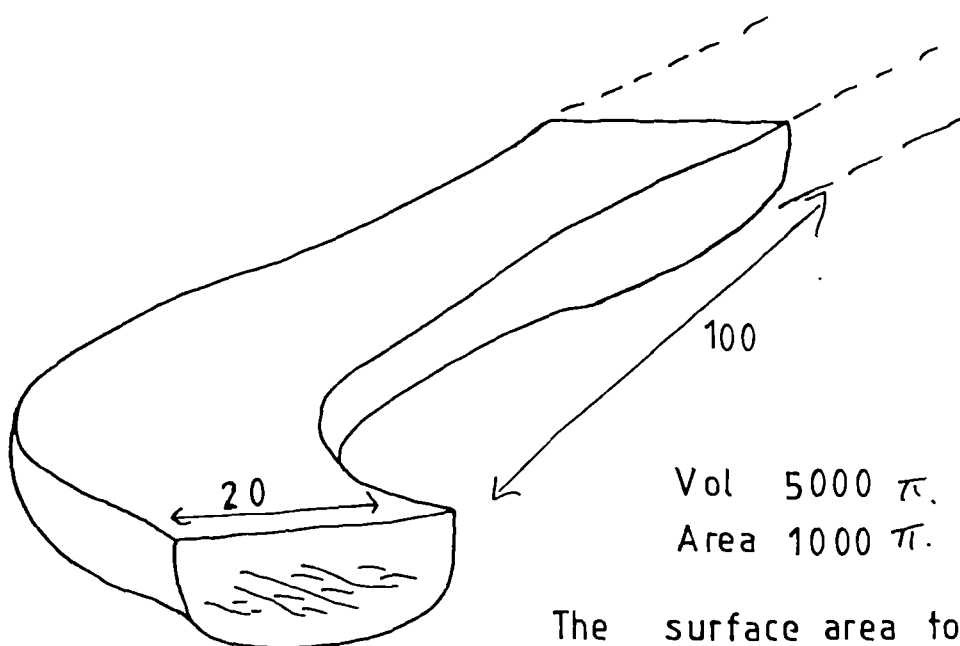
FIG. 3.13 NON MARINE SANDBODY GEOMETRY.

The surface area to volume ratio of a typical 2 m thick overbank sandstone, is 1:1

Vol. 20,000  
Area 20,000



THE SURFACE AREA TO VOLUME RATIO  
OF OVERBANK SANDS IS FIVE TIMES  
THAT OF CHANNELS



Vol  $5000 \pi$ .  
Area  $1000 \pi$ .

The surface area to  
volume ratio of a 10 m  
deep channel is 1:5



FIG. 3.14 SCHEMATIC FLOODPLAIN EOGENESIS MODEL FOR THE RAVENSCAR GROUP. TYPE AND INTENSITY OF DIAGENETIC MODIFICATION RELATED TO MOVEMENT AND CHEMISTRY OF THE WATER TABLE.

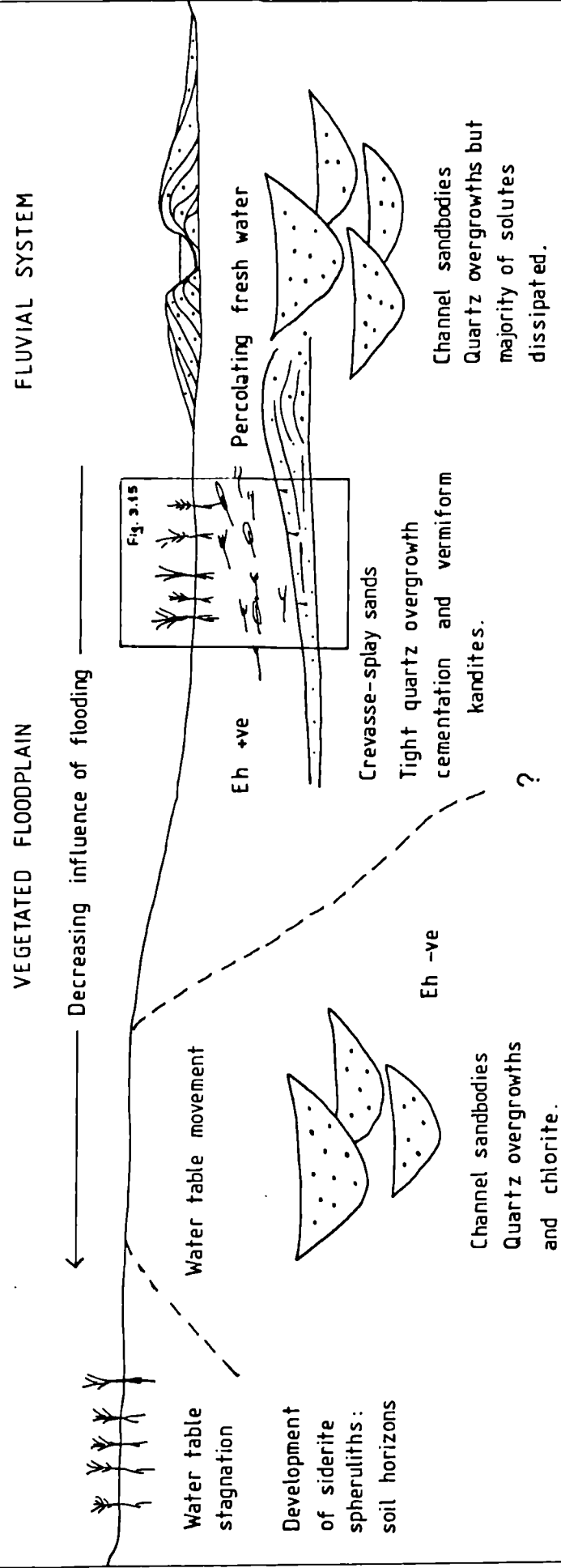
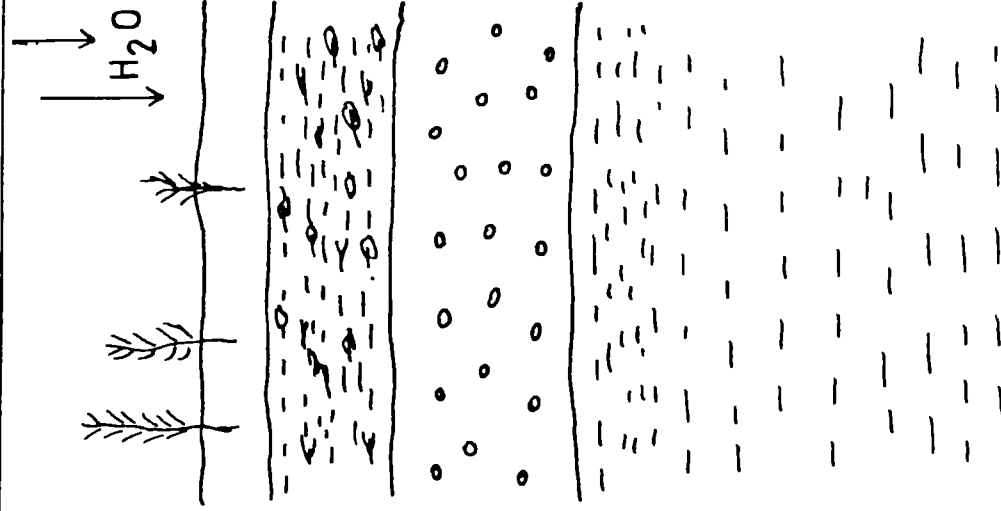
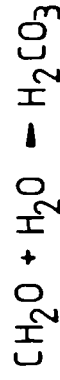


FIG 3.15

TROPICAL "SILCRETE" MODEL FOR THE EOGENESIS OF OVERBANK SANDSTONES  
IN WELL DRAINED OXYGENATED SEDIMENTS.



BACTERIAL DEGRADATION OF ORGANIC  
MATTER



DISSOLUTION OF FELDSPARS AND

AMORPHOUS ALUMINA AND SILICA

PRECIPITATION OF VERMIFORM  
KANDITES AND QUARTZ

OVERGROWTHS

PRECIPITATION OF  
KANDITES

FIG. 3.16 Flow chart to summarise eogenesis of non-marine sediments  
in the Ravenscar Group.

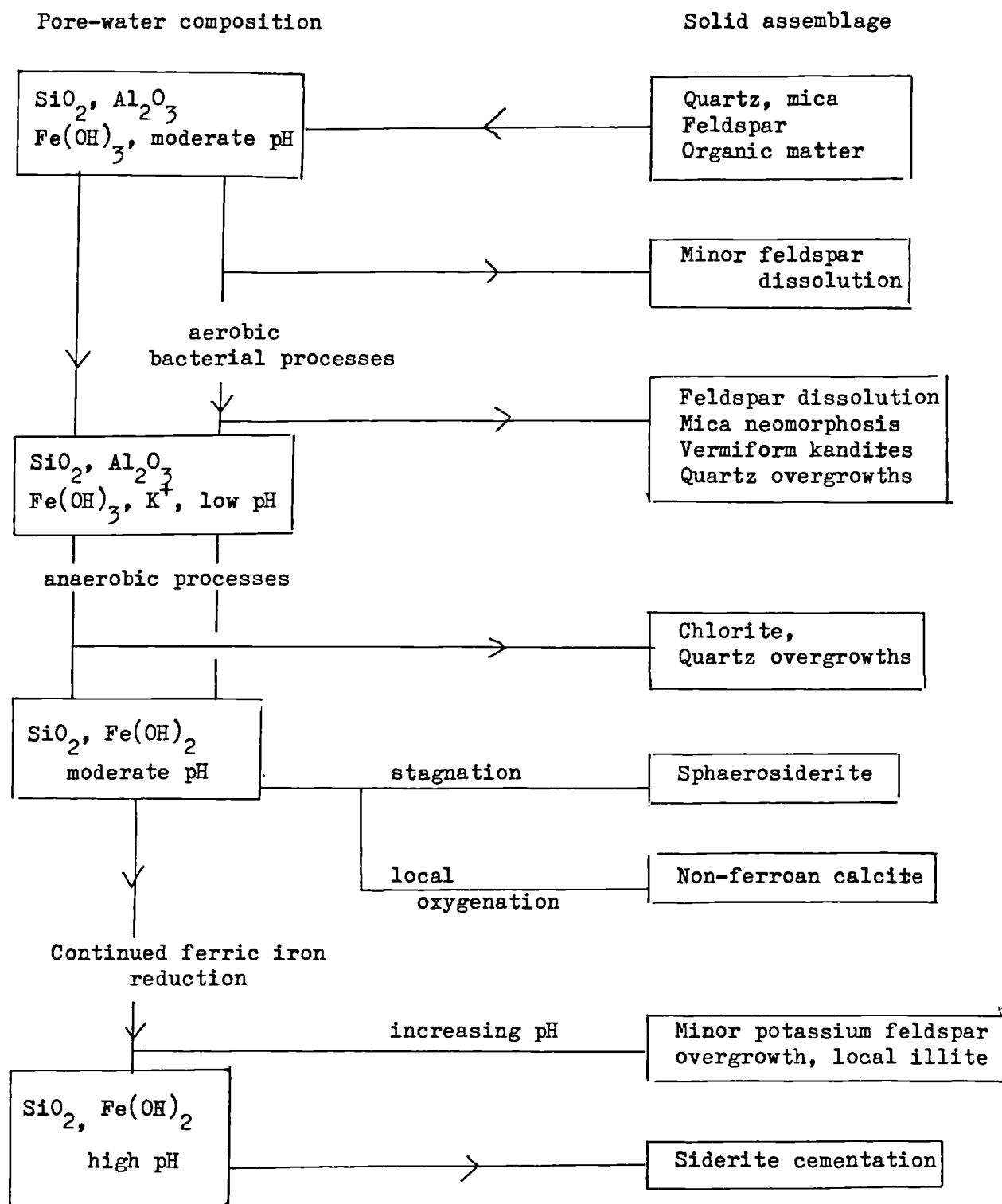
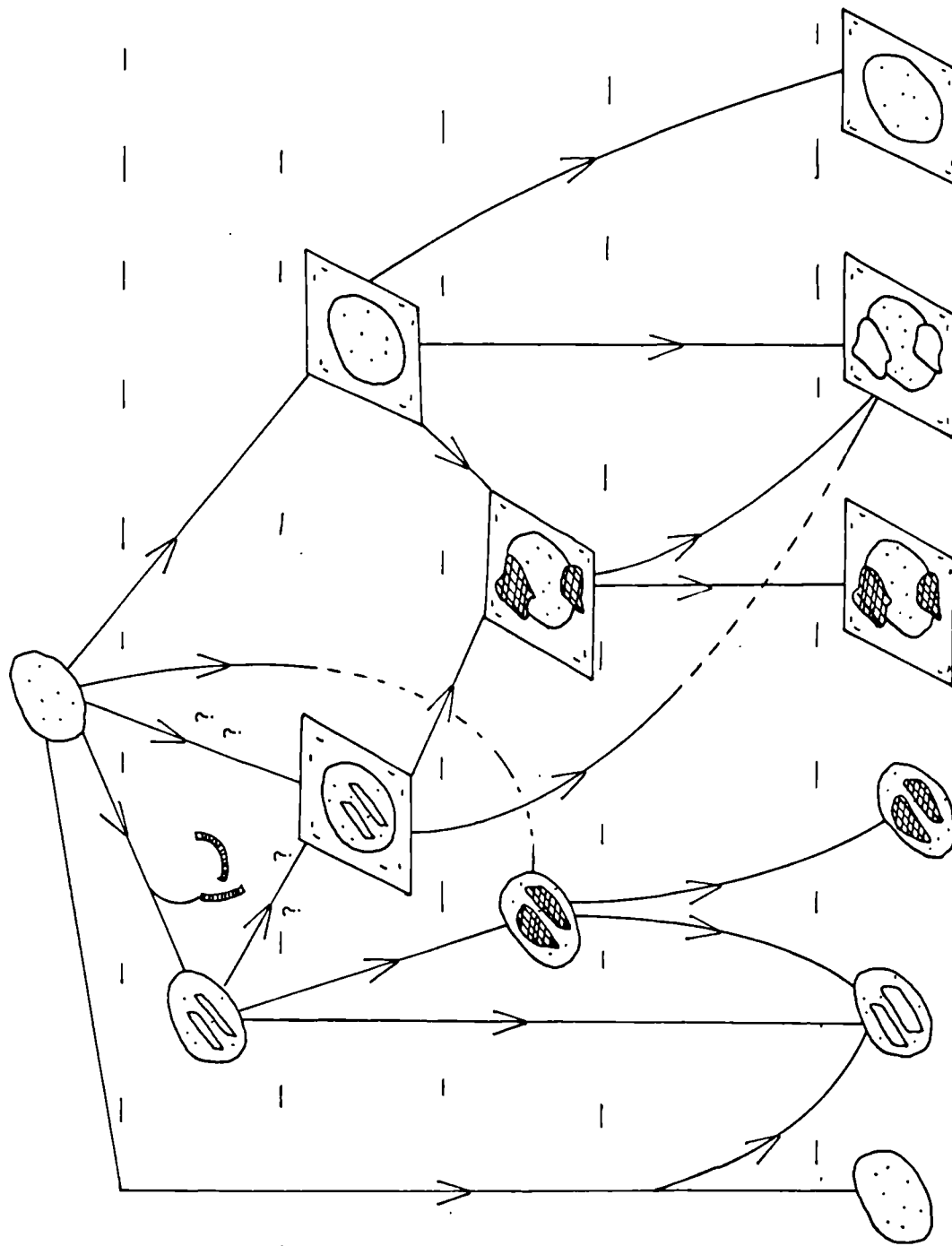


FIG. 3.17 FLOW CHART OF POSSIBLE DIAGENETIC PATHWAYS TAKEN BY DETRITAL FELDSPAR GRAINS IN NON - MARINE SANDSTONES.



Detrital grains

Eogenetic dissolution  
(precipitating kandites)

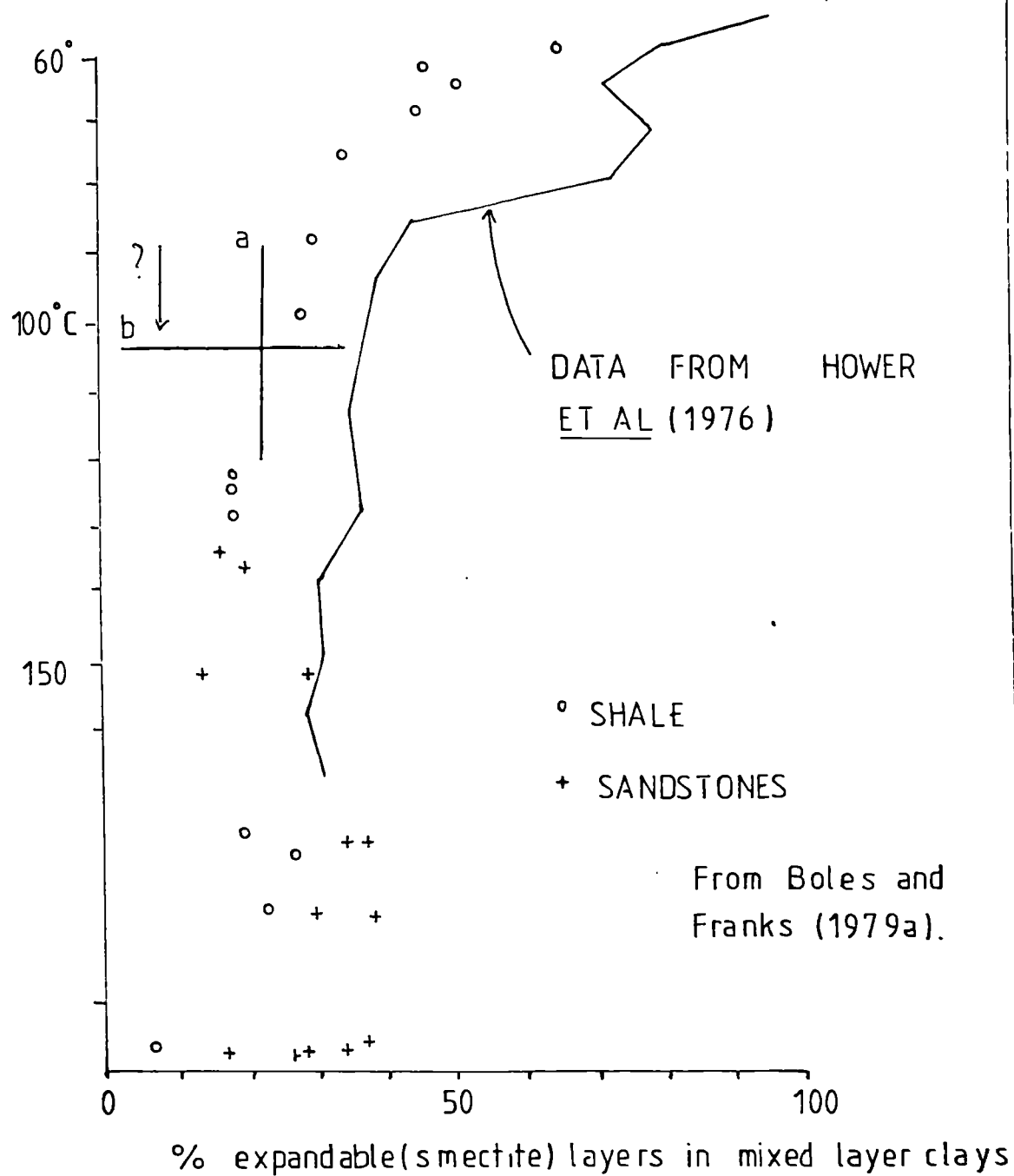
Simultaneous reprecipitation  
as overgrowths: or direct  
authigenesis

Carbonate replacement

Carbonate and further  
feldspar dissolution, due  
to either aggressive pore  
solutions or surface  
weathering, or both.

Extant feldspathic features.

FIG 3.18 COMPARISON OF XRD DATA FROM  
YORKSHIRE AND FROM TERTIARY  
SEDIMENTS IN THE GULF COAST



a Thesis data from appendix E

b Maximum palaeoburial temperature  
(Cooper, pers. comm. 1980).

FIG. 3.19 Flow chart to illustrate the burial diagenesis of sandstones  
in the Ravenscar Group

Non-marine sediments

Marine sediments

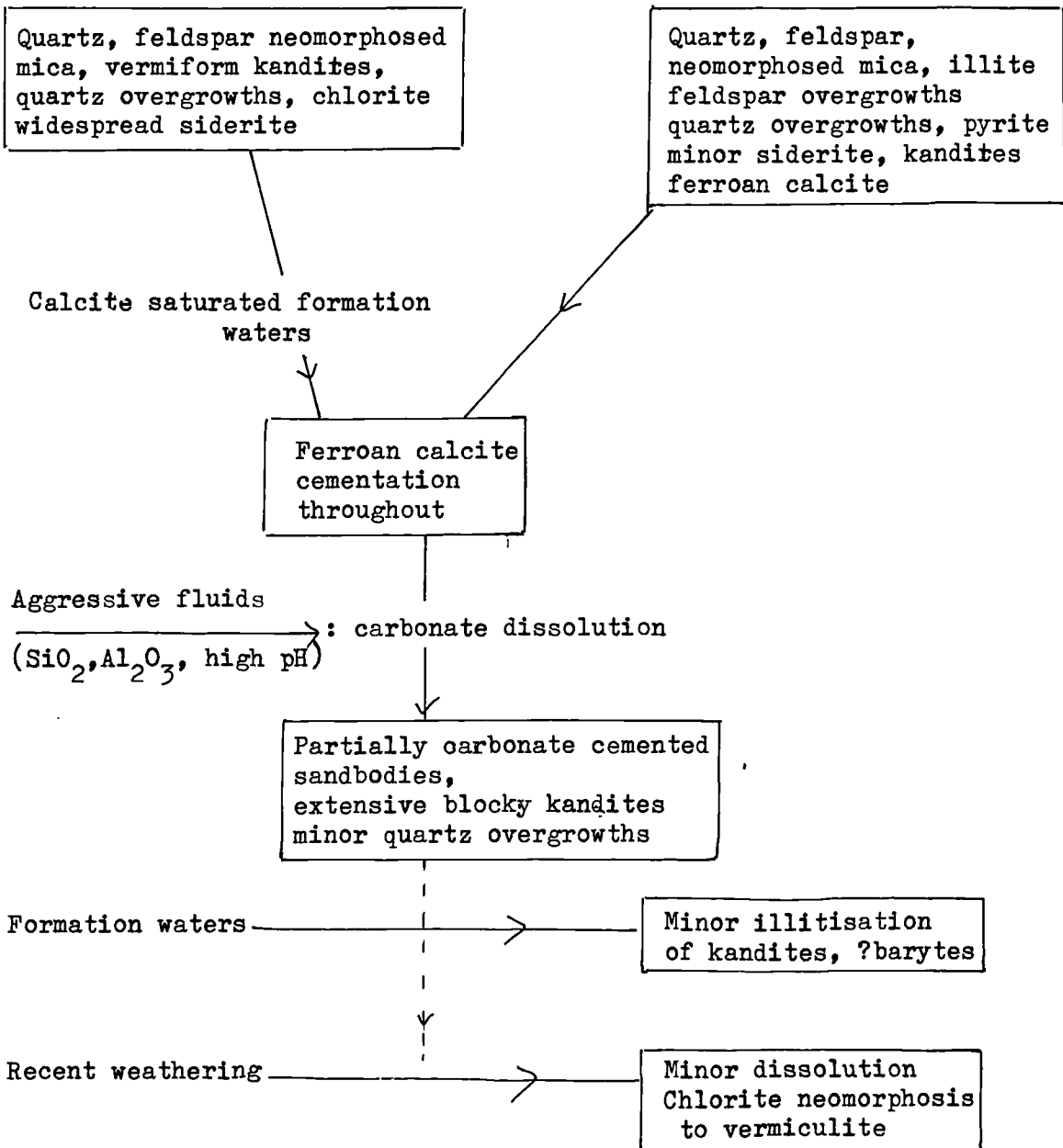


Plate 3.1

- A        Berthierine oolite nucleated on a quartz grain. The oolite and surrounding detrital quartz grains are cemented by siderite. Sample 683. Basal ironstone conglomerate, Dogger Formation, Egton Bridge. Plate width 550  $\mu\text{m}$
- B and C   Euhedral terminations of quartz overgrowths remaining although the majority of the overgrowths have been intensively corroded. In C siderite occurs in the space previously occupied by the overgrowth. B and C sample 603, shallow marine sandstone, Dogger Formation NZ 677076.
- D        Detail of pore-lining vermiculite plates. Sample 654, shallow marine sandstone, Dogger Formation, Thorgill Bank, Rosedale.
- E        Intimately intergrown rhombic siderite cement, and berthierine plates. Both phases occur between berthierine oolites. Sample 684 basal ironstone conglomerate, Dogger Formation, Egton Bridge.
- F        Quartz overgrowth. Sample 602 shallow marine sandstone Dogger Formation NZ 677076'.
- G and H   Small sphaerosiderite spherulites, filling pore space, and replacing detrital grains. The spherulites are oxidised to goethite in G. G, sample 602, shallow marine sandstone Dogger Formation, Thorgill Bank, Rosedale. H, sample 348, beach sandstone, Dogger Formation, Whitby East Cliff. Plate width 875  $\mu\text{m}$ .



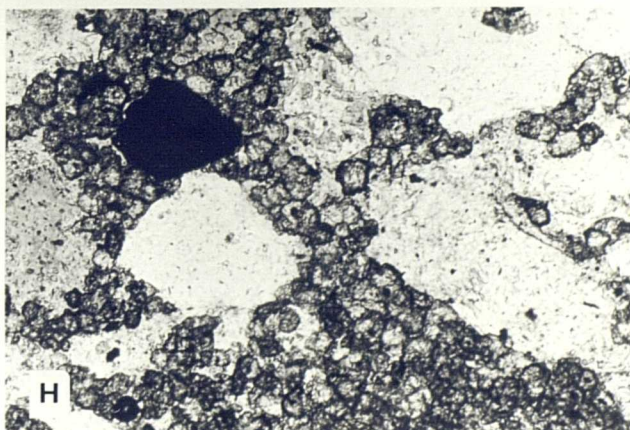
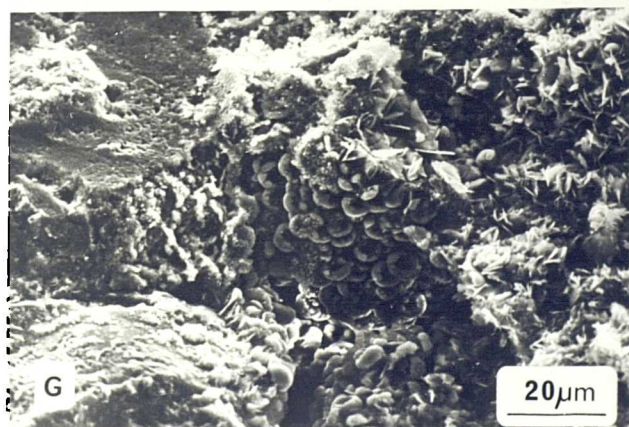
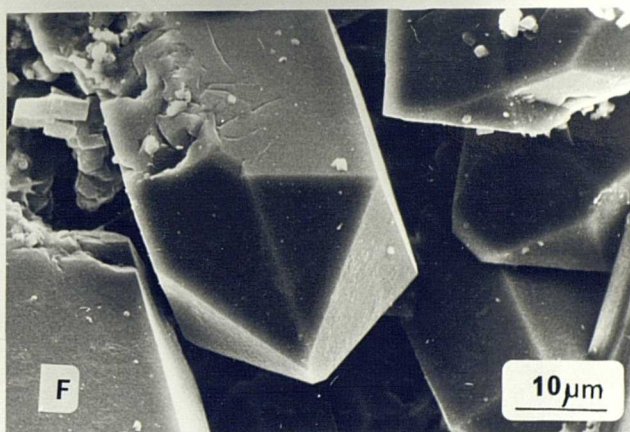
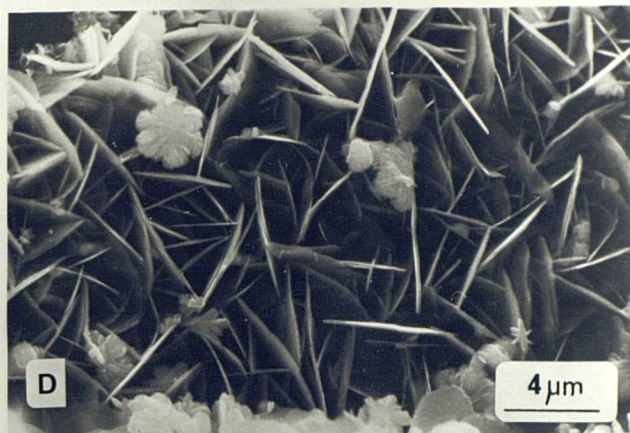
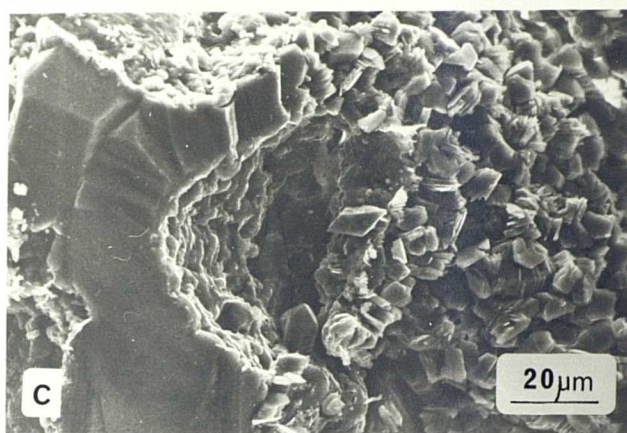
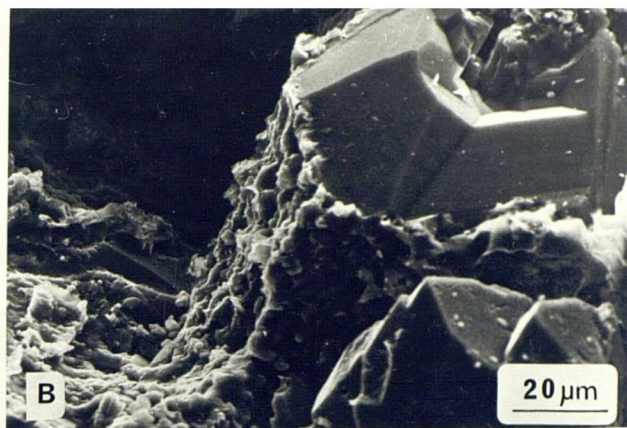
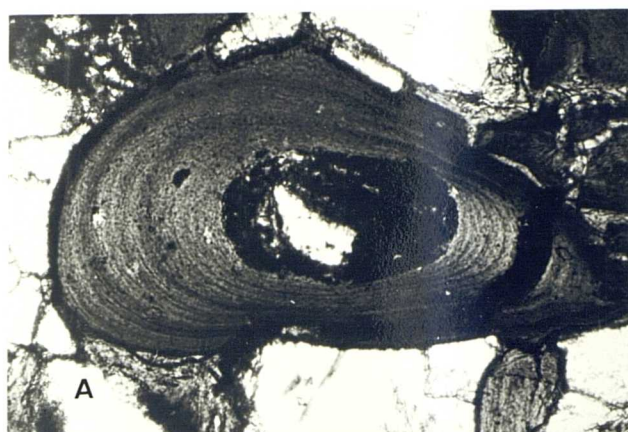




Plate 3.2

- A and B Authigenic vermiculite, occurring as a perpendicular pore lining, coating pore walls (detrital quartz grains) and preventing nucleation of overgrowths. Sample 654. Plate A width 220  $\mu\text{m}$  cross-polarised light. Shallow marine sandstone, Dogger Formation, Thorgill Bank, Rosedale.
- C General view of poorly-sorted fine-grained sandstone. Here authigenesis was inhibited by matrix clay. Sample 320. Plate width 875  $\mu\text{m}$  cross-polarised light. Crevasse-splay sandstone, Saltwick Formation, Whitby West Cliff.
- D Illite neomorphism of detrital matrix clay and perhaps of authigenic kaolinites. Sample 563. Crevasse-splay sandstone, Saltwick Formation, Uggelbarnby Moor.
- E Dissolution of detrital feldspar grain, and authigenesis of feldspar overgrowth. Sample 552. Crevasse-splay sandstone, Saltwick Formation, Alum Quarry, Ravenscar.
- F Stepped euhedral overgrowth surface on detrital quartz grain.
- G and H Incipient quartz overgrowths, nucleation of which is partially inhibited by pore-lining vermiculite which is itself being enclosed by the overgrowths. F, G and H, sample 444, crevasse-splay sandstone, Saltwick Formation, Hayburn Wyke.

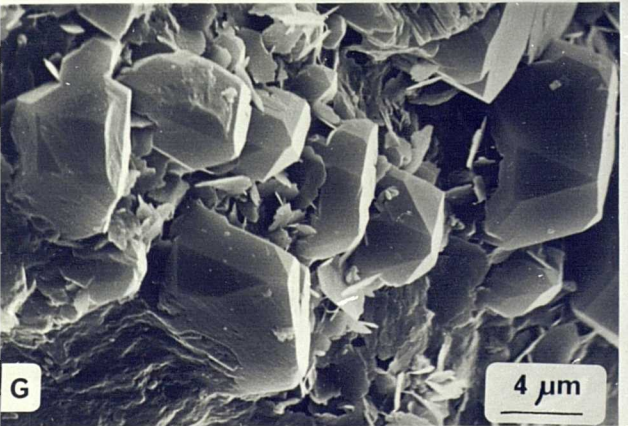
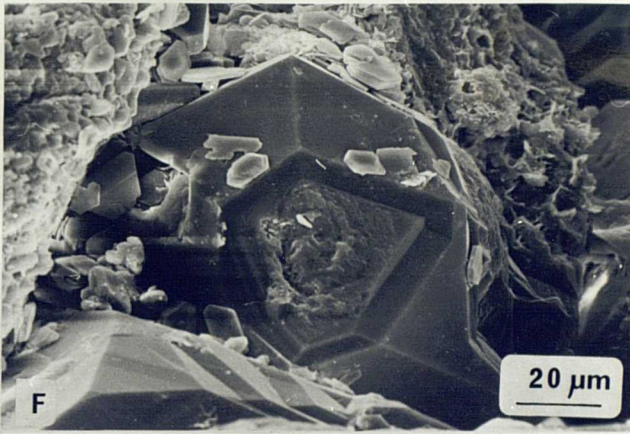
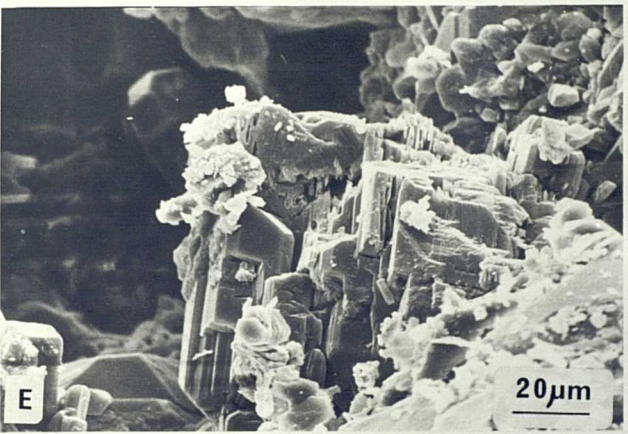
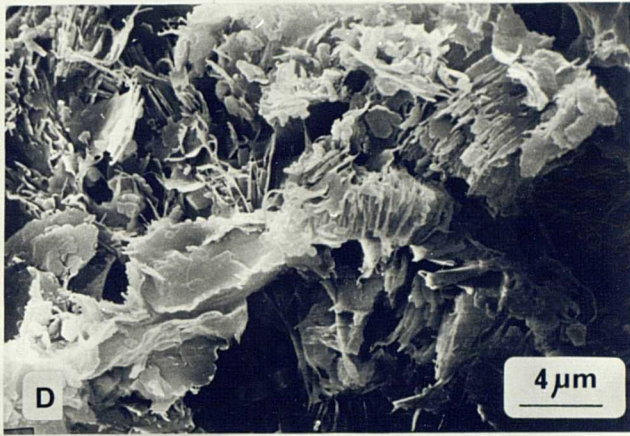
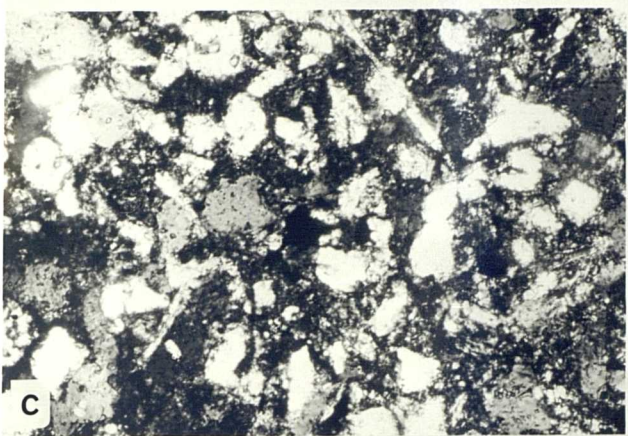
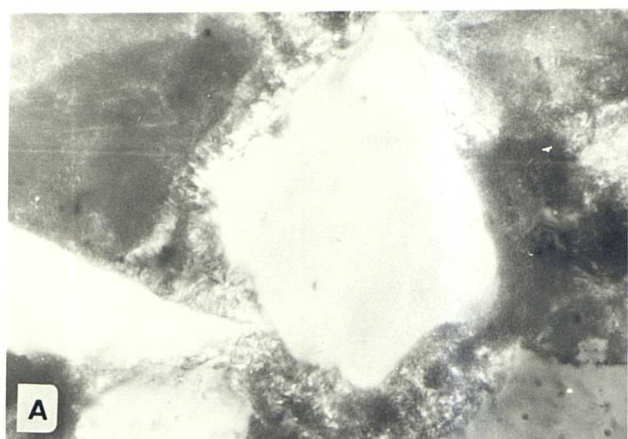


Plate 3.3

- A      Deeply etched or corroded quartz overgrowth and detrital quartz grain. Note the rounded surface of the detrital grain separated from the overgrowth by a dust rim. Sample 444. Plate width 875  $\mu\text{m}$  cross-polarised light. Crevasse-splay sandstone, Saltwick Formation, Hayburn Wyke.
- B      Replacement and corrosion of quartz overgrowth by (?) oxidised siderite. Sample 661 channel sandstone, Saltwick Formation, Rosedale.
- C      Rhombs of authigenic siderite, filling pore space, and replacing quartz overgrowth. Sample 661 channel sandstone, Saltwick Formation, Rosedale.
- D      Subsequently oxidised siderite replacing quartz overgrowth. Sample 659 channel sandstone, Saltwick Formation, Rosedale.
- E      Siderite replacement of quartz overgrowths and grains. Sample 322. Plate width 700  $\mu\text{m}$  cross-polarised light. Channel sandstone, Saltwick Formation, Whitby West Cliff.
- F      Corroded quartz overgrowth (q) and siderite replacement of feldspar (f) grain. Sample 314. Plate width 1.9 mm. Plane-polarised light. Channel sandstone, Saltwick Formation, Whitby West Cliff.
- G      "V" shaped notches in quartz overgrowth. Sample 312. Channel sandstone, Saltwick Formation Whitby West Cliff.
- H      Deeply corroded quartz overgrowth. Amorphous material filling etched hollow is probably goethite, an oxidation product of the original siderite. Sample 661. Channel sandstone, Saltwick Formation, Rosedale.



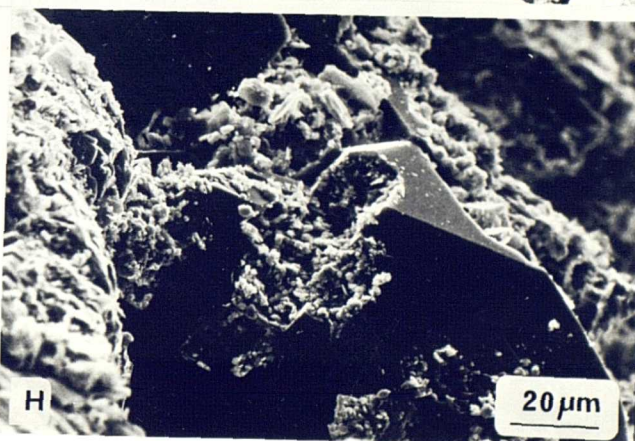
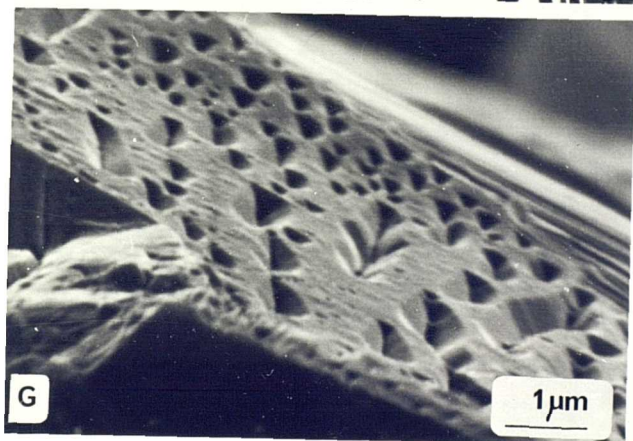
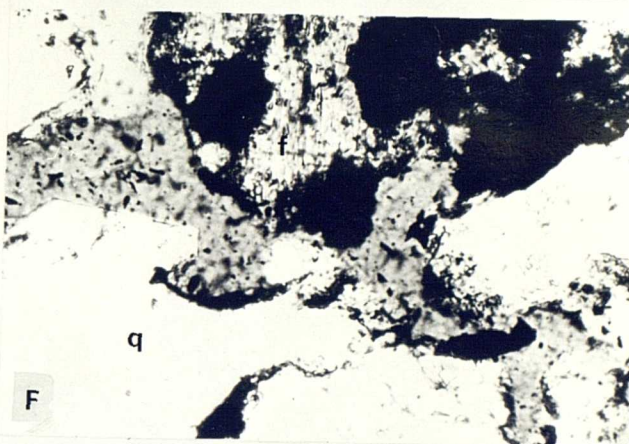
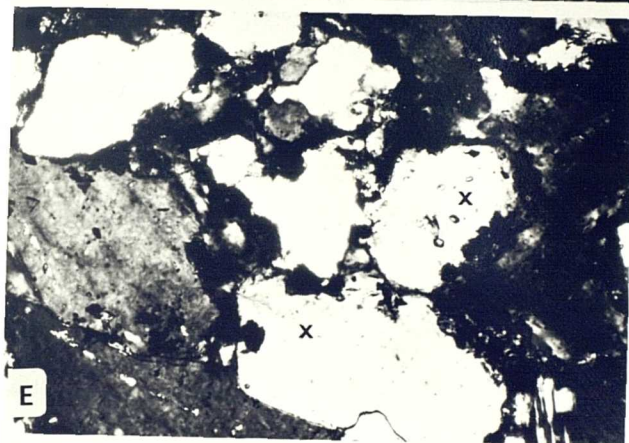
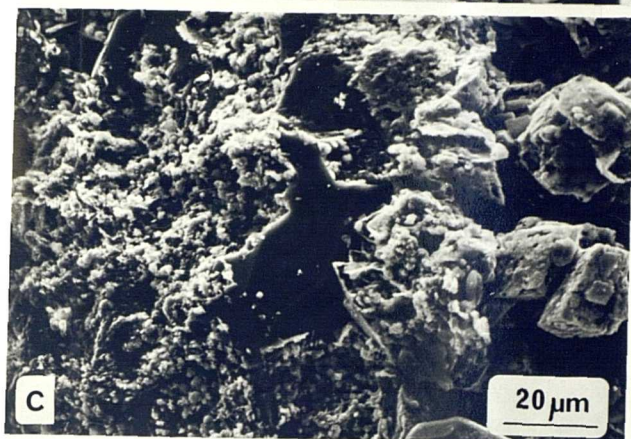
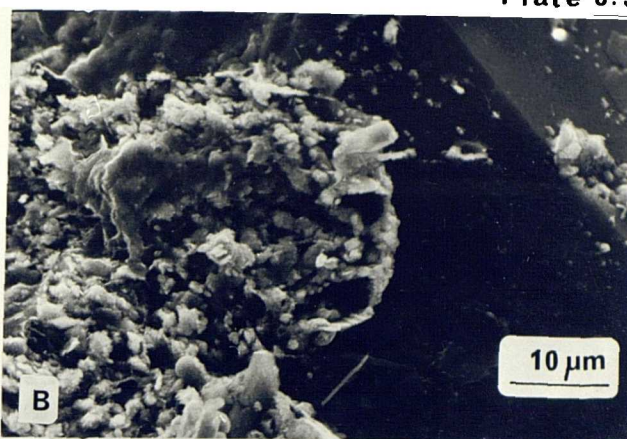
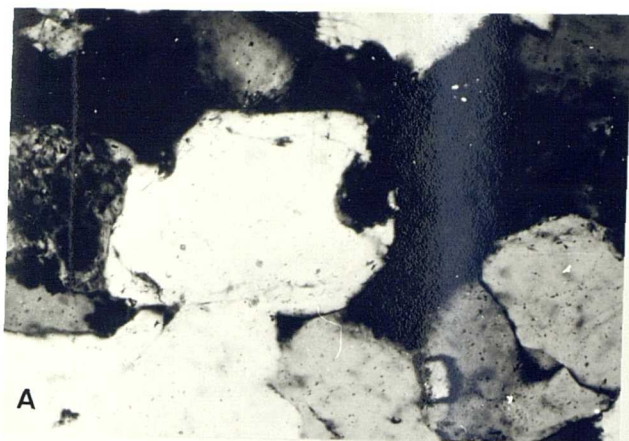


Plate 3.4

- A and B Muscovite neomorphosed to kandites. Plate B, width 550  $\mu\text{m}$ , plane polarised light. Channel sandstones, Saltwick Formation, Samples 355 and 306, Whitby East and West Cliffs respectively.
- C and D Dissolution of feldspar grains, corroding the framework parallel to lamellae. Plate D, width 875  $\mu\text{m}$ . Channel sandstones, Samples 567 and 606. Saltwick Formation (NZ 966059) and (NZ 682060) respectively.
- E and F Intergranular pore-filling vermiform kandites. Note the number of individual plates in E, and nucleation of the aggregate on a muscovite in Plate F. Plate F width 350  $\mu\text{m}$ . Plane polarised light. Channel sandstones, Samples 606 and 638. Saltwick Formation (NZ 682060) and Roseberry Topping respectively.
- G and H Oversized pore-filling of blocky kandites. Those in G mantle quartz grains with overgrowths completely, and are not confined to one pore. Those in H occupy a pore equivalent to several detrital grains. Note kandite filling of corroded quartz grain (x). Plate H width 875  $\mu\text{m}$ , cross-polarised light. Channel sandstones, Samples 329 and 606. Saltwick Formation, Whitby West Cliff and (NZ 682060) respectively.



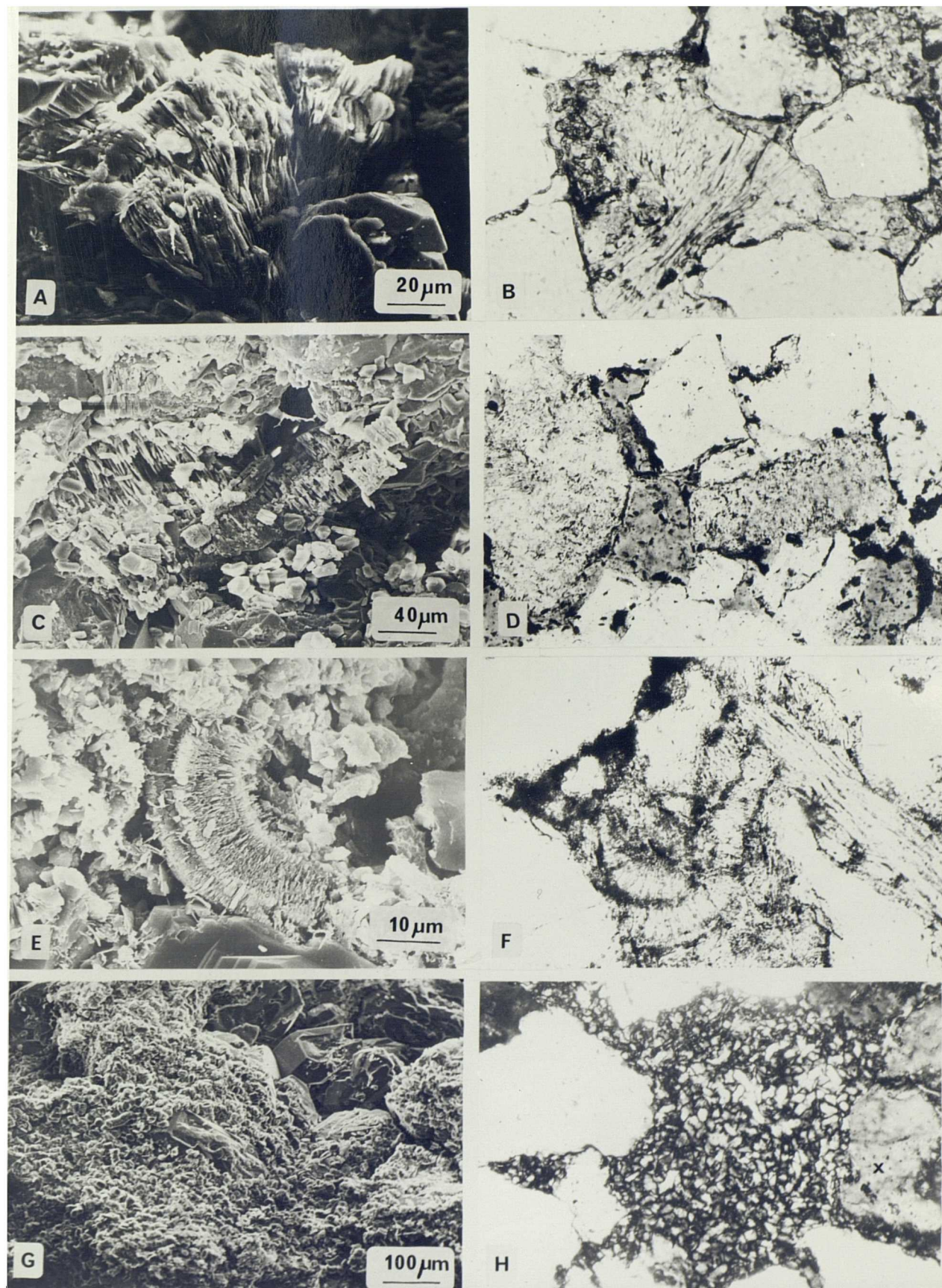


Plate 3.5

- A        Enclosure of blocky kandites by quartz overgrowth.  
         Individual aggregates of kandites are one plate  
         in diameter. Sample 596. Channel sandstone,  
         Saltwick Formation, Glaisdale.
- B        Incipient illitisation of blocky kandites. Sample 355.  
         Channel Sandstone, Saltwick Formation, Whitby West Cliff.
- C        General view, to show generally porous nature, with  
         predominant quartz overgrowth cementation. Sample 604.  
         Channel sandstone, Saltwick Formation (NZ 682060).
- D        Nucleation of illitic hairs on detrital mica. Sample 596.  
         Channel sandstone, Saltwick Formation, Glaisdale.
- E        Individual and coalescing "blobs" of goethite covering  
         a quartz overgrowth. Sample 549. Channel sandstone,  
         Saltwick Formation, Alum Quarry, Ravenscar.
- F        Small authigenic pyrite crystals covering a quartz  
         overgrowth. Sample 549. Channel sandstone, Saltwick  
         Formation, Alum Quarry, Ravenscar.
- G        Sodium-feldspar overgrowth.
- H        Dissolved titanium oxide grain, probably rutile. G and H  
         channel sandstones, Sample 606, Saltwick Formation  
         (NZ 682060).



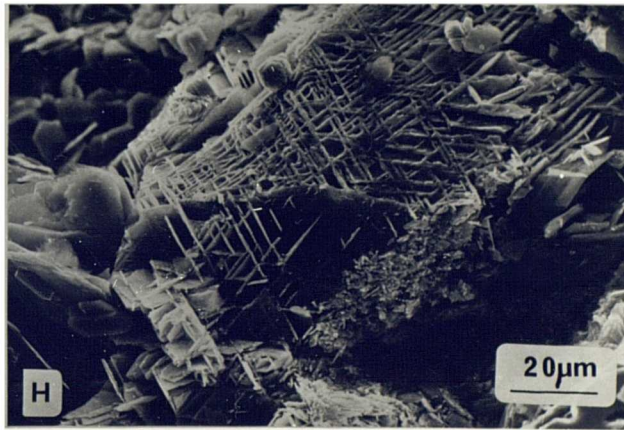
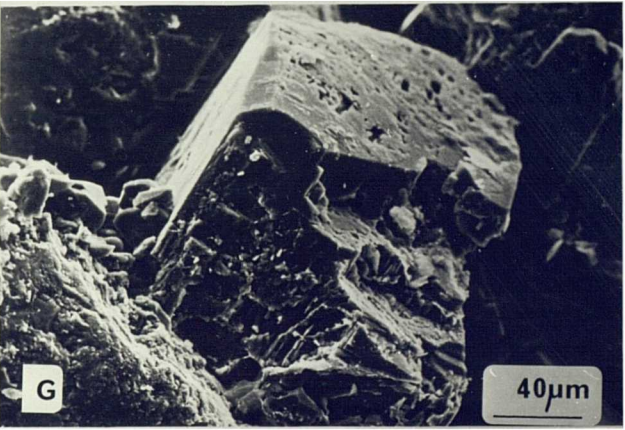
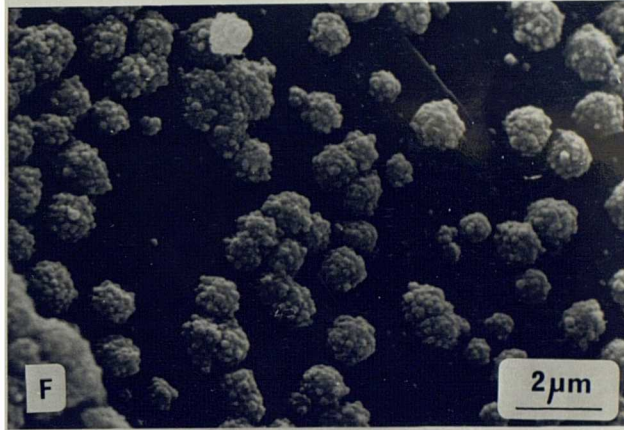
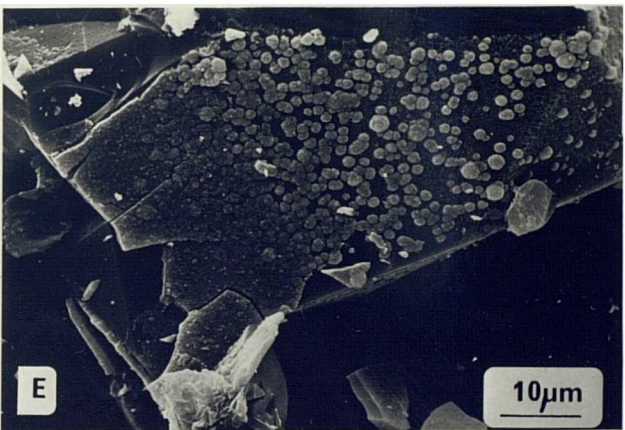
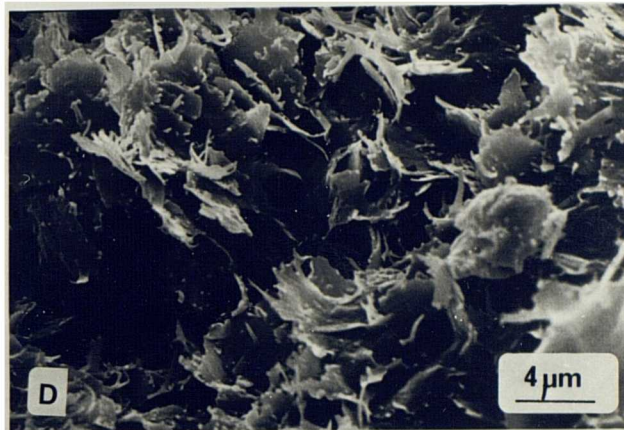
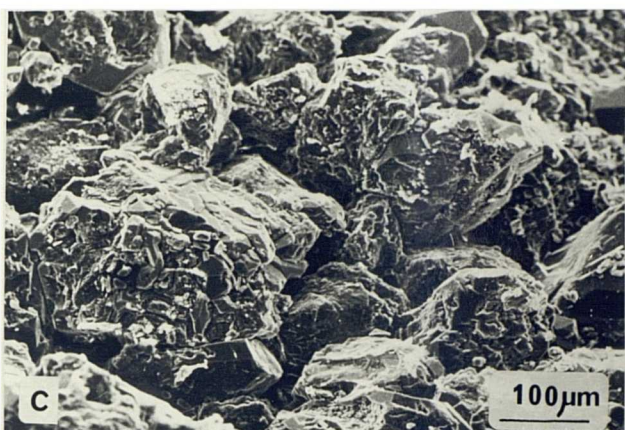




Plate 3.6

- A Authigenic titanium oxide, with orthorhombic form,  
probably brookite. Sample 355. Channel sandstone,  
Saltwick Formation, Whitby East Cliff.
- B Authigenic titanium oxide, with tetragonal form,  
probably anatase. Sample 306. Channel sandstone,  
Saltwick Formation (NZ 682060).
- C and D Plane-polarised light and CL of bryozoan fragment and  
brightly luminescent intraparticle pore-filling calcite.  
Blocky interparticle porosity contains non-luminescent  
sparry-ferroan calcite. Plate width 3.75 mm.
- E, F,
- G and H Close up. Plane polarised light and CL views of bryozoan  
chambers to show zoned nature of brightly luminescent  
pore filling. Sample 201. Oolitic dune complex,  
Millepore Bed, Yons Nab. Plate width 925  $\mu\text{m}$ .
- C - H Photographed at Nottingham University on the  
J A D Dickson Cathodoluminiser. Operating conditions:  
beam energy 30 kV  
beam current 5  $\mu\text{A}$   
beam diameter 5-10 mm  
gun type, cold cathode  
ambient gas, air  
working vacuum  $10^{-1}$  torr  
microscope, Zeiss Photomicroscope II with Type CS  
Photomicrographic camera attachment  
exposures, 4 minutes  
film, 125 ASA

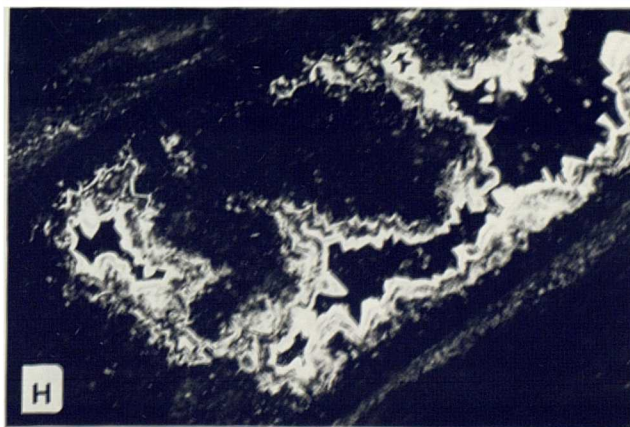
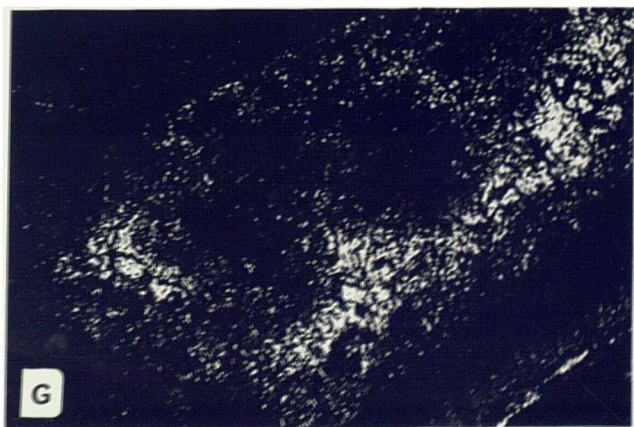
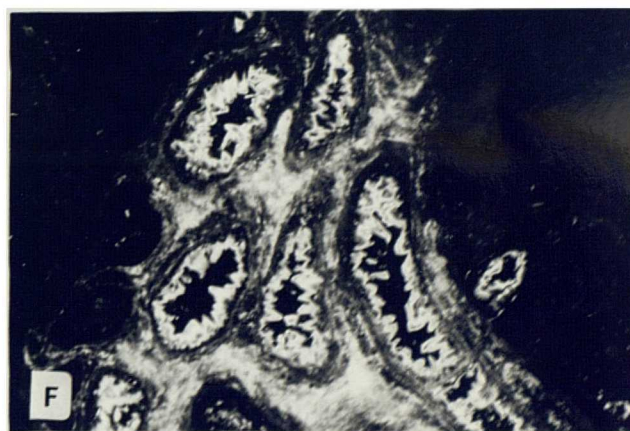
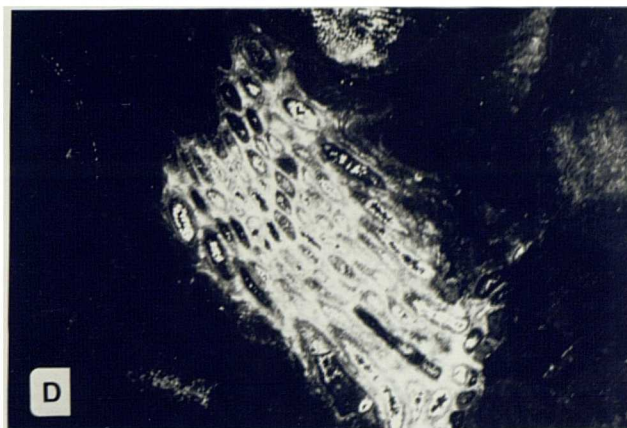
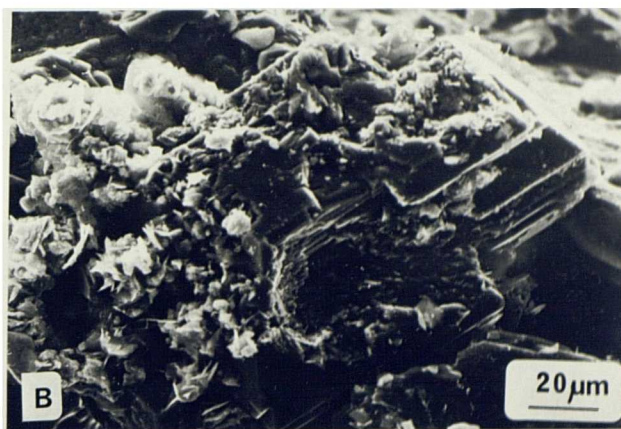


Plate 3.7

- A        Calcite rim cement (r), and sparry interparticle  
         pore filling (s) within oolitic limestone.
- B        Ferroan calcite enclosing vermiform kandites.  
         A and B sample 201. Millepore Bed, Yons Nab.  
         Plate width 140  $\mu\text{m}$ .
- C        Authigenic pyrite, enclosed in ferroan calcite.
- D        Vermiform kandites (k) enclosed in ferroan calcite.
- E        Ferroan calcite (c) cementing and replacing quartz  
         overgrowths on adjacent grains. Corrosion of quartz  
         overgrowths visible where calcite is removed.
- F, G, H   Close ups of notch-shaped etch pits and their  
         coalescence into larger hollows.
- C, D, E,   Sample 203. Interdistributary bay filling sandstones,  
F, G, H   Yons Nab Beds, Yons Nab.



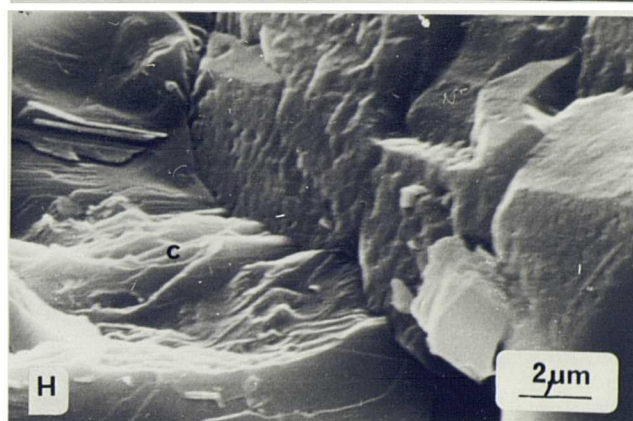
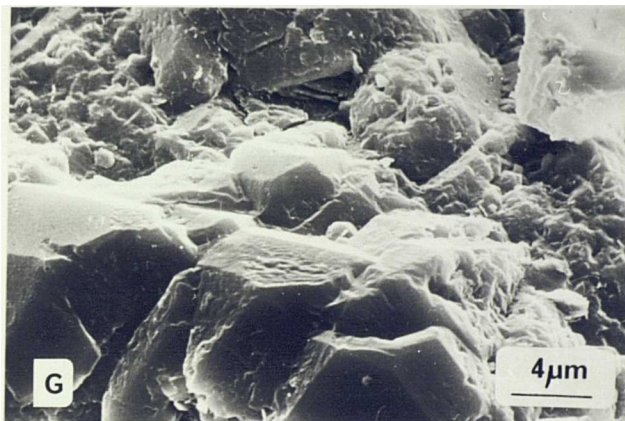
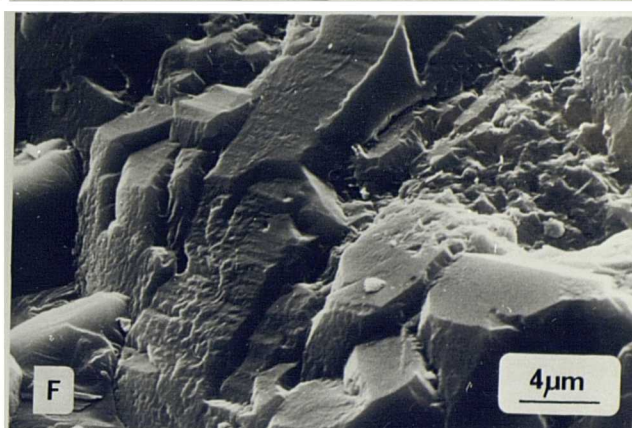
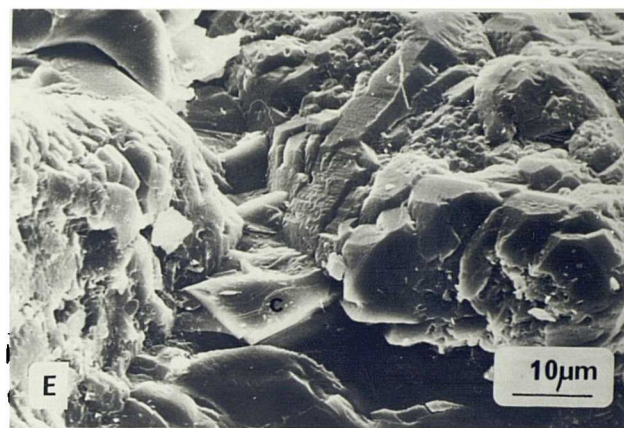
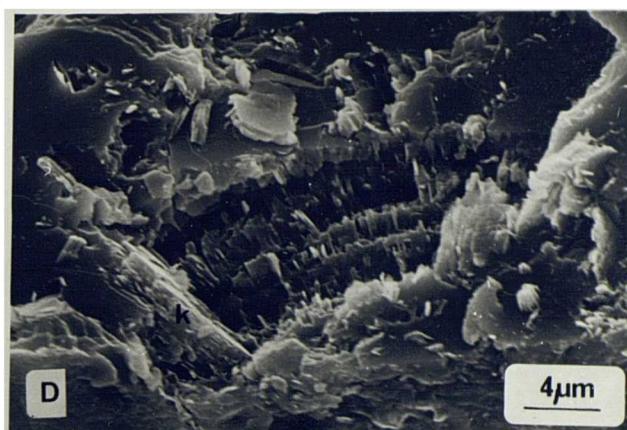
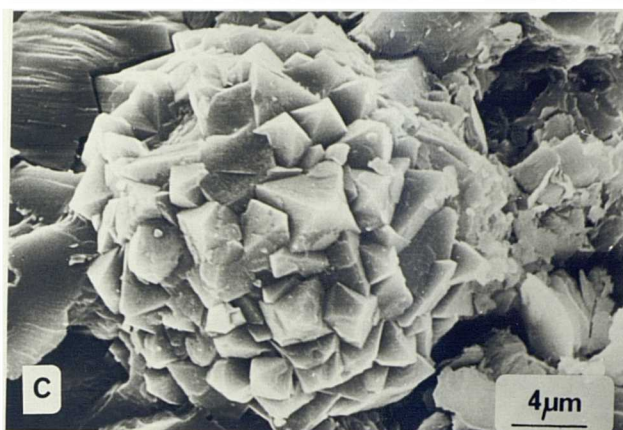
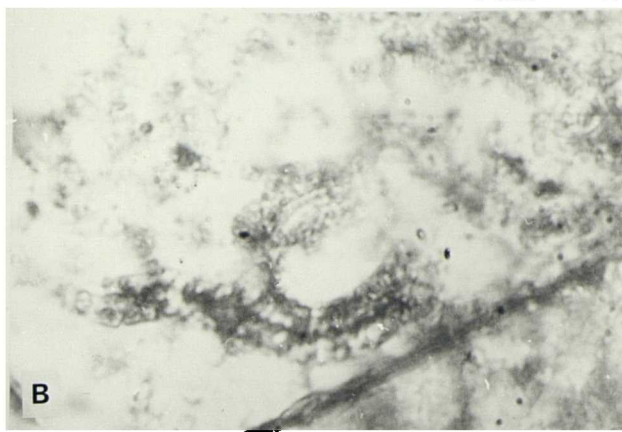


Plate 3.8

- A        General view to show quartz overgrowth cementation, and scattered pockets of blocky kandites (k), but generally open pore throats. Sample 232. Tidally influenced bar, Yons Nab Beds, Osgodby Nab.
- B        Pore-filling rhombic siderite cementation. Siderite also replaces authigenic quartz (q). Sample 272. Ironstone capping interdistributary bay filling sequence, Yons Nab Beds, Yons Nab.
- C and D   Illitic hairs nucleated on, and neomorphosing plates of detrital matrix clay.. Sample 581. Crevasse-splay sandstone, Gristhorpe Member (NZ 682090).
- E and F   Pore-lining chlorite, enclosed by subsequent quartz overgrowths. Most extensive developments of chlorite rosettes inhibit nucleation of overgrowths, and are not enclosed. Sample 382 and 383. Tidal bar, Gristhorpe Member, Cloughton Wyke.
- G        Vermiform kandite aggregate, comprising numerous individual plates. Sample 594. Crevasse-splay sandstone, Gristhorpe Member, (NZ 660110).
- H        Quartz overgrowth enclosing chlorite plates and cementing grains together. Euhedral faces reveal slight steps and pits. Sample 383. Tidal bar, Gristhorpe Member, Cloughton Wyke.



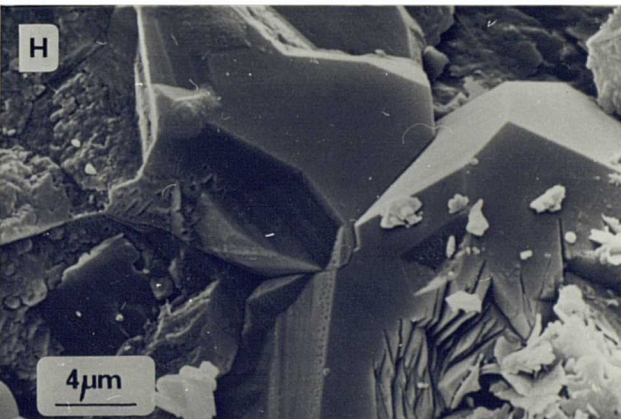
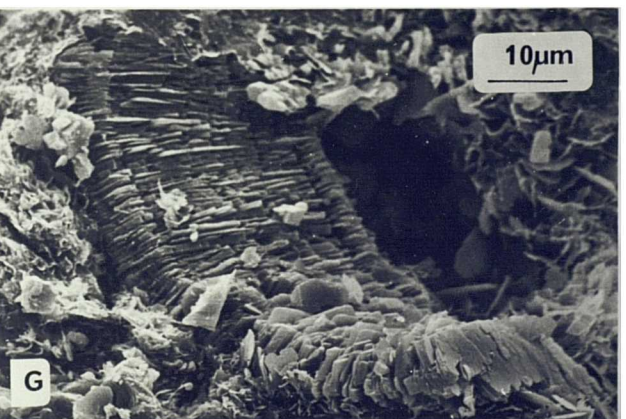
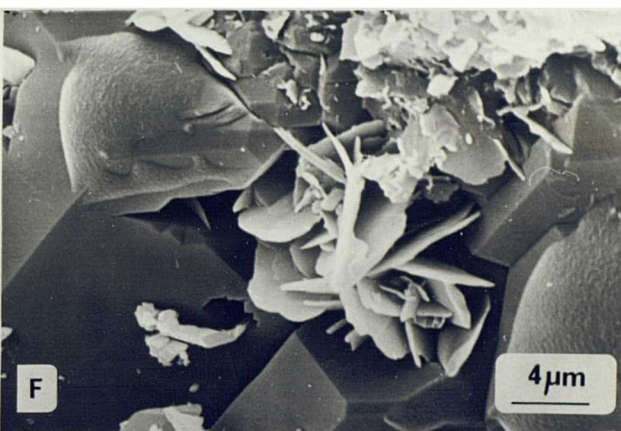
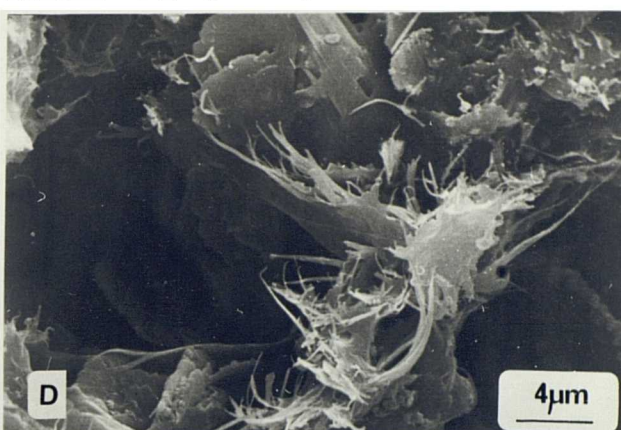
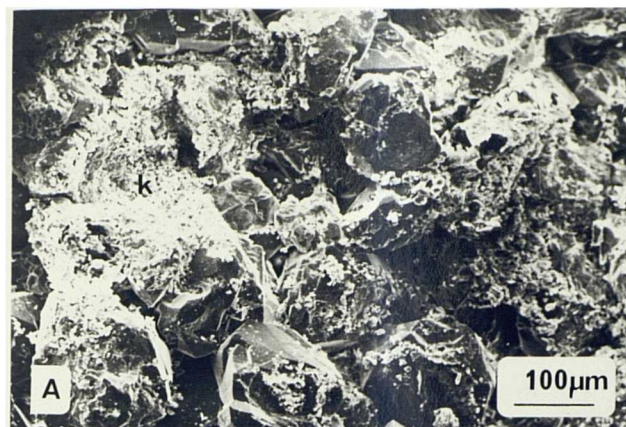


Plate 3.9

- A        Plant debris. Sample 594. Crevasse-splay sandstone, Gristhorpe Member, (NZ 660110).
- B        Rosette of chlorite plates. Sample 380. Sheetflood sandstone, Gristhorpe Member, Cloughton Wyke.
- C        Poorly developed pore-lining vermiculite, enclosed by subsequent quartz overgrowths. Sample 594. Crevasse-splay sandstones, Gristhorpe Member (NZ 660110).
- D        Tightly interlocking quartz overgrowths, completely cementing grains together, and filling pore space. Note late development of amorphous aluminosilicate, described as "toffee-cracking" when observed in Middle Jurassic Brent Group sandstones by McTurk (pers. comm. 1980).
- E and F   Pore-filling pocket of blocky kaolinites. D, E, and F, sample 689, crevasse-splay sandstone, Cloughton Formation, Danby.
- G        Quartz overgrowth cemented sheetflood sandstone. Sample 385. Gristhorpe Member, Cloughton Wyke.
- H        Pore-filling gypsum. Sample 203. Crevasse-splay sandstones, Gristhorpe Member, Yons Nab.



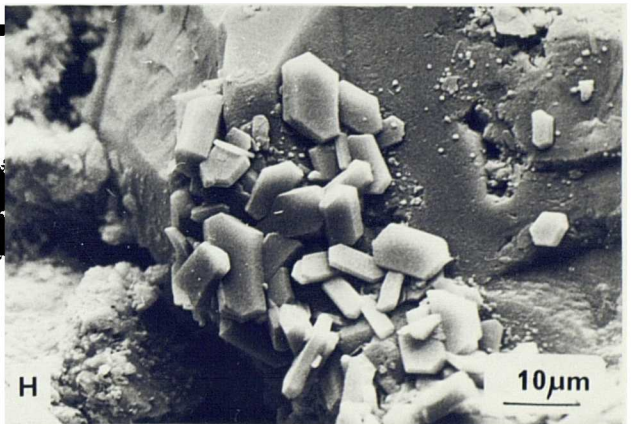
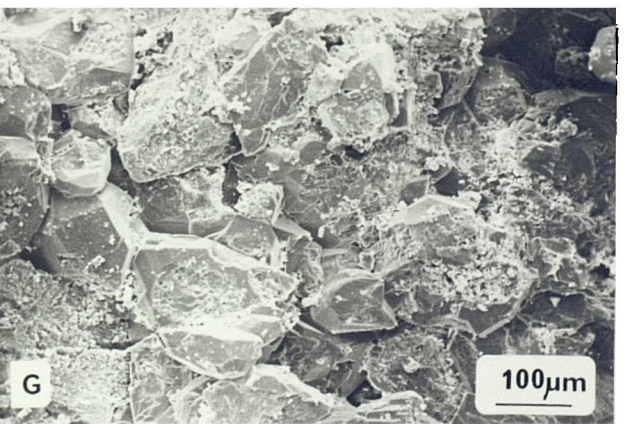
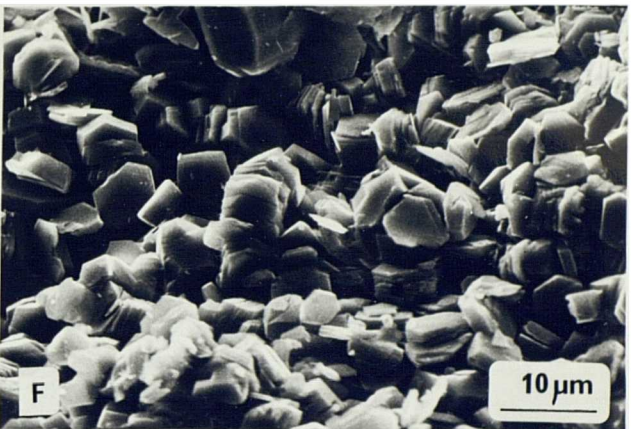
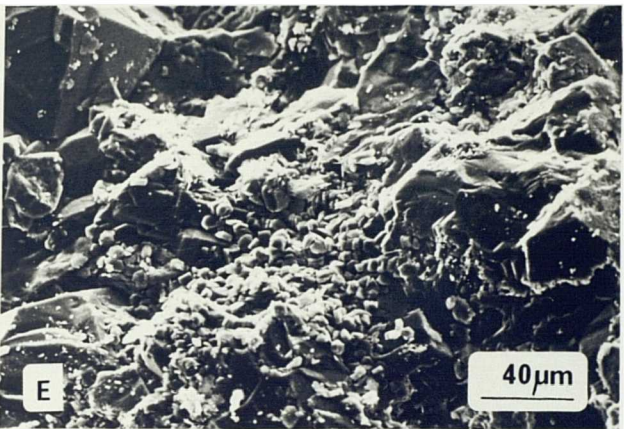
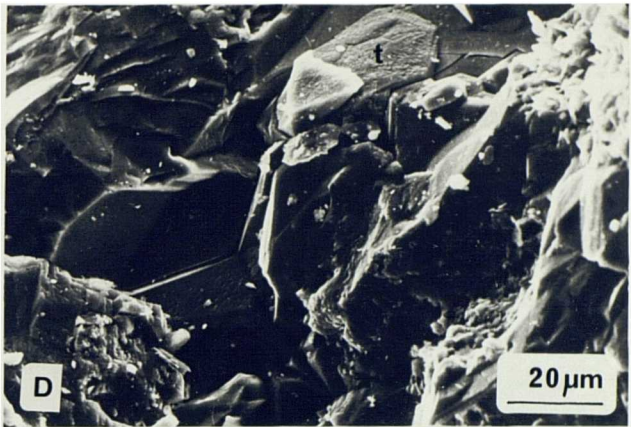
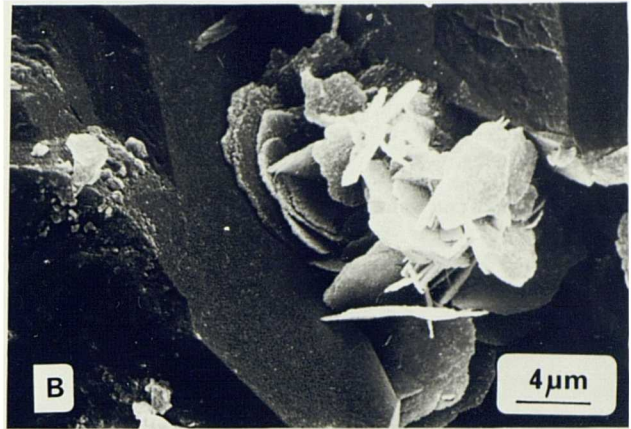




Plate 3.10

- A and B Dense pore-lining vermiculite, enclosed by subsequent  
C and D quartz overgrowths where thinnest. Quartz overgrowths  
not extensively developed because of inhibition by  
vermiculite. Sample 558. Beach sandstone, Scarborough  
Formation, Sneaton Quarry.
- E Authigenic sodium feldspar (f), and later illitic  
clays and blocky kaolinites. Sample 547. Intertidal  
sheet sandstone, Scarborough Formation, Bloody Beck.
- F Authigenic titanium oxide with orthorhombic form,  
probably brookite. Sample 393. Intertidal sheet  
sandstone, Scarborough Formation, Cloughton Wyke.
- G and H Pyrite crystals and pyrite framboid. Sample 263.  
Shallow-marine mudrocks. Scarborough Formation,  
Yons Nab.

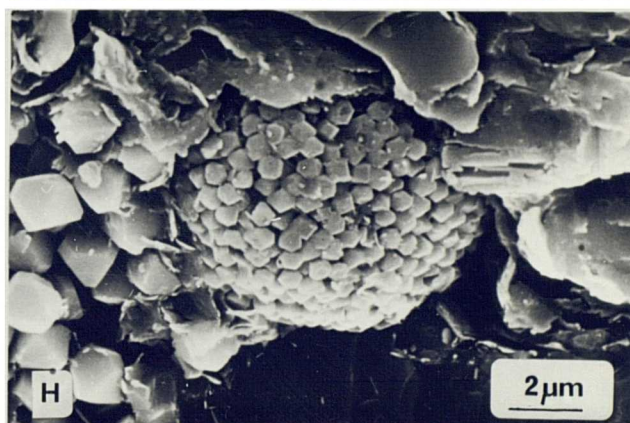
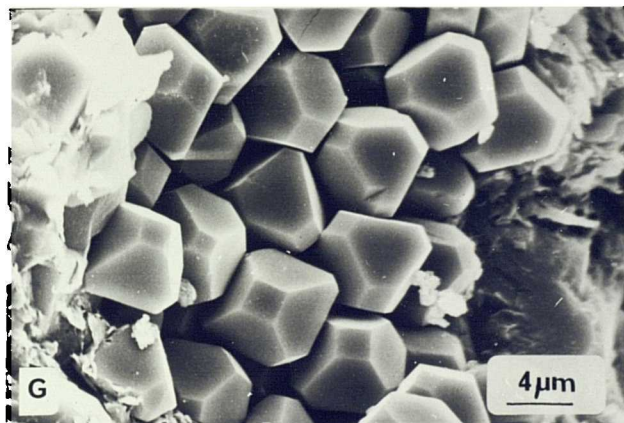
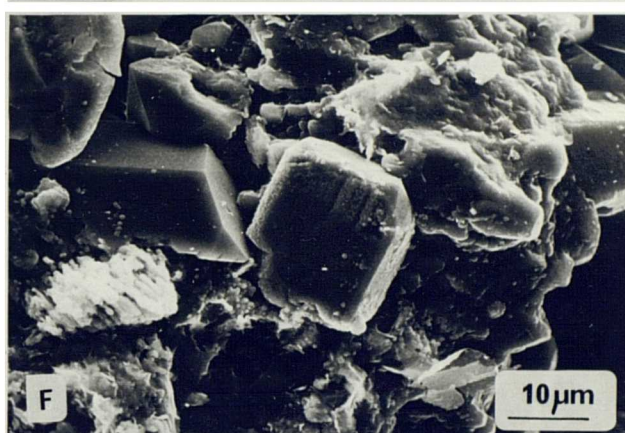
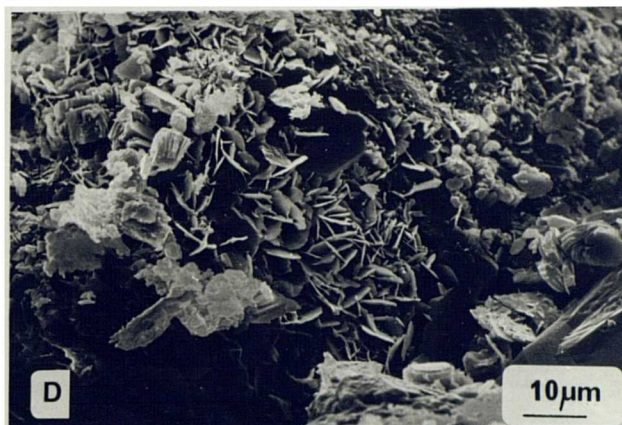
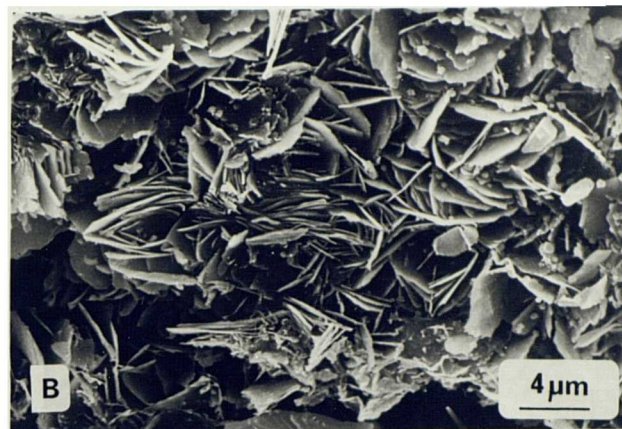
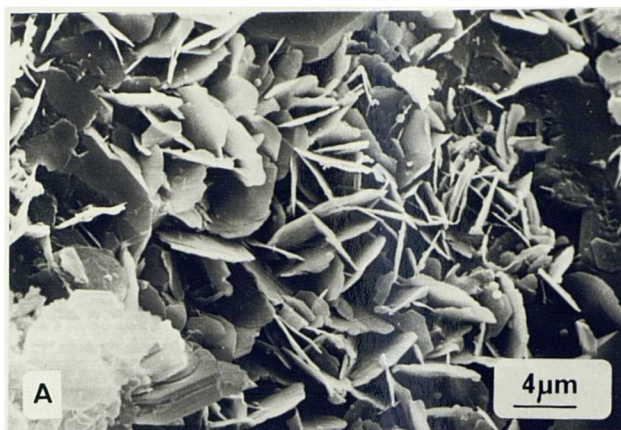


Plate 3.11

- A            Authigenic sodium feldspar (f).
- B            Pore-lining pyrite crystals. A and B intertidal  
sheet sandstone, sample 547, Scarborough Formation,  
Bloody Beck.
- C, D, E    Radiating, displacive calcite cement. Sample 401.
- F            General view of intertidal sheet sandstone with  
patchy calcite cement. Plate width 700  $\mu\text{m}$ .  
Sample 392.
- G and H    Slightly dissolved halite crystals irregularly  
filling pore space. Sample 395. C to H intertidal  
sheet sandstones, Scarborough Formation, Cloughton Wyke.



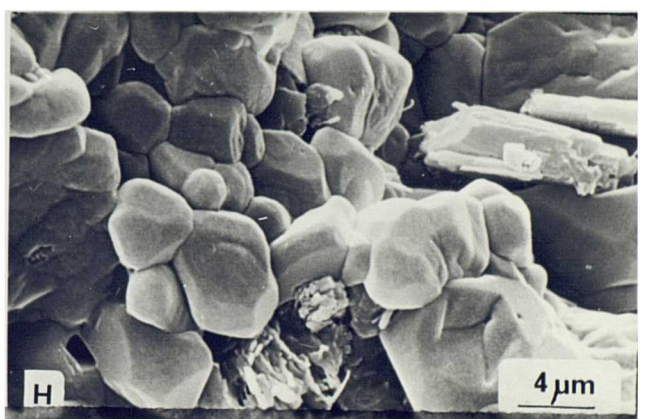
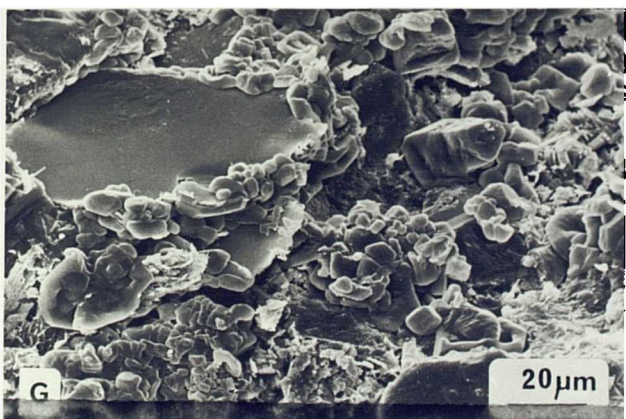
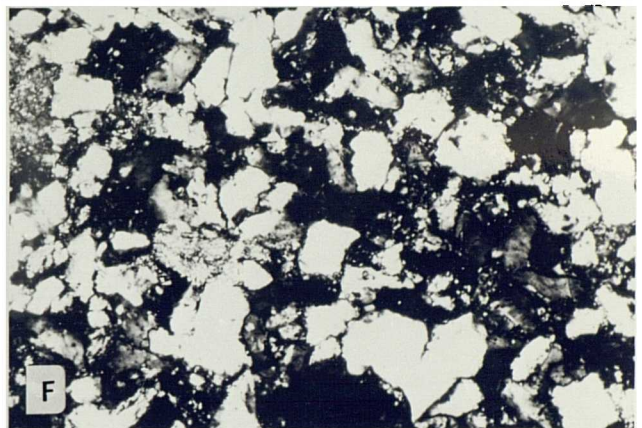
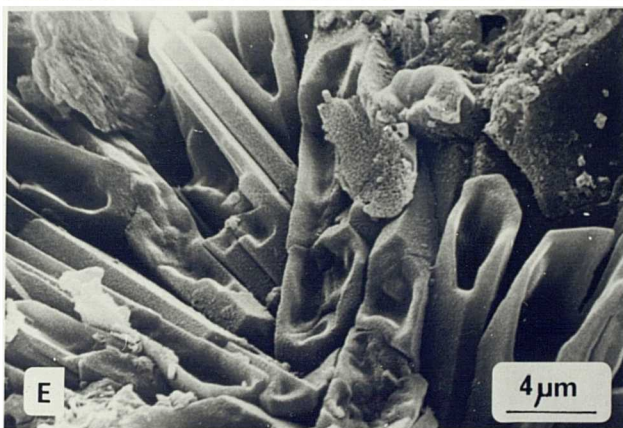
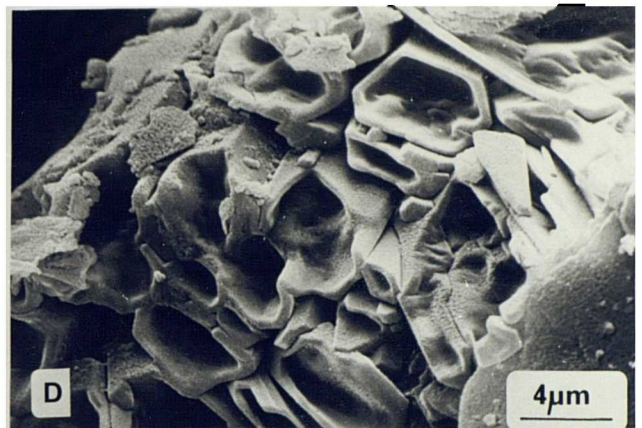
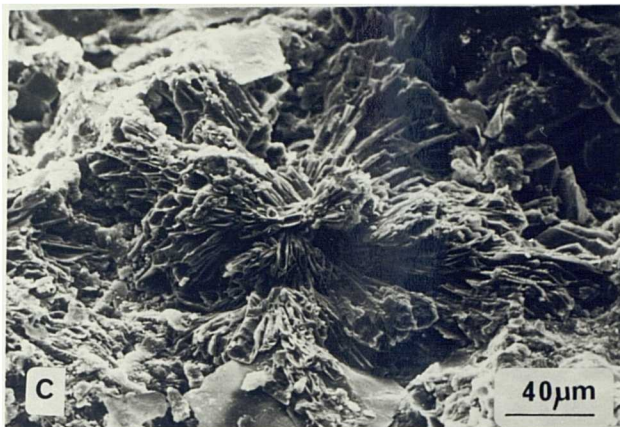
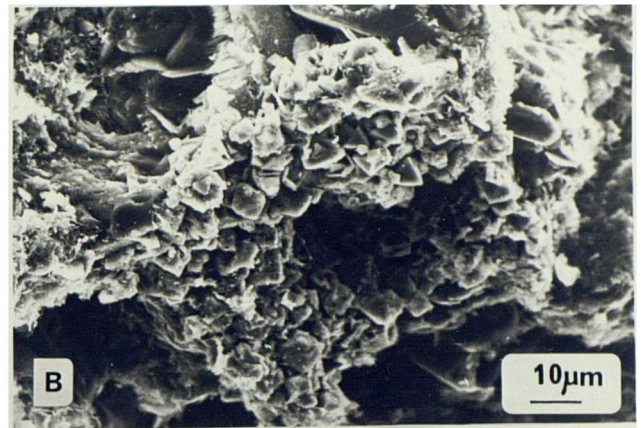
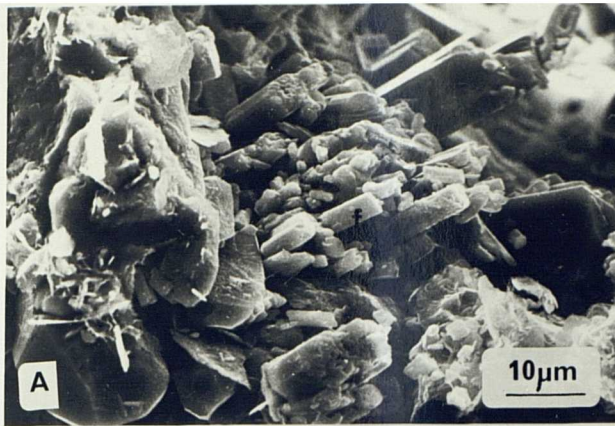


Plate 3.12

- A and B Illitic hairs. Sample 547. Intertidal sheet sandstone, Scarborough Formation, Bloody Beck.
- C General view showing quartz overgrowth cementation preserving wide, open pore throats. Sample 583. Braided channel sandstones, Moor Grit Member (NZ 682095).
- D Blocky pore-filling kandites. Sample 471.
- E General view showing porous nature of Moor Grit Member, also illustrating large euhedral overgrowths on simple detrital quartz grains (s), and numerous small, incipient overgrowths on polycrystalline detrital grains (p). Sample 507.
- F Corroded quartz overgrowth. Plate width 550  $\mu$ m. Cross-polarised light. Sample 491.
- G Tight quartz overgrowth cementation. Plate width 2.8 mm. Cross-polarised light. Sample 448.
- D, E,  
F and G Braided-channel sandstone, Moor Grit Member, Hundale Point.
- H Siderite spheruliths from a soil horizon. Sample 703. Floodplain mudrocks, Long Nab Member, Crook Ness. Plate width 3.5 mm. Plane-polarised light.



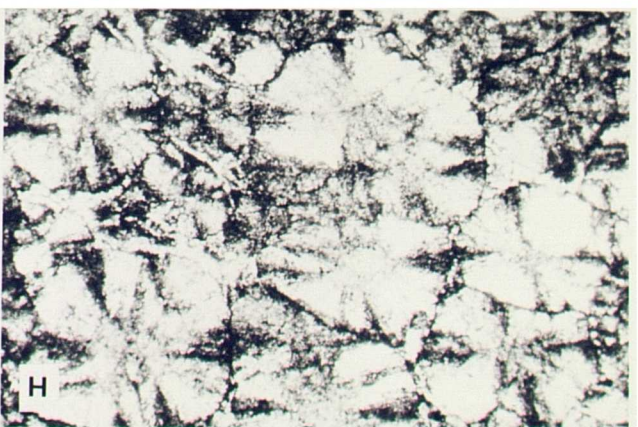
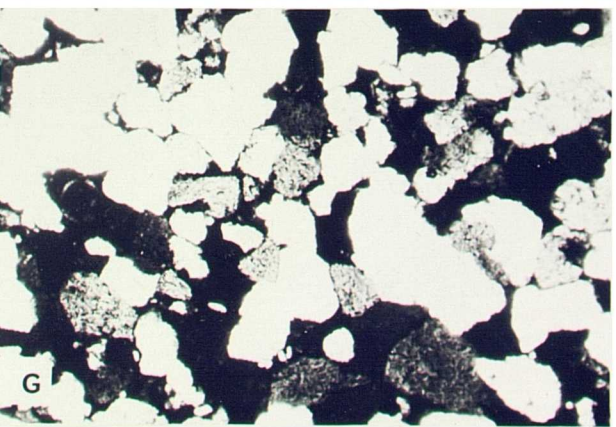
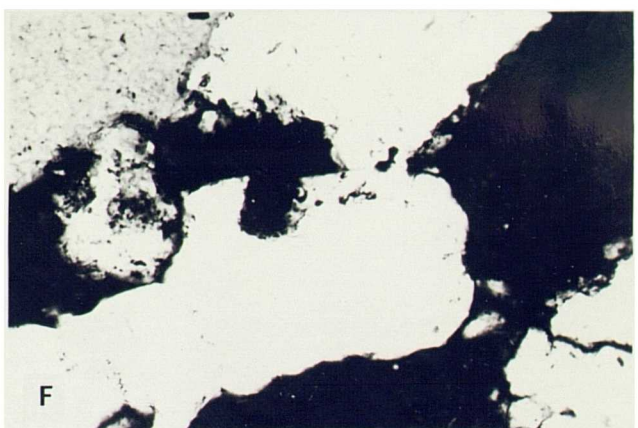
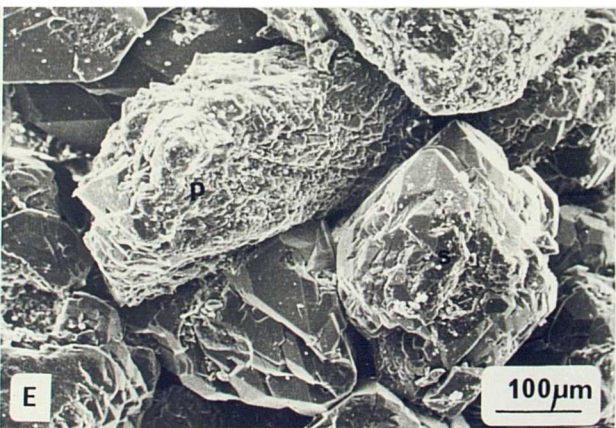
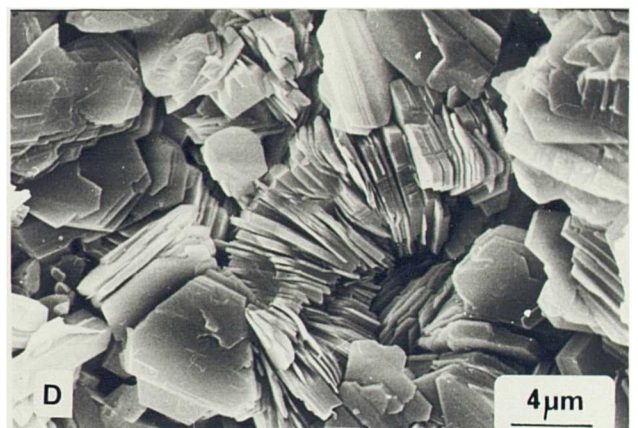
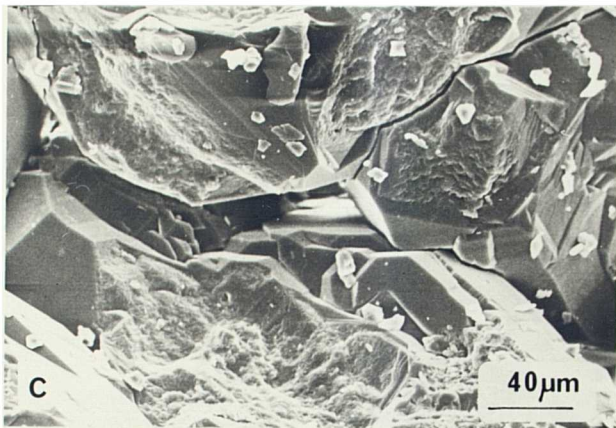
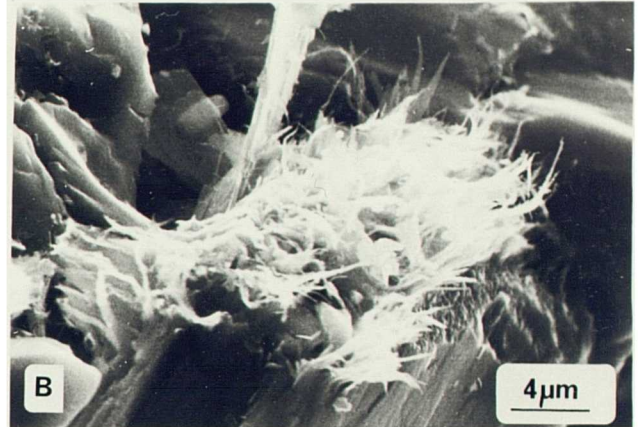


Plate 3.13

- A        Pore-lining chlorite, enclosed by subsequent quartz overgrowths Sample 540. Braided channel sandstone, Moor Grit Member, Bloody Beck.
- B        Pore-lining vermiculite inhibiting overgrowths on detrital grains, and preserving intergranular pore space. Sample 645. Braided-channel sandstone, Moor Grit Member, May Beck.
- C and D   Pore-lining chlorite, forming rosettes, but enclosed beneath quartz overgrowths. Braided channel sandstones, Moor Grit Member, Eller Beck Bridge, and Bloody Beck respectively. Samples 701 and 542.
- E and F   Extensive pore filling of blocky kandites, adjacent to a stepped face on quartz overgrowth. Sample 698.
- G and H   Extensive pore-filling blocky kandites. Filling pore space created by corrosion of quartz (c) in G. Blanketing pore space in H. Note stepped face on quartz overgrowth (s). Plate G, Width 875µm.
- E,F,G and H, braided-channel sandstones, Moor Grit Member, Eller Beck Bridge, and Hundale Point respectively. G Sample 472, H Sample 471.



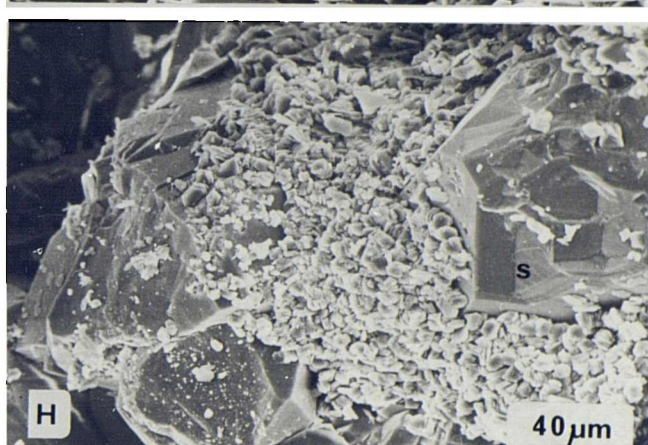
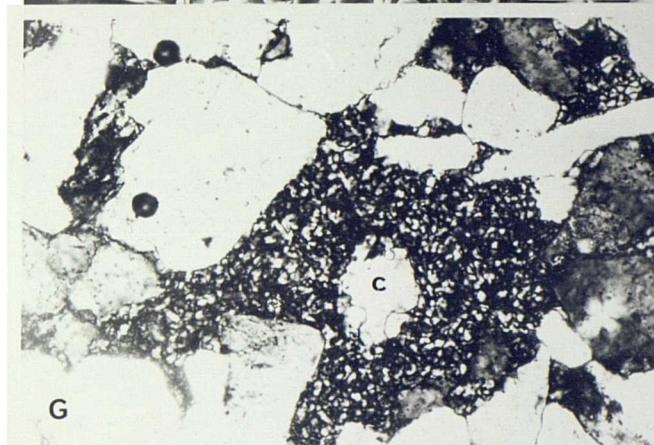
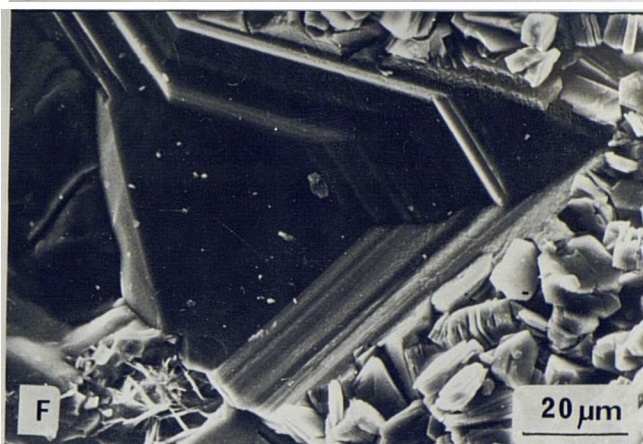
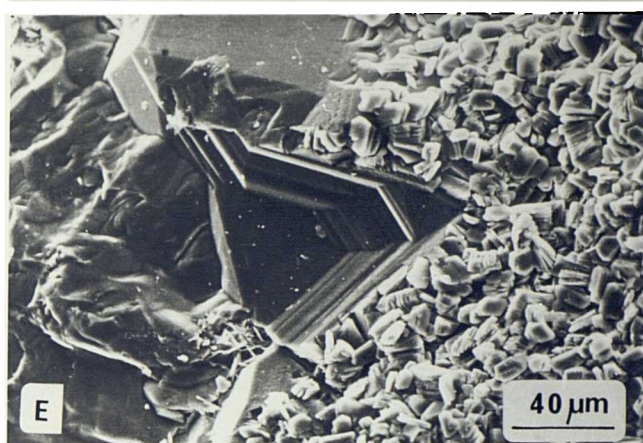
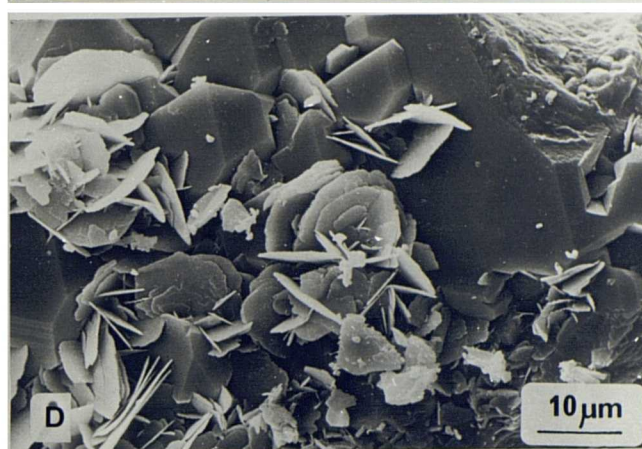
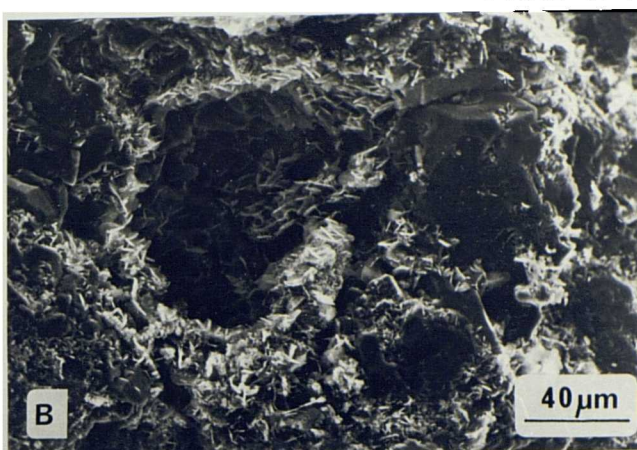
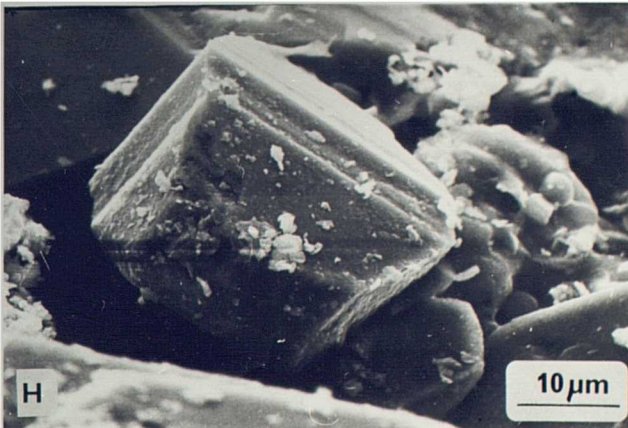
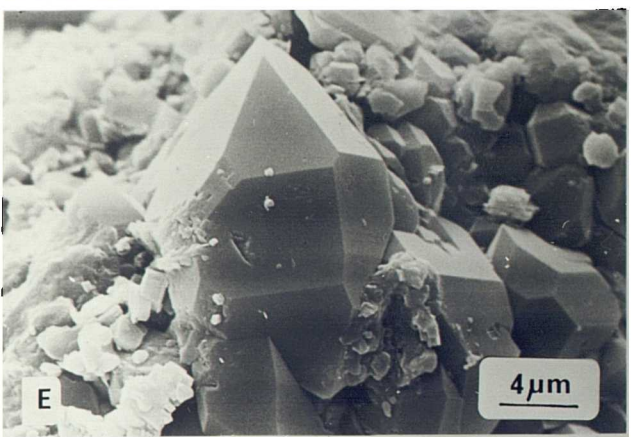
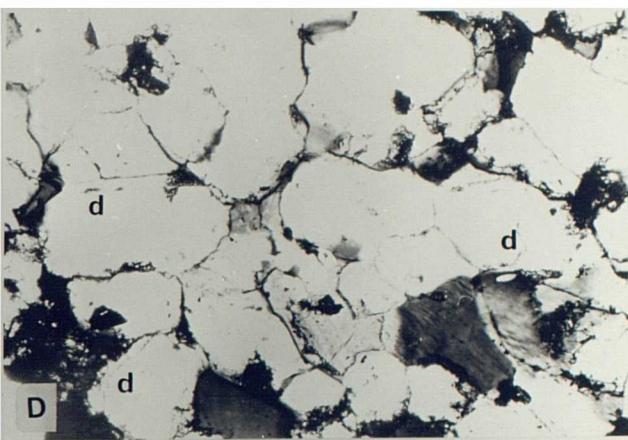
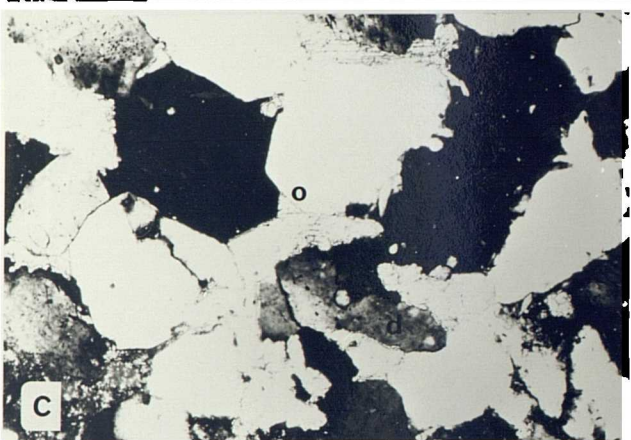
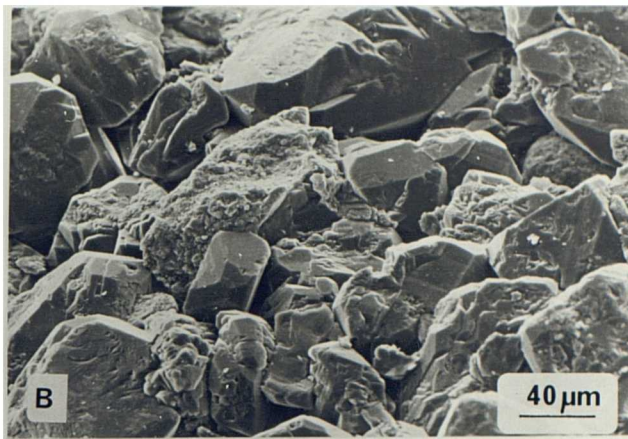
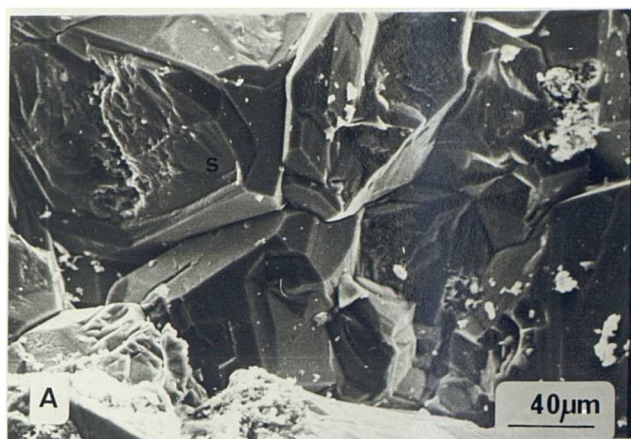




Plate 3.14

- A and B Contrast of tight quartz overgrowth cementation in A, loose cement preserving an open framework in B. Note stepped faces on quartz overgrowths (s) in A. Crevasse-splay sandstone and channel sandstone, Long Nab Member, Cromer Point, and Boltby Reservoir respectively. Samples 452 and 410.
- C Quartz overgrowth cementation, and subsequent corrosive calcite cementation. Calcite replaces edges of detrital grains (d), but not overgrowths (o). Sample 247. Channel sandstone, Moor Grit Member, White Nab. Plate width 875 $\mu$ m.
- D Tight quartz overgrowth cementation, in which detrital grains may be distinguished from overgrowths by dust rims between the two (d). Sample 452. Crevasse-splay sandstone, Long Nab Member, Cromer Point. Plate width 875 $\mu$ m.
- E Authigenic quartz. Sample 435. Channel sandstone, Long Nab Member, Scarborough Quarry.
- F Pore-lining chlorite. Sample 485. Crevasse-splay sandstone, Long Nab Member, Crook Ness.
- G Pore-filling barytes crystals. Sample 701. Braided channel sandstone, Moor Grit Member, Eller Beck Bridge.
- H Authigenic titanium oxide with tetragonal form, probably anatase. Sample 650. Braided channel sandstone, Moor Grit Member (SE 71/92).



CHAPTER FOUR: SEDIMENTOLOGY AND DIAGENESIS OF MIDDLE JURASSIC BRENT GROUP  
CORES FROM WELLS 3/3-1, 3/3-2 AND 3/3-3, NINIAN FIELD,  
EAST SHETLAND BASIN

"...it is astonishing and incredible to us, but not to Nature,  
for she performs with utmost ease and simplicity things which  
are even infinitely puzzling to our minds, and what is very  
difficult for us to comprehend is quite easy for her to perform!"

Galileo

In this chapter I should like to record both the description of sedimentological logs and their environmental interpretations, and the results of petrographical analyses of three cores through the Middle Jurassic Brent Group from the Ninian Field. The sedimentological logs and interpretations serve two purposes, firstly to revise and refine the depositional model proposed by Albright et al, (1980), and secondly, to facilitate comparison of petrography and diagenesis between differing depositional environments. Subsequently, petrographical analysis is summarised within the context of the depositional framework established from facies analysis of the three cores, further enhancing comparison of the results from specific environments.

I should like, briefly, to make two points. Firstly, 'facies' is used in a descriptive sense here. Secondly, these sandstones are all texturally and mineralogically mature, and so these criteria cannot be used in support of any later sedimentological interpretations. Composite lithological and wireline logs of the three cored wells are recorded in Figs. 4.1, 4.2, and 4.3 for 3/3-1, -2, and -3 respectively. Finally, petrographical data are compiled in Appendix F.

## SEDIMENTOLOGY

Cores from Wells 3/3-2 and 3/3-3 (Figs. 4.4 and 4.5 respectively) are discussed together in the succeeding sections. The core from 3/3-1 is too short to be of sedimentological value and is discussed separately below.

### Core Description

Coarse-basal sandstone facies. This facies overlies dark grey, locally micaceous mudrocks which contain both siderite and pyrite nodules. These mudrocks are inferred to be Liassic in age, although the nature of the contact is not clear: it is sharp and irregular rather than gradational. It is not possible, however, to deduce from either the data provided or from the cores themselves, what thickness, if any, of Liassic strata has been eroded. The coarse-basal facies, 39' thick in 3/3-2, (10607'-10568') and 41' 10" thick in 3/3-3 (10654' 10"-10613'), can be subdivided into two sub-facies. The lower subfacies, 14' thick in 3/3-2 (10606'-10593') and 24' 10" thick in 3/3-3 (10654' 10"-106301'), is a very coarse-grained sandstone and is almost conglomeratic in places. In this facies sedimentary structures differ slightly between the two wells. In 3/3-2, very coarse to coarse sand laminations occur. They have scoured erosive contacts and are characterised by basal laminae of well-rounded pebbles and wavy lamination. In 3/3-3, this basal subfacies is more massive but contains similar well-rounded, pebble-based lags of very coarse sand which pass upwards into coarse sand. Wavy and horizontal lamination, the latter occurring particularly towards the base, are characteristics of this subfacies. The coarse sand and pebbles observed either at the basal contact, or in the overlying pulses, are composed of quartz, and therefore have not been derived from the underlying grey and black mudrocks. Finally, although suggestions of bioturbation were observed at the base of each core, only one distinctive burrow was recognised.



Brown concentric clasts occur scattered around 10632' in 3/3-3.

This subfacies passes gradationally upwards into medium- to coarse-grained sandstones. These are locally massive, but sedimentary structures, such as horizontal lamination and low-angle cross-bedding, occur throughout. In the laminated sections scattered woody debris rather than pebbles mark the lags of individual beds. Although this subfacies is burrowed, intensive bioturbation, resulting in the destruction of primary sedimentary structures was not observed. Burrows, including the presence of recognisable Diplocraterion and Teichichnus occur. Other burrows preserved are both vertical and horizontal types, although the latter predominate. Furthermore, bioturbation increases upwards through these sequences, with recognisable escape burrows increasing towards the top of 3/3-2. No fine parting laminations or intercalated mudrocks were observed in these coarse-basal sandstones, although couplets of mica and fine sand occur as laminae towards the top, and pass gradually into the overlying micaceous sandstone.

Micaceous sandstone facies. The coarse-basal and sandy-laminated sandstone subfacies pass upwards into 50' of micaceous sandstone in both cores (3/3-2, 10518-10568' and 3/3-2, 10567-10613'). This facies is medium grained in the lowermost two feet, but fine grained throughout the remainder. The strata at the base are bioturbated, with horizontal, transverse and vertical burrows. However, bioturbation decreases upwards and was not observed above the lowest 10'. The whole facies, from its base and through the bioturbated subfacies is characterised by either low-angle cross-lamination or horizontal lamination. Within these laminae, each fine-grained layer of sand, 3-10 mm thick, is separated by a discrete layer of mica and fragmented plant debris. Minor infrequent erosion surfaces were observed, particularly between cosets of laminae with noticeably different angles. In addition, the few traces of woody debris present are concentrated at the bases of individual sets.

Although the contact between the micaceous sand facies and the underlying facies is generally gradational, the former is overlain erosively by a massive sandstone facies in 3/3-2. The junction between the two is not present in 3/3-3, where the relevant core is missing, but the overlying strata are distinctly coarser.

"Massive" sandstone. I should like to point out that this sandbody is not sedimentologically massive, sensu strictu: it is laminated and locally cross-bedded. The term "massive" has been used here to denote a thick sandbody with no lithological variations. This follows the original sense of Bowen (1975), and retains a degree of consistency with existing stratigraphical divisions.

The micaceous sandstone is overlain, and incised into, by a thick or "massive" sandstone. This sequence, 47' thick in 3/3-2 (10471-10518') and 51' thick in 3/3-3 (10517-10568'), contains coarse- to fine-grained sand, which is only occasionally micaceous, and is generally subdivisible into fining-upwards facies units. Two repeated units of this facies are observed in 3/3-2 (10507-10578' and 10471-10507' respectively). Within each unit the sediments 'fine' from a very coarse lag to a medium-grained sandstone. Woody debris occurs in both, whilst the lower one is based on a pebble-lag deposit. This lower unit also contains low-angle cross-bedding throughout, and has concentrations of micaceous and leafy plant debris as partings between sand-dominated laminae. In addition, prominent erosion surfaces occur between sets of laminae at distinctly different angles. The upper unit in this core also contains low-angle cross-lamination at its base, and horizontal lamination towards the top.

A similar pattern was observed in 3/3-3 where two cross-bedded sandstones fine upwards from coarse bases into medium-grained sandstone (10534-10547'

and 10547-10565' respectively). Both are more massive than those in 3/3-2, although micaceous partings were not observed. In these units laminations are best developed in finer grained parts. The upper unit passes or coarsens upwards gradually into a significantly different facies. This is a 15' thick medium-grained sandstone which is locally massive, but contains a wavy laminated portion with micaceous partings in which bioturbation was observed. This sandstone facies is also bioturbated at the top. In both cores the massive sandstone has a sharp top, and is overlain by fine sandstones and mudrocks.

Coarsening-upwards facies. The "massive" sandstone is overlain by repeated coarsening-upwards units with a combined thickness of 41' in 3/3-2 (10429-10471) and 52' in 3/3-3 (10465-10517'). The units immediately overlying the massive sandstone occur above a fine sandstone of uncertain affinity. These and all the other units, have basal mudrocks, and coarsen upwards through sequences of silty mudrocks and silty sandstone to fine- or medium-grained, sharp-topped sandstones. All the units are bioturbated, with vertical, inclined and horizontal burrows preserved in places, whilst elsewhere, primary sedimentary structures have been destroyed. Bioturbation is particularly common in the lower portions of each unit, where preserved primary sedimentary structures pass from horizontally laminated and wave-rippled mudrocks and silty mudrocks through low-angle climbing-ripple laminated silts and sands, into climbing ripple, cross-laminated and low-angle cross-bedded sandstones.

Plant debris occurs throughout the units, especially in the mudrock sequences where a whole leaf was observed (3/3-2, at 10465'). Although rootlets are absent at the base, they occur more frequently towards the top. Indeed, the uppermost unit in 3/3-2 is overlain by a coal. These units do not coarsen gradually or smoothly upwards; in several places within otherwise mudrock-rich sequences, discrete 1-2' thick climbing-ripple laminated fine sandstone

subfacies units occur, with sharp bases and sharp tops.

These sequences of coarsening-upwards units are succeeded by sequences of fining-upwards units. Unfortunately, apart from sporadic coal deposits, it is not clear whether the intervening mudrock subfacies has more affinity sedimentologically to those either above or below. The boundary between the two has, therefore, been taken, albeit arbitrarily, above the coarsening-upwards facies sequences.

Fining-upwards facies. In both cores, units of fining-upwards sandstone, siltstone, and mudrock erosively overlie the coarsening-upwards units. In general, the remaining 127' of 3/3-2 (10307-10429') is comprised of these units. A massive sandstone, however, (see below) which separates two sequences of fining-upwards units (10397-10465' and 10278-10323' respectively), also occurs in 3/3-3. Each fining-upwards facies unit invariably has a sharp, erosive base and fines from very coarse-grained sandstone with a pebble- or woody-lag deposit, through coarse- and medium-grained sandstone, fine sandstone, and siltstone, to silty mudrocks and mudrocks. In addition, within the uppermost mudrock subfacies, small 1-2' thick sharp-topped and sharp-based subfacies of fine- to medium-grained sand occur. Moreover, in places, short, intercalated coarsening-upwards facies occur, for example, 7' in 3/3-2 (10328-10335'), capping mudrocks and underlying further units of fining-upwards facies. The arbitrary nature of the junctions selected between these fining-upwards facies units and the underlying coarsening-upwards facies units is exemplified in 3/3-3, where there is no complete fining-upwards facies in the first 30' of the sequence. This horizontally laminated subfacies is, however, included here, rather than below, because coals also occur in horizontally laminated subfacies higher in the sequences, within fining-upwards units, whereas they do not occur in the coarsening-upwards facies below.



Bioturbation was observed in both cores, especially within finer grained subfacies where primary sedimentary structures are often obliterated. Both vertical and horizontal burrows are preserved in these bioturbated sediments. Fining-upwards facies units typically have erosive bases, marked with a lag of woody debris and pebbles. Similar lags occur between cross-laminated cosets in the coarse subfacies. From their erosive bases, units pass upwards through massive, locally micaceous sandstones, and cross-bedded coarse- to medium-grained sandstones, to horizontally laminated or ripple-laminated fine sandstones and siltstones, and finally, mudstones. Climbing-ripple lamination was recognised in several sharp-based and sharp-topped sandstone units from both the lower mudrock dominated part of 3/3-3 and towards the top of 3/3-2, 10446' and 10343' respectively.

The fining-upwards facies is only locally micaceous, with few concentrations or discrete partings either in the mudrocks or in the intercalated sandstones. Coarse woody debris occurs in lag deposits, and fragmented stems and leafy plant debris occurs in the finer subfacies. In addition, rootlets are common, especially in the finer mudrock dominated subfaces, and beneath poorly developed coals, for example, in 3/3-3 at 10438'. "Fining upwards" is particularly well demonstrated on an extremely small scale, at the top of 3/3-2 (10307-10320'), where a sandstone occurs, comprising numerous discrete 2-8 cm thick laminae, which grade upwards from very coarse bases, often only one or two sand grains thick, with occasional pebbles, to coarse- or medium-grained sand. The two sequences of fining-upwards facies units are separated in 3/3-3 by a massive sandstone facies.

3/3-3 sandbody (10323-10397'). This 74' thick sandbody has an abrupt, although not noticeably erosive, contact with the underlying mudrock. It fines very slightly from medium sand at the base to fine sand at the top. Vague low-angle cross-bedding was observed in a few places only, although most of this

facies is massive, with no visible sedimentary structures. No erosion surfaces were observed within this sequence. The sand is uniformly well sorted throughout, with no micaceous partings or horizons, and no local coarse concentrations or pebble lags. No plant debris and no evidence of bioturbation, pedogenic deformation or rootlet development was observed.

### Interpretation

In the following sections I would like to propose, and discuss, an interpretation of the Brent Group in the Ninian Field. On the basis of the cores examined in this study, the Brent Group is interpreted as a shoreface-lag and possible beach deposit, overlain by predominantly storm-driven foreshore and shoreface sediments, dissected by distributary-channel sands, and succeeding interdistributary bay-filling sequences and finally, floodplain deposits, including fine-grained alluvium, coals, and channel sandstones. The sequence is therefore inferred to record an initial transgression, and subsequent shoreline progradation. It is unclear whether this progradation is actually related to regression.

Coarse-basal sandstone facies. This facies is interpreted as accumulating following an erosive transgression onto Liassic strata. Above the shoreface erosion plane occur lag deposits and a possible beach with succeeding storm-driven and fairweather foreshore to shoreface sediments, reflecting deepening water. Interpretation of ichnofaunal evidence and sedimentary structures suggests that most of the sediments were deposited in high-energy nearshore environments. The extremely well sorted nature of the sediments also supports a high-energy setting.

The coarse-basal sandstone may be subdivided into two subfacies: a lower subfacies of erosively based beds, graded from coarse sand and granules, to

medium-grained sand, and an upper subfacies of horizontally and low-angle, cross-bedded micaceous sandstone, bioturbated and fining upwards. The contact between the coarse-basal sandstone facies and the underlying Liassic mudrock is abrupt, and slightly angular or undulating. Furthermore, the mudrock was, presumably, already lithified during deposition of the sand, as there is no evidence of the soft sediment deformation one would expect from deposition of such a thick sequence of clastic sediments onto unconsolidated clays (Fitzgerald and Bouma, 1972). Although this basal sand is conglomeratic in places, with scattered pebbles, it is not a basal conglomerate, sensu strictu, as the coarse clasts were not derived from the underlying mudrocks.

This lower subfacies is interpreted as transgressive. It overlies a distinct erosion plane, and its initial deposits are probably a shoreface lag (Clifton et al., 1971). However, there is insufficient evidence to confirm or deny the suggestion (Gray and Barnes, 1981) that this sandstone marks a transgression onto a previously subaerially exposed surface.

The fining-upwards, massive or horizontally-laminated units, each with a scoured base, and coarse lag, in the lower subfacies could be indicative of channel deposits, with each bed reflecting waning flow events. Deposits such as these occur in meandering (Allen, 1965), braided (Rust, 1978), or tidal channels (Klein, 1970). In addition, the textural maturity of these sediments is consistent with tidal channel deposition (Balazs and Klein, 1972) following intense abrasion in nearshore high-energy environments. Moreover, tidal delta progradation in the modern Ossabow Sound has generated an analogous sequence (Greer, 1975), whilst Saunders and Kumar (1974) interpret thin, granule rich laminated sandstones at the base of a similar succession as tidal inlet lag deposits. Conversely, coarse pebbly lag deposits are also interpreted from ancient sediments as high-energy deposits from the swash zone during transgression (Bridges, 1976). Furthermore, coarse gravels and

sands occur as lags in the swash zone of modern high-energy beaches (Clifton et al, 1971) and are similarly interpreted from ancient deposits (Bluck, 1967). Finally, Clifton et al, (1973) report small-scale braided rivulets and channels which locally rework beach sediments.

Both tidal-channel deposits or coarse washovers (Elliott, 1978) should be succeeded by an erosive plane beneath the succeeding transgressive, storm-driven foreshore sediments. Moreover, ancient analogues, in which basal tidal lags occur, contain tidal flat sediments or intertidal sands and mudflats (Greer, 1975, and Johnson, 1975, respectively), evidence for which does not exist here. There is, therefore, no evidence for preservation of landward deposits beneath this transgression. The lower subfacies is consequently interpreted as a shoreface-lag deposit, in a high-energy environment, deposited during a transgression similar to that inferred by Bourgeois (1980). She describes a coarse-conglomeratic sandstone, cross bedded in places, which is interpreted as a beach to foreshore deposit. This deposit is overlain by successively finer grained storm-driven inner-shelf, and fairweather outer-shelf sediments.

Between the coarse beds at the base and the succeeding bioturbated, horizontally laminated facies occur massive sandstones. It is tentatively proposed that these are the remains of a beach, their destratification possibly being a pedogenic process (Bigarella et al, 1969, Budding and Inglin, 1981), and the scattered siderite spheruliths the remains of a poorly developed soil.

The horizontally and low-angle cross-laminated subfacies above is typical of high-energy shoreface and foreshore deposits (Howard and Reineck, 1972; Reineck and Singh, 1973). In isolation, this combination of horizontal and low-angle cross-lamination is not specific within the range of possible shallow-marine environments. However, these sediments are texturally mature,

and contain Diplocraterion, and, consequently, are probably nearshore deposits. Although this subfacies accumulated in a high-energy environment, the preservation of burrows, and the range of other sedimentary structures preserved is indicative of predominantly fairweather rather than storm-driven sedimentation.

The bioturbation observed in this upper subfacies only occasionally destroys primary sedimentary structures and is preserved as horizontal, inclined and predominantly vertical burrows. These include the presence of Diplocraterion, Teichichnus and escape structures. Teichichnus is not indicative of any particular shallow-marine environment, indeed, it is almost ubiquitous in marine sediments. Diplocraterion is interpreted as a marine indicator, but occurs typically in either intertidal (Mackenzie, 1963, 1965, 1971; Chamberlain, 1976), or shallow-marine shoreface environments (Hubert et al, 1972; Spencer, 1976). Conversely, escape structures are indicative of rapid sedimentation.

Beach, foreshore and upper-shoreface environments are characterised by a wide range of sedimentary structures. These include horizontal, wave-rippled, and antidune lamination, low- and high-angle cross lamination. Nevertheless, these and the associated bioturbation are generally only preserved during fairweather deposition, being destroyed during storm conditions when the potential for preservation of only low-angle cross- and horizontal-lamination is greatest (Thompson, 1937). These structures are, consequently, typical of storm-driven upper-shoreface or foreshore environments (Thompson, 1937; Hoyt and Weimer, 1963). Furthermore, Clifton (1969) describes discrete 1-2 cm thick laminations, comprising couplets of fine-grained (or high-density) minerals and coarse-grained (or low-density) minerals, which are directly analogous to the mica:sand couplets observed towards the top of this subfacies and in the overlying micaceous sandstone. Finally, similar sedimentary structures are interpreted by Embry et al, (1979), as resulting from deposition in beach or shoreface environments. Also, low-angle cross-lamination between

parallel bedding surfaces has been recorded from modern foreshores (Straaten, 1959; Andrews and Lingen, 1969). In addition, Thompson (1937) and Hoyt and Weimer (1963) discuss the preservation potential of these probably storm-driven deposits in comparison to the diverse range of fairweather deposits observed on modern foreshores. They conclude that storm-driven deposits are more likely to be preserved in the geological record.

Howard and Reineck (1972), as well as Kumar and Sanders (1976), report similar alternations of storm-driven parallel laminated and bioturbated fairweather deposits. Thus, the upper subfacies of the coarse-basal sandstone is interpreted as a nearshore deposit, accumulated during fairweather conditions with occasional storms generating horizontally laminated sediments.

Micaceous-sandstone facies. The coarse-basal sandstone passes upwards into 50' of micaceous horizontally- and low-angle cross-laminated fine sandstone. This facies is interpreted as the result of foreshore to shoreface deposition during storm conditions, on the basis of both lithology and bioturbation, as well as sedimentary structures.

The bioturbation which occurs at the top of the underlying coarse-basal sandstone facies decreases in intensity through the lower 10' of this facies, and is absent from the remainder. Vertical and inclined burrows predominate, with relatively fewer horizontal burrows. This general decrease in bioturbation upwards through the coarse-basal and micaceous sandstone could reflect increasing wave energy, due perhaps to the relative proximity of the shoreline towards the top of the sequence (Elliott, 1978). However, in combination with decreasing grain size (and hence, waning flow), it is more likely that this facies reflects deepening water, and more frequent storm activity, removing fairweather sedimentation. The remainder of the micaceous sandstone comprises discrete couplets of mica and fine sand,

analogous to those described by Clifton (1969) and interpreted as storm-driven sediments (see discussion above). The micaceous sandstone is, therefore, probably a shoreface deposit, resulting from storm conditions and deepening water above the coarse-basal sandstone. The micaceous sandstone is not interpreted as a prodelta deposit, indeed transgression rather than regression is inferred at this time.

In general, the vertical sequence of subfacies interpreted from these cores is identical to the lateral sequence of environments in modern and ancient high-energy wave-dominated shoreline (Clifton et al, 1971; Howard and Reineck, 1972; Johnson, 1975; and Hunter et al, 1979 respectively). In addition, the inferred sequence reflects progressively deepening water following the initial transgression recorded by the coarse-basal sandstone facies below. Consequently, the micaceous sandstone is interpreted as a foreshore to upper shoreface storm-driven accumulation, following an initial transgression, and during continued transgression.

"Massive" sandstone. This sandbody, comprising erosively based fining-upwards facies units and a possible reworked top, is interpreted as a distributary channel deposit. Consequently, a major environmental change is inferred, from the transgressive sequence below, accumulated in progressively deepening water to the prograding sequence above, initiated by these distributary channels, and culminating in a fluvio-deltaic complex.

Facies units are locally massive (s.s.) in both cores, but fine upwards through a sequence of high-angle cross bedding to horizontal lamination. This facies could be generated by either deepening water (Frazier, 1974), typified by meandering-channel deposits on point bars (Allen, 1965), waning channel flow, or low-sinuosity channel bars (Cant and Walker, 1976). Moreover, irrespective of whether they accreted laterally or vertically, repetition

of fining-upwards facies units occurs more commonly on floodplains (Allen, 1965; Nami, 1976b; Livera and Leeder, 1981).

Channel deposits are not restricted to fluvial settings, but may also occur in tidal or estuarine environments. Here the tidal or fluvial channel, carrying coarser grained sediments, migrates across finer tidal flats and muds, generating a coarsening-upwards sequence (Coleman and Wright, 1975; Howard and Frey, 1975a, 1975b). Tidal accumulations are typified by a high proportion of fine-grained sediment, which coarsens upwards into the actual channel deposits. Tidal-channel deposits themselves usually have scoured bases and internal scoured surfaces between cosets, as well as higher angle cross bedding (Klein, 1970; Mackenzie, 1972; and Reineck and Singh, 1973). Similarly, meandering or braided channels with their associated floodplains would accumulate characteristic sediments. The sequence here does not support any such concept. These channel deposits are incised into a transgressive sequence, and are succeeded by interdistributary-bay deposits. They are, therefore, interpreted as progradational distributary channel deposits.

The more massive coarsening-upwards facies at the top of 3/3-3 probably reflects shallow marine winnowing or reworking of the top of the distributary-channel sand. Local reworking during fairweather conditions would certainly account for the wavy-ripple cross-lamination and bioturbation observed (Kumar and Sanders, 1976).

The occurrence of distributary-channel deposits beneath the delta sensu strictu, reflects progradation, a marked change from the transgressive sequence below. There is no compelling evidence towards interpreting this sequence as coalescing mouth bars (cf. Albright et al, 1980), nor from which regression as well as progradation can be inferred.



Coarsening-upwards facies. Several coarsening-upwards facies units occur in both cores above the massive sand and are directly analogous to repeated interdistributary bay-filling sequences (Baganz et al, 1975; Elliott, 1975). Thus, the sequences in both cores begin with fine sand, probably reworked from the underlying coarser, massive deposits. These are overlain by bioturbated, wave-rippled, and horizontally laminated mudrocks with silty lenses, interpreted as having been deposited from suspension, and subsequently rippled in a relatively low-energy environment, restricted to either coarse clastic fluvial supply, or high-energy wave action. Nevertheless, the bioturbated nature of basal mudstones in these sequences is indicative of marine influence.

This facies coarsens upwards and its sedimentary structures record a progressive increase in energy. Therefore, above basal mudrocks, succeeding siltstones are ripple-laminated and contain climbing-ripple lamination whilst the overlying sands are horizontally laminated or contain low-angle cross-bedding. Conversely, bioturbation decreases in intensity upwards, with preserved burrows also decreasing in frequency upwards. At the base, primary sedimentary structures are often destroyed, and the remaining burrows are predominantly horizontal. Higher in the facies, burrow form changes to inclined and then vertical with an associated increase in escape structures. This sequence may reflect increasing rates of sedimentation and energy, as well as a decreasing ratio of sediment to organic matter - the mudrocks certainly contain a greater percentage of plant debris compared to the silts and sands. In addition, as the coarsest strata which cap each facies unit are rooted from above, one may infer that the changing environment was influenced relatively less by saline water. Proximity to a vegetated coastal or deltaic plain at this time is suggested by the concentration of locally derived whole and fragmented plant debris.

One such facies unit in isolation could have been deposited by progradation into a lagoon (Elliott, 1975), or delta front progradation, with the final sands representing a beach. However, a lagoonal environment would not be so easily re-established above the beach, whereas a further interdistributary bay could be (Coleman and Gagliano, 1964; Coleman and Wright, 1975). Thus, continuing subsidence following filling of any bay sequence, whilst the major distributary disgorged its sediment elsewhere, would regenerate the bay in the same area (Frazier, 1967; Frazier and Osanik, 1969). The interbedded sharp-based and sharp-topped sandstone subfacies, often characterised by climbing-ripple lamination, are interpreted as crevasse-splay sandstones, deposited from minor crevassing events deposited rapidly from arrested sediment laden suspension (Ashley et al, 1982), and emanating from a major proximal distributary channel (Elliott, 1975). Each coarsening upwards facies unit is rooted from above, and occasionally capped by a poorly developed coal. Consequently, each unit marks complete filling of the interdistributary bay to sea level, and subsequent emergence. Assuming continuing subsidence throughout this period, rather than intermittent bursts, each represented by a coarsening upwards unit, one may conclude that interdistributary-bay filling reflects an equilibrium between subsidence and sediment supply. Hence, continued sedimentation - crevasse splaying from adjacent distributaries - filled bays rapidly to sea level and emergence. Conversely, during periods of quiescence with only occasional crevasse-splay episodes, sedimentation either matched subsidence and maintained water depths, or water depth increased. Consequently, periods of emergence are succeeded by continuing subsidence and hence renewed marine influence above coals, unless fluvial supply maintained a wholly alluvial environment. These coarsening-upwards units lowest in the sequence are overlain by pyritic mudrocks, implying renewed open marine influence, whilst those higher in the sequence and succeeded by alluvial sediments reflect more pronounced fluvial influence.

The significance of pyrite is discussed at length elsewhere, but it is summarised here to elucidate the genesis inferred above. Pyrite only forms under anoxic, reducing conditions (Berner, 1971), from solutions rich in sulphate ions, which fresh and meteoric waters are not. Whilst sea water contains sulphate ions, it is not normally anoxic. Conversely, restricted lagoonal and interdistributary bay areas are often density stratified or have poor circulation; here anoxic conditions frequently develop.

The repeated coarsening upwards facies above the massive sandstone are, therefore, interpreted as interdistributary bay-filling sequences formed adjacent to the distributary. The overall environment had changed from one of wave domination to fluvial domination.

Fining-upwards facies. This facies is interpreted as a fluvial channel deposit. Consequently, its repetition throughout the sequence is indicative of continued fluvial supply and floodplain accretion. Coarse-member subfacies within individual units have erosive bases, woody- and pebbly-lag deposits overlain by massive and high-angle or trough cross-bedded sandstones which fine upwards. Similar deposits occur in a range of channel situations from high- and low-sinuosity river systems on alluvial plains (Allen, 1965; Puigdefabregas and van Vliet, 1978; Smith, 1970; Miall, 1977 respectively), as well as in tidal estuaries (see above). These are interpreted as fluvial because sedimentary structures are unidirectional, and the sediments in the coarse member are texturally mature, whilst those in the fine member subfacies are plant colonised, indicating a probable floodplain setting.

Fining-upwards units may be subdivided into coarser sandy subfacies - channel fills - and finer mudrock dominated subfacies - floodplain or overbank deposits. It is not really possible from cored sequences to distinguish between vertically accreted channel filling (Moody-Stuart, 1966; Campbell, 1976) or laterally accreted point bars (Allen, 1965; Moody-Stuart, 1966). Individual

channel deposits vary in size, presumably reflecting their original depths, from between 10' on average, to the extremely coarse, 21' thick member, in 3/3-2 (10328-10307'), the top of which is not seen. Finally, a high- rather than low-sinuosity system may be inferred tentatively from the high fine- to coarse-member ratio in these sediments (Moody-Stuart, 1966).

The fine-member subfacies comprises horizontally and ripple-laminated mudrocks and siltstones, typical deposits of low-energy systems. These deposits are interpreted as having been deposited on a floodplain from suspension and probably in standing water. The floodplains were poorly drained and probably not subaerially exposed in this area, hence the poorly developed soil profiles, and lack of desiccation cracks. Bioturbation, which occasionally destroys primary sedimentary structures, is preserved as horizontal and inclined burrows in places. These mudrocks are also commonly rooted, although unlike the coarsening-upwards facies below, rootlets are not associated with coals. Thus the floodplain environment is interpreted as one of standing water with lagoons, lakes and vegetated swamps, with poor drainage and infrequent sediment supply from the major distributary channels.

Associated with the fine-member subfacies are two interbedded subfacies: sharp-based and sharp-topped climbing-ripple laminated sandstones, and short coarsening-upwards facies units. The former are interpreted as crevasse-splay sandstones (see discussion above) produced by decelerating flow during minor avulsion events, and the latter as filling lakes, lagoons, or bays, by the same essential process of crevassing and overbank flooding. Indeed, the short coarsening-upwards unit beneath a fluvial-channel sand at 10330' in 3/3-2 may be the channels levee.

3/3-3 sandbody. In view of the complete absence of diagnostic features within this sandbody, it is not possible to interpret its depositional environment.

However, a fluvial, possibly distributary channel origin may be inferred from the association of floodplain sediments above and below, and the lack of any significant sedimentological changes either at the onset or cessation of its deposition. It is not possible to evaluate the suggestion that this sandbody is a "dune sand" (Eynon, 1981), although this interpretation is not favoured here.

In general, the fining-upwards facies and floodplain association above the interdistributary-bay filling sequences is analogous to the modern, progradational, fluvial-dominated Mississippi delta (Coleman and Wright, 1975). These Brent Group sediments are probably lower delta plain deposits, supplied by distributary channels from a larger river system to the south, meandering through a vegetated coastal plain. Hence, the juxtaposition of coarse woody debris in channel lag deposits and small rootlet developments on the floodplain at this time.

3/3-1. This core is too short to be of value in facies analysis of the Brent Group as a whole, although its depositional environment may be inferred by analogy to the facies described above. The cored interval, therefore, passes through an interdistributary-bay fill (9927-9920'), and two fining-upwards channel deposits, interbedded with floodplain mudrocks (9909-9920', and 9893-9909' respectively - Fig. 4.6).

Summary. Although some of the more general conclusions reached above are at variance with interpretations from elsewhere within the East Shetland Basin, this is perhaps to be expected when one considers the variations that may occur laterally and temporally in a deltaic complex covering at least 1200 km<sup>2</sup> (cf. Coleman and Wright, 1975; Elliott, 1975, 1976; Livera, 1981).

The Brent Group in the Ninian Field is interpreted as having been deposited

in a wave- and fluvial-dominated, initially transgressive and subsequently progradational shoreline. A shoreface lag, and beach deposit at the base, represents the transgressive episode onto the Liassic. This was succeeded by progressively deeper water environments during the subsequent transgression, producing a fining-upwards sequence of alternating fairweather and storm-driven foreshore, and upper shoreface sediments. These pass gradationally from the coarse-basal sandstone, into and through the micaceous sand. However, the massive sandstone incision represents a major change in the hydrodynamic regime at this time, to fluvial domination. The subsequent deposits represent an erosively incised, possibly distributary channel, cut into the shoreface sequence. Subsequently, during progradation distributary channel breaching of this high-energy shoreface created a coastline dominated here by interdistributary bays. The coarsening-upwards facies results from progressive filling of these bays with crevasse-splays and peat accumulations produced with each successive filling to sea level.

Subsequently, the fluvial distributary system prograded over these sequences, as a wide floodplain with possible high-sinuosity or meandering channels incised into finer member floodplain deposits. The floodplain at this time was probably permanently flooded with standing water, lakes and with an extensive vegetation. The channel deposits are, therefore, intercalated with poorly developed soils, crevasse-splay sands, and coarsening upwards bay-, lagoonal-, and lake-filling sands. Whilst absence is not a particularly valid scientific criterion to use, the absence of garnet from these sediments is consistent with its absence elsewhere in Brent Group sediment, derived from the southeast (Gray, in discussion to Gray and Barnes, 1981).

This study has not generated sufficient data to allow comment on the salinity of interdistributary bay and floodplain environments, or on the proposed marine incursion at the top of the Brent Group, although it is not clear whether or

not these cores extend to the Tarbert Formation.

### Discussion

I should like to discuss briefly three topics: a comparison of this facies interpretation with other models for Brent Group sedimentation; whether progradation here actually reflects regression; and the relationship between facies divisions in this study and conventional Brent stratigraphy.

Although the model proposed differs from that of Albright et al (1980), the differences are not significant. Both models propose a transgression and progradation of a fluvial system, although this study suggests a distributary channel rather than mouth bar origin for the massive sand. Furthermore, although Albright et al (1980) interpret their Zones I and II as marine, they refer to them as prodelta sands, whereas in this study a transgressive origin unrelated to deltaic progradation is inferred. Elsewhere in the basin, coarsening upwards sequences are reported and interpreted as barrier islands or other regressive features. It is likely that the discrepancy between these conclusions and published results reflects the erosive nature of the distributary system in which the massive sand accumulated. Hence, whilst the micaceous sand may subsequently coarsen upwards elsewhere, here this ultimate event has been removed by distributary incision. However, some sequences reported are similar to those described here, with a general fining upwards beneath the massive sand. Although these sequences fine upwards and are occasionally identified as marine, they are widely reported as prodelta sediments and inferred to be regressive rather than progradational.

This leads to the second point. The model above suggests transgression recording "a vertical sequence of deepening-upwards facies", followed by progradation: "a seaward shift in shoreline location caused by deposition",

(Bourgeois, 1980, p. 681). Progradation, however, is not necessarily related to regression - a lowering of sea level (Elliott, 1978; Bourgeois, 1980). The paradox of published interpretations is exemplified by Eynon (1981, p. 203): "the succeeding deltaic facies is a regressive pulse in an otherwise ... transgressive regime." Hallam (1978) recognises transgression beginning in the Bajocian and continuing to the Bathonian after a short-lived intra-Bajocian regression. He suggests a general regression in the early Bathonian, but a sea-level rise before the Callovian. In comparison, the complexity of differentiating progradational and regressive changes is exemplified by the Ravenscar Group (Livera and Leeder, 1981), which has three marine incursions during the Bajocian, which do not correlate with Hallam's (1978) two. Can one extrapolate Hallam's curves to the Brent Group and relate progradation to regression? The answer appears to be "No". This study has recognised one transgressive event, and one subsequent progradation. Even allowing for marine influence at the top of the sequence, not recognised in this study, there is no evidence for the intra-Bajocian regression recognised by Hallam (1978). To summarise, although the transgression and progradation inferred in this study could be correlated with the general Bajocian transgression and Bathonian regression recognised by Hallam (1978), a specific correlation may not be made and consequently progradation cannot be unequivocally related to regression. Further complications arise if the Brent Group is extended into the Aalenian.

In this final section I should like to compare the facies and divisions recognised in this study with conventional Brent stratigraphy (see Table 4.1). Although there is a general correlation between the lower three units, it is not clear whether the laminated subfacies included here in the coarse-basal sandstone should be included in the Broom or Rannoch Formation. Moreover, correlation within the overlying sequences is even more problematical. Firstly, both cores begin in mid-facies and so may not represent the entire Brent Group.



Secondly, the Ness Formation contains "interbedded sandstones, siltstones and coals. It is carbonaceous with a number of rootlet horizons," (Brown and Deegan, 1981, p. 11), whilst the Tarbert Formation consists of "grey-brown massive, well sorted sandstone with subordinate bands of siltstone, shale, and coal. Commonly recorded features include small and large scale cross-stratification, scour and fill structures and highly micaceous laminae" (Brown and Deegan, 1981, p. 12). There does not appear to be much difference between the two. The interdistributary bay-filling sequences contain rootlets, but are bioturbated. The sandstones above are cross-laminated etc, but contain rootlets. Here they are not interpreted as marine. Also, it is not obvious whether either or both formations occur here, or where any boundary occurs. Finally, it is not obvious whether the Tarbert Formation should occur in these cores: both composite logs (Figs. 4.2 and 4.3) reveal an unconformity beneath the overlying sediments, which may be erosive, whilst the actual cores themselves begin within the Brent Group. Conventional Brent stratigraphy has not, therefore, been adopted in this study.

#### DIAGENESIS

In the following sections I should like to describe in detail the petrography and diagenesis of sediments from the Ninian Field. Subsequently, I should like to establish a paragenetic sequence of diagenetic events and interpret these in terms of interaction between detrital minerals and pore waters. Finally, I should like to discuss these diagenetic reactions, and address myself to the question - what controls diagenesis?

In order to avoid repetition, constant reference to data supporting mineralogical identifications and chemistry will not be made. However, these data are compiled in Appendix F, which lists results of XRD, modal and microprobe analysis.

## Petrography

Beach sandstones (3/33 10643-10632'). Samples taken from this interval are mature and supermature coarse-grained quartz arenites (Fig. 4.7A). Detrital components, comprising 60-75% of the rock, consist of simple and polycrystalline quartz, with up to 3% feldspar and traces of mica, rutile, tourmaline and zircon. Authigenic phases include kandites (dickite and kaolinite), illite, quartz overgrowths, calcite, siderite, ankerite, pyrite, and chlorite; they comprise 16-35% of the rock. Porosity in these samples is moderate or low, ranging from 2-8%, although these values are probably slight underestimates in view of the high proportion of microporosity contained within pores full of authigenic clay. Sutured contacts commonly occur between detrital quartz grains, and apparently those with quartz overgrowths also.

Each sample differs significantly from the others diagenetically, and few generalisations can be made. All the samples contain a framework of quartz grains cemented with a trace of quartz overgrowths, and welded together with sutured contacts. Furthermore, all the samples contain significant quantities of kandites and illite, 8-11% and 3-5% respectively. Kandites occur in two morphologies: as large vermiform aggregates (Plate 4.1A) each comprising numerous pseudo-hexagonal plates, stacked in aggregates of approximately four plates per layer; and as smaller dense pockets of blocky aggregates, each aggregate being one plate in diameter. Vermiform aggregates comprise a greater percentage of the kandite total. They are present throughout, and are enclosed by calcite at 10637' and 10640'. Microprobe analysis and SEM examination supplemented with EDS failed to detect any illitisation of either kandite morphology (Fig. 4.7B). Illite occurs in all the samples, as a discrete pore-lining and pore-filling phase. It appears to occupy grain shaped pores, but was not observed replacing or nucleating on kandites. Interpretation of XRD traces suggests that some of the illite in these samples

is randomly interstratified with approximately 20% smectite. Chlorite occurs as a pore filling at 10640' and 10645'.

Siderite occurs in all the samples, as small rhombs, cementing the lower two, and as discrete spheruliths of sphaerosiderite in the upper two, 10632' especially (Plate 4.1 B, C and D). These spheruliths occur in intergranular pore space, and are enclosed by either calcite or ankerite or both. Within individual spheruliths concentrations of manganese and iron decrease from the cores to the margins, whilst concentrations of magnesium, and especially calcium increase in this direction (Fig. 4.8). Poikilotopic-ferroan calcite occurs extensively at 10637' and 10640' enclosing siderite and vermiform kandites. It comprises 14-20% of these two rocks, and replaces detrital quartz and feldspar grains. Terminations of calcite crystals are not perfect rhombs, being invariably corroded and irregular. Ankerite occurs in all four samples, comprising from a trace to 3% of the whole rock. It forms small rhombs, which occasionally replace detrital quartz grains. Porosity is comprised almost entirely of enlarged or regularly shaped intergranular pore space. However, a significant amount of microporosity occurs within clay mineral pore fillings, but is not reflected in the total estimated by modal analysis. Little grain dissolution porosity occurs.

Foreshore sandstones (3/3-3, 10628' 6" - 10613' 6"). Samples from this interval are mature, medium-grained, quartz arenites (Fig. 4.7A). They consist of 70-75% detrital grains, quartz comprising 65-70% of the rock, feldspars (orthoclase and albite) 2-3%, and mica up to 3%, 10-20% authigenic phases, including quartz overgrowths, kandites, illite, ankerite, siderite, and calcite, and 5-10% porosity. Detrital phases are variably affected by physical processes: dissolved feldspar grains and neomorphosed micas are not further deformed, micas are compressed between detrital grains; finally, contacts between quartz grains and quartz overgrowths are occasionally sutured.

Diagenetic modifications are consistent within these samples. Quartz overgrowths on detrital quartz grains occur throughout, especially in laminae consisting predominantly of quartz grains. They comprise up to 5% of the rock, and occasionally completely fill pore spaces, although they generally only cement grains together and reduce pore throats. Quartz overgrowths were not observed in areas containing significant quantities of mica. They do not enclose other authigenic phases, but are conversely replaced by siderite, ankerite and calcite, or corroded and etched where they abut open pores in the absence of carbonate cements (Plate 4.1 E).

Kandites occur in three morphologies, comprising 8-11% of the whole rock. These are: neomorphosed muscovite, and possibly biotites; vermiform aggregates, which are the <sup>most</sup>/volumetrically significant phase, and blocky aggregates of pseudo-hexagonal plates. Neomorphism of micas occurs throughout the samples. Neomorphism is often associated with siderite authigenesis, especially neomorphism of biotite. Vermiform aggregates occur in large intergranular pore spaces sometimes associated with detrital micas (Plate 4.1 F and G). The less common blocky variety also occurs, but is locally concentrated, forming discrete pockets. Individual plates forming blocks within these pockets are 20  $\mu$ m in diameter (Plate 4.1 H). Although illite occurs in these samples, comprising 1-2% of the whole rock, there is no obvious relationship between the two minerals. Illite occurs in discrete grain shaped pores, and as linings on detrital quartz pore walls (Plate 4.2A). No neomorphism of kandites to illite or nucleation of illite on authigenic kandites is observed in these samples. Furthermore, no in situ neomorphism of detrital feldspar grains to either illite or kandites is observed in this study.

The carbonate phases calcite, ankerite and siderite each comprise up to 3% of the samples, and they comprise up to 5% in total, with the exception of 10627' 6", which contains only traces of vermiform kandites, siderite and

quartz overgrowths, completely enclosed in poikilotopic-ferroan calcite, which comprises half of the rock. In other samples, siderite occurs as small, incipient nodules, and discrete cementing rhombs. These replace quartz grains and overgrowths, and are associated with altered biotite wherever it occurs. Where it only comprises a small percentage of the rock, ferroan calcite also forms large poikilotopic cementing crystals. However, these crystals do not have discrete rhombohedral terminations, but are commonly corroded, or irregularly terminated. Ferroan calcite encloses vermiform kandites, and quartz overgrowths, but not blocky kandites. Ankerite occurs as discrete pore-filling or cementing rhombs, replacing the quartzose framework. It replaces or encloses all other authigenic phases in these samples except blocky kandites. Feldspar overgrowths on detrital feldspar grains occur as a trace in several samples. Their distribution and paragenetic relationship to other minerals is similar to that of quartz overgrowths (Plate 4.2 B).

Porosity in these samples is moderate, ranging from 6-10%. It consists almost entirely of intergranular pore space, with very little obvious grain dissolution porosity. These totals are probably low in view of the microporosity within pores full of clay minerals, especially vermiform kandites.

Foreshore to upper shoreface sandstone (3/3-3, 10565-10610'). Samples from the micaceous sandstone are petrographically and diagenetically similar. They are all fine to medium-grained quartz arenites consisting of alternating laminations of quartz grains, and flakes of mica (Fig. 4.7C). Individual laminae are generally only 1-2 mm thick. Diagenetic modifications are consistent within each lamina, but differ significantly between micaceous and quartzose members. Detrital components comprise 75-90% of the rock, including 40-70% simple quartz, up to 3% feldspar and 15-40% mica (muscovite and biotite in similar proportions, with traces of chlorite), and traces of debris. Authigenic phases include quartz and feldspar overgrowths, illite,

kandites, neomorphosed micas, calcite, ankerite and siderite. Porosity is generally low, ranging from 1-10%. Finally, the effects of compaction are evident in the micaceous laminae, in which flakes of mica are often crushed between, or around detrital grains.

In order to illustrate the differences between the two lithologies, I should like to describe their diagenesis separately, rather than considering the rock as a whole. Quartz-rich laminae contain quartz overgrowths on detrital quartz grains, comprising up to 10% of these laminae. These overgrowths do not enclose other authigenic phases, but, generally, tightly cement grains together, especially fine sand-sized grains. In coarser samples overgrowths are spread thinly on detrital quartz grains. Where they do not completely fill intergranular pore space, overgrowths are either replaced by carbonates, or occasionally corroded. The remaining intergranular pore space is filled with carbonates, particularly ferroan calcite, and, to a lesser extent, ankerite. Where these carbonates are present they comprise no more than 2-3% of any sample. They also enclose or replace mica and vermiform kandites where they occur adjacent to micaceous laminae. Although ankerite forms perfect rhombs, calcite crystals are usually corroded or irregularly terminated. Finally, almost all the pore space in these samples occurs within quartz rich laminae. It ranges from 1-10% of the whole rock, and is almost entirely intergranular pore space, frequently isolated from adjacent pore space or connected through much reduced pore throats. Feldspar overgrowths occur on detrital feldspar grains in these laminae, but they comprise no more than a trace of the whole rock (Plate 4.2 C). Detrital grains are commonly dissolved or corroded, even when they act as nuclei for overgrowths. Blocky kandites occur within some intergranular pore spaces in quartz rich laminae, but they comprise no more than 1% of the whole rock, less than a third of the total kandite content of the samples.

Micaceous laminae consist almost entirely of detrital micas, neomorphosed micas, authigenic clay and siderite. Quartz and feldspar overgrowths were not observed within these laminae. All the micas are compacted or compressed and deformed between quartz grains in the enclosing laminae. Neomorphosed mica probably comprises 2-3% of the rock, although it is difficult to quantitatively estimate whether partially altered portions of flakes are still, for example, muscovite, or effectively clay minerals. Diagenetic modifications of micas, however, vary with their mineralogy. Muscovite is typically partially or wholly altered to kandites, although some may be neomorphosed to illite. Biotites vary from completely fresh to partially or wholly altered to kandites, although some may be neomorphosed to illite. Biotites vary from completely fresh to partially or wholly altered. Biotite does not appear to alter to any specific mineral, XRD analysis failing to detect either chlorite or vermiculite in these samples. However, neomorphosed or altered biotites are commonly associated with siderite, either as discrete rhombs within expanding lattices or concentrated between flakes. Siderite also occurs as incipient concretions, which, together with rhombic cements, comprise up to 11% of the whole rock, generally restricted to the micaceous laminae, and completely filling pore space between micaceous flakes. A trace of pyrite also occurs in one or two samples, associated with these micaceous laminae. Wholly authigenic kandites occur in two morphologies in micaceous laminae, comprising 2-3% of the whole rock. The majority occur as large vermiform aggregates of pseudo-hexagonal plates, filling pores remaining after neomorphosis of muscovites. The second, much less frequent form occurs as blocky stacked plates in small pockets. Apparently, only the vermiform type is neomorphosed to illite, and no alteration or nucleation of illite on blocky kandites was observed (Plate 4.2D). As well as pseudomorphing vermiform kandites, illite occurs within micaceous laminae as a discrete pore filling. There is no macroporosity within micaceous laminae. Intergranular pore space is predominantly full of products of mica neomorphism, and wholly authigenic

clays (Plate 4.2E).

Distributary channel sandstones (3/3-3, 10563' 9" - 10517' 3"). This interval consists of medium to coarse-grained quartz arenites (except for one subarkose) (Fig. 4.9 A), containing simple and polycrystalline quartz (comprising 60-80% of the whole rock), feldspars (up to 6%), and micas (a trace or 1%). Traces of plant debris, rutile, tourmaline, zircon and opaque grains also occur. Detrital components comprise 60-85% of the whole rock. Authigenic phases, including quartz and feldspar overgrowths, illite, kandites, siderite, pyrite, and ankerite, comprise 5-30% of the rock, whilst porosity ranges from 10-20% averaging 12%. The solid detrital framework has been modified by occasional extensive suturing of quartz grains, and dissolution or neomorphosis of less significant feldspar and mica constituents respectively.

The most volumetrically significant and ubiquitously distributed authigenic phases are quartz overgrowths and kandites. Quartz overgrowths occur throughout the samples as a thin cementing veneer on detrital quartz grains, comprising up to 5% of the rock. They do not enclose other authigenic phases, except occasional vermiform kandites (Plate 4.3D), and are sometimes either replaced by carbonates, or corroded and etched (Plate 4.2 F and G). Feldspar overgrowths which occur on detrital feldspar grains comprise no more than a trace of the whole rock. Both authigenic potassium feldspar and albite occur in these samples (Plate 4.2 G and H, and Plate 4.3 A respectively). Kandites occur in three morphologies: rare neomorphosed muscovite, its scarcity being a function of the mica content; vermiform kandites, which also comprise a small percentage of the kandite total; and blocky kandites which constitute the more abundant form. Vermiform kandites are occasionally illitised, although the majority are not. Even those which appear to possess hairy projections, which grow from individual plates were found by EDS to contain no potassium. Vermiform kandites are large, well ordered stacks of



pseudo-hexagonal plates, each plate some 10  $\mu$ m in diameter. Each stack, however, contains approximately four plates per layer and although the overall morphology is one of less regularity than a blocky stack, each individual plate is morphologically similar to a blocky plate (Plate 4.3B, C and D). Blocky kandites constitute most of the 2-7% total kandite content of the rock. They also occur as stacks, but each stack is only one pseudo-hexagonal plate in diameter. These plates are sometimes also partially illitised, (Plate 4.3E), and sometimes apparently totally illitised, although no potassium was detected by EDS analysis, they are also sometimes unaltered. Vermiform kandites are too rare to allow generalisation about their distribution. Blocky kandites, however, tend to occur in small dense pore-filling pockets, spread regularly throughout the rock.

The remaining authigenic phases occur as irregularly distributed traces. In addition to replacing or nucleating on kandites, illite occurs as a pore lining, around the edges of pores filled with kandites. Siderite occurs in one or two samples, replacing detrital and authigenic quartz. It is usually rhombic, although these rhombs are often corroded. Ankerite is more widespread, occurring as a trace of most samples and almost completely cementing 3/3-3, at 10538' (Plate 4.3F). Ankerite was not observed to enclose blocky kandites. It is usually rhombic, cementing samples, and replacing detrital and authigenic quartz and feldspar.

Interdistributary-bay filling sequences. The majority of these samples are mature quartz arenites or subarkoses (Fig. 4.9B). Some, however, are mineralogically immature, with high concentrations of micaceous laminae, while others are mudrocks. Grain size varies with depth within each genetic unit, coarsening upwards from mudrocks through immature fine silty sandstones, to rooted mature medium-grained sandstones overlain by poorly developed coals. The mudrocks consist of kandites, micas and silt-sized quartz grains.

In the lowermost samples in each unit - the mudrocks and immature siltstones - diagenetic modifications are rare, being confined to illitisation of detrital clays and micas, and muscovite neomorphism to kandites, but little else. Finely scattered pyrite crystals also occur, and porosity is low, averaging 1-2% (Plate 4.3G).

Towards the top of each unit occur coarser-grained quartz arenites. Within these sandstones quartz grains are dominantly monocrystalline, (they comprise 30-75% of the rock and average 60%), rock fragments are rare, and feldspar (comprising 2-6%) is typically orthoclase or microcline with only traces of plagioclase. Muscovite is the dominant mica, although traces of biotite are present. Heavy minerals present are rutile, tourmaline and zircon. Traces of plant debris also occur, concentrated in micaceous laminae, especially towards the top of each unit.

Interdistributary-bay siltstones and sandstones generally have moderate porosity of 0-11% within a quartzose framework containing a wide range of diagenetic minerals. These minerals comprise 15-65% of the rock. Quartz overgrowths, ferroan calcite, siderite, ankerite, and kandites are the most volumetrically significant, although feldspar overgrowths, illites, barytes and pyrite are also present.

The dominantly quartzose detrital components are relatively stable, whilst the feldspars and micas display varying degrees of instability. Muscovites are neomorphosed to kandites, and show splayed ends and a progressive loss of cations (Plate 4.4A and B, Fig. 4.9C). In these samples, kandites display two distinct morphologies. Large vermiform kandites occur frequently; they are usually associated with laminae of muscovite and plant debris, but are also found as large discrete pore fillings up to 2 mm in diameter (Plate 4.3H). In this habit they are often enclosed by quartz overgrowths. Alternatively,

kandites are sometimes found as a more blocky pore filling, within both intergranular and oversized pore spaces. These are also occasionally enclosed by overgrowths, and are sometimes illitised (Plate 4.4 C and D). Together these two types occur in the majority of samples and comprise up to 6% of the rocks. Although feldspar dissolution is common throughout the samples examined, there is no qualitative relationship between feldspar content, feldspar dissolution and blocky or vermiform kandites. Indeed, oversized pore fillings of blocky kandites are commonly found adjacent to fresh feldspar grains.

Authigenic illitic clays are widespread, although not quantitatively significant. Illites occur as coatings on quartz grains, which are sometimes enclosed by later overgrowths, as neomorphosed detrital clays, and on, or replacing both vermiform or blocky kandites (Plate 4.4E and F). Approximately 30% of the pore filling kandites are illitised to varying degrees, but in the remainder, potassium uptake was not detected.

Quartz and rare feldspar overgrowths are found throughout all samples, unless carbonate concretions and nodules are well developed. Quartz overgrowths occur as a thin veneer on detrital quartz grains, evenly distributed within the sandstone samples and comprising 4-23% of the rock. Quartz overgrowths are often euhedrally developed (Plate 4.4G and H) and appear to enclose both kandites and illite. Where overgrowths are best developed primary pore space is almost fully occluded. However, both thin section and SEM evidence reveal occasionally ragged and corroded rather than perfectly euhedral overgrowths (Plate 4.5A).

Pyrite nodules up to 2 cm in diameter occur throughout the interdistributary-bay sequences with a concentration towards the top of each unit, and especially towards 10420-10440'. Where a nodular habit has developed quartz grains with quartz overgrowths and neomorphosed muscovite flakes are often enclosed.

Smaller, local developments occur, filling pore spaces between quartz grains and within spaces in plant debris. Traces of pyrite are also found enclosed within small siderite concretions. When present as nodules, pyrite may comprise 50-60% of the rock, although it is normally present only as 1% or less.

Carbonate minerals occur in a variety of forms in these samples. Whilst 1-2 cm diameter siderite concretions occur irregularly throughout the core, small discrete 1-5 mm diameter concretions occur frequently, concentrated along laminae rich in plant debris. These small concentrations enclose pyrite, vermiform kandites and neomorphosed muscovite. Rhombic siderite also occurs as a cement, occasionally extensively, but usually in irregular, scattered pore filling patches.

Calcite, always ferroan, occurs as both small concretions and a cement. The concretions are discrete and tightly cemented to the exclusion of all other diagenetic features. Calcite cements, however, whether present as scattered patches or extensive poikilotopic crystals, enclose small siderite concretions, vermiform kandites, neomorphosed micas and quartz overgrowths. Both these calcite and the siderite concretions comprise up to 50% of the rock where they occur.

Ankerite is not as abundant as calcite, although its distribution is similar, forming either small pore-filling patches or poikilotopic cements enclosing quartz grains with overgrowths, neomorphosed micas, and small siderite concretions. Ankerite and calcite do not occur together; their compositions are shown in Fig. 4.10A. All carbonates are seen to replace quartz and feldspar grains and overgrowths. Barytes was found as an anhedral pore filling in several samples. Sutured contacts between quartz grains were observed in two samples. These sutures were not developed well enough to be seen in hand

specimen. Examination under cathodoluminescence indicated that sutured contacts occurred between both grains and overgrowths. There is no association of suturing and subsequent quartz overgrowth development.

Crevasse-splay sandstones. These deposits are variable texturally, though reasonably consistent mineralogically. The variations may be attributed to fining and rapid deposition with decreasing velocity away from levees and onto the floodplain. The coarsest, medium-grained sandstones are mature quartz arenites and subarkoses; finer samples contain appreciable amounts of silt and clay and range from immature subarkoses to arkosic wackes and mudstones (Fig. 4.10B). Quartz grains are mostly simple with few recognisable polycrystalline grains; they comprise 60-70% of the rock. Feldspar is dominantly orthoclase and microcline, with only traces of albite, and comprises up to 7% of the rock. Micas are mostly muscovite with some biotite. Heavy minerals, such as rutile and zircon are rare. Plant debris is present throughout and is especially concentrated in finer samples. These occasional deposits of sand and silt interrupted more continuous sedimentation of a clay fraction containing micas, kaolinites and traces of mixed layer clays. This detrital clay comprises from a trace to 15% of the rock.

In finer, or immature samples where there is little porosity, authigenic phases comprise 5-20% of the rock. Coarser samples contain up to 15% porosity and 10-25% authigenic phases. The predominant minerals present are quartz overgrowths, calcite and kaolinites. Volumetrically less significant feldspar overgrowths, pyrite, illite, siderite, ankerite, gypsum and barytes also occur.

These finer grained and immature samples have little diagenetic modification where concentrations of detrital matrix clay occur, (itself often incipiently illitised); quartz overgrowths and kaolinites are only rarely present (Plate 4.5C).

Coarser and more mature samples, however, have undergone a more diverse diagenesis. Thin illitic clay coatings are frequent, and often enclosed by later quartz overgrowths (Plate 4.5D). Quartz overgrowths occur on detrital quartz and feldspar grains. They are occasionally "etched". Feldspar grains range from extremely fresh to highly dissolved with only a skeletal framework remaining. Although feldspar overgrowths occur rarely on detrital feldspar grains, quartz overgrowths on feldspar grains are even more rare, only being observed at 3/3-3 (10447') (Plate 4.5E). Overgrowths occur throughout the majority of samples as a thin, evenly spread veneer and comprise up to 17% of the rock.

Scattered pyrite crystals also occur, although they are less common in coarser samples. Localised concentrations of pyrite, small siderite concretions and muscovite are common. The muscovite is frequently neomorphosed to "poorly" crystalline, flaky kandites similar to those of the vermiform kandites (Plate 4.5F). Vermiform kandites are present in the majority of samples, comprising a small percentage of most rocks. They occupy large intergranular pore spaces. Blocky kandites also occur, although their distribution varies. Vermiform kandites only occur in intergranular pore spaces. They are often illitised but not when enclosed within calcite. They are sometimes enclosed within quartz overgrowths (Plate 4.5G). Blocky kandites are more widespread and occupy both intergranular pore spaces and larger, irregular pore spaces; they are sometimes illitised (Plate 4.5H). However, blocky kandites are not seen enclosed by carbonates. Kandites comprise up to 7% of the rock.

Siderite occurs in a few samples, both as small discrete concretions, and as a rhombic cement. Siderite cements replace quartz and feldspar grains and overgrowths (Plate 4.6A and B). Calcite occurs as irregularly distributed anhedral or corroded patches of cement, also replacing quartz grains and overgrowths. Poikilotopic calcite cements, where found, enclose small siderite concretions, quartz grains with overgrowths, partially dissolved feldspars, vermiform kandites,

and neomorphosed muscovite. Small, irregularly distributed subhedral or slightly corroded patches of ankerite also occur. However, calcite and ankerite are not found together. Calcite and siderite usually comprise a trace of each sample, but, in one, calcite comprises 25%. SEM analysis revealed traces of authigenic, anhedral gypsum, one authigenic brookite crystal, and patches of barytes.

Channel sandstones. This group of samples has a noticeably uniform texture. The majority are mature, whilst the exceptions are supermature. Mineralogically, quartz arenites predominate, with only occasional subarkoses (Fig. 4.10C). Grain size varies from medium to coarse sand, with occasional granules in channel-lag deposits. There are few noticeable variations of mineralogy with grain sizes, although the percentage of polycrystalline quartz grains tends to rise with increasing grain size. Most quartz grains are simple, although a small amount of polycrystalline quartz occurs; quartz comprises 60-80% of the rock. Cathodoluminescence of quartz reveals a variety of violet, violet tinged blue, blue and brown simple grains, as well as more complicated polycrystalline grains with blue and brown segments as well as black veins.

Feldspar grains include orthoclase and microcline, with subordinate amounts of albite. They average 2% and comprise no more than 4% of the rock. Rare fragments of sandstone and siltstone occur also. Rutile, tourmaline and zircon are present as traces in most samples. These sandstones are uniformly moderate to highly porous, values ranging from 8-20%, and averaging 14%. Authigenic phases comprise 3-16% of the rock, and are dominated by quartz overgrowths (up to 12%) and kandites (1-4%). Less volumetrically significant diagenetic minerals include illite, siderite, ankerite and barytes.

Quartz overgrowths are found in almost all samples. They are uniformly thin and occur as an even veneer on detrital quartz grains. Pore spaces and pore

throats are generally partially rather than fully occluded. Overgrowths are normally euhedral (Plate 4.6D) and sometimes display etch pits (Plate 4.6E). The relationship between overgrowths and the widespread sutured contacts is unclear even with the aid of cathodoluminescence. Sutured contacts are common in most coarse grained and some medium grained sandstones. Moreover, they are sometimes sufficiently well developed to be seen in hand specimen, for example, in 3/3-2 at 10380'. The relative timing of overgrowths and suturing is unclear. Some appear to post-date overgrowths, whilst others precede overgrowths. Furthermore, there is no positive qualitative or quantitative correlation between sutured contacts and overgrowths. Plate 4.6F shows that there are no overgrowths associated with the best developed sutures.

Kandites occur in two morphologies: as large vermiform pore fillings, occupying only intergranular pore spaces and smaller, more blocky dense pockets in both regular and irregularly shaped pore spaces. In addition to the rare illitic alteration of some kandites, illitic coats are found along most, but not all, of the sutured grain contacts, as well as enclosed beneath overgrowths on a few quartz grains (Plate 4.6G). Muscovite, where present, has been partly altered or neomorphosed to kandites, with characteristically splayed ends and reduced birefringence. Vermiform kandites are most frequent in the area of altered micas.

The behaviour of feldspar grains appears to be a function of mineralogy. Microcline grains are rarely altered; orthoclase grains sometimes have orthoclase overgrowths and dissolved cores, but others are perfectly fresh; albite grains usually have completely dissolved cores. In situ neomorphosis of feldspar grains to illite or kandites was not observed.

Scattered throughout the samples are small patches of calcite and siderite with occasional ankerite. All three carbonates occur as replacive and pore-



filling phases. Quartz and feldspar grains and overgrowths are replaced or corroded by carbonates (Plate 4.6H). The carbonates are irregularly distributed, usually as traces, and comprise no more than 2% of any sample. Calcite and ankerite occur with siderite, but not together. Irregularly scattered traces of pyrite and barytes were observed, the former especially below 10400'.

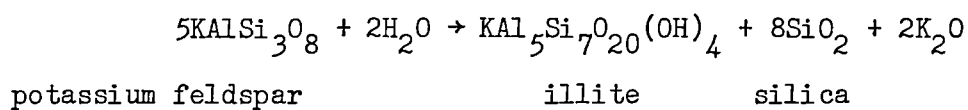
### Interpretation

Elucidation of the paragenetic sequence of events during diagenesis in these rocks is complicated by multiple generations of illite and kandites, the presence of chlorite, and the lack of significant variations between marine and non-marine sediments. Sedimentary clastic assemblages are fundamentally unstable in either fresh or sea water, and dissolve to form, respectively, kandites (Curtis and Spears, 1971), or illite (Kastner and Siever, 1979). Muscovite is also unstable in either, neomorphosing to illite or kandites, or simply dissolving (Fanning and Keramides, 1977; Lin and Clemency, 1981). Biotite contains ferric and ferrous iron and is consequently unstable at any Eh (Curtis, 1976). Finally, organic matter is oxidised by bacteria releasing bicarbonate ions into solution (Curtis, 1980).

Eogenesis of marine sediments. The initial diagenetic reactions of these marine clastic sediments resulted in precipitation of illite and then both potassium-feldspar and quartz overgrowths. The next diagenetic modifications resulted from a lowering of pH and then Eh.

Illite is interpreted as forming in two generations: the first from saline depositional pore fluids; the second, later, from formation waters during burial. The first generation is, therefore, eogenetic, and probably formed from interstitial waters, but before potassium-feldspar and quartz overgrowths. This illitic clay (often with some irregularly interstratified smectite) forms the

first authigenic phase in the foreshore, shoreface, interdistributary bay-filling and some crevasse-splay sandstones. In each case it is succeeded by quartz overgrowths, which enclose the least extensive illitic coats, but are inhibited by more extensive pore linings. Illite may form, and is stable in, saline waters with high pH, that is, essentially sea water (Harder, 1974). In addition, although interstitial marine fluids rapidly equilibrate with feldspars. Feldspars are initially unstable and dissolve to form illite (Kastner and Siever, 1979). Illite may, therefore, precipitate directly from solution or form from the initial breakdown products of feldspars in sea water. Thus:



Some detrital potassium feldspar grains, although not observed neomorphosing directly to illite, appear to have dissolved and directly reprecipitated as grain-shaped illitic pore fillings. Such feldspar dissolution releases silica into solution, the build up of which eventually inhibits the formation of illite (Harder, 1974). Consequently, and especially with detrital grains to act as nuclei for overgrowths, quartz precipitates (Harder, 1974). Similarly, interstitial marine pore waters move towards equilibrium with potassium feldspar, and so following an initial period of illite precipitation, increasing quartz concentration would promote feldspar overgrowths as well as inhibiting illite formation (see Fig. 4.11, modified after Kastner and Siever, 1979). Although this may explain the interpretation of initial diagenetic modifications to the wholly marine sediments, it does not explain illite authigenesis of the floodplain sediments.

The only exceptions to this general pattern occur in the transgressive sands at the base of the sequence. These contain pore-lining chlorite and concentrations of sphaerosiderite spheruliths, the latter especially in 3/3-3 at 10632'. Chlorite is interpreted as a wholly authigenic precipitate, although favourable conditions for its formation only occurred locally. I would suggest that here, at the base of the sequence, the bacterial processes responsible for lowering

pH and consequent aluminosilicate dissolution, also removed oxygen. Thus, some pore waters became anoxic, ferric iron was reduced and chlorite precipitated. Budding and Inglin (1981) also report authigenic chlorite in the coarse-basal sandstone, but nowhere else, which suggests a possible environmental control on its distribution in the Brent Group.

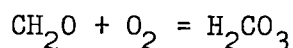
The spheruliths are somewhat more problematical, resembling closely pedogenic horizons observed elsewhere. Nagtegaal (1980), however, interprets these features in the Broom Formation as shallow-burial phases, and does not include them amongst the pedogenic features he describes. His interpretation is compatible with a freshwater origin as suggested below for the rhombic cement in floodplain sediments. Pedogenesis, unfortunately, is more difficult to explain. Although the underlying Liassic mudrocks were presumably sufficiently impermeable to allow stagnation in the water table, these spheruliths occur in a porous sandstone. Secondly, rootlets were not observed in these cores. This interpretation necessitates a period of relative quiescence following beach development, for pedogenesis to occur prior to continued transgression. A possible situation is demonstrated in Fig. 4.12. Also, (although this perhaps stretches the point) the succeeding storm-driven sediments could have removed any well developed pedogenic structures above. Moreover, these sediments do contain large and abundant vermiform kandites, similar to those formed in modern soils (Fitzpatrick, 1980). It is possible, therefore, that these features record pedogenesis in these sediments.

Continued marine eogenesis or freshwater diagenesis? Authigenesis of illite, quartz and potassium-feldspar overgrowths is followed by diagenetic modifications to these marine sediments which are interpreted as continuing in acidic rather than alkaline pore waters. There are two possible explanations for this progression. In the first, bacterial processes degraded organic matter, as a result of which first pH was lowered and later Eh became negative. The former

would explain the origin of kandites, the latter, siderite and local pyrite. Also, calcium carbonate originally in solution could have remained to precipitate eventually in the subsequent ferroan calcite. This model requires no changes of pore-fluid composition, only of chemistry. In the second explanation, pores could have been flushed by the water table of the overlying delta. As the water table is inferred to have been initially acidic and thereafter anoxic, kandites and then siderite, and perhaps pyrite, could have formed. A second change of pore fluid composition is inferred to explain the subsequent ferroan calcite.

The choice between these two models - the simpler one requiring no changes of pore fluids, the other requiring two - is complicated by reference to the non-marine sediments. Here, the inferred second change of pore fluids is also required. Thus, ferroan calcite may have been introduced into the whole system simultaneously. This problem cannot, however, be solved here, as this study has not included suitable stable isotope analysis to determine the origin of carbonates in these marine sediments.

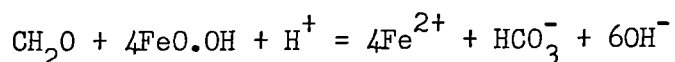
In the following paragraphs I intend to describe diagenetic modifications of these marine sediments, but, in view of the problems outlined above, without reference to the origin of their pore waters. Following deposition, these sediments began to equilibrate with their depositional pore waters, and consequently illite, and potassium feldspar and quartz overgrowths precipitated. Thereafter, pore waters became acidic as a result of aerobic bacterial processes.



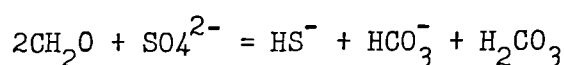
Detrital and authigenic phases stable previously, now became unstable. As a consequence, muscovite neomorphosed to kandites and feldspars were probably partially dissolved, resulting in vermiform kandite precipitation (Fig. 4.11). If diagenesis reflected in situ porewater evolution, these pores were effectively

sealed from the overlying sea water, because where diffusion across the sediment-water interface is possible, products of bacterial processes are lost (Curtis, 1980).

Upon completion of aluminosilicate diagenesis, continuing bacterial degradation of organic matter removed free oxygen and caused ferrous iron and sulphate reduction (Curtis, 1980).



and



Although iron reduction and, consequently, siderite precipitation should precede sulphate reduction (Froelich et al, 1979), ferrous iron reacts more readily with sulphate ions to form pyrite, than with carbonates to form siderite (Berner, 1971). Pyrite consequently marks the onset of anoxic conditions in these sediments, and its formation would have continued until all sulphate ions in solution had been removed. Thereafter, the remaining ferrous iron reacted with continuously evolving bicarbonates to form siderite (Berner, 1971). Whilst some ferric iron may have been present in the sediment, very little siderite actually occurs here. Moreover, the majority appears to be directly associated with neomorphosing micas. Thus adjacent to, and between, the lamellae of neomorphosing micas, one finds siderite rhombs. In addition, this rhombic siderite differs in habit from the spheruliths at the base of the sequence. This suggests that their origin may differ. Furthermore, the spheruliths do not enclose pyrite, but it occurs around their edges, suggesting that they formed from pore waters devoid of sulphate ions. Could this be fresh water perhaps? It should be mentioned here that not all the pyrite is interpreted as eogenetic and enclosed by ferroan calcite. A second generation occurs, scattered widely throughout pore space, but concentrated below 10420'. This second phase is probably related to the oil-water contact at 10430' (Albright et al, 1980) and is discussed below.

Ferroan calcite cementation occurred subsequently, enclosing and replacing all the phases described above as well as the remaining sediments. If the preceding modifications occurred in fresh water, this calcite was probably introduced in formation waters. If they occurred as the result of in situ bacterial processes, calcium may have been present the whole time, and only precipitated when pH and, more especially, carbonate concentration reached favourable levels.

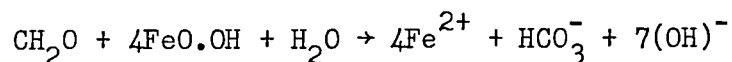
Eogenesis of non-marine sediments. Quartz overgrowths, vermiform kandites and neomorphosed muscovite are the first diagenetic modifications in most of the non-marine sediments, and are products of freshwater diagenesis. In floodplain and channel-filling sandstones, depositional pore waters were presumably meteoric, and dilute with a pH of 7-7.5 (White et al, 1963). However, aerobic bacterial oxidation of organic matter would have released bicarbonate ions into solution, and so generated acidic fresh water, climate permitting (Curtis, 1977). Consequently, partial dissolution of feldspars and amorphous aluminosilicates, especially in thick sequences of compacting muds, generated kandites, and liberated silica (Helgeson et al, 1969; Curtis and Spears, 1971; Huang, 1977). These alternative aluminosilicate equilibria are also illustrated in Fig. 4.13. As a result large vermiform kandites and quartz overgrowths precipitated. This quartz overgrowth cementation may also have incorporated silica from the ground water: analogous modern ground waters are typically saturated with respect to quartz (White et al, 1963). Furthermore, muscovite, which is also unstable in fresh water, neomorphosed to kandites (Fanning and Keramides, 1977). It must be emphasised that the inferred timing of these processes is immediately following deposition and during shallow burial. Quartz overgrowths (Breese, 1960), and vermiform kandites (Fitzpatrick, 1980) have been reported from modern soils. Indeed, kandite formation requires specific conditions which may be satisfied in fresh water following deposition. These are low pH, oxygenated pore waters, and continuous flushing to remove

$K^+$ ,  $Ca^{2+}$ ,  $Mg^{2+}$  and other cations (Bucke and Mankin, 1971).

Whilst this adequately explains observations of all the non-marine sediments, and the probable channel deposits in the massive sand, it does not account for the presence of illite enclosed by quartz overgrowths in crevasse-splay sandstones. However, as mentioned above, this study has not produced any data on the nature and salinity of "floodplain sediments". Consequently, whilst some may be wholly non-marine, having accumulated in lakes, others may have accumulated in waters open to and influenced by sea water. Hence, the coarsening-upwards facies, including crevasse-splay sandstones, interspersed with channel deposits, may have filled saline-interdistributary bays.

The simplest explanation of sediments containing illitic pore linings, therefore, is that they were deposited in shallow saline interdistributary bays. Thus, initial diagenetic reactions in these sediments reflect interaction with their saline depositional pore waters. Subsequent diagenetic modifications are similar to those of non-marine sediments and presumably result from freshwater flushing of pore space.

All the reactions above involving aluminosilicates release potassium and tend to increase pH. In the non-marine sediments potassium-feldspar overgrowths are interpreted as forming from this potassium. Following aerobic bacteriological degradation of organic matter, suboxic processes take over. The former lowers pH, but the latter increases it (Curtis, 1980)



Consequently, with rising pH, any potassium in solution or being released concomitantly from aluminosilicates could form overgrowths on detrital potassium-feldspar grains. It is also possible that the traces of authigenic illite discussed above also resulted from a build-up of potassium in solution.

Traces of pyrite occur locally in the non-marine sediments either in association with organic matter, or within finer sediments. Although sulphate ions are not abundant in fresh water, some occur. Also, sulphate ions may be introduced in saline bays, and from degraded organic matter. Whilst ferric iron reduction yields bicarbonates as well as ferrous iron, pyrite rather than siderite precipitation is favoured thermodynamically from a solution which also contains sulphates. This local pyrite, therefore, records the onset of reducing conditions in these sediments. Siderite which encloses it, and generally cements samples as well as replacing the quartzose framework, formed subsequently from further ferrous iron ions, and bicarbonates in solution. This siderite is rhombic rather than sphaeroidal, perhaps further support for an exotic origin for the spheruliths observed in 3/3-3 at 10632'. The occasional authigenic brookite observed in these sediments is interpreted as precipitating following the dissolution of its detrital high-temperature polymorph, rutile.

Mesogenesis of non-marine sediments. Poikilotopic ferroan calcite which occurs enclosing siderite and also replacing the quartzose framework, is interpreted as forming from formation waters introduced into the system subsequently. The basis of this explanation is that calcium carbonate originally in solution should have precipitated before rather than after siderite (Curtis, 1978). This suggests that calcium carbonate was not present in the original pore fluids and so calcite cementation cannot be directly related to the evolution of connate or fresh water: the argument is tenuous. Unfortunately, stable isotope analysis of siderites and calcites failed to produce unequivocal data interpretable either in favour of, or against, this hypothesis.

Throughout the sequence, two varieties of tight ferroan calcite cementation occur. The first generally fills pores and comprises up to 30% of the rock. The second is extensively replacive and comprises 50% of the rock. This second variety is interpreted as concretionary rather than cementing (s.s.),



and is probably not laterally continuous. Although the majority of the core is oil stained, these calcite cemented portions are not, suggesting that elsewhere carbonates were absent during hydrocarbon migration.

Ubiquitous mesogenetic changes. The remaining diagenetic modifications post-date ferroan calcite cementation. These commence with carbonate dissolution, and so later authigenic phases occur in secondary porosity. These changes are unaffected by the depositional environment and occur ubiquitously. Although some samples remain tightly cemented with quartz overgrowths, siderite and ferroan calcite, it is not clear whether or not the remainder were also fully cemented with carbonates. In these samples pore space exhibits evidence of enlargement by corrosion, recognised by etched and irregularly notched quartz overgrowths. These features are interpreted as the result of carbonate replacement of the quartzose framework, and subsequent dissolution of the carbonates. It is again difficult to evaluate whether carbonates merely lined pore space. However, as evidence suggests that a replacive cement has occupied much of the pore space this extant porosity is, therefore, interpreted as secondary (Schmidt and McDonald, 1979b). It is significant that dissolution of this presumably carbonate cement recreated the original framework of the rocks, following minor physical compaction and cementation with quartz overgrowths.

Carbonate dissolution, blocky kandite precipitation, authigenic albite, barytes, illitisation, grain-contact suturing and ankerite precipitation are all related to changes in pore-fluid composition during burial. Whilst their relative timing may be established, absolute timing as well as depths of formation etc, may not.

Blocky kandites occur in secondary porosity and are interpreted as forming from the same "aggressive" solutions that dissolved the original carbonate

cements. This interpretation is based on the size and shape of pore spaces filled by blocky kandites, pore walls often exhibiting evidence of corrosion, and the fact that this kandite morphology is not seen enclosed by carbonates, it is therefore inferred to follow carbonate dissolution. In order to form kandites and effect dissolution, these fluids must have had a low pH, and contained both alumina and silica. Their origin is probably related to diagenetic processes in source or mudrocks. Bacteriological degradation of organic matter continued during burial (Curtis, 1978). When the resulting bicarbonates are not fixed to form carbonate concretions or cements (Irwin et al, 1977; Curtis, 1980), they form acidic solutions and act aggressively (Curtis, pers. comm. 1982). Thus, during burial acidic solutions may be generated. When these migrated into carbonate cemented rocks, they dissolved the carbonates and created secondary porosity. Furthermore, these solutions were probably saturated with respect to alumina and silica, a consequence of illitisation of aluminous smectites in the source rock (Boles and Franks, 1979a). As they equilibrated with carbonates in the reservoir, pH increased, the solution entered the field of kandite stability and so precipitated blocky kandites in this new-born porosity. An alternative explanation is that during structural inversion and unroofing of the reservoir in the Cretaceous, meteoric water was introduced, and acted in a similar fashion to the aggressive fluids (Hancock and Taylor, 1978; Sommer, 1978). There is, nevertheless, no evidence to suggest that this meteoric water would have been acidic or that it would have contained alumina or silica. Unfortunately, this alternative cannot be dismissed because this study has not revealed sufficient data either to confirm or deny the increased kandite concentration one would expect towards the exposed crest of the horst as this theory predicts.

The second phase of quartz overgrowths observed with CL is interpreted as forming after blocky kandites. It follows that enclosure of blocky kandites

by overgrowths, rather than etching of overgrowths by kandites, is the preferred explanation of the texture shown in Plate 4.4C and cf. Sommer (1978). These overgrowths may have formed from silica also introduced by the aggressive fluids responsible for kandite precipitation.

Ankerite, which occurs throughout the cores, is interpreted as forming after  $Mg^{2+}$  and  $Fe^{2+}$  bearing solutions were introduced into the reservoir. These solutions equilibrated with the remaining carbonates to precipitate ankerite, probably after the formation of blocky kandites, and at an elevated temperature (see Chapter Six). The cations were probably also released from source rocks or enclosing mudrocks during illitisation of smectites (Boles and Franks, 1979a; Pearson et al, in press), but before hydrocarbon maturation and migration, as they occur within both the oil and water zones. Both blocky and vermiform kandites are occasionally illitised. The illitisation, as well as authigenesis of albite, is interpreted as occurring following equilibration and dissipation of aggressive fluids, and reintroduction of saline formation waters into the reservoir, possibly similar in composition to those present today. Illitisation requires little more than a source of potassium, low silica concentrate and a high pH (Harder, 1974), conditions satisfied by typical formation waters (White, 1965; Collins, 1975). It must be stressed that there is no indication on the basis of visual inspection, quantified petrographical analyses, or semi-quantitative XRD of clay fractions throughout 3/3-3 to suggest that illitisation is at all related to the position of the oil-water contact (cf. Hancock and Taylor, 1978). As outlined above, most illite appears to be related to the depositional environment and mineralogy, very little is related to any processes during burial. Indeed, microprobe analyses confirm SEM observation of completely unaltered kandites throughout the 200' of 3/3-3 below the oil-water contact.

Although it represents no more than a trace of any one sample, authigenic

albite occurs throughout the cores. It is not clear, however, whether the absence of sodic plagioclase reflects original detrital composition, hence source rock composition or diagenetic processes following deposition (Boles, 1982). Albitisation of plagioclase according to Boles (1982) takes place in dilute alkaline solutions, undersaturated with respect to clay minerals. Whilst high temperatures are required for relatively young strata (Boles, 1982), albitisation may take place at lower temperatures in relatively older strata (Boles, pers. comm. 1982). Present Ninian formation waters (Table 4.2, Larsen, pers. comm. 1981) plot outside Boles' (1982) field of albite stability (Fig. 4.14). Consequently, if albitisation has taken place in this reservoir, it is not active at present, and has operated at less than 100°C, the present and maximum reservoir temperature (Albright et al, 1980). Nevertheless, evidence suggests that albitisation has not taken place here. There is no calcite within albite grains, nor does any of the albite contain broad lamellae due to pseudomorphing of calcic plagioclase (cf. Boles, 1982). This evidence suggests, therefore, that the purely sodic plagioclase present here is primary and reflects an originally plutonic or metamorphic source area rather than a volcanic one.

The second generation of pyrite, a major pore-filling cement around 10420' and below is interpreted as the last major authigenic phase in these samples. Pyrite forms in reducing conditions (Berner, 1971). Its concentration around the oil-water contact suggests that sulphate reducing bacteria occur at this level, reducing ions from the water zone below and degrading hydrocarbons in the anoxic oil-filled pores above (Sharma, 1969; Evans et al, 1971). The only other authigenic phase observed, barytes, is supersaturated in the existing formation water and may be forming presently.

Sutured contacts occur throughout the sequences, but in particular in the coarser grained sandstones. They postdate quartz overgrowths and are thus

one of the last diagenetic modifications to the framework. Sutured contacts were not observed in the finer and tightly cemented sandstones, they appear to occur only in coarse grained quartz arenites with, coincidentally, little or no quartz overgrowth cementation. Suturing is clearly significant here, as it changes grain-to-grain contacts from points to (albeit irregular) lines and reduces intergranular pore volumes. Consequently, minus cement porosity<sup>1</sup> values for coarse sands are significantly lower than those for finer ones. It should be emphasised that in these samples where rare overgrowths occur, sutured contacts are found between quartz grains and between overgrowths, hence they postdate overgrowths. Moreover, there is no evidence of authigenic quartz precipitating elsewhere in the sequence as a result of quartz dissolution at these contacts. Thus, there is no evidence to suggest that quartz dissolution at grain-to-grain contacts contributes to the formation of quartz overgrowths at any stage during the diagenesis of these sediments. This conclusion is at variance with established doctrine in some texts, which consider "pressure solution" as the origin of sutured contacts and, therefore, of quartz cements (see Weyl, 1959 for review).

Cathodoluminescence observations. In addition to suggesting that suturing of these sediments postdates the final quartz overgrowths, CL also allows an insight into the complexity of the source area, not apparent from standard petrographical observation. CL observation reveals simple quartz grains which luminesce blue, violet, and brown. In addition, polycrystalline grains are found to contain portions of violet and brown or blue luminescent quartz. Furthermore, some grains contain fractures annealed with non-luminescent quartz. The majority of grains, however, are simple, and either violet or blue, but ringed with brown luminescent quartz. Interpretation of these various features

---

<sup>1</sup> Minus cement porosity is the sum of porosity and authigenic phases present in the rock, and is an approximate estimate of the porosity remaining after mechanical compaction.

(Zinkernagel, 1978; Ramseyer, pers. comm. 1981) is based on the following scheme: authigenic quartz is generally non-luminescent; blue luminescence results from a volcanic origin, violet from plutons, and brown from regional metamorphism. Consequently, the origin or provenance of monochromatic quartz is unequivocal. The majority of quartz here is not so easily interpreted. Basically, violet or blue quartz with a brown tinge is evidence of either regional metamorphism of the primary body, or of a subsequent sedimentary deposit. Conversely, polycrystalline grains comprising violet and blue components must reflect recycled sediments. The origin of quartz annealing is equally complex. The cracks observed here are filled with authigenic quartz, which, however, does not extend into an overgrowth. Annealing has not, therefore, taken place in the sediment, but in a previous sediment or during telogenesis of a primary source area. In summary, CL reveals that the source area of these Brent Group sediments was either varied, including plutons, volcanics, and recycled sediments, or possibly relatively monotonous sediments, themselves possibly recycled.

Summary. Whilst the coarse-basal sands may have developed poor soil profiles, eogenetic modifications of the succeeding transgressive sands reflected their alkaline depositional pore waters. Initially, precipitation and equilibration produced illite, potassium-feldspar and quartz overgrowths. Subsequently, after isolation from the overlying sea water, bacterial processes reduced pH and then Eh. Consequently, muscovite neomorphosed to kaolinite and then siderite precipitated locally, often associated with pyrite. These phases were all enclosed and partially replaced by ferroan calcite.

In the non-marine sediments meanwhile, bacterial processes immediately lowered pH, causing muscovite neomorphosis, vermiform kaolinite and quartz overgrowth precipitation. Subsequently, they lowered Eh and raised pH, causing siderite cementation and probably potassium-feldspar overgrowths.

Following diagenetic modifications related to depositional pore waters, and the possible influence of the water table on the underlying marine sediments, similar diagenetic reactions occurred throughout the Brent Group in response to ubiquitous changes in pore-water composition. These reactions are probably mesogenetic (Schmidt and McDonald, 1979b). Cementation by ferroan calcite was the first of such processes, reducing remaining pore space. Pore waters at this time were alkaline, reducing and saturated with bicarbonates. The relative timing of the following events is uncertain, but the proposed scheme requires few changes of pore-water chemistry. During burial, aggressive solutions generated by bacterial degradation of organic matter in the surrounding mudrocks migrated into the reservoir, dissolving carbonates, reaching equilibration and precipitating blocky kandites.

Subsequently, pore waters became dilute and mildly alkaline. Under these conditions firstly minor illitisation of kandites, and secondly authigenesis of albite occurred. Finally, prior to and perhaps during the migration of hydrocarbons from the source rock into the reservoir,  $Mg^{2+}$  and  $Fe^{2+}$  bearing solutions equilibrated with carbonates in situ and precipitated ankerite. Following emplacement of hydrocarbons above 10430', anoxic conditions developed at the oil-water contact, and pyrite precipitated. However, in the zone, beneath the oil-water contact, minor illitisation of kandites may have proceeded. Diagenetic modifications in the Brent Group are summarised in Fig. 4.15.

### Discussion

What controls diagenesis? A number of factors which may or may not influence diagenesis have been mentioned during interpretation of diagenetic modifications of the Brent Group in the Ninian Field. These include depositional mineralogy, environment and texture; climate; formation waters during burial; solutions migrating from hydrocarbon source rocks, and the subsequent oil-water contact;

and, finally, formation waters. In the following discussion I should like to emphasise some of the preceding interpretations, and highlight factors which influence diagenesis. However, I intend demonstrating that during eogenesis especially, no single factor can be identified as controlling diagenesis.

Sedimentary clastic assemblages are fundamentally unstable when deposited. Consequently, immediately following deposition, they react and attempt to reach an equilibrium with their interstitial pore waters. The relative degree to which detrital minerals interact is a function of their relative stability. Thus, although thermodynamically metastable, quartz grains persist whilst relatively less stable aluminosilicates such as feldspars and micas begin to dissolve, or react. As Goldich (1938) pointed out, the relative stability of minerals is the reverse of Bowen's reaction series. Besides, these reactions are essentially weathering processes, and may take place at the earth's surface (Curtis, 1976), either in the source rock or, in the case of minerals surviving erosion, when deposited.

Assuming correct interpretation of depositional environments, theoretical predictions based on the discussion above, and thermodynamic equilibria (e.g. Helgeson et al, 1969) adequately explain eogenetic reactions in all the sediments. It is not possible, however, to distinguish between depositional environment, that is, pore-fluid chemistry, and depositional mineralogy, as the control on these processes. For example, muscovite is unstable in fresh or marine pore waters, and neomorphoses to either kandites or illite respectively. Pore-fluid chemistry influences the end product, but the mica itself is prerequisite to the discussion. Similarly, feldspars dissolve to form either kandites or illite under similar conditions.

What controls diagenesis? The assumption that fresh water per se will always



equilibrate with these aluminosilicates to form kandites is erroneous. This system, a tropical delta probably containing abundant sedimentary organic matter and with a high level of precipitation (rainfall), is significantly different to an arid alluvial fan with little sedimentary organic matter, and less precipitation. In the former, organic matter survives aerobic processes, and generates bicarbonates during burial. In the latter system, conversely, organic matter is rapidly oxidised, red beds form, and ground waters are not necessarily acidic (Curtis, 1977). Walker et al, (1978), for example, describe saline ground waters from a semi-arid alluvial fan in which detrital feldspars dissolve to form either illites or authigenic feldspars. Consequently, an additional factor, climate, must be taken into account when assessing controls on diagenesis.

Both marine and non-marine sedimentary clastic assemblages in the Ninian Field have attempted to reach an equilibrium with their depositional pore fluids. The processes involved, however, cannot be solely related to the influence of any single factor. In addition, these marine sediments exemplify the difficulty of achieving equilibrium with their interstitial pore waters, and so they, and the remaining detrital components reacted and moved towards a new equilibrium. This paradox is illustrated further by reference to the diagenesis of biotite. Biotite contains ferric and ferrous iron. Consequently, it is unstable in oxidising and reducing conditions. Deposition in oxidising pore waters resulted, therefore, in reaction to the ferrous iron. However, under subsequent anoxic conditions both the extant ferric iron and the reaction products of the original ferrous iron became unstable and reduced to ferrous iron.

In addition to reacting with interstitial pore waters, detrital minerals can act as nuclei for overgrowths and so add a further dimension to controls on diagenetic processes. In the marine sediments the first carbonate phase was

siderite. As sea water usually has a high pH at which calcium carbonate precipitates, one must assume that the solution was not supersaturated. As Berner (1980) points out, precipitation onto a pre-existing nucleus requires saturation with respect to a phase, whilst crystallisation requires supersaturation. Consequently, whilst pore fluids may have been saturated with respect to calcium carbonate, it would have been unable to precipitate. Silica conversely, either in ground water solution, or released by other reactions involving aluminosilicates, was able to precipitate as overgrowths on detrital quartz grains from saturated solutions and would not need supersaturation.

It follows that diagenetic reactions in regimes influenced by surface waters are not controlled by environment or mineralogy alone. These results also illustrate the possible influence of hydrostatic head on diagenesis in fluvio-deltaic sediments. Assuming that pore waters changed rather than evolved in situ during diagenesis of the marine sediments, these marine sediments at the base of the complex contain more freshwater reaction products such as kandites, than marine ones, such as illite. The inferred cause of this may be the hydrostatic head of fresh water from the overlying delta. This is the driving force which causes the movement of water through the water table. In this instance, it is inferred that the water table extended into these marine sediments. Consequently, continued freshwater flushing through pores, removed liberated ions and maintained a relatively poor equilibrium between the sediments and their pore waters. As a result, aluminosilicates remained unstable for a prolonged period and freshwater reactions continued, causing significant amounts of kandite formation.

Diagenesis is the sum of those processes by which an originally sedimentary assemblage attempts to reach, and maintain, an equilibrium with its environment. This working definition of diagenesis is illustrated by processes in these sediments. The marine sediments attempted to equilibrate with interstitial

sea water. Feldspars and micas began to dissolve, illite and quartz and feldspar overgrowths began to precipitate. The environment thereafter changed and became acidic, and the remaining sediments as well as solid authigenic phases reacted and moved towards a new equilibrium. Changes in pore-water chemistry during diagenesis illustrate indirectly the influence of climate, but more directly, the influence of formation waters. Suboxic bacterial processes commence following aerobic processes, assuming that organic matter remains (e.g. Curtis, 1978). It follows that ferric iron is reduced and pH rises (Curtis, 1978). As a result, equilibria reached at a low pH, and the phases precipitated at low pH became unstable. Consequently, throughout the delta, ferrous iron combined with suboxic bicarbonates to precipitate siderite. Thus, replacement of the pre-existing aluminosilicate framework began, and continued with the introduction of formation waters supersaturated with respect to calcite. The suggestion that this ferroan calcite formed from formation waters, and not depositional pore fluids must remain tentative in view of the indeterminate results from stable isotope analysis.

What controls diagenesis? As well as local relationships between grains and interstitial fluids, larger scale factors should be considered. Both depositional texture, and alluvial architecture, the geometry and connectivity of sandbodies, affect diagenesis. The relatively poor sorting of floodplain sediments affects their cementation with quartz overgrowths. Channel sandstones are well sorted, and so the detrital framework has large pores, and a large surface area. Precipitation of 5-8% quartz cemented grains together and reduced pore throats, but did not fill pore space significantly. Crevasse-splay sandstones, however, were not as well sorted, and contained more detrital pore-filling clay-sized particles. As a consequence of this, precipitation of a similar amount of quartz cemented grains together, and completely filled pore spaces. Thus, the latter are tightly cemented by quartz overgrowths in places, whilst the former are not. Subsequently, formation water circulating through the

reservoir only affected those porous sandbodies connected to the main conduits, and not completely cemented with quartz overgrowths and siderite. As a result, those thin texturally immature sands, such as crevasse splays, in which porosity was cemented during eogenesis, were unaffected by formation waters. Similarly, any sandbodies not connected through an open pore system to major conduits, would have been unaffected by formation waters.

Porosity throughout the reservoir is interpreted as secondary. The reservoir potential of these sediments can be attributed to their eogenetic cementation, as well as the subsequent aggressive fluids responsible for the porosity. During eogenesis, sandbodies throughout the Brent Group were cemented with quartz overgrowths. Thus, a rigid quartzose framework of grains and overgrowths was established. This may have taken place following minor physical compaction, during the first few metres of burial. Later, during carbonate cementation of the remaining 25-30% porosity, some replacement of quartz took place. Thereafter, when aggressive fluids removed the carbonates, they created a porosity system which mimicked the original pore space. Creation of this porosity established a system of sandbodies with a high reservoir potential (Nagtegaal, 1980). These sandbodies must have been connected in order to act as conduits for the aggressive fluids. The resulting potential reservoir, therefore, comprised connected sandbodies consisting of a rigid quartz framework containing an open pore system. Unfortunately, as interpreted above, kandites were also precipitated throughout the system.

What controls diagenesis? It is likely, in my opinion, that aggressive fluids dissolved carbonates, created secondary porosity, and precipitated kandites. The proposed influence of meteoric water on these processes is not preferred here. Bacterial degradation of organic matter generates bicarbonates. When these are not fixed they act aggressively (Curtis, pers. comm. 1982). Most probably, in the source rocks surrounding the reservoir (Kimmeridgian above,

and down faulted Kimmeridgian below, as well as possible Liassic) aggressive solutions were generated prior to hydrocarbon maturation, the eventual fate of any remaining organic matter. Pearson et al, (in press) report progressive conversion of smectites to illites in these source rocks. Their data agree with the results and trends established by Boles and Franks (1979a). As they point out, illitisation requires potassium. The postulated source of this potassium in the source rock is dissolution of aluminosilicates such as clays, micas, and fine feldspar particles (Hower et al, 1976). Although in the illitisation reaction preferred by Boles and Franks (1979a) aluminium is immobile and silica is released into solution, the silica and alumina released from other aluminosilicates is not involved. Also, illitisation of smectites is a two-stage process: the first stage, consuming potassium and releasing silica, proceeds above 60°C; the second stage, involving ordering of poorly crystalline illites, takes place above 100°C and releases  $Mg^{2+}$  and  $Fe^{2+}$ .

It follows that aggressive fluids generated during burial above 60°C would be saturated with alumina and silica. More significantly, this initial illitisation reaction releases water (Pearson et al, in press) which would, therefore, act as a transporting medium for all the reaction products. It must be stressed again that this process removes potassium from the system, it does not release potassium into hydrocarbon bearing solutions subsequently (cf. Hancock and Taylor, 1978). The introduction of these aggressive fluids containing alumina and silica into carbonate cemented reservoirs may explain carbonate dissolution, creation of secondary porosity, blocky kankar precipitation, and finally further quartz overgrowth cementation. During continued burial, and before hydrocarbon migration, continued illitisation of smectites in the source rock released  $Fe^{2+}$  and  $Mg^{2+}$  into solution. Stable isotope analysis suggests that ankerite in the Ninian Field formed at around 115°C. Although this value is not absolute, it is of the right order of magnitude and certainly suggests that ankerite formation here took place at an elevated

temperature. Boles (1978) estimates ankerite formation by a similar process at 120-160°C. Whilst the trace of chlorite at the base of 3/3-3 is interpreted as eogenetic here, an alternative explanation is that it too results from the introduction of  $\text{Fe}^{2+}$  and  $\text{Mg}^{2+}$  bearing solutions. These solutions could have reacted with pre-existing authigenic kaolinite, neomorphosing it to chlorite. In spite of this, eogenesis is preferred here because if ankerite and chlorite are attributable to the same solutions, why is their distribution dissimilar?

To summarise, ferroan calcite cements throughout the reservoir have been affected by solutions generated from two stages of illitisation of source rock smectites. The first generated aggressive solutions which dissolved carbonates, created secondary porosity and precipitated kandites and quartz. The second released  $\text{Fe}^{2+}$  and  $\text{Mg}^{2+}$ , which converted some of the remaining carbonates into ankerite.

What controls diagenesis? The discussion above has added further complicating factors to the processes affecting assemblages during burial. Mesogenetic processes, that is, processes unaffected by the regime at the surface, operated throughout these porous sandbodies irrespective of their depositional environment.

Similarly, other diagenetic processes operating during burial affected all the remaining porous sandbodies. These processes include illite and albit authigenesis, and grain-to-grain contact dissolution. These may have begun before ankerite precipitation, but appears to have operated with increasing dilution of pore waters. The amount of formation water illitisation is negligible by comparison to eogenetic illite throughout the sediments. Indeed, this illite does not appear to have significantly affected kandite either above or below the oil-water contact.

Semi-quantitative XRD data, and modal analyses from 3/3-3 are compiled in Table 4.3. Although there is a discrepancy between the two sets of data, this does not affect the overall picture. This discrepancy is affected by two things: kandite plates are generally 5-20  $\mu\text{m}$  in diameter, whilst illitic hairs are a fraction of a micron in diameter and thus occupy a larger proportion of the less than 2 $\mu\text{m}$  fraction than they do of the whole rock; secondly, large clay plates are readily counted during modal analysis, whereas fibrous hairs are not. Furthermore, pore-filling clays contain up to 50% porosity and so do not readily reflect their actual content in the rock (Sarkisyan, 1971). The data in Table 4.3 demonstrate a concentration of illite in the marine sediments below 10570', and in the marginal marine interdistributary bay-filling sands between 10464' and 10510'. Kandites, however, predominate in the inferred non-marine sediments. Whilst there is more illite below the oil-water contact it does not increase gradually downwards. Furthermore, illite concentration does not increase at the expense of kandites, which occur unaltered below the oil-water contact, and indeed are more abundant in the coarse-basal sandstone than in the oil zone.

In addition, the gamma ray logs (Turner, pers. comm. 1980; Figs. 4.2 and 4.3) do not reveal any marked increase of radioactivity and possibly, therefore, potassium content directly below the oil-water contact. What these logs do reveal is a distinct increase through mudrock horizons, and a smaller peak in the micaceous sandstone. Thus, none of the available techniques has confirmed the hypothesis of illitisation intensity increasing downwards through the oil zone and into the water zone.

Sommer (1978) also discusses this problem, and whilst he too suggests that illitisation is related to hydrocarbon migration, he does not propose as simplistic a model as Hancock and Taylor (1978). Moreover, Sommer (1978) states that in some wells illitisation increases into the oil zone. In addition,

he breaks down analysed sequences into lithological units and notes that the clean coarse basal sands are not illitised, whilst illite concentrations are greatest in micaceous sands. This suggests that lithology (depositional mineralogy) and possibly eogenetic processes may better explain the distribution of illite in the Brent Group.

Illite precipitation might have occurred after oil migration, but not for the reasons suggested by Hancock and Taylor (1978), nor producing the sequence they predict. Most of the illite in the Ninian Field can be related to eogenetic processes, not formation waters. Its precipitation presumably diluted formation waters with respect to alumina and silica, and especially potassium. I would tentatively suggest that albite authigenesis, which requires dilute saline waters undersaturated with respect to clays (Boles, 1982), took place subsequently.

Quartz is increasingly soluble at high pH (Berner, 1971), but it is generally metastable, not possessing sufficient free energy to dissolve. However, it is possible that the combination of dilute silica undersaturated pore waters, high pH, high temperature and poorly cemented grains, with stressed contacts lined with clays is sufficient to promote quartz dissolution. Recent work suggests that pressure does not contribute significantly to suturing grain-to-grain contacts. Firstly, De Boer et al (1977, p. 257) state:

"experiments revealed that when samples have undergone some consolidation, the presence of water is essential for continuation of the compaction process."

Removal of water does not remove any stresses to which the sediment may be subject, but removes the medium in which material can diffuse away down "chemical-potential gradients" (Robin, 1978). Consequently, dissolution at grain contacts takes place when these contacts are stressed, and when a medium exists in which material can diffuse away. Stress, however, is not necessarily a function of pressure or burial depth. Borak and Friedman (1981, p. 144)



describe textures from the Anadarko Basin in Oklahoma, and report that

"in summary, at a depth of approximately 9100 m, many of the textural features described from these quartz sandstones duplicate those found at much shallower depths of burial, including features present under near surface conditions."

In addition, intense sutures throughout the Ninian Field are lined with micaceous material, which is believed to aid the diffusion of dissolved material away from grain-to-grain contacts (Hancock, 1978a).

I would conclude, therefore, that relatively poor cementation with quartz overgrowths retained a high proportion of stressed grain contacts in coarse samples. Consequently, with suitable pore-water composition dissolution occurred, generating sutured contacts and releasing silica into solution. Displacement of pore waters by hydrocarbons above the oil-water contact may have inhibited suturing, but dissolution would have continued to the present day elsewhere. Hence grain-margin dissolution has operated in the Brent Group, at depth, but has not contributed to its cementation by quartz overgrowths, which predate suturing.

One final point I should like to discuss briefly is the marked discrepancy between petrophysical data from Albright et al (1980), and modal analyses from this study (Table 4.4). Essentially, results from modal analyses of porosity only approach petrophysical values in the most permeable samples, channel sandstones from Zones III, IVB and V. Results from relatively impermeable samples which contain large percentages of clay are 50-200% in error. The reasons for the discrepancy are probably related to porosity types and clay content. Sarkisyan (1971) estimates that clay-filled pores contain up to 50% porosity. Visual observation of clays in this study, for example, Plates 4.1H, and 4.3E, certainly does not contradict this estimate. Clay-filled pores, therefore, contain significant porosity. Similarly, samples containing large percentages of matrix clay, fine-grained sediment, or

neomorphosed micas may contain significant amounts of microporosity. Microporosity is difficult to evaluate visually during modal analysis, but is measured petrophysically. However, clays tend to limit permeability, and the micropores they enclose are often fully occluded. Consequently, the correlation of low permeability and high clay content may help to explain this discrepancy, for example Zone II. Furthermore, permeability in fine-grained sandstones with small pore throats may be affected by migrating clays. Whilst coarse sands have large open pore throats, those of fine and tightly cemented sands are often only 10  $\mu\text{m}$  wide. Thus, loose pore-filling kaolinites up to 20  $\mu\text{m}$  in diameter may block pore throats and reduce permeability if they migrate during fluid flow through pores (Hancock, 1978b). Hence the low permeability of porous sands with a high clay content such as Zones I, IVA and VI.

#### CONCLUSIONS

Following their lithification, Liassic mudrocks were transgressed by mature coarse clastic sediments during the Middle Jurassic. The resulting sequence fines upwards through beach, foreshore, and shoreface deposits. Afterwards, fluvio-deltaic progradation incised distributary channels into these marine sediments, and established a low-lying coastal plain on which interdistributary bay filling sequences, floodplain muds and sands, and channel-filling sands accumulated.

Diagenetic modifications of these sediments reflect numerous influences. Marine and non-marine sediments generally contain illite and kaolinites respectively, following attempted equilibration of pore fluids with the sediments. Although the data may be interpreted to suggest in situ processes were responsible for continued modifications in the marine sediments, inferred allochthonous pore waters are perhaps a better explanation in view of the consistency

between diagenesis here and on the floodplain. Consequently, all the sediments probably reflect the influence of the water table driving fresh water through the sequence, precipitating kandites and subsequently siderite. During burial, formation waters precipitated ferroan calcite throughout the remaining porous sandbodies. The reservoir was then affected by source rock reactions. Firstly, bacterial bicarbonate production and illitisation of smectites in the source rock, generated aggressive fluids which both created secondary porosity and precipitated kandites and quartz. These were succeeded from the source rock by  $\text{Fe}^{2+}$  and  $\text{Mg}^{2+}$  bearing solutions, which resulted in ankerite precipitation, and finally oil. Meanwhile, following illite precipitation, increasing dilution of the formation waters promoted albite authigenesis and finally grain-margin dissolution of quartz.

FIG. 4.1 NORTHERN NORTH SEA  
NINIAN FIELD,  
WELL 3/3 -1, COMPOSITE  
LOG. (Turner, pers.comm. 1980 )

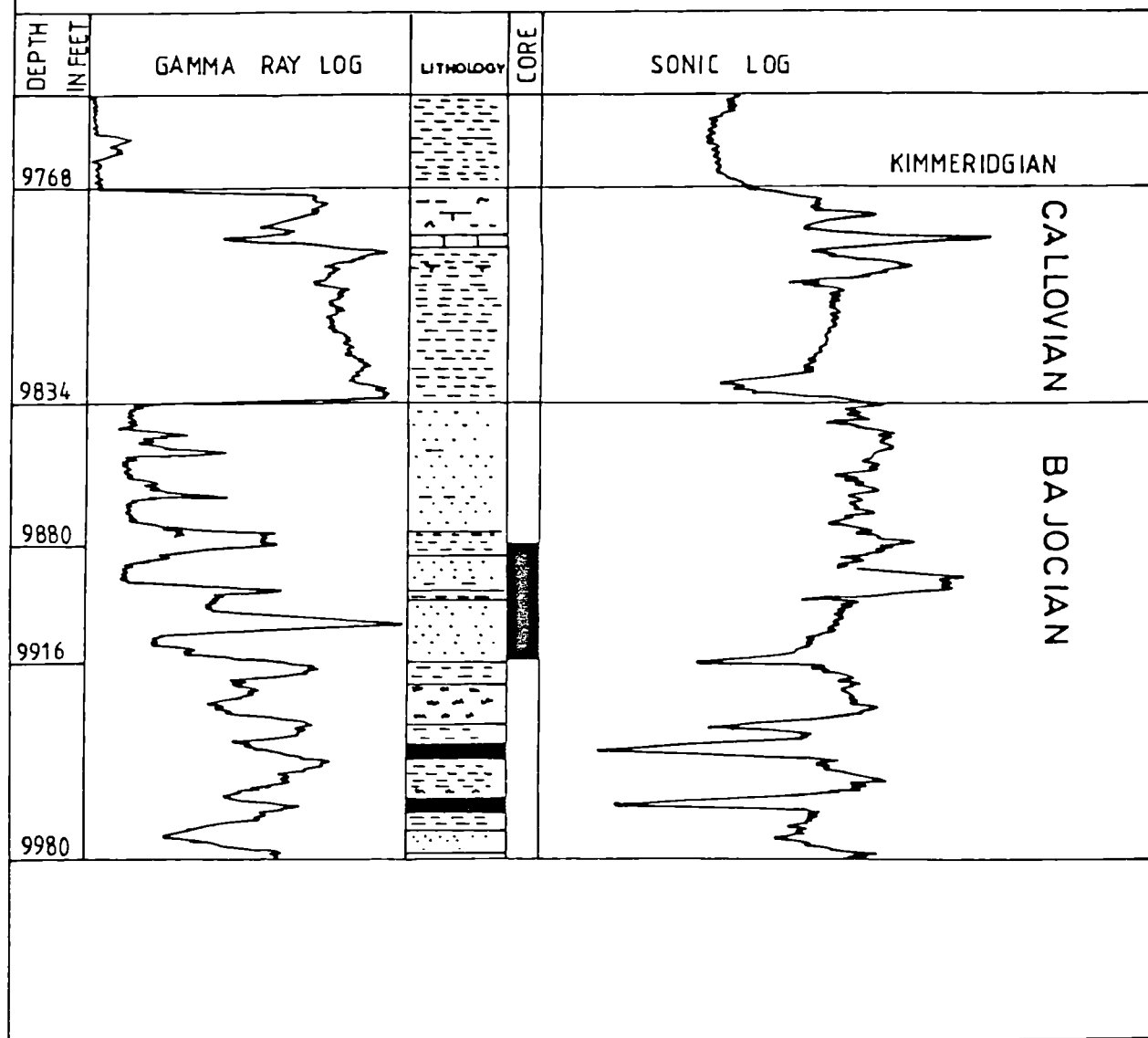


FIG. 4.2 NORTHERN NORTH SEA, NINIAN FIELD,  
WELL 3/3-2, COMPOSITE LOG

(Turner. pers. comm. 1980).

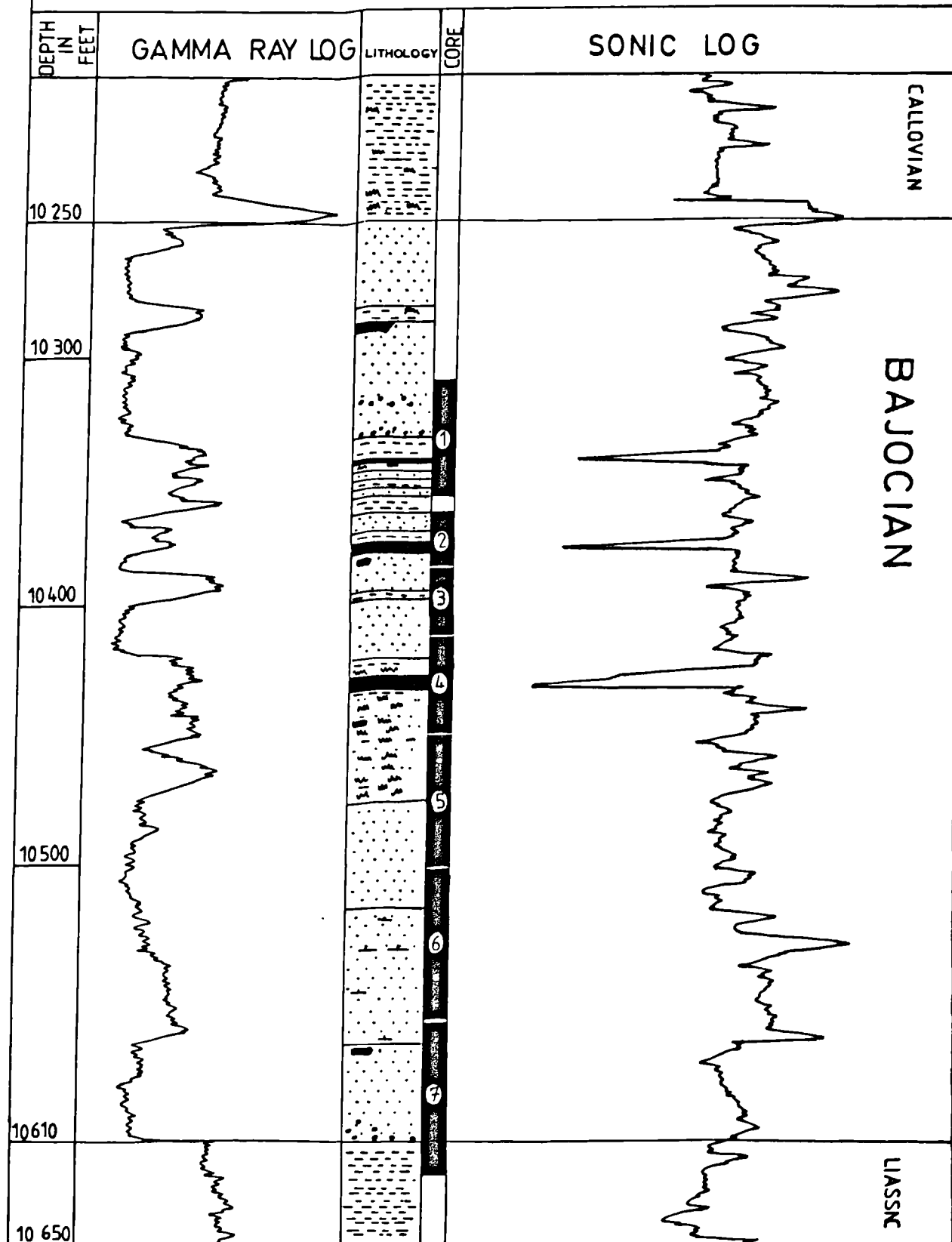


FIG. 4.3 NORTHERN NORTH SEA, NINIAN FIELD.  
WELL 3/3-3 COMPOSITE LOG (Turner, pers.comm.  
1980)

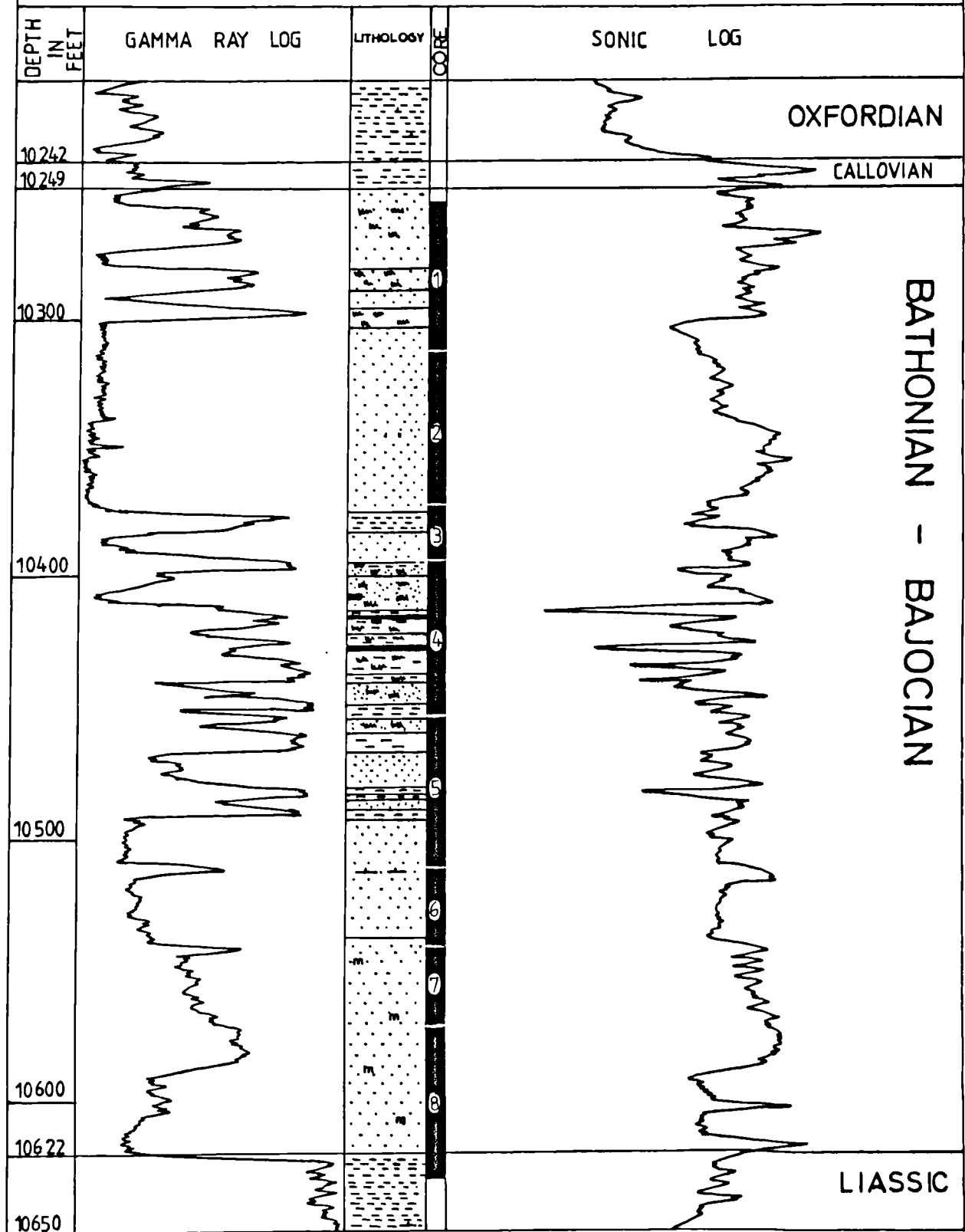




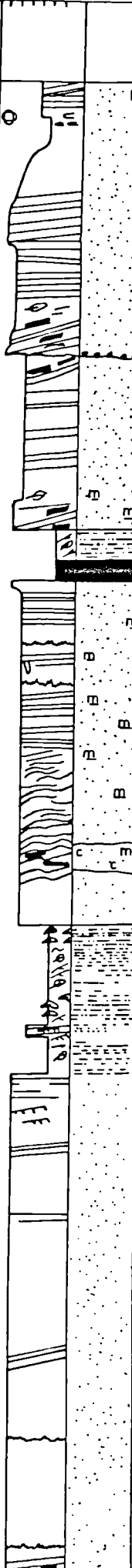
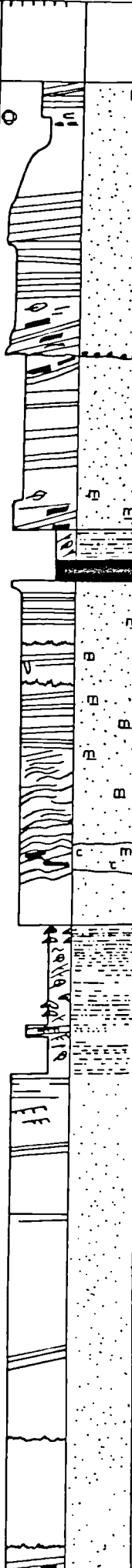
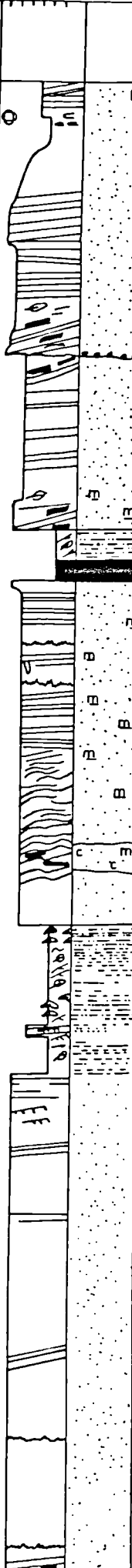
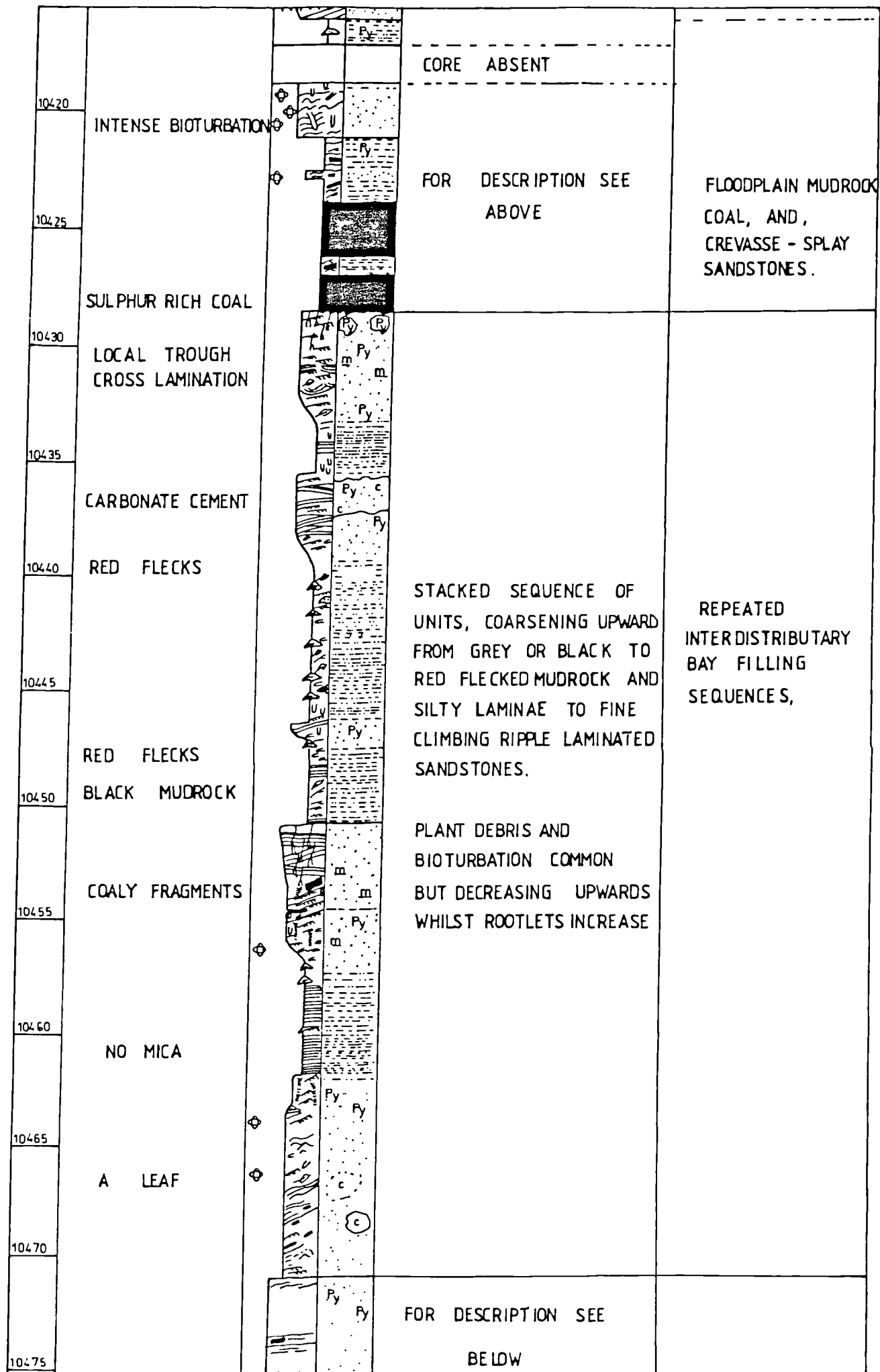


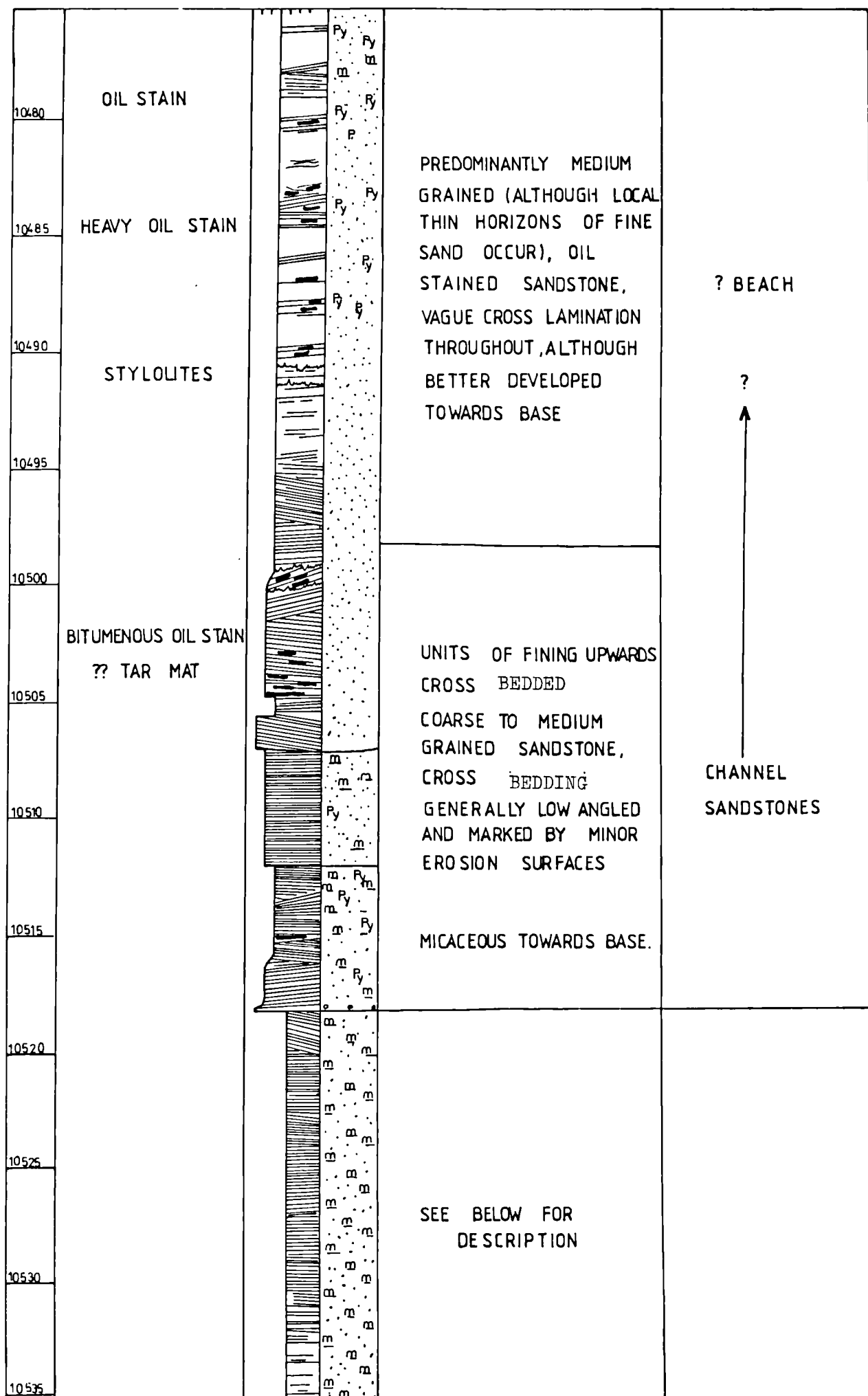
FIG.4.4 NORTHERN NORTH SEA NINIAN FIELD, BRENT GROUP, CORE 3/3-2. LITHOLOGICAL AND SEDIMENTOLOGICAL LOG.

DEPTH IN FEET	SPECIFIC COMMENTS	GRAIN-SIZE SEDIMENTARY STRUCTURES V-C-M-F-S-Ch	GRAPHIC LITHOLOGY	DESCRIPTION	INTERPRETATION
10307					
10310	OIL-STAIN			REPEATED VERY COARSE TO COARSE, SUCCEEDED BY COARSE TO MEDIUM GRAINED FINING UPWARDS UNITS. OVERALL SECTION FINES UPWARDS, FROM LAG DEPOSIT OF PLANT DEBRIS AND PEBBLES.	CHANNEL SANDSTONE
10315					
10320					
10325					
10330	LAG DEPOSITS			COARSENING UPWARDS UNIT, CAPPING SEQUENCE OF INTERBEDDED SHARP TOPPED AND ABRUPTLY BASED FINE SANDSTONE UNITS, WITH SILTY GREY AND BLACK MUDROCKS. PLANT DEBRIS COMMON THROUGHOUT. ROOTLETS AND BIOTURBATION IN SANDS AND MUDROCKS.	LEVEE OR LAKE FILLING ----- FLOODPLAIN MUDROCK AND CREVASSE SPLAY SANDSTONES
10335	MICACEOUS LAMINAE				
10340	CONTORTED BEDDING				
10345	VERY BLACK MUDROCKS				
10351	LITTLE MCA ABUNDANT PLANT DEBRIS				
				CORE ABSENT	

10359	RED STAIN		CORE ABSENT	
10365	OIL STAIN		REPEATED CROSS-LAMINATED FINING UPWARDS UNITS, WITH LAG DEPOSITS OF WOODY AND PLANT DEBRIS AND PEBBLES.	CHANNEL SANDSTONE
10370				
10375				
10380	MICACEOUS		INTERCALATED GREY PYRITOUS MUDROCKS, SILTY MUDROCKS AND COALS WITH ABUNDANT PLANT DEBRIS : WITH THICK LOCALLY MASSIVE SHARP TOPPED AND ABRUPTLY BASED CROSS-LAMINATED SANDSTONES	FLOODPLAIN SEDIMENTS
10385	WAVY LAMINATION			CHANNEL SANDSTONE
10390	CALCAREOUS CEMENT NO OIL STAIN			FLOODPLAIN SEDIMENTS
10395				FLOODPLAIN SEDIMENTS
10400	OIL STAIN		INTERCALATED GREY PYRITOUS MUDROCKS, SILTY MUDROCKS AND COALS WITH ABUNDANT PLANT DEBRIS : WITH THICK LOCALLY MASSIVE SHARP TOPPED AND ABRUPTLY BASED CROSS-LAMINATED SANDSTONES	CHANNEL SANDSTONE
10405				CHANNEL SANDSTONE
10410				CHANNEL SANDSTONE
10415	STYLOLITES			CHANNEL SANDSTONE

















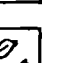
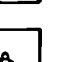


10540				
10545				
10550				
10555				
10560				
10565				
	RED MUDROCK CLAST			
10570				
10575	STYLOLITES ESCAPE BURROWS HAEMATITIC HORIZON			
10580				
10585				
10590				
10595	END/TOP OF PEBBLES			
		<p>VERY FINE GRAINED PALE GREY MICACEOUS SANDSTONE. PREDOMINANTLY WELL CROSS LAMINATED ALTHOUGH LOWER TEN FEET BIOTURBATED INTENSIVELY. SCATTERED WOODY DEBRIS</p> <p>INDIVIDUAL SAND LAMINAE SEPARATED BY MICACEOUS LAMINAE</p>	<p>STORM - DRIVEN (? MIDDLE TO) UPPER SHOREFACE DEPOSITS.</p> <p>-----</p> <p>INTERMITTENT FAIR, WEATHER SANDSTONE</p>	
		<p>FINING UPWARDS COARSE TO MEDIUM GRAINED SANDSTONE, WITH LOW ANGLE CROSS, AND HORIZONTAL BEDDING . BIOTURBATED TOWARDS TOP, WITH A VARIETY OF BURROWS AND ESCAPE STRUCTURES PRESERVED.</p>	<p>INCREASINGLY STORM INFLUENCED FORESHORE TO UPPER SHOREFACE SANDSTONE</p> <p>-----</p> <p>FORESHORE/BEACH</p>	
		FOR DESCRIPTION SEE BELOW		

10600			COARSE GRAINED PEBBLY SANDSTONE WITH VERY COARSE PEBBLY LAG DEPOSITS BETWEEN COSETS	BEACH SWASH ZONE OR FORESHORE CHANNEL SANDSTONE (SEE TEXT)
10605			WAVY CROSS-LAMINATION	
10610			DARK GREY HORIZONTALLY LAMINATED MUDROCK	"LIASSIC"
10615				

## KEY

### SEDIMENTARY STRUCTURES

-  HORIZONTAL LAMINATION
-  LOW ANGLE CROSS BEDDING
-  WAVY LAMINATION
-  RIPPLE LAMINATION
-  CLIMBING RIPPLE LAMINATION
-  CLIMBING RIPPLES
-  STYLOLITES
-  BURROWS
-  ESCAPE STRUCTURES
-  ROOTLETS
-  SILTSTONE CLAST
-  WOODY DEBRIS
-  PLANT DEBRIS
-  BIOTURBATION

### GRAPHIC LITHOLOGY

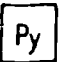


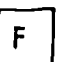



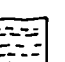


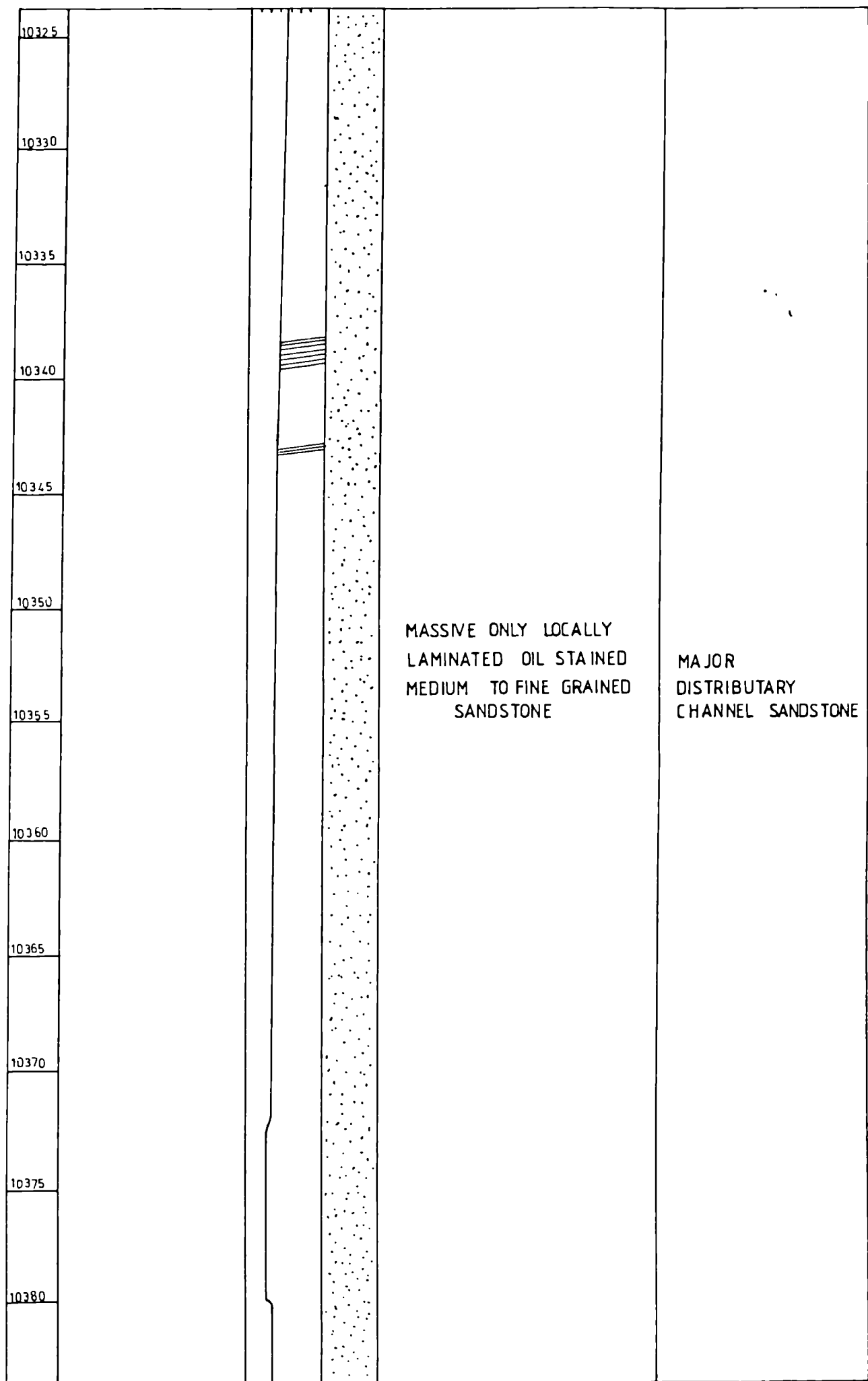
-  PYRITE
-  MICACEOUS LAMINATION
-  CARBONATE CONCRETIONS
-  FERROUS CARBONATE CONCRETIONS
-  SANDSTONE
-  SILTSTONE
-  SILTY MUDROCK
-  MUDROCK
-  GRANULES
-  COAL

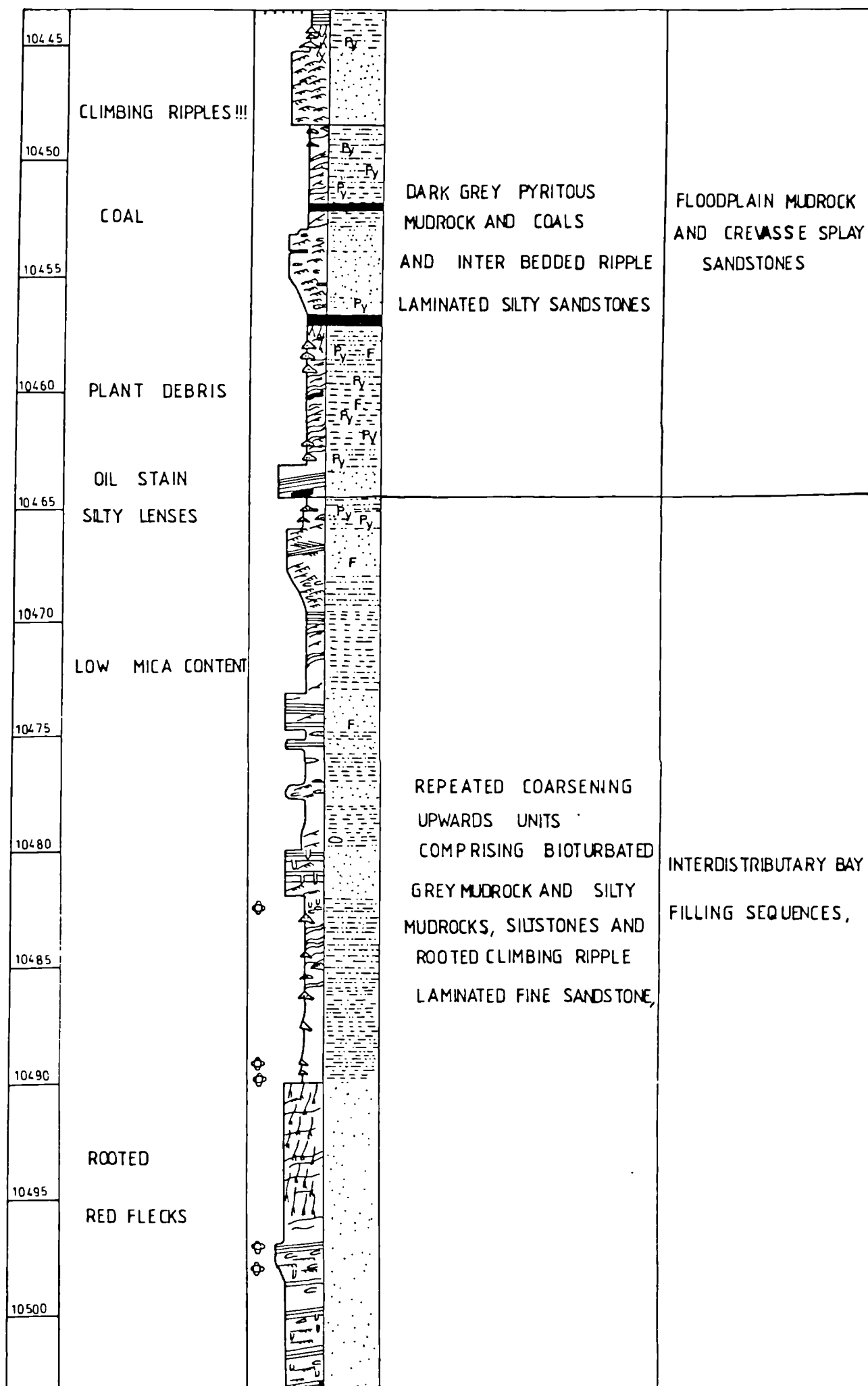
FIG. 4.5 NORTHERN NORTH SEA NINIAN FIELD, BRENT GROUP, CORE 3/3-3 LITHOLOGICAL AND SEDIMENTOLOGICAL LOG.

(SEE FIG. 4.4 FOR KEY)

DEPTH IN FEET	SPECIFIC COMMENTS	GRAIN SIZE SEDIMENTARY STRUCTURES M.C.M.F. SCHV	GRAPHIC LITHOLOGY	DESCRIPTION	INTERPRETATION
10278					
10280			Ry m		CHANNEL SANDSTONE
10285			m		
10290				COARSE TO MEDIUM AND FINE GRAINED FINING UPWARDS UNITS, WITH WAVY AND LOW ANGLE CROSS BEDDING :	FLOODPLAIN MUDROCK AND CREVASSE SPAY SANDSTONES
10295			Py Ry	ALTERNATING WITH HORIZONTALLY LAMINATED GREY AND BLACK PYRITOUS SILTY MUDROCKS, INTER-BEDDED WITH THIN SHARP TOPPED AND SHARP BASED RIPPLE LAMINATED FINE SANDSTONES AND SHORT COARSENING UPWARDS BIOTURBATED UNITS.	CHANNEL SANDSTONE
10300					
10305			Ry Ry Ry Ry		FLOODPLAIN MUDROCK AND LAKE FILLING SANDSTONES
10310					
10315			Py		CHANNEL SANDSTONE
10320			Py Py Py		FLOODPLAIN MUDROCK
				SEE BELOW	



10390			SEE ABOVE FOR DESCRIPTION	
10395	? TAR MAT			
10400				
10405	LARGE OIL STAIN		COARSE TO MEDIUM GRAINED FINING UPWARDS UNIT (BASE ABSENT), OVERLAIN BY SILTY WAVE RIPPLE LAMINATED MUDROCKS	FLOODPLAIN MUDROCK
10410	OIL STAIN			CHANNEL SANDSTONE
10415			CORE BROKEN	
10417			CORE ABSENT	
10420				FLOODPLAIN MUDROCK
10425			COARSE TO MEDIUM GRAINED FINING UPWARDS SANDSTONE WITH COARSE BASAL LAG DEPOSIT OVERLAIN BY BLACK MICACEOUS MUDROCK	CHANNEL SANDSTONE
10430	OIL STAIN			
10435				
10440	COAL		DESCRIPTION BELOW	





10505				
10510			FOR DESCRIPTION SEE ABOVE	
10515				
10520				
10525	HEAVY OIL STAIN			FORESHORE / BEACH ? SANDSTONE
10530	? BITUMEN		WHITE TO BUFF PREDOMINANTLY MEDIUM GRAINED NON-CALCAREOUS SANDSTONE. LOWER UNITS FINE UPWARDS FROM COARSE BASAL LAG DEPOSIT WITH LOCAL CROSS- LAMINATED BASE AND VAGUE WAVY LAMINATION ABOVE. UPPER UNIT MASSIVE WITH LOCAL HORIZONTAL LAMINATION ABOVE FINE BASE WITH LOW ANGLE CROSS BEDDING	UPPER SHOREFACE ? CHANNEL SANDSTONE
10535				
10540				
10545				CHANNEL SANDSTONE
10550				
10555				
10560				

			SEE ABOVE	
			CORE ABSENT	
10570				
10575				
10580				
10585			WHITE TO LIGHT GREY VERY FINE GRAINED MICACEOUS SANDSTONE WITH MINOR FINE SAND DEVELOPMENTS.	
10590			HORIZONTAL AND LOW ANGLE CROSS LAMINATION THROUGHOUT, WITH MINOR EROSION SURFACES EVIDENT. SANDSTONE MICACEOUS THROUGHOUT BUT PARTICULARLY TOWARDS THE INTENSIVELY BIOTURBATED BASE.	STORM DRIVEN (UPPER) SHOREFACE SANDSTONE
10595				
10600				
10605				
10610				
10615	NOTE COLOUR MOTTLING		PALE GREY, MEDIUM GRAINED HORIZONTALLY LAMINATED SANDSTONE.	BEACH/FORESHORE SANDSTONE
10620				

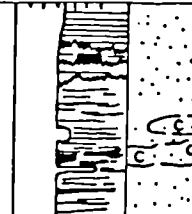
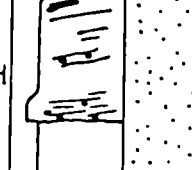

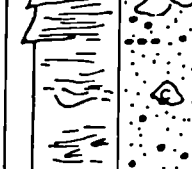
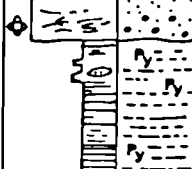
	STYLOLITES		CARBONATE CONCRETIONS. MICACEOUS IN PLACES WITH WOODY DEBRIS	
10630				
	SIDERITE SPHERULITH HORIZON ??		WHITE TO GREY, MAINLY COARSE GRAINED SANDSTONE WITH VERY COARSE SAND HORIZONS AND SCATTERED PEBBLES. LARGELY MASSIVE, BUT WITH WAVY LAMINATION IN LOWER PART AND VAGUE HORIZONTAL LAMINATION AT BASE. MOSTLY POROUS BUT WITH OCCASIONAL CONCRETIONS.	? BEACH FORESHORE OR SWASH ZONE (SEE TEXT).
10635				
				
10640				
	? BURROWS			
10645				
			DARK GREY MUDROCKS WITH COMMON PYRITE NODULES	LIASSIC
10650				
10654.10				

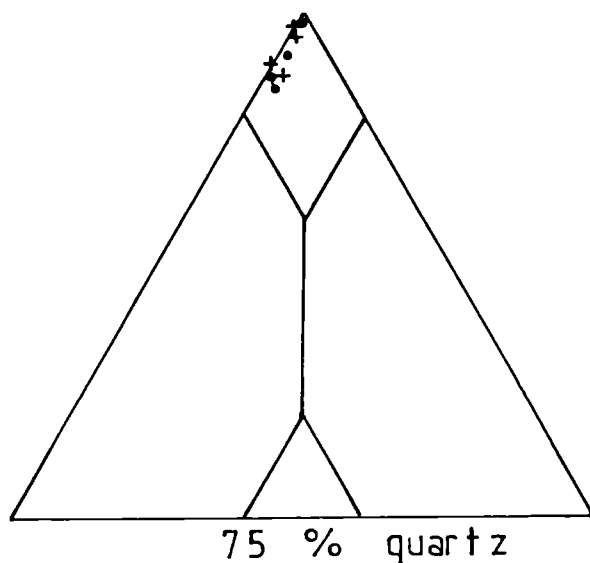
FIG. 4.6 NORTHERN NORTH SEA NINIAN  
FIELD, BRENT GROUP, CORE 3/3-1.  
LITHOLOGICAL AND SEDIMENTOLOGICAL  
LOG.

(SEE FIG 4.4 FOR KEY)

DEPTH IN FEET	SPECIFIC COMMENTS	GRAIN SIZE, SEDIMENTARY STRUCTURES VEGETATION & Clay	GRAPHIC LITHOLOGY	DESCRIPTION	INTERPRETATION
9853					
9900					FLOODPLAIN MUDROCKS
9905	OIL STAIN				
9910	CARBONATE CONCRETIONS 2" COAL			FINING UPWARDS UNITS: COMPRISING COARSE TO MEDIUM GRAINED, CROSS BEDDED SANDSTONES; FINE GRAINED SANDSTONE AND SILTY SANDSTONE OVERLAIN BY ROOTED SILTY MUDROCKS.	CHANNEL SANDSTONE
9915					FLOODPLAIN MUDROCKS
9920	ABUNDANT PLANT DEBRIS				CHANNEL SANDSTONE
9927	OIL STAIN			? MASSIVE COARSENING UPWARDS MEDIUM GRAINED CROSS BEDDED SANDSTONE	?? BAY FILLING

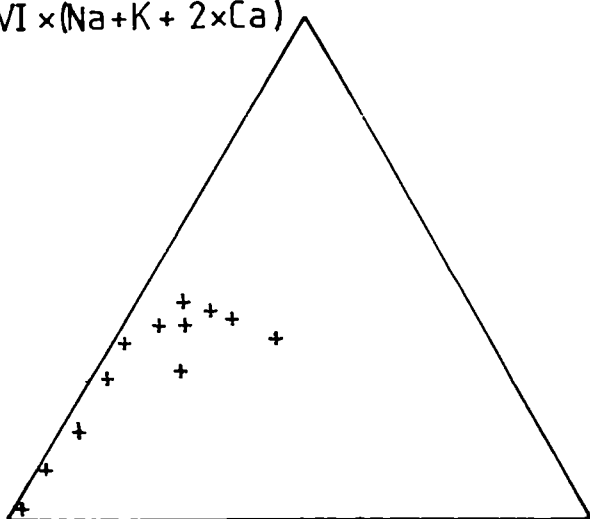
FIG 4.7

SANDSTONE COMPOSITION AND CLAY  
MINERAL ANALYSIS



(a) Sandstone composition  
+ Beach  
• Shoreface

Al VI  $\times$  (Na + K + 2Ca)

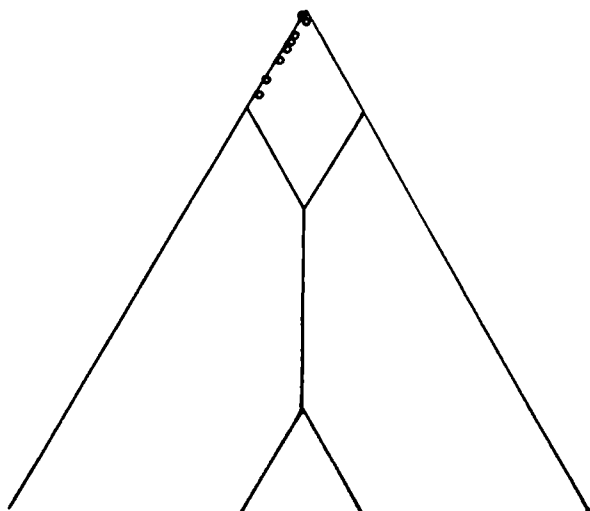


(b) Clay mineralogy of  
beach sandstones.

+ neomorphosing micas

Al VI  $\times$  2

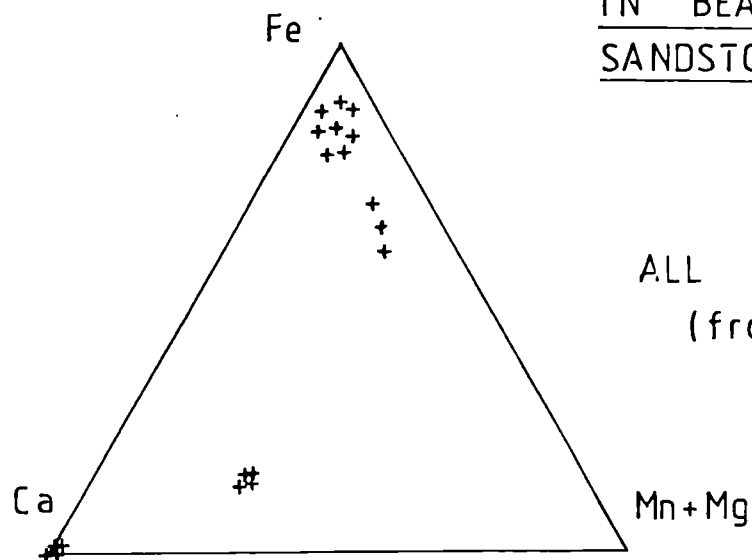
3  $\times$  (Fe + Mn + Mg)



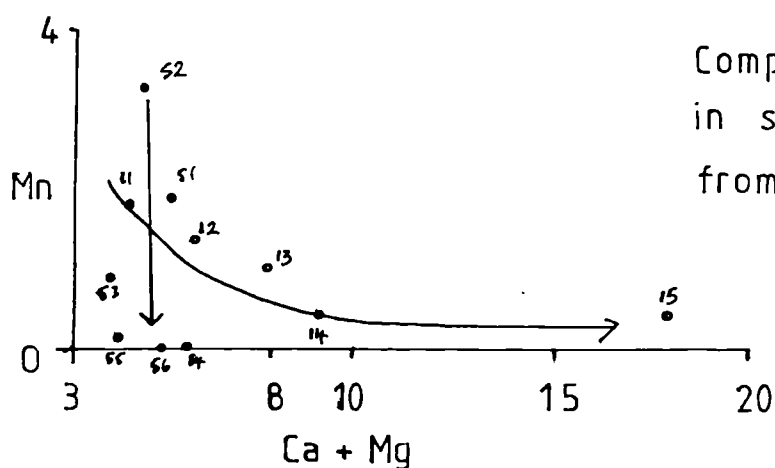
(c) Modal analysis of  
micaceous sandstone

FIG. 4.8

MINERALOGICAL COMPOSITION AND  
VARIATIONS OF CARBONATE CEMENTS  
IN BEACH AND FORESHORE  
SANDSTONES , 3/3-3



ALL DATA  
 (from appendix F)

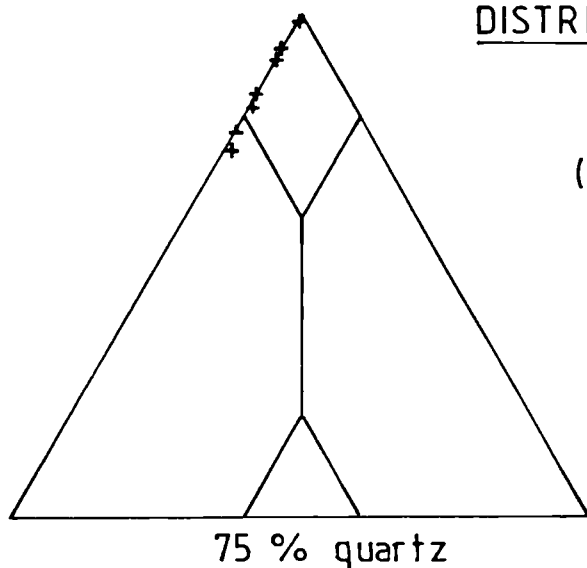


Compositional variations  
 in siderite spheruliths  
 from - 10,632

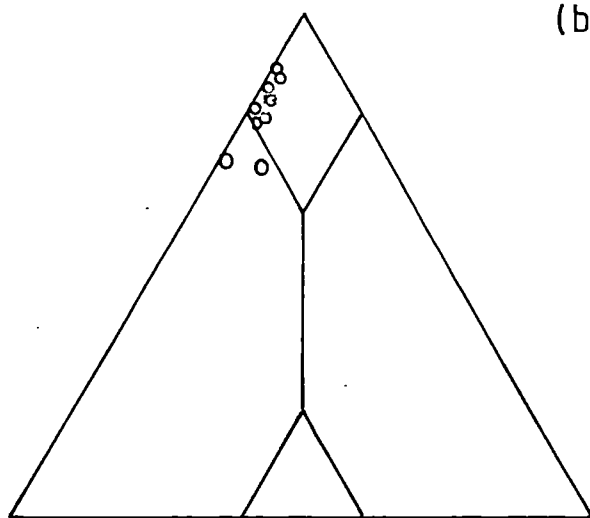
Sample	10632	10632	10632	10632	10632	Sample	10632	10632	10632	10632	10632	10632
Code	C..	C..	C..	C..	C..	Code	C..	C..	C..	C..	C..	C..
Spot	11	12	13	14	15	Spot	51	52	53	54	55	56
SiO <sub>2</sub>	4.03	2.67	0.63	1.09	0.70	SiO <sub>2</sub>	n.d.	n.d.	0.27	0.32	0.25	n.d.
TiO <sub>2</sub>	n.d.	n.d.	n.d.	n.d.	n.d.	TiO <sub>2</sub>	n.d.	n.d.	n.d.	n.d.	n.d.	n.d.
Al <sub>2</sub> O <sub>3</sub>	0.27	2.02	0.40	0.48	0.25	Al <sub>2</sub> O <sub>3</sub>	n.d.	n.d.	n.d.	n.d.	n.d.	n.d.
FeO	53.08	51.00	52.13	51.29	51.85	FeO	55.79	53.69	57.76	55.50	56.80	57.63
MgO	1.30	1.27	1.79	2.42	11.97	MgO	1.53	1.24	1.39	0.89	0.59	1.15
MnO	1.77	1.31	1.20	0.43	0.45	MnO	1.85	3.43	0.93	n.d.	0.36	n.d.
CaO	3.03	4.61	5.97	6.65	5.96	CaO	3.88	3.12	2.47	4.83	3.66	4.00
Na <sub>2</sub> O	0.56	n.d.	n.d.	0.46	n.d.	Na <sub>2</sub> O	0.43	n.d.	n.d.	0.42	n.d.	0.46
K <sub>2</sub> O	0.13	0.42	0.14	n.d.	n.d.	K <sub>2</sub> O	n.d.	n.d.	n.d.	n.d.	n.d.	n.d.
TOTAL	64.17	63.30	62.26	62.82	71.18	TOTAL	63.48	61.48	62.82	61.96	61.66	63.24

FIG 4.9

SANDSTONE COMPOSITION AND CLAY  
MINERALOGY OF DISTRIBUTARY AND INTER-  
DISTRIBUTARY SEDIMENTS.

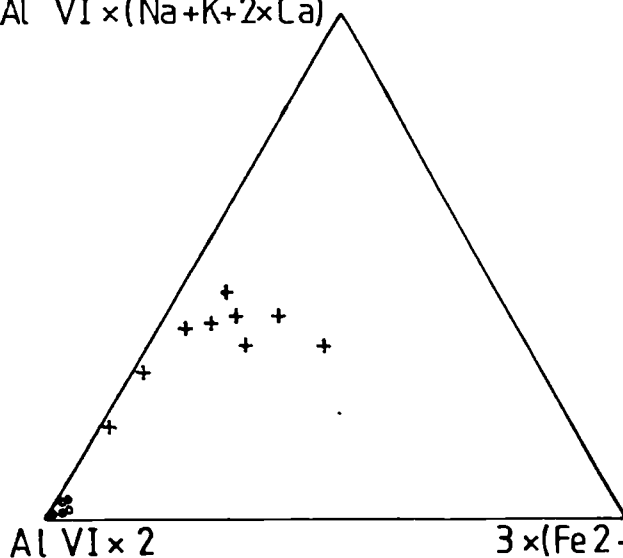


(a) Sandstone composition of distributary sandstones



(b) Composition of bay-filling sandstones

Al VI  $\times$  (Na+K+2 $\times$ Ca)

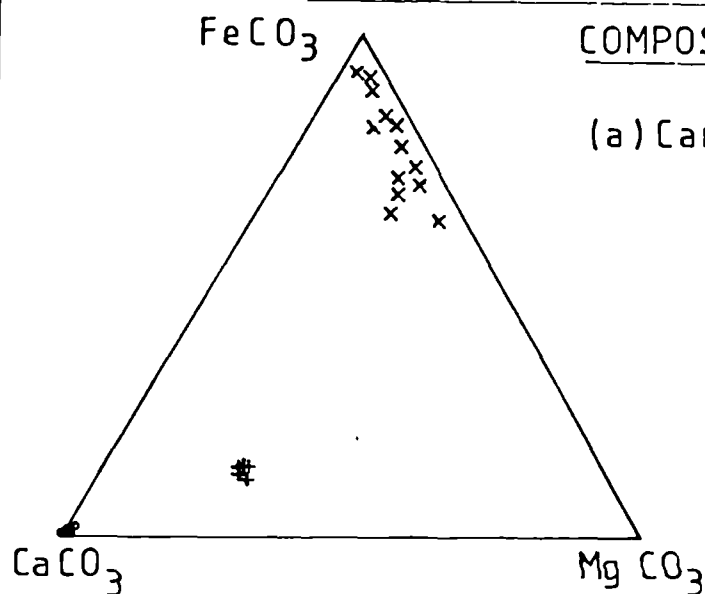


(c) Clay mineralogy of bay-filling sandstones  
+ neomorphosing micas  
• kandites.

FIG 4.10

CARBONATE COMPOSITIONS THROUGHOUT THE  
NINIAN FIELD AND SANDSTONE

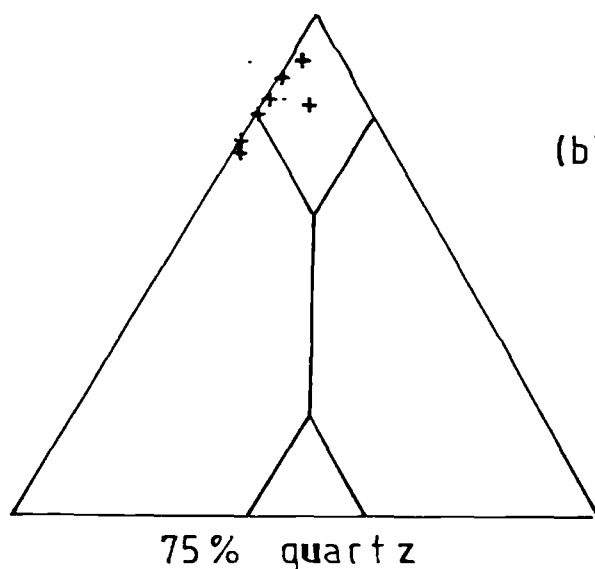
COMPOSITION AND CLASSIFICATION



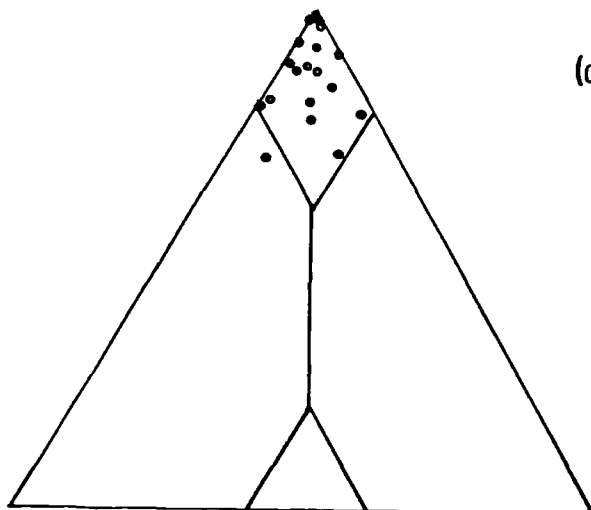
(a) Carbonate composition

- Calcite
- + Ankerite
- x Siderite

(the spheruliths from  
10 632 are not  
included here).



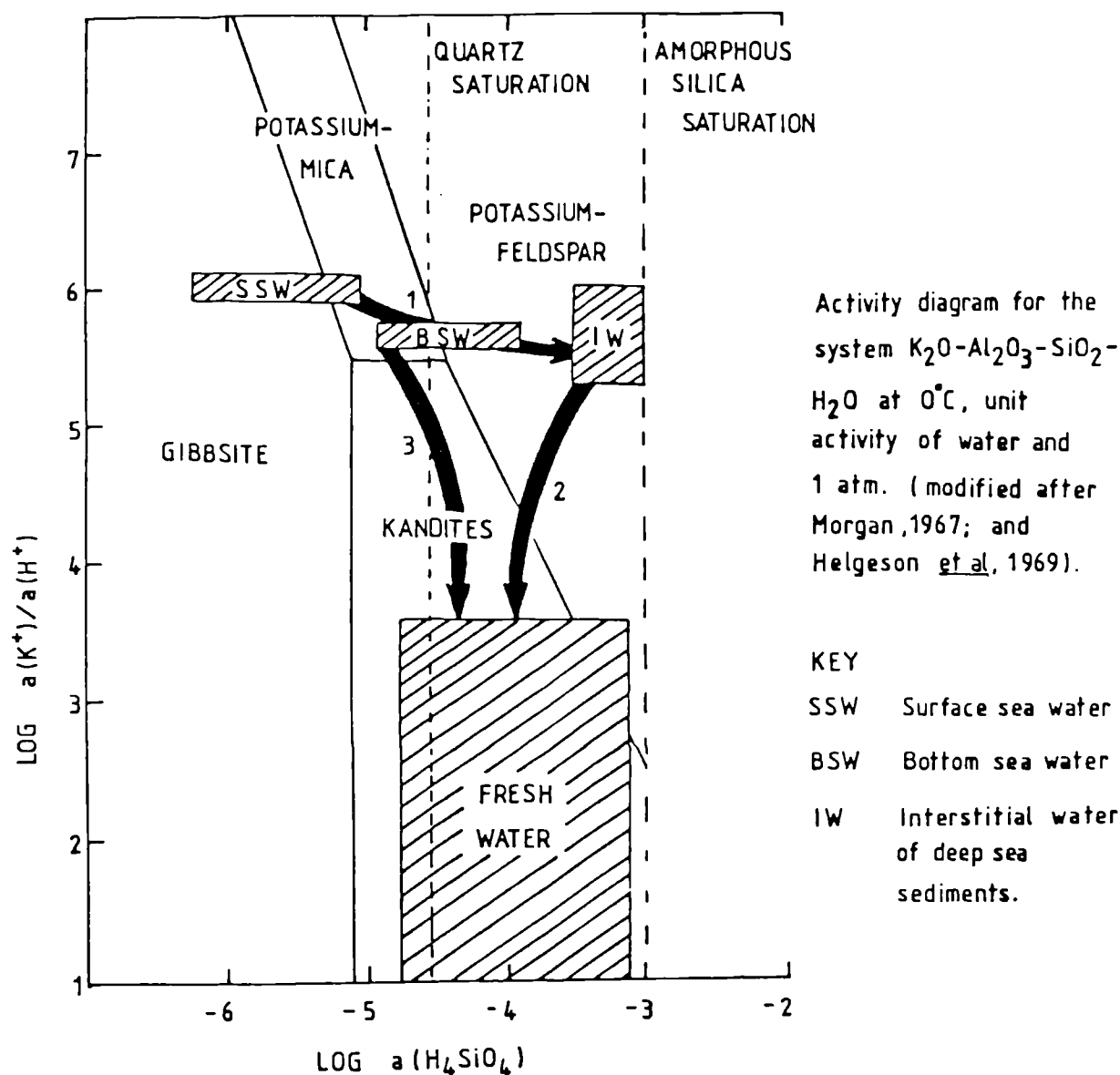
(b) Modal analysis of  
crevasse splay sandstones



(c) Modal analysis of channel  
sandstones.



Fig. 4.11 Eogenesis of aluminosilicates in marine clastic sediments in the Ninian Field.

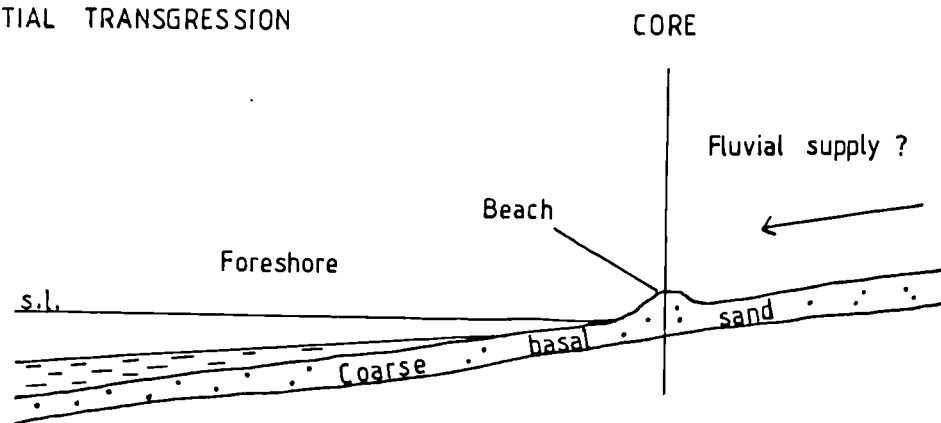


(1) Illite precipitated immediately following deposition as it is the only aluminosilicate phase stable in sea water. Detrital kandites and feldspars may have dissolved at this time. As pore-fluid composition evolved, potassium feldspar became stable, and illite precipitation ceased. Consequently, overgrowths formed.

(2+3) Subsequently, as pore fluids became acidic, both potassic phases became unstable with respect to kandites and so micas neomorphosed whilst both detrital and authigenic feldspars dissolved.

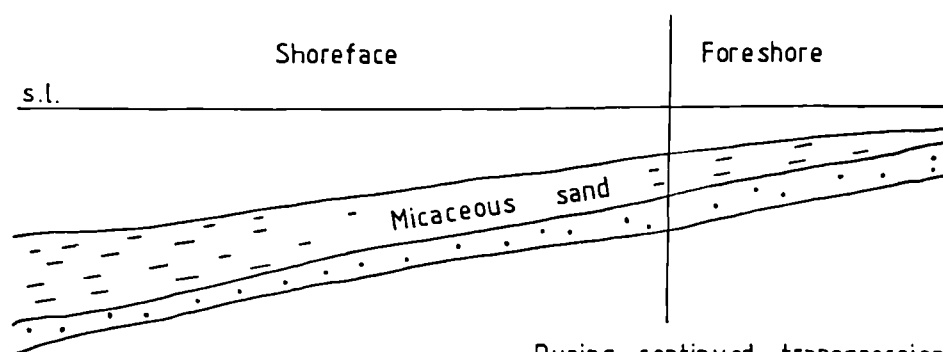
FIG. 4.12 A POSSIBLE MODEL FOR THE ORIGIN AND PRESERVATION OF A SIDERITE SOIL IN THE COARSE-BASAL SAND.

(a) INITIAL TRANSGRESSION



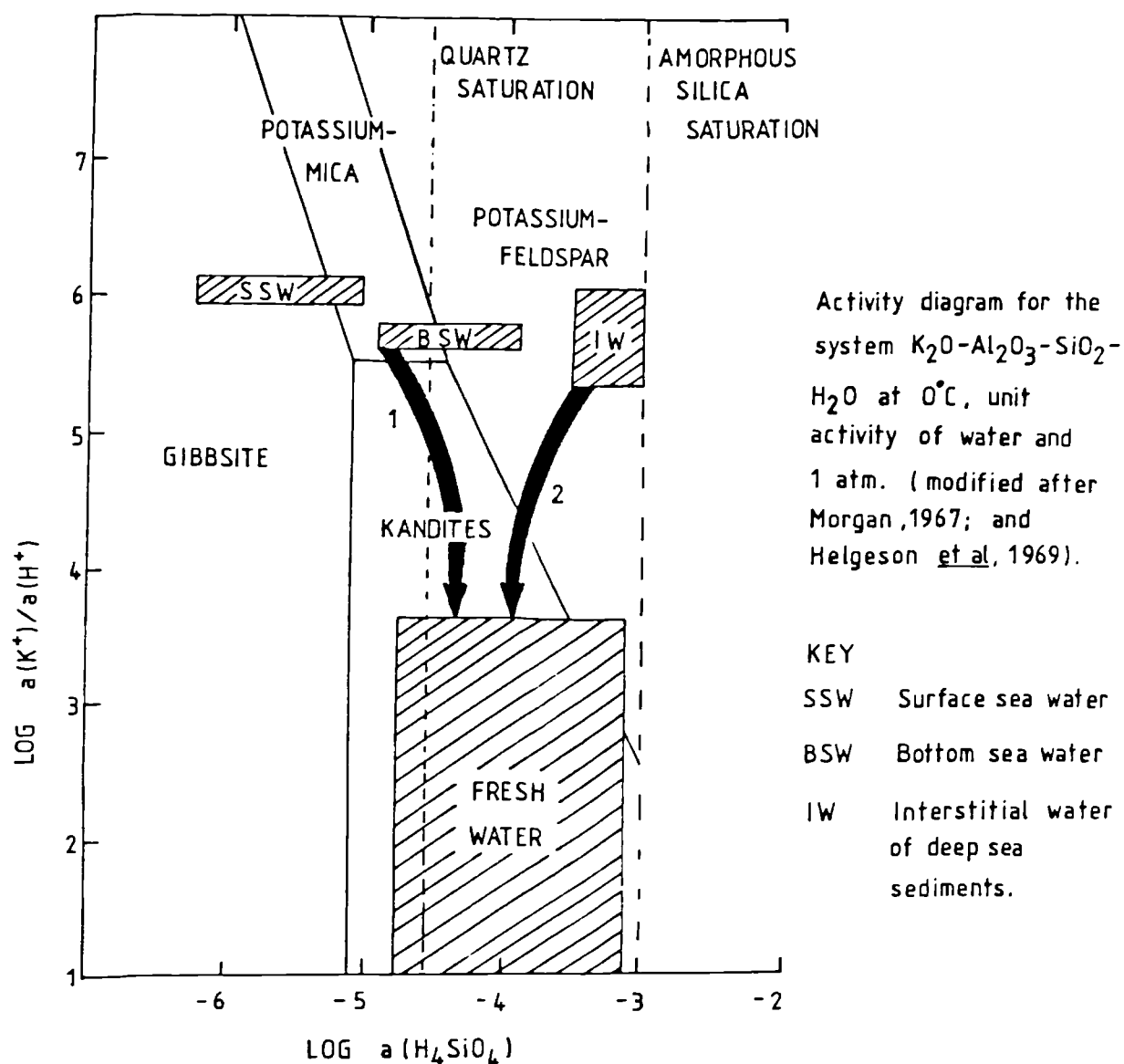
During the initial transgression soil horizons may have developed on or in the beach perhaps due to oxygen depletion or stagnation on the floodplain

(b) PROGRESSIVELY DEEPENING WATER



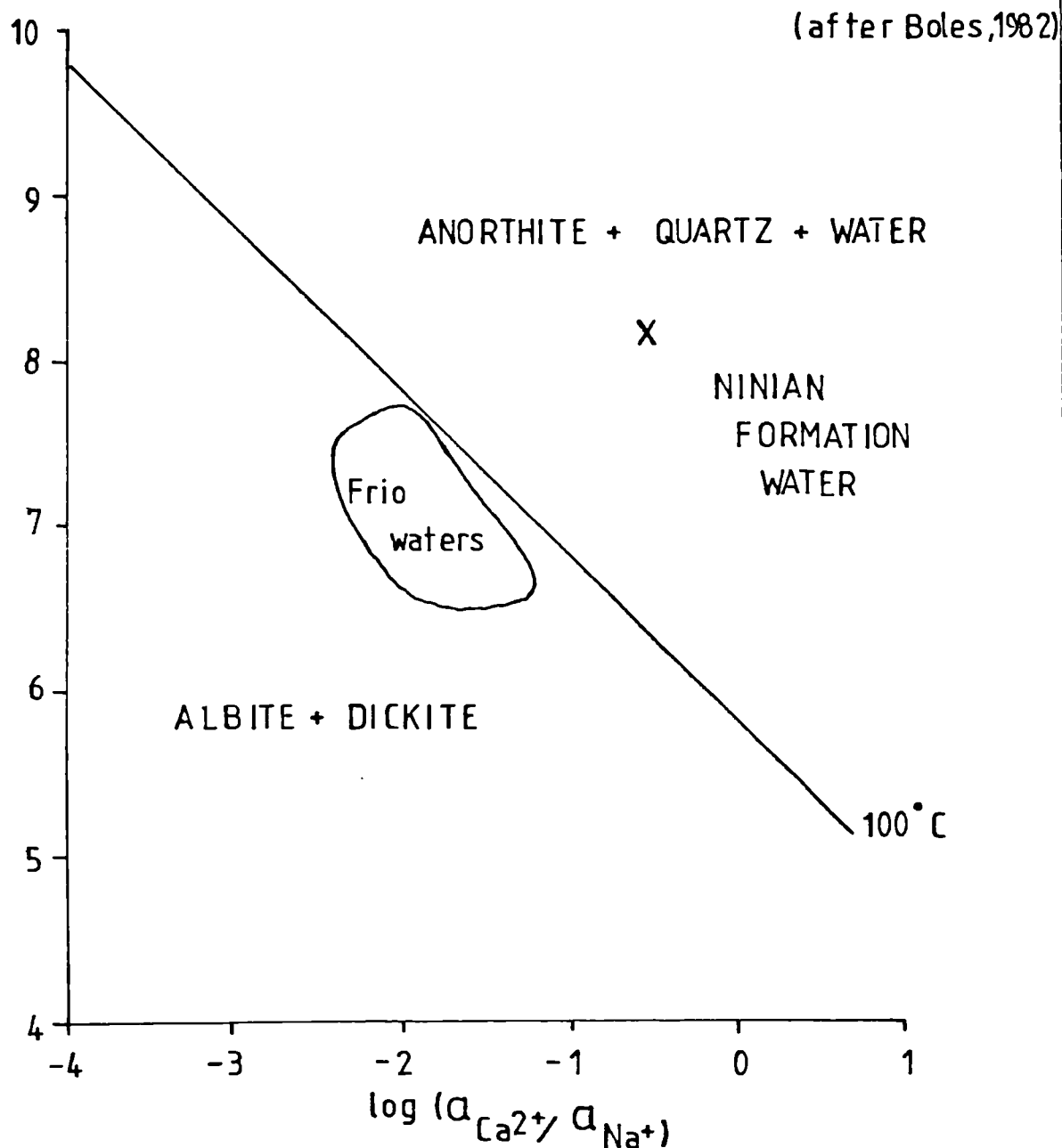
During continued transgression erosion removed part of the coarse-basal sand.

Fig.4.13 Eogenesis of aluminosilicates in non-marine clastic sediments from the Ninian Field.



1. Neomorphism of micas and illitic clays to kandites, the more stable phase in fresh water.
2. Hydration and dissolution of feldspars as they equilibrate with their fresh water pore fluids.

FIG 4.14 COMPARISON OF FORMATION WATERS  
FROM THE NINIAN FIELD WITH THOSE  
FROM THE FRIO FORMATION, TEXAS  
AND THE EQUILIBRIUM BOUNDARY FOR  
THE ALBITISATION REACTION.



Basic diagram after Boles (1982, Fig. 6),

Ninian analyses from Table 4.2 (Larsen, pers.comm.1981)

FIG. 4.15 Flow chart to summarise diagenetic reactions in the Ninian Field

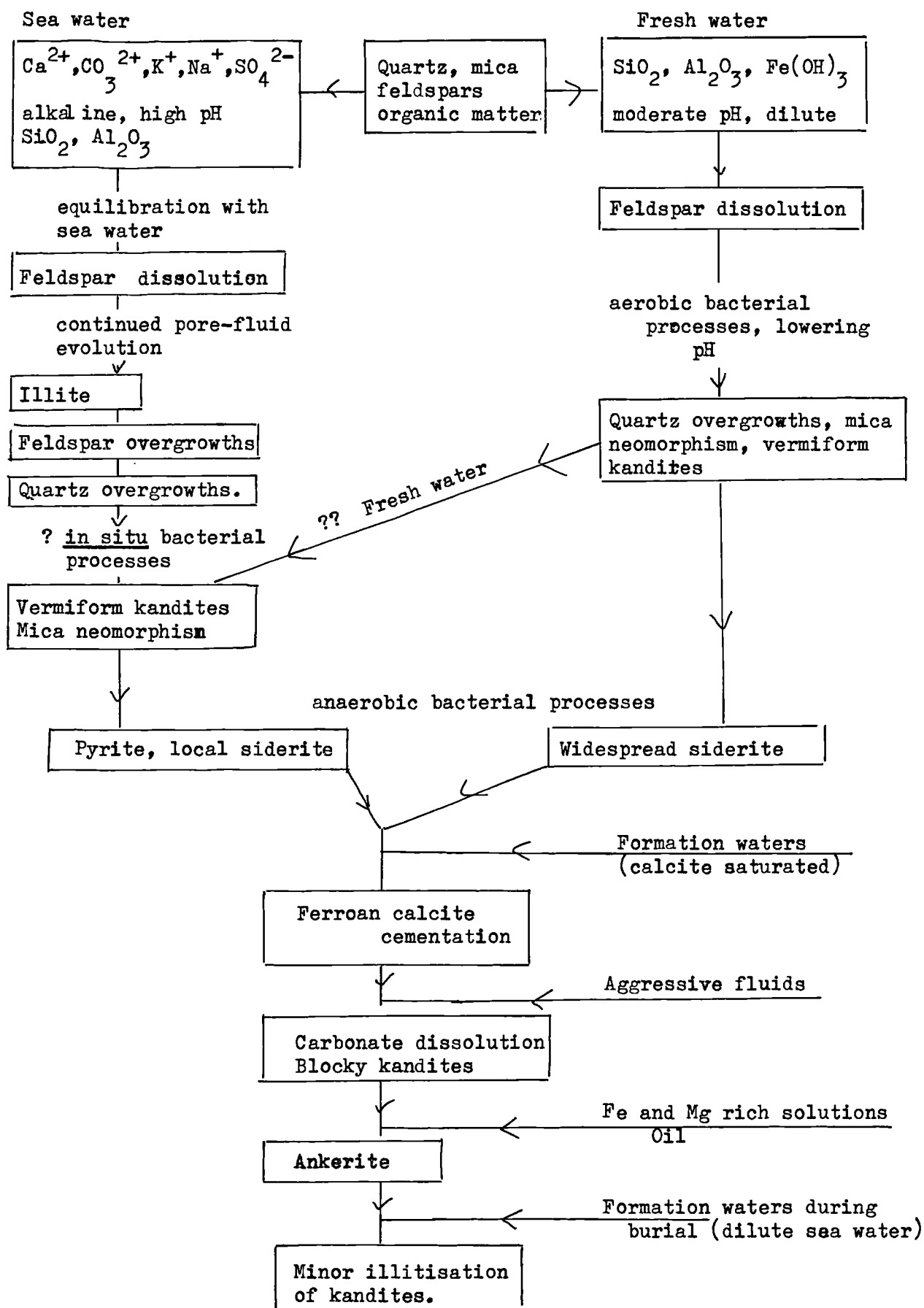


Table 4.1 Comparison of the sedimentological facies recognised in the Ninian Field, with existing stratigraphical proposals for the Brent Group.

Bowen (1975)	Deegan and Scull (1977)	Albright <u>et al</u> , (1980)	This study
Upper Brent Sand	Tarbert Formation	Zone VI	↑ ?    Fining-upwards units: channels and floodplain sediments
		Zone V	
Middle Brent Sand	Ness Formation	Zone IV	Coarsening-upwards units: interdistributary bay filling sediments
Lower Brent Sand	Etive Formation	Zone III	Massive sand: distributary channel sands
	Rannoch Formation	Zone II	Micaceous sandstone: shoreface sandstones
	Broom Formation	Zone I	Coarse-basal sandstone: Beach/foreshore sands

Table 4.2      Composition of Ninian Field formation waters,  
in comparison with other data

	Ninian Field (Larsen, pers.comm.1981)	Sea water (White, 1965)	Frio Formation Wells C and D (Boles, 1982)	
Na <sup>+</sup>	8,600	10,560	2,680	9,420
K <sup>+</sup>	175	380	46	240
Ca <sup>+</sup>	165	400	150	4,225
Mg <sup>2+</sup>	30	1,272	3.3	18
Ba <sup>2+</sup>	51	0.05	1.5	256
Sr <sup>+</sup>	32	13.3		
Cl <sup>-</sup>	12,730	18,980	3.950	22,000
SO <sub>4</sub> <sup>2-</sup>	90	2,649	57	7
HCO <sub>3</sub> <sup>-</sup>	1,800	140	400	114
CO <sub>3</sub> <sup>2-</sup>				
pH	8.2	8.1	7.3	6.8
T.D.S. (mg/L)	23,690	34,475	7,500	36,000

Table 4.3 Clay mineralogy of 3/3-3 from XRD and modal analysis

Depth	and Depositional environment	Quantified XRD		Modal analysis	
		Kandite	Illite	Kandite	Illite
10295	Channel	75	25	2	0
10323	"	100		1.5	0
10350	"	100		2	0
10365	"			1	0
10385	"			1	0
10406	"	85	15	2	0
10425	"				
<hr/>					
		Oil-water contact 10430			
10434	"			3	0
10447	Crevasse splay			7	0
10454	"	85	15	3	2
10464	Bay filling			5	1
10474	"	85	15	3	0
10495	"	60	30	3	1
10497	"			6	2
10502	"			0	0
10510	"	55	45	0	0
10519	Distributary channel	85	12		
10525	"			5	0
10529	"	100		2	0
10538	"	90	9	7	0
10547	"	90	10	7	0
10552	"			5	0
10562	"	90	10		
10563	"			7	2
10570	Shallow marine	80	15	3	1
10575	"			4	0
10580	"	80	20	4	1
10590	"	80	15		
10594	"			4	0
10599	"	75	16	4	0
10608	"			8	-
10610	"	80	15	6	2
10616	Foreshore			8	2
10620	"	90	10		
10624	"			11	1
10628	"			11	2
10632	Beach ?	85	10	10	5
10637	"			8	3
10640	"	85	10	11	3
10645	"			8	3



Table 4.4      A comparison of petrophysical data and modal analyses  
                                  from the Ninian Field

Information presented in this thesis		Data from Albright <u>et al</u> (1980)			
Sedimentological lithological divisions	Porosity %	Clay content %	Permeability md.	Porosity %	Chevron zones
Coarse basal sand	7.1	12.7	50-150	14.5-22	I
Micaceous sand	3.3	4 (Mica 25%)	15-35	10.8-18.9	II
Massive sand	12	5.8	4-500	14-24.6	III
Bay filling sequences	5	3.6	20-800	17.8-24.8	IV
Floodplains	4.3	7.8			
Channel sands			400-2850	16.1-21.3	IVB
	14	1.8			
Massive channel sand (3/3-3)			1550-1800	15.6-20.9	V
Overbank sands	4.3	7.8	225	16.4	VI

Modal analyses only approach the petrophysical values in the cleanest sandstones - the channel sandstones.

Plate 4.1

- A Pore-filling vermiform kandites, comprising aggregated, stacked pseudo-hexagonal plates. Beach sandstone, 3/3-3, 10640'.
- B and C Large siderite spheruliths between and cementing quartz grains. Plate widths 700  $\mu\text{m}$ .
- D Characteristic lozenge shaped aggregate of siderite, possibly replacing plant debris. Plate width 2.2 mm.
- B, C, D Beach sandstone 3/3-3, 10632'.
- E Quartz arenite with tight quartz overgrowth cementation. Overgrowths are separated from detrital grains by dust rims (x). Foreshore sandstone 3/3-3, 10642'.
- F and G Vermiform kandites, aggregates of pseudo-hexagonal plates, intergrown with an ordered stacking sequence of individual plates and filling intergranular pore space. Plate G, width 350  $\mu\text{m}$ . Foreshore sandstones 3/3-3 10620' and 10624' respectively.
- H Oversized or secondary pore filling of blocky kandites. Each short dense stack of pseudo-hexagonal kandite plates is one plate in diameter, and unrelated to other stacks within the pore. Note that no evidence of illitisation was observed or detected in these or the vermiform kandites (F and G) from these samples. Foreshore sandstone 3/3-3, 10624'

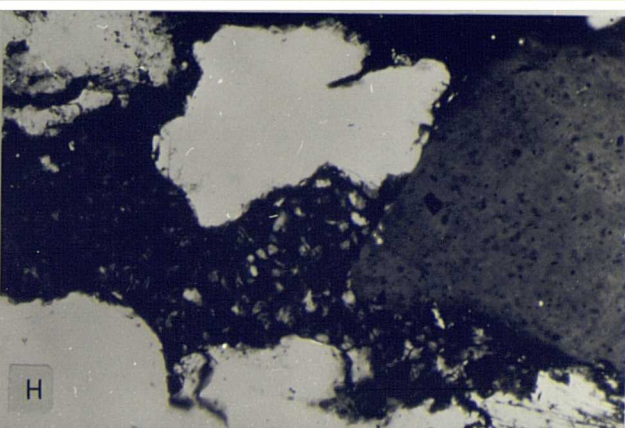
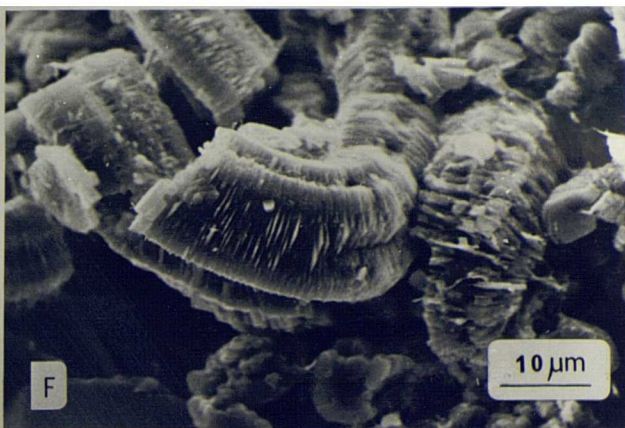
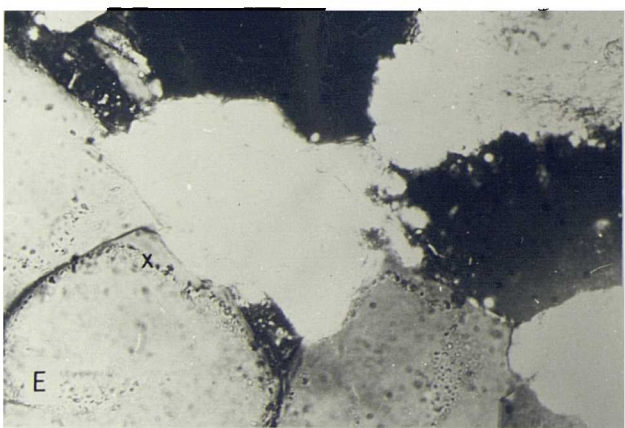
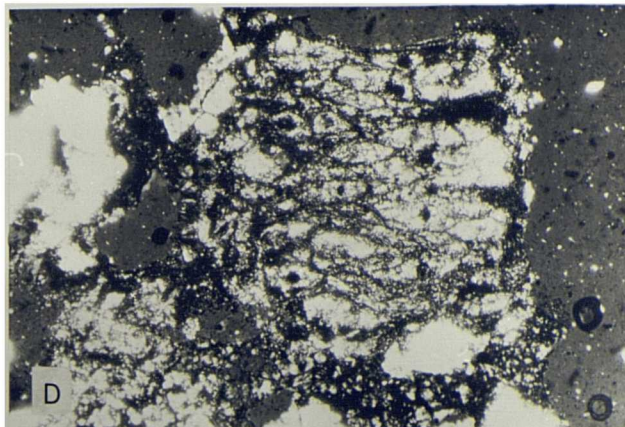
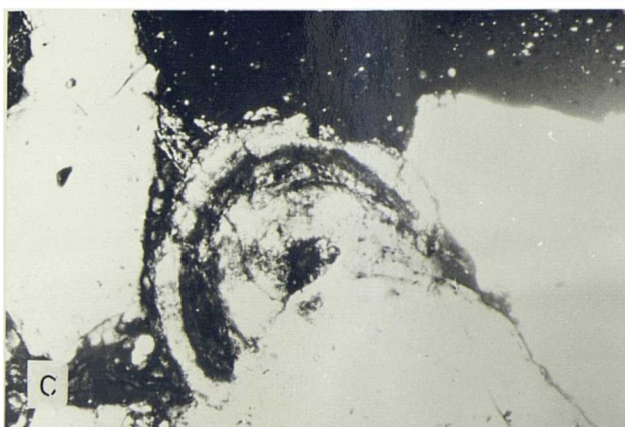
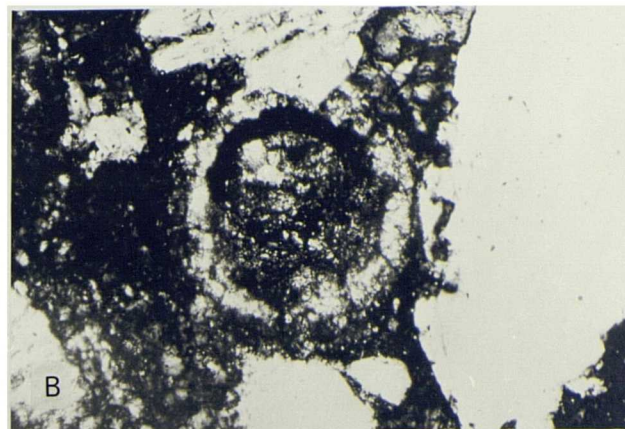
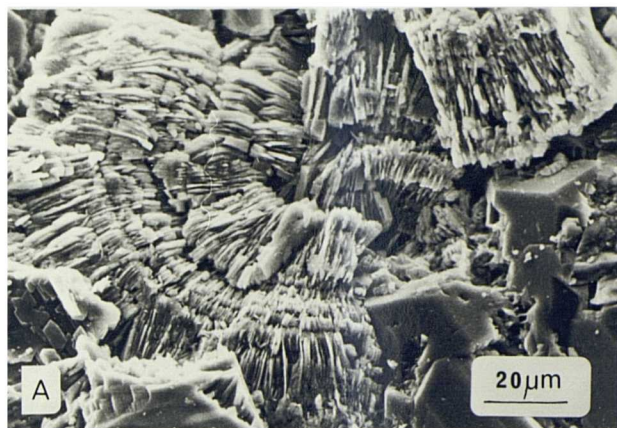


Plate 4.2

- A      Pore-lining illite, apparently nucleated directly on the pore wall, a quartz grain.
- B      Dissolution of the core of a detrital feldspar grain, whilst an overgrowth also occurs (o). This pore also contains quartz overgrowths, and blocky kandites (k) which are apparently unrelated to the feldspar grain. A and B foreshore sandstones 3/3-3, 10620'.
- C      Potassium feldspar overgrowth, and dissolved detrital grain core. Dissolution has also occurred subsequent to overgrowth precipitation. Foreshore sandstone 3/3-3, 10580'.
- D      Pore-filling blocky kandites. Each short aggregate is typically one plate in diameter. There is no evidence of illitisation of these plates.
- E      Intergranular porosity full of illitic clays and kandites. D and E shoreface sandstones, 3/3-3, 10590' and 10599' 6" respectively.
- F      Quartz overgrowths with a deeply etched surface. (This example should not be confused with the surface revealed by removal of the surrounding grain which should be convex rather than concave, and exhibit sharp quartz overgrowth boundaries). Channel sandstone 3/3-3, 10547' 9".
- G      Secondary pore filling of blocky kandites, with corroded quartz overgrowths on pore walls (o), and potassium feldspar overgrowth. Possible crevasse-splay sandstone (?). 3/3-3, 10525'.
- H      Authigenic potassium feldspar, with a typical rhombic form. Channel sandstone, 3/3-3, 10562'.



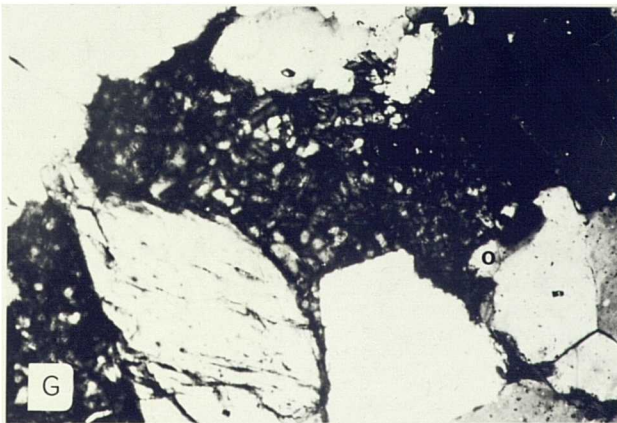
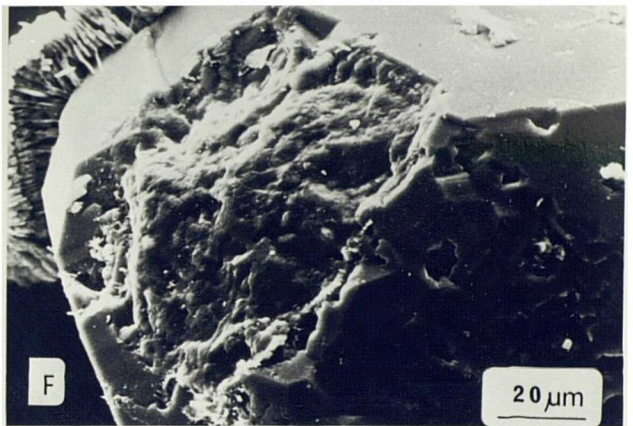
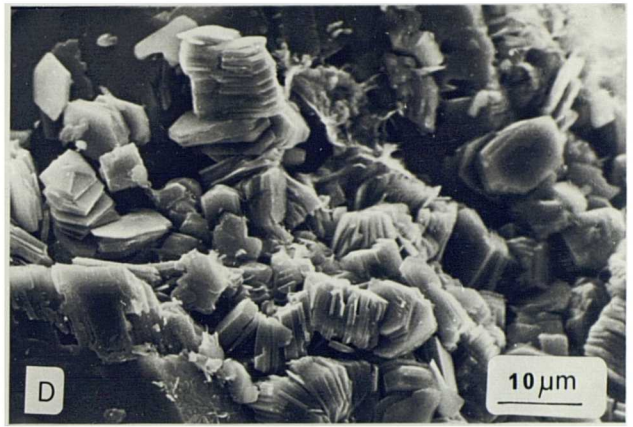
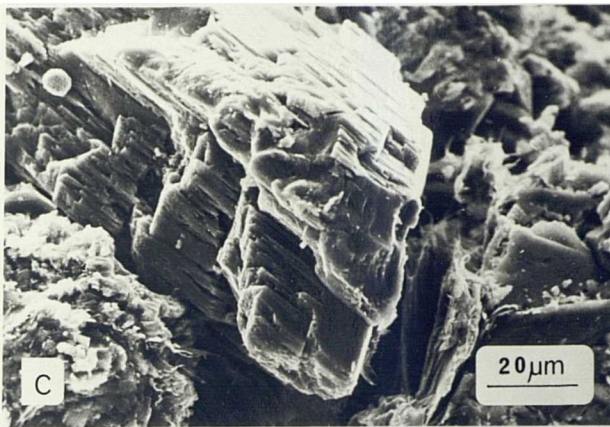
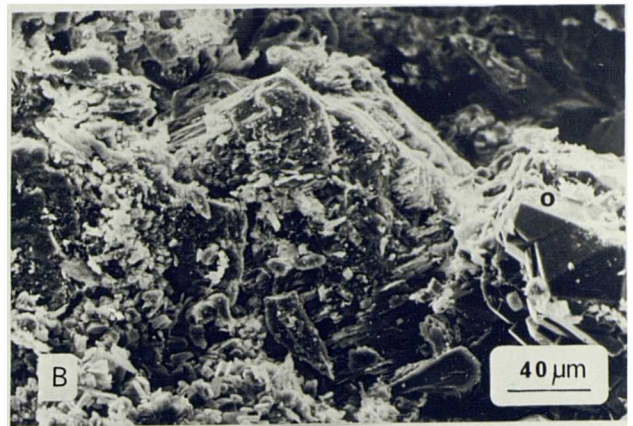
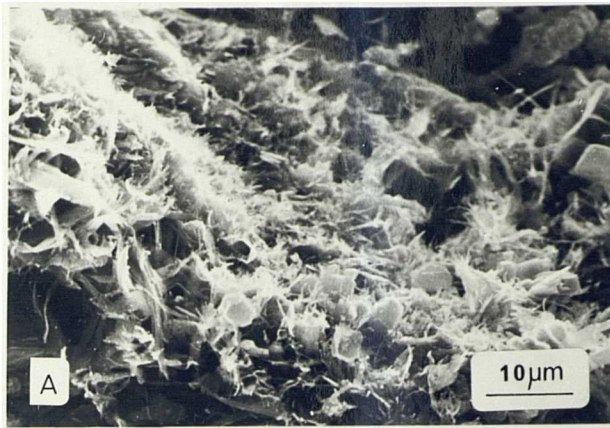


Plate 4.3

- A        Authigenic sodium feldspar (a) filling pore space remaining following incomplete quartz overgrowth (o) cementation (background) of the original pore. Channel sandstone, 3/3-3, 10562'.
- B        Vermiform kandite aggregate, filling intergranular pore space. Note stalked plates within whole aggregate.
- C        Close up of base of aggregate in B to show the pseudo-hexagonal morphology of individual plates within vermiform aggregates. B and C channel sandstone 3/3-3, 10547' 9".
- D        Extremely long vermiform kandite aggregate, enclosed by subsequent quartz overgrowth cementation. Bay filling sandstone, 3/3-3, 105178 3". Note the absence of apparent illitisation in B, C, and D.
- E        Illitised blocky kandite aggregate. Note that illitic hairs appear to be nucleated on rather than pseudomorphing the actual kandite plates.
- F        Pore-filling ankerite. Rhombic morphology exhibited here is not characteristic of this mineral, and may be confused on the basis of morphology, with other carbonates and feldspars. E and F channel sandstones 3/3-3, 10563' 9" and 10538' respectively.
- G        A general view of a texturally immature siltstone, containing a high percentage of fine quartz grains, mica and matrix clay. Diagenetic modifications are limited, with some authigenic clay, and pore-filling siderite. Interdistributary filling sandstone 3/3-3, 10470'.
- H        Vermiform kandite within pore partially filled with illitic clay. Interdistributary-bay filling sandstone 3/3-3, 10497'.



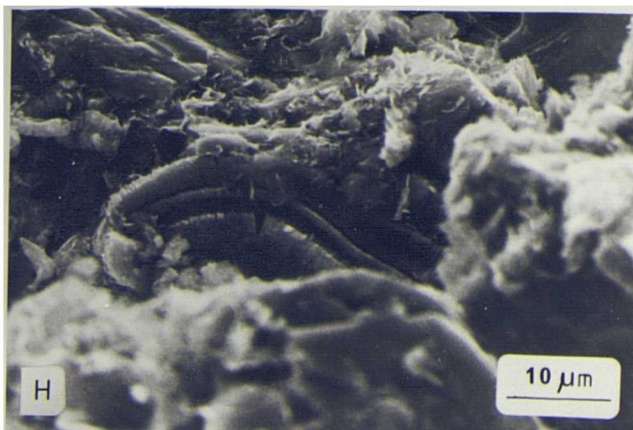
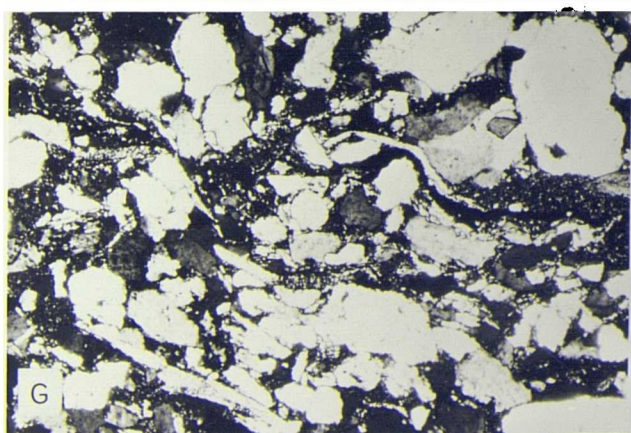
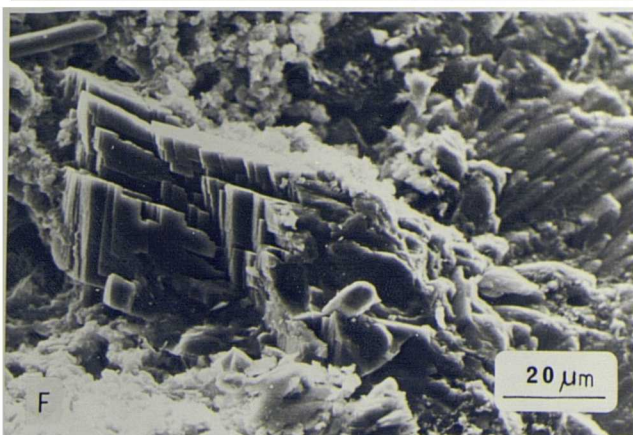
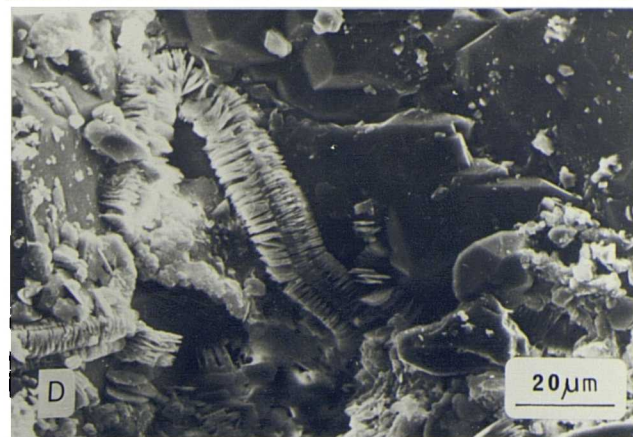
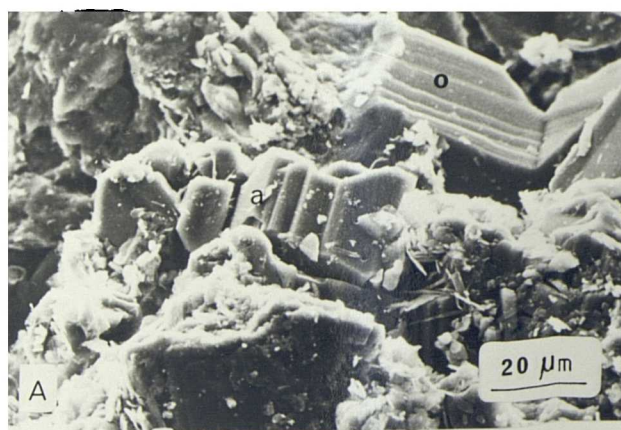


Plate 4.4

A and B Neomorphosis of muscovite to kandites. Plate B width 875  $\mu\text{m}$ . Interdistributary bay filling sandstones, 3/3-3 10474' and 10497' respectively.

C and D Blocky kandites; stacked pseudo-hexagonal plates, enclosed by later quartz overgrowths. Those in C are illitised, those in D are not. Interdistributary bay filling sandstones 3/3-2 10447' and 10465' respectively.

E and F Pore-filling vermiform kandites. Those in E are relatively intensively illitised, with discrete illitic hairs. Those in F are less intensively illitised, although the surrounding illitic clays are. E and F interdistributary bay filling sandstone 3/3-3 10497'.

G and H Quartz overgrowth cementation, preserved here as euhedral terminations on detrital grains. Where pore space is not fully cemented, open pore throats remain within a quartzose framework. G and H interdistributary filling sandstone 3/3-3 10517' 3".



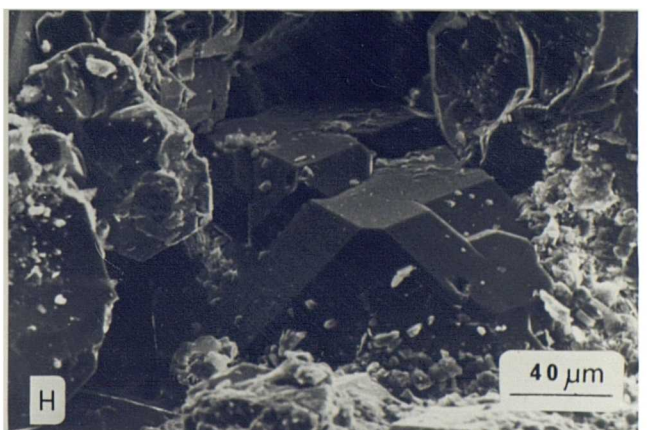
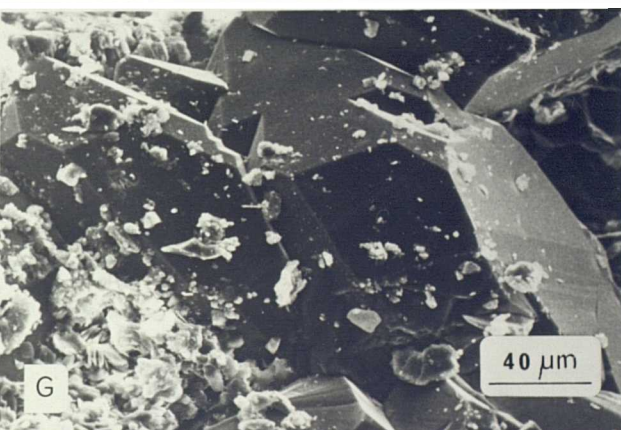
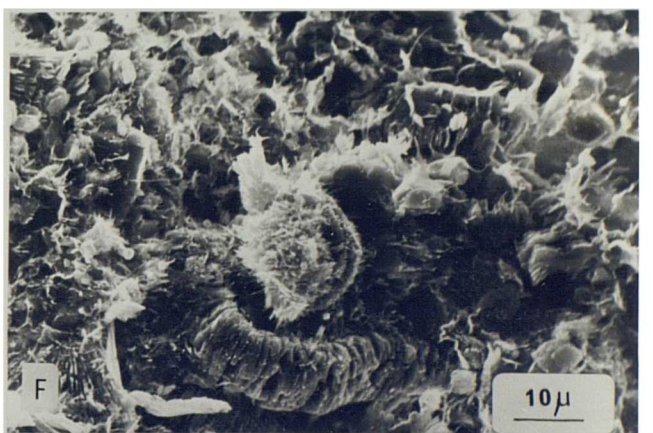
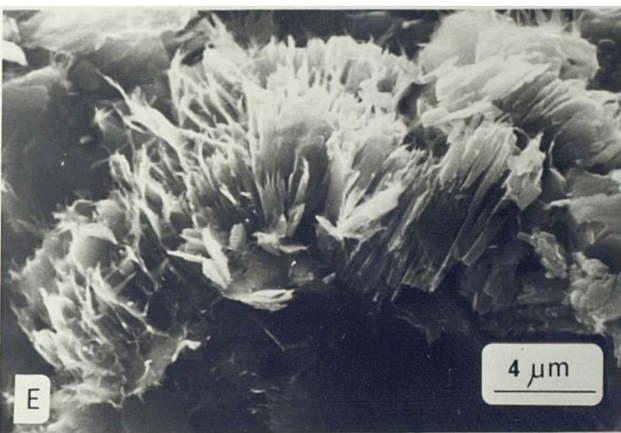
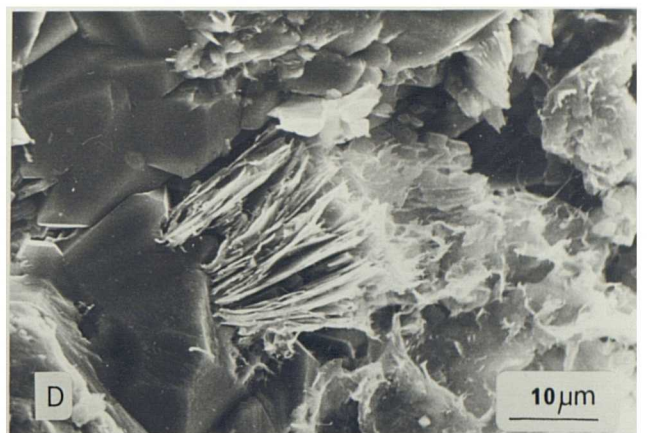
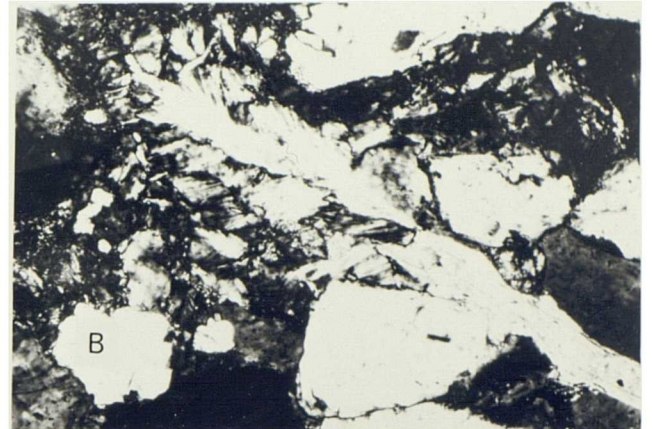
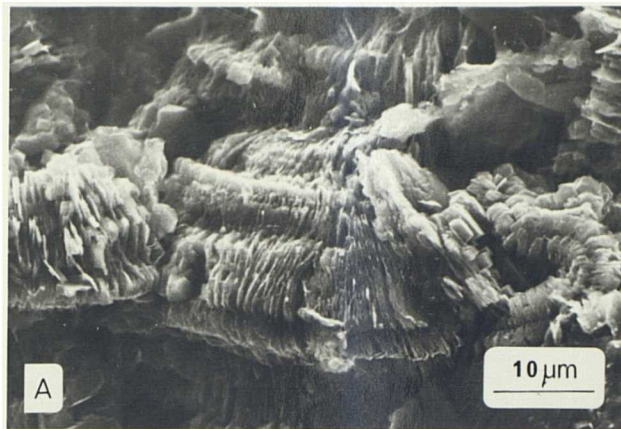


Plate 4.5

- A Corroded quartz overgrowth.
- B Rhombic siderite cement.
- A and B Interdistributary bay filling sandstones 3/3-2 10452' and 10465'.
- C Illitic clay enclosing authigenic pyrite cubes, and filling pore space.
- D Illitic clay coating detrital quartz grain and subsequently enclosed by quartz overgrowth.
- C and D Crevasse-splay sandstones 3/3-2 10420' and 3/3-3 10447' respectively.
- E Quartz overgrowth (inferred from Si peak during EDS analysis), on a corroded or dissolved potassium feldspar grain (K, Al and Si peaks with EDS analysis).
- F Neomorphosed muscovite flake within pore space almost fully occluded by quartz overgrowths.
- E and F crevasse-splay sandstones 3/3-3, 10447' and 3/3-3, 10315' respectively.
- G and H Blocky kaolinites. G enclosed within quartz overgrowths and partially illitised, H pore filling and serving as nucleus for illitic hairs. In neither case are the pseudo-hexagonal plates altered. EDS analysis detected K in the short hairs only. Crevasse-splay sandstone, 3/3-3, 10447'.



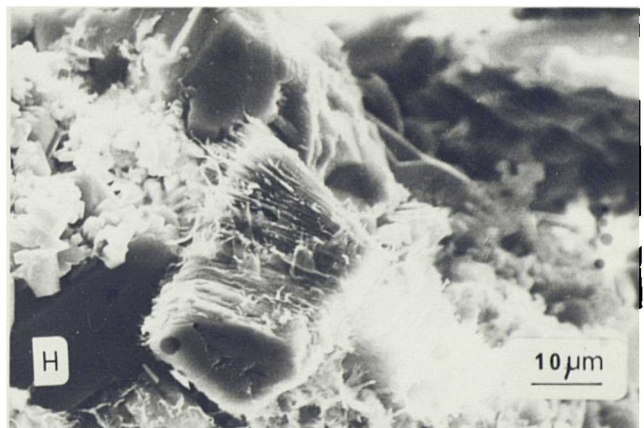
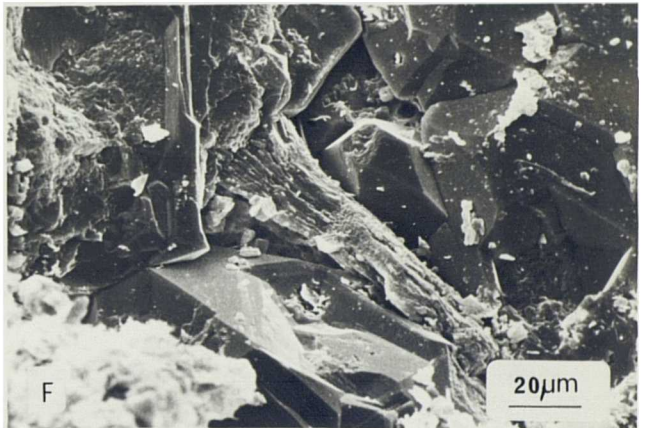
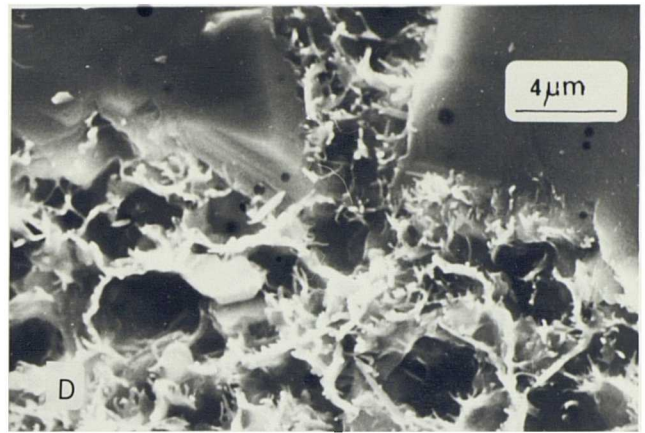
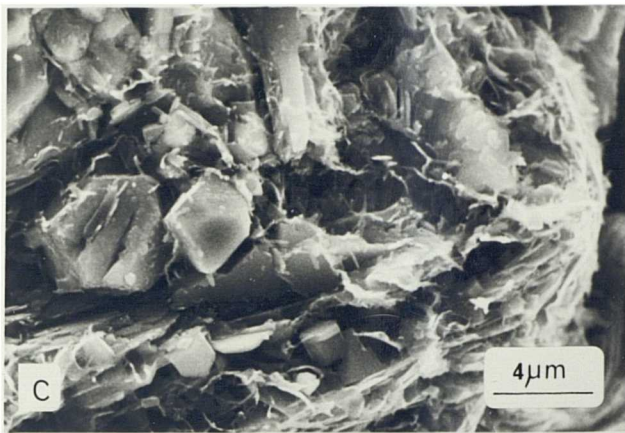
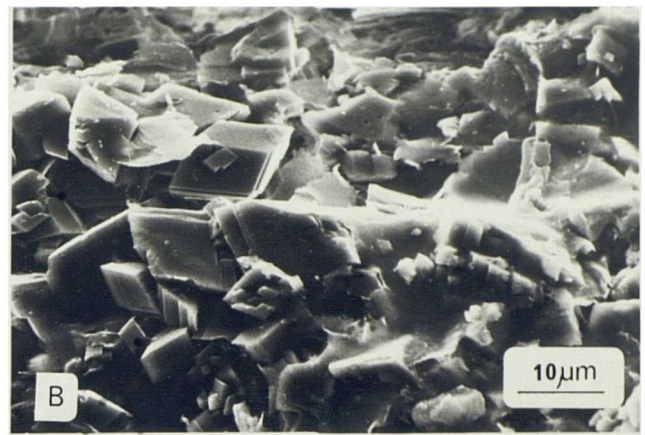
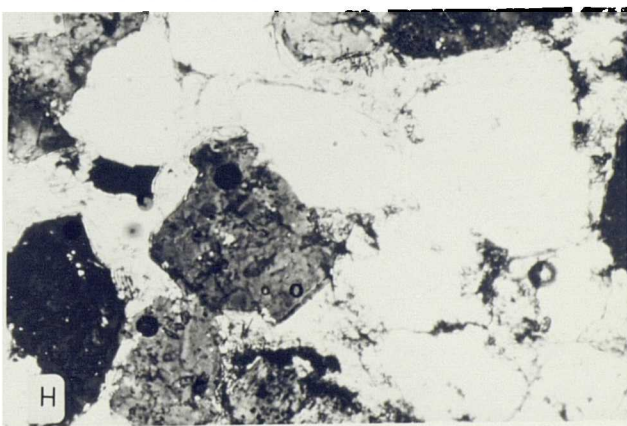
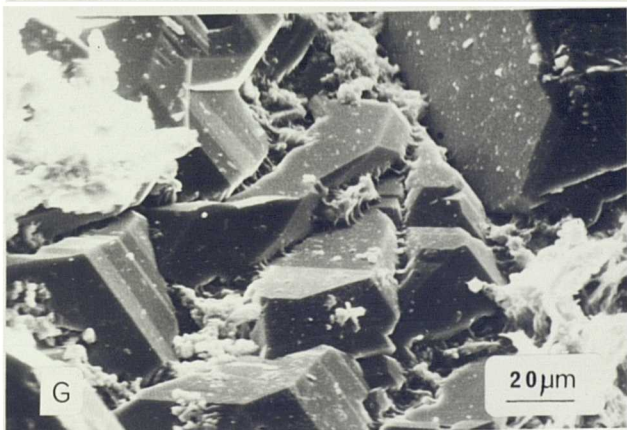
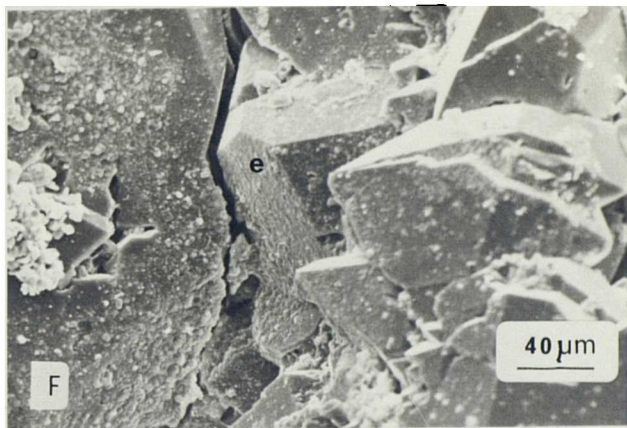
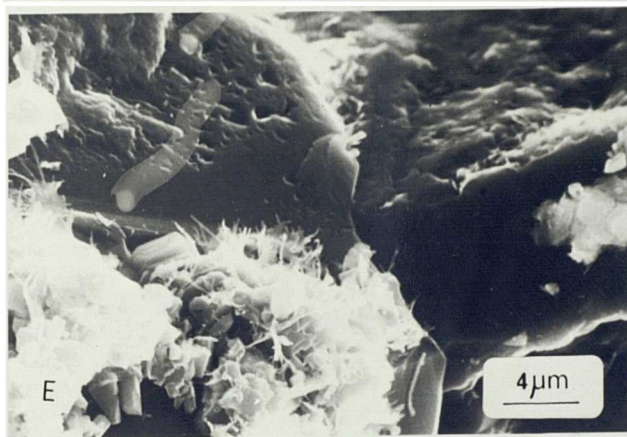
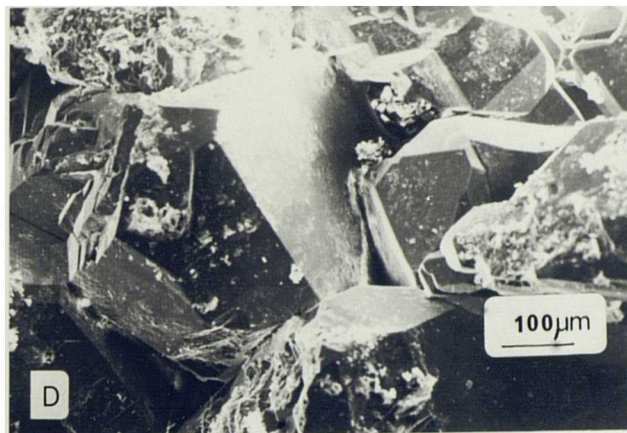
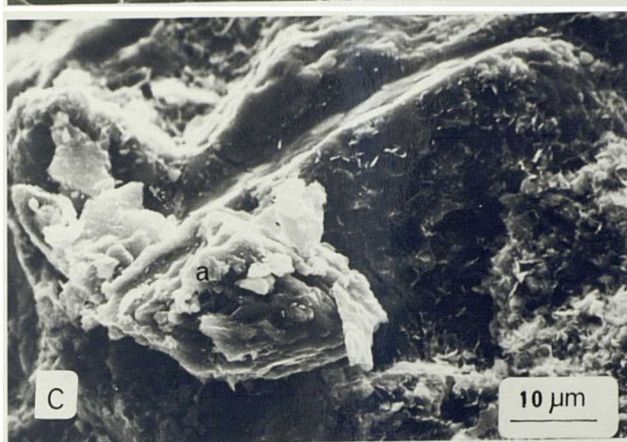
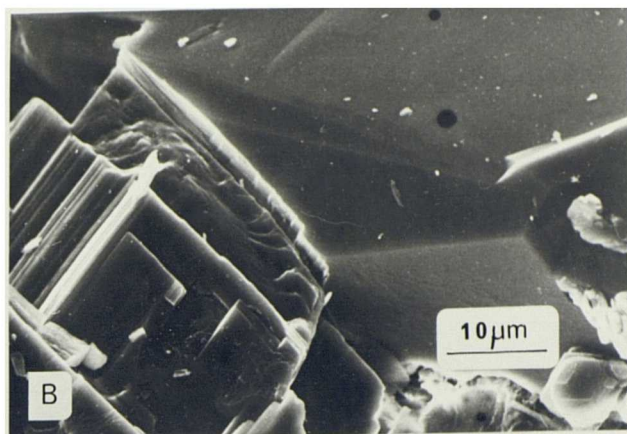
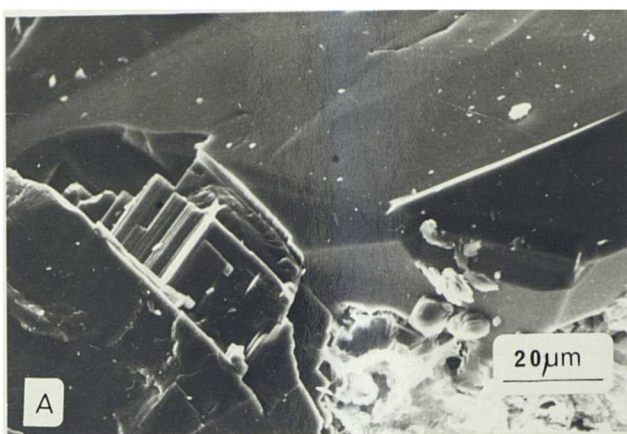


Plate 4.6

- A and B Rhombic siderite cementation, and replacement of a quartz overgrowth.
- C Corroded patch of ankerite (a) within a pore space lined with illitic clay.
- A and B 3/3-3, 10447', and C 3/3-2, 10330' respectively.
- D Euhedral quartz overgrowth cementation generating a quartzose framework resistant to overburden pressures. Pore throats reduced but remain up to 60  $\mu\text{m}$  in diameter. Channel sandstone 3/3-3, 10425'.
- E Small "v" shaped notches in a quartz overgrowth. The overgrowths themselves enclose illitic clays.
- F A sutured contact between quartz grains with overgrowths. The suture line, along which dissolution has presumably taken place passes obliquely across one euhedral termination (e) and therefore postdates the overgrowth.
- E and F Channel sandstones 3/3-2, 9916' and 3/3-3, 10295' respectively.
- G Small incipient overgrowths enclosing, but inhibited by illitic clay covering the detrital grain beneath
- H Tight ferroan calcite cementation of a sandstone with minor quartz overgrowth (o). Plate width 700  $\mu\text{m}$ .
- G and H Channel sandstones 3/3-2 10465' and 3/3-1 9916' respectively.





CHAPTER FIVE: SEDIMENTOLOGY AND DIAGENESIS OF THE MIDDLE JURASSIC  
BRENT GROUP CORE FROM WELL 210/15-2

In this chapter I should like to describe a cored sequence through the Brent Group from Well 210/15-2 in the west of the East Shetland Basin. This is followed by an interpretation of the depositional environment of this sequence and a discussion on its relationship to other Middle Jurassic sequences in the basin. I should then like to describe the diagenetic modifications in these sediments, interpret their paragenetic sequence, and finally discuss the relationship between their diagenesis and depositional environment.

SEDIMENTOLOGY

Core Description

A logged section through the Brent Group cored in 210/15-2 is shown in Fig. 5.1.

Micaceous facies 6899-6933'. The base of this sequence was not cored and, as a consequence, the micaceous facies represents the lowest thirty-four feet of available core. This facies fines upwards slightly from a medium-grained sandstone, through fine-grained sandstone at 6925', with a short coarsening upwards profile to 6914', above which it fines again to fine-grained sandstone. Fine-grained sandstone persists throughout the remaining fifteen feet. This facies contains no coarse-grained sandstone laminations, or pebble lags and neither mudrock partings nor other lithological variations. The majority of the core, with the exception of 6900-6906' (six feet of clean sand), consists of couplets of fine- or medium-grained sandstone and micaceous laminae, which are characteristic of the micaceous facies. These couplets consist of distinct layers of fine- to medium-grained, white or grey sandstone, 1-3 mm thick, separated by a distinct micaceous lamination containing fragmented leafy plant

debris. These couplets are, in a sense, graded beds.

Sedimentary structures throughout vary with grain size. The lowermost medium-grained sandstone exhibits well developed low-angle cross-bedding which passes upwards into horizontal lamination in the overlying fine-grained sandstone. The short succeeding coarsening-upwards sandstone begins with further low-angle cross-bedding and ripple-lamination, although the core at this point is badly broken. However, the fine-grained sandstone overlying horizontally laminated medium-grained sandstones at 6914' is also predominantly horizontally laminated with local ripple and climbing-ripple lamination, especially towards 6900'. Rootlets occur in the fine-grained sandstone at 6910' and from 6900-6904', but each individual rootlet is truncated by laminae above. Elsewhere, neither rootlets nor bioturbation are observed.

Fining-upwards facies 6876-6899'. This facies occurs as two repeated fining-upwards units with a combined thickness of twenty-three feet. The lower facies unit (6884-6889') passes upwards from coarse-grained sandstone, through medium sand and two distinct beds of very coarse sand to medium-, and ultimately fine-grained sandstone. The lowermost few feet show bimodal low-angle cross-bedding with occasional, very coarse laminae. These fine upwards through horizontally laminated sand into six feet of ripple-, climbing-ripple, and locally horizontally-laminated sandstone, which contains Equisitites-like rootlets throughout. The overlying facies unit fines upwards from a coarse-grained, erosively based sandstone with low-angle cross-bedding, with woody debris between cosets, to a medium-grained low-angle cross- and horizontally-bedded sandstone. Both these units are locally micaceous, with abundant leafy-plant debris. The top of the upper facies unit is absent.

Bioturbated micaceous sandstone facies 6793-6868'. In spite of the large gap which exists within this facies (between 6818' and 6841'), the twenty-five feet

of strata above and the twenty-seven feet below may be described together in view of their similarity. The lowermost few feet are medium-grained sandstone, which fines upwards into twenty-one feet of fine-grained sandstone. This coarser sandstone is horizontally laminated and bioturbated, with vertical and inclined burrows preserved. The succeeding fine sand is predominantly horizontally laminated with some climbing ripple lamination. This horizontally laminated sandstone is locally micaceous, with further distinct sand:mica-plant debris couplets. It is also bioturbated locally, and especially towards the top, where horizontal and inclined burrows are more frequently preserved. However, there is only occasional obliteration of primary lamination by bioturbation. Above the gap in the cored sequence occurs almost entirely horizontally-laminated fine-grained sandstone. In addition, in this sandstone, which does not contain particularly abundant plant debris or mica, discrete, coarse, pebble-rich laminae occur, especially towards the top. The only exceptional section is <sup>6</sup>806-<sup>6</sup>810', a discrete, locally coarse-, but predominantly horizontally-laminated medium-grained sandstone containing abundant mica, woody debris and scattered granules. Bioturbation is not observed in the upper twenty-five feet, except for local burrows at 6811' immediately below the coarse intercalation. The sequence contains rootlets penetrating from the overlying coal at 6793'.

Coal-bearing facies 6785-6793'. This facies consists of three poorly developed coals at 6785', 6789', 6793' respectively, separated by horizontally-laminated siltstones containing abundant woody and leafy plant debris.

Fining-upwards facies 6780-6785'. The top of this facies unit is absent, but it fines upwards through the existing five feet, from very coarse-grained cross-laminated sandstones, to coarse-, medium- and fine-grained sandstones above. The upper three feet are horizontally laminated, with some bioturbation, vertical burrows being preserved.



### Interpretation

Micaceous facies. The facies described from 6899-6933', and 6793-6868', are sedimentologically similar, and may be interpreted together. Unequivocal interpretation is hampered here, firstly, by the presence of only one core, and secondly, by the absence of complete genetic units whose internal features, and relationships to surrounding units, are clearly visible. This facies is interpreted as having accumulated during either fairweather or storm-driven sedimentation on a beach foreshore, or shoreface for the reasons discussed below.

Horizontal lamination is not indicative of any particular depositional environment, but its repetition, particularly as couplets of fine sand and micaceous laminae, is typical of shoreface and beach deposits (Howard and Reineck, 1972; Reineck and Singh, 1973). Similarly, primary sedimentary structures produced on beach foreshores and shorefaces are diverse and not characterised by any particular structure or assemblage of structures (e.g. Clifton et al, 1971). Nevertheless, both the shoreface and foreshore are high-energy environments within which the potential for preservation of most primary sedimentary structures is low (Thompson, 1937; Clifton et al, 1971). Consequently, fairweather deposits characterised by wave ripples, low- and high-angle cross-bedding, and bioturbation are not commonly preserved. They are destroyed during storm conditions, under which the potential for preservation of low-angle cross-bedding and especially horizontal lamination is greater (Thompson, 1937; Hoyt and Weimar, 1963). The latter are analogous to structures described from modern foreshore and upper shoreface deposits by Straaten (1959) and Andrews and Lingen (1969). In addition, the discrete couplets of mica and sand grain laminae found here are analogous to the 1-2 cm thick laminations described by Clifton (1969) from the Oregon coast. He describes laminae of fine-grained or high-density minerals and of coarse-grained or low-density minerals, forming in the swash

zone of a modern beach. Furthermore, Clifton et al, (1971) interpret horizontal lamination with discrete pebble laminae within sand sequences as forming in the surf zone or beach foreshore. These are similar to the granule laminations between 6785' and 6804', and the coarser sand at 6806-6810'. Finally, this coarse sand is also similar to the coarse shoal between cross-laminated upper-shoreface sediments and horizontally laminated foreshore deposits described by Vos (1977), and is indicative of high-energy conditions. Thus, the horizontal and low-angle cross-laminated micaceous sandstone which occurs through this facies is interpreted as a storm-driven shoreface and foreshore deposit.

The remainder of this facies is interpreted as accumulating during fairweather conditions. It is significant to note the general association of fairweather foreshore and shoreface sedimentary structures such as climbing-ripple lamination (e.g. 6843') with bioturbation and preserved burrows, (cf. Clifton et al, 1971). This association indicates that some fairweather sediments are preserved, and under these conditions, faunal colonisation took place (cf. Kumar and Sanders, 1976). The presence of rootlets below the fining-upwards facies at 6900' is also perhaps environmentally significant. Within this sequence, individual rootlets are truncated, indicating that the surface from which they penetrated has not been preserved. In foreshore sediments such as these, that is, horizontally-laminated fine-grained sandstones which the rootlets penetrate, this is not out of context. Thus, plant colonisation of the beach crest may have taken place during fairweather conditions, perhaps even annually between spring tides. Subsequently, during storm conditions, superficial sediments such as poorly developed soils, plant remains and the underlying rippled sands and silts were perhaps removed and horizontally-laminated sediments accumulated. This assumes that on each occasion rootlets from the plant colony had penetrated to below the level reached during erosion. As a result, the foreshore built up a sequence of horizontally-laminated sandstones containing truncated rootlets recording the intervening periods of less energetic sedimentation.

These sediments are all interpreted, therefore, as foreshore, or perhaps upper-foreshore deposits. The variation between rippled and bioturbated horizontally-laminated sandstones probably reflects alternating storm-driven and fairweather sedimentation. It is postulated that rootlets penetrated into these sediments during their deposition from generally unpreserved fairweather plant colonies on the beach itself. However, the uppermost unit is succeeded by a coal at 6793', indicating that here at least, storm conditions did not remove the overlying plant colony, and subsequent progradation allowed the accumulation of fine-grained sediments (see below).

Fining-upwards facies. This facies occurs in two intervals between 6876-6899' and 6780-6785'. Unequivocal interpretation is difficult here because neither sequence includes a complete genetic unit, since in both, strata are truncated by succeeding units or absent core. This facies may be interpreted as a channel deposit, or, less probably, a transgressive foreshore to shoreface accumulation.

Fining-upwards facies may be generated in a range of environments. Their development requires decreasing energy due to either deepening water, or waning flow. Nonetheless, the repetition of fining-upwards facies units is more typical of channel deposits. Fining upwards occurs in deposits from braided (Rust, 1978), meandering (Allen, 1965), and tidal channels (Klein, 1970), and marine sediments with increasing water depth, for example, following transgression (Johnson, 1975). In spite of this, it is difficult to reconcile a wholly marine model with the presence of rootlets in the climbing-ripple laminated sequences between 6885' and 6890'. The only available explanation would entail interpreting the underlying sediments as swash zone deposits, similar to the rivulets reworking beach sediment described by Clifton et al (1973), and storm-driven foreshore deposits. It follows that these rooted sandstones would have to be fairweather deposits in which rootlets penetrating

from a plant colonised beach above are preserved.

The preferred explanation is that the fining-upwards facies accumulated in channels, and in view of the bimodal cross bedding at 6894', possibly tidal channels. Consequently, their fining-upwards nature reflects waning channel flow. In addition, the occurrence of rootlets in the finer portions of the units could be analogous to modern plant colonisation of exposures on point bars (Baganz et al, 1975). It is not clear what type of channel deposits these are: they may be distributary channels or possibly fluvial ones, although a tidal origin is preferred here.

Tidal deposits in low energy environments often contain significant quantities of fine material (e.g. Klein, 1970), whilst tidal deposits in high-energy environments may be well sorted and coarse, especially those in actual channels themselves. Kumar and Sanders (1976) interpret thin granule-rich laminated sandstones at the base of a similar fining-upwards facies unit, as tidal inlet lag deposits. The deposits here are interpreted similarly, although it must be stressed that even a channel interpretation of the depositional origin of these sequences must remain tentative.

The upper unit (6780-6785') may, alternatively, represent a renewed transgression following peat accumulation. Its base, therefore, represents the lag of a shoreface erosion plane, with fining upwards shoreface deposits accumulated above during continued transgression (Johnson, 1975).

Coal-bearing facies. This thin sequence may be interpreted as either an alluvial deposit, or possibly a lagoonal accumulation. The development of rootlets beneath the lowermost coal is evidence of an autochthonous rather than an allochthonous origin. Hence, these sediments may have accumulated in a peat bog (cf. Carter, 1978).

### Discussion

It is perhaps unfortunate that only one core was available for study from this area, because even consideration of these facies in relation to each other does not allow any less equivocal interpretation to be made than that based on each facies in isolation. The most conclusive point that can be made is that this sequence probably accumulated extremely close to sea level, on a beach and either behind the beach in a protected environment, or in front on its foreshore. This conclusion is not affected by the uncertain origin of the fining-upwards facies. If these are channel sands, they dissect the beach and so remain proximal to the inferred setting. Moreover, the whole sequence is undoubtedly condensed with erosive contacts, truncated rootlets and a predominance of storm-driven rather than fairweather foreshore deposits.

In view of the considerable breaks within this cored sequence, these conclusions must remain tentative within the general framework of shallow marine storm-driven and fairweather deposits. The presence of rootlets perhaps restricts the setting to actual shoreface and foreshore accumulation rather than a protective barrier environment similar to that described by Carter (1978). Exclusion of this type of alternative is hindered by the absence of the underlying sediments.

This sequence is unlike those described elsewhere in the Brent Group from the East Shetland Basin (Albright et al, 1980; Moiola and Jones, 1980; Budding and Inglin, 1981; Eynon, 1981; Parry et al, 1981). It is difficult, consequently, to evaluate its significance in terms of reconstructing regional Middle Jurassic facies distribution. Moreover, it is not clear from the composite log (Fig. 5.2) where exactly these sediments occur within the Middle Jurassic sequence in this area. It is probable that the large increase in gamma rays detected below 7060' as well as the transition from a predominantly sandstone to a

predominantly "claystone" lithology, marks the boundary between the Liassic and the Middle Jurassic. However, it is not possible to elucidate either from this log or especially lithostratigraphical considerations, where exactly in the sequence these sediments come from, or to what formation they should be ascribed .

Middle Jurassic sediments elsewhere in the East Shetland Basin are interpreted as accumulating in a range of transgressive shallow marine environments, subsequently overlaid by a prograding fluvio-deltaic sequence (see Chapter Two). Progradation occurred from the south, although various authors (e.g. Eynon, 1981) discuss the influence of additional fluvial systems from either the east (off the Scandinavian Shield) or the west (off the Shetland Platform). Consequently, the shallow-marine nearshore sediments described here could have accumulated during several possible periods. Firstly, during Broom to Etive time, on the shoreline between the open sea to the northeast, and land on the Shetland Platform. Secondly, during Ness to Tarbert time as the high-energy shoreline between a fluvial system depositing floodplain sediments in the south, and open sea to the north. Alternatively, throughout Brent Group time, these sediments may have accumulated on a structural high, hence their condensed nature, irrespective of the palaeogeography of the basin. These sediments are also unusual in view of the presence of garnets, suggesting derivation from the southwest, possibly from the Shetland Platform, whilst Brent Group sequences elsewhere lack garnet and have an inferred source in the southeast (Gray, in discussion to Gray and Barnes, 1981).

#### Summary

The Brent Group cored in Well 210/15-2 is a condensed accumulation of predominantly storm-driven nearshore sediments, dissected by possibly tidal-channel deposits. The sequence is interpreted as a shallow-marine, nearshore

and possibly foreshore accumulation, breached by channels and subsequently overlaid by a peat bog. It is not clear whether this sequence is regressive as well as progradational. Also, the overlying fining-upwards facies may either represent renewed transgression, or a further tidal-channel deposit. This Brent Group sequence differs from other published sequences in the East Shetland Basin. However, uncertainty regarding its stratigraphical position within the Group itself precludes any positive statements concerning facies distribution throughout the basin.

### DIAGENESIS

The results of semi-quantitative XRD, modal, and electron microprobe analysis are compiled in Appendix G.

### Petrography

All the samples analysed from this well are similar and are mature, medium-grained subarkoses (Fig. 5.3A). Detrital components, which comprise 37-76% of the rock, include simple quartz (20-50%) and polycrystalline quartz (3-23%); feldspars, apparently entirely potassium (3-18%); mica (up to 13%); local concentrations of matrix clay; and traces of rutile, tourmaline, zircon, garnet and plant debris. Authigenic components, which comprise 1-62% of the rock include kandites (up to 20%); quartz overgrowths, (up to 3%); a trace of feldspar overgrowths; calcite (often absent, but locally comprising up to 53%); siderite (up to 7%); and traces of brookite, anatase, gypsum, barytes and pyrite. A quarter of the samples are completely cemented with ferroan calcite (irrespective of facies), the remainder, however, are highly porous, with most containing 20-25% porosity. This porosity is predominantly enlarged intergranular porosity in most samples, but in those which contain abundant kandites, a high proportion of the total porosity is microporosity.

Quartz overgrowths occur throughout as a thin cementing veneer on detrital quartz grains (Plate 5.1A). They are also observed on dissolved detrital feldspar grains, although not as frequently (Plate 5.1B). These overgrowths do not completely enclose any authigenic or detrital phases. Indeed, overgrowths only loosely cement samples, many of which are friable, unless they are also cemented with calcite. In one sample, a quartz overgrowth is observed to enclose an authigenic potassium feldspar overgrowth, and an apparently wholly authigenic potassium feldspar crystal (Plate 5.1G and H). Quartz overgrowths are replaced by ferroan calcite and siderite where carbonates occur (Plate 5.3D and E) and are corroded elsewhere, recognised by deep etch pits and hollows. A second phase of authigenic quartz is observed in some samples as scattered pore-filling crystals, unrelated to quartz overgrowths on the pore walls (Plate 5.1C).

Feldspar overgrowths also occur throughout the samples as a thin cementing veneer on detrital feldspar grains. Only potassium-feldspar grains and overgrowths were observed in these samples. Feldspar overgrowths do not enclose other authigenic or detrital phases (Plate 5.1D and 5.2A). Feldspars, however, have undergone dissolution as well as overgrowth. Furthermore, dissolution appears to have affected both grains and some overgrowths, many of which have corroded euhedral terminations (Plate 5.1D, E and F, 5.3F). Nevertheless, not all grains have undergone dissolution. Many of those observed in thin section are perfectly fresh, as are their euhedral overgrowths.

Kandites occur in four forms: neomorphosed micas, principally muscovite; large vermiform aggregates, comprising numerous layered and stacked pseudo-hexagonal plates; small, often independent rather than stacked or aggregated plates, filling grain-shaped pores and apparently replacing feldspar grains; and fourthly, large, blocky aggregates of pseudo-hexagonal plates, each aggregate one plate in diameter. Almost all the muscovite present in the samples is



partially or wholly altered to kandites. The degree of alteration varies, from the extremities of individual flakes, and flakes with characteristically splayed ends (Plate 5.2B and H), to completely altered "flakes" now represented by huge expanded kandite sheets, often the size of fine-sand grains. Microprobe analyses of spots along splaying flakes indicates a progressive loss of potassium from typical muscovite chemistry through an illitic chemistry, to kandite chemistry with no potassium (Fig. 5.3B). Large, vermiform aggregates also occur in almost all the samples and are the predominant kandite form present (Plates 5.2C, D, E, F, and G; Plate 5.3G and H). These aggregates occur, typically, in intergranular pore space. They are often enclosed by ferroan calcite and associated with neomorphosing muscovite, and small sphaeroid siderite spheruliths. The two remaining kandite forms are not as common as the two above. Pseudomorphic kandite replacement of feldspar grains comprises no more than a trace of any sample. These grain-shaped replacements may also be replaced or enclosed by ferroan calcite. Incomplete replacement also occurs (Plate 5.3A and B), although there is no evidence to suggest that kandites are neomorphosing rather than simply replacing the actual feldspar grains in these samples (Plate 5.3C). The paragenetic sequence of this kandite replacement and feldspar overgrowths is not clear from the textural evidence available. In their fourth form, kandites occur as blocky aggregates of thick plates, each aggregate one plate in diameter only. These comprise a trace of the samples. Blocky kandites do not occur where complete ferroan calcite cementation occurs. They fill intergranular and enlarged intergranular pore space.

There is no evidence of illitisation of kandites in these samples, indeed illite was neither detected by XRD, nor observed in thin section or with the SEM in any form or in any sample.

Siderite and calcite occur scattered throughout the samples (Fig. 5.3C). The former is more evenly distributed, comprising a few per cent of each sample,

whilst the latter is either absent, or comprises 20-50% of the sample and cements it completely. These carbonates enclose and replace quartz and feldspar grains and overgrowths, vermiform kandites, neomorphosed muscovite, and kandite replacements of feldspar grains. Although homogeneous throughout the core, siderite distribution is heterogeneous within any particular sample. It is concentrated around micaceous laminae or neomorphosing micas and finer grained parts of samples. The sample from 6858' contains scattered sphaero-siderite spheruliths, whilst elsewhere siderite is rhombic. Where ferroan calcite also occurs it encloses siderite. Ferroan calcite is usually absent, but where present it completely cements samples. This complete cement is either "pore filling" and only slightly replacive, hence comprising 20-30% of the rock, or extensively replacive, comprising 50% of the rock. Oil staining does not occur in the calcite cemented samples, although it does occur elsewhere.

The remaining authigenic phases are present only as traces. These include pyrite, which is often associated with plant debris and enclosed by carbonates; gypsum and barytes, which occur as discrete pore-filling crystals and a minor cement respectively; and brookite and anatase, identified on the basis of their respective morphologies, and scattered throughout almost all the samples as discrete pore-filling crystals, often associated with heavy mineral rich laminae.

In the porous samples porosity is predominantly intergranular with an increasing proportion of microporosity where clay concentration increases. Moreover, grain dissolution porosity does not contribute significantly to the total. The majority of intergranular pore space is slightly enlarged by corrosion of the pore walls, although in most instances these walls are in fact quartz or feldspar overgrowths. Consequently, porosity does not actually comprise the whole intergranular volume. In addition to being occasionally corroded,

a number of grains in each thin section examined are actually floating, or only in contact with surrounding grains at one point.

### Interpretation

The paragenetic sequence of events interpreted in these samples is as follows: precipitation of feldspar overgrowths; dissolution of feldspars and overgrowths, and neomorphosis of muscovite to kandites, with simultaneous quartz overgrowth and vermiform kandite precipitation; replacement of feldspars by kandites, and probable continued quartz overgrowth cementation; siderite and subsequent ferroan calcite authigenesis, replacing pre-existing components; carbonate dissolution and partial filling of this secondary porosity with blocky kandites; and finally, migration of oil into the remaining porespace.

Pore water composition during this sequence changed from initially potassium-rich and mildly alkaline (sea water), to acidic before pH rose and carbonates precipitated. Subsequently, aggressive fluids, acidic and saturated with respect to alumina and silica dissolved carbonates, created secondary porosity and precipitated kandites. This diagenetic sequence is interpreted as reflecting initially interstitial sea water, and subsequently the influence of acids, generated in situ by bacterial degradation of organic matter. As anoxic bacterial processes raised pH, they affected diagenetic modifications up to the ferroan calcite cementation stage, after which migrating aggressive fluids influenced the sediment. These initial changes are summarised in Fig. 5.4.

Potassium-feldspar overgrowths formed from alkaline pore fluids, rich in potassium and silica (Kastner and Siever, 1979). Although they require silica saturation with respect to quartz at low pH, with increasing potassium concentration less silica is required in solution (Garrels and Christ, 1965). Although these conditions are not satisfied by sea water, interstitial sea

water rapidly moves into equilibrium with potassium feldspars (Kastner and Siever, 1979). Sea water, however, is initially in equilibrium with illite and so illite would be expected to precede feldspar overgrowths precipitation (Harder, 1974; Kastner and Siever, 1979). Three possible explanations for the absence of illite may be considered. Firstly, illite may have been formed and subsequently removed when pH changed. This is unlikely in view of the metastability of low temperature authigenic phases. Secondly, pore waters may have been saturated with respect to quartz and consequently inhibited illite formation (Harder, 1974). Thirdly, without a suitable nucleus, pore fluids saturated but not supersaturated with respect to illite would not allow illite precipitation (Berner, 1980). These sediments are extremely well sorted and may not have contained any detrital nuclei such as matrix clays, on which illite could precipitate (see Fig. 5.5).

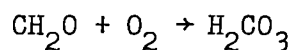
Thus, following deposition, with interstitial sea water saturated with respect to quartz and potassium feldspars, both phases probably precipitated as overgrowths. The order in which they precipitated is not immediately obvious from either petrological evidence, or theoretical considerations. However, the quartz overgrowth in Plate 5.1G and H appears to enclose authigenic feldspars, suggesting that they are the later phase.

Subsequent diagenetic modifications require a lower pH (see Fig. 5.5). Throughout the core, both detrital and authigenic feldspars are partially dissolved, with dissolution concentrating along composition planes (cf. Berner and Holdren, 1979). In addition, intergranular pore space contains abundant vermiform kandites. Both feldspar dissolution and precipitation of kandites require low pH (Helgeson et al, 1969; Curtis and Spears, 1971). Moreover, both processes require continued acidic conditions, feldspar dissolution to remove reaction products and prevent equilibration of grains and pore fluids (Berner, 1981), kandites to maintain a low pH and prevent a build up of basic cations (Bucke

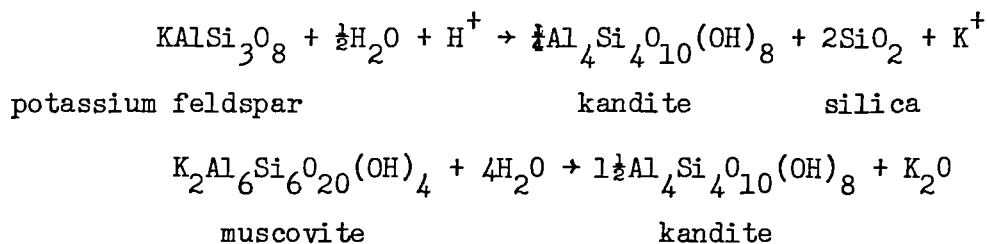
and Mankin, 1971). Replacement of feldspars with overgrowths, either partial or wholly, by kandites also requires acidic pore waters (Curtis and Spears, 1971). Finally, neomorphosis of micas to kandites requires similar conditions (Fanning and Keramides, 1977).

Acidic pore fluids may have occurred for either of two reasons. Firstly, in situ bacterial degradation of organic matter may have lowered pH (Curtis, 1980). This process also leads to a lowering of Eh and could, therefore, explain the subsequent siderite and ferroan calcite. Nonetheless, the alternative explanation of fresh water flushing is perhaps more suitable here for the reasons stated below. Fresh water may have flushed through all the sediments as the delta prograded over them. This fresh water would not have been capable of precipitating the subsequent ferroan calcite. This phase requires a further change of pore-fluid composition. In spite of this added complication, this may have been the case, because ferroan calcite occurs throughout all the sediments, irrespective of their depositional environment.

Fresh or allochthonous water caused the subsequent diagenetic modifications in these sediments. However, it should be pointed out that fresh water here would have been initially acidic and later reducing for the same reasons, that is, bacterial degradation of organic matter. The reactions related to aerobic bacterial processes are probably all connected:



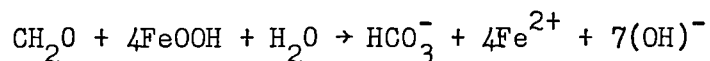
Consequently, dissolution of feldspars and neomorphism of muscovite occur:



These processes, resulting in partial dissolution of feldspars, lead to replacement of feldspars by kandites, vermiform kandite and quartz overgrowth precipi-

tation.

Following initial, and probably during continued diagenesis of aluminosilicates in these sediments, siderite precipitated. Siderite authigenesis requires reducing conditions and generally occurs at a high pH (Berner, 1971), although it has been reported from modern peat bogs with a pH of 5 (Fitzpatrick, 1980). Assuming that climatic conditions do not promote complete oxidation of organic matter and red bed formation (Curtis, 1977), bacterial activity continues after removal of free oxygen from the system. The water table here became anoxic as a consequence, and nitrates, manganese and iron oxides were reduced in order to oxidise organic matter:



When the water table became reducing, quartz overgrowth cementation may have continued. However, kaolinite precipitation must have stopped because in the presence of ferrous iron, chlorite precipitates (Velde, 1977). Siderite is interpreted as the first major authigenic phase to form following the onset of reducing conditions and minor pyrite authigenesis. Its local concentration in laminae rich plant debris and around neomorphosing muscovite suggests that some iron may have been locally derived from micas. The significance of siderite authigenesis prior to calcite is that this interpretation contradicts the general principles established by Curtis (1978, 1980) in his reviews of diagenetic processes in marine sediments. Nevertheless, two points may be made in support of this interpretation. As a brief review of its occurrence, it can be stated that siderite occurs principally as incipient nodules around pyrite crystals and in association with plant debris. Neomorphosing muscovites, which release iron, also occur in these laminae, and siderite crystals often occur within splayed muscovite sheets. Aerobic bacterial processes lower pH but, as anoxic processes involving iron reduction raise pH, one would expect higher pH values within pores containing iron. I would suggest, therefore,

that with the onset of reducing conditions, pyrite formation, in effect, removed sulphate ions from solution. Subsequently, as pH rose, siderite precipitated in pore spaces preferentially enriched with ferrous iron. The two points are as follows: firstly, sulphate ions are not generally present in fresh water, but may be derived locally from degraded plant debris; pyrite forms preferentially before siderite from anoxic solutions containing sulphates. Secondly, fresh waters are not generally saturated with calcium carbonate. Indeed, even if they were, it is unlikely that it would not have precipitated when pH rose and siderite precipitation began. A change of pore-water composition, as well as simple chemistry, is thus also inferred at this stage. The inferred source of calcium carbonate introduced into this anoxic water table and precipitating as ferroan calcite, is formation water unrelated to surface processes.

Porosity throughout the sequence is interpreted as secondary (Schmidt and McDonald, 1979b), created by the activity of aggressive pore fluids (Curtis, pers. comm. 1982). Both carbonate phases replace quartz and feldspar grains and overgrowths. Elsewhere in the porous samples, overgrowths are often pitted and etched, whilst feldspar grains are highly corroded. These features are inferred to result from replacement by carbonates and subsequent dissolution of the carbonates. The major part of this porosity is intergranular and results from the inferred removal of a replacive cement. It is, therefore, secondary cement dissolution and replacement dissolution porosity, respectively (Schmidt and McDonald, 1979b). Dissolution of carbonates requires acidic solutions (Blatt, 1966). Continued degradation of organic matter during burial, however, generates bicarbonates, which, unless fixed and precipitated as carbonates, are released to form acidic solutions (Irwin et al, 1977; Curtis, 1980), which may then act aggressively. If these solutions are saturated with respect to alumina and silica, they will precipitate kandites and quartz following their equilibration with carbonates. Blocky kandites, which only occur in porous

samples, and the discrete pore-filling quartz crystals are interpreted as forming in this fashion. It is not possible to exclude the possibility that further in situ dissolution of feldspars took place at this time, contributing alumina and silica to the resulting phases. The possible, and complicated, diagenetic pathways of feldspars in these sediments are summarised in Fig. 5.6.

Although one quarter of the samples remain completely calcite cemented, they differ in two important ways. In some of them, calcite fills pore space without replacing much of the detrital or cementing framework (those with 20-30% calcite), whilst in others the calcite is extensively replacive (50% of the rock). There appears to be a distinct difference between the two. Removal of the cement from the former would leave a texture similar to that seen in the porous samples. The latter calcite, however, has corroded grains so intensively that none are in contact. I would suggest, as inferred above, that the cementing calcite is a cement sensu strictu, and secondary porosity results from its removal, whilst the replacive calcite is, possibly, concretionary. Creation of secondary porosity preceded the arrival of oil, hence calcite cemented sandstones are not oil stained. These diagenetic modifications are summarised in Fig. 5.7.

Of the remaining minor phases, anatase and brookite are probably derived from local dissolution of rutile. Finally, barytes and gypsum may both have formed from formation waters, following the creation of secondary porosity.

### Discussion

What controls diagenesis? Elucidation of exact controls on some of the diagenetic processes in these sediments is hampered by the uncertain interpretation of their depositional environment. Diagenetic modifications begin, throughout the sequence, with processes which operate under alkaline rather



acidic conditions. These are clearly compatible with the depositional environment of the foreshore and shoreface deposits, but only compatible with a brackish or marine influenced rather than wholly fluvial interpretation of the fining-upwards facies.

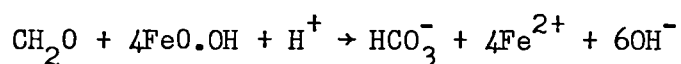
Whilst feldspar and quartz overgrowths may be the result of eogenetic processes, the succeeding diagenetic modifications are not. They require a radical change in pore-fluid chemistry, with a marked lowering of pH. Acidic conditions in marine sediments may result from a range of processes, principal amongst which are in situ bacterial degradation of organic matter (Curtis, 1980), and flushing with acidic fresh water (Bjørlykke et al, 1979). Bacterial degradation of organic matter generates bicarbonates and, unless they are fixed, acidic solutions.

As pointed out above, if organic matter is oxidised at the surface, products diffuse across the sediment-water interface and are dissipated and the system remains alkaline. However, where compaction and cementation, or, possibly, depositional textures, occlude pore space and reduce vertical permeability, acidic solutions may be generated within, or migrate into and operate within the sediment. This bacterial process has little to do with depositional environment and everything to do with the climate and the composition of the sediment. This is because organic matter was supplied from the lush tropical vegetation at this time, and accumulated in the sediment. Here, this bacterial process is mesogenetic, resulting from the introduction of fresh water from the adjacent alluvial sediments. The reactions which occur as a consequence of this process are initially oxygenated, but as organic matter slowly removes oxygen, they become anoxic. Alkaline pore fluids were thus succeeded by acidic ones. Consequently, feldspar overgrowths, the result of equilibration of the sediment with interstitial sea water, became unstable with respect to these pore waters and began to dissolve. Kankrites and quartz

overgrowths throughout the sequence probably resulted from this dissolution as well as alumina and silica in the ground water.

Diagenetic modifications have, therefore, been affected by pore-fluid composition. However, here, as elsewhere, they have also been affected by the presence or absence of nuclei for authigenic crystal growth. Sea water is generally saturated with respect to calcium carbonate (Berner, 1971), especially in the tropics (Bathurst, 1975). It is also in equilibrium with illite (Harder, 1974). Conversely, neither calcite nor illite occur as authigenic phases that may be related directly to precipitation from initial interstitial waters. One must assume that either these interstitial waters were undersaturated with respect to the two phases, or, if they were saturated, that nuclei were absent (Berner, 1980). It follows that, as well as pore-fluid composition, detrital mineralogy plays a part in determining which authigenic phases precipitate. This influence of detrital solids is highlighted by subsequent phases: authigenic quartz forming overgrowths, whereas ferroan calcite occurs as an intergranular pore-filling cement.

The importance of climate must again be emphasised as an influence on diagenesis. Pore waters become acidic when organic matter is not completely removed during superficial oxidation, and releases bicarbonates into solution (Curtis, 1977). Furthermore, where sufficient organic matter occurs, and some survives aerobic bacterial processes, anoxic bacterial processes take over, and reducing conditions are established (Curtis, 1977, 1978). Siderite precipitation is probably the direct result of these reducing conditions with iron reduction resulting in an increase in pH, and bicarbonate and ferrous iron production.

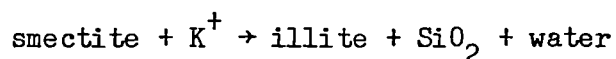


Thus, within each diagenetic regime, such as the depositional environment in which surface conditions directly influence pore-fluid chemistry, a number of factors can be identified as influencing diagenesis. These are as follows:

depositional pore-water chemistry; depositional mineralogy, and in the case of burial regimes, the solid framework; the relative saturation of pore waters and the availability of suitable nuclei; and finally, the presence of organic matter, which is a function of climate, and the influence of which is a function of sediment texture. During burial processes, that is, those unrelated to the regime at the surface, the relative stability of the extant solid assemblage becomes significant.

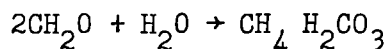
Ferroan calcite cemented most, if not all, of the sequence. Even excluding the exceptional "replacive" cements which may be concretions, this ferroan calcite partially replaces the existing solid framework. Consequently, where it has been dissolved, the secondary porosity system created closely mimics the original pore space. Moreover, whilst the original solid components were unconsolidated and unlithified, pore space created at depth exists within a generally rigid overgrowth cemented framework. Unfortunately, from the available data it is not possible to assess the depth at which this dissolution took place. In spite of this, the solutions responsible were probably aggressive solutions generated during burial by bacterial methanogenic fermentation (Curtis, pers. comm. 1982).

The generation of aggressive solutions again reveals the complex inter-relationship between factors during diagenesis. Aggressive fluids are probably generated at above 60°C during the initial conversion of smectites to illites in organic rich mudrocks. As a consequence, these mudrocks require a specific depositional mineralogy and the survival of organic matter during burial. Above 60°C aluminous smectites convert to illite (Boles and Franks, 1979a) releasing silica and water.



The possible source of potassium is dissolution of aluminosilicates, thus releasing further alumina and silica into solution (Hower, et al, 1976).

Furthermore, if fermentation carbonates produced at this stage are not fixed, they too will be released into solution.



The resulting solutions are acidic, aggressive, and saturated with alumina and silica (Curtis, pers. comm. 1982). Also, as they migrate into sandstones dissolving carbonates, they equilibrate and pH rises. Consequently, kandites are precipitated in the secondary porosity created by dissolution of the carbonates. The pore-filling crystals of quartz observed in samples may also have been introduced at this time.

In addition, therefore, to those processes operating at the surface, a number of diagenetic processes operated during the burial of these Brent Group sediments. Their effect on the sediments is similar to those operating at the surface: where phases are in equilibrium, they are unaffected, whilst where they are not, replacement and dissolution may take place. These meso-genetic processes do not appear to follow a uniform pattern: up to, and including, blocky kandite precipitation, mesogenetic processes are similar to those in Brent Group sediments from the Ninian Field. Whilst hydrocarbons have migrated into both, these sediments reveal none of the intervening effects of continued illitisation of smectites in the source rock, that is, the conversion of calcite to ankerite.

The discussion above has highlighted the problems of attempting to answer the question "What controls diagenesis?" Throughout this discussion no obvious overriding "control" has emerged. Certainly, within one specific regime, such as during the migration of aggressive fluids, the regime itself can be identified and, in this instance, isolated from the effects of those before and after. Nevertheless, to say that aggressive fluids control diagenesis, even at this time, is an over-simplification. Their concentration depends upon the composition of the source rock, and their effect on the composition

of the reservoir into which they migrate. Subsequently, the relative saturation of phases determines whether they precipitate or not. Finally, surviving detrital and authigenic minerals may not be stable in these waters, those that are may act as nuclei for further authigenic phases, those which are not may either dissolve or neomorphose. In these sediments, the complex interaction of numerous factors "controls" diagenesis. These factors may be grouped into regimes only around mutually exclusive regimes, such as depositional environment, or perhaps burial, but only where these regimes can be identified.

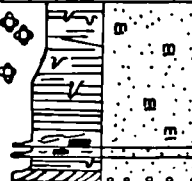



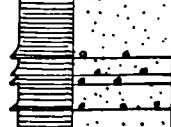



### CONCLUSIONS

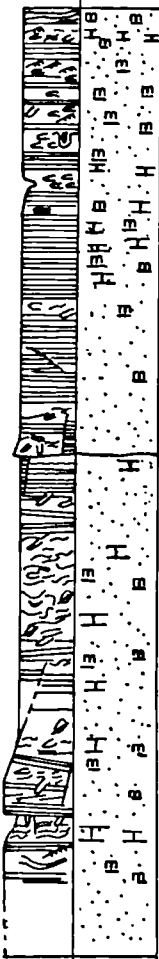
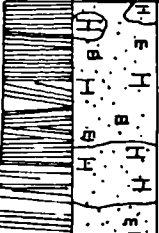
Following deposition in a nearshore shallow marine complex, the Brent Group sediments from 210/15-2 partially equilibrated with their depositional pore waters. As a result, they are cemented with feldspar and quartz overgrowths. The remainder of their diagenetic modification, however, resulted from, firstly, flushing with fresh water, secondly, cementation from formation waters, and thirdly, the action of aggressive fluids prior to hydrocarbon migration. Bacterial generation of acidic solutions resulted in dissolution of feldspars and overgrowths, replacement of feldspars by kandites and neomorphism of muscovite to kandites, and precipitation of quartz overgrowths and vermiform kandites. Subsequently, anoxic bacterial processes began, pore fluids became reducing and more alkaline, with local siderite cementation occurring. As pH rose further, the relative stability of calcite to siderite changed, and resulted in widespread ferroan calcite cementation, either as a pore-filling phase, or in a more intensively replacive, concretionary habit. Later, during bacterial methanogenic fermentation,  $\text{CO}_2$  combined with water from illitisation of smectites in the surrounding mudrocks to form acidic or aggressive solutions. These migrated into the reservoir and dissolved carbonate cement throughout the sequence, creating secondary porosity, recognisable by floating grains and corroded and etched overgrowths. They also precipitated

blocky kandites and pore-filling crystals of quartz after equilibrating with the carbonates. No further major diagenetic modifications to the sequence occurred, either before, during or after the migration of oil into the reservoir. Thus, the resulting rocks are subarkoses, one quarter tightly cemented with ferroan calcite, the remainder highly porous and containing substantial quantities of kandites.

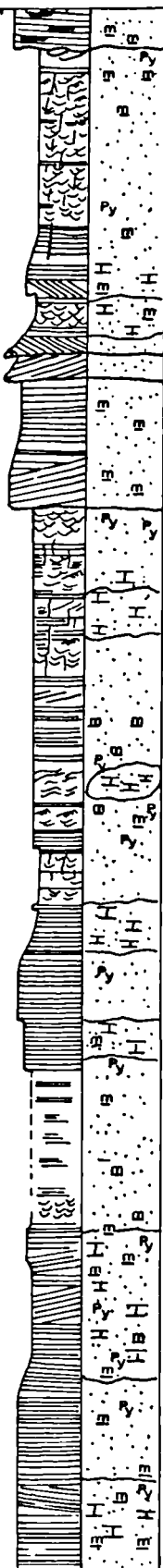
FIG. 5.1 SEDIMENTOLOGICAL AND LITHOLOGICAL LOG OF BRENT GROUP CORE, WELL 210/15-2, NORTHERN NORTH SEA.

(FOR KEY SEE FIG. 4.4)

DEPTH IN FEET	COMMENTS	GRAIN SIZE, SEDIMENTARY STRUCTURES V-CMF & Clay TTTTT	GRAPHIC LITHOLOGY	CORE DESCRIPTION	INTERPRETATION
6780				TOP OF CORED INTERVAL	
6785	OIL STAINED			WHITE TO GREY BIOTURBATED, CROSS LAMINATED, FINING UPWARDS SANDSTONE.	? CHANNEL SANDSTONE.
6790				HORIZONTALLY LAMINATED SILTSTONES AND COALS.	FLOODPLAIN OR MARSH DEPOSIT
6795	ROOLETS				
6800	OIL STAINED			GREY, HORIZONTALLY LAMINATED, FINE-GRAINED SANDSTONE. HIGHLY MICACEOUS WITH ABUNDANT PLANT DEBRIS AND SCATTERED GRANULES.	
6805				LOCALLY FRIABLE.	
6810					
6815					
6818					

6830				
6835			CORE ABSENT	
6840				
6845				
6850	ABUNDANT LEAFY PLANT DEBRIS IN MICACEOUS LAMINAE		WHITE TO GREY, MEDIUM TO FINE GRAINED, WAVY AND PREDOMINANTLY HORIZONTALLY LAMINATED SANDSTONE. LOCALLY BIOTURBATED. HIGHLY MICACEOUS PARTINGS THROUGHOUT, RICH IN PLANT DEBRIS	PREDOMINANTLY STORM DRIVEN FORE SHORE ACCUMULATION.
6855				
6860	OIL STAIN			
6865				
6870				
6875			CORE ABSENT	
6880			SEE BELOW	



6885	WOODY DEBRIS ON FORESETS		WHITE TO GREY, FINING UPWARDS COARSE TO FINE GRAINED SANDSTONE	CHANNEL SANDSTONE ? TIDAL CHANNEL
6890	LIGHT OIL STAIN		LOW ANGLE CROSS BEDDING AT BASE, WITH ROOTED RIPPLE LAMINATED SANDSTONE ABOVE.	
6895				
6900	ROOTLETS		MEDIUM TO FINE GRAINED HORIZONTALLY AND LOW ANGLE CROSS BEDDED SANDSTONE.	FAIRWEATHER FORESHORE SANDSTONE
6905	ROOTLETS			
6910				
6915	CORE BROKEN		SAND GRAIN LAMINAE SEPARATED BY LAMINAE OF MICA AND PLANT DEBRIS.	STORM - DRIVEN FORESHORE SANDSTONE
6920			OCCASIONAL TIGHT CALCITE CEMENTATION, REMAINDER OF CORE FRIABLE AND LIGHTLY OIL STAINED.	
6925				
6930				

ADDITIONAL SYMBOL



CARBONATE CEMENTATION

# FIG. 5.2 COMPOSITE LOG, WELL 210/15-2 NORTHERN NORTH SEA

(Warwick, pers.comm. 1981)

STRATIGRAPHICAL DETAILS NOT GIVEN

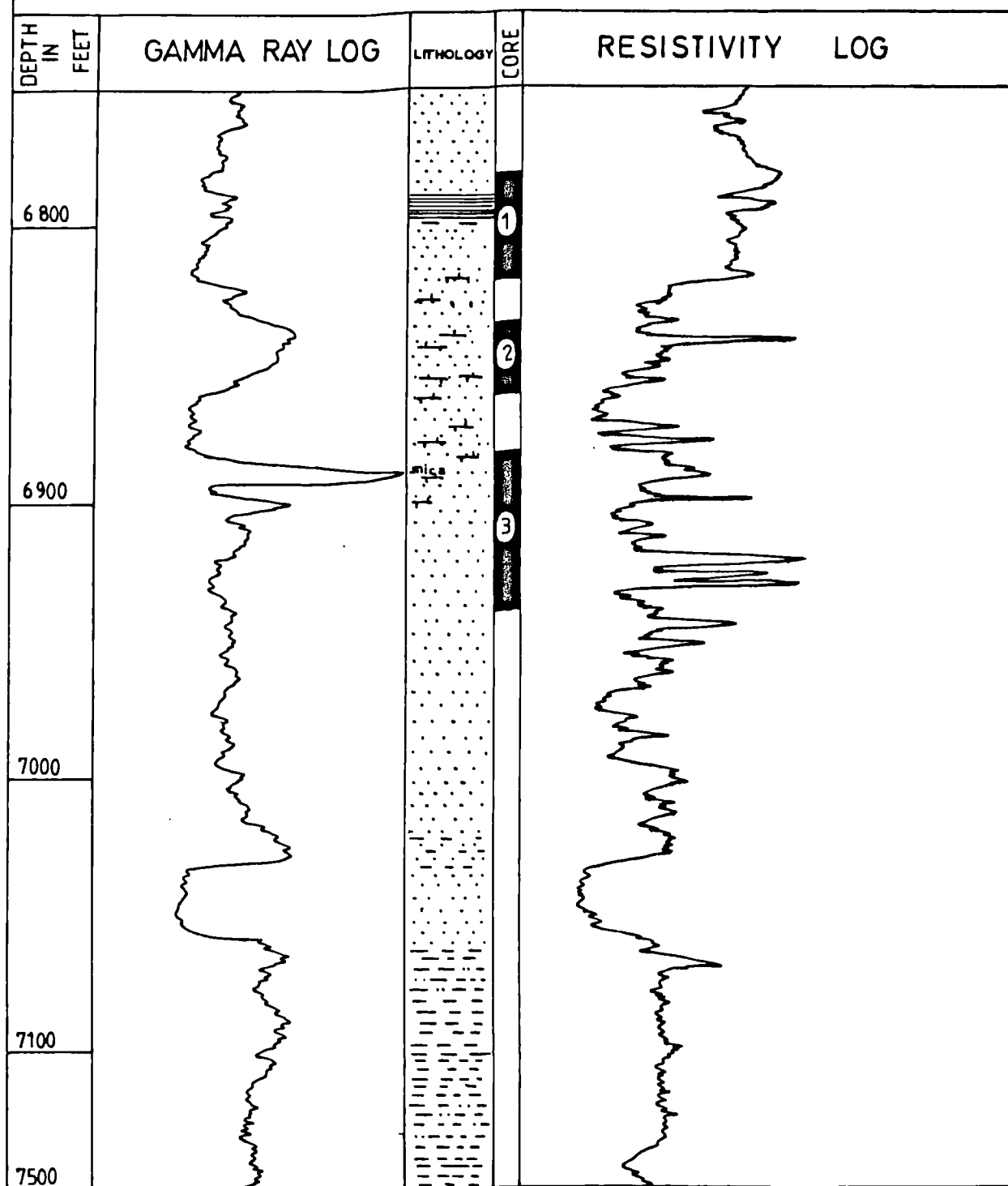
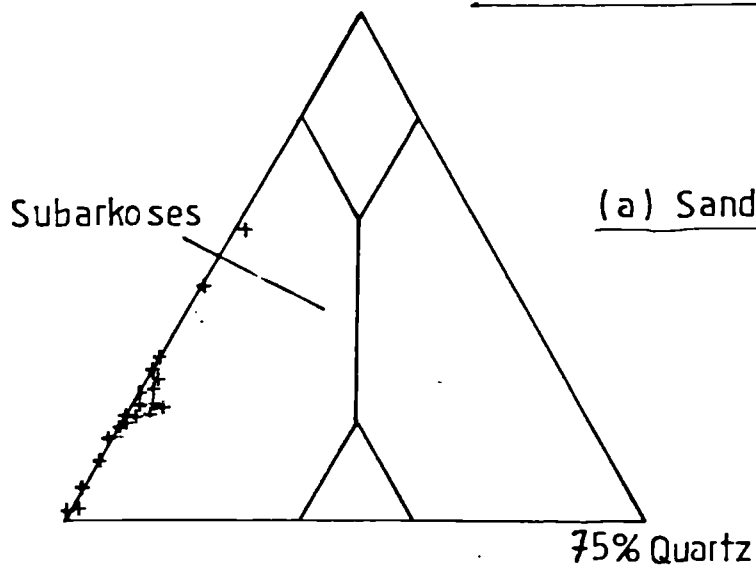
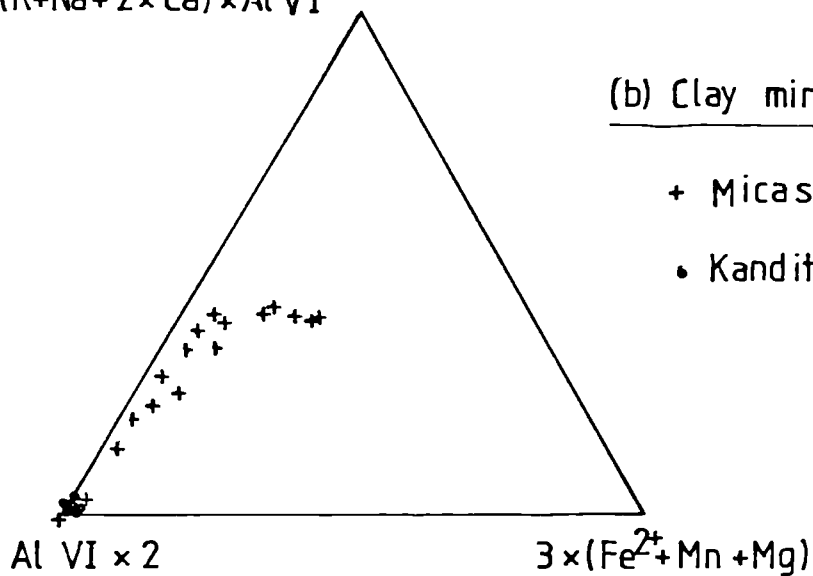


FIG 5.3 COMPOSITION OF FRAMEWORK MINERALS, CLAYS  
AND CARBONATES FROM 210/15-2



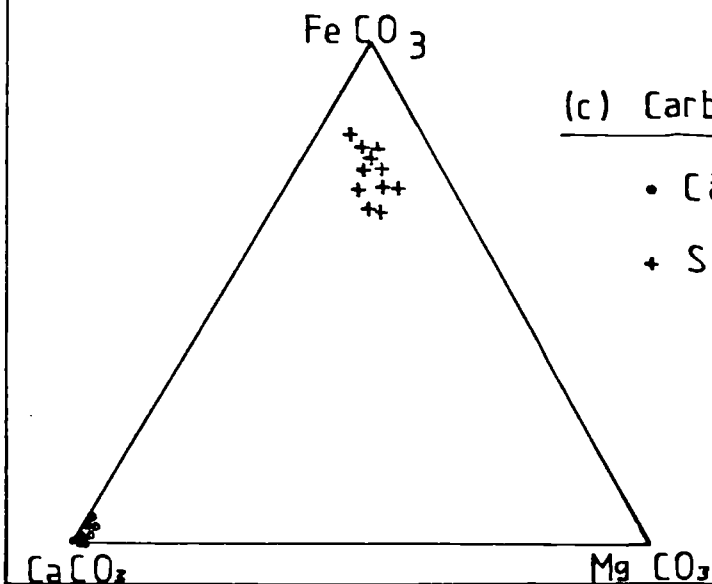
(a) Sandstone classification

$(K+Na+2 \times Ca) \times Al\ VI$



(b) Clay mineral classification

- + Micaceous and altered micaceous
- Kaolinites



(c) Carbonate composition

- Calcite
- + Siderite

FIG. 5.4 Flow chart to illustrate the possible origins of diagenetic reactions in 210/15-2.

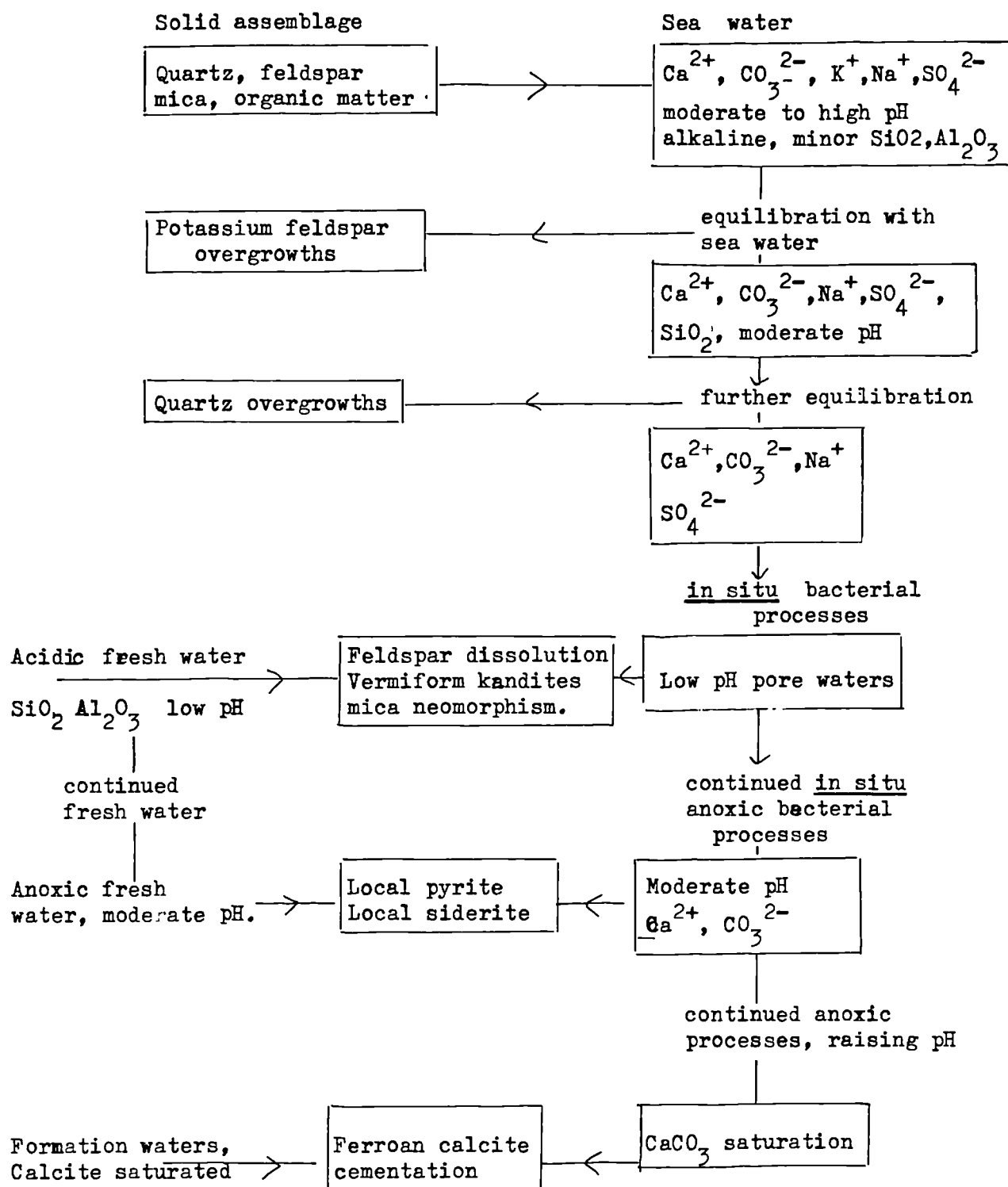
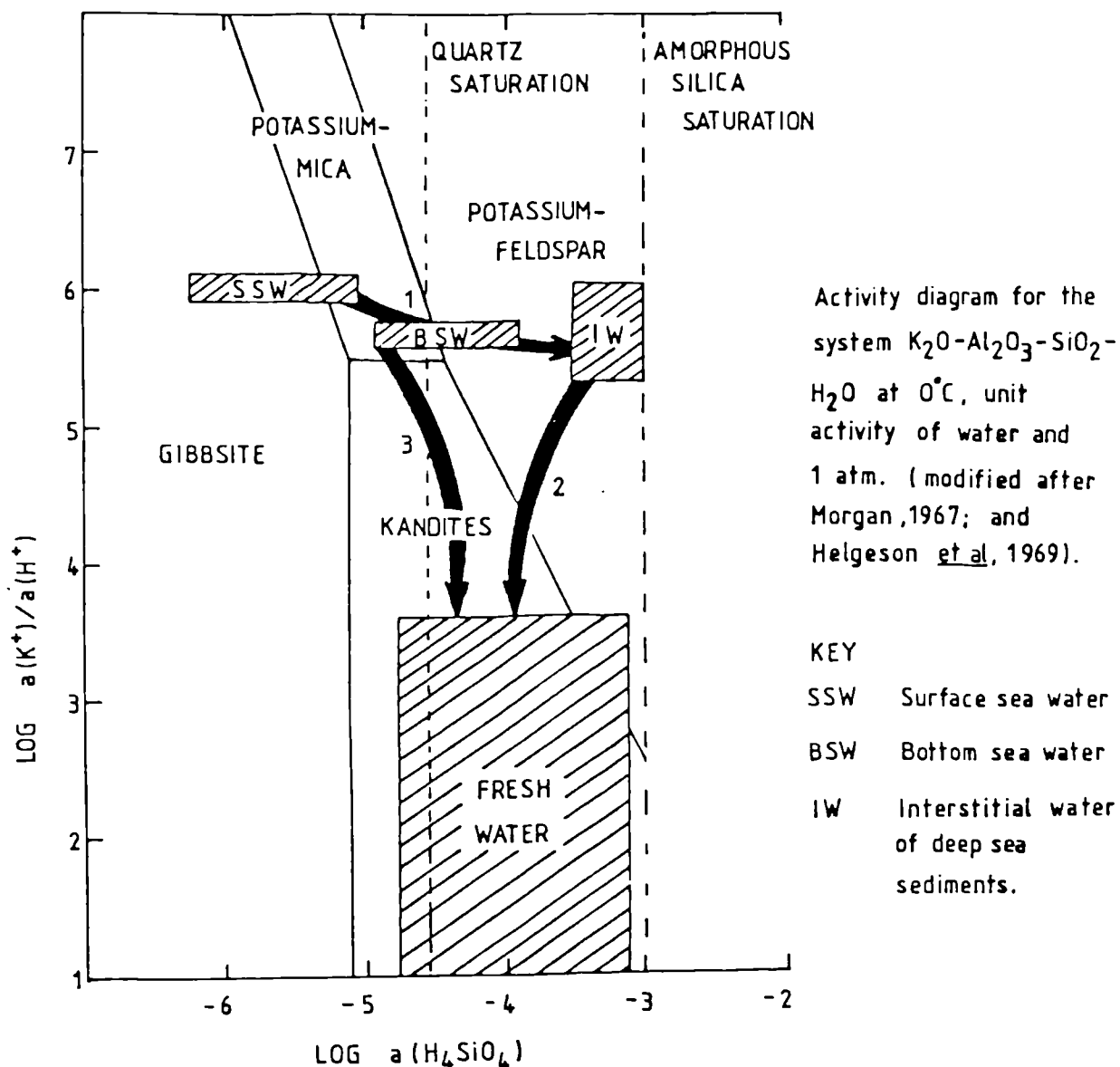


Fig. 5.5 Aluminosilicate diagenesis in clastic sediments from  
210/15-2



- (1). Although deposited in sea water initially, no illite precipitated. Pore waters must, therefore, have evolved to equilibrium with potassium feldspar whilst illite precipitation was inhibited. Potassium-feldspar overgrowths subsequently formed. Then:
- (2+3) pore fluids became acidic, micas neomorphosed to kandites, and potassium feldspars dissolved. Vermiform kandites probably precipitated as a result of the latter.

FIG. 5.6 FLOW CHART OF DIAGENETIC MODIFICATIONS TO POTASSIUM FELDSPARS,  
BRENT GROUP, 210/15-2

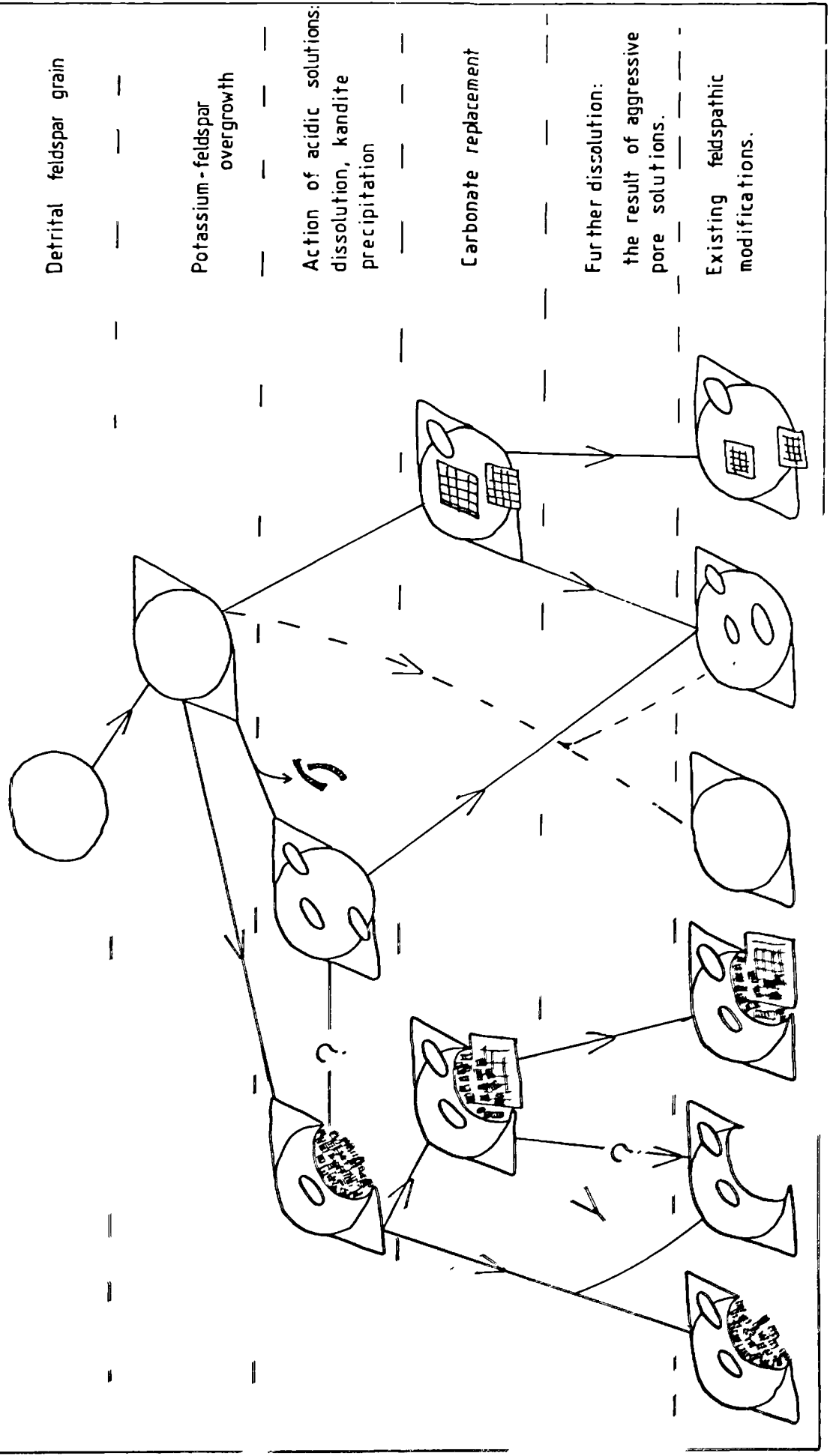


FIG. 5.7 Summary flow chart to demonstrate the diagenetic evolution  
of samples from 210/15-2

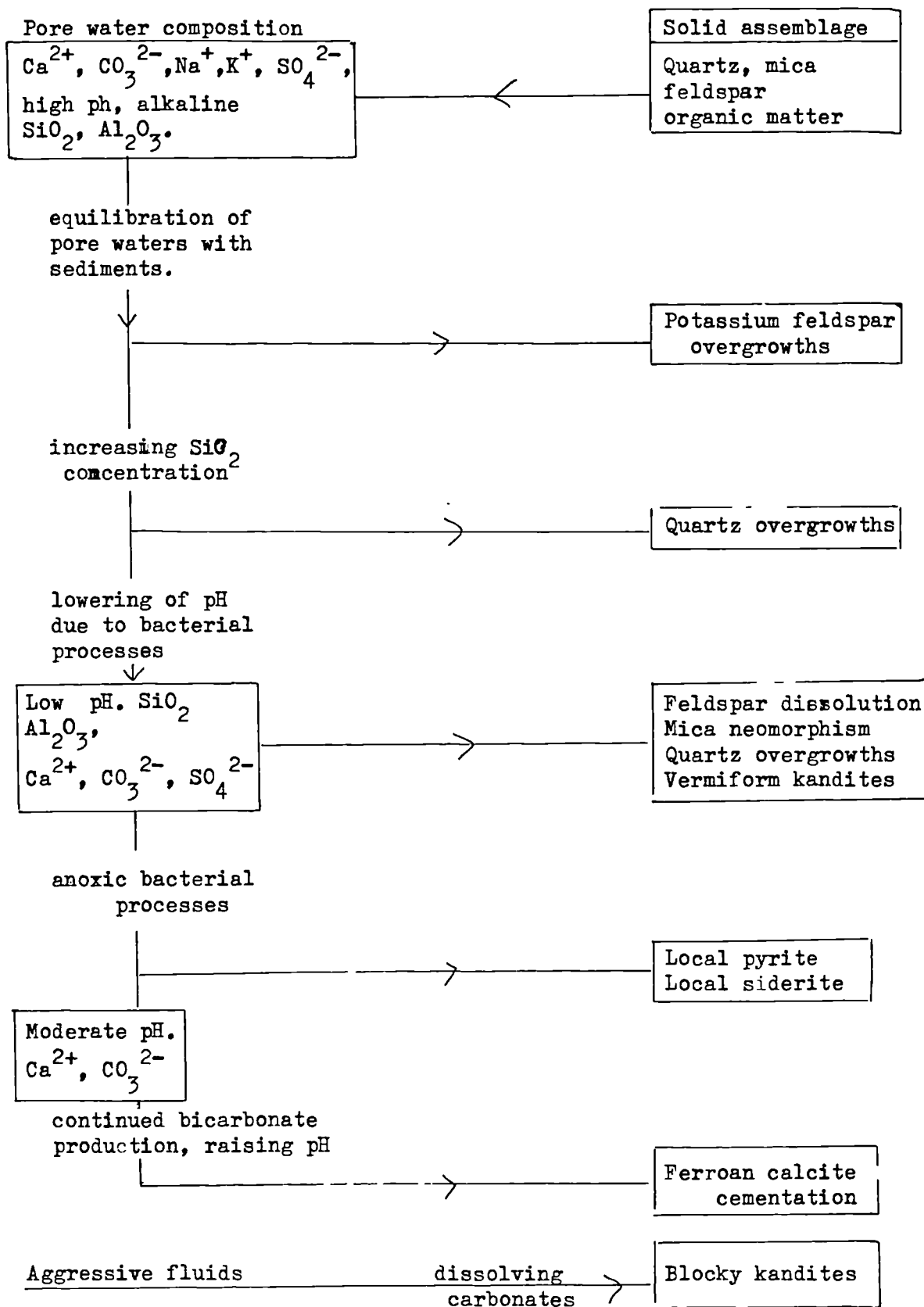


Plate 5.1

- A        A thin veneer of authigenic quartz occurring as overgrowths on detrital quartz grains, cementing grains together, and creating a quartzose framework perforated by a labyrinth of large pores, and open pore throats. Foreshore sandstones 6918'.
- B        A quartz overgrowth on a partially dissolved potassium feldspar grain. Foreshore sandstone 6854'.
- C        Small quartz crystals (c) clustered, as a late pore filling, on an earlier phase of authigenic quartz, an overgrowth (o). Foreshore sandstone 6810' 3".
- D        Two aspects of potassium-feldspar diagenesis: sharp euhedral crystal terminations occur on this feldspar, suggesting the development of an overgrowth, although both the overgrowth and the detrital grains are partially dissolved. Foreshore sandstone 6810' 3".
- E and F    Detail of potassium feldspar lamellae following partial dissolution of the original detrital grain. Foreshore sandstone 6846'.
- G and H    Quartz overgrowth (q) apparently enclosing wholly authigenic potassium feldspar crystals, (c), whilst replacing overgrowths (o) on the detrital grain below. Foreshore sandstone 6904'.



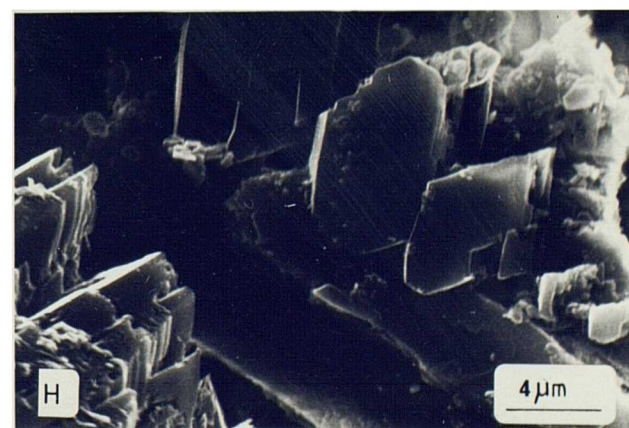
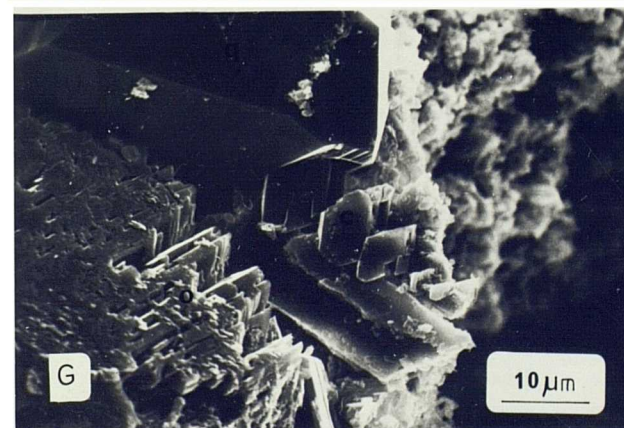
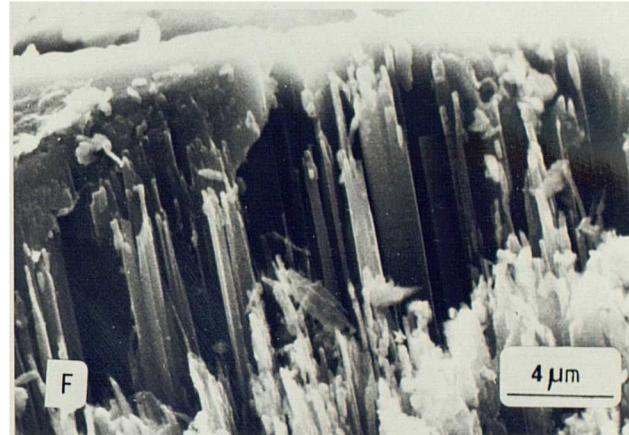
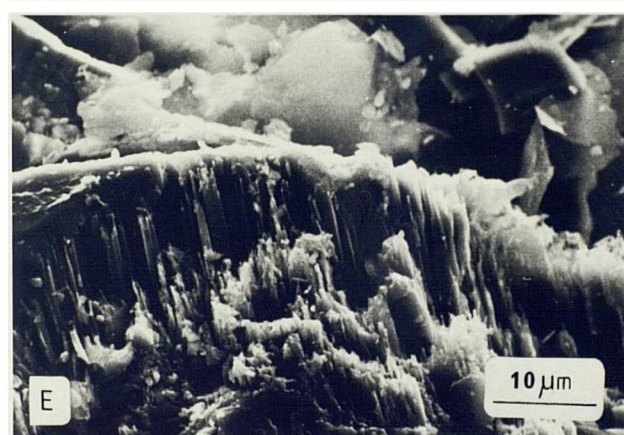
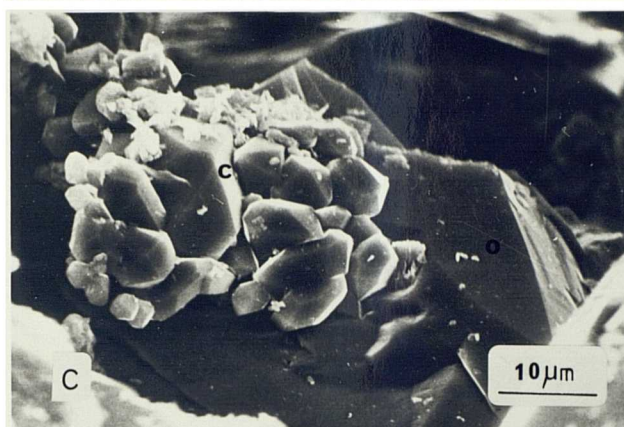
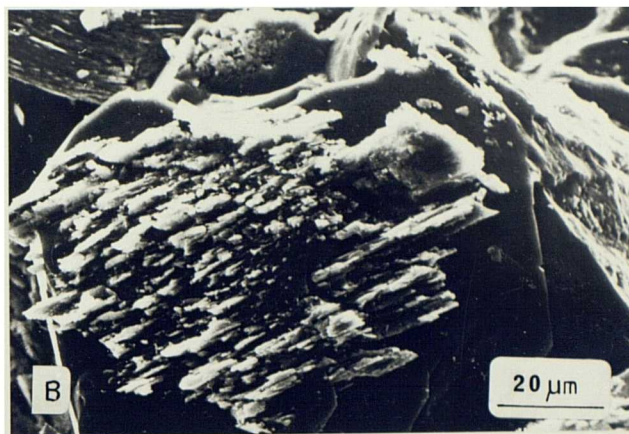
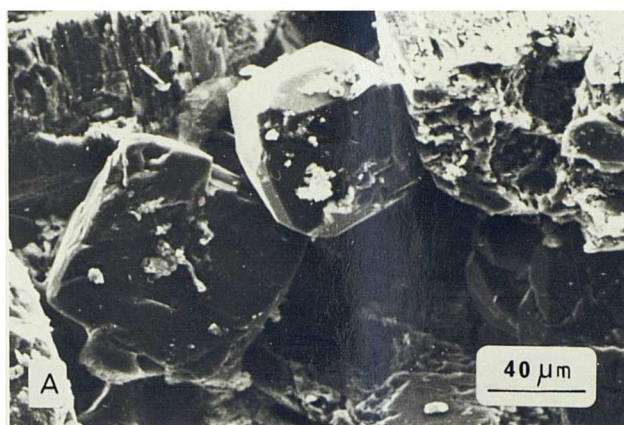


Plate 5.2

- A Potassium-feldspar overgrowths, as small rhombic terminations on a detrital grain which is partially dissolved. The paragenetic relationship between this overgrowth and the quartz overgrowth on the left is unclear. Foreshore sandstone 6818'.
- B An extensive aggregate of stacked kandite sheets, 60  $\mu\text{m}$  thick, and 150  $\mu\text{m}$  long, possibly a neomorphosed detrital muscovite. Foreshore sandstone 6928'.
- C and D A large vermiform kandite aggregate. Although the whole aggregate is over 100  $\mu\text{m}$  long, it is actually composed of numerous, small, regularly stacked pseudo-hexagonal plates, each perhaps only 5  $\mu\text{m}$  in diameter. Foreshore sandstone 6846'.
- E and F Whole sale pore filling by vermiform kandites, each aggregate extensive, but again comprising numerous small plates regularly arranged within each layer, and regularly stacked. Foreshore sandstone 6818'.
- G A small vermiform kandite aggregate.
- H The splayed end of a muscovite flake neomorphosed to kandites. G and H foreshore sandstone 6810' 3".



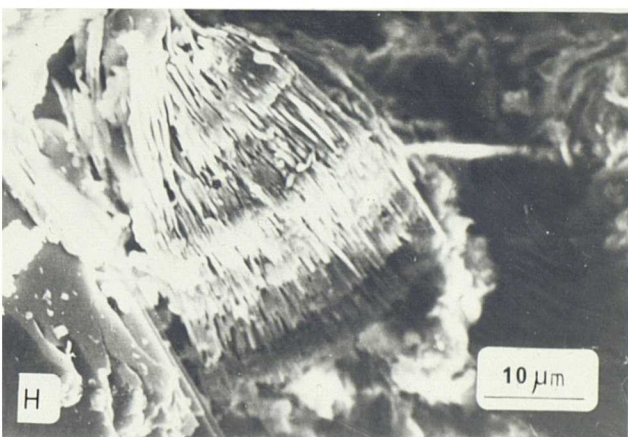
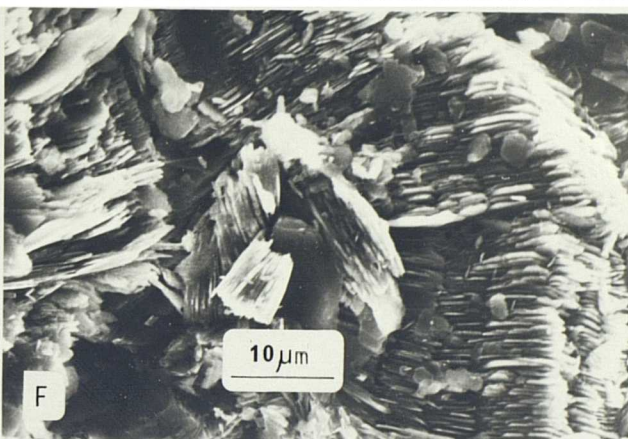
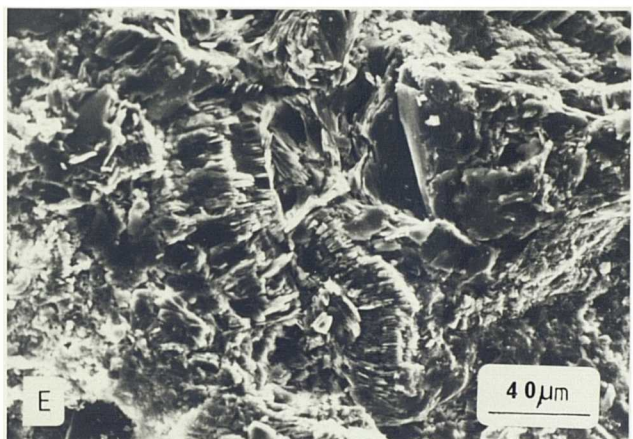
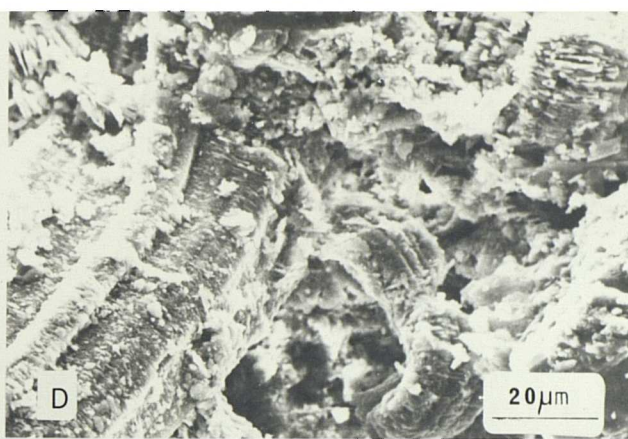
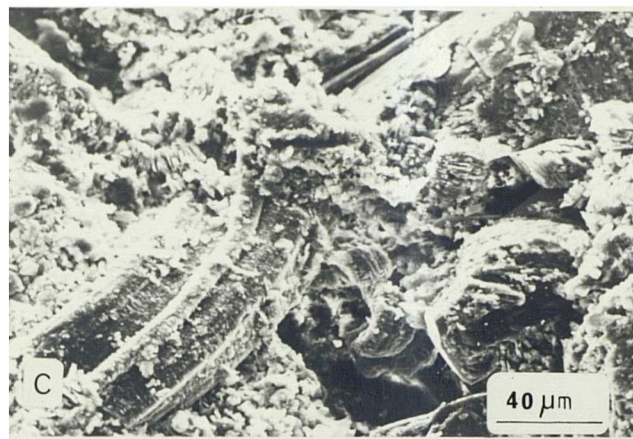
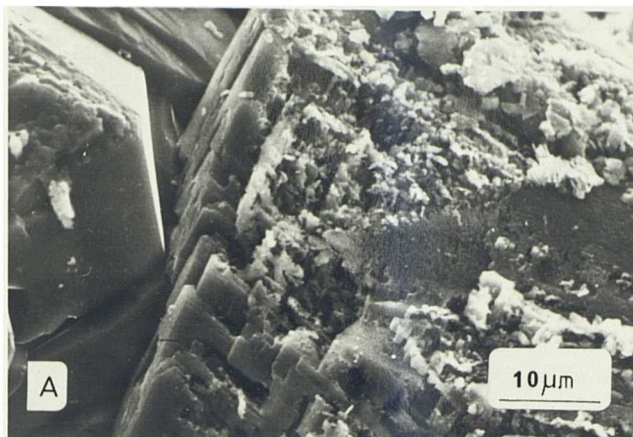


Plate 5.3

A and B Thermodynamically unstable and unpredictable assemblage of a potassium feldspar overgrowth or a grain, most of which has been dissolved and reprecipitated as small kandite plates. There is no evidence visible to suggest that transformation of the former to the latter occurs as a solid state reaction with any inheritance of the original structure as expected from neomorphism. Foreshore sandstone 6928'.

C Fine, pseudo-hexagonal plates of kandites, not arranged in either blocky or vermiform aggregates, filling a pore space between quartz grains with overgrowths. This pore-filling kandite may have replaced a detrital feldspar grain. Needles of authigenic brookite occur on the left hand quartz grain. Foreshore sandstone 6846'.

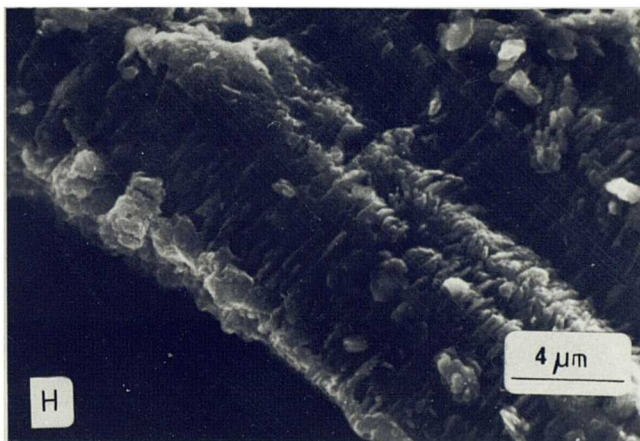
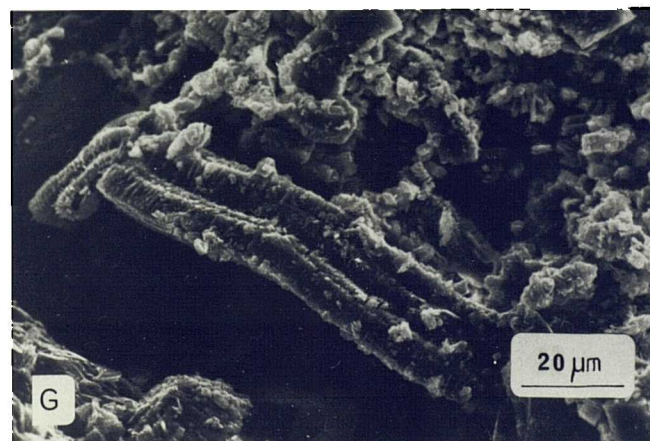
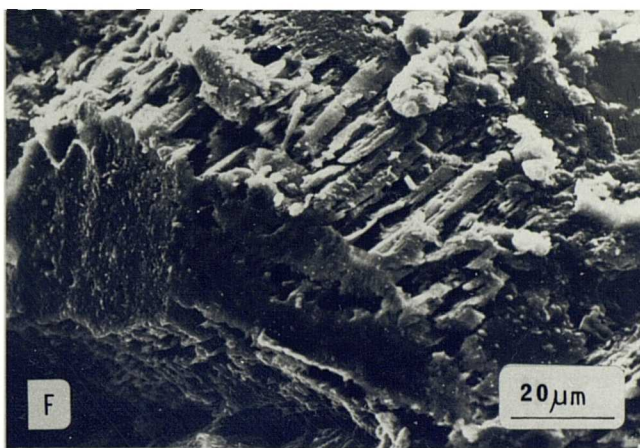
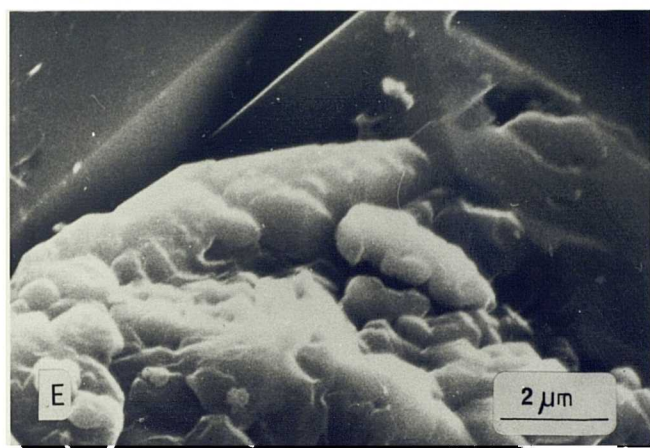
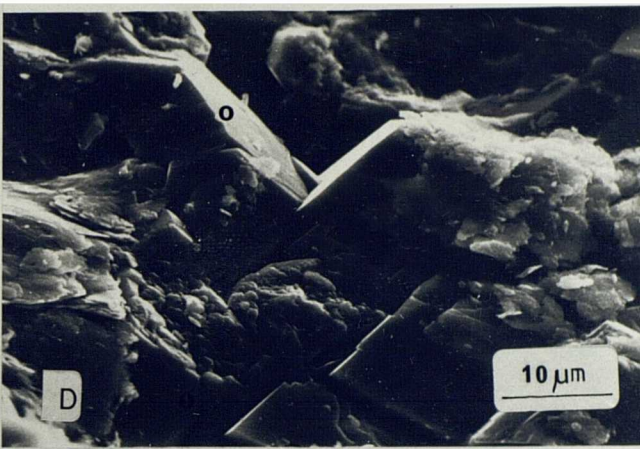
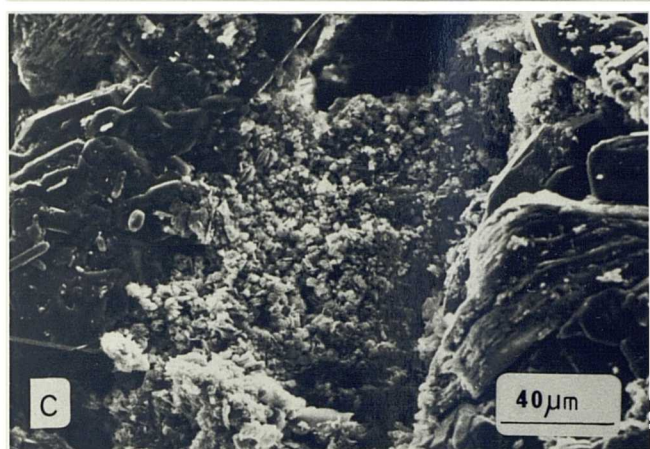
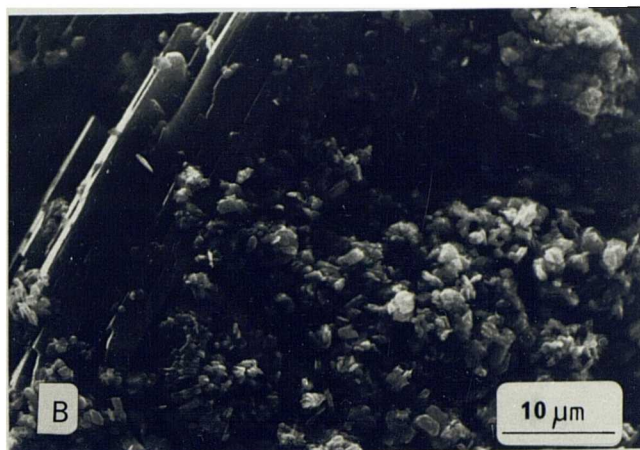
D and E Replacement of a quartz grain, with its overgrowth (o) by rhombic calcite cement. The quartz surface, where the calcite is now absent, is intensively pitted and corroded. Foreshore sandstone 6818'.

F A euhedral potassium-feldspar overgrowth termination, with the effects of subsequently dissolution, which also affected the detrital grain.

G and H Vermiform kandites.

F, G, H Fining upwards facies sandstone 6878'.





CHAPTER SIX: THE STABLE ISOTOPE INVESTIGATION OF AUTHIGENIC CARBONATES  
AND KANDITES FROM THE RAVENSCAR GROUP, YORKSHIRE, AND THE  
BRENT GROUP, NINIAN FIELD, NORTHERN NORTH SEA.

"I often say that when you can measure what you are speaking about, and express it in numbers, you know something about it; but when you cannot measure it, when you cannot express it in numbers, your knowledge is of a meagre and unsatisfactory kind."

Kelvin

Stable isotope analysis lends a degree of sophisticated quantification to petrological problems unavailable with basic petrography. At its simplest, it allows a distinction to be made between sources of elements such as carbon, oxygen and sulphur (see Hudson, 1977). Carbon may be derived from bacterial processes which impart characteristic ratios of  $C^{12}$  to  $C^{13}$  to the resulting minerals (see Table 6.2) or from water; calcite precipitated from sea water and from fresh water has different but characteristic  $\delta^{13}C$  values. Thus, one may distinguish between carbonates forming from bacterial processes and those precipitating from simple natural waters. Mixtures of sources complicate and hamper investigation. Oxygen isotope ratios are generally unaffected by organic processes. However, the ratios in mineral phases are determined by the temperature of the solutions from which they formed. Analysis is often undertaken to assess temperatures of mineral formation. Investigation is complicated here too, because absolute measurement and reference to a standard requires precipitation from "sea water" against which standards are usually measured: as pore waters do not always have the composition of sea water, values may not be true reflections of their temperatures. Nevertheless, trends in oxygen values may be internally significant.

Standard petrographical analysis of non-marine sandstones from the Ravenscar Group (Chapter Three), and the Brent Group in the Ninian Field (Chapter Four),

reveals broadly comparable sequences of diagenetic events. These are: quartz and feldspar overgrowths, and vermiform kandites; widespread rhombic carbonate cementation replacing authigenic quartz; dissolution of carbonate cements; and widespread precipitation of pore-filling blocky kandites. Ankerite also occurs in the Ninian Field.

In addition to cementing non-marine sandstones, siderite occurs throughout the Ravenscar Group in a number of habits. These are: sphaerosiderite spheruliths, 1 mm in diameter, forming laterally extensive horizons, and probably representing palaeosols, in the Saltwick Formation and in the Long Nab Member; nodules 2-50 cm in diameter, formed by coalescence and replacement of spheruliths, in the Long Nab Member at Crook Ness; large ellipsoidal concretions, up to one metre in diameter, also at Crook Ness, either in mudrock sequences, or replacing the spheruliths; as replacive ironstones at the tops of the Yons Nab Beds at Yons Nab, the Millepore Bed at Cloughton Wyke and Osgodby Nab, and in the Scarborough Formation.

Stable isotope analysis was undertaken in an attempt to quantify and elucidate the nature of the diagenetic sequence described above. All the calcite cemented non-marine sandstones were investigated, as were kandites from rocks containing only the blocky variety (dickite?). Furthermore, a diverse suite of siderite samples was selected from sandstones, and ironstones, and the spheruliths, nodules and concretions at Crook Ness to investigate the origin of these differing occurrences and to investigate the relationship between concretion growth and burial (cf. Hudson, 1977; Irwin et al, 1977).



## METHODOLOGY

Wherever possible, throughout this study, sample preparation and analytical techniques have followed procedures established in the literature to ensure a degree of standardisation between these and published results.

Kandites were isolated from disaggregated sandstones by sedimentation, separating the less than 2  $\mu\text{m}$  fraction of the selected samples. Carbonate cements were not separated from detrital siliciclastic grains in view of the latter's stability over the range of experimental conditions outlined below. Siderite concretions and nodules were dissected, and samples of unoxidised centres, tops, and edges were removed for analysis. Both kandites and carbonate cements from outcrop were treated to remove free iron oxides (Mehra and Jackson, 1960). Cole (pers. comm. 1981) reports that kandites and other clays are unaffected by this treatment, although no data were found concerning the stability of carbonates. All samples were washed with 1% sodium hypochlorite solution to remove organic compounds and hydrocarbons. Forester, et al (1973), Dickson and Coleman (1980), and others report that this treatment does not affect carbonate analyses significantly.

Kandite analysis followed the methodology of Clayton and Mayeda (1963). Duplicate samples were preheated to 100°C and 250°C to remove interstitial and structural water, then reacted with 100%  $\text{BrF}_5$  at 400°C for twelve hours. The oxygen evolved during this reaction was reacted with a hot graphite rod to generate carbon dioxide. The carbon dioxide from both samples and a quartz standard reacted at the same time was analysed with a Micromass 903 Mass Spectrometer. The corrected data are presented relative to SMOW.

Calcite and ankerite were reacted with 100% phosphoric acid at 25°C for two hours, and siderite at 55 C for 96 hours. The carbon dioxide evolved was



separated from water-vapour in a refrigerated acetone trap (at 95°C), and analysed with a Micromass 903 Mass Spectrometer. The resulting raw data were corrected following the methods of Craig (1957), and Deines (1970). The ratios are reported in parts per thousand difference between the sample and PDB standard in conventional notation:

$$\delta^{13}\text{C}_{\text{sample}} = \frac{^{13}\text{C}/^{12}\text{C}_{\text{sample}} - ^{13}\text{C}/^{12}\text{C}_{\text{standard}}}{^{13}\text{C}/^{12}\text{C}_{\text{standard}}} \times 1000$$

and similarly for  $\delta^{18}\text{O}$ .

All samples were corrected with reference to carbon dioxide from a standard calcite prepared and analysed at the same time.

Calcite and ankerite analyses have been corrected with fractionation factors of 1.01025 and 1.01109 respectively (Sharma and Clayton, 1965). Unfortunately, both Coleman (pers. comm. 1981) and Gautier (pers. comm. 1981) report considerable uncertainty regarding the accuracy of the published siderite fractionation factor of 1.01169 (Clayton, in Fritz et al, 1971), as well as extrapolation from this value at 25°C, to 1.01131 at 59°C (Hangari et al, 1980). In view of this uncertainty and the high temperature of reaction, the data have been corrected with a fractionation factor of 1.025 to allow comparison with published calcite data. Appendix H contains the raw gas values for future reference.

Most of the carbonate cemented samples and especially those from Ninian contain both siderite and calcite or ankerite. Gases were, therefore, extracted from the samples after two hours at 25°C and a further 94 hours at 55°C. It is necessary to assume that calcite and ankerite reactions were completed after two hours and siderite reaction had not begun. It is most likely that this assumption is incorrect and the gases extracted at each stage were contaminated with the gas from the other reaction. Consequently, the results from samples containing a mixture of carbonates must be treated with caution.

It should be noted that the outermost margins of nodules and concretions were not sampled, as these had been heavily oxidised. This work may, therefore, suffer from the selective sampling described by Curtis et al (1972).

## RESULTS

The results are presented in Table 6.1, relative to PDB unless stated. The corrected results of siderite concretion analyses are presented in Fig. 6.1. Isolated spheruliths average  $\delta^{13}\text{C}$   $-16.2\%$  and  $\delta^{18}\text{O}$   $-3.1\%$ , whilst the concretions and nodules are scattered irregularly around  $\delta^{13}\text{C}$   $-6$  to  $-9\%$  and  $\delta^{18}\text{O}$   $-1$  to  $-5\%$ . Ravenscar Group carbonate cement results are shown relative to the concretions in Fig. 6.2 and relative to published data in Fig. 6.3. Siderite cements and hardgrounds have  $\delta^{13}\text{C}$  and  $\delta^{18}\text{O}$  values similar to those of the concretions, that is,  $-2$  to  $-10\%$ , and  $-2$  to  $-8\%$  respectively. The non-ferroan calcite cement falls within the range of siderite results, whilst the ferroan calcite cements have similar  $\delta^{13}\text{C}$  values to the siderites but have lighter  $\delta^{18}\text{O}$  values of  $-12$  to  $14\%$ . Kandite values are presented relative to SMOW. Carbonate cements from the Brent Group are presented in Fig. 6.4 and in Fig. 6.5 for comparison with published data for cements.

## INTERPRETATION AND DISCUSSION

### Ravenscar Group

Siderite spheruliths. The siderite spheruliths are interpreted as soil horizons forming in poorly drained suboxic or stagnant reducing conditions. Whilst this interpretation confirms an origin inferred from outcrop studies, it relies on analogy to environments where a mixing of carbon sources occurs, and has to overcome the slightly problematical presence of pyrite within the spheruliths. These spheruliths are single sphaerosiderite crystals around a ring of pyrite

crystals and an "amorphous" siderite core. In spite of this, the conditions under which siderite can form are severely restricted. They are: high  $\text{pS}^{2-}$ , low Eh, Ca:Fe ratio of less than 20:1, and moderately high pH (Berner, 1971), although Fitzpatrick (1980) records siderite formation in peat bogs at a pH of 5. These conditions are most easily satisfied in terrestrial environments. Following deposition, organic matter passes through stages of oxidation involving initial oxygen, and subsequently reduction of nitrates, manganese oxides, ferric iron oxides and sulphates (Froelich et al, 1979). The bicarbonates generated in each of these stages has a typical  $\delta^{13}\text{C}$  value (Table 6.2). Nevertheless, the  $\delta^{13}\text{C}$  values of -16‰ from these spheruliths are not typical of either aerobic or reducing bacterial activity - Table 6.2 (Irwin et al, 1977; Curtis, 1978, 1980), nor are they typical of phases precipitated from fresh water (see discussion below). They are, however, typical of conditions involving a mixture of fresh water,  $\delta^{13}\text{C}$  -9‰, and suboxic or sulphate reducing bicarbonate  $\delta^{13}\text{C}$  -25 (Oana and Deevey, 1960). Also, Whelan and Roberts (1973) report similar results from carbonate concretions in poorly drained environments in the Mississippi delta.

Coleman et al (1979) point out that burial rate is the key to the timing of these bacterial processes. If the rate of removal from the system, fixing, of a species equals the rate of sedimentary supply, the zone or depth at which this process takes place remains constant, relative to the surface. If, however, sedimentation rate does not supply reducing species sufficiently quickly, their zones will migrate upwards through the sediment, exhausting the respective species until bacterial methanogenic fermentation occurs beneath a superficial zone of effective oxygen diffusion from above. Indeed, methane commonly occurs in swamps, and beneath stagnant water (Oana and Deevey, 1960; Whelan, 1974; Whelan et al, 1975).

The formation of siderite under these conditions before and after pyrite is,

however, problematical, especially in the absence of calcite. As the concentration of iron to calcium in fresh water is relatively high, siderite commonly precipitates rather than calcite. In addition, bicarbonate production under oxidising conditions generates and maintains a low pH, at which calcite is not stable, until ferric iron reduction increases pH and, simultaneously, increases the ratio of ferrous iron to calcium in solution. Siderite, consequently, becomes stable relative to calcite (Bostrom, 1967; Stumm and Morgan, 1970). Siderite precipitation from fresh water is not, therefore, too difficult to explain. However, although zones of bacterial processes are not completely mutually exclusive (Curtis, 1980), sulphate reduction should only take place after the exhaustion of ferric iron in solution (Froelich et al, 1979). Furthermore, in a closed system following sulphate reduction, one would expect bacterial methanogenic fermentation and more positive  $\delta^{13}\text{C}$  values (Curtis, 1978, 1980).

The results above, however, are not consistent with closed system evolution controlled by bacterial processes. Also, the widespread occurrence of the ring of pyrite after an approximately equal amount of siderite growth suggests widespread rather than local, sulphate reducing conditions (cf. Kaplan et al, 1963; Hudson and Palframan, 1969). Two alternative explanations are possible, therefore. Firstly, there may have been a fluctuation in the water table, mixing a temporarily waning supply of meteoric water, with ferric iron depleted pore fluids, although this too is difficult to reconcile with isotopic data. Secondly, as high tide is the optimum condition for overbank flooding (Fisher and Brown, 1972), brackish or marine sulphate rich waters may have been introduced onto the floodplain. As pyrite rather than siderite is stable in the presence of free sulphate ions, the ring of pyrite would, therefore, mark the effective removal of pore-water sulphate ions, introduced in flood waters prior to continued stagnant fresh water diagenesis.

Siderite nodules and concretions.

"The accurate, detailed study of concretions is a promising enquiry, likely to yield interesting and unexpected results."

Sorby (1908, p. 215)

These nodules and concretions are interpreted as forming from fresh water following improved drainage of poorly developed soil horizons. Outcrop and petrological evidence suggests that nodules have grown by the coalescence and replacement of isolated spheruliths. The trend from  $\delta^{13}\text{C}$  -16‰ in the spheruliths to -9 to -6‰ in the nodules therefore reflects changing pore-fluid composition during this process. However, the unsystematic scatter of points (Fig. 6.1) may be interpreted as demonstrating that no discernable trends of pore-fluid composition occurred during simultaneous nodule and concretion growth. Siderite and calcite concretions occur widely in the geological record (for discussion see Hudson, 1977). Whilst calcite occurs ubiquitously, siderite can form freely in freshwater environments but usually only in marine sediments during burial. Therefore, siderite concretions in marine sediments tend to reflect sources of bicarbonate throughout burial, whilst those formed in terrestrial environments may reflect their depositional environment and shallow- as well as deep-burial diagenesis. Previous studies of siderite concretions from freshwater sediments demonstrate the possible variations in isotopic compositions. Weber et al (1964) conclude that  $\delta^{13}\text{C}$  values of  $-4.75 \pm 1.13\text{‰}$  are related to fresh water whilst Fritz et al (1971) attribute  $\delta^{13}\text{C}$  values of -1.1 to -7.7‰, averaging -3.4‰, to bacterial processes rather than the depositional environment. Curtis et al (1972), in a more detailed study, relate bicarbonate production to bacterial fermentation. Finally, Gould and Smith (1979), attribute siderite spheruliths associated with a coal bearing sequence to early diagenetic bacterial fermentation.

Values found in this study of  $\delta^{13}\text{C}$  -6 to -9‰ agree with environmental control rather than diagenetic or bacterial activity. Also, these values fall within the range of freshwater cements (I.G.S. Annual Report 1979, p. 57) and agree

with published data from freshwater cements and fossils, and meteoric waters (Oana and Deevey, 1960; Keith and Weber, 1964; Keith et al, 1964; Murata et al, 1969; Tan and Hudson, 1974; Salomons et al, 1978). Perhaps more significantly, Whelan and Roberts (1973) relate values of  $\delta^{13}\text{C}$  -10 to -19‰ to bacterial processes in poorly drained environments, whilst values of -9 to -10‰ are attributed to "renewed surface water."

Laminations may be traced from the mudrocks and through the concretions without any change in thickness. However, they are compacted around the tops and edges of individual concretions. This suggests that compaction took place after, but not during, growth. Concretions typically contain at least 90% siderite, which suggests that they grew before significant compaction had taken place (Raiswell, 1971). Although this conclusion may not be directly applicable, as siderite replaces as well as encloses detrital clays, it suggests from the ellipsoidal shape of the concretions that horizontal permeability greatly exceeded vertical permeability even at very shallow depths. This apparent lack of compaction may have been aided during shallow burial by iron oxide "propping" (Curtis, pers. comm. 1982). The concept of iron oxide propping is based on the work of Coleman and Ho (1968).

Coleman and Ho (1968) describe Recent alluvium from the Atchafalaya Basin which is being cemented with iron and manganese oxides and, hence, losing porosity by precipitation rather than compaction. This sequence contains up to 30 year old concretions at depths of up to 150'. These concretions are progressively enclosing the surrounding muds, although laminae may be traced through the concretions irrespective of depth without any apparent physical compaction. It is concluded, therefore, that iron and manganese oxides are propping open pores within clay laminae prior to their cementation by the concretions. Whilst this may have been the case initially during the Middle Jurassic in Yorkshire, the iron and manganese iron oxide cementation described

by Coleman and Ho (1968) would not have resisted later overburden pressures, hence the consequent evidence of compaction.

Following Whelan and Roberts (1973) one may conclude that during stagnation the speruliths grew, but subsequent percolation of fresh water with improved drainage caused the precipitation of further siderite and, hence, the growth of dense siderite concretions and nodules.

Siderite cements. The siderite cements from the Ravenscar Group are freshwater cements. As shown in Fig. 6.3,  $\delta^{13}\text{C}$  values from both rhombic siderite cements, and the ironstones, closely overlap both the concretions discussed above, and previously reported freshwater carbonates (Keith and Weber, 1964; Bathurst, 1975; I. G. S. Annual Report, 1979). These results also differ markedly from values for marine cements (Hudson, 1977), and the range of marine hardgrounds discussed by Schlager and James (1978). However, an average value for the ironstones of  $\delta^{13}\text{C} -5.9\text{‰}$  is similar to the freshwater diagenesis of Quaternary to late Tertiary carbonate sediments discussed by Gavish and Friedman (1969).

The  $\delta^{18}\text{O}$  values of meteoric waters are generally lighter than those of sea water (Dansgaard, 1964). The average  $\delta^{18}\text{O}$  values of these concretions, nodules, cements, and ironstones, of -2 to  $-8\text{‰}$  may also reflect precipitation from tropical Jurassic fresh water. Furthermore, the ironstone  $\delta^{13}\text{C}$  values of -4 to  $-8\text{‰}$  could reflect equilibration of freshwater bicarbonate  $\delta^{13}\text{C} -9$  to  $-6\text{‰}$  (Murata et al, 1969), with the "primary" marine limestones which they replace  $\delta^{13}\text{C}$  0 to  $2\text{‰}$  (Marshall and Ashton, 1980).

Calcite cements. The non-ferroan calcite is interpreted as a freshwater cement, whilst the ferroan calcite formed later from isotopically light fluids, probably formation waters. Although  $\delta^{13}\text{C}$  values overlap, the  $\delta^{18}\text{O}$  for non-ferroan

calcite is distinctly different from those of the ferroan calcite, -11.9 to -13.8‰. The non-ferroan calcite values for both carbon and oxygen fall within the field of siderite concretions, ironstones and cements, and therefore agree with published analyses of freshwater cements (see discussion above). Why does this calcite postdate siderite precipitation? Siderite is stable in reducing conditions with a ratio of  $\text{Ca}^{2+} : \text{Fe}^{2+}$  of less than 20:1. When ferrous iron is removed to form siderite, this ratio may increase, although some calcium is removed from solution, into the resulting non-stoichiometric siderite. However, when ferrous iron becomes sufficiently depleted and calcium forms, 5% ferrous iron would be present, and one might expect ferroan, rather than non-ferroan calcite to precipitate. Alternatively, if oxygenated pore fluids were locally introduced, oxidation of ferrous iron would promote non-ferroan calcite precipitation. The latter explanation of non-ferroan calcite formation is, therefore, preferred. It is also significant because this calcite only encloses ~~sphaer~~sphaerosiderite (although not the spheruliths analysed here). If sphaerosiderite forms in stagnant environments, it is plausible that, in this case, subsequently improved drainage which elsewhere produced freshwater siderite, here introduced oxygenated pore waters, which precipitated non-ferroan calcite.

The ferroan calcite, whilst having  $\delta^{13}\text{C}$  values/typical of fresh water, is significantly lighter in oxygen. The  $\delta^{13}\text{C}$  results do not support cementation by bacterial sulphate reducing or methanogenic fermentation bicarbonates. Furthermore, they do not fall within any fields of eogenetic calcite precipitation (Fig. 6.3). The discussion above suggests that evolving pore fluids should precipitate ferroan calcite following the fixing of ferrous iron by siderite. In addition, temperature increases with burial, consequently precipitation of ferroan calcite lighter in  $\text{O}^{18}$  might be expected in a closed system (Hudson and Friedman, 1976; Dickson and Coleman, 1980). Several lines of evidence, however, suggest that ferroan calcite is mesogenetic, that is, it has formed from formation water, and



evolving depositional pore fluids in a closed system. Firstly, the effect of increasing temperature producing more negative  $\delta^{18}\text{O}$  values would be countered by pore-fluid composition which would tend to become enriched with heavier isotopes, and therefore produce more positive calcite following precipitation of light siderites (Hudson, 1977). Secondly, whilst the difference in fractionation between siderite and water, and calcite and water, is not known, it is not as great as the 3.7‰ break between the two found here. Thirdly, precipitation from a hypothetical Jurassic sea water ( $\delta^{18}\text{O} = 0 - 1\text{‰}$ ) would suggest non-ferroan calcite formation at 40°C, and ferroan calcite at 85°C (Table 6.3), an increase which is not realistic in terms of a simple burial model. This suggests that an open-changing pore-water system precipitated the second phase of cement. The introduction during burial of isotopically light,  $\text{Ca}^{2+}$  bearing pore waters from elsewhere in the basin may explain these values.

Kandites. Analyses of kandites (Tables 6.1 and 6.3) are difficult to evaluate in isolation. As the clay minerals replace carbonates, some modification of pH is required in this paragenetic sequence, which again suggests the introduction of pore waters rather than the simple evolution of a pore-fluid system. Assuming their precipitation from a Jurassic sea water, ( $\delta^{18}\text{O SMOW} = -1.2\text{‰}$ ), the kandites precipitated at 108°C, whilst the calcite formed at 85°C, a discrepancy not expected from simple pore-fluid evolution (cf. Dickson and Coleman, 1980). Nonetheless, a modified fluid of some kind is required because these values of  $\delta^{18}\text{O SMOW} +14$  to  $+16$  do not support precipitation at or near the earth's surface:  $\delta^{18}\text{O}$  for sea water is 0, and fresh water is only slightly lighter. These data do not necessarily support formation at 108°C either, but more probably precipitation from isotopically light pore waters.

Irrespective of whether these hypothetical calculations suggest pore-fluid evolution, both petrographical evidence and geochemical considerations require

that pore-fluids changed at this time. The origin of these pore fluids, and the resulting kandites is conjectural. Whilst these data exclude formation from low-temperature dissolution of feldspars, they do not exclude the influence of meteoric water introduced during structural inversion and unroofing in the Lower Cretaceous (Kent, 1980), and subsequently fractionated during reactions prior to introduction into Middle Jurassic sandstones. However, there is no reason why this water would have been acidic (Curtis, in press). The preferred interpretation is one of continued degradation of organic matter and generation of "aggressive fluids" during burial.

Stable isotope analysis of extant carbonates records bicarbonates generated under suboxic and sulphate reducing conditions and from fresh and formation water. Organic matter in the surrounding mudrocks is now marginally mature (Cooper, pers. comm. 1980) and has generated oil, filling chambers in the underlying Liassic, for example (Hemingway, 1974). These extant carbonate cements do not record bicarbonate from the intervening bacterial methanogenic fermentation zone proposed by Irwin et al (1977). It is therefore proposed that fermentation took place, generating acidic or aggressive solutions, which migrated into the sandbodies and dissolved carbonates. Consequently, as pore-fluid rose, these solutions entered the field of kandite stability and from supersaturated solutions, possibly enhanced by dissolution of feldspars, precipitated blocky kandites (Curtis, pers. comm. 1982).

#### Brent Group

Brent Group results from the Ninian Field (Fig. 6.4) do not demonstrate any consistency within carbonate species or between species, either from the same or different samples. Furthermore, whilst some  $\delta^{13}\text{C}$  values could be explained in terms of fresh water, -6 to -9‰, and soil processes or bacterial sulphate reduction, -20 to -25‰ etc, none of these would explain the relatively light

oxygen values  $\delta^{18}\text{O}$  -10 to -14‰, averaging -12‰. Results from 3/3-3, 10468' are distinctly different from other samples' results, and may reflect early diagenetic concretion growth during bacterial sulphate reduction (Irwin et al, 1977). This possibility may be confirmed by  $\delta^{18}\text{O}$  values of -5.8 to -7.6 which are not dissimilar to those from interpreted freshwater phases in the Ravenscar Group. Furthermore, a "temperature" of 40°C (Table 6.3) may result from the relatively isotopically light nature of meteoric water (Dansgaard, 1964).

The remaining data, however, cannot be explained by a model similar to that invoked for the petrographically similar Ravenscar Group. Moreover, straightforward interpretation of these data leading to an unequivocal model for their origin is not possible. It must be stressed, however, that because of the problems of analysing mixtures of carbonates from samples, all the proposals below must be considered cautiously.

High-heat flow, combined with intense advection along active faults in the East Shetland Basin at this time may have influenced the conditions under which other cements formed. Whilst the  $\delta^{13}\text{C}$  values of -6 to -9‰ of the remaining siderites could have resulted from freshwater precipitation, their  $\delta^{18}\text{O}$  values may, therefore, reflect not only  $\text{O}^{18}$  depletion of fresh or meteoric water, but also hotter and lighter pore fluids during burial (Coleman, pers. comm. 1982).

Ferroan calcite occurs as a cement throughout the reservoir, and formed after siderite. It too has relatively light  $\delta^{18}\text{O}$  values. However, whilst in the Ravenscar Group there is a marked break between the freshwater siderites, and inferred formation water calcites, no such break occurs here. Consequently, although  $\delta^{18}\text{O}$  values of these ferroan calcites are similar to those from the Ravenscar Group, they cannot be interpreted as formation water cements by

direct analogy. Their lightness may also reflect high-heat flow during shallow burial.

These results and their interpretations do not readily conform to a simple model of pore-fluid evolution (cf. Dickson and Coleman, 1980), nor do they agree with previously published data for cements from a variety of origins (Fig. 6.5). However, both high-temperature precipitation, and precipitation from isotopically fractionated pore-fluid systems could help to explain these relatively negative  $\delta^{18}\text{O}$  values. Whilst these suggestions may explain calcite values, they do not explain fully light siderite values, nor indeed the presence of ankerite.

Ankerite occurs in a number of samples as a late stage pore filling, scattered irregularly throughout the cores with not apparent relationship to either depositional environment or depth. Ankerite is interpreted here as forming from carbonates in situ equilibrating with  $\text{Mg}^{2+}$  and  $\text{Fe}^{2+}$  released during illitisation of smectites in the surrounding source rocks. Boles (1978) discusses the ankerite which occurs below 3-4000 m in the Wilcox Sandstone from south-west Texas. He records  $\delta^{18}\text{O}$  values of -8 to -11‰, and  $\delta^{13}\text{C}$  values of -5 to -9‰, which are remarkably similar to those reported here (Table 6.1). Also, Boles and Franks (1979a) correlate the replacement of calcite by ankerite with depth, and the conversion of ordered smectites to illite releasing  $\text{Fe}^{2+}$  and  $\text{Mg}^{2+}$  at approximately 120°C in the surrounding mudrock sequence. Interpretation of Boles' (1978) Fig. 8 suggests that ankerite in the Ninian Field formed at 150°C, whilst calculations (Table 6.3) give a value of 115°C. These "values" are not unreasonable in view of the likely Tertiary migration (Cooper et al, 1975) of hydrocarbons from a hotter source rock, into a reservoir currently at 100°C (Albright et al, 1980). Furthermore, Pearson et al (in press) report progressive illitisation of smectites in mudrocks from the Northern North Sea, including wells in Block 3. They suggest that clay mineral diagenesis

in the Northern North Sea is following a similar path to that reported by Boles and Franks (1979a). Consequently, Jurassic smectites have been illitised and released  $\text{Fe}^{2+}$  and  $\text{Mg}^{2+}$ , which probably equilibrated with calcite in the reservoir, and subsequently precipitated ankerite.

Previous studies of hydrocarbon-bearing (Carothers and Kharaka, 1980) or hydrocarbon-related sequences (Donovan, 1974) indicate that  $\delta^{13}\text{C}$  values of -20 to 25‰ may result from the introduction of hydrocarbons or their subsequent oxidation and interaction with the local carbonates. Core examination, however, indicates that the surviving tight calcite cements are not oil stained. In view of this and the values obtained in this study there is, therefore, no isotopic evidence to suggest that hydrocarbon-bearing fluids are recorded directly in the samples studied here.

#### SUMMARY AND CONCLUSIONS

##### Ravenscar Group

Before and during shallow burial, siderite spheruliths formed in a soil horizon in the Long Nab Member. These diagenetic spheruliths probably resulted from the combination of aerobic and suboxic zone bicarbonate with ferrous iron in reducing conditions in stagnant water. Scattered pyrite crystals indicate that sulphate reduction also took place at this time, probably after the introduction of sea or brackish water during flooding, but the fermentation zone was not generally reached. Replenishment of stagnant waters with fresh water resulted in the nucleation and growth of siderite concretions as well as the formation of nodules by the coalescence and replacement of the diagenetic spheruliths. Possibly simultaneously, widespread freshwater siderite cementation took place under suboxic or anaerobic conditions at shallow depths, further consolidating sediments previously cemented with quartz overgrowths,

and preventing more pronounced compaction of mud sequences around the nodules and concretions before significant burial. The occasional introduction of oxygenated fresh water led to the precipitation of non-ferroan calcite cement.

During freshwater diagenesis the percolation of ground water into intercalated marine sequences caused the replacement of calcite by siderite and the formation of ironstone horizons from limestones at the tops of the Yons Nab Beds, the Millepore Bed and the Sarborough Formation. Subsequently, during burial, ferroan calcite cement precipitated from isotopically light formation waters, introduced into pores. Burial diagenesis models of aerobic, suboxic, sulphate reducing and fermentation zones do not apply in these sediments.

Petrographical evidence suggests that one or more extensive carbonate phases have been precipitated, and subsequently removed by presumably acidic solutions. Unfortunately, the isotopic nature of these carbonates and later fluids is not known. Following dissolution of these carbonate cements, kaolinites precipitated. Isotopic data support an erratic rather than steady state evolution towards more negative  $\delta^{18}\text{O}$  values. Calcite and siderite dissolution could be related to delayed bacterial methanogenic fermentation and thermal decarboxylation of the remaining organic matter, generating aggressive fluids which subsequently precipitated the clay minerals. The data do not support a surface or near surface origin by feldspar dissolution for these clays.

#### Brent Group

Although results from one sample are similar to the eogenetic data from the Ravenscar Group, the problematic siderite values do not allow confirmation or denial of their suspected eogenetic origin. Similarly, whilst calcite values may be interpreted as mesogenetic in isolation, they do not easily fit in with

siderite data. Ankerite, however, may be interpreted as the result of equilibration of either eogenetic or mesogenetic carbonates, with  $Mg^{2+}$  and  $Fe^{2+}$  bearing solutions migrating from source rocks during illitisation of smectites, but prior to hydrocarbon migration. In conclusion, therefore, whilst stable isotope investigation of Brent Group carbonates confirms burial related diagenesis, it does not allow complete elucidation of other diagenetic controls. The situation is complicated by high-heat flow during the late Jurassic, and inherent problems in analysing mixtures of carbonates.

FIG 6.1 CARBON AND OXYGEN ISOTOPE VALUES,  
FROM SPHERULITES, NODULES, AND  
CONCRETIONS, LONG NAB MEMBER,  
RAVENSCAR GROUP, YORKSHIRE.

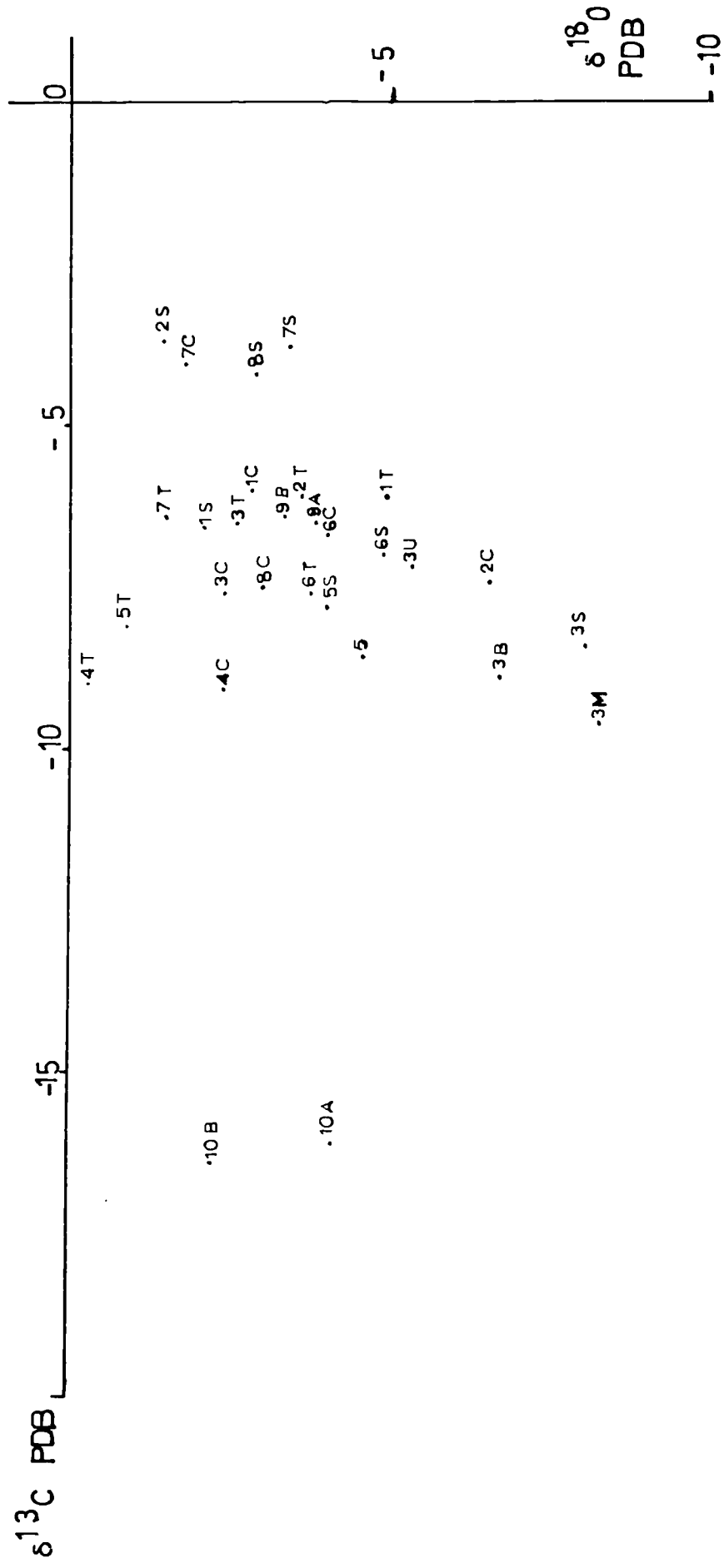




FIG. 6.2 CARBON AND OXYGEN ISOTOPE VALUES,  
CARBONATE CEMENTS, RAVENSCAR GROUP,  
YORKSHIRE

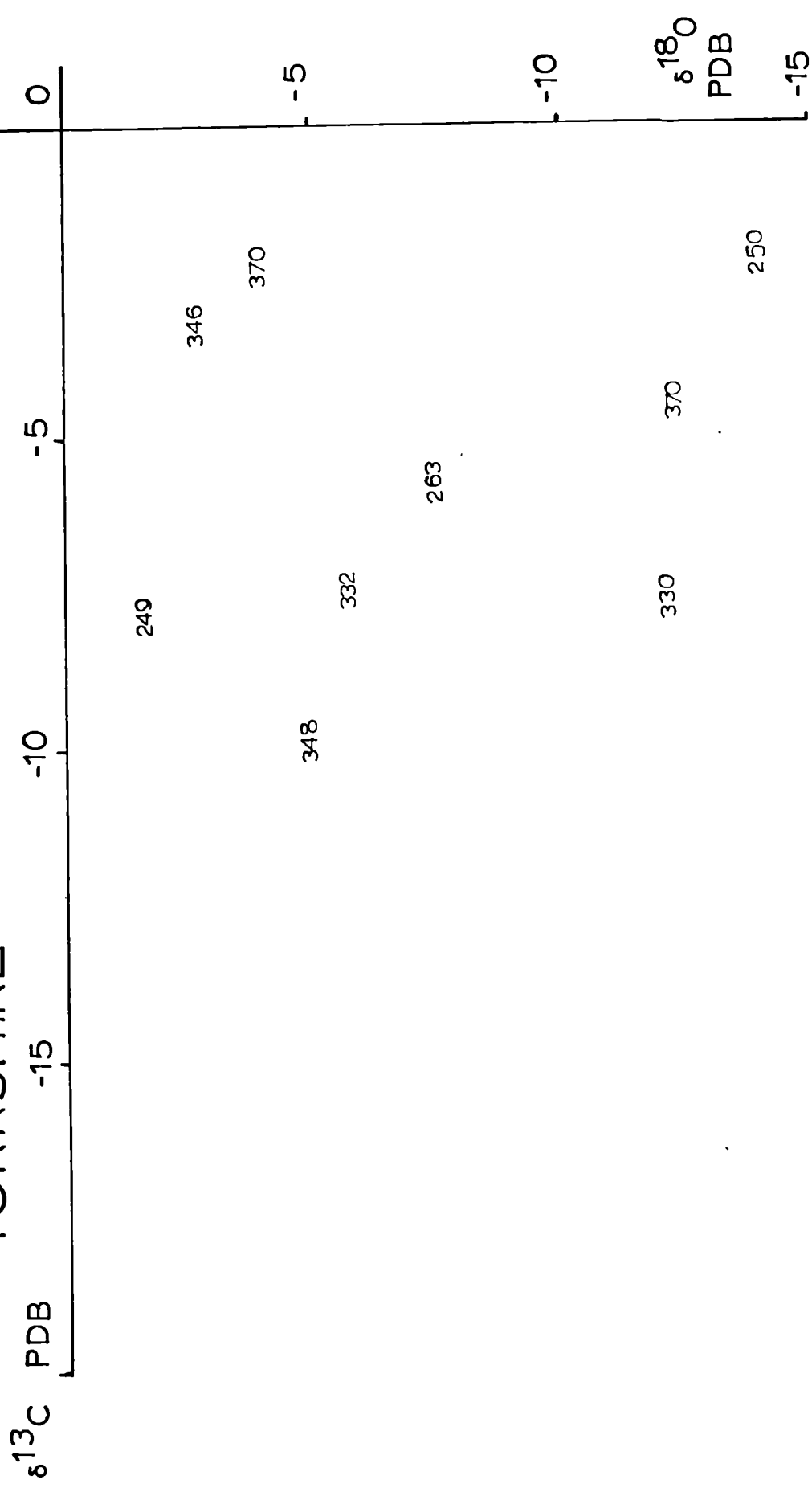


FIG 6.3 COMPARISON OF OXYGEN AND CARBON ISOTOPE VALUES OF RAVENSCAR GROUP RESULTS, WITH PUBLISHED DATA.

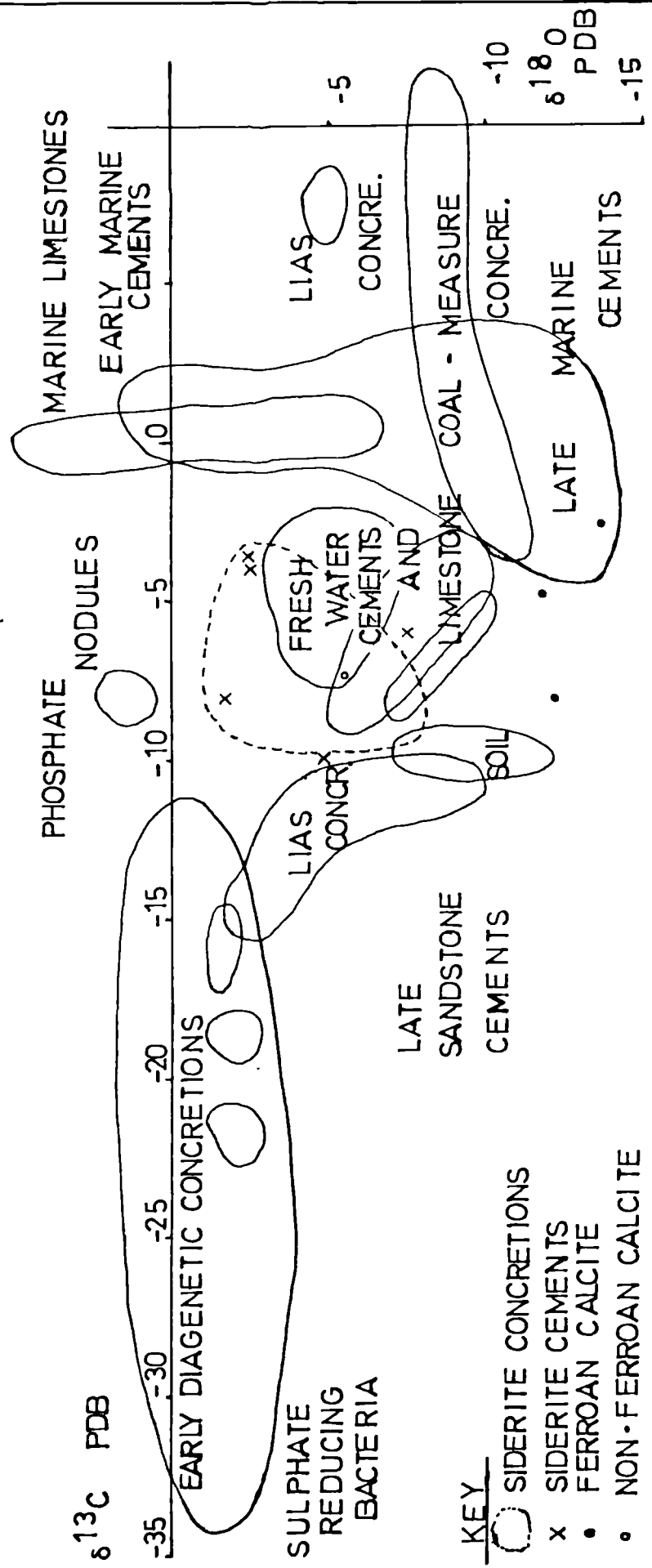


FIG 6.4 COMPARISON OF OXYGEN AND CARBON ISOTOPE VALUES OF BRENT GROUP RESULTS, WITH PUBLISHED DATA.

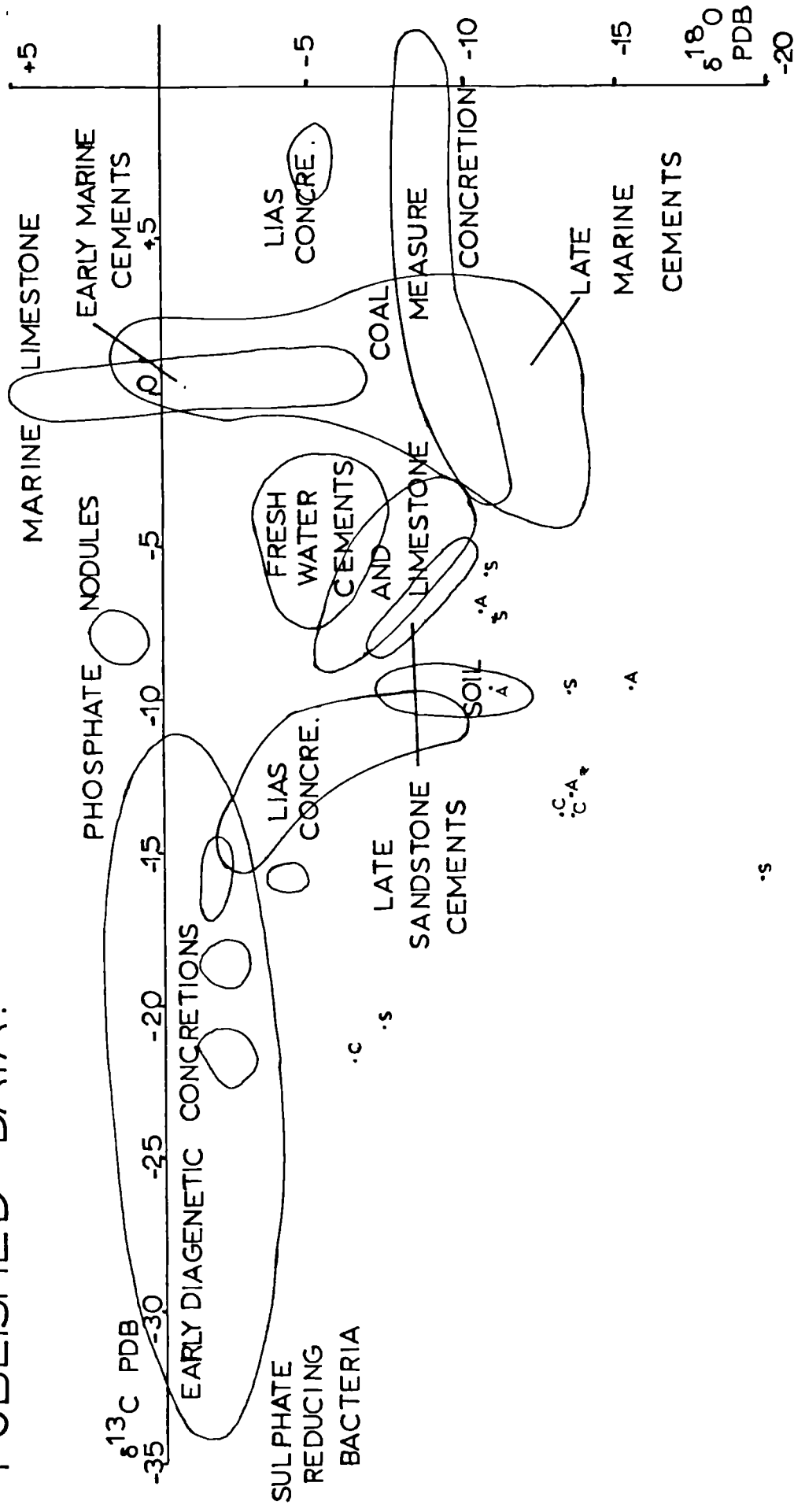


FIG. 6.5 BRENT GROUP  
CARBON AND OXYGEN  
ISOTOPE VALUES.

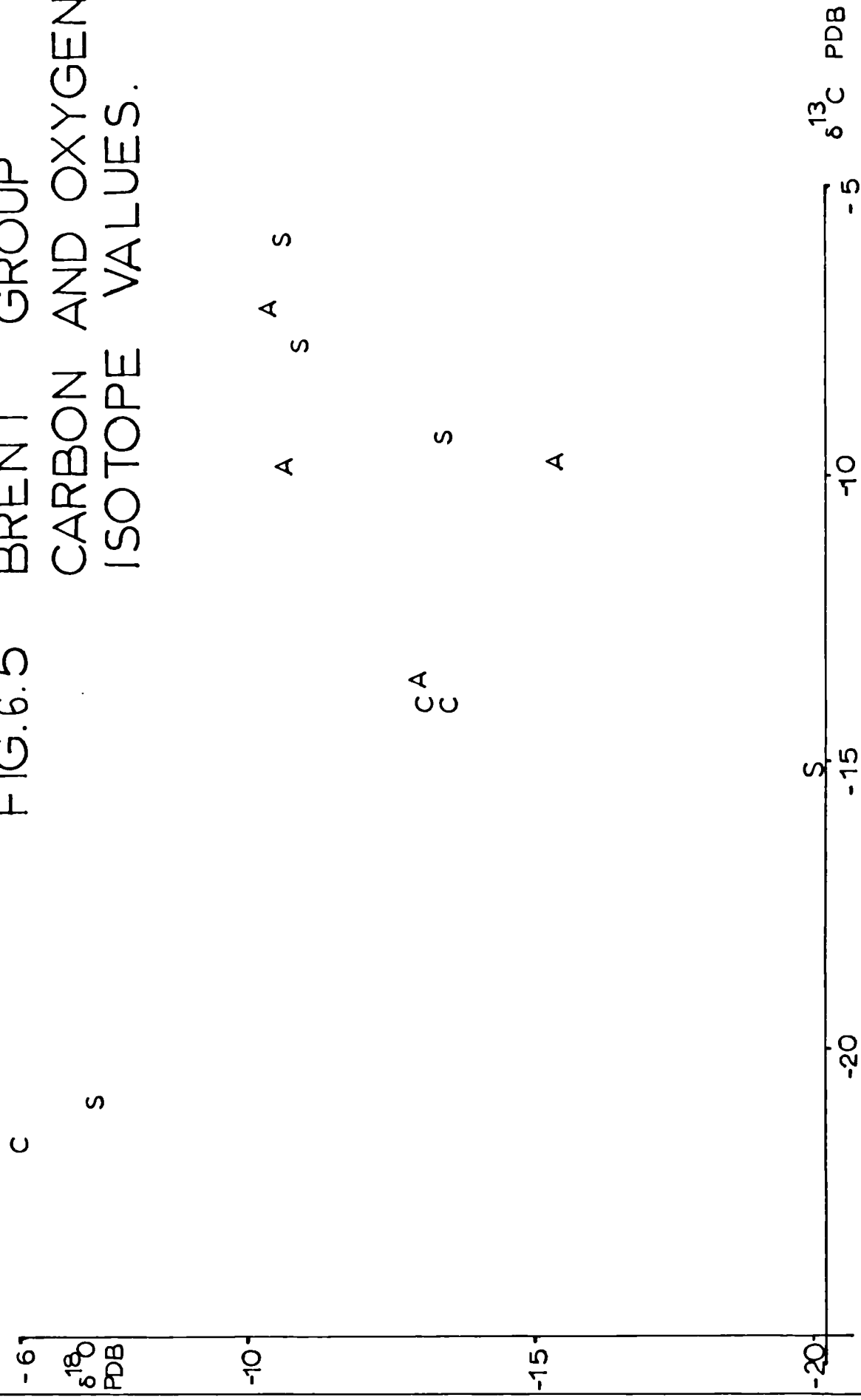


Table 6.1 Corrected results of stable isotope analyses.

<u>Description</u>	<u>Sample number</u>	$\delta^{13}\text{C}$ PDB	$\delta^{18}\text{O}$ PDB
<u>Ravenscar Group</u>			
Siderite spheruliths	10A	-16.1	-4.4
(outcrop No 703)	10B	-16.4	-2.4
Siderite nodules, top	5T	-8.1	-1.2
side	5S	-7.9	-4.3
core	5C	-8.6	-4.8
top	7T	-6.5	-1.8
side	7S	-3.7	-3.6
core	7C	-4.2	-2.1
Small siderite nodules	9A	-6.5	-4.2
	9B	-6.5	-3.6
Siderite concretions, top	1T	-6.1	-5.2
side	1S	-6.6	-2.3
core	1C	-6.0	-3.0
top	2T	-6.2	-3.9
side	2S	-3.8	-1.7
core	2C	-7.4	-6.7
top	3T	-6.6	-2.8
above core	3U	-7.2	-5.6
core	3C	-7.5	-2.7
beside core	3M	-9.6	-8.5
side	3S	-8.5	-8.3
base	3B	-8.9	-6.8
top	4T	-9.0	-0.6
core	4C	-9.1	-2.7
top	6T	-7.6	-4.0
side	6S	-7.0	-4.5
core	6C	-6.7	-4.2
core	8C	-7.5	-3.3
side	8S	-4.3	-3.1
Siderite cement	346	-3.3	-2.8
	348	-10.2	-5.0
Siderite ironstone	249	-8.0	-1.5
	263	-5.8	-7.7
	370	-3.9	-2.4
Non-ferroan calcite	332	-7.6	-5.7
Ferroan calcite	250	-2.4	-13.8
	330	-7.9	-12.2
	370	-4.7	-11.9

Kandites

$\delta^{18}\text{O}$  SMOW  
250°C 100°C  
pre-treatment heating

251	16.3	15.7
314	14.0	15.1
410	16.2	
480	15.1	14.4
502	14.2	

<u>Brent Group, Ninian Field</u>		$\delta^{13}\text{C}$ PDB	$\delta^{18}\text{O}$ PDB
Siderite	3/3-2, 10465	-16.0	-20.4
	3/3-3, 10480	-9.4	-13.9
	3/3-2, 10456	-7.8	-11.3
	3/3-3, 10468	-20.9	-7.6
	3/3-3, 10502	-5.9	-10.9
Calcite	3/3-2, 10388	-14.0	-13.3
	3/3-2, 10438	-14.0	-13.0
	3/3-3, 10468	-21.7	-5.8
Ankerite	3/3-1, 9916	-9.7	-15.2
	3/3-2, 10330	-7.1	-10.3
	3/3-2, 10456	-13.6	-12.9
	3/3-3, 10502	-9.4	-10.5

Table 6.2 Summary chart of reactions related to bacterial processes and the stable isotope ratios of their products.

Zone	Activity	Processes	Mineral reactions	Ideal $\delta^{13}C$ values for pure components
I	Suboxic	Bacterial aerobic oxidation $CH_2O + O_2 \rightarrow H_2CO_3$ Oxygen depletion	Clay exchange reactions	-20 to -30‰
IIIi	Suboxic	Nitrate, Iron and Manganese reduction $CH_2O + 4FeOOH + H_2O \rightarrow 4Fe^{2+} + HCO_3^- + 7OH^-$	Carbonate precipitation	-20 to -30‰
IIIi	Sulphate reducing	Bacterial sulphate reduction $2CH_2O + SO_4^{2-} \rightarrow 2HCO_3^- + HS^- + H^+$	Soil colloid destruction Pyrite and iron free calcite precipitation	-20 to -30‰
III	Fermentation	Bacterial methanogenic fermentation $2CH_2O \rightarrow CH_4 + CO_2$ Phosphate reduction	Amorphous carbonates Clay exchange Ferroan calcite Dolomite, siderite	$\approx +15‰$
IV	Decarboxylation	Abiotic thermal decarboxylation $RCO_2H \rightarrow RH + CO_2$	Siderite      Ferroan dolomite	-20 up to 0‰

Table 6.3    Estimated formation temperatures from a hypothetical  
Jurassic sea water equivalent at depth

Kandites

-from solution  $\delta^{18}\text{O}$  SMOW = -1.2‰

Dickson and Coleman's (1980) modification of Savin and Epstein (1970)

$$1000 \ln a = 2.58 \times 10^6 \times T^{\circ}\text{K}^{-2} - 3.57$$

average value    107°C

Land and Dutton (1978)

$$1000 \ln a = 2.5 \times 10^6 \times T^{\circ}\text{K}^{-2} - 2.87$$

average value    109°C

Ravenscar Group calcites

-from solution  $\delta^{18}\text{O}$  PDB = -1.0‰

Craig (1965)

$$T^{\circ}\text{C} = 16.9 - 4.21(d - w) + 0.14(c - w)^2$$

average value    ferroan calcite    85°C  
                     non-ferroan calcite    40°C

Shackleton and Kennett (1975)

$$T^{\circ}\text{C} = 16.9 - 4.38(c - w) + 0.10(c - w)^2$$

average value    ferroan calcite    81°C  
                     non-ferroan calcite    40°C

North Sea ankerite

(assuming ankerite fractionation similar to dolomite)

Fritz and Smith (1970)

$$T^{\circ}\text{C} = 31.9 - 5.55(d - w) + 0.17(c - w)^2$$

average value    115°C

North Sea calcite

	3/3-3 10468	others
-Shackleton and Kennett (1975)	40°C	89°C
-Craig (1965)	40°C	85°C



Plate 6.1

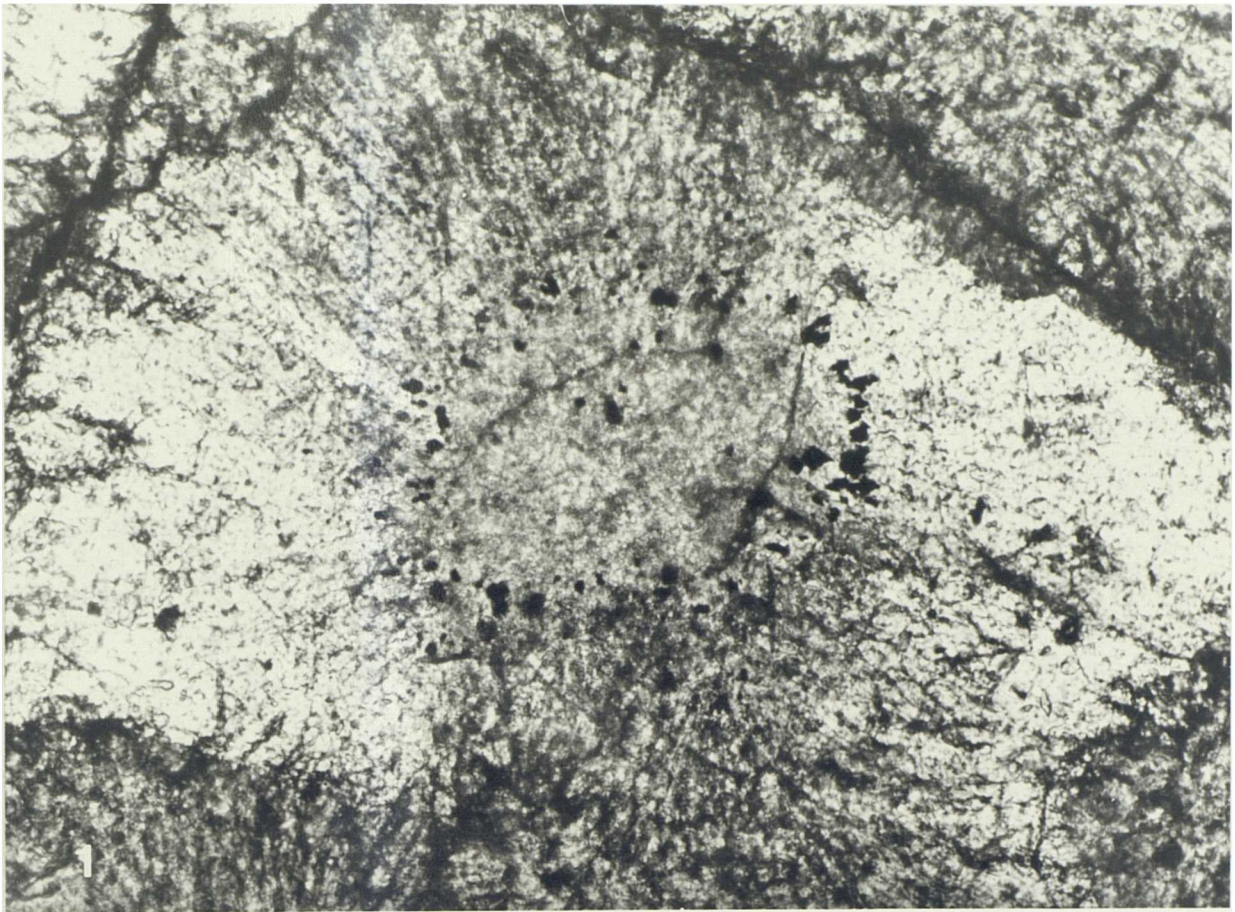
Thin section photograph of a siderite spherulith, 1 mm in diameter comprising a single crystal of sphaerosiderite around a ring of pyrite crystals and an 'amorphous' siderite core.

Plane polarised light, Plate width 1 mm.

Plate 6.2

Siderite concretions in a mudrock sequence, between Crook Ness and Cromer Point, Long Nab Mamber, Note compaction of the laminated muds around the concretion.

Hammer length 30 cm.



CHAPTER SEVEN: THE DIAGENESIS OF CLASTIC SEDIMENTS: CONTROLLING PROCESSES,  
PREDICTIVE MODELS AND GENERAL THESIS CONCLUSIONS.

"In our endeavours to understand reality, we are somewhat like a man trying to understand the mechanism of a closed watch. He sees the face and the moving hands, even hears its ticking, but he has no way of opening the case. If he is ingenious, he may form some picture of the mechanism which could be responsible for all he observes, but he may never be quite sure his picture is the only one which could account for all his observations."

Einstein

The rocks studied in this thesis accumulated as predominantly clastic assemblages in Middle Jurassic fluvio-deltaic complexes in Yorkshire and in the North Sea. Their gross depositional environments are, therefore, similar. The same climate was probably effective throughout the whole area. Furthermore, the differences in their burial histories appear to have had little effect on their burial diagenesis. In broad terms, diagenetic modifications of these sediments are strikingly similar in that the vast majority have undergone acidic diagenesis of their aluminosilicates, experienced siderite and more extensive ferroan calcite cementation, carbonate leaching and blocky kandite precipitation. Most, but by no means all, the differences which occur are eogenetic: they may be related to equilibration of depositional pore waters and the initial sediments. The gross similarities that follow eogenesis suggest that certain processes were effective throughout the North Sea Basin during the burial of these sediments. What was responsible for the local variations seen within each area, and why are there minor variations in the diagenesis of these sediments in response to burial?

In this final section I should like to address myself to the question "What controls diagenesis?" and to expand on the perhaps more specific question "Does the depositional environment control diagenesis?". In order to consider

these questions effectively in view of the results reported and the interpretations made in this thesis, it will be necessary to review and reconsider the controls on diagenesis discussed earlier. Diagenesis is the sum of those processes by which originally sedimentary assemblages attempt to reach equilibrium with their environments. In this extended discourse I intend demonstrating that diagenesis is a multifactorial process: that numerous factors affect and influence diagenesis, but that none of them may be isolated as wholly controlling diagenesis. These factors are illustrated in Fig. 7.1, 7.2 and 7.3.

I should like to point out that this thesis is not intended to be the definitive work on the diagenesis of clastic sediments. It is intended to resolve and refine some of the problems provoked by previous research, and provoke further questions itself. The interpretations made and models erected in this thesis are based broadly on the textural relationships between detrital grains, authigenic minerals and porosity. Some of the ideas presented on the basis of these relationships are novel, others agree with trends established elsewhere. However, alternative explanations may be made and, in the future, refinements will be made, and so I do not propose to offer the answer, but rather, to pose the question

#### WHAT CONTROLS DIAGENESIS?

In his brief review of the prediagenetic conditions which affect diagenesis, Hayes (1979) cites the tectonic setting as a fundamental influence on provenance and depositional environment. These factors in turn influence mineralogical partitioning and, hence, detrital mineralogy. They also influence the texture of the resulting sediments and, consequently, their fluid flow characteristics, that is, their initial porosity and permeability. The resulting sedimentary clastic assemblages are fundamentally unstable when deposited. I should like

to reiterate as discussed in Chapter One that the inherent instability of detrital minerals is a natural function of their source and, hence, their genesis. However, the influence of the climate in both generating detritus and affecting its immediate post depositional diagenesis cannot be overlooked. With this in mind, I should like to restrict my discussion to the factors which influence the diagenesis of sediments rather than the innate mineralogical reasons for it.

### Climate?

I should like to suggest that the climate of the source area and of the depositional basin, that is, the area of weathering, transport and deposition, is of fundamental importance to diagenesis. Indeed, rather than simply being added to the criteria outlined previously, I should like to propose that climatic importance cannot be overemphasised and an understanding of its role in diagenesis is vital, especially in non-marine clastic sediments. Its effects are twofold.

Inorganic effects. Climate determines the weathering processes which operate in the source area. The intensity of these processes affects the initial size and shape of the resulting clastic grains and their chemical stability, degrading progressively more stable minerals, and removing their soluble constituents (Curtis, 1976). In spite of this, the mineralogy of most of the sediments reported in this thesis probably reflects the mineralogy of their source area rather than its climate. The coarse sediments in all the deposits studied are quartz rich and are either subarkoses or quartz arenites. They are also texturally mature. As they contain feldspars, with up to 20% in some samples, it is probable that their maturity does not reflect selective weathering in their source areas. For example, feldspars should not survive intense tropical weathering (Thomas, 1974; Curtis, 1976). It follows that the sources of these



of these sediments were probably acidic plutonics or sedimentary rocks themselves, derived from similar acidic and feldspathic plutonics. Conversely, the sediments which probably do reflect source area weathering are the detrital clays. Throughout the Ravenscar Group and Brent Group these are kandites and micas, typical tropical weathering products.

The effects of tropical weathering in the source area are also inferred during eogenesis in all the non-marine sediments. Tropical fresh water is typically saturated with respect to alumina and silica as the result of reactions throughout the hinterland. It also transports amorphous alumina, silica and iron hydroxides (e.g. Gibbs, 1977). As emphasised previously, these solutions, dissolving amorphous constituents and percolating through overbank sandstones, precipitated extensive quartz overgrowths as well as vermiform kandites. Although in situ reactions may have contributed to this process, consideration of mass balances within the system dictates that some of the material had an external source. In the Ravenscar Group the relationship between the thick mudrock sequences from which suitable waters may have been expelled and tightly cemented overbank sandstones is more obvious than in the cores from the Brent Group where it must be inferred.

Two other features which I should like to relate to the tropical climate's inorganic effects are the abundant iron incorporated into siderite cements, and the presence of berthierine oololiths. There are no in situ sources of iron in these sediments. Nonetheless, it comprises up to 12% of the rocks siderite cements, and 40% of the spherulith horizons. The most likely source of iron is lateritic weathering throughout the drainage basin, which concentrates iron rather than other elements present, establishing iron pans, ferruginous horizons and iron coated clay micelles, all of which could have been eroded and subsequently deposited on the floodplains. Further evidence for a tropical weathering origin of iron is given by Gibbs (1977) who reports that 6-7% of

the material presently transported by the Amazon and Yukon Rivers is iron and that some 90% of this is transported as solid particles or as grain coatings. Gibbs (1977) considers that the most likely origin of both the iron-coated clay particles, and the iron particles is (lateritic) weathering in the source area. Berthierine oolites may be derived from lateritic weathering profiles (Nahon et al., 1980). Nevertheless, berthierine generally occurs in the tropics only, further evidence of the effect of climate on eogenesis (Odin and Matter, 1981).

Climatic effects influence weathering processes directly and depositional and source area ground waters indirectly. The more direct effects were those implied above due to the temperature, and type, rate and frequency of precipitation. In addition, indirect effects were equally significant, and perhaps more so in the depositional basin. In the prevailing climatic conditions, floras flourished. Although significant geomorphologically, at the time the floral contribution to soils of stabilising local sediments and of physical weathering by rootlets is almost insignificant diagenetically. What is relevant is the amount of organic matter contributed to the sediments by plants.

Organic effects. Where no organic matter accumulates, diagenetic reactions at the surface are affected directly by the climate, whilst below the surface ground water chemistry is influenced predominantly by diagenetic reactions. This is the case in red beds where iron is oxidised at the surface to haematite and, as detrital grains dissolve, basic cations are released into solution, raising pH.

Where organic matter accumulates, atmospheric conditions affect only superficial sediments, or those above the water table. In these sediments no ferric iron phases exist. It follows that an anoxic water table probably extended to the surface on floodplains except where a continual flow of water removed

ferric iron. The unstable nature of clastic sediments is enhanced, even before significant burial, by the reaction products of the least stable constituents (Curtis, 1980). One of these processes, bacterial degradation of organic matter, commences immediately following deposition. This takes place in two stages: at or near the earth's surface, aerobic bacteria operate, removing free oxygen from the system. Subsequently, anaerobic bacteria reduce ferric oxides, sulphates, nitrates, and phosphates. Then bacterial methanogenic fermentation degrades the remaining debris. With the exception of ferric iron reduction, these reactions all tend to lower pH, whilst the anaerobic processes tend to lower Eh also. As a result, both the chemistry and composition of ground water reflects equilibration of sediments and pore waters. Black mudrocks are the extreme consequence of these processes in fine-grained sediments, especially where a significant proportion of the rock is extant organic matter.

In mineralogically mature clastic sediments, effects such as these which influence colour, through the precipitation of a variety of possible iron compounds, may be preserved at depth. The climate may, therefore, fingerprint diagenetically immature sediments. As a result of this, the likely depositional climate of Carboniferous (Hawkins, 1978; Besly, 1980), Rotliegendes (Glennie et al, 1978), and Triassic sediments (Burley, pers. comm. 1982) may be inferred.

I should like to argue that eogenesis in most of the clastic sediments studied in this thesis was strongly influenced by the climate in which they accumulated, that is, the tropics. I should like, however, to emphasise the influence of several other factors on the composition and arrangement of these sediments. In the Jurassic, the tropical lowlands of north-west Europe drained a hinterland of predominantly acidic plutonics or perhaps arkosic sedimentary rocks. Both source area mineralogy and weathering affected eventual detrital mineralogies. Transportational and, moreover, depositional processes controlled both the



gross and local texture of the resulting sediments, i.e. alluvial sediments comprising tubes of mature channel sandstones, and sheets of texturally less mature overbank sandstones all encased in floodplain mudrocks; sheets of shallow-marine sandstones from high-energy environments, and occasional pockets of interdistributary bay-filling mudrocks.

For the non-marine clastic sediments, climate influenced the supply of both water and organic matter to the sediment, the former influencing the water table position and, conversely, the effects of aerobic organic and inorganic processes. Marine reworking of coarser clastics may have diminished indirect climatic influence locally by removing some organic matter. However, abundant organic matter - a consequence of the tropical climate - occurs throughout the majority of these sediments.

Diagenesis of the majority of these Middle Jurassic non-marine sediments, therefore, reflects both the direct and indirect influence of the tropical climate. Alumina, silica and iron hydroxides may all have been derived from depositional pore waters. In addition, bacterial degradation of organic matter reduced pH and, consequently, catalysed the in situ reaction of detrital aluminosilicates. These may also have released alumina and silica into solution. Feldspar dissolution and muscovite neomorphism to kaolinites are the most significant direct consequences of lowering pH. As a result, quartz overgrowths and vermicular kaolinites precipitated from alumina and silica probably both in solution, and released by dissolution. Where aluminosilicate diagenesis finished before anaerobic bacterial processes commenced, siderite followed. This is the case in the Brent Group and throughout most of the Ravenscar Group. The significance of climate/organic matter as an influence on diagenesis is exemplified by the wide ranging occurrence of these effects. Elsewhere in the Ravenscar Group, however, anoxic conditions occurred closer to the sediment surface and chlorite rather than kaolinites precipitated. The

aluminosilicates in solution and organic matter present throughout the sediments, which reduces Eh, may be related directly to the climate. However, the varying temporal relationship between aluminosilicate diagenesis Eh and pH cannot be so related.

The multifactorial nature of diagenesis here is further exemplified by the final response of diagenesis to climate, that is, extensive freshwater siderite cements. The source area's climate was responsible for the abundant iron in the sediments. In addition, the climate of the depositional basin was responsible for the presence and perhaps the preservation of organic matter. Preservation is also a function of the burial rate with greater potential in areas with initially fast burial. Following deposition, organic matter decayed and affected pore-fluid Eh and pH. Subsequently, during burial and anaerobic bacterial processes, ferric iron was reduced and pH increased as bicarbonate ions were liberated. This led to pore-fluid saturation with respect to siderite and resulted in its precipitation.

In all the marine sediments, initial cements probably precipitated directly from solution. Later, as burial or lithification sealed pore fluids from the overlying sea water, they began to evolve. This resulted in bacterial processes lowering pH and then Eh. Following the formation of authigenic illite and potassium-feldspar overgrowths, the same effects of eogenesis in the non-marine clastics also occur in marine sediments. Here, too, they resulted from bacterial degradation of organic matter, either in situ or in the water table of the overlying alluvial plains.

The importance of climate as an influence on diagenesis cannot be overemphasised. Moreover, it often predominates over other influences such as the depositional environment. For example, one finds authigenic haematite in red beds, in alluvial (Walker et al, 1978), aeolian (Glennie et al, 1978) and both ancient

(McBride, 1974) and modern deltaic sediments (Johnson, 1982). Nonetheless, not all eogenetic processes or modifications can be explained in terms of the prevalent hot and wet conditions during deposition. An analogous situation has been described by Besly (1980), who describes haematite from inferred locally aerated Carboniferous alluvium whilst more typical sediments are cemented with siderite (e.g. Hawkins, 1978). In the following sections, the effects on diagenesis of other factors will be examined.

#### Depositional environment?

It is not clear from the literature whether authors referring to the depositional environment mean the macroenvironment, in this case a fluvio-deltaic complex, or the microenvironment, that is, the interstitial pore fluids surrounding individual grains. Despite this uncertainty, there is some degree of overlap. After all, depositional pore fluids are either fresh water in non-marine environments, or sea water in marine ones. In spite of this, further complications arise when one considers that weathering processes throughout a drainage basin affect fresh water composition, whereas sea water in enclosed basins becomes either concentrated with net-water loss through evaporation, or diluted with a continual influx of fresh water. Unfortunately, one major area of uncertainty remains, and that is that the chemistry and composition of depositional pore fluids in transitional environments between the land and the sea is extremely variable.

The effects of the environment are not solely chemical, as depositional processes control the sorting and hence the texture, shape and distribution of grain sizes within deposits. Moreover, here the distribution of sandbodies controlled the movement of formation waters during later burial and, consequently, the distribution of mesogenetic modifications of the surviving sediments, and eogenetic phases.

In this section I shall argue that the depositional environment influenced and affected diagenesis in a number of ways. It did not "control" diagenesis, however, because of the multifactorial nature of the whole process. Moreover, whilst some aspects of eogenesis affected the sediments during their continued burial, these are only preserved because of these sediments' inherent stability.

Sandbody texture and distribution. These fluvio-deltaic sediments were deposited in a plethora of subenvironments of either marine or non-marine affinity. To assess the importance of the "macroenvironment", the concept of a fluvio-deltaic complex should be discarded, and, instead, the depositional environment of individual sandbodies considered. Wholly non-marine sediments can be grouped into channel-filling sandstones - tubes of coarser sediment - meandering through occasional sheets of crevasse-splay or sheetflood sandstones - finer and often less mature than the channels - and thick sequences of floodplain mudrocks which enclose all the sandbodies.

Wholly marine sediments generally occur as sheets, those in the Brent Group being stacked on one another, whilst those in the Ravenscar Group are generally associated with, and enclosed by, mudrocks. These differences are a function of the overall depositional regime. Thus, Brent Group sediments reflect their relatively higher energy environment, whilst the tidally- and fluviably-dominated sediments in the Ravenscar Group accumulated under calmer conditions.

The relationship between sandbodies is more complicated at the interface between the land and the sea. Beach sediments occur in the Ravenscar and in the Brent Group. They accumulated as diachronous sheets between further wholly marine sheet sands and heterogeneous non-marine sediments. Interdistributary bay-filling sequences, however, comprise pockets of mudrocks which are replaced upwards by progressively coarser sediments, culminating in sands.

As outlined above, and in the relevant sections of each chapter, there are marked differences between eogenetic modifications of the non-marine overbank and channel-filling sandstones. These differences are a function of their differing depositional textures. Essentially, the finer and less mature overbank sandstones were tightly cemented by quartz except where overgrowths were inhibited by matrix clay. Supermature and coarser channel sandstones, conversely, were equally rigidly cemented, but connected intergranular porosity remains. The effects of local textural variations in (mineralogically) immature clastic sediments are also reported by Hawkins (1978) and Nagtegaal (1979) who both record diagenetic inhibition in texturally immature areas of sediments.

I should like to emphasise the extremely small scale at which sediment texture affected diagenesis. Those crevasse-splay sandstones, which are relatively well sorted and "clean", that is, texturally more mature, contain quartz overgrowths. Overbank sandstones which contain quantities of matrix clay do not. These distinctions do not necessarily apply only to different sandbodies. In both the Ravenscar Group and the Brent Group these differences may be seen in graded laminations perhaps a centimetre thick. Hence, the medium-grained sand at the base is quartz overgrowth cemented, whilst matrix clay filling pore space at the top inhibited overgrowths. The scale of this inhibition is such that overgrowths may occur on one end of a grain in an open pore, but not the other.

In the Ravenscar Group, the fine-grained alluvium accumulating on the floodplain was, presumably, relatively impermeable, and, in view of the inferred frequency of flooding, poorly drained. The depositional environment, consequently, affected the threefold eogenetic model proposed here for these non-marine sediments. On the floodplain itself, stagnation of the standing water allowed the development of soil horizons, comprising siderite spheruliths. Where drainage was improved, quartz overgrowths and vermiform kandites precipitated.

Similarly, where pore fluids were sealed from the aerated pore waters above and became anoxic, chlorite rather than kandites precipitated.

Pore-water chemistry. The response of diagenesis to depositional environment reflects both the physical distribution of sediments and the chemistry of depositional pore fluids. In general, in oxygenated non-marine sediments, kandites and quartz overgrowths precipitated, whilst in the marine ones, illites and potassium-feldspar overgrowths were precipitated. Although these events were in a sense controlled by the depositional environment, the conditions under which they formed were only effective until pore waters were sealed from the effects of the overlying waters. Subsequently, equilibration of pore water and sediments effected diagenetic modifications. Unfortunately, these simplistic models are complicated in places, for example, whilst marine sediments from the Ravenscar Group and the Ninian Field contain authigenic illite, those from 210/15-2 do not: an additional factor must exert some influence here.. Secondly, almost all the marine sediments examined contained kandites, quartz overgrowths and minor traces of siderite prior to ferroan calcite cementation. In the Ravenscar Group the calcite is occasionally succeeded and replaced by rhombic siderite cements, which were precipitated from fresh water.. In the Brent Group, however, it is not clear whether this paragenetic sequence had a similar origin, that is, in situ pore-fluid evolution during bacterial degradation of organic matter, or whether it resulted from fresh water flushing through the sediments prior to widespread mesogenetic ferroan calcite cementation. In both the Ninian Field, and 210/15-2, the choice must be based on inference and the need to select a simplistic model, one that does not require too many changes of pore-fluid composition. This problem is mentioned here because of the possible significance of the gross environmental setting: marine Brent Group sediments accumulated beneath a prograding delta. They may all, therefore, have been flushed by fresh ground water as the system evolved.

A similar mechanism of freshwater flushing by the "head" or "drive" of the water table has been proposed elsewhere, but on a larger scale by Bjørlykke et al (1979). Whilst here this model probably applies to the lower formations of the Brent Group as the upper formations prograded over them, Bjørlykke et al (1979) ignore possible facies variations within the Brent Group and the underlying Statfjord Formation in the Statfjord Field, and proposed that fresh water flushed through the whole system. All the results reported by Bjørlykke et al (1979) are similar to those reported in this thesis from the Ninian Field. Also, with the exception of ankerite, they are similar to those from the Ravenscar Group. Nevertheless, none of the interpretations made by Bjørlykke et al (1979) agree with those made in this thesis.

Sandbody geometry. The influence on diagenesis of the physical distribution of sediments in any accumulation is significant not only during eogenesis. In these sediments, sandbodies acted as conduits for solutions during burial. The effects of changing pore-fluid compositions are demonstrable throughout all but the least mature marine sandstones. This is not true, however, of non-marine sandstones. Most of the overbank sandstones are tightly cemented with quartz overgrowths and unaffected by later events. Moreover, some channel sandstones remain tightly cemented with calcite or siderite. These differences appear to be a function of sandbody geometry.

During their deposition, marine sands accumulated as mature sheets which were succeeded by further sheets as the environment changed. The resulting sandbodies are intimately connected in three dimensions and, consequently, their porosity is also interconnected. During the accumulation of sediments from the highly sinuous fluvial systems channel-filling sandstones were either stacked on one another (e.g Whitby West Cliff, Yorkshire, or 10323-10397' in 3/3-3, Ninian Field), or they are isolated. Overbank sandstones, alternatively, although sheet-like, are texturally less mature, isolated, laterally impersistent

and enveloped in mudrocks. In view of their connectivity, channel sandstones may have acted as pore-fluid conduits during burial, overbank sandstones, conversely, did not. Mesogenetic formation waters and aggressive fluids did not pass through the latter, although they did affect both the former and most of the marine sandbodies. Depositional sandbody geometry has, therefore, played a significant role throughout diagenesis.

#### Sediment composition?

In general, the composition of these sediments has affected their diagenesis in three ways. Firstly, by the dissolution and the reaction of relatively unstable constituents affecting pore-water chemistry and composition. Secondly, by grains acting as nuclei for precipitation. Thirdly, by determining how stable the originally sedimentary assemblage was during burial.

Dissolution of sedimentary constituents. In these rocks the only remnants of the original assemblage are modified grains, flakes and plates of mica and clay minerals respectively, and occasional plant debris. Nevertheless, it is likely that the original sediments, especially the finer grained ones, contained considerable quantities of amorphous material, such as soil colloids and plant debris which was subsequently degraded. Although the visible results are associated with detrital grains, these amorphous constituents are likely to have had a most significant effect on diagenesis, especially during the first few metres of burial. They were probably the least stable constituents of the original sediment. Consequently, they will have begun to dissolve immediately following deposition, affecting pore-fluid composition, and, in the case of organic debris, pore-fluid chemistry. The effects of degradation of organic matter have been amplified throughout the thesis. These were probably most effective immediately following burial. However, the breakdown products of organic matter continued to influence diagenesis in all the samples studied



throughout their burial. In all the sediments, depositional pore waters were either fresh (dilute and neutral) or marine (mildly saline and mildly alkaline). Subsequently, they became acidic as organic matter was degraded. Later, also, as anaerobic processes commenced, Eh was lowered and pH rose again. It has been suggested throughout this thesis that these processes were probably effective close to the surface, especially on the alluvial plains where the net rate of sediment accumulation appears to have been low. As a result, their effects will have been most significant in promoting, catalysing, and even effecting diagenetic reactions immediately following deposition. In this sense, vermiform kandites, muscovite neomorphism, feldspar dissolution, siderite and pyrite precipitation are influenced by the composition of the original sediment. Nevertheless, they are not "controlled" by the sediments' composition, because this is a function of the source rock mineralogy, climate, and depositional environment also.

In both the Brent and the Ravenscar Group, quartz overgrowths and other less quantitatively significant phases are interpreted as predating freshwater siderite cementation. In all these sediments there are no obvious sources at this stage of either the abundant silica precipitated as quartz overgrowths or the iron incorporated into siderite cements. Nonetheless, amorphous silica and iron hydroxides were probably present in the original sediments. Moreover, in view of their inferred amorphous state, they will have been more readily dissolved and hence available for precipitation than, for example, solid components involved in reactions elsewhere. Whilst they influence diagenesis significantly, the presence or absence of amorphous and similar fine-grained constituents is itself a function of depositional environment and source area weathering, further support for the multifactorial nature of diagenesis.

Amorphous material is inferred to influence diagenesis immediately following deposition. The effects which may be related to processes involving organic

matter are demonstrable during eogenesis also. In addition, however, organic matter affects diagenesis until it is destroyed. Continuing maturation of organic matter influenced all the sediments studied here because carbonate cementation is followed by dissolution and blocky kandite precipitation: it is unlikely that this results from the action of aggressive fluids. To recap, aggressive fluids are generated during bacterial methanogenic fermentation when the resulting bicarbonates are not fixed into carbonate phases. In the Ravenscar Group this is significant diagenetically because blocky kandites are the most abundant authigenic phases in some samples, as well as occupying secondary porosity. It is also important economically in the Ninian Field where the generation of extensive cement dissolution porosity has created an effective hydrocarbon reservoir. Whilst it is possible that the aggressive fluids active in both Brent and Ravenscar Group sandbodies were generated in their surrounding muds, the hydrocarbons which now occupy the Brent Group were most probably not. Their effect on diagenesis is, therefore, discussed below.

Nucleation on detrital grains. The effects of amorphous and organic constituents described above may have profoundly modified these sediments. More immediately obvious, however, is the influence of detrital grains on diagenesis. The coarser sediments studied in this thesis are quartz rich with small quantities of feldspars and micas. The finer ones are dominated by detrital kandites and micas. The influence of detrital grains is exemplified in the Ravenscar Group. Here quartz overgrowths occur on quartz grains in marine and non-marine sediments. Calcite, conversely, occurs as a relatively late phase in all the marine clastic sediments, whilst it is the first in the Millepore Bed. I should like to suggest that the presence or absence of nuclei determines whether saturated rather than supersaturated phases in the original pore waters were precipitated here. Hence, whilst depositional pore waters in the marine clastic sediments may have been saturated with respect to

calcite, it did not precipitate. Precipitation was prohibited until later during eogenesis when bacterial processes increased bicarbonate concentration. Conversely, the Millepore Bed contains carbonate ooliths cemented with an isopachous rim of calcite. Here the ooliths acted as nuclei for precipitation. Similarly, detrital quartz grains acted as nuclei for overgrowths. It follows that the solutions need only have been saturated, but not supersaturated with respect to quartz.

Detrital minerals also influenced diagenesis by their dissolution and neomorphism. Hence, in these sediments, potassium, alumina and silica were released into solution by feldspar dissolution, and potassium also during muscovite neomorphism. In spite of this, there is little evidence to suggest that elements derived from in situ dissolution have played a significant role in the diagenesis of any of these sediments. The major eogenetic phases, kandites, quartz overgrowths and siderite, in non-marine, and illite and potassium-feldspar overgrowths in marine sediments can almost all be derived from amorphous constituents and pore fluids. Similarly, later phases, such as calcite and blocky kandites, probably precipitated from solution, although kandites may have incorporated some alumina and silica from in situ dissolution of feldspar grains. This general conclusion is in marked contrast to the model suggested by Walker et al (1978) who appear to derive all their authigenic constituents from in situ reactions.

I should like to digress briefly and, in this section, consider the relationship between kandites and feldspars. Both minerals occur in almost all the sediments. Furthermore, feldspar dissolution is common and so one cannot exclude the possibility that alumina and silica derived from the latter has been precipitated in kandites. Nevertheless, even allowing for complete removal of some hypothetical feldspar grains, the quantities of kandites present exceed the amount that could be generated by in situ dissolution. Whilst Rossel (1982) reports

that the quantities of the two minerals present in the Rotliegende of the Southern North Sea are inversely proportional and infers a genetic relationship, other authors appear to be indoctrinated with the notion that "kaolinite replaces feldspars". Nevertheless, in these sediments, vermiform kandites occur within limestones in the Millepore Bed. Secondly, the quantities of the respective minerals (Moor Grit: no feldspar, 2-5% kandites; Saltwick Formation: 2-5% and 15%; and 210/15-2 both exceed 10% in some samples) do not suggest that kandites develop at the expense of feldspar. Indeed, the most abundant kandites occur where feldspars are also most abundant. Moreover, the samples from 210/15-2 contain the only apparent kandite replacement of feldspars.

Framework stability. Diagenesis is the sum of those processes by which an originally sedimentary assemblage attempts to reach and maintain an equilibrium with its environment. It is in this context that the significance of this working definition of diagenesis will be amplified. The assemblage in question during diagenesis is only the original sediment for a short while. After eogenetic modification, the evolving assemblage contains a variety of diagenetic phases whilst some of the unstable components of the original assemblage may have been removed.

These sediments were all quartz rich and, consequently, generally stable. Where they are cemented with eogenetic quartz overgrowths they now have a rigid quartzose framework propping open up to 30% intergranular porosity. Their quartz cementation itself reflects partially their detrital mineralogy: quartz overgrowths rather than other phases forming preferentially on quartz grains. Later, during their burial, these sediments have been exposed to elevated temperatures and pressures (approximately 100°C and 3 km of overburden presently in the Ninian Field; 2 km in 210/15-2; and 100°C and perhaps 2 km previously in Yorkshire). Nevertheless, apart from minor suturing in

the coarsest channel sandstones in the Ninian Field, and occasionally in Yorkshire, the framework established during eogenesis in all these sediments does not appear to have been modified either physically or chemically during burial. It follows that overburden pressures have not been sufficient to effect grain-to-grain dissolution or further mechanical compaction. Similarly, changes in pore-fluid composition as well as precipitation of replacive cements have not affected the framework significantly. It appears, therefore, that quartz overgrowth cementation of these quartzose sandstones created a metastable framework. Thus, during burial, no environments were encountered in which the framework was unstable.

In a sense, these sediments have reached an equilibrium with their environments although this is by no means a thermodynamic equilibrium (s.s.). Nonetheless, it has important implications. The significance of cementation of this type is that even if subsequently carbonate cemented, leaching may recreate the intergranular pore system. The rigid framework houses an effective porosity network - a labyrinth of hydraulic pipes - which is only destroyed by extreme physical or chemical compaction, or the precipitation of stable pore-filling phases such as clays. In conclusion, therefore, quartz overgrowth cementation of these originally quartz rich deposits created assemblages which subsequently maintained a metastable equilibrium with their changing environments during burial.

By contrast, less stable detrital assemblages, such as those studied by Galloway (1974, 1979) or by Walker et al (1978) subsequently become greywackes. All their unstable components break down into clays, carbonates and zeolites. Then, as temperatures and pressures increase during burial, these assemblages, stable at the earth's surface, become unstable and react to form further diagenetic "facies" assemblages. Unless extensive phases, such as calcretes or evaporites, were precipitated under the influence of the depositional

environment; in this type of sediment only the original composition is of any consequence.

There is, therefore, a marked difference in the behaviour of stable and unstable detrital assemblages during burial. The composition of the original assemblage is extremely important. It affects the type and distribution of initial cements and, consequently, the stability of the resulting assemblage during burial. The influence of the depositional environment on diagenesis is affected by these various possible variations in assemblage stability. In the Middle Jurassic sediments studied here, the effects of eogenesis are still visible in most samples. Similarly, the rocks retain a significant amount of either intergranular or minus-cement porosity. The consequence of the detrital framework's stability in these coarser sediments is, therefore, that at depth they still resemble the original deposits and unless permanently cemented up, they have acted as conduits for pore fluids during burial. By contrast, Galloway's (1974) greywackes bear no resemblance to the original sediments and have no porosity.

Almost all the effects discussed above are most effective in the eogenetic realm. Their influences are most profound if the sediments are not rapidly buried. Moreover, their overall result is to prepare an assemblage which may or may not survive burial. In the burial realm the minor variations operating previously become less significant as processes are effective on all the available sediments.

#### Burial?

The final factors which have been identified in this thesis as influencing diagenesis operate during burial. Burial, in this sense, is the realm of mesogenesis - the realm in which the chemistry of pore fluids is unaffected

by surface agents. In this section I should like to mention briefly the effects of changing pore-fluid composition, formation water migration, burial temperatures and pressures, and hydrocarbons. Here the limitations of studying small intervals in isolation may become apparent. Whilst most of the effects discussed earlier may be related to the original deposits and their setting, factors which influence diagenesis during burial may originate elsewhere within the sedimentary basin in which they accumulated. In this sense, the complete geological evolution of the North Sea Basin from its inception to the present day must be considered, as it may have contributed to various aspects of the diagenesis of these sediments. I should stress once again, that almost all the samples examined were subjected to most, if not all, of the influences below.

Changing pore-water composition. Following eogenetic modifications to non-marine sediments, pore waters changed and ferroan calcite cementation took place. Although the ferroan calcite in the Millepore Bed appears to be an early phase, the remainder in both Yorkshire and in the North Sea may be a later introduction into the system. This calcite could be the apparent "carbonate curtain" (Schmidt and McDonald 1979a) through which most sediments pass before both calcite solubility increases (Curtis, pers. comm. 1982) and aggressive fluids are generated. Where this cement remains, diagenesis has effectively, been completed. Elsewhere, carbonate cements have been removed, but their replacive effects on the remaining framework are most marked, causing enlarged intergranular pore space and more significantly, pore throats. In general, the volume of cement that may be derived from one pore volume of solution is insignificant compared to the size of most pores. Consequently, changing pore fluids were most important in supplying, as well as producing, calcite cements in all these sandstones.

In addition, this illustrates the significance of basinal studies; calcium

is not available in situ in these non-marine sediments and must have been derived from elsewhere. The origin of the calcium bearing solutions is not immediately obvious, but down dip marine connate water is a possibility, either in older sediments deeper in the basin, or in *contemporaneously* deposited ones. In the marine sediments, ferroan calcite may have precipitated from the original depositional pore fluids. This illustrates the diversity of diagenetic processes, the same mineral being produced for different reasons.

Later, during burial, pore-fluid composition changed again, from bicarbonate saturated waters in equilibrium with these cements, to acidic aggressive fluids. This resulted in dissolution of the cements and the recreation of the porosity they filled. It also precipitated blocky kandites (dickite) in the majority of samples analysed. Again, whilst changing pore fluids were responsible for these modifications, where did they come from? Aggressive fluids are generated when bacterial methanogenic fermentation coincides with illitisation of smectites in mudrocks. The potential sources of these fluids are diverse. They may have come from either marine or non-marine Middle Jurassic mudrocks enclosing the respective deposits. Alternatively, widely quoted source rocks, such as Liassic, Kimmeridgian, or even Carboniferous mudrocks are possible sources in the North Sea Basin. As the organic matter in the Ninian and Yorkshire sandbodies is marginally mature, these muds are likely to have passed through at least one phase of smectite illitisation. Hence, they cannot be excluded as possible sources of these fluids.

The importance of a complete understanding of a basin's evolution has been stressed in this section. In the North Sea Basin, Middle Jurassic sediments in all the study areas were partially exhumed in the Cretaceous and possibly exposed to fresh water or perhaps to sea water. This has led various authors to suggest that fresh water was responsible for the leaching seen in the North Sea Basin (e.g. Hancock and Taylor 1978; Sommer, 1978). Nonetheless, Curtis,



(in press) believes that fresh water is probably not capable of producing these effects, typified by carbonate leaching and kandite precipitation. He favours the evolution of pore water from reactions in mudrocks during their burial diagenesis. Although the significance of the correlation between kandite precipitation and secondary porosity development has only recently been realised in terms of burial processes, the occurrence of secondary porosity in sandstones is neither a new concept nor a new discovery. For example, Evans (1864, p. 159) states that

"... the cavities have probably been caused sometimes by uplift and sometimes by erosion and dissolving action of water."

In general, the Kimmeridgian is the only one of the sources quoted above to have undergone complete hydrocarbon maturation. Also, only under these conditions is the second phase of smectite illitisation likely to have occurred (Boles and Franks, 1979a). It follows that this source, rather than the enclosing muds, must have produced at least the second phase of fluids which affected the Ninian Field, altering calcite to ankerite and, moreover, supplied the oil which is now found there. A cautionary note must be added here, because hydrocarbon maturation is not necessarily synonymous with the second phase of smectite illitisation. Organic matter in the muds enclosing and occurring below the Ravenscar Group is mature, but no alteration of calcite to ankerite was observed here, although ankerite occurs below in the Liassic (Hallam, 1967). Similarly, oil has passed through 210/15-2, but no chlorite replacement of kandites or ankerite replacement of calcite was observed.

The final changes of pore fluids appear to have been effective to the present. In 210/15-2 there are no further diagenetic modifications, and no further changes need to be inferred. In Yorkshire, only traces of illitisation occurred after the formation of blocky kandites, although surface weathering has affected some samples. Lastly, in the Ninian Field also, some blocky kandites are

slightly illitised and the remaining pore fluids are effectively dilute sea water. Both here and in Yorkshire solutions of this kind may have been responsible for the minor amount of illitisation present.

Temperature and pressure. These appear to have had little effect on the major sandbodies. The effects of overburden pressures are most obvious in the mudrock sequences in each area, where porosity has been reduced to zero and laminae have been compacted around concretions. XRD analysis suggests that any smectite originally present in the muds enclosing the sediments has since been almost completely illitised. This too is a response to pressure and temperature and is in fact one of the few mineralogical phase changes that can be related solely to burial.

All the rigidly cemented sandbodies except coarse channel sandstones in the Ninian Field, and in the Moor Grit and beach sediments in the Dogger Formation in Yorkshire, have been virtually unaffected by burial. It is likely, therefore, that because of their relatively poor cementation these coarse sands were more susceptible to grain-to-grain dissolution than the others. Whether this was a purely physical process is debatable. After all, the sutured contacts between oolites in the Millepore Bed predate replacement by freshwater siderite during subsequent progradation. In the coarse clastics, overburden pressures may have been significant, or, alternatively, the stressed grain contacts here may have allowed dissolution here when pore fluids became undersaturated with respect to quartz, whilst elsewhere the relatively more stable overgrowth surfaces did not.

Hydrocarbons. The effects of hydrocarbon migration into and through these sediments appear restricted to widespread pyritisation of the oil-water contact in the Ninian Field, and a trace of pyritisation in Yorkshire. There is no evidence to suggest that oil has affected diagenesis in 210/15-2

nor that it has had any other fundamental effects on the other rocks.

#### GENERAL THESIS CONCLUSIONS

This thesis reports the results of an investigation into the controls on diagenesis in clastic sediments from the Middle Jurassic Dogger Formation and Ravenscar Group in Yorkshire, and the Middle Jurassic Brent Group in the Northern North Sea. Its objectives have been, firstly, to define and delineate where possible those diagenetic processes which may be directly related to the depositional environment, and, secondly, to distinguish quantitatively these processes from those operating subsequently.

In the Ravenscar Group eogenesis of non-marine sediments resulted in vermiform kandite (kaolinite) or chlorite precipitation, followed by the formation of quartz overgrowths and then freshwater siderite in sandstones. Both Eh and pH were reduced during bacterial degradation of organic matter, as a result of which the originally fresh water became acidic and the anoxic. At the same time, siderite soil horizons grew on and in the surrounding muds which were also saturated with anoxic pore waters. During burial replacive ferroan calcite cemented the remaining porosity. In the marine clastic sediments illite and potassium-feldspar and quartz overgrowths precipitated from interstitial pore waters before bacterial processes lowered the pH and Eh of pore waters which consequently precipitated vermiform kandites or chlorite and then siderite. As pH rose, ferroan calcite cementation took place. Later, during burial, aggressive fluids migrated into the major sandbodies, leaching carbonates and precipitating blocky kandites (dickite). The Ravenscar Group is exposed on the surface today and has undergone weathering which has resulted in the oxidation of siderite, alteration of chlorite to vermiculite and perhaps leached further carbonates.

In the Brent Group from the Ninian Field, eogenetic modifications were similar except that Eh was not reduced during diagenesis of aluminosilicates and so only vermiform kandites, but not chlorite, precipitated before quartz overgrowths and siderite. Also, illite occurs widely in the lowermost marine formations. Burial diagenesis was also similar, with ferroan calcite cementation followed by leaching and blocky kandite precipitation in the larger sandbodies. In addition, however, Fe and Mg rich solutions migrated into the strata prior to hydrocarbons. These equilibrated with the existing carbonates and precipitated ankerite. The presence of oil has only resulted in pyrite precipitation at the oil water contact.

The sandstones in 210/15-2, although deposited in similar environments and subsequently invaded by hydrocarbons, have not undergone similar diagenesis. Extensive potassium-feldspar overgrowths as well as vermiform kandites preceded ferroan calcite cementation. This was then leached and more kandites were precipitated. Hydrocarbons later migrated into the remaining pore space. There is no illite nor any ankerite in these deposits.

Diagenesis reflects the original textures of and gross distribution of sandbodies within these deposits. Similarly, their composition has influenced the phases which precipitated and the preservation of the original siliciclastic framework. Overprinting all this, however, the tropical climate of the original environments ensured a plentiful supply of organic matter to and a high water table in the non-marine sediments, which consequently determined pore fluid pH and Eh throughout eogenesis. Continuing diagenesis during burial was affected by various solutions migrating from adjacent mudrocks.

On a broad scale, this research, in comparison with existing publications, suggests that a diagenetic "facies" model may exist. Firstly, depositional mineralogy, and hence overall framework stability, determines whether the

effects of early diagenetic processes survive burial. Immature sediments become diagenetically mature. Conversely, mature sediments may be fingerprinted by their depositional climate and their burial portrayed as passage through the zones of the carbonate curtain, aggressive fluids, dilute alkaline formation waters, Fe and Mg rich solutions, and perhaps hydrocarbon migration. Nonetheless, the overriding conclusion that I have reached on the basis of this research is that whilst numerous factors affect the diagenesis of clastic sediments, they are all inexorably intertwined and none may be identified as wholly controlling diagenesis.

"In every work regard the writer's end,  
For none can compass more than they intend."

Pope

- THE END -

FIG. 7.1 Flow chart to demonstrate the interaction of prediagenetic factors which affected initial reactions in the Ravenscar Group.

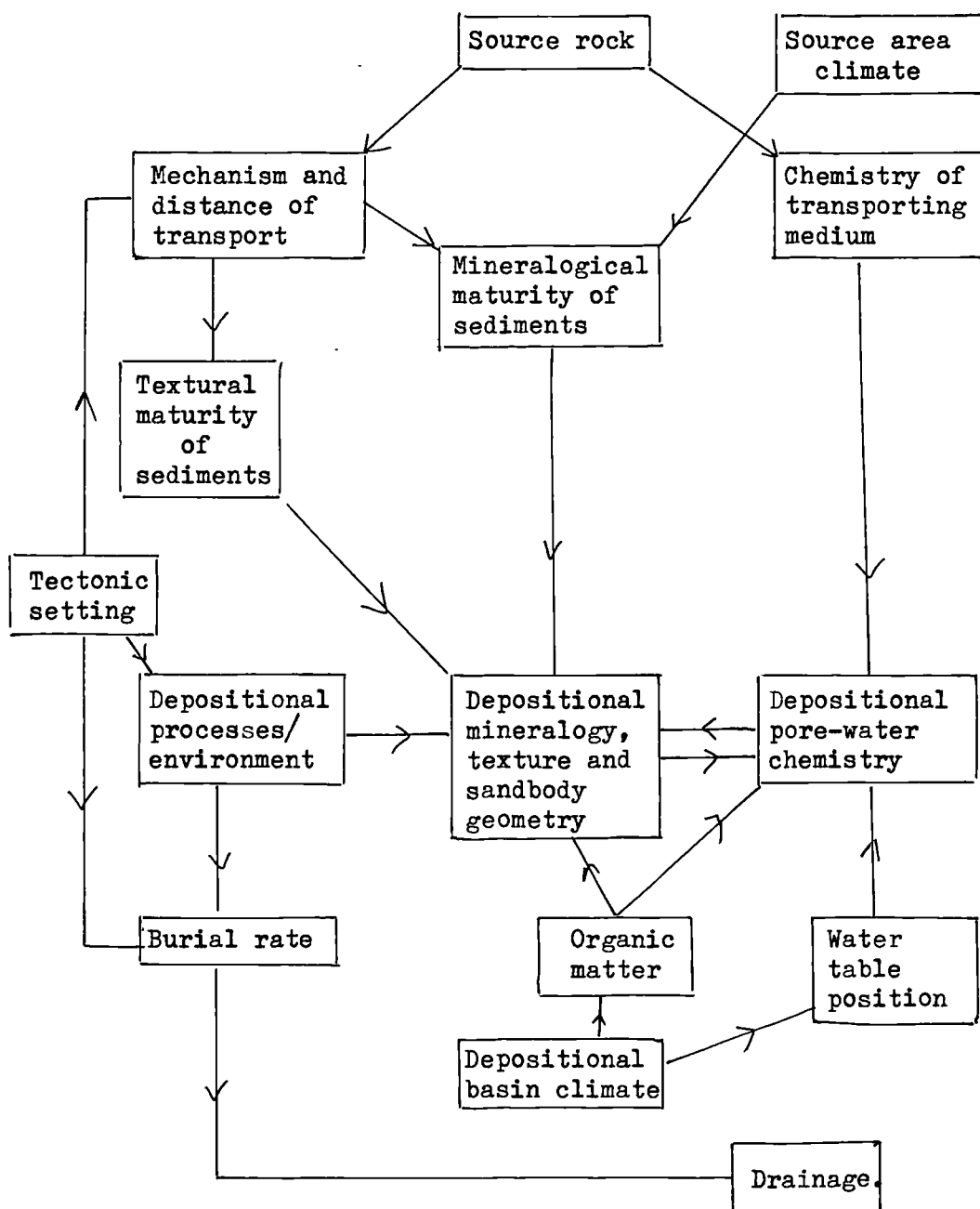


FIG. 7.2 Flow chart to demonstrate the possible pathways of clastic sediments during eogenesis in the Ravenscar Group.

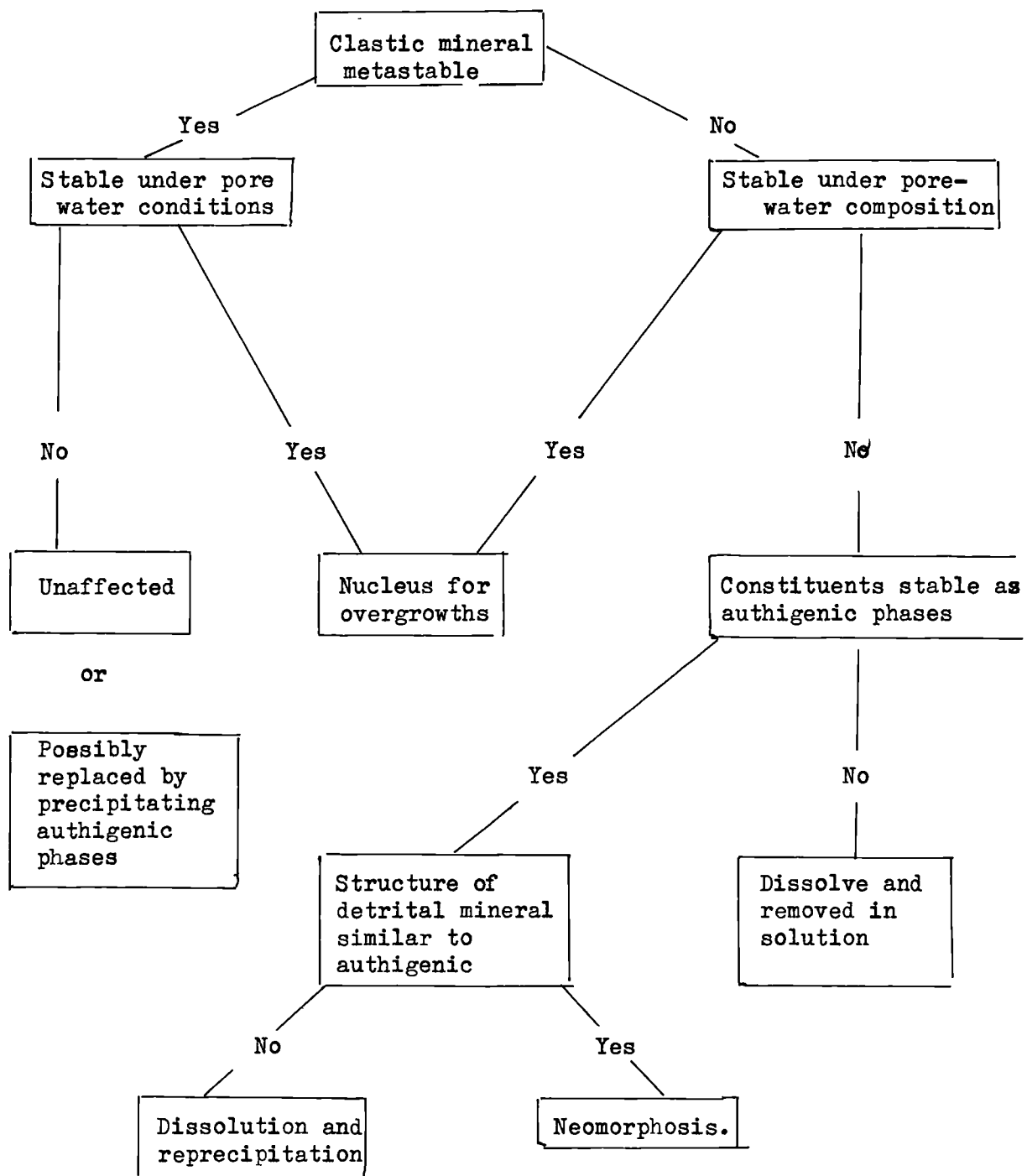
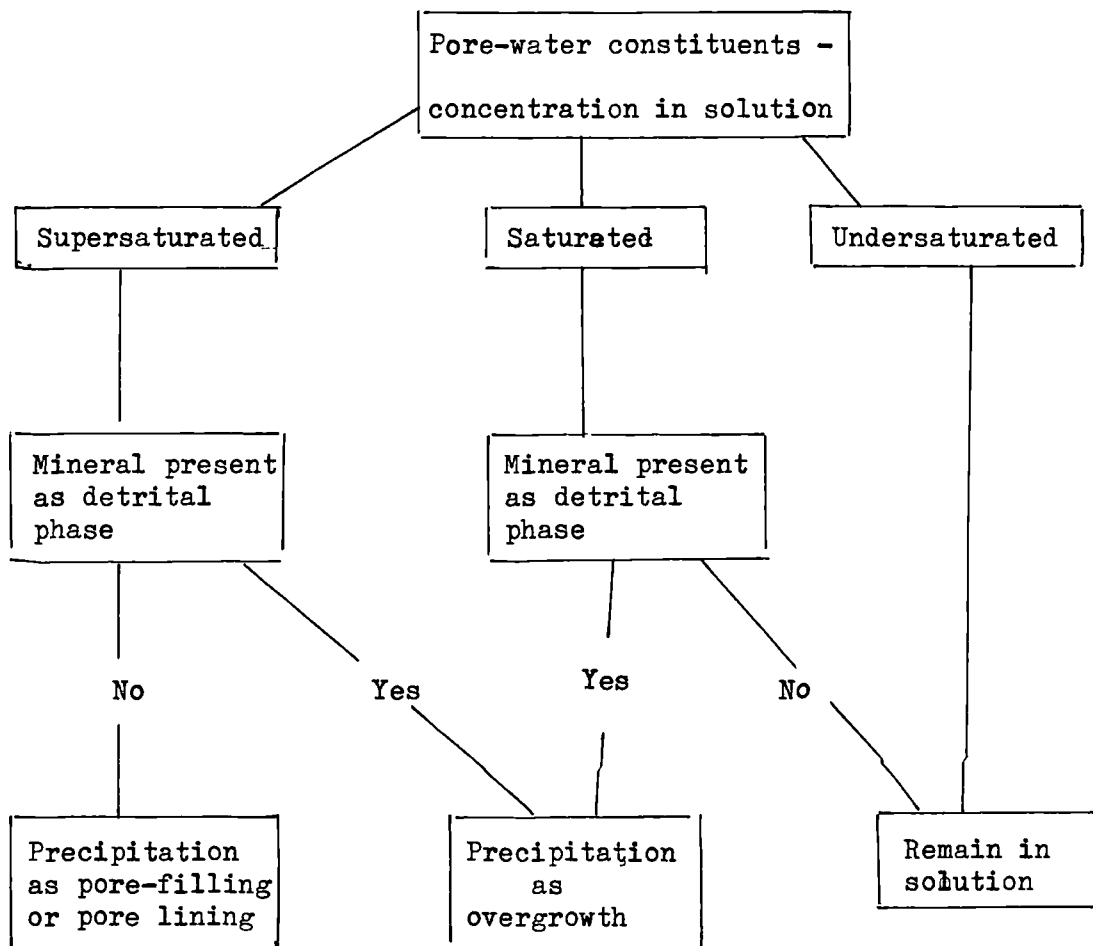


FIG. 7.3 Flow chart to demonstrate the schematic paths of ionic species in pore fluids during eogenesis of the Ravenscar Group.





## REFERENCES

- ALBRIGHT, W.A., TURNER, W.L. and WILLIAMSON, K.R. 1980 Ninian Field, U.K. sector, North Sea. In HALBOUTY, M.T. (ed) Giant Oil and Gas Fields of the decade 1968-1978. Mem. Am. Ass. Petrol. Geol. 30 173-193
- ALLEN, J.R.L. 1965 A review of the origin and characteristics of Recent alluvial sediments. Sedimentology 5 89-191
- ALMON, W.R., FULLERTON, L.B. and DAVIES, D.K. 1976 Pore space reduction in Cretaceous sandstones through chemical precipitation of clay minerals. J. sedim. Petrol. 46 89-96
- \_\_\_\_\_ and DAVIES, D.K. 1979 Regional diagenetic trends in the Lower Cretaceous Muddy Sandstone, Powder River Basin. In: SCHOLLE, P.A. and SCHLUGER, P.R. (eds) q.v. 379-400
- ANDERTON, R., BRIDGES, P.H., LEEDER, M.R. and SELLWOOD, B.W. 1979 A dynamic stratigraphy of the British Isles. George Allen and Unwin, London 301pp.
- ANDREWS, P.B. and LINGEN, G.J. van der 1969 Environmentally significant sedimentologic characteristics of beach sands. N.Z.J. Geol. Geophys. 12 119-137
- ARCHER, D.J. 1969 X-ray diffraction analysis of deep-sea clay minerals Unpublished PhD Thesis, University of Manchester 108pp
- ASHLEY, G.M., SOUTHARD, J.B. and BOOTHROYD, J.C. 1982 Deposition of climbing ripple beds: a flume simulation. Sedimentology 29 67-79
- BAILEY, S.W. 1980 Summary of recommendations of AIPEA nomenclature committee. Clay Miner. 15 85-93
- BAGANZ, B.P., HORNE, J.C. and FERM, J.C. 1975 Carboniferous and Recent Mississippi lower delta plains; a comparison. Gulf Coast Assoc. Geol. Soc. Trans. 25 183-191

- BALAZS, R.J. and KLEIN, G. deVries 1972 Roundmass-mineralogical relations of some intertidal sands. J.sedim.Petrol. 42 425-433
- BARNARD, P.C. and COOPER, B.S. 1981 Oils and source rocks of the North Sea area. In: ILLING, L.V. and HOBSON, G.D. (eds) q.v., 169-175
- BASS BECKING, L.G.M., KAPLAN, F.R. and MOORE, D. 1960 Limits of the natural environment in terms of pH and oxidation-reduction potentials. J.Geol. 68 243-384
- BATE, R.H. 1967 Stratigraphy and palaeogeography of the Yorkshire oolites and their relationship with the Lincolnshire Limestone. Bull.Br.Mus.nat.Hist.(Geol.) 14 111-141
- BATHURST, R.G.C. 1975 Carbonate sediments and their diagenesis. Developments in Sedimentology 12 658pp
- BEARD, D.C. and WEYL, P.K. 1973 Influence of texture on porosity and permeability of unconsolidated sand. Bull.Am.Assoc.Petrol. Geol. 57 349-369
- BERNER, R.A. 1971 Principles of chemical sedimentology. McGraw Hill, New York. 240pp
- \_\_\_\_\_ 1974 Kinetic models for the early diagenesis of nitrogen, sulfur, phosphorous, and silicon in anoxic marine sediments. In: GOLDBERG, E.D. (ed.) The Sea v5, Wiley and Sons, New York. 427-450
- \_\_\_\_\_ 1980 Early diagenesis. A theoretical approach. Princeton University Press, Princeton New Jersey. 241pp
- \_\_\_\_\_ 1981 Kinetics of weathering and diagenesis. In: LASAGA, A.C. and KIRKPATRICK, R.J. (eds) Kinetics of geochemical processes. Reviews in mineralogy 8 111-134 Mineralogical Society of America.
- \_\_\_\_\_ and HOLDREN, G.R.Jr. 1979 Mechanism of feldspar weathering.II Observations of feldspars from soils. Geochim. Cosmochim.Acta 43 1173-1186

- BESLY, B.M. 1980 The catenary relationship of tropical palaeosols in the Westphalian Coal Measures of central England. Internat.Assoc. Sedimentologists 1st Europ.Mtg. Bochum 1980 Abs. p150
- BIGARELLA, J.J., BECKER, R.D. and DUARTE, G.M. 1969 Coastal dune structures from Paraná (Brazil). Mar.Geol. 7 5-55
- BJØRLYKKE, K. 1979 Cementation of sandstone - discussion. J.sedim. Petrol. 49 1358-1439
- \_\_\_\_\_ ELVERHOI, K.A. and MALM, A.O. 1979 Diagenesis in Mesozoic sandstones from Spitsbergen and the North Sea, a comparison. Geol.Rdsch. 68 1152-1171
- BLACK, M. 1928 'Washouts' in the Estuarine Series of Yorkshire. Geol. Mag. 65 301-307
- \_\_\_\_\_ 1929 Drifted plant beds of the Upper Estuarine Series of Yorkshire. Q.Jl.geol.Soc.Lond. 85 389-437
- \_\_\_\_\_ 1934 The Middle Jurassic rocks. In: WILSON, V., BLACK, M. and HEMINGWAY, J.E. 1934 A synopsis of the Jurassic rocks of Yorkshire. Proc.Geol.Ass. 45 247-306
- BLATT, H. 1966 Diagenesis of sandstones: processes and problems. Wyoming Geol.Assoc.Ann.Conf. 65 a-o
- \_\_\_\_\_ 1979 Diagenetic processes in sandstones. In: SCHOLLE, P.A. and SCHLUGER, P.R. (eds) q.v., 141-157
- \_\_\_\_\_ MIDDLETON, G. and MURRAY, R. 1972 Origin of sedimentary rocks. Prentice-Hall, New Jersey. 634pp
- BLUCK, B.J. 1967 Sedimentation of beach gravels - examples from South Wales. J.sedim.Petrol. 37 128-157
- BOLES, J.R. 1978 Active ankerite cementation in the subsurface Eocene of south-west Texas. Contrib.Mineral.Petrol. 68 13-22
- \_\_\_\_\_ 1981 Clay diagenesis and effects on sandstone cementation (case histories from the Gulf Coast Tertiary). In: LONGSTAFFE, F.J. (ed) q.v., 148-168

- BOLES, J.R. 1982 Active albitization of plagioclase, Gulf Coast Tertiary.  
Am.J.Sci. 282 165-180
- \_\_\_\_\_ and FRANKS, S.G. 1979a Clay mineral diagenesis in Wilcox of south-west Texas: implications of smectite diagenesis in sandstone cementation. J.sedim.Petrol. 49 55-70
- \_\_\_\_\_ 1979b Cementation of sandstones - reply.  
J.sedim.Petrol. 49 1362
- BORAK, B. and FRIEDMAN, G.M. 1981 Textures of sandstones and carbonate rocks in the worlds deepest wells (in excess of 30,000ft. or 9.1km) Anadarko Basin, Oklahoma. Sediment.Geol. 29 133-151
- BOSTROM, K. 1967 Some pH controlling redox reactions in natural waters.  
Advances in Chemistry Ser. 67 286-311
- BOURGEOIS, J. 1980 A transgressive shelf sequence exhibiting hummocky stratification: the Cape Sebastin sandstone (Upper Cretaceous), southwestern Oregon. J.sedim.Petrol. 50 681-702
- BRADSHAW, M.J., JAMES, S.J. and TURNER, P. 1980 Origin of oolitic ironstones - discussion. J.sedim.Petrol. 50 295-299
- BREESE, B.E. 1960 Quartz overgrowths as evidence of silica deposition in soils. Aust.J.Sci. 23 18-20
- BRIDGE, J.S. and LEEDER, M.R. 1979 A simulation model of alluvial stratigraphy. Sedimentology 26 617-644
- BRIDGES, P.H. 1976 Lower Silurian transgressive barrier islands, southwest Wales. Sedimentology 23 347-362
- BRINDLEY, G.W. 1982 Chemical composition of berthierines. Clays Clay Miner. 30 153-155
- \_\_\_\_\_ and BROWN, G. (eds) 1980 Crystal structures of clay minerals and their x-ray identification. Mineralogical Society Monograph No.5, Mineralogical Society, London. 455pp
- BROWN, S. and DEEGAN, C.E. 1981 Jurassic In: Introduction to the petroleum geology of the North Sea. JAPEC Course Notes 1 (G)1-30

- BUCKE, D.P. and MANKIN, C.J. 1971 Clay mineral diagenesis within interlaminated shales and sandstones. J.sedim.Petrol. 41 971-981
- BUDDING, M.C. and INGLIN, H.F. 1981 A reservoir geological model of the Brent Sands in Southern Cormorant. In: ILLING, L.V. and HOBSON, G.D. (eds) q.v., 326-334
- BURKE, K. 1977 Aulacogens and continental break up. Ann.Rev.Earth Planet.Science 5 371-396
- BURNS, L.K. and ETHRIDGE, F.G. 1979 Petrology and diagenetic effects of lithic sandstones: Palaeocene and Eocene Umpqua Formation, southwest Oregon. In: SCHOLLE, P.A. and SCHLUGER, P.R. (eds) q.v., 307-317
- BURST, J.F. 1959 Post diagenetic clay mineral environmental relationships in the Gulf Coast Eocene. Clays Clay Miner. 6 327-341
- \_\_\_\_\_ 1969 Diagenesis of Gulf Coast clayey sediments and its possible relation to petroleum migration. Bull.Am.Assoc.Petrol. Geol. 53 73-93
- CAMPBELL, C.V. 1976 Reservoir geometry of a fluvial sheet sandstone. Bull.Am.Assoc..Petrol.Geol. 60 1009-1020
- CANT, D.J. and WALKER, R.G. 1976 Development of a braided-fluvial facies model for the Devonian Battery Point. Can.Jl.Earth Sci. 13 102-119
- CAROTHERS, W.W. and KHARAKA, Y.K. 1980 Stable carbon isotopes of  $\text{HCO}_3^-$  in oilfield waters: implications for the origin of  $\text{CO}_2$ . Geochim. Cosmochim.Acta 44 323-332
- CARROLL, D. 1958 Role of clay minerals in the transportation of iron. Geochim.Cosmochim.Acta 14 1-27
- CARTER, C.H. 1978 A regressive barrier and barrier-protected deposit: depositional environments and geographic setting of the late Tertiary Cohansey Sand. J.sedim.Petrol. 48 933-950

- CHALLINOR, A. and OUTLAW, B.D. 1981 Structural evolution of the North Viking Graben. In: ILLING, L.V. and HOBSON, G.D. (eds) q.v., 104-109
- CHAMBERLAIN, C.K. 1976 Field guide to the trace fossils of the Cretaceous Dakota hogback along Alameda Avenue, west of Denver, Colorado. In: EPIS, R.C. and WEIMER, R.J. (eds) Studies in Colorado Field Geology. Prof.Contrib.Colorado School Mines 8: 242-250
- CHRISTIE, P.A.F. and SCLATER, J.G. 1980 An extensional origin for the Buchan and Witchground Graben in the North Sea. Nature 283 729-732
- CLAYTON, R.N. and MAYEDA, T.K. 1963 The use of bromine pentafluoride in the extraction of oxygen from oxides and silicates for isotopic analysis. Geochim.Cosmochim.Acta 27 43-52
- CLIFTON, H.E. 1969 Beach lamination - nature and origin. Mar.Geol. 7 553-559.
- \_\_\_\_\_, HUNTER, R.E. and PHILLIPS, R.L. 1971 Depositional structures and processes in the non-barred high energy near-shore. J.sedim.Petrol. 41 651-670
- \_\_\_\_\_, PHILLIPS, R.L. and HUNTER, R.E. 1973 Depositional structures and processes in the mouths of small coastal streams, southwest Oregon. In: COATES, D.R. (ed) Coastal geomorphology. Publications in Geomorphology, State University of New York, Binghamton, New York. 115-140
- COLEMAN, M.L., CURTIS, C.D. and IRWIN, H. 1979 Burial rate a key to source and reservoir potential. World Oil 5 83-92
- COLEMAN, J.M. and GAGLIANO, S.M. 1964 Cyclic sedimentation in the Mississippi River delta plain. Gulf Coast Assoc.Geol.Socs. Trans. 14 67-80

- COLEMAN, J.M. and HO, C. 1968 Early diagenesis and compaction in clays. Proc.Symp. Abnormal Subsurface pressures, Louisiana State University. 23-50 (Louisiana Coastal Studies Institute Technical Report 62 AD No. 687 550)
- \_\_\_\_\_ and WRIGHT, L.D. 1975 Modern river deltas: variability of processes and sandbodies. In: BROUSSARD, M.L.R. (ed) Deltas: models for exploration. Houston Geological Society, Houston, Texas. 99-149
- COLLINS, A.G. 1975 Geochemistry of oilfield waters. Developments in petroleum science 1 Elsevier publishing company 496pp
- COPE, J.C.W., DUFF, K.L., PARSONS, C.F., TORRENS, H.S., WIMBLEDON, W.A., and WRIGHT, J.K. 1980 A correlation of Jurassic rocks in the British Isles.Part Two: Middle and Upper Jurassic. Geol.Soc. London Special Report 15 109pp
- COOPER, B.S., COLEMAN, S.H., BARNARD,P.C. and BUTTERWORTH, J.S. 1975 Palaeotemperatures in the Northern North Sea Basin. In: WOODLAND, A.W. (ed) q.v., 487-492
- CRAIG, H. 1957 Isotopic standards for carbon and oxygen correction factors for mass spectrometric analysis for carbon dioxide. Geochim.Cosmochim.Acta 12 133-149
- \_\_\_\_\_ 1965 The measurement of oxygen isotope palaeotemperatures. In: TONGIORGI, E. (ed) Stable isotopes in oceanographic studies and palaeotemperatures. Consiglio Nazionale delle Ricerche, Pisa. 3-24
- CURTIS, C.D. 1976 Stability of minerals in surface weathering reactions: a general thermochemical model. Earth Surf.Proc. 1 63-70
- \_\_\_\_\_ 1977 Sedimentary geochemistry: environments and processes dominated by involvement in an aqueous phase. Phil.Trans.R. Soc. A286 353-371

- CURTIS, C.D. 1978 Possible links between sandstone diagenesis and depth related geochemical reactions occurring in enclosing mudstones. J.geol.Soc.Lond. 135 107-117
- \_\_\_\_\_ 1980 Diagenetic alteration in black shales. J.geol.Soc.Lond. 137 189-194
- \_\_\_\_\_ in press. Geochemical studies on development and destruction of secondary porosity. Petroleum geochemistry and exploration of Europe, 23-24/9/82 Glasgow University. Geol.Soc.Lond. Spec.Pub.
- \_\_\_\_\_ and SPEARS, D.A. 1968 Formation of sedimentary iron minerals Pt. II. Econ.Geol. 63 262-270
- \_\_\_\_\_ 1971 Diagenetic development of kaolinite Clays Clay Miner. 19 219-227
- \_\_\_\_\_, PETROWSKI, C. and OERTEL, G. 1972 Stable carbon isotopes within carbonate concretions: a clue to place and time of formation. Nature 235 98-100
- DANSGAARD, W. 1964 Stable isotopes in precipitation. Tellus 16 436-468
- DAVIES, D.K., ALMON, W.R., BONIS, S.B. and HUNTER, B.E. 1979 Deposition and diagenesis of Tertiary-Holocene volcanoclastics, Guatemala. In: SCHOLLE, P.A. and SCHLUGER, P.R. (eds) q.v., 281-306
- DAY, G.A., COOPER, B.A., ANDERSON, C., BURGERS, W.F.J., RØNNEVIK, H.C. and SCHONEICH, H. 1981 Regional seismic structure maps of the North Sea. In: ILLING, L.V. and HOBSON, G.D. (eds) q.v., 76-84
- DEBOER, R.B., NAGTEGAAL, P.J.C. and DUYVIS, E.M. 1977 Pressure solution experiments on quartz sand. Geochim.Cosmochim.Acta 41 257-264
- DEEGAN, C.E. and SCULL, B.J. 1977 A standard lithostratigraphical nomenclature for the Central and Northern North Sea. Report 77/25 Inst.Geol.Sci. H.M.S.O. 36pp



- DEINES, P. 1970 Mass spectrometer correction factors for the determination of small isotopic composition variations of carbon and oxygen. Int.Jl.Mass Spectrometry and Ion Physics 4 283-295
- DICKINSON, W.R. and SUCZEK, C.A. 1979 Plate tectonics and sandstone compositions. Bull.Am.Assoc.Petrol.Geol. 63 2164-2182
- DICKSON, J.A.D. and COLEMAN, M.L. 1980 Changes in carbon and oxygen isotope composition during limestone diagenesis. Sedimentology 27 107-118
- DIMROTH, E. 1977 Facies models 6.Diagenetic facies of iron formation. Geoscience Canada 4 83-88
- DINGLE, R.V. 1971 A marine geological survey off the north-east coast of England (western North Sea) J.geol.Soc.Lond. 127 303-338
- DIXON, J.B. and WEED, S.B. (eds) 1977 Minerals in soil environments. Soil Science Society of America, Madison, Wisconsin. 948pp
- DIXON, J.E., FITTON, J.G. and FROST, R.T.C. 1981 The tectonic significance of post-Carboniferous igneous activity in the North Sea Basin. In: ILLING, L.V. and HOBSON, G.D. (eds) q.v., 121-137
- DOMENICO, P.A. 1977 Transport phenomena in chemical rate processes in sediments Ann.Rev.Earth Planetary Sci. 5 287-317
- DONOVAN, T.J. 1974 Petroleum microseepage at Cement Oklahoma: evidence and mechanism. Bull.Am.Assoc.Petrol.Geol. 58 429-446
- DUNHAM, A.C. and WILKINSON, F.W.F. 1978 Accuracy, precision and detection limits of energy dispersive electron microprobe analyses of silicates. X-ray Spectrom. 7 50-56
- DUNHAM, K.C. 1960 Syngenetic and diagenetic mineralisation in Yorkshire. Proc.Yorks.geol.Soc. 32 229-284
- DUTTON, S.P. 1977 Diagenesis and secondary porosity distribution in deltaic sandstone, Strawn Series (Pennsylvanian) north-central Texas. Gulf Coast Assoc.Geol.Socs.Trans. 27 272-277

- EBERL, D. and HOWER, J. 1976 Kinetics of illite formation. Bull.geol. Soc. Am. 87 1326-1330
- EDWARDS, M.B. 1978 Composition, provenance and diagenesis of sandstones in the Lower Cretaceous Helvetiafjellet Formation, Svalbard. Continental Shelf Institute Trondheim. Publication 98 1-29
- \_\_\_\_\_ 1979 Sandstone in Lower Cretaceous Helvetiafjellet Formation, Svalbard. Bearing on reservoir potential of Barents Shelf. Bull.Am.Assoc.Petrol.Geol. 63 2193-2203
- ELLIOTT, R.E. 1968 Facies, sedimentation successions and cyclotherms in productive Coal Measures in the East Midlands, Great Britain. Mercian Geologist 2 351-372
- ELLIOTT, T. 1975 The sedimentary history of a delta lobe from a Yoredale (Carboniferous) cyclothem. Proc.Yorks.geol.Soc. 40 505-536
- \_\_\_\_\_ 1976 Morphology, magnitude and regime of a Carboniferous fluvial-distributary channel. J.sedim.Petrol. 46 70-76
- \_\_\_\_\_ 1978 Clastic shorelines. In: READING, H.G. (ed) Sedimentary environments and facies. Blackwells Scientific Publications London. 143-177
- ELSBERG, J.N. Van 1978 A new approach to sediment diagenesis. Can.Pet. Geol.Bull. 26 57-86
- EMBRY, A.F., REINSON, G.E., and SCHLUGER, P.R. 1979 Shallow marine sediments - a brief review. In: SHAWA, M.S. (ed) Use of sedimentary structures for recognition of sedimentary environments. 2nd Edition. Can.Soc.Pet.Geol. 53-64
- EVANS, C.R., ROGERS, M.A. and BAILEY, N.J.L. 1971 Evolution and alteration of petroleum in western Canada. Chem. Geol. 8 147-170
- EVANS, E.W. 1864 On the action of oil wells Am.J.Sci. 42 159-166
- EYNON, G. 1981 Basin development and sedimentation in the Middle Jurassic of the Northern North Sea. In: ILLING, L.V. and HOBSON, G.D. (eds) q.v., 196-204

- FAIRCHILD, I.J. 1980 Stages in a Precambrian dolomitisation, Scotland: cementing versus replacement textures. Sedimentology 27 631-650
- FANNING, D.S. and KERAMIDES, V.Z. 1977 Micaceous. In: DIXON, J.B. and WEED, S.B. (eds) q.v., 195-258
- FEININGER, T. 1971 Chemical weathering and glacial erosion of crystalline rocks and the origin of till. U.S.Geol.Surv.Prof.Pap. 750-C 65-81
- FETH, J.H., ROBERSON, C.E., and POLZER, W.L. 1964 Sources of mineral constituents in water from granitic rocks, Sierra Nevada, California and Nevada. U.S.Geol.Surv.Water Supply Pap. 1535-1 170pp
- FISHER, W.L. and BROWN, L.F. 1972 Clastic depositional systems - a genetic approach to facies. Bur.of Econ.Geol., University of Texas at Austin, Texas. 211pp
- FITZGERALD, D.M. and BOUMA, A.H. 1972 Consolidation studies of deltaic sediments. Gulf Coast Assoc.Geol.Socs.Trans. 22 165-173
- FITZPATRICK, E.A. 1980 Soils. Their formation, classification and distribution. 2nd edition. Longman, London. 353pp
- FOLK, R.L. 1968 Petrology of sedimentary rocks. Hemphills Bookstore, Austin, Texas. 170pp
- FORESTER, R.M., SANDBERG, P.A. and ANDERSON, T.F. 1973 Isotopic variability of cheilostome bryozoan skeletons. In: LARWOOD, G.P. (ed) Living and fossil bryozoa. Academic Press, London. 79-94
- FRAZIER, D.E. 1967 Recent deltaic deposits of the Mississippi, their development and chronology. Gulf Coast Assoc.Geol.Socs.Trans. 17 287-311
- \_\_\_\_\_ 1974 Depositional episodes: their relationship to the Quaternary stratigraphic framework in the northwest portion of the Gulf Basin. Bur.Econ.Geol., Univ.Texas.Geol.Circ. 74-1 28pp
- \_\_\_\_\_ and OSANIK, A. 1961 Ponit-bar deposits, Old River Locksite, Louisiana. Gulf Coast Assoc. Geol.Socs.Trans. 11 121-137

- FRIEDMAN, G.M., ALI, S.A. and KRINSLEY, D.H. 1976 Dissolution of quartz accompanying carbonate precipitation and cementation in reefs: example from the Red Sea. J.sedim.Petrol. 46 970-973
- FRITZ, P. and SMITH, D.G.W. 1970 The isotopic composition of secondary dolomite. Geochim.Cosmochim.Acta 34 1161-1173
- \_\_\_\_\_, BINDA, P.L., FOLINSBEE, F.E. and KROUSE, H.R. 1971 Isotopic composition of diagenetic siderites from Cretaceous sediments in western Canada. J.sedim.Petrol. 41 282-288
- FROELICH, P.N., KLINKHAMMER, G.P., BENDER, M.L., LUEDTKE, N.A., HEATH, G.R., CULLEN, D., DAUPHIN, P., HAMMOND, D., HARTMAN, B. and MAYNARD, V. 1979 Early oxidation of organic matter in pelagic sediments of the eastern equatorial Atlantic: suboxic diagenesis. Geochim.Cosmochim.Acta 43 1075-1090
- GAC, J.Y. and TARDY, Y. 1980 Geochemistry of a tropical landscape on granitic rocks: the Lake Chad Basin. In: CAMPBELL, A. (ed) Proceedings 3rd International Symposium on Water-Rock interaction Alberta Research Council. 8-10
- GALLOWAY, W.E. 1974 Deposition and diagenetic alteration of sandstones in northeast Pacific arc-related basins: implications of greywacke genesis. Bull.geol.Soc.Am. 85 379-390
- \_\_\_\_\_ 1979 Diagenetic control of reservoir quality in arc-derived sandstones: implications for petroleum exploration. In: SCHOLLE, P.A. and SCHLUGER, P.R. (eds) q.v., 251-262
- GARRELS, R.M. and CHRIST, C.L. 1965 Solutions, minerals and equilibria. Harper and Row, New York. 450pp
- GAUNT, G.D., IVEY-COOK, H.C., PENN, I.E. and COX, B.M. 1980. Mesozoic rocks proved by I.G.S. boreholes in the Humber and Acklam areas. Rep.Inst.geol.Sci.London, 79/13 34pp

- GAVISH, E. and FRIEDMAN, G.M. 1969 Progressive diagenesis in Quaternary to late Tertiary carbonate sediments: sequence and time scale. J.sedim.Petrol. 39 980-1006
- GIBBS, H.J. 1977 Transport phases of transition metals in the Amazon and Yukon Rivers. Bull.geol.Soc.Am. 88 829-843
- GLENNIE, K.W., MUDD, G.C. and NAGTEGAAL, P.J.C. 1978 Depositional environment and diagenesis of Permian Rotliegendes sandstones in Leman Bank and Sole Pit areas of the U.K. Southern North Sea. J.geol.Soc.Lond. 135 25-34
- \_\_\_\_\_ and BOEGNER, P.L.E. 1981 Sole Pit inversion tectonics. In: ILLING, L.V. and HOBSON, G.D. (eds) q.v., 110-120
- GOLDICH, S.S. 1938 A study in rock weathering. J.Geol. 46 17-58
- GOULD, K.W. and SMITH, J.W. 1979 The genesis and isotopic composition of carbonates associated with some Australian coals. Chem. Geol. 24 137-150
- GRAY, W.D.T. and BARNES, G. 1981 The Heather Oilfield. In: ILLING, L.V. and HOBSON, G.D. (eds) q.v., 335-341
- GREENLAND, D.J. 1975 Charge characteristics of some kaolinite-iron hydroxide complexes. Clay Miner. 10 407-416
- GREENSMITH, J.T., RAWSON, P.F. and SHALABY, S.E. 1980 An association of minor fining-upward cycles and aligned gutter marks in the Middle Lias (Lower Jurassic) of the Yorkshire coast. Proc. Yorks.geol. Soc. 42 525-538
- GREER, S.A. 1975 Sandbody geometry and sedimentary facies at the estuary marine transition zone. Senckenberg Mar. 7 105-135
- GRIM, R.E., BRAY, R.H. and BRADLEY, W.F. 1937 The mica in argillaceous sediments. Am.Miner. 22 813-829
- GUVEN, N., HOWER, W.F. and DAVIES, D.K. 1980 Nature of authigenic illites in sandstone reservoirs. J.sedim.Petrol. 50 761-766

- HALLAM, A. 1967 Siderite- and calcite-bearing concretionary nodules in the Lias of Yorkshire. Geol.Mag. 104 222-227
- \_\_\_\_\_ 1975 Jurassic environments. Cambridge University Press, Cambridge. 269pp
- \_\_\_\_\_ 1978 Eustatic cycles in the Jurassic. Palaeogeog. Palaeoclimatol. Palaeoecol. 23 1-32
- \_\_\_\_\_ 1981 A revised sea-level curve for the early Jurassic. J.geol. Soc.Lond. 138 735-743
- \_\_\_\_\_ and BRADSHAW, M.J. 1979 Bituminous shales and oolitic ironstones as indicators of transgressions and regressions. J.geol.Soc.Lond. 136 157-164
- HALLET, D. 1981 Refinement of the geological model of the Thistle Field. In: ILLING, L.V. and HOBSON, G.D. (eds) q.v., 315-325
- HALLIMOND, A.F. 1925 Iron ores: bedded ores of England and Wales. Great Britian Geol.Surv.Spec.Repts Min.Res. 29 139pp
- HANCOCK, J.M. and SCHOLLE, P.A. 1975 Chalk of the North Sea. In: WOODLAND, A.W. (ed) q.v., 413-425
- HANCOCK, N.J. 1978a Discussion on pressure solution. J.geol.Soc.Lond. 135 134
- \_\_\_\_\_ 1978b An application of scanning electron microscopy in pilot water injection studies for oilfield development. In: WHALLEY, W.B. (ed) Scanning electron microscopy in the study of sediments. GeoAbstracts, Norwich. 61-70
- \_\_\_\_\_ and TAYLOR, A.M. 1978 Clay mineral diagenesis and oil migration in the Middle Jurassic Brent Sand Formation. J.geol. Soc,Lond. 135 69-72
- \_\_\_\_\_ and FISHER, M.J. 1981 Middle Jurassic North Sea deltas with particular reference to Yorkshire. In: ILLING, L.V. and HOBSON, G.D. (eds) q.v., 186-195

- HANGARI, K.M., AHMAD, S.N. and PERRY, E.C. Jr. 1980 Carbon and oxygen isotope ratios in diagenetic siderite and magnetite from Upper Devonian Ironstone, Wadi Shatti District, Libya. Econ.Geol. 75 538-545
- HANSON, R.F., ZAMORA, R. and KELLER, W.D. 1981 Nacrite, dickite and kaolinite in one deposit in Nayarit, Mexico. Clays Clay Miner. 29 451-453
- HARDER, H. 1974 Illite mineral synthesis at surface temperatures. Chem. Geol. 14 241-253
- HARRIS, T.M. The geology of the Yorkshire Flora. Proc.Yorks.geol.Soc. 29 63-71
- HARRISS, R.C., SEBACHER, D.I. and DAY, F.P.Jr.. 1982 Methane flux in the Great Dismal Swamp. Nature 297 673-674
- HAWKINS, P.J. 1978 Relationship between diagenesis, porosity reduction and oil emplacement in late Carboniferous sandstone reservoirs: Bothamsall Oilfield, East Midlands. J.geol.Soc.Lond. 135 7-24
- HAYES, J.B. 1979 Sandstone diagenesis - the hole truth. In: SCHOLLE, P.A. and SCHLUGER, P.R. (eds) q.v., 127-139
- HAYS, J.D. and PITMAN, W.C. III 1973 Lithospheric plate motion, sea-level changes, and climatic and ecological consequences. Nature 246 18-22
- HEALD, M.T. and BAKER, G.F. 1977 Diagenesis of the Mt. Simon and Rose Run sandstones in western West Virginia and Southern Ohio. J.sedim.Petrol. 47 66-77
- HELGESON, H.C., GARRELS, R.M. and MACKENZIE, F.T. 1969 Evaluation of irreversible reactions in geochemical processes involving minerals and aqueous solutions. II Applications. Geochim. Cosmochim. Acta 33 455-481
- HEM, J.D. 1970 Study and interpretation of the chemical characteristics of natural water. U.S.Geol.Surv. Water Supply Pap. 1473 (2nd ed.)

- HEMINGWAY, J.E. 1968 Sedimentology of coal bearing strata. In:  
MURCHISON, D. and WESTOLL, T.S.(eds) q.v., 43-69
- \_\_\_\_\_ 1974 Jurassic. In: RAYNER, D.H. and HEMINGWAY, J.E.  
(eds) q.v., 161-223
- \_\_\_\_\_ and BRINDLEY, G.W. 1952 The occurrence of dickite in some  
sedimentary rocks. Rep.int.geol.Congr.1948 (18th, London.) 13 308
- \_\_\_\_\_ and KNOX, R.W.O'B. 1973 Lithostratigraphic  
nomenclature of The Middle Jurassic strata of the Yorkshire  
Basin of north-east England. Proc.Yorks.geol.Soc. 39 527-535
- \_\_\_\_\_ and OWEN, J.S. 1975 William Smith and the Jurassic coals  
of Yorkshire. Proc.Yorks.geol.Soc. 40 297-308
- HEROUX, Y., CHAGNON, A. and BERTRAND, R. 1979 Compilation and correlation  
of major thermal maturation indicators. Bull.Am.Assoc.Petrol.  
Geol. 63 2128-2144
- HILL, C.R. 1974 Palaeobotanical and sedimentological studies on the Lower  
Bajocian (Middle Jurassic) flora of Yorkshire. Unpublished PhD  
Thesis, University of Leeds.
- HOWARD, J.D. and REINECK, H-E, 1972 Georgia coastal region, Sapelo Island,  
U.S.A.: sedimentology and biology. IV Physical and biogenic  
sedimentary structures of the nearshore shelf. Senckenberg. Mar.  
4 81-123
- \_\_\_\_\_ and FREY, R.W. 1975a Estuaries of the Georgia coast, U.S.A.:  
sedimentology and biology. 1 Introduction. Senckenberg.Mar. 7 1-31
- \_\_\_\_\_ 1975b Regional animal sediment characteristics  
of Georgia estuaries. Senckenberg,Mar. 7 33-103
- HOWER, J. 1981 Shale diagenesis. In: LONGSTAFFE, F.J. (ed) q.v., 60-80
- \_\_\_\_\_, ESLINGER, E.V., HOWER, M.E. and PERRY, E.A. 1976 Mechanism  
of burial and metamorphism of argillaceous sediment: 1.  
Mineralogical and chemical evidence. Bull.geol.Soc.Am. 87 725-737



- HOYT, J.H. and WEIMER, R.J. 1963 Comparison of modern and ancient beaches central Georgia coast. Bull.Am.Assoc.Petrol.Geol. 47 529-531
- HUANG, P.M. 1977 Feldspars, olivines, pyroxenes and amphiboles. In: DIXON, J.B. and WEED, S.B. (eds) q.v., 553-602
- HUBERT, J.F., BUTERA, J.G. and RICE, R.F. 1972 Sedimentology of Upper Cretaceous Cody-Parkman delta, southwestern Powder River Basin, Wyoming. Bull.geol.Soc.Am. 83 1649-1670
- HUDSON, J.D. 1977 Stable isotopes and limestone lithification. J.geol.Soc.Lond. 133 637-660
- \_\_\_\_\_ and PALFRAMAN, D.F.B. 1969 Ecology and preservation of the Oxford Clay fauna at Woodham, Buckinghamshire. Q.Jl.geol.Soc. Lond. 124 387-418
- \_\_\_\_\_ and FRIEDMAN, I. 1976 Carbon and oxygen isotopes in concretions: relationship to pore-water changes during burial. In: CADEK, J. and PACES, T. (eds) Proc.Int. Symp. Water Rock Interaction, Geol.Surv. Prague. 331-339
- HUNTER, R.E., CLIFTON, H.E. and PHILLIPS, R.L. 1979 Depositional processes sedimentary structures, and predicted vertical sequences in barred nearshore systems, southern Oregon coast. J.sedim.Petrol. 49 711-726
- HURST, A.R. 1980 Occurrence of corroded authigenic kaolinite in a diagenetically modified sandstone. Clays Clay Miner. 28 393-396
- \_\_\_\_\_ 1981 A scale of dissolution for quartz and its implications for diagenetic processes in sandstones. Sedimentology 28 451-460
- \_\_\_\_\_ and IRWIN, H. 1982 Geological modelling of clay diagenesis in sandstones. Clay Miner. 17 5-22
- HUTCHEON, I., OLDERSHAW, A. and GHENT, E.D. 1980 Diagenesis of Cretaceous sandstones of the Kootenay Formation at Elk Valley (southeastern British Columbia) and Mt. Allan (southwestern Alberta). Geochim.Cosmochim.Acta. 44 1425-1435

- ILLING, L.V. and HOBSON, G.D. (eds) 1981 Petroleum geology of the continental shelf of north-west Europe. Institute of Petroleum and Heydon and Sons, London. 521pp
- INSTITUTE OF GEOLOGICAL SCIENCES. 1979 Annual Report. Institute of Geological Sciences, London. 122pp
- IRWIN, H., CURTIS, C.D. and COLEMAN, M.L. 1977 Isotopic evidence for source of diagenetic carbonates formed during burial of organic-rich sediments. Nature 269 209-213
- JAMES, H.E. and HOUTEN, F.B. VAN 1979 Miocene goethite and chamositic oolites, northeastern Colombia. Sedimentology 26 125-134
- JEANS, C.V. 1978 The origin of the Triassic clay assemblages of Europe with special reference to the Keuper Marl and Rhaetic of parts of England. Phil.Trans.R.Soc.(A) 289 549-639
- JOHNSON, D.P. 1982 Sedimentary facies of an arid zone delta: Gascoyne Delta, western Australia. J.sedim.Petrol. 52 547-563
- JOHNSON, H.D. 1975 Tide- and wave-dominated inshore and shoreline sequences from the late Precambrian, Finnmark, north Norway. Sedimentology 22 45-74
- KAPLAN, I.R., EMERY, K.O. and RITTENBURG, S.C. 1963 The distribution and isotopic abundance of sulphur in Recent marine sediments off Southern California. Geochim.Cosmochim.Acta 27 297-331
- KASTNER, M. and SIEVER, R. 1979 Low temperature feldspars in sedimentary rocks. Am.J.Sci. 279 435-479
- KEITH, M.L., ANDERSON, G.M. and EICHLER, R. 1964 Carbon and oxygen isotopic composition of mollusc shells from marine and fresh water sediments. Geochim.Cosmochim.Acta 28 1757-1786
- \_\_\_\_\_ and WEBER, J.N. 1964 Carbon and oxygen isotopic composition of selected limestones and fossils. Geochim.Cosmochim.Acta 28 1787-1816
- KENDALL, P.F. and WROOT, H.E. 1924 The geology of Yorkshire. 2 vols  
Printed privately, Vienna. xxii and 985pp

KENT, P.E. 1980 Subsidence and uplift in East Yorkshire and Lincolnshire:  
a double inversion. Proc.Yorks geol.Soc. 42 505-524

KIMBERLEY, M.M. 1979 Origin of oolitic iron formations. J.sedim.Petrol.  
49 111-132

\_\_\_\_\_ 1980a Origin of oolitic iron formations - reply. J.sedim.  
Petrol. 50 299-302

\_\_\_\_\_ 1980b Origin of oolitic iron formations - reply. J.sedim.  
Petrol. 50 1003-1004

KLEIN, G.DE VRIES 1970 Depositional and dispersal dynamics of intertidal  
sand bars. J.sedim.Petrol. 40 1095-1127

KNOX, R.W.O'B. 1969 Sedimentology and studies of the Eller Beck Bed and  
Lower Deltaic Series in north-east Yorkshire. Unpublished PhD  
Thesis, University of Newcastle-upon-Tyne.

\_\_\_\_\_ 1970 Chamositic ooliths from the Winter Gill Ironstone  
(Jurassic) of Yorkshire, England. J.sedim.Petrol. 40 1216-1225

KUMAR, N. and SANDERS, J.E. 1976 Characteristics of shoreface storm  
deposits: modern and ancient examples. J. sedim.Petrol. 46 145-162

LAND, L.S. and DUTTON, S.P. 1978 Cementation of a Pennsylvannian Deltaic  
sandstone: isotopic data. J.sedim.Petrol. 48 1167-1176

\_\_\_\_\_ 1979 Cementation of sandstones - reply.  
J.sedim.Petrol. 49 1359-1361

LANGFORD-SMITH, T. (ed) 1978 Silcrete in Australia. Department of Geography,  
University of New England. 304pp

LEEDER, M.R. 1978 A quantitative stratigraphic model for alluvium; with  
special reference to channel deposit density and interconnectedness.  
In: MIALL, A.D. (ed) q.v., 587-596

LEEDER, M.R. and NAMI, M. 1979 Sedimentary models for the non-marine  
Scalby Formation (Middle Jurassic) and evidence for late  
Bajocian/Bathonian uplift of the Yorkshire Basin. Proc. Yorks  
geol.Soc. 43 461-482

- LEMOALLE, J. and DUPONT, B. 1973 Iron-bearing oolites and the present conditions of iron sedimentation in Lake Chad. In: AMSTUTZ, G.C. and BERNARD, A.J. (eds) Ore in sediments. Springer-Verlag, Berlin. 167-178
- LIN, F-C, and CLEMENCY, C.V. 1981 The kinetics of dissolution of muscovite at 25°C and 1 atm. CO<sub>2</sub> partial pressure. Geochim. Cosmochim. Acta 45 571-576
- LINDQUIST, S.J. 1977 Secondary porosity development and subsequent reduction overpressed Frio Formation (Oligocene) south Texas. Gulf Coast Assoc. Geol. Soc. Trans 27 99-107
- LIVERA, S.E. 1981 Sedimentology of Bajocian rocks from the Ravenscar Group of Yorkshire. Unpublished PhD Thesis, University of Leeds 298pp
- \_\_\_\_\_ and LEEDER, M.R. 1981 The Middle Jurassic Ravenscar Group (Deltaic Series) of Yorkshire: recent sedimentological studies as demonstrated during a recent Field Meeting, 2-3 May 1980. Proc. Geol. Ass. 92 241-250
- LIVINGSTONE, D.A. 1963 Data on geochemistry. Chapter G. Chemical composition of rivers and lakes. U.S. Geol. Surv. Prof. Pap. 440G 64pp (ed)
- LONGSTAFFE, F.J./1981 Clays and the resource geologist. Min. Assoc. Canada, Short Course Handbook 7 199pp
- LOUCKS, R.G., BEBOUT, D.G., and GALLOWAY, W.E. 1977 Relationship of porosity formation and preservation to sandstone consolidation history. Gulf Coast Assoc. Geol. Soc. Trans. 27 109-120
- MackENZIE, D.B. 1963 Dakota Group on west flank of Denver Basin. In: Geology of the north Denver Basin and adjacent uplifts. 14th Field. Conf. Rocky Mtn. Assoc. Geol. 135-148
- \_\_\_\_\_ 1965 Depositional environment of Muddy Sandstone, western Denver Basin, Colorado. Bull. Am. Assoc. Petrol. Geol. 49 186-206
- \_\_\_\_\_ 1971 Post-Lyttle Dakota Group on west flank of Denver Basin. Mountain Geol. 8 91-131

- MacKENZIE, D.B. 1972 Tidal sand flat deposits in Lower Cretaceous Dakota Group near Denver, Colorado. Mountain Geol. 9 269-277
- MacKENZIE, F.T. and GEES, R. 1971 Quartz synthesis at earth surface conditions. Science. 173 533-535
- MARSHALL, J.D. and ASHTON, M. 1980 Isotopic and trace element evidence for submarine lithification of hardgrounds in the Jurassic of eastern England. Sedimentology 27 271-290
- McBRIDE, E.F. 1963 A classification of common sandstones. J.sedim.Petrol. 33 664-669
- \_\_\_\_\_ 1974 Significance of colour in red, green, purple, olive-brown and grey beds of Difunta Group, northeastern Mexico. J.sedim. Petrol. 44 760-773
- \_\_\_\_\_ 1977 Secondary porosity importance in sandstone reservoirs in Texas. Gulf Coast Assoc.Geol.Socs.Trans. 27 121-122
- McHARDY, W.J., WILSON, M.J. and TAIT, J.M. 1982 Electron microscope and x-ray diffraction studies of filamentous illitic clay from sandstones of the Magnus Field. Clay Miner. 17 23-29
- McKENZIE, D.P. 1978 Some remarks on the development of sedimentary basins. Earth and planet. Sci.Lett. 40 25-32
- MEADE, R.H. 1966 Factors influencing the early stages of the compaction of clays and sands - review. J.sedim.Petrol. 36 1085-1101
- MEHRA, O.P. and JACKSON, M.L. 1960 Iron oxide removal from soils and clays by a dithionite-citrate system buffered with sodium bicarbonate. Clays Clay Miner. 7 317-327
- MIAL, A.D. 1977 A review of the braided river depositional environment. Earth Sci.Rev. 13 1-62
- \_\_\_\_\_ (ed) 1978 Fluvial sedimentology. Can.Soc.Petrol.Geol. Mem. 5 859pp
- MILLIKEN, K.L., LAND, L.S. and LOUCKS, R.G. 1981 History of burial diagenesis determined from isotopic geochemistry, Frio Formation, Brazoria County, Texas. Bull.Am.Assoc.Petrol.Geol. 65 1397-1413

- MOIOLA, R.J. and JONES, E.L. 1981 Sedimentology of Brent Formation  
(Middle Jurassic) Statfjord Field, Norway - United Kingdom.  
(Abstract). Bull.Am.Assoc.Petrol.Geol. 65 959
- MOODY-STUART, M. 1966 High- and low-sinuosity stream deposits, with  
examples from the Devonian of Spitsbergen. J.sedim.Petrol. 36  
1102-1117
- MOORE, L.R. 1968 Some sediments closely associated with coal seams.  
In: MURCHISON, D. and WESTOLL, T.S. (eds) q.v., 105-123
- MORGAN, J. 1967 Applications and limitations of chemical thermodynamics  
in natural water systems. Advances in Chemistry Ser. 67 1-29
- MORRIS, K.A. 1979 An integrated facies analysis of Toarcian organic-rich  
shales and contiguous deposits in Great Britain. Unpublished  
PhD Thesis, University of Reading
- MURATA, K.J., FRIEDMAN, I. and MADSEN, B.M. 1969 Isotopic composition  
of diagenetic carbonates in marine Miocene formations of  
California and Oregon. U.S.Geol.Surv.Prof.Pap. 614B 24pp
- MURCHISON, R.I. 1832 On the occurrence of the stems of fossil plants in  
vertical positions in the sandstones of the inferior oolite  
of the Cleveland Hills. Proc.Geol.Soc.Lond. 1 391-392
- NAGTEGAAL, P.J.C. 1978 Sandstone framework instability as a function of  
burial diagenesis. J.geol.Soc.Lond. 135 101-105
- \_\_\_\_\_ 1979 Relationship of facies and reservoir quality in  
Rotliegendes desert sandstones, Southern North Sea region.  
J.Petrol.Geol. 2 145-158
- \_\_\_\_\_ 1980 Diagenetic models for predicting clastic reservoir  
quality. Revista Instituto Investigaciones Geologicas 34 5-19
- NAHON, D., CARROZI, A.V. and PARRON, C. 1980 Lateritic weathering as a  
mechanism for the generation of ferruginous ooids. J.sedim.  
Petrol. 50 1287-1298

- NAMI, M. 1976a Sedimentology of the Scalby Formation (Upper Deltaic Series) in Yorkshire. Unpublished PhD Thesis, University of Leeds. 195pp
- \_\_\_\_\_ 1976b An exhumed Jurassic meander belt from Yorkshire, England. Geol.Mag. 113 47-52
- \_\_\_\_\_ and LEEDER, M.R. 1978 Changing channel morphologies and magnitude in the Scalby Formation (Middle Jurassic) of Yorkshire England. In: MIALL, A.D. (ed) q.v., 431-440
- NEALE, J.W. 1974 Cretaceous In: RAYNER, D.H. and HEMINGWAY, J.E. (eds) q.v., 225-243
- NICOLAS, J. and BILDGEN, P. 1979 Relations between the location of the karst bauxites in the northern hemisphere, the global tectonics, and the climatic variations during geological time. Palaeogeog.Palaeoclimatol.Palaeoecol. 28 205-239
- NISHIYAMA, T., OINUMA, K. and SATO, M. 1978 An interstratified chlorite-vermiculite in weathered red shale near Toyoma, Japan. (Abstract) Proc.6th Int.Clay Conf, Oxford. 157
- OANA, S. and DEEVEY, E.S. 1960 Carbon 13 in lake waters and its possible bearing on palaeolimnology. Am.J.Sci. 258A 253-272
- ODIN, G.S. and MATTER, A. 1981 De glauconiarum origin. Sedimentology 28 611-641
- ODOM, I.E., WILLARD, T.N., and LASSIN, R.J. 1979 Paragenesis of diagenetic minerals in the St.Peter Sandstone (Ordovician), Wisconsin and Illinois In: SCHOLLE, P.A. and SCHLUGER, P.R. (eds) q.v., 425-443
- ORCEL, J., HENIN, S. and CALLIERE, S. 1949 Sur les silicates phylliteux des mineraux de fer oolithiques. C.R.Acad.Sci.Paris 229 134-135
- PARKER, C.A. 1974 Geopressures and secondary porosity in the deep Jurassic of Mississippi. Gulf Coast Assoc.Geol.Socs. Trans. 24 69-80
- PARRY, C.C., WHITLEY, P.K.J. and SIMPSON, R.D.H. 1981 Integration of palynological and sedimentological methods in facies analysis of the Brent Formation. In: ILLING, L.V. and HOBSON, G.D. (eds) q.v., 205-215

- PARSONS, C.F. 1977 A stratigraphical revision of the Scarborough Formation (Middle Jurassic) of northeast Yorkshire. Proc.Yorks Geol. Soc. 41 203-222
- PEARSON, M.J., WATKINS, D. and SMALL, J.S. in press Clay diagenesis and organic maturation in Northern North Sea sediments. Proc. Int.Clay Conf. (1981)
- PERRY, J. and HOWER, J. 1970 Burial diagenesis in Gulf Coast pelitic sediments. Clays Clay Miner. 18 165-178
- PHILLIPS, J. 1829 Illustrations of the geology of Yorkshire, or a description of the strata and organic remains. Part 1. The Yorkshire Coast. Printed privately, York xvi + 192pp
- PIERSON, B.J. 1981 The controls of cathodoluminescence in dolomite by iron and manganese. Sedimentology 28 601-610
- PICARD, G.L. and FELBECK, G.T.Jr 1976 The complexation of iron by marine humic acid. Geochim.Cosmochim.Acta 40 1347-1350
- PITTMAN, E.D. 1979 Porosity, diagenesis, and productive capability of sandstone reservoirs. In: SCHOLLE, P.A. and SCHLUGER, P.R. (eds) q.v., 159-173
- PORRENGA, D.H. 1965 Chamosite in recent sediments of the Niger and Orinoco Deltas. Geologie Mijnb. 44 400-403
- \_\_\_\_\_ 1967 Glauconite and chamosite as depth indicators in the marine environment. Mar. Geol. 5 495-501
- POWELL, J.H. and RATHBONE, P.A. in press The stratigraphical relationship of the Eller Beck Formation and the supposed Blowgill Member in the Middle Jurassic strata of the Hambleton Hills (Yorkshire Basin). Proc.Yorks.geol.Soc.
- PRYOR, W.A. 1973 Permeability - porosity patterns and variations in some Holocene sandbodies. Bull.Am.Assoc.Petrol.Geol. 57 162-189



- PUIDEFABREGAS, C. and VLIET, A.VAN 1978 Meandering stream deposits from the Tertiary of the Southern Pyrenees. In: MIAL, A.D. (ed) q.v., 469-485
- RAISWELL, R. 1971 The growth of Cambrian and Liassic concretions. Sedimentology 17 147-171
- RAYNER, D.H. and HEMINGWAY, J.E.(eds) 1974 Geology and mineral resources of Yorkshire. Yorkshire Geological Society, Leeds. 405pp
- REINECK, H.E. and SINGH, I.B. 1973 Depositional sedimentary environments with reference to terrigenous clastics. Springer-Verlag, Berlin. 439pp
- REYNOLDS, R.C. 1980 Interstratified clay minerals. In: BRINDLEY, G.W. and BROWN, G. (eds) q.v., 249-303
- ROBIN, P-Y,F. 1978 Pressure solution at grain-to-grain contacts. Geochim. Cosmochim.Acta 42 1383-1389
- ROSSEL, N.C. 1982 Clay mineral diagenesis in Rotliegendes aeolian sandstones of the Southern North Sea. Clay Miner. 17 69-77
- RUST, B.R. 1978 Depositional models for braided alluvium. In: MIAL, A.D. (ed) q.v., 605-625
- SALOMONS, W., GOUDIE, A.S. and MOOK, W.G. 1978 Isotopic composition of calcrete deposits from Europe, Africa and India. Earth Surf. Proc. 3 43-57
- SANDERS, J.E. and KUMAR, N. 1975 Evidence of shoreface retreat and in place 'drowning' during Holocene submergence of barriers, shelf off Fire Island, New York. Bull.geol.Soc.Am. 86 65-76
- SARKISYAN, S.G. 1971 Application of the scanning electron microscope in the investigation of oil and gas reservoir rocks. J.sedim.Petrol. 41 289-292
- SAVIN, M. and JACKSON, M.L. 1975 Scanning electron microscopy of cherts in relation to the oxygen isotopic variation of soil chert. Clays Clay Miner. 23 365-368

- SAVIN, S. and EPSTEIN, S. 1970 The oxygen and hydrogen isotope geochemistry of clay minerals. Geochim.Cosmochim.Acta 34 25-42
- SAWKINS, F.J. 1966 Ore genesis in the North Pennine Orefield in the light of fluid inclusion studies. Econ.Geol. 61 385-401
- SCHMIDT, V. and McDONALD, D.A. 1979a The role of secondary porosity in the course of sandstone diagenesis. In: SCHOLLE, P.A. and SCHLUGER, P.R. (eds) q.v., 175-207
- 
- 1979b Texture and recognition of secondary porosity in sandstones. In: SCHOLLE, P.A. and SCHLUGER, P.R. (eds) q.v., 209-225
- SCHLAGER, W. and JAMES, N.P. 1978 Low magnesian calcite limestones forming at the deep-sea floor, Tongue of the Ocean, Bahamas. Sedimentology 25 675-702
- SCHOLLE, P.A. and SCHLUGER, P.R. (eds) 1979 Aspects of diagenesis. Spec.Pub.Soc.econ.Miner.Palaeont. Tulsa 26 443pp
- SCLATER, J.G and CHRISTIE, P.A.F. 1980 Continental stretching: an explanation of the post-mid-Cretaceous subsidence of the central North Sea Basin. J.Geophys.Res. (B)85 3711-3739
- SEDGWICK, A. 1826 On the classification of the strata which appear on the Yorkshire coast. Ann.Phil. xi 339-362
- SELLWOOD, B.W. and PARKER, A. 1978 Observations on diagenesis in North Sea reservoir sandstones. J.geol.Soc.Lond. 135 133-134
- SHACKLETON, N.J. and KENNETT, J.P. 1975 Palaeotemperature history of the Cenozoic and the initiation of the Antarctic glaciation: oxygen and carbon isotope analysis in DSDP Sites 277, 279, and 281 In: KENNETT, J.P. and HOUTZ, R.E. (eds) Initial reports of the Deep-Sea Drilling Project 29 U.S.Government Printing Office, Washington. 743-755
- SHARMA, G.D. 1969 Paragenetic evolution in Peejay Field, British Columbia, Canada. Miner.Deposita 4 346-354

- SHARMA, T. and CLAYTON, R.N. 1965 Measurement of  $O^{18}/O^{16}$  ratios of total oxygen of carbonates. Geochim.Cosmochim.Acta 29 1347-1354
- SIEVER, R. 1979 Plate-tectonic controls on diagenesis. J.Geol. 87 127-155
- \_\_\_\_\_ and WOODFORD, N. 1973 Sorption of silica by clay minerals. Geochim.Cosmochim.Acta 37 1851-1880
- SIMPSON, R.D.H. and WHITLEY, P.K.J. 1981 Geological input to reservoir simulation of the Brent Formation. In: ILLING, L.V. and HOBSON, G.D. (eds) q.v., 310-314
- SLEEP, N.H. 1971 Thermal effects of the formation of Atlantic continental margins by continental breakup. Geophys.J.R.astr.Soc. 24 325-350
- SMITH, A.G., BRIDEN, J.C. and DREWRY, G.E. 1973 Phanerozoic World maps. In: HUGHES, N.F. (ed) Organisms and continents throught time. Palaeont.Ass.Sp.Paper 12 1-42
- SMITH, N.D. 1970 The braided stream depositional environment: comparison of the Platte River with some Silurian clastic rocks, north-central Appalachians. Bull.geol.Soc.Am. 81 2993-3014
- SMITHSON, F. 1942 The Middle Jurassic rocks of Yorkshire, a petrological and palaeogeographical study. Q.Jl.geol.Soc.Lond. 98 27-59
- \_\_\_\_\_ and BROWN, G. 1954 The petrography of dickitic sandstones in North Wales and Northern England. Geol.Mag. 41 177-188
- \_\_\_\_\_ 1957 Dickite in Northern England and North Wales. Mineral.Mag. 31 381-391
- SOMMER, F. 1975 Histoire diagénétique d'une série gréseuse de Mer du Nord Datation de l'introduction des hydrocarbours. Revue del'institut Francais du Pétrole 30 729-741
- \_\_\_\_\_ 1978 Diagenesis of Jurassic sandstones in the Viking Graben. J.geol.Soc.Lond. 135 63-67
- SORBY, H.C. 1857 On the origin of the Cleveland Hill ironstone. Geological and Polytechnic Soc. West Riding of Yorkshire 3 457-461

- SORBY, H.C. 1908 On the application of quantitative methods to the study of the structure and history of rocks. Q.Jl.geol.Soc.Lond. 64 171-232
- SPEARS, D.A. 1980 Towards a classification of shales. J.geol.Soc.Lond 137 125-129
- SPENCER, C.W. 1976 Hydrodynamic-energy classification for the interpretation of cores of Cretaceous sandstones deposited in wave dominated environments. In: Wyoming Geol.Assoc. 28th Ann. Field Conf. Symposium. Geology and energy resources of the Powder River Basin. Symposium Abstracts 3-4
- STALDER, P.J. 1975 Cementation of Pliocene-Quaternary fluviatile clastic deposits in and along the Oman Mountains. Geologie Mijnb. 54 148-156
- STANTON, G.D. 1977 Secondary porosity in sandstones of the Lower Wilcox (Eocene), Kames County, Texas. Gulf Coast Assoc.Geol.Socs. Trans 27 197-207
- STAUB, J.R. and COHEN, A.D. 1978 Kaolinite-enrichment beneath coals; a modern analog, Snuggedy Swamp, South Carolina. J.sedim.Petrol. 48 203-210
- STEWART, D.J. 1978 Ophiomorpha: a marine indicator? Proc.Geol.Ass. 89 33-41
- STRAATEN, M.J.U.VAN 1959 Minor structures of some Recent littoral and neritic sediments. Geologie Mijnb. 21 197-216
- STUMM, W. and MORGAN, J.J. 1970 Aquatic chemistry. Wiley Interscience, New York. 583pp
- SURLYK, F. 1978 Submarine fan sedimentation along fault scarps on tilted fault blocks (Jurassic/Cretaceous boundary, East Greenland). Bull. Grønlands Geologiske Undersøgelse 128 108pp
- TAN, F.C. and HUDSON, J.D. 1974 Isotopic studies of the palaeoecology and diagenesis of the Great Estuarine Series (Jurassic) of Scotland. Scott.Jnl.Geol. 10 91-128

- TARDY, Y. 1971 Characterisation of the principal weathering types by the geochemistry of waters from European and African crystalline massifs. Chem.Geol. 7 253-271
- TAYLOR, G. 1978 Silcretes in the Walgett Camborah region of New South Wales. In: LANGFORD-SMITH, T. (ed) q.v., 187-193
- TAYLOR, J.H. 1949 The Mesozoic Ironstones of England. Petrology of the Northampton Sand Ironstone Formation. Mem.Geol.Surv.G.B. 111pp
- THOMAS, M.F. 1974 Tropical geomorphology. A study of weathering and landform development in warm climates. MacMillan Press Ltd, London. 332pp
- THOMPSON, W.O. 1937 Original structures of beaches, bars, and dunes. Bull.geol.Soc.Am. 48 723-752
- VAIL, P.R., MITCHUM, R.M.Jr. and TODD, R.G. 1977 Eustatic model for the North Sea during the Mesozoic. Mesozoic Northern North Sea Symposium. 12 1-35
- VELDE, B. 1977 Clays and clay minerals in natural and synthetic systems. Developments in Sedimentology 21 218pp
- VOS, R.G. 1977 Sedimentology of an Upper Palaeozoic River wave and tide influenced delta system in southern Morocco. J.sedim.Petrol 47 1242-1260
- WALKER, T.R., WAUGH, B. and CRONE, A.J. 1978 Diagenesis in first cycle desert alluvium of Cenozoic age, southwestern United States and northwestern Mexico. Bull.geol.Soc.Am. 89 19-32
- WATTS, N.L. 1980 Quaternary pedogenic calcretes from the Kalahari (southern Africa): mineralogy, genesis and diagenesis. Sedimentology 27 661-686
- WEBER, J.N., WILLIAMS, E.G. and KEITH, M.L. 1964 Palaeoenvironmental significance of carbon isotopic composition of siderite nodules in some shales of Pennsylvanian age, J.sedim.Petrol 34 814-818

- WEIR, A.H., OMEROD, E.C. and MANSEY, I.M.I. 1975 Clay mineralogy of sediments of the Western Nile Delta. Clay Miner. 10 369-386
- WEYL, P.K. 1959 Pressure solution and the force of crystallisation - a phenomenological theory. J.Geophys.Res. (B) 64 2001-2025
- WHELAN, T. 1974 Methane, carbon dioxide and dissolved sulphate from interstitial water of coastal marsh sediments. Estuarine and Coastal Marine Science 2 407-415
- \_\_\_\_\_ and ROBERTS, H.H. 1973 Carbon isotopic composition of diagenetic carbonate nodules from freshwater swamp deposits. J.sedim.Petrol 43 54-58
- \_\_\_\_\_, COLEMAN, J.M., SUHAYDA, J.N. and GARRISON, L.E. 1975 The geochemistry of Recent Mississippi River delta sediments: gas concentration and sediment stability. 7th Ann. Offshore Technology Conf. Houston Texas. May 5-8th 1975. 71-84. Paper OTC 2342
- WHITE, D.E. 1965 Saline waters of sedimentary rocks. In: YOUNG, A. and GALLEY, J.E. (eds) Fluids in subsurface environments. Mem. Am.Assoc.Petrol.Geol. 4 342-366
- \_\_\_\_\_, HEM, J.D. and WARING, G.A. 1963 Data of geochemistry. 6th ed. U.S.Geol.Surv. Prof.Paper 440-F 67pp
- WILSON, M.D. and PITTMAN, E.D. 1977 Authigenic clays in sandstones: recognition and influence on reservoir properties and palaeoenvironmental analysis. J.sedim.Petrol. 47 3-31
- WINDLE, T.M.F. 1979 Reworked Carboniferous spores: an example from the Lower Jurassic of northeast Scotland. Rev.Palaeobot. Palynol. 27 173-184
- WOOD, R.J. 1981 The subsidence history of Conoco Well 15/30-1, central North Sea. Earth and Planet.Sci.Lett. 54 306-312
- WOODHALL, D. and KNOX, R.W.O'B. 1979 Mesozoic volcanism in the northern North Sea and adjacent areas. Bull. Geol.Surv. G.B. 70 34-56

- WOODLAND, A.W. (ed) 1975 Petroleum and the continental shelf of north-west Europe. 1 Geology. Applied Science Publishers, London. 501pp
- WOPFNER, H. 1978 Silcretes of Northern South Australia and adjacent ref regions. In: LANGFØRD-SMITH, T. (ed) q.v., 93-141
- YEH, H. and SAVIN, S, 1977 The mechanism of burial diagenetic reactions in argillaceous sediments: 3 Oxygen isotope evidence.  
Bull.geol.Soc.Am. 88 1321-1330
- ZIEGLER, P.A. 1981 Evolution of sedimentary basins in northwest Europe.  
In: ILLING, L.V. and HOBSON, G.D. (eds) q.v., 3-39
- ZINKERNAGEL, U. 1978 Cathodoluminescence of quartz and its applications to sandstone petrology. Contributions to Sedimentology 8 69pp
- BOWEN, J.M. 1975 The Brent Oil-field. In: WOODLAND, A.W. (ed) q.v., 353-361

## APPENDIX A:

## LOCALITY DETAILS

The grid references are unambiguous within the outcrop area shown in Fig. AI and include the National Grid Reference Grid letters NZ, SE, and TA.

Locality details	Interpretation	Sample numbers
DOGGER FORMATION		
(860060)	Shallow-marine sandstone	574
(677076)	"	597, 598, 599, 600, 601, 602
(570117)	"	626
Rosedale Chimney (725955)	"	652, 653
Thorgill Bank	"	654, 655
East Rosedale (705985)	"	656
(683023)	"	609, 610
Whitby East Cliff		
(905114)	?beach deposit	345, 347, 348, 353, 354
Beck Hole (823023)	Conglomeratic ironstone	678, 681, 682, 683, 684, 685
SALTWICK FORMATION		
Whitby West Cliff	Meandering-channel	301, 302, 303, 304, 305, 306
(905114)	sandstones	307, 308, 309, 310, 311, 312
		313, 314, 315, 316, 322, 323
		324
	Crevasse-splay sediments	317, 318, 319, 320, 331
	Overbank mudrocks	321
Whitby West Cliff	Meandering-channel	326, 327, 328, 329, 330, 332
(Khyber Pass)	sandstones	333
	Floodplain mudrocks	325
Whitby East Cliff	Channel sandstones	355, 356
(905114)	Crevasse splay sediments	350, 357, 358, 359
	Floodplain mudrocks	349, 360
Ravenscar (995016)	Channel sandstones	525, 526, 527, 528
	Floodplain mudrock	529
Alum Quarry Ravenscar	Channel sandstone	549, 550, 551
(868017)	Crevasse-splay sands	552
	Floodplain mudrock	553
Stoupe Brow (962024)	Channel sandstone	554, 555, 556, 557
Hayburn Wyke (012975)	"	441, 442, 443, 445, 446, 447
	Crevasse splay sands	440, 444
(860059)	Channel sandstone	567, 568
Ugglebarnby Moor		
(883075)	Crevasse splay sand	563, 564, 565, 566
(860060)	Channel sandstone	569, 570, 571
	Crevasse splay sand	573
	Floodplain mudrock	572
Aislaby Quarry (854086)	Channel sandstone	575, 576
	Crevasse splay sands	577



Glaisdale (778056)	Crevasse splay sand	597
(681974)	Channel sandstone	596
(682060)	"	603,604
(683989)	"	605,606
(684058)	Crevasse splay sandstone	607,608
Hollins Hall (745055)	Channel sandstone	611
Hasty Bank (567036)	"	613,614
Boulby (759178)	"	622,623,624,625
Boulby Alum Quarry	"	628,629,630
Guisborough (632145)	"	631,632,633
Roseberry Topping	"	634,635,636,637
(579126)	"	638,639,640
Rosedale East (705985)	"	657,658,659,660,661
Rosedale (732967)	Floodplain mudrocks	662
Mallyan Spout (820005)	Channel sandstone	663,664,665
Beck Hole (823023)	"	666,667,668,669
	"	676,677,679,680,688
	Floodplain mudrock	687

## MILLEPORE BED

Yons Nab (085844)	Shallow-marine	201
Osgodby Nab (065855)	oolitic limestone	220,221
Cloughton (020950)	Beach sandstone	370,371,372,373

## YONS NAB BEDS

Yons Nab (085844)	Bay filling sediments	202,203,204,205,206,265 272,420,438
	Bay filling mudrock	437
Osgodby Nab (065855)	Mouth/tidal bar sands	222,226,227,228,229,230 231,425
Cloughton (020950)	"	382,383
	Lagoon muds	375,376
	Lagoon sands	374,377,378,379

## GRISTHORPE MEMBER

Yons Nab (085844)	Channel sandstone	207,208,209,266,267,268
	Overbank sands	211,264,269,270
	Floodplain mudrocks	210,271
Osgodby Nab (065855)	Channel sandstones	223,224,225,233,234,426
	Crevasse splay sands	427,428
Cloughton (020950)	Sheetflood sands	380,381,384,385,386,387 388,389,390,470
Bloody Beck (942983)	Crevasse splay sands	548
(683086)	"	578,579
(682090)	"	581,582
(684112)	"	593
(660110)	"	591,594
(6601'3)	Floodplain mudrocks	592

## CLOUGHTON FORMATION (inland outcrops undifferentiated)

Silton Forest (452935)	Channel sandstone	620,621
(713912)	"	647,648
	Floodplain mudrock	649
Goathland Station	Crevasse-splay sands	670,671,672,673,674,675
	Floodplain mudrock	671
Danby Moor (71/09)	Crevasse splay sand	689,690,691,692

## SCARBOROUGH FORMATION

Yons Nab (084844)	?tidal shhet sand	261,421
	Mudrocks	262,263
Cloughton (020950)	Sheet sand ? subtidal	392,393,394,397,398,399
		400,401
	Slumped sheet	391,395,396
Scarborough (050870)	Shallow-marine lst.	249
Bloody Beck (942983)	Sheet sand	545,546,547
Sneaton Quarry (891078)	Beach sand	558,559,560,561,562

## MOOR GRIT MEMBER

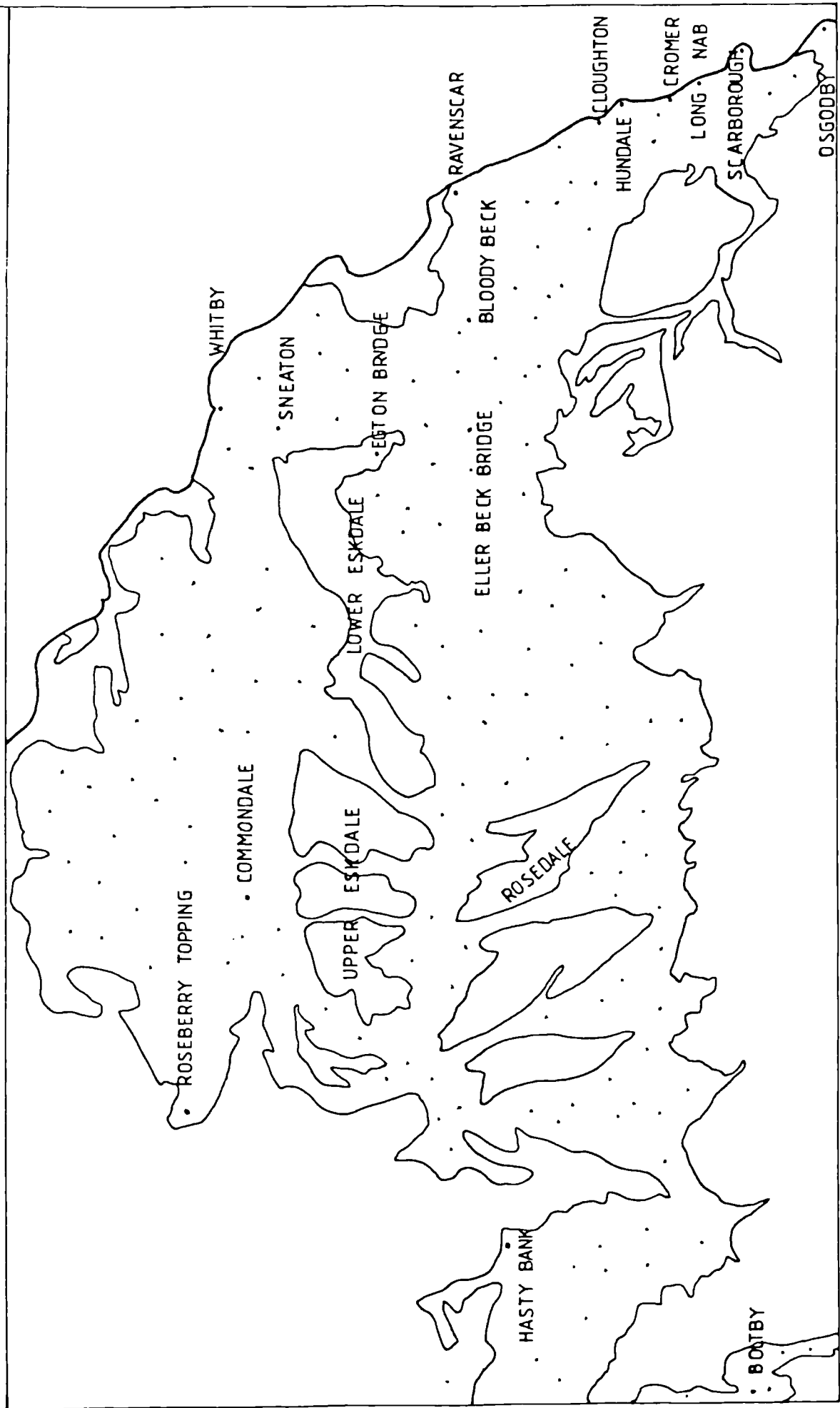
Cornelian Bay (060860)	Channel sandstone	240,241,242,243,244,245
White Nab (058865)	"	246,247
Scarborough (050870)	"	248,250,251,252,253
(045877)	Braided-channel sands	254,255
Hundale Point (025950)		471,472,473,474,475,476
		477,478,479,480,481,486
		487,488,489,490,491,492
		493,494,495,497,498,499
		500,507,508,509,510,511
		512
	Floodplain/bar top mud	496
Bloody Beck (942983)	Braided-channel sandstone	540,541,542,543,544
(682095)	"	583,584,585,586
(682093)	"	587,588
(686091)	"	589,590
May Beck (890024)	"	642,643,645,646
(71/92)	"	650,651
Low Moor (850993)	"	693,694,695
Eller Beck Bridge		696,697,698,699,700,701
(858984)	Braided-channel lag	702
Yons Nab (085844)	Meandering channel sand	212,213,214,215,422,423
		424

## LONG NAB MEMBER

Boltby Reservoir	Channel sandstone	410,411,412,413,414,415
(492886)		416
Crook Ness (027935)	Crevasse splay sands	404,522,523
	Floodplain mudrocks	405,483,484,703
	'Concretions'	1,2,3,4,5,6,7,8,9,
Scalby Mills (036908)	Floodplain mudrocks	406
	Channel sandstones	460,461,462,463,464,465,
Scarborough Quarries	"	431,432,433,434,435,436
(040870)	Overbank sands	429
Cromer Point (030928)	Meandering-channel sand	449,450,451
	Crevasse splay sand	452,453
	Floodplain mudrock	454,455,448
Long Nab/Hundale	Meandering channels	501,502,503,504,505,506
(030940)	complex	513,514,515,516
	Channels	518,519,520,521

LOCALITY DETAILS

(Outcrop of Ravenscar Group stippled).



## APPENDIX B: METHODOLOGY

## THIN-SECTION PREPARATION AND MODAL ANALYSIS

Samples were blue-dye impregnated, and thin sections were then prepared. These were visually examined, and representative examples subjected to modal analysis of 300 or 400 points on a Swift Point Counter. The following procedure was used to impregnate samples for all thin-sections and polished thin-sections. Firstly, 5-10 mm thick slices were cut, unless samples were poorly cemented, in which case thicker pieces were used. Sample numbers were painted on one side or edge with a typing correction fluid and the slices heated to between 90° and 100°C. This serves to both expel absorbed water and facilitate the "inhaling" of the impregnating fluid. Slices were heated for at least four hours. The blue impregnating fluid was prepared by, firstly, dissolving 1 g of blue dye in 100 ml of acetone; secondly, mixing 50 ml of an epoxy resin with 50 ml of hardner, and finally mixing the two together. This fluid has a watery consistency. Heated and numbered slices were then immersed in the fluid, either for 5-10 seconds for porous samples, or longer, and under vacuum for finer and less permeable samples. When dry, thin sections were prepared from the blue chips in the normal way, and mounted with a similar epoxy system to prevent damage to the thin section as the result of differential thermal expansion and contraction. This impregnation serves to bind friable samples, allowing easier thin-section preparation and colour pore-space blue, thus enhancing its visual recognition and facilitating the identification of holes created during thin-section preparation.

## ELECTRON MICROPROBE ANALYSIS

Thin sections for electron microprobe analyses were highly polished, coated with carbon, and their mineral chemistry quantitatively analysed with a Link Systems Model 290 Energy Dispersive Analyser fitted to a Cambridge Instruments Geoscan. The data was corrected and processed with a Link Systems Software ZAF 4 package.

Operating conditions are detailed below:

Beam voltage 15 kV

Specimen current 2.5 nA measured on Cobalt

Beam width 1  $\mu\text{m}$  (expanded to 10  $\mu\text{m}$  for calcites).

The minimum detection limits of the Cambridge Instruments Geoscan are listed below (from Dunham and Wilkinson, 1978: Table 5).

These electron microprobe detection limits for energy dispersive analysis are based on a range of common geological materials. Weight percentage of each element is expressed for 100 seconds livetime.

Element	Minimum limit	Maximum limit
Na	0.15	0.26
Mg	0.07	0.08
Al	0.06	0.11
Si	0.05	0.08
K	0.07	0.11
Ca	0.07	0.12
Ti	0.07	0.12
Mn	0.09	0.17
Fe	0.10	0.19

An unfocussed beam was used for analyses of calcites because recalculating data from a 1  $\mu\text{m}$  beam originally produced calcite totals of 110%. The recalculated results for the remaining carbonates, ankerite and siderite, approximate to 100% in total. Detrital components such as feldspars and micas, unless highly altered, produced satisfactory high totals. However, authigenic clay minerals as well as the breakdown products of detrital micas gave low totals ranging from 40-90%. Justification of the use of these low totals is given in the text.

## X-RAY DIFFRACTION ANALYSIS

### Sample preparation

Sample preparation and analysis was based on a scheme adapted from Jeans (1978). Approximately 250-400 g of each sample was crushed or disaggregated as gently as possible. Samples were either wet ground with a pestle and mortar, or when well cemented, broken with a fly-press prior to wet grinding, and subsequently disaggregated in 500 ml of water either in a food mixer or in a sonic bath for 10 minutes, with either DISPEX or tetrasodium pyrophosphate as a dispersing agent, and washed if necessary. The dispersed solutions were allowed to settle and the upper 10 cm decanted after eight hours. Working with smaller samples required scaling down this operation to a test-tube and decanting the upper 5 cm portion after four hours. This portion is assumed to contain the less than 2  $\mu\text{m}$  e.s.d. fraction. This 2  $\mu\text{m}$  fraction was selected for two reasons, despite the 4-30  $\mu\text{m}$  diameter of authigenic clay plates observed throughout this study. Firstly, publications to date (see Brindley and Brown, 1980) have assumed that the 2  $\mu\text{m}$  fraction is wholly authigenic. Secondly, selection of this size fraction should avoid the inclusion of silt sized quartz particles and any subsequent interference with clay mineral peak intensities, and hence allow semi-quantification of clay proportions.

The irrelevance of this size fraction is demonstrated by data from different size fractions (see Appendix E). In sample 356, for example, the ratio of kandites to illites changes from a 50:50 mixture in the 2  $\mu\text{m}$  fraction to 90:10 in the 10  $\mu\text{m}$  fraction. This latter size reflects more realistically kandite percentages in view of the size of platelets observed during this study. (See Plate 3.4H, for example, where individual clay plates are greater than 10  $\mu\text{m}$  in diameter.).

The decanted solutions were evaporated to dryness. Then, small portions of the dried clay were dispersed in a sonic bath for 2 minutes prior to the preparation of oriented mounts. Both glass slides and ceramic tiles were used during this study. Redispersed slurries were allowed to evaporate to dryness on glass slides or pipetted onto warm unglazed ceramic tiles to facilitate rapid drying and to enhance the preferred orientation of basal spacings. Two mounts were prepared from each sample. One mount was run after drying in air 2-60°2 $\theta$ , then glycolated and rerun from 2-35°2 $\theta$ . The second was heated to 440°C, run for two hours from 2-35°2 $\theta$ , then heated to 550°C for a further two hours and rerun.

#### Running conditions and machine settings

40 kV, 25 mA

Chart speed 10 mm/minute

Scanning speed 1°2 $\theta$ /minute

Co K radiation, Fe filter

Time constant 4 seconds

X-ray Diffractogram Interpretation

Clay mineral identifications are based on the scheme outlined below.

Chlorites. Air dried 14 Å (001) peak, unresponsive to glycolation or heating to 440°C. Heating to 550°C, however, reduces the 7 Å (002) peak whilst increasing the intensity of the 14 Å (001) reflection. Chlorites may be destroyed by boiling in dilute hydrochloric acid.

Berthierine. Air dried 7.2 Å (001) peak, unresponsive to glycolation or heat-treatment to 440°C, but destroyed by heating to 550°C. Identification of mineral species is based on supplementary microprobe analysis.

Kandites. Air dried 7.1 Å (001) peak, unresponsive to glycolation or heat-treatment to 440°C, but destroyed by heating to 550°C. Resistant to acid boiling. Identification of dickite, kaolinite, or nacrite species was attempted for several samples with powder or cavity mounts based on data from Brindley and Brown (1980).

Micas. Air dried 10 Å (001) peak, unresponsive to glycolation or heat treatment.

Smectites. Air dried (001) peak between 14 and 17 Å, expanded to 17 Å on glycolation, and collapsing to 10 Å on heat treatments.

Vermiculites. Air dried 14 Å (001) peak, only slightly affected by glycolation, but contracting through 12 Å and 11 Å towards 10 Å with progressive heating.

Interstratified clay minerals. The only mixed-layer clays encountered in this study were the currently controversial illite-smectite interstratifications (McHardy et al, 1982). In these samples, either a symmetrical 10 Å peak, or



or a discrete saddle occurs between the 10 Å and 14 Å peaks. Those which, on glycolation, generated a small low angle peak of up to 27 Å may be identified as regular interstratifications with a superstructure. However, in the majority of cases in this study, this saddle or asymmetrical peak was reduced by glycolation at 100°C but no other peak generated. These may be either random interstratifications with too little discrete smectite to be detected, or artefacts of sample preparation, resulting from absorbed layers of water as suggested by McHardy *et al*, (1982). Whilst this problem has not been resolved at present, one point which can be made supporting the artefact theory is that a qualitative examination suggests less asymmetric peaks or saddles occur with ceramic tile mounts, that is, with preparations in which water is drawn out of the sample.

Quantification of interstratified illite/smectite percentages does not follow the method of Perry and Hower (1970). In this study percentages of illite and collapsed illite /smectite have been determined following the method of Weir *et al* (1975) and the latter identified as irregularly or regularly interstratified in the presence or absence of a superstructural 27 Å peak.

Representative XRD traces are shown in Fig. I. Whilst interpretation of kandites, illites, chlorites and smectites is unequivocal within the criteria detailed by Brindley and Brown (1980), identification of vermiculite remains problematical. According to Brindley and Brown (1980) and other standard text books, vermiculite should expand on glycolation, and collapse to 10 Å on treating. The mineral here only expands from 13.9 to 14.4 Å on glycolation, although it does collapse on heating, but not to 10 Å. This mineral collapses to 12 Å at 440°C and 11.5 Å at 550°C. As it does not behave as perfect vermiculite it has been suggested that it is an interstratified vermiculite-chlorite. Thus, incomplete collapse on heating is attributed to the presence of chlorite layers (Jeans, pers. comm. 1982). Unfortunately, no superstructure exists here. However,

this does not preclude the possibility that this mineral is irregularly interstratified, hence it collapses towards 10 Å but is propped up by the chlorite. A similar mineral has been reported by Nishiyama *et al* (1978) who describe the incomplete collapse to 11.8 Å of irregularly interstratified chlorite-vermiculite on heating to 450°C. The inferred origin of this mineral is weathering of chlorite. Further support for a weathering interpretation comes from Curtis (pers. comm. 1982), who has observed a similar phenomenon. In addition, whilst by no means quantitative, EDS spectra of vermiculite reveal varying quantities of potassium, and those of chlorite reveal traces of potassium. Thus, neomorphism of chlorite to vermiculite may involve little more than the uptake of potassium.

This identification of irregularly interstratified chlorite-vermiculite is hampered by two things. Firstly, the size of the potassium ion may account for the response of this mineral to expansion or collapse, preventing assimilation of glycol, or collapse of the lattice. Secondly, vermiculite may spontaneously rehydrate on exposure to the atmosphere or on cooling. In the absence of a heated stage it is not, therefore, possible to exclude the possibility that this mineral is pure vermiculite whose behaviour is governed by the presence of potassium as its interlayer cation. Although its inferred origin is also by weathering of chlorite, the process is assumed to be complete.

#### Semi-quantification of XRD Results

Semi-quantification of XRD traces follows the method outlined by Weir *et al* (1975).

The method involves:

Measuring the air dried 7 Å peak				
"	"	"	10 Å	"
"	"	440°C	14 Å	"
"	"	"	10 Å	"
"	"	"	12 Å	"

Calculating the relative intensities of the main clay mineral groups:

Berthierine and Kandites =  $7 \text{ \AA}$  air dried peak / 2.5

Chlorites =  $440 \text{ C } 14 \text{ \AA}$  peak / 2

Vermiculites =  $440 \text{ C } 12 \text{ \AA}$  peak / 2

Micas =  $10 \text{ \AA}$  air dried peak

Smectites =  $440 \text{ C } 10 \text{ \AA}$  peak -  $10 \text{ \AA}$  air dried peak

and adjusting these ratios to percentages of the clay fraction.

#### CATHODOLUMINESCENCE

Luminescence observations of clastic sedimentary rocks were made at the Geologisches Institut, Universität Bern, Switzerland, by Karl Ramsmeier.

Operating conditions and photographic conditions are detailed below:

Machine Type: "Home-made" Hot cathode luminescence microscope

Beam Energy: 30 kV (negative)

Beam Current: 1-3  $\mu\text{A}$

Beam Diameter: 5 mm

Gun Type: Hot cathode

Ambient Gas: air

Working Vacuum: less than  $10^{-5}$  mbar

Standard highly polished thin sections were prepared and coated with aluminium prior to luminescence.

Film Type: Kodak 135/36

Development: equivalent to 800 ASA

Exposure times: 1-3 minutes

Luminescence observations of carbonate sedimentary rocks were made at Nottingham

University on the Cathodoluminiser built by Tony Dickson.

#### SCANNING ELECTRON MICROSCOPY

Samples were mounted on aluminium stubbs, coated with either gold or carbon, and examined at magnifications of up to 10,000x in a Cambridge 600 Scanning Electron Microscope. Qualitative elemental analysis was performed with a Link Systems 860 Energy Dispersive analyser, and recorded graphically.

FIG. 1a REPRESENTATIVE XRD TRACE DEMONSTRATING  
KANDITES, CHLORITE, MICA AND ORDERED MICA/SMECTITE

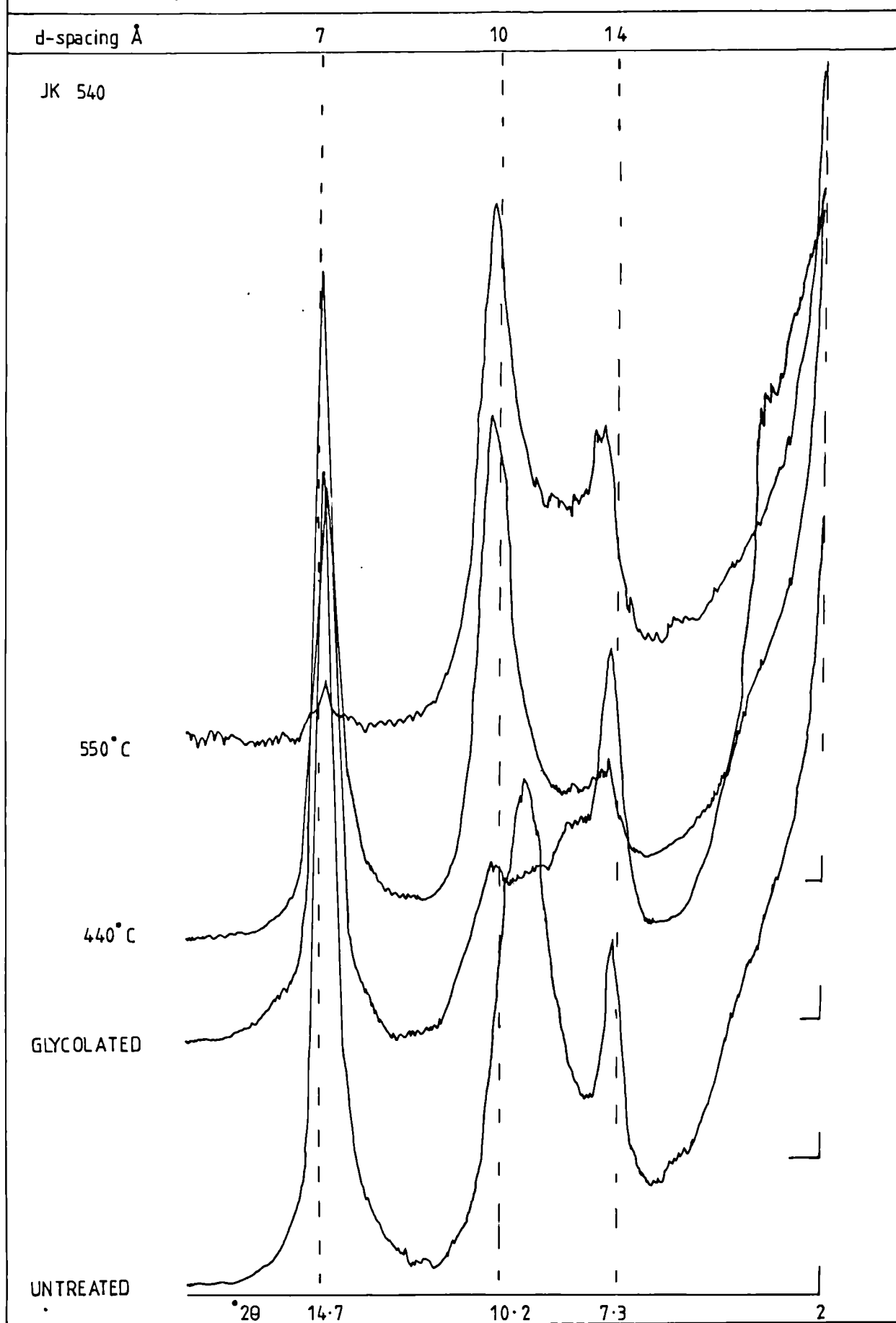


FIG 1b REPRESENTATIVE XRD TRACE DEMONSTRATING  
KANDITES, MICA, AND ?VERMICULITE

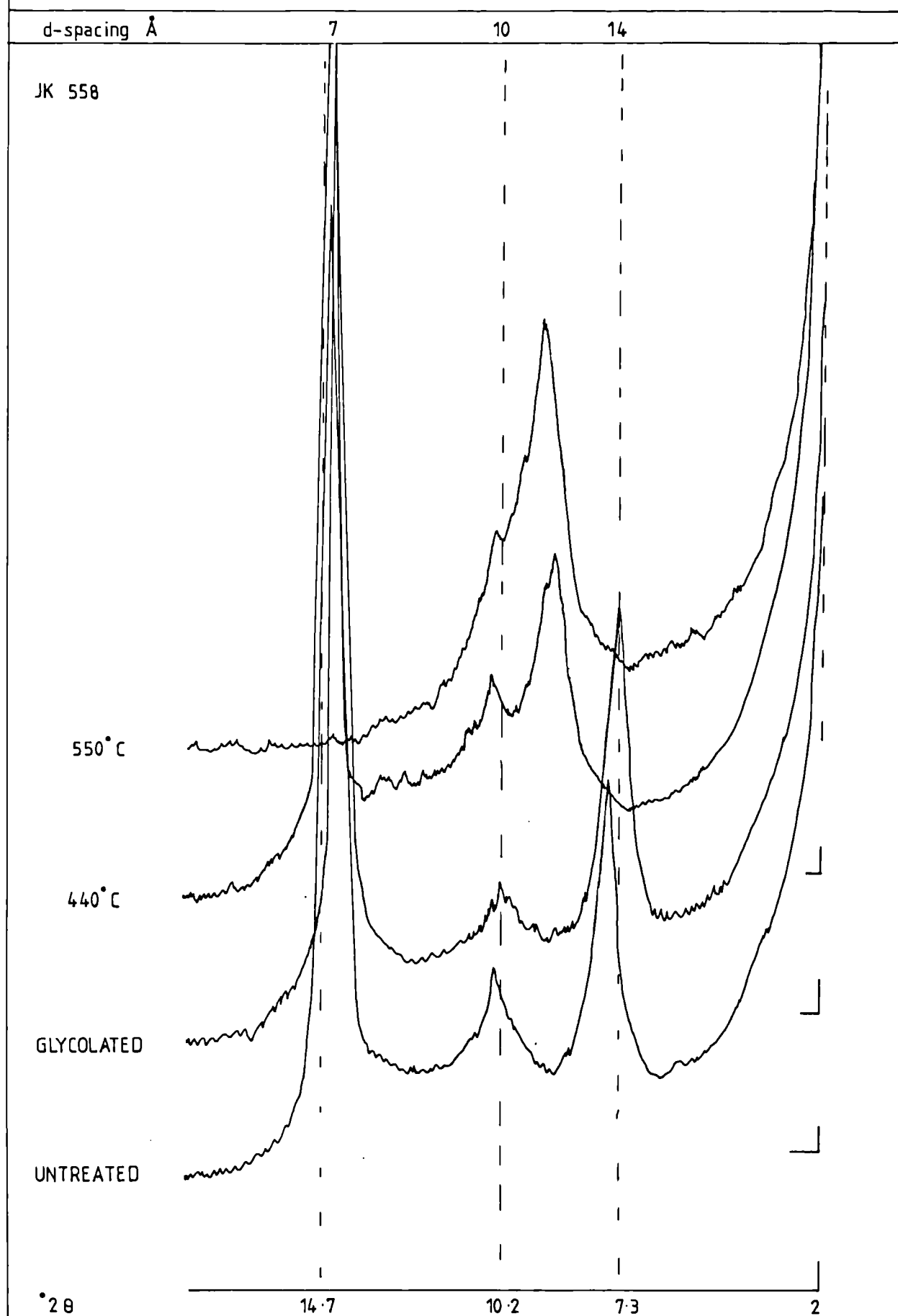
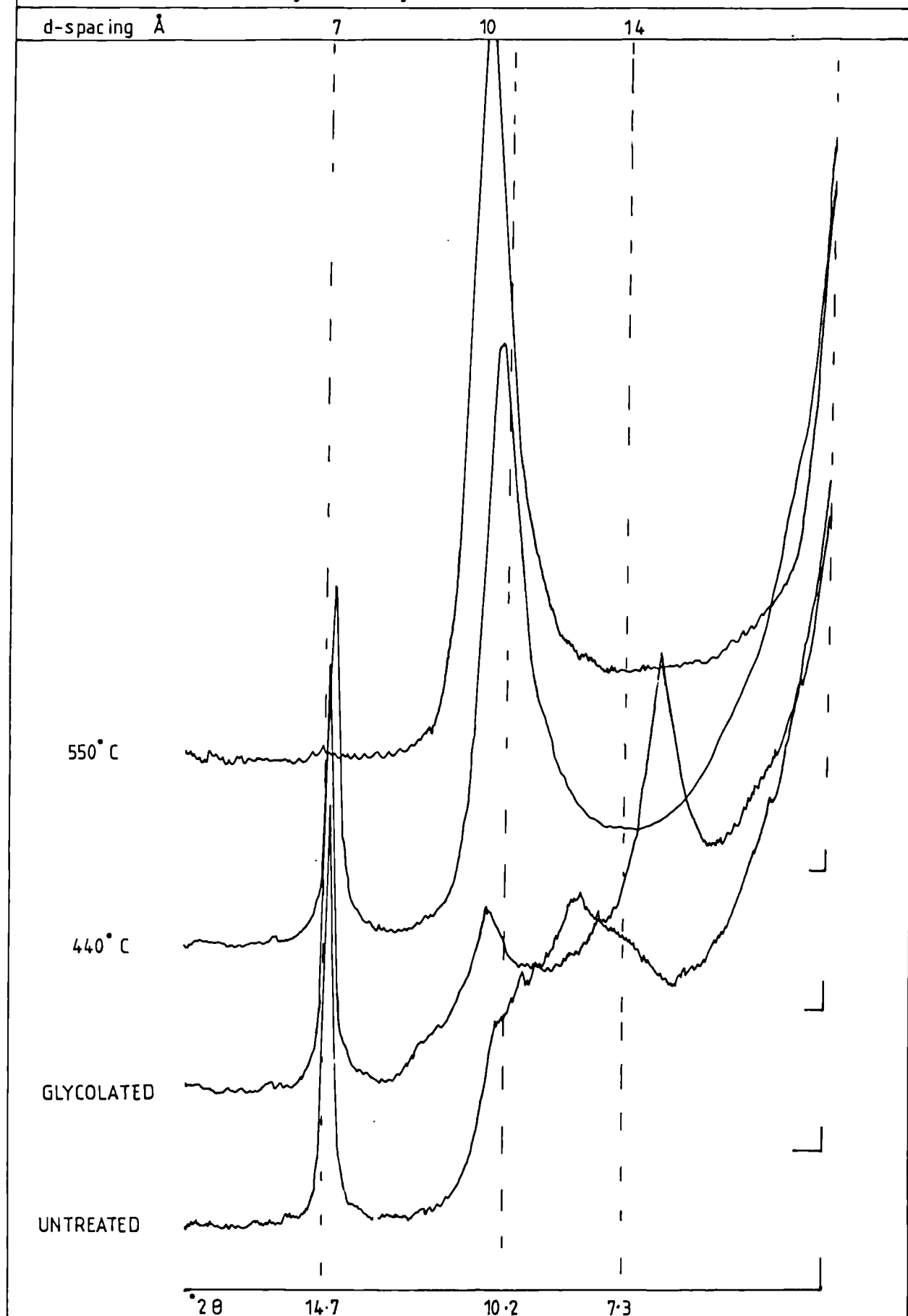


FIG 1c REPRESENTATIVE XRD TRACE DEMONSTRATING  
KANDITES, MICA, AND SMECTITES.



APPENDIX C: MODAL ANALYSIS DATA FROM YORKSHIRE SAMPLES





Sample details Saltwick Formation, crevasse splay sandstones

Sample number	317	320	331	350	358	359	444	552	563	573	577	595	607
Quartz - simple	62	71	70	59	44	59	64	71	70	53	70	63	60
Quartz - polycrystalline	2	2	1	-	2	-	-	1	-	2	-	2	-
Rock Fragments	-	-	-	-	-	-	1	-	1	1	-	2	2
Feldspars	5	-	2	1	-	-	6	5	2	5	2	8	2
Mica	1	3	2	4	1	-	-	-	-	-	2	1	-
Clay matrix	-	6	10	-	-	-	-	-	-	-	-	-	4
Opaque and heavy minerals	-	1	1	-	-	-	-	1	-	-	-	-	-
Fossils (plant debris)													
Chlorites													
Illite					1				4	3		2	
Kandites	5	6	2	7	4		6	3	10	3	11	6	7
Vermiculite								3					
Quartz overgrowths	9	3	4	7	1	14	7	10	6	3	3	4	10
Feldspar overgrowths	-	-	-	-	1	-	1	-	-	-	-	-	-
Calcite													
Siderite (goethite)	8	1	3	21	44	26	7	1	1	28	6	5	1
Ankerite													
Pyrite	-								-				
Intergranular porosity	6	7	5	1	3	1	7	4	5	1	3	5	8
Grain dissolution porosity	2	-	-	-	-	-	-	-	1	-	2	2	6
Total detritus	71	83	86	64	47	59	71	79	73	61	74	76	68
Total authigenics	21	10	9	35	51	40	21	17	21	37	20	17	18
Total porosity	8	7	5	1	3	1	7	4	6	1	5	7	14

Sample details Saltwick Formation, Channel sandstones, Whitby:															Hayburn Wyke:			
Sample number	301	306	309	312	314	316	322	327	332	355	442	445						
Quartz - simple	67	53	64	63	66	63	58	54	56	61	52	58						
Quartz - polycrystalline	5	2	3	1	2	3	3	8	1	4	7	4						
Rock Fragments	-	1	1	1	-	-	-	-	-	-	-	1						
Feldspars	2	4	1	6	2	3	4	3	3	4	7	3						
Mica	-	-	-	1	-	-	-	-	-	-	-	-						
Clay matrix	-	-	-	-	1	-	-	-	2	1	-	-						
Opaque and heavy minerals	-	-	-	1	1	-	1	-	1	-	-	1						
Fossils (plant debris)	-	-	-	-	-	-	-	-	-	-	-	-						
Chlorites																		
Illite		3	1		-	1	1			1								
Kandites	11	9	14	8	8	9	10	4	11	8	4	3						
Vermiculite																		
Quartz overgrowths	3	5	2	6	1	2	1	3	2	4	5	7						
Feldspar overgrowths	-	-	-	-	-	-	-	-	-	-	-	-						
Calcite									19									
Siderite (goethite)	-	6	-	2	-	4	14	12	4	3	11	7						
Ankerite																		
Pyrite																		
Intergranular porosity	5	13	13	11	18	13	7	14	-	11	11	16						
Grain dissolution porosity	6	3	1	1	1	4	1	4	-	4	3	3						
Total detritus	75	61	69	72	72	67	66	65	64	70	66	67						
Total authigenics	14	23	17	16	9	16	26	19	36	16	20	14						
Total porosity	11	16	14	12	19	17	8	18		15	14	19						





Sample details Yons Nab Beds, Interdistributary bay-fill:										Tidal bar:				
Sample number	202	203	205	375	379	226	232							
Quartz - simple	57	52	54	47	69	70	60							
Quartz - polycrystalline	-	-			1	-	3							
Rock Fragments	-	-			-	-	-							
Feldspars	1	-	1	3	4	-	1							
Mica	1	1	1	5	1	1	-							
Clay matrix	7	2	1	11	-	1	2							
Opaque and heavy minerals	1	-	1		-	3	-							
Fossils (plant debris)		-		2		-								
Chlorites														
Illite					2									
Kandites				4	3	8	11							
Vermiculite														
Quartz overgrowths				-	5	5	8							
Feldspar overgrowths														
Calcite	31	42	40											
Siderite (goethite)				28	7									
Ankerite														
Pyrite						1								
Intergranular porosity	2	2	2	-	7	11	15							
Grain dissolution porosity					1		1							
Total detritus	66	56	58	68	76	75	66							
Total authigenics	31	42	40	32	17	14	19							
Total porosity	2	2	2	-	8	11	16							

Sample details Cloughton Formation, Channel Sandstones: Floodplain sediments															
Sample number	208	209	233	223	224	620		381	385	390	427	211	383	548	578
Quartz - simple	65	63	64	63	59	61		60	62	72	71	77	71	72	64
Quartz - polycrystalline	-	-	-	-	-	2		1	1	2	1			1	2
Rock Fragments	-	-	-	-	-	-		1	-	-			-	-	-
Feldspars	3	2	1	1	1	7		3	1	1	3	1	2	1	2
Mica	1	1		-	1	-		1	1	1			1		2
Clay matrix	1		1		-					1			4		3
Opaque and heavy minerals	3	6	-	1	-	-		1	-	2					-
Fossils (plant debris)															
Chlorites								4		8			4		
Illite									2						1
Kandites	7	7	7	8	10	2		-	-	1	-	1		3	
Vermiculite														13	4
Quartz overgrowths	8	5	4	7	7	3		19	16	6	4	5	5	6	9
Feldspar overgrowths						-		-							
Calcite															
Siderite (goethite)	2					10		-	1	-	-	-	4	3	8
Ankerite															
Pyrite											-		-		
Intergranular porosity	10	16	22	19	22	13		7	12	6	16	16	8	1	4
Grain dissolution porosity			2			1		2	3		3		1		
Total detritus	73	72	66	66	62	71		67	65	79	75	78	79	74	73
Total authigenics	17	12	11	15	17	15		23	20	15	4	6	13	25	22
Total porosity	10	16	24	19	22	14		9	15	6	19	16	9	1	4





Sample details			Moor Grit Member,				Hundale Point:				Low Moor:				Bloody Beck: NZ (68/09):			
Sample number	472	478	489	494	499	508	650	693	698	701	540	544	584	587	590			
Quartz - simple	72	70	70	73	66	79	74	73	77	68	76	67	70	76	76			
Quartz - polycrystalline	2	3	1	1	2	1	5	3	9	8	-	2	1	1	-			
Rock Fragments	-			1			-	-	-	-	-	-	-	1	-			
Feldspars	-	2	4	2	1		1	2		3	-	-	1	-	1			
Mica	1	1	1		-													
Clay matrix			1		1													
Opaque and heavy minerals	-	-	-	-	-	-	-	-	-	-	-	-	-	-	-			
Fossils (plant debris)																		
Chlorites			-		-					9	7	4	1					
Illite																		
Kandites	1		3	1	2	3	-		4	1	-	1	1	2	-			
Vermiculite																		
Quartz overgrowths	4	5	16	10	1	-	11	12	3	6	12	12	11	13	16			
Feldspar overgrowths							-	-										
Calcite																		
Siderite (goethite)		-	1	-	5		1	-	4	-	1	2						
Ankerite																		
Pyrite										4			-					
Intergranular porosity	17	15	2	10	19	15	8	9	4	2	4	11	11	5	6			
Grain dissolution porosity	2	3		1	3	1	1					2		2				
Total detritus	76	76	77	77	70	80	80	78	86	79	76	69	72	78	77			
Total authigenics	5	5	20	11	8	4	12	12	11	20	20	19	13	15	16			
Total porosity	19	18	2	11	22	16	9	9	4	2	4	13	11	7	6			

Sample details		May Beck:				South of Scarborough.					Long Nab Member, Channels				
Sample number		642	646		243	247	250	255	422		410	413	416	431	434
Quartz - simple		62	69		50	65	67	65	62		73	68	73	62	59
Quartz - polycrystalline		2	1			1						3		1	4
Rock Fragments			-			-									-
Feldspars		3	4			2		-	5		3	2	1	4	5
Mica			-			-		-							-
Clay matrix						4			4						
Opaque and heavy minerals		-	-			1		-	1		-	-	1		
Fossils (plant debris)															
Chlorites															
Illite												1			1
Kandites		5	2			1		1	2				1		
Vermiculite			8												
Quartz overgrowths		6	4			5		6	8		5	8	8	5	7
Feldspar overgrowths															
Calcite						5	32								
Siderite (goethite)		8	2		48		1	9				7	-	2	-
Ankerite															
Pyrite					2										
Intergranular porosity		12	9			14		17	16		18	7	15	21	18
Grain dissolution porosity		2	1			1						2		5	5
Total detritus		67	74		50	74	67	66	72		76	73	75	67	69
Total authigenics		19	16		50	11	33	16	10		5	16	9	7	8
Total porosity		14	10			15		17	16		18	9	15	26	23

Sample details		Channels continued										Crevasse splays.				
Sample number		436	450	460	463	519	502	505	516	452	429	485				
Quartz - simple		61	61	62	57	71	77	73	69	76	68	774				
Quartz - polycrystalline		1	2	3	3	1	-	-	1	2	-					
Rock Fragments		-	-	1	2	-	-	-	-		-					
Feldspars		4	5	4	2	-	-	-	-	6	4	3				
Mica		-	-	1	-	-	-	-	-		1	1				
Clay matrix			10	2	-	-	-	-	-		10	11				
Opaque and heavy minerals			3	-	-	-	-	-	-							
Fossils (plant debris)																
Chlorites																
Illite		4	1		2	3					5					
Kandites			1	1	4	1	-		1	1						
Vermiculite																
Quartz overgrowths		5	4	5	7	3	8	4	11	7	3	1				
Feldspar overgrowths																
Calcite																
Siderite (goethite)		2		8	3	4	1			-	2	1				
Ankerite																
Pyrite																
Intergranular porosity		20	10	9	13	12	14	23	19	3	4	6				
Grain dissolution porosity		2	2	4	7	3	1			3		2				
Total detritus		66	81	73	65	73	77	73	70	84	84	87				
Total authigenics		11	6	14	16	11	9	4	12	10	11	4				
Total porosity		22	12	13	20	15	15	23	19	6	4	8				

## APPENDIX D: MICROPROBE ANALYSIS OF SAMPLES FROM YORKSHIRE

Notes

Sample numbers. These refer to samples collected by the author, with the exception of the two provided by Professor Hemingway. These are JEHD and JEHR from the Dogger Formation at Cold Moor and the Rosedale Oolite/magnetite respectively.

Codes. The following codes are used

Column A: M Micas

I Illitic clay

C Chlorite

K Kandites

N Neomorphosing micas <sup>1</sup>

B Berthierine

G "

F Feldspar

carbonates are generally

C Calcite <sup>2</sup>

S Siderite

1 Codes for neomorphosing micas include both the general scheme with stratigraphical and environmental codes as well as specific codes NO1, NO2 etc which refer to the specific flake of mica. Spot numbers for these micas record individual analyses on each flake.

2 Sample 201 has the following third column codes:

R Isopachous rim cement

I Intragranular pore-filling cement

B Blocky, sparry pore-filling cement

P Pyrite

A Apatite

Column B: A Long Nab Member

B Moor Grit Member

C Scarborough Formation

D Gristhorpe/Cloughton

E Yons Nab Beds

F Saltwick Formation

G Dogger Formation

Column C: C Channels

O Overbank sands

M Meander Belt (Long Nab Member)

N Normal Moor Grit

U Moor Grit south of Scarborough

T Tidal sands

B Beach

S Shallow marine sands

P Pebble lag conglomerate - basal Dogger Formation

Spot numbers. These generally refer to different spots on different grains, or in different pores full of clays. However, where sequences number from, for example, 11 to 15 and 21 to 24 etc, these numbers refer to spots on the same grains. These sequences are most significant in berthierine ooliths and siderite spheruliths where they generally number from the centres outwards.

MICAS

Sample Code	394 NCT 21	394 NCT 22	394 NCT 23	934 NCT 24	394 NCT 31	394 NCT 32	672 NDO 41	672 NDO 81	672 NDO 82	672 NDO 83	672 NDO 84	672 NDO 91	672 NDO 92	672 NDO 93	672 NDO 101	690 NDO 21	690 NDO 22	690 NDO 23
SiO2	44.79	45.87	45.28	47.09	41.81	43.23	45.14	38.51	42.32	25.44	37.15	44.08	45.98	47.16	41.16	37.50	33.23	35.21
TiO2	0.33	n.d.	0.52	n.d.	n.d.	n.d.	0.55	n.d.	0.28	n.d.	n.d.	0.56	0.35	0.56	n.d.	n.d.	n.d.	0.42
Al2O3	29.58	37.44	33.46	36.68	31.99	33.24	30.56	23.41	24.12	17.17	22.72	33.01	33.67	34.97	29.06	18.07	16.61	18.26
FeO	0.84	n.d.	0.75	0.83	0.38	0.98	4.02	2.67	1.60	2.10	2.17	1.03	1.00	1.04	0.87	19.65	17.30	13.09
MgO	1.57	n.d.	0.54	0.58	n.d.	0.57	1.35	1.66	2.27	0.38	1.50	0.93	0.97	0.69	0.76	2.24	3.60	6.25
MnO	n.d.	n.d.	n.d.	n.d.	n.d.	n.d.	n.d.	n.d.	n.d.	n.d.	n.d.	n.d.	n.d.	n.d.	n.d.	n.d.	n.d.	n.d.
CaO	0.16	0.15	n.d.	0.33	0.20	0.16	n.d.	0.20	0.20	0.21	n.d.	n.d.	n.d.	n.d.	0.17	0.93	0.98	0.88
Na2O	1.56	n.d.	0.91	2.73	0.38	0.85	0.65	n.d.	n.d.	n.d.	n.d.	1.74	1.41	0.97	0.54	n.d.	n.d.	n.d.
K2O	7.87	0.12	6.62	3.58	0.69	4.47	10.06	6.47	8.07	2.28	6.20	9.09	9.00	8.18	6.04	0.79	0.74	1.17
TOTAL	66.70	83.58	88.08	91.82	75.45	83.50	92.35	72.92	78.86	47.58	69.74	90.44	92.38	93.57	78.60	79.18	72.46	75.28

Recalculated formula on the basis of 22 oxygens

Si	6.478	6.380	6.344	6.240	6.500	6.309	6.302	6.647	6.757	6.566	6.673	6.173	6.267	6.287	6.463	6.434	6.239	6.183
AlIV	1.522	1.620	1.656	1.754	1.560	1.691	1.698	1.353	1.243	1.434	1.327	1.827	1.733	1.713	1.537	1.566	1.761	1.817
AlVI	3.520	4.518	3.869	3.980	4.361	4.027	3.333	3.410	3.296	3.789	3.484	3.622	3.676	3.780	3.841	2.089	1.914	1.962
Fe2	6.102	0.000	0.068	0.092	0.049	0.120	0.469	0.385	0.214	0.453	0.326	0.121	0.114	0.116	0.114	2.820	2.716	1.922
Mg	0.338	0.000	0.113	0.115	0.000	0.124	0.281	0.427	0.540	0.146	0.402	0.194	0.197	0.137	0.178	0.573	1.007	1.636
Mn	0.000	0.000	0.000	0.000	0.000	0.000	0.000	0.000	0.000	0.000	0.000	0.000	0.000	0.000	0.000	0.000	0.000	0.000
Ca	0.025	0.022	0.000	0.047	0.033	0.025	0.000	0.037	0.034	0.058	0.000	0.000	0.000	0.000	0.029	0.171	0.197	0.166
Na	0.437	0.000	0.247	0.762	0.115	0.241	0.176	0.000	0.000	0.000	0.000	0.472	0.373	0.251	0.164	0.000	0.000	0.000
K	1.452	0.021	1.183	0.606	0.137	0.632	1.791	1.425	1.644	0.751	1.421	1.624	1.565	1.391	1.210	0.173	0.177	0.262

Total aluminum

Al	5.042	6.138	5.525	5.734	5.861	5.718	5.031	4.762	4.539	5.223	4.810	5.448	5.409	5.494	5.378	3.654	3.675	3.779
----	-------	-------	-------	-------	-------	-------	-------	-------	-------	-------	-------	-------	-------	-------	-------	-------	-------	-------

Sample Code	690 NDO 24	690 NDO 25	690 NDO 26	690 NDO 41	690 NDO 42	690 NDO 43	548 NDO 91	206 NDO 41	206 NDO 42	206 NDO 51	206 NDO 52	206 NDO 53	206 NDO 54	206 NDO 55	683 NDO 131	606 NDO 13	606 NDO 14	606 NDO 16
SiO2	34.20	33.03	29.51	33.66	40.32	44.92	48.96	44.71	41.60	42.74	44.07	46.92	43.77	42.02	45.95	38.13	24.39	47.06
TiO2	0.22	0.00	n.d.	n.d.	n.d.	n.d.	0.55	0.97	0.87	1.12	1.56	1.84	1.55	1.31	n.d.	0.46	0.75	0.32
Al2O3	17.23	15.59	13.75	23.20	29.71	32.45	28.53	33.83	30.56	26.63	23.52	24.82	24.26	21.88	30.40	19.39	11.84	31.14
FeO	16.00	20.56	17.21	1.14	1.52	1.08	2.73	1.75	1.51	4.79	5.86	6.04	4.96	5.33	5.36	5.91	4.46	1.27
MgO	3.39	2.04	2.10	0.49	0.42	0.43	2.75	0.73	0.63	1.46	1.95	2.26	1.83	1.89	1.53	1.75	1.26	2.43
MnO	n.d.	n.d.	n.d.	n.d.	n.d.	n.d.	0.24	n.d.	0.29	n.d.	n.d.	n.d.	n.d.	n.d.	n.d.	n.d.	n.d.	n.d.
CaO	0.94	0.85	0.77	0.19	n.d.	0.23	n.d.	n.d.	n.d.	n.d.	n.d.	n.d.	n.d.	n.d.	n.d.	n.d.	0.17	n.d.
Na2O	n.d.	n.d.	n.d.	0.30	0.86	0.74	0.50	0.48	0.36	0.36	0.35	0.47	0.27	0.26	n.d.	n.d.	n.d.	n.d.
K2O	1.23	0.39	0.54	5.90	6.64	7.09	10.77	6.89	5.24	8.38	10.81	10.76	8.78	9.55	10.82	9.01	5.48	10.79
TOTAL	73.21	72.46	63.88	64.88	79.47	86.94	95.03	89.36	81.00	85.48	88.12	92.91	85.42	82.24	94.06	74.65	48.36	93.01

Recalculated formula on the basis of 22 oxygens

Si	6.301	6.318	6.364	6.480	6.330	6.407	6.603	6.222	6.331	6.435	6.591	6.620	6.618	6.684	6.345	6.736	6.696	6.422
AlIV	1.699	1.682	1.636	1.520	1.670	1.593	1.397	1.778	1.669	1.565	1.409	1.380	1.382	1.316	1.655	1.264	1.304	1.578
AlVI	2.042	1.832	1.858	3.744	3.828	3.862	3.138	3.776	3.801	3.161	2.736	2.748	2.942	2.786	3.293	2.774	2.528	3.430
Fe2	2.465	3.289	3.104	0.184	0.200	0.129	0.308	0.204	0.192	0.603	0.733	0.713	0.627	0.709	0.619	0.873	1.024	0.145
Mg	0.931	0.582	0.675	0.141	0.098	0.091	0.553	0.151	0.143	0.328	0.435	0.475	0.412	0.446	0.315	0.461	0.518	0.493
Mn	0.000	0.000	0.000	0.000	0.000	0.000	0.027	0.000	0.037	0.000	0.000	0.000	0.000	0.000	0.000	0.000	0.000	0.000
Ca	0.186	0.174	0.178	0.039	0.060	0.035	0.060	0.060	0.060	0.000	0.000	0.000	0.000	0.000	0.000	0.000	0.051	0.000
Na	0.000	0.000	0.000	0.112	0.262	0.205	0.131	0.130	0.106	0.105	0.101	0.129	0.079	0.080	0.006	0.000	0.000	0.000
K	0.289	0.095	0.149	1.449	1.330	1.290	1.853	1.223	1.017	1.609	2.062	1.937	1.693	1.938	1.906	2.029	1.918	1.879

Total aluminum

Al	3.741	3.515	3.495	5.264	5.497	5.455	4.535	5.548	5.470	4.725	4.146	4.127	4.323	4.102	4.948	4.038	3.832	5.008
----	-------	-------	-------	-------	-------	-------	-------	-------	-------	-------	-------	-------	-------	-------	-------	-------	-------	-------

Sample Code	666	666	666	666	666	666	677	677	677	355	355	355	609	609	476	470	470	470	470	470	470
Spot	NFC	NFC	NFC	NFC	NFC	NFC	NFC	NFC	NFC	NFC	NFC	NFC	N6S	N6S	NDO	NDO	NDO	NDO	NDO	N6U	N6U
Spot	20	21	23	24	31	34	4	5	6	16	17	20	2	3	11	12	13	14	15	16	21
S102	45.85	43.39	43.05	42.98	45.17	42.87	45.85	37.81	43.83	43.60	45.90	45.69	47.04	23.98	45.77	45.04	44.05	45.14	45.23	44.69	45.66
T102	n.d.	n.d.	0.68	0.68	n.d.	0.54	0.40	n.d.	n.d.	0.93	1.44	0.50	0.41	0.25	0.60	n.d.	0.27	n.d.	n.d.	n.d.	n.d.
AL203	32.03	30.14	25.04	24.93	30.45	29.13	31.05	24.08	27.80	28.51	33.00	34.39	27.66	13.79	35.06	35.76	33.48	37.78	37.03	36.36	34.12
FeO	3.81	5.17	6.04	6.32	2.28	4.12	3.47	8.96	6.94	5.45	1.46	1.40	3.26	1.64	0.86	0.56	0.68	n.d.	0.25	n.d.	1.29
MO	0.69	0.86	1.52	1.54	1.17	1.25	0.99	1.44	1.28	1.58	1.06	0.79	1.93	0.99	0.46	n.d.	0.37	n.d.	n.d.	n.d.	0.53
MAO	n.d.	n.d.	n.d.	n.d.	n.d.	n.d.	n.d.	n.d.	n.d.	n.d.	n.d.	n.d.	n.d.	n.d.	n.d.	n.d.	n.d.	n.d.	n.d.	n.d.	n.d.
CAO	n.d.	n.d.	n.d.	n.d.	n.d.	n.d.	0.19	0.20	0.19	n.d.	n.d.	n.d.	n.d.	n.d.	n.d.	n.d.	n.d.	n.d.	n.d.	0.15	n.d.
MA2O	n.d.	0.36	0.28	n.d.	n.d.	0.45	0.73	0.68	n.d.	0.84	0.78	1.67	n.d.	n.d.	1.68	1.08	0.92	n.d.	n.d.	n.d.	0.83
K2O	10.60	10.55	10.01	10.36	8.97	8.80	4.45	3.93	5.02	9.90	10.26	8.85	10.72	5.45	8.59	5.25	6.02	0.67	0.74	0.23	6.63
TOTAL	93.17	90.47	86.02	86.82	88.04	87.16	87.12	77.10	85.06	90.82	93.91	93.29	91.01	46.11	93.02	87.69	85.79	83.59	82.25	81.43	89.28

Recalculated formula on the basis of 22 oxygens

Si	6.327	6.249	6.515	6.510	6.472	6.313	6.495	6.340	6.519	6.267	6.218	6.184	6.633	6.675	6.180	6.265	6.312	6.305	6.354	6.366	6.349
Aliv	1.673	1.751	1.465	1.490	1.528	1.687	1.505	1.660	1.481	1.733	1.782	1.816	1.367	1.325	1.820	1.735	1.668	1.695	1.646	1.614	1.651
Alv1	3.537	3.365	2.981	2.950	3.614	3.368	3.679	3.098	3.391	3.097	3.486	3.669	3.229	3.198	3.759	4.127	3.965	4.525	4.485	4.505	3.914
FE2	0.439	0.623	0.765	0.801	0.273	0.507	0.410	1.256	0.863	0.655	0.165	0.152	0.384	0.383	0.097	0.665	0.081	0.000	0.029	0.006	0.149
MO	0.142	0.185	0.343	0.348	0.251	0.273	0.208	0.360	0.284	0.339	0.214	0.160	0.406	0.411	0.093	0.000	0.079	0.000	0.000	0.000	0.105
MA	0.000	0.000	0.000	0.000	0.000	0.000	0.000	0.000	0.000	0.000	0.000	0.000	0.000	0.000	0.000	0.000	0.000	0.000	0.000	0.000	0.000
CA	0.000	0.000	0.000	0.000	0.000	0.000	0.028	0.036	0.030	0.000	0.000	0.000	0.000	0.000	0.000	0.000	0.000	0.000	0.000	0.000	0.000
MA	0.000	0.101	0.082	0.006	0.000	0.129	0.201	0.222	0.000	0.235	0.205	0.438	0.000	0.000	0.440	0.291	0.256	0.000	0.000	0.000	0.223
K	1.901	1.938	1.933	2.001	1.640	1.653	0.805	0.840	0.952	1.816	1.774	1.529	1.927	1.934	1.480	0.932	1.100	0.119	0.132	0.042	1.176

Total aluminum

AL	5.205	5.110	4.460	4.450	5.142	5.055	5.183	4.758	4.872	4.836	5.268	5.466	4.596	4.523	5.579	5.662	5.654	6.220	6.131	6.122	5.565
----	-------	-------	-------	-------	-------	-------	-------	-------	-------	-------	-------	-------	-------	-------	-------	-------	-------	-------	-------	-------	-------

Sample Code	Spot	470 NDO	470 NDO	470 NDO	470 NDO	470 NDO	470 NDO	470 NDO	470 NDO	613 NFC	613 NFC	613 NFC	613 NFC	613 NFC	613 NFC	613 NFC	613 NFC	613 NFC	613 NFC	613 NFC
Spot	22	51	52	111	121	121	181	182	183	41	141	142	143	144	145	161	162	171	172	191
S102	45.03	44.81	44.74	46.47	44.84	45.16	45.42	45.12	45.73	44.65	43.35	37.68	44.04	15.79	42.02	44.93	38.57	45.05	45.74	44.67
T102	n.d.	n.d.	0.00	0.50	n.d.	n.d.	n.d.	n.d.	0.45	0.53	n.d.	n.d.	n.d.	n.d.	n.d.	0.49	n.d.	1.36	1.15	0.81
AL2O3	36.21	36.75	36.58	26.57	34.09	35.25	30.16	36.69	34.81	26.73	35.23	30.42	36.19	10.86	29.12	34.85	27.05	27.09	26.69	31.66
FeO	0.79	n.d.	0.32	521.00	1.57	0.44	2.08	n.d.	0.87	5.96	n.d.	0.38	n.d.	1.59	4.75	0.86	0.90	5.12	5.32	3.40
MO	n.d.	n.d.	n.d.	2.00	0.43	0.29	1.63	n.d.	0.53	1.36	n.d.	n.d.	n.d.	0.22	0.55	0.68	0.79	1.93	2.20	0.76
MAO	n.d.	n.d.	0.23	n.d.	n.d.	n.d.	n.d.	n.d.	n.d.	n.d.	n.d.	n.d.	n.d.	n.d.	n.d.	n.d.	n.d.	n.d.	n.d.	n.d.
CAO	n.d.	n.d.	n.d.	n.d.	n.d.	n.d.	n.d.	n.d.	n.d.	n.d.	n.d.	n.d.	n.d.	0.16	0.25	n.d.	n.d.	n.d.	n.d.	n.d.
MA2O	n.d.	n.d.	0.96	n.d.	0.95	0.34	3.00	n.d.	0.64	n.d.	n.d.	n.d.	n.d.	n.d.	0.55	1.12	0.56	0.32	0.37	1.07
K2O	2.76	1.46	3.58	11.04	6.95	2.40	8.89	0.69	6.55	11.04	0.16	0.23	0.20	1.41	6.65	6.36	5.77	10.47	10.85	9.37
TOTAL	85.39	83.02	86.35	607.58	88.83	83.62	91.18	82.50	89.58	92.27	76.74	68.71	80.43	30.03	63.89	89.29	73.64	91.34	92.32	91.76

Recalculated formula on the basis of 22 oxygens

Si	6.306	6.339	6.239	1.743	6.273	6.358	6.368	6.382	6.288	6.340	6.397	6.396	6.366	6.492	6.360	6.214	6.472	6.428	6.475	6.238
Aliv	1.634	1.661	1.761	1.175	1.727	1.602	1.632	1.618	1.712	1.660	1.603	1.604	1.634	1.508	1.640	1.786	1.528	1.572	1.525	1.762
Alv1	4.320	4.466	4.251	0.000	3.894	4.283	3.352	4.498	3.930	3.148	4.524	4.482	4.532	3.755	3.555	3.894	3.821	2.984	2.929	3.451
FE2	0.092	0.090	0.037	16.347	0.184	0.052	0.244	0.000	0.160	0.708	0.000	0.054	0.060	0.547	0.601	0.099	0.126	0.611	0.630	0.397
MO	0.000	0.000	0.000	0.112	0.090	0.061	0.341	0.000	0.109	0.288	0.000	0.000	0.000	0.135	0.124	0.140	0.198	0.410	0.464	0.158
MA	0.000	0.000	0.027	0.000	0.000	0.000	0.000	0.000	0.000	0.000	0.000	0.000	0.000	0.000	0.000	0.000	0.000	0.000	0.000	0.000
CA	0.000	0.000	0.000	0.000	0.000	0.000	0.000	0.000	0.000	0.000	0.000	0.000	0.000	0.070	0.041	0.000	0.000	0.000	0.000	0.000
MA	0.000	0.000	0.243	0.000	0.258	0.093	0.816	0.000	0.171	0.000	0.000	0.096	0.000	0.000	0.160	0.300	0.162	0.085	0.102	0.290
K	0.491	0.263	0.637	0.526	1.240	0.434	1.590	0.124	1.149	2.000	0.030	0.050	0.037	0.740	1.284	1.122	1.235	1.906	1.959	1.669

Total aluminum

AL	5.954	6.127	6.012	1.175	5.621	5.685	4.964	6.116	5.641	4.806	6.127	6.066	6.166	5.263	5.195	5.666	5.349	4.556	4.453	5.214
----	-------	-------	-------	-------	-------	-------	-------	-------	-------	-------	-------	-------	-------	-------	-------	-------	-------	-------	-------	-------

Sample Code Spot	613 MFC 211	613 MFC 212	613 MFC 213	613 MFC 214	431 MAC 31	431 MAC 32	431 MAC 61	431 MAC 71	254 MPN 11	254 MPN 12	254 MPN 21	254 MPN 22	254 MPN 31	254 MPN 32	254 MPN 41	254 MPN 42	254 MPN 61	254 MPN 62	254 MPN 63	254 MPN 71	254 MPN 72
S102	42.94	39.15	43.30	45.54	44.08	44.46	45.24	45.96	45.59	42.82	43.97	44.93	46.66	47.56	45.97	45.76	46.21	46.64	47.06	42.16	43.34
T102	n.d.	0.36	n.d.	n.d.	n.d.	0.34	0.67	0.81	0.98	0.70	0.88	1.06	0.86	0.97	0.53	0.75	0.50	0.29	0.49	1.13	1.13
AL203	33.79	31.10	33.79	36.92	33.00	33.68	35.52	30.62	33.62	28.84	32.93	33.31	26.71	23.30	33.75	35.09	31.31	29.26	32.49	27.86	29.32
FE2	1.60	1.92	1.84	n.d.	2.26	2.25	1.34	2.46	3.01	3.86	2.32	2.79	5.76	1.13	0.86	2.26	2.26	2.30	3.52	3.35	
MG0	n.d.	0.40	n.d.	0.22	0.34	0.44	0.92	1.37	0.53	1.12	0.57	0.58	2.62	2.89	0.87	0.66	1.12	1.94	1.51	1.22	1.15
MNO	n.d.	n.d.	n.d.	n.d.	n.d.	n.d.	n.d.	n.d.	n.d.	n.d.	n.d.	n.d.	n.d.	n.d.	n.d.	n.d.	n.d.	n.d.	n.d.	n.d.	n.d.
CA0	n.d.	n.d.	n.d.	n.d.	n.d.	n.d.	n.d.	n.d.	n.d.	n.d.	n.d.	n.d.	n.d.	n.d.	n.d.	n.d.	n.d.	n.d.	n.d.	n.d.	n.d.
NA2O	1.09	1.21	0.94	n.d.	1.97	1.90	0.83	1.09	0.64	0.43	0.58	0.97	n.d.	n.d.	0.64	0.46	0.55	0.66	0.92	0.45	n.d.
K2O	6.72	7.69	6.43	0.42	8.35	8.34	9.58	8.99	9.26	6.42	8.30	9.79	11.08	10.24	10.04	8.46	7.90	8.36	8.24	10.06	9.17
TOTAL	86.14	81.83	86.30	83.10	90.00	91.41	94.10	91.30	93.63	84.19	89.55	93.43	93.69	91.80	92.93	92.04	89.85	89.40	92.01	86.42	87.46
Recalculated formula on the basis of 22 oxygens																					
Si	6.203	6.061	6.231	6.384	6.211	6.164	6.080	6.393	6.194	6.405	6.196	6.150	6.513	6.780	6.256	6.206	6.448	6.570	6.367	6.314	6.222
ALIV	1.797	1.939	1.769	1.616	1.789	1.836	1.920	1.607	1.806	1.595	1.804	1.850	1.487	1.220	1.744	1.794	1.552	1.430	1.637	1.666	1.666
ALVI	3.956	3.736	3.961	4.483	3.691	3.668	3.707	3.413	3.578	3.489	3.665	3.524	2.906	2.694	3.669	3.814	3.598	3.427	3.547	3.231	3.381
FE2	0.193	0.249	0.221	0.000	0.266	0.261	0.151	0.286	0.342	0.483	0.273	0.319	0.672	0.815	0.129	0.098	0.264	0.266	0.260	0.441	0.400
MG	0.000	0.092	0.000	0.046	0.071	0.091	0.184	0.284	0.107	0.250	0.120	0.118	0.545	0.614	0.176	0.133	0.233	0.407	0.304	0.277	0.25
MN	0.000	0.000	0.000	0.000	0.000	0.000	0.000	0.000	0.000	0.000	0.000	0.000	0.000	0.000	0.000	0.000	0.000	0.000	0.000	0.000	0.000
CA	0.000	0.000	0.000	0.000	0.000	0.000	0.000	0.000	0.000	0.000	0.000	0.000	0.000	0.000	0.000	0.000	0.000	0.000	0.000	0.000	0.000
NA	0.305	0.363	0.262	0.000	0.538	0.511	0.216	0.294	0.169	0.125	0.158	0.257	0.090	0.000	0.169	0.121	0.149	0.180	0.247	0.131	0.000
K	1.278	1.519	1.180	0.075	1.501	1.475	1.642	1.595	1.605	1.225	1.492	1.709	1.973	1.862	1.747	1.463	1.406	1.510	1.427	1.926	1.706
Total aluminium																					
AL	5.753	5.675	5.731	6.000	5.480	5.504	5.626	5.020	5.383	5.094	5.469	5.374	4.394	3.915	5.413	5.608	5.140	4.858	5.180	4.917	5.040

Sample Code Spot	254 MPN 81	254 MPN 82	254 MPN 101	254 MPN 111	254 MPN 112	254 MPN 121	254 MPN 122	254 MPN 151	254 MPN 152	254 MPN 171	254 MPN 172	254 MPN 173
S102	43.75	44.48	45.57	45.69	39.54	63.68	61.88	44.93	40.41	42.45	46.20	48.69
T102	1.10	0.78	0.65	0.77	0.80	n.d.	0.00	1.02	0.89	0.32	0.30	0.61
AL203	28.35	26.14	31.99	28.63	26.03	18.38	17.47	25.02	23.77	30.45	27.24	25.65
FE2	4.22	5.06	2.79	5.84	3.10	n.d.	n.d.	4.04	3.98	2.26	3.37	3.74
MG0	1.25	1.89	1.13	1.58	1.22	n.d.	n.d.	2.22	1.69	0.67	0.82	0.87
MNO	n.d.	n.d.	n.d.	n.d.	n.d.	n.d.	n.d.	n.d.	0.23	n.d.	n.d.	n.d.
CA0	n.d.	n.d.	n.d.	n.d.	n.d.	n.d.	n.d.	n.d.	n.d.	n.d.	n.d.	n.d.
NA2O	n.d.	n.d.	0.28	n.d.	0.41	0.40	0.42	n.d.	n.d.	0.30	0.36	n.d.
K2O	7.68	7.86	6.98	10.51	9.59	16.55	16.05	9.35	8.07	8.12	9.78	9.57
TOTAL	86.35	86.21	88.49	93.02	80.69	99.01	95.82	86.58	79.03	84.57	88.16	86.13
Recalculated formula on the basis of 22 oxygens												
Si	6.435	6.594	6.392	6.399	6.339	8.203	8.236	6.666	6.568	6.329	6.708	6.948
ALIV	1.565	1.496	1.608	1.601	1.661	0.000	0.000	1.334	1.432	1.671	1.292	1.057
ALVI	3.350	3.161	3.681	3.124	3.257	2.790	2.740	3.041	3.121	3.679	3.360	3.262
FE2	0.519	0.627	0.327	0.684	0.416	0.000	0.000	0.501	0.541	0.287	0.408	0.446
MG	0.274	0.418	0.236	0.330	0.292	0.000	0.000	0.491	0.409	0.149	0.177	0.195
MN	0.000	0.000	0.000	0.000	0.000	0.000	0.000	0.000	0.032	0.000	0.000	0.000
CA	0.000	0.000	0.000	0.000	0.000	0.000	0.000	0.000	0.000	0.000	0.000	0.000
NA	0.000	0.000	0.076	0.000	0.127	0.100	0.108	0.000	0.000	0.067	0.101	0.000
K	1.441	1.486	1.088	1.878	1.961	2.719	2.725	1.770	1.673	1.544	1.808	1.747
Total aluminium												
AL	4.915	4.567	5.289	4.725	4.918	2.790	2.740	4.375	4.553	5.350	4.652	4.314



NEOMORPHOSING MICAS

Sample Code Spot	605 NFC 3	605 NFC 11	605 NFC 12	605 NFC 13	605 NFC 15	605 NFC 19	605 NFC 20	605 NFC 21	605 NFC 22	605 NFC 23	605 NFC 24	605 NFC 26	605 NFC 27	605 NFC 28	605 NFC 29	605 NFC 30	605 NFC 31	605 NFC 34	605 NFC 35
SiO <sub>2</sub>	44.87	46.75	46.16	46.29	46.37	45.28	45.80	44.15	46.64	13.70	39.62	46.72	43.92	44.26	31.55	43.62	44.96	33.71	46.10
TiO <sub>2</sub>	0.32	0.78	0.77	0.82	0.75	0.33	0.46	n.d.	0.49	n.d.	0.76	0.46	0.63	1.04	n.d.	0.27	n.d.	n.d.	n.d.
Al <sub>2</sub> O <sub>3</sub>	34.01	27.09	26.66	26.70	26.49	29.46	26.13	25.36	23.57	6.93	20.92	27.31	25.77	26.86	19.29	21.82	22.96	26.64	26.55
FeO	1.11	5.38	5.56	5.21	5.58	2.29	2.34	2.38	2.05	1.64	6.02	4.63	4.28	4.31	2.90	6.19	6.22	0.58	4.46
MgO	0.55	1.89	1.86	1.93	2.06	1.56	2.25	2.22	2.11	0.36	1.44	2.36	2.21	1.78	1.19	1.28	1.21	n.d.	2.26
MnO	n.d.	n.d.	n.d.	n.d.	n.d.	n.d.	n.d.	n.d.	n.d.	n.d.	n.d.	n.d.	n.d.	n.d.	n.d.	n.d.	n.d.	n.d.	n.d.
CaO	n.d.	n.d.	n.d.	n.d.	n.d.	n.d.	0.18	n.d.	n.d.	n.d.	0.18	n.d.	n.d.	n.d.	n.d.	0.23	n.d.	0.62	n.d.
Na <sub>2</sub> O	0.45	n.d.	n.d.	n.d.	n.d.	0.69	0.65	0.46	0.40	n.d.	n.d.	0.45	0.28	0.40	n.d.	n.d.	n.d.	0.23	n.d.
K <sub>2</sub> O	6.99	10.60	10.61	10.86	10.71	9.38	9.02	8.70	7.81	1.54	1.19	10.20	9.31	9.80	7.23	4.93	5.43	0.25	10.70
TOTAL	66.29	92.49	91.65	91.81	91.96	88.99	86.83	83.28	77.27	24.16	70.14	92.13	86.40	88.45	62.17	78.34	86.78	62.03	90.09

Recalculated formula on the basis of 22 oxygens

Si	6.269	6.566	6.558	6.562	6.570	6.468	6.701	6.725	6.676	7.085	6.944	6.557	6.554	6.471	6.548	7.020	7.016	6.396	6.625
Al <sub>IV</sub>	1.711	1.434	1.442	1.438	1.430	1.532	1.299	1.275	1.316	0.915	1.056	1.443	1.446	1.529	1.452	0.980	0.984	1.616	1.375
Al <sub>VI</sub>	3.965	3.051	3.024	3.023	2.994	3.427	3.206	3.276	3.239	3.311	3.267	3.076	3.067	3.100	3.265	3.166	3.238	4.343	3.122
Fe <sup>2+</sup>	0.136	0.631	0.660	0.618	0.661	0.273	0.286	0.304	0.281	0.709	0.883	0.543	0.534	0.527	0.502	0.833	0.812	0.092	0.536
Mg	0.114	0.395	0.399	0.407	0.435	0.333	0.491	0.504	0.516	0.275	0.376	0.493	0.490	0.386	0.368	0.307	0.282	0.060	0.468
Mn	0.003	0.006	0.006	0.006	0.000	0.000	0.000	0.000	0.000	0.000	0.000	0.000	0.000	0.000	0.000	0.000	0.000	0.006	0.006
Ca	0.000	0.000	0.000	0.000	0.000	0.000	0.000	0.000	0.000	0.000	0.034	0.000	0.000	0.000	0.000	0.000	0.000	0.126	0.000
Na	0.123	0.000	0.000	0.000	0.000	0.190	0.185	0.137	0.128	0.000	0.000	0.124	0.082	0.114	0.000	0.000	0.000	0.085	0.000
K	1.250	1.899	1.922	1.935	1.936	1.710	1.684	1.691	1.631	1.015	0.267	1.827	1.772	1.828	1.915	1.013	1.082	0.061	1.966

Total aluminium

Al	5.617	4.465	4.466	4.461	4.424	4.959	4.505	4.553	4.556	4.225	4.323	4.518	4.533	4.629	4.718	4.139	4.222	5.953	4.497
----	-------	-------	-------	-------	-------	-------	-------	-------	-------	-------	-------	-------	-------	-------	-------	-------	-------	-------	-------

Sample Code Spot	605 NFC 36	606 NFC 27	606 NFC 28	606 NFC 29	606 NFC 30	606 NFC 40	606 NFC 41	606 NFC 42	606 NFC 43	306 NFC 1	306 NFC 2	306 NFC 3	306 NFC 4	306 NFC 5	306 NFC 6	306 NFC 1	306 NFC 2	306 NFC 3	306 NFC 4
SiO <sub>2</sub>	47.62	47.40	41.93	42.51	45.28	47.41	32.84	47.72	46.47	39.61	37.86	39.80	37.24	39.23	36.29	38.39	41.21	40.46	40.25
TiO <sub>2</sub>	n.d.	0.71	0.40	n.d.	0.34	n.d.	n.d.	n.d.	n.d.	0.32	0.28	0.36	n.d.	n.d.	n.d.	0.69	n.d.	0.31	n.d.
Al <sub>2</sub> O <sub>3</sub>	24.77	32.57	31.63	29.56	31.79	31.53	26.27	29.72	36.34	26.95	27.32	28.14	24.77	31.99	31.42	29.42	34.15	32.35	31.99
FeO	5.25	1.75	2.53	2.26	2.46	2.18	1.93	0.86	2.09	1.51	1.22	1.58	1.47	0.27	n.d.	0.80	n.d.	0.37	0.27
MgO	2.07	1.63	0.62	0.51	0.41	0.73	0.79	1.18	1.13	1.13	0.79	0.96	0.86	n.d.	n.d.	0.52	n.d.	0.25	0.34
MnO	n.d.	n.d.	n.d.	n.d.	n.d.	n.d.	n.d.	n.d.	n.d.	n.d.	n.d.	n.d.	n.d.	n.d.	n.d.	n.d.	n.d.	n.d.	n.d.
CaO	n.d.	n.d.	0.26	n.d.	n.d.	n.d.	0.25	n.d.	0.25	n.d.	n.d.	n.d.	n.d.	n.d.	n.d.	n.d.	n.d.	n.d.	0.16
Na <sub>2</sub> O	0.27	1.15	1.19	0.48	0.35	n.d.	0.35	n.d.	n.d.	0.71	0.69	0.73	0.36	n.d.	n.d.	0.95	n.d.	0.57	0.63
K <sub>2</sub> O	9.70	9.23	7.86	7.23	8.33	9.70	6.23	8.87	9.26	8.04	5.19	7.72	6.50	0.16	n.d.	7.75	0.16	4.61	1.82
TOTAL	89.46	94.42	86.42	82.66	88.96	91.55	62.66	88.35	89.54	78.27	73.35	79.33	71.23	71.67	69.71	78.52	75.53	78.91	75.47

Recalculated formula on the basis of 22 oxygens

Si	6.857	6.346	6.155	6.448	6.403	6.533	6.635	6.725	6.546	6.403	6.377	6.331	6.538	6.376	6.375	6.158	6.344	6.239	6.337
Al <sub>IV</sub>	1.142	1.654	1.845	1.552	1.597	1.467	1.365	1.275	1.454	1.597	1.623	1.669	1.462	1.624	1.625	1.842	1.656	1.761	1.663
Al <sub>VI</sub>	3.661	3.485	3.628	3.734	3.706	3.654	3.462	3.661	3.562	3.537	3.800	3.606	3.664	4.504	4.542	3.722	4.540	4.110	4.273
Fe <sup>2+</sup>	0.668	0.196	0.310	0.296	0.291	0.251	0.326	0.101	0.247	0.204	0.171	0.210	0.216	0.037	0.006	0.107	0.060	0.047	0.035
Mg	0.444	0.324	0.136	0.115	0.085	0.145	0.237	0.248	0.237	0.271	0.199	0.233	0.231	0.000	0.000	0.123	0.000	0.057	0.080
Mn	0.000	0.000	0.000	0.000	0.000	0.000	0.000	0.000	0.000	0.000	0.000	0.000	0.000	0.000	0.000	0.000	0.000	0.000	0.000
Ca	0.000	0.000	0.040	0.000	0.000	0.000	0.055	0.000	0.038	0.000	0.000	0.000	0.000	0.000	0.000	0.000	0.000	0.000	0.028
Na	0.075	0.299	0.336	0.141	0.095	0.000	0.137	0.000	0.000	0.221	0.226	0.226	0.122	0.000	0.000	0.296	0.000	0.172	0.191
K	1.782	1.576	1.476	1.399	1.563	1.706	1.605	1.594	1.664	1.658	1.114	1.567	1.456	0.037	0.000	1.586	0.035	0.967	0.367

Total aluminium

Al	4.204	5.139	5.472	5.287	5.297	5.121	4.827	4.936	5.037	5.134	5.423	5.275	5.126	6.126	6.166	5.563	6.196	5.871	5.936
----	-------	-------	-------	-------	-------	-------	-------	-------	-------	-------	-------	-------	-------	-------	-------	-------	-------	-------	-------

Sample Code	355 No3 Spot 1	355 No3 Spot 2	355 No3 Spot 3	355 No3 Spot 4	355 No4 Spot 1	355 No4 Spot 2	355 No4 Spot 3	355 No4 Spot 4	355 No5 Spot 1	355 No5 Spot 2	355 No5 Spot 3	577 No6 Spot 1	577 No6 Spot 2	577 No6 Spot 3	577 No6 Spot 4	577 No6 Spot 5	577 No7 Spot 1	577 No7 Spot 2
S102	44.42	43.60	35.27	46.11	45.90	45.43	44.29	43.58	44.61	44.04	39.97	45.03	42.47	44.66	44.60	46.10	45.61	45.47
T102	0.62	0.93	n.d.	0.97	1.44	n.d.	0.38	n.d.	1.11	0.46	0.40	n.d.	0.42	n.d.	n.d.	n.d.	1.32	1.10
AL203	29.44	26.51	27.75	33.50	33.00	34.44	3.03	35.60	26.27	31.47	30.49	35.15	31.77	35.92	36.62	38.02	25.82	25.38
FeO	4.53	5.45	1.03	0.72	1.46	1.27	1.50	0.22	5.17	1.20	0.78	0.36	2.66	0.62	0.30	n.d.	6.35	6.46
MgO	1.11	1.58	0.07	0.89	1.06	0.54	0.73	n.d.	1.48	1.07	0.48	0.28	0.60	n.d.	n.d.	0.23	1.83	2.02
MnO	n.d.	n.d.	n.d.	n.d.	n.d.	n.d.	n.d.	n.d.	n.d.	n.d.	n.d.	n.d.	n.d.	n.d.	n.d.	n.d.	n.d.	n.d.
CaO	n.d.	n.d.	n.d.	n.d.	n.d.	n.d.	n.d.	n.d.	n.d.	n.d.	n.d.	n.d.	n.d.	n.d.	n.d.	n.d.	n.d.	n.d.
Na2O	0.54	0.84	n.d.	0.74	0.78	0.81	1.50	n.d.	n.d.	1.18	0.85	n.d.	1.16	n.d.	n.d.	n.d.	n.d.	0.43
K2O	10.26	9.90	0.72	6.83	10.26	9.03	8.05	0.49	10.38	8.30	6.35	1.51	7.43	2.22	0.19	n.d.	16.72	16.63
TOTAL	90.87	90.62	64.84	89.76	93.91	91.53	59.48	79.89	91.01	87.72	79.38	82.34	86.50	83.41	81.71	84.36	91.65	91.52

Recalculated formula on the basis of 22 oxygens

Si	6.334	6.267	6.411	6.344	6.216	6.241	9.420	6.367	6.373	6.314	6.249	6.437	6.200	6.349	6.358	6.348	6.527	6.534
Aliv	1.662	1.733	1.589	1.656	1.782	1.759	0.000	1.633	1.627	1.686	1.751	1.563	1.800	1.651	1.642	1.652	1.473	1.466
Alvi	3.280	3.097	4.356	3.776	3.466	3.816	0.759	4.497	3.132	3.632	3.866	4.360	3.665	4.368	4.512	4.519	2.863	2.832
Fe2	0.540	0.655	0.156	0.083	0.165	0.146	0.267	0.026	0.618	0.144	0.103	0.043	0.325	0.073	0.035	0.000	0.760	0.779
Mg	0.235	0.339	0.020	0.183	0.214	0.110	0.231	0.000	0.315	0.229	0.113	0.060	0.130	0.000	0.000	0.048	0.391	0.433
Mn	0.000	0.000	0.000	0.000	0.000	0.000	0.000	0.000	0.000	0.000	0.000	0.000	0.000	0.000	0.000	0.000	0.000	0.000
Ca	0.000	0.000	0.000	0.000	0.000	0.000	0.000	0.000	0.000	0.000	0.000	0.000	0.000	0.000	0.000	0.000	0.000	0.000
Na	0.154	0.235	0.000	0.197	0.205	0.217	0.620	0.000	0.000	0.329	0.258	0.000	0.328	0.000	0.000	0.000	0.000	0.121
K	1.856	1.816	0.167	1.198	1.774	1.582	2.185	0.091	1.892	1.517	1.275	0.276	1.384	0.402	0.034	0.000	1.956	1.949

Total aluminium

AL	4.947	4.830	5.945	5.432	5.268	5.575	0.759	6.130	4.759	5.318	5.617	5.922	5.465	6.019	6.154	6.170	4.355	4.296
----	-------	-------	-------	-------	-------	-------	-------	-------	-------	-------	-------	-------	-------	-------	-------	-------	-------	-------

Sample Code	577 No8 Spot 1	577 No8 Spot 2	577 No8 Spot 3	577 No8 Spot 4	577 No9 Spot 1	577 No9 Spot 2	577 No10 Spot 1	577 No10 Spot 2	577 No10 Spot 3	577 No11 Spot 1	577 No11 Spot 2	577 No11 Spot 3
S102	45.71	46.21	45.50	45.82	46.39	43.56	46.42	46.00	45.63	45.41	45.57	55.56
T102	0.30	n.d.	n.d.	0.27	0.68	n.d.	0.32	0.41	n.d.	0.46	0.38	0.40
AL203	35.86	35.96	37.50	36.50	26.17	22.93	35.93	34.80	37.83	32.40	35.20	25.57
FeO	1.11	1.21	0.34	0.35	4.57	3.61	1.35	1.80	n.d.	2.46	1.43	n.d.
MgO	0.67	0.91	n.d.	0.38	1.93	1.59	0.67	0.83	n.d.	1.22	0.54	n.d.
MnO	n.d.	n.d.	n.d.	n.d.	n.d.	n.d.	n.d.	n.d.	n.d.	n.d.	n.d.	n.d.
CaO	n.d.	n.d.	n.d.	n.d.	n.d.	n.d.	n.d.	n.d.	n.d.	n.d.	n.d.	0.14
Na2O	2.07	1.31	n.d.	0.40	0.54	0.17	0.43	0.81	n.d.	0.81	1.03	0.29
K2O	8.76	8.06	0.14	2.45	10.52	5.90	3.70	4.85	n.d.	9.56	6.42	n.d.
TOTAL	94.49	93.67	82.48	86.16	92.74	77.75	88.82	89.50	83.46	92.34	90.57	81.96

Recalculated formula on the basis of 22 oxygens

Si	6.102	6.170	6.349	6.325	6.481	6.997	6.314	6.295	6.348	6.261	6.226	7.768
Aliv	1.698	1.830	1.651	1.675	1.519	1.603	1.686	1.705	1.652	1.739	1.774	0.232
Alvi	3.744	3.829	4.516	4.263	3.119	3.337	4.074	3.907	4.551	3.527	3.893	3.981
Fe2	0.124	0.135	0.039	0.040	0.534	0.465	0.153	0.266	0.000	0.284	0.164	0.000
Mg	0.134	0.181	0.000	0.078	0.395	0.381	0.136	0.170	0.000	0.256	0.111	0.000
Mn	0.000	0.000	0.000	0.000	0.000	0.000	0.000	0.000	0.000	0.000	0.000	0.000
Ca	0.000	0.000	0.000	0.000	0.000	0.000	0.000	0.000	0.000	0.000	0.000	0.021
Na	0.536	0.340	0.000	0.108	0.146	0.052	0.114	0.216	0.000	0.215	0.272	0.076
K	1.492	1.373	0.024	0.431	1.874	1.209	0.641	0.646	0.000	1.684	1.119	0.000

Total aluminium

AL	5.642	5.659	6.167	5.938	4.638	4.340	5.760	5.612	6.203	5.265	5.668	4.213
----	-------	-------	-------	-------	-------	-------	-------	-------	-------	-------	-------	-------

ILLITIC CLAYS

Sample Code Spot	605 1FC 1	605 1FC 2	605 1FC 6	605 1FC 7	605 1FC 10	605 1FC 38	605 1FC 39	605 1FC 33	606 1FC 36	606 1FC 37	355 1FC 18	355 1FC 19	306 1FC 8	306 1FC 9	306 1FC 10	306 1FC 11
SiO <sub>2</sub>	35.22	27.80	43.13	43.02	18.43	43.03	34.11	36.39	28.64	42.30	45.13	43.43	36.06	36.54	37.75	35.15
TiO <sub>2</sub>	n.d.	n.d.	0.46	0.29	n.d.	n.d.	n.d.	n.d.	n.d.	n.d.	n.d.	n.d.	n.d.	n.d.	n.d.	n.d.
Al <sub>2</sub> O <sub>3</sub>	19.21	15.63	31.04	32.81	12.44	31.03	22.89	20.41	17.28	29.79	36.87	35.83	25.31	27.73	30.01	26.93
FeO	2.64	2.23	1.27	0.84	0.48	1.33	5.39	2.47	0.85	1.08	n.d.	0.26	1.24	1.01	0.43	0.91
MgO	1.43	1.01	0.80	0.48	0.37	0.65	0.93	1.09	0.63	0.92	n.d.	n.d.	0.68	0.44	0.22	0.31
MnO	n.d.	n.d.	n.d.	n.d.	n.d.	n.d.	n.d.	n.d.	n.d.	n.d.	n.d.	n.d.	n.d.	n.d.	n.d.	n.d.
CaO	0.23	n.d.	n.d.	0.09	0.20	n.d.	n.d.	n.d.	0.27	n.d.	n.d.	n.d.	n.d.	n.d.	n.d.	n.d.
Na <sub>2</sub> O	n.d.	n.d.	0.58	n.d.	n.d.	0.38	n.d.	n.d.	n.d.	n.d.	n.d.	n.d.	0.52	0.88	0.31	1.20
K <sub>2</sub> O	5.93	4.60	8.94	5.55	2.08	8.05	5.11	5.27	3.96	5.11	0.21	2.46	6.72	6.91	2.11	5.32
TOTAL	64.87	51.47	66.21	83.08	34.91	84.47	68.43	65.64	51.56	79.20	82.21	81.97	70.55	73.51	70.82	69.83

Recalculated formula on the basis of 22 oxygens

Si	6.860	6.804	6.312	6.330	6.607	6.375	6.368	6.907	6.830	6.517	6.382	6.287	6.414	6.238	6.345	6.252
Al <sup>IV</sup>	1.140	1.196	1.688	1.670	1.393	1.625	1.632	1.093	1.170	1.483	1.618	1.713	1.586	1.762	1.655	1.748
Al <sup>VI</sup>	3.271	3.370	3.665	4.019	3.867	3.793	3.405	3.472	3.687	3.926	4.527	4.399	3.718	3.818	4.291	3.897
Fe <sup>2</sup>	0.463	0.456	0.155	0.103	0.145	0.165	0.642	0.393	0.169	0.139	0.000	0.031	0.184	0.145	0.060	0.135
Mg	0.416	0.370	0.174	0.105	0.260	0.142	0.259	0.308	0.223	0.212	0.000	0.000	0.179	0.112	0.054	0.082
Mn	0.000	0.000	0.000	0.000	0.000	0.000	0.000	0.000	0.000	0.000	0.000	0.000	0.000	0.000	0.000	0.000
Ca	0.048	0.000	0.000	0.015	0.076	0.000	0.000	0.000	0.070	0.000	0.000	0.000	0.000	0.000	0.000	0.000
Na	0.000	0.000	0.165	0.000	0.000	0.116	0.000	0.000	0.000	0.000	0.000	0.000	0.178	0.291	0.099	0.415
K	1.474	1.435	1.669	1.042	0.953	1.522	1.216	1.277	1.187	1.004	0.038	0.454	1.525	1.504	0.453	1.207

Total aluminium

Al	4.411	4.500	5.353	5.689	5.259	5.419	5.037	4.565	4.857	5.409	6.145	6.112	5.304	5.579	5.946	5.645
----	-------	-------	-------	-------	-------	-------	-------	-------	-------	-------	-------	-------	-------	-------	-------	-------

Sample Code Spot	306 1FC 12	577 1FC 1	577 1FC 2	310 1FC 1	310 1FC 3	310 1FC 4	310 1FC 5	310 1FC 6	431 1AC 101
SiO <sub>2</sub>	41.71	45.32	45.69	44.39	45.58	44.21	40.99	45.25	34.39
TiO <sub>2</sub>	n.d.	n.d.	n.d.	0.77	0.64	n.d.	n.d.	n.d.	n.d.
Al <sub>2</sub> O <sub>3</sub>	30.90	35.82	35.63	35.02	35.34	34.90	34.82	35.86	13.88
FeO	1.46	0.54	1.04	1.01	1.00	0.67	1.13	0.58	1.10
MgO	0.59	0.23	0.25	0.57	0.59	n.d.	0.36	n.d.	0.41
MnO	n.d.	n.d.	n.d.	n.d.	n.d.	n.d.	n.d.	n.d.	n.d.
CaO	n.d.	n.d.	n.d.	n.d.	n.d.	n.d.	2.16	n.d.	0.22
Na <sub>2</sub> O	0.58	0.36	0.81	0.87	1.02	0.33	0.64	0.28	n.d.
K <sub>2</sub> O	7.50	3.34	7.48	10.06	9.31	4.67	5.44	4.10	6.14
TOTAL	81.84	85.61	90.90	92.68	93.46	84.77	85.52	86.07	56.14

Recalculated formula on the basis of 22 oxygens

Si	6.377	6.341	6.236	6.073	6.143	6.317	5.956	6.324	7.642
Al <sup>IV</sup>	1.623	1.659	1.764	1.927	1.857	1.683	2.044	1.671	0.358
Al <sup>VI</sup>	3.783	4.247	3.969	3.720	3.756	4.194	3.918	4.242	3.277
Fe <sup>2</sup>	0.187	0.053	0.119	0.116	0.113	0.080	0.138	0.067	0.204
Mg	0.134	0.045	0.051	0.116	0.119	0.000	0.078	0.060	0.136
Mn	0.000	0.000	0.000	0.000	0.000	0.000	0.000	0.000	0.000
Ca	0.000	0.000	0.000	0.000	0.000	0.000	0.336	0.000	0.052
Na	0.172	0.098	0.216	0.230	0.267	0.091	0.179	0.077	0.000
K	1.462	0.596	1.302	1.755	1.601	0.851	1.607	0.732	1.740

Total aluminium

Al	5.466	5.967	5.732	5.647	5.613	5.877	5.963	5.913	3.635
----	-------	-------	-------	-------	-------	-------	-------	-------	-------

## KANDITES

Sample Code	644 KBN	644 KBN	644 KBN	644 KBN	644 KBN	644 KBN	354 KCT	672 KDO	672 KDO	690 KDO	548 KBN	548 KBN	548 KBN	548 KBN	548 KBN	548 KBN	548 KBN	266 KFI	266 KFI
Spot	21	22	23	24	25	26	61	21	51	31	61	71	72	73	74	111	112	31	32
S102	45.50	30.34	30.04	37.61	44.94	44.31	45.59	46.05	45.53	44.28	41.75	45.94	44.36	46.86	24.23	46.14	42.32	44.97	45.50
T102	n.d.	n.d.	n.d.	n.d.	n.d.	n.d.	n.d.	n.d.	n.d.	n.d.	n.d.	n.d.	n.d.	n.d.	n.d.	n.d.	n.d.	n.d.	n.d.
AL203	37.28	29.67	24.45	30.92	30.91	36.09	37.57	38.15	36.96	36.14	33.93	37.52	32.72	37.83	19.11	37.91	34.27	36.78	37.38
FEO	n.d.	1.34	0.26	1.39	n.d.	0.64	n.d.	0.26	n.d.	n.d.	n.d.	n.d.	0.50	n.d.	n.d.	n.d.	n.d.	n.d.	0.25
MO	n.d.	n.d.	n.d.	n.d.	n.d.	n.d.	n.d.	n.d.	n.d.	n.d.	n.d.	n.d.	n.d.	n.d.	n.d.	n.d.	n.d.	n.d.	n.d.
MAE	n.d.	n.d.	n.d.	n.d.	n.d.	n.d.	n.d.	n.d.	n.d.	n.d.	n.d.	n.d.	n.d.	n.d.	n.d.	n.d.	n.d.	n.d.	n.d.
CAO	n.d.	n.d.	0.15	n.d.	n.d.	n.d.	n.d.	n.d.	n.d.	n.d.	n.d.	n.d.	n.d.	n.d.	n.d.	0.23	n.d.	n.d.	n.d.
MA20	n.d.	n.d.	n.d.	n.d.	n.d.	n.d.	n.d.	n.d.	n.d.	n.d.	n.d.	n.d.	0.32	n.d.	n.d.	n.d.	n.d.	n.d.	n.d.
K20	n.d.	n.d.	n.d.	0.13	n.d.	n.d.	0.17	n.d.	n.d.	n.d.	0.13	0.19	0.55	n.d.	n.d.	n.d.	0.24	0.66	0.33
TOTAL	82.78	67.35	54.90	70.05	81.85	81.04	83.33	84.46	82.49	80.42	75.81	83.65	78.45	84.69	43.34	84.28	76.83	82.41	83.46

Recalculated formula on the basis of 14 oxygens

S1	4.060	4.030	4.056	4.016	4.056	4.056	4.047	4.035	4.076	4.066	4.071	4.062	4.206	4.085	4.125	4.049	4.075	4.052	4.044
AL	3.920	3.678	3.891	3.891	3.926	3.893	3.931	3.940	3.899	3.911	3.900	3.910	3.657	3.887	3.834	3.921	3.890	3.905	3.916
FE2	0.000	0.124	0.029	0.124	0.000	0.049	0.000	0.019	0.000	0.000	0.000	0.000	0.040	0.000	0.000	0.000	0.000	0.000	0.019
MO	0.000	0.000	0.000	0.000	0.000	0.000	0.000	0.000	0.000	0.000	0.000	0.000	0.000	0.000	0.000	0.000	0.000	0.000	0.000
CA	0.000	0.000	0.022	0.000	0.000	0.000	0.000	0.000	0.000	0.000	0.000	0.000	0.000	0.000	0.000	0.022	0.000	0.000	0.000
MA	0.000	0.000	0.000	0.000	0.000	0.000	0.000	0.000	0.000	0.000	0.000	0.000	0.059	0.000	0.000	0.000	0.000	0.000	0.000
K	0.000	0.000	0.000	0.018	0.000	0.000	0.019	0.000	0.000	0.000	0.016	0.021	0.067	0.000	0.000	0.000	0.029	0.076	0.037

Sample Code	681 KBP	681 KBP	681 KBP	681 KBP	681 KBP	683 KBP	683 KBP	683 KBP	683 KBP	605 KFC	605 KFC	605 KFC	605 KFC	605 KFC	605 KFC	605 KFC	605 KFC	606 KFC	606 KFC
Spot	61	62	63	81	82	61	62	101	111	4	5	8	9	14	18	25	32	15	17
S102	44.94	45.42	40.96	46.04	42.89	45.00	44.65	43.85	46.20	44.91	44.66	45.11	44.39	37.25	44.52	44.94	16.31	40.99	40.92
T102	n.d.	n.d.	0.32	n.d.	n.d.	n.d.	n.d.	n.d.	n.d.	n.d.	n.d.	n.d.	n.d.	n.d.	n.d.	n.d.	n.d.	n.d.	1.26
AL203	36.86	37.48	31.64	38.09	34.89	37.86	36.90	35.79	37.53	37.16	35.73	36.96	35.82	29.95	36.86	37.10	12.10	32.77	33.85
FEO	0.44	0.31	1.70	n.d.	0.27	n.d.	0.22	0.37	0.46	n.d.	0.30	n.d.	n.d.	n.d.	n.d.	0.23	0.34	n.d.	n.d.
MO	n.d.	n.d.	n.d.	n.d.	0.31	n.d.	n.d.	n.d.	n.d.	n.d.	n.d.	n.d.	n.d.	n.d.	n.d.	n.d.	n.d.	n.d.	n.d.
MAE	n.d.	n.d.	n.d.	n.d.	n.d.	n.d.	n.d.	n.d.	n.d.	n.d.	n.d.	n.d.	n.d.	n.d.	n.d.	n.d.	n.d.	n.d.	n.d.
CAO	n.d.	n.d.	n.d.	0.13	0.15	0.15	n.d.	0.22	0.14	n.d.	n.d.	n.d.	0.20	0.17	n.d.	n.d.	n.d.	0.12	0.16
MA20	n.d.	n.d.	0.51	n.d.	n.d.	n.d.	n.d.	n.d.	n.d.	n.d.	n.d.	n.d.	n.d.	n.d.	0.24	n.d.	n.d.	0.22	n.d.
K23	0.19	0.38	3.57	n.d.	n.d.	n.d.	n.d.	n.d.	n.d.	0.58	1.42	n.d.	0.16	n.d.	n.d.	0.10	n.d.	0.10	n.d.
TOTAL	82.45	83.56	78.71	84.26	78.31	83.01	81.76	80.22	84.33	82.66	82.10	82.06	80.57	67.37	81.62	82.38	26.75	74.20	76.22

Recalculated formula on the basis of 14 oxygens

S1	4.044	4.035	4.037	4.040	4.041	4.011	4.041	4.052	4.061	4.033	4.069	4.060	4.077	4.066	4.036	4.040	4.206	4.090	4.038
AL	3.912	3.924	3.676	3.939	3.892	3.976	3.935	3.898	3.887	3.934	3.837	3.920	3.878	3.872	3.936	3.931	3.677	3.853	3.937
FE2	0.033	0.023	0.140	0.000	0.021	0.000	0.016	0.029	0.034	0.000	0.023	0.000	0.000	0.000	0.000	0.018	0.072	0.000	0.000
MO	0.000	0.000	0.000	0.000	0.044	0.000	0.000	0.000	0.000	0.000	0.000	0.000	0.000	0.000	0.000	0.000	0.000	0.000	0.000
CA	0.000	0.000	0.000	0.013	0.016	0.014	0.000	0.022	0.014	0.000	0.000	0.000	0.020	0.020	0.000	0.000	0.000	0.013	0.019
MA	0.000	0.000	0.097	0.000	0.000	0.000	0.000	0.000	0.000	0.000	0.000	0.000	0.000	0.000	0.043	0.000	0.000	0.043	0.000
K	0.022	0.043	0.449	0.000	0.000	0.000	0.000	0.000	0.000	0.067	0.165	0.000	0.019	0.000	0.000	0.012	0.000	0.012	0.000

Sample Code	606 KFC	606 KFC	606 KFC	606 KFC	606 KFC	606 KFC	677 KFC	677 KFC	677 KFC	355 KFC	355 KFC	355 KFC	355 KFC	355 KFC	355 KFC	355 KFC	306 KFC	306 KFC	609 KES
Spot	19	25	26	33	35	36	7	8	9	7	8	10	11	13	14	15	3	5	1
S102	45.89	42.77	31.03	41.73	44.57	39.75	20.03	38.32	30.01	45.03	16.34	45.57	37.70	42.51	43.89	45.86	45.33	46.01	29.23
T102	n.d.	n.d.	n.d.	n.d.	n.d.	n.d.	n.d.	n.d.	n.d.	n.d.	n.d.	n.d.	n.d.	n.d.	n.d.	n.d.	n.d.	n.d.	n.d.
AL203	37.53	34.98	24.90	33.46	36.26	31.51	15.30	30.87	24.42	37.46	12.41	37.26	30.62	34.42	35.47	38.03	37.51	38.32	23.71
FEO	n.d.	n.d.	0.20	0.31	n.d.	0.39	1.04	0.63	2.47	n.d.	0.36	n.d.	0.42	0.52	n.d.	n.d.	n.d.	n.d.	n.d.
MO	n.d.	n.d.	n.d.	n.d.	n.d.	n.d.	n.d.	n.d.	n.d.	n.d.	n.d.	n.d.	n.d.	n.d.	n.d.	n.d.	n.d.	n.d.	n.d.
MAE	n.d.	n.d.	n.d.	n.d.	n.d.	n.d.	n.d.	n.d.	n.d.	n.d.	n.d.	n.d.	n.d.	n.d.	n.d.	n.d.	n.d.	n.d.	n.d.
CAO	n.d.	n.d.	0.14	0.15	n.d.	n.d.	0.41	0.15	0.39	n.d.	n.d.	n.d.	0.13	0.21	n.d.	n.d.	n.d.	0.20	n.d.
MA20	n.d.	n.d.	n.d.	0.26	n.d.	n.d.	n.d.	n.d.	n.d.	n.d.	0.24	n.d.	n.d.	n.d.	n.d.	n.d.	0.26	n.d.	n.d.
K20	n.d.	n.d.	n.d.	0.42	0.10	0.98	n.d.	0.20	0.13	n.d.	n.d.	n.d.	n.d.	0.13	n.d.	n.d.	n.d.	n.d.	n.d.
TOTAL	83.42	77.75	56.27	76.33	80.93	72.64	36.78	70.18	57.41	82.49	29.35	82.84	66.87	77.79	79.35	83.89	83.16	84.53	52.94

Recalculated formula on the basis of 14 oxygens

S1	4.063	4.063	4.063	4.076	4.071	4.067	4.099	4.063	3.973	4.034	4.147	4.063	4.059	4.059	4.063	4.039	4.037	4.026	4.077
AL	3.916	3.916	3.661	3.846	3.902	3.819	3.669	3.856	3.810	3.955	3.713	3.915	3.886	3.874	3.889	3.948	3.936	3.952	3.897
FE2	0.000	0.000	0.022	0.025	0.000	0.034	0.177	0.056	0.273	0.000	0.077	0.000	0.037	0.042	0.000	0.000	0.000	0.000	0.000
MO	0.000	0.000	0.000	0.000	0.000	0.000	0.000	0.000	0.000	0.000	0.000	0.000	0.000	0.000	0.000	0.000	0.000	0.000	0.000
CA	0.000	0.000	0.020	0.016	0.000	0.000	0.090	0.017	0.055	0.000	0.000	0.000	0.016	0.021	0.000	0.000	0.000	0.019	0.000
MA	0.000	0.000	0.000	0.050	0.000	0.000	0.000	0.000	0.000	0.000	0.118	0.000	0.000	0.000	0.000	0.000	0.046	0.000	0.000
K	0.000	0.000	0.000	0.053	0.012	0.129	0.000	0.026	0.021	0.000	0.000	0.000	0.000	0.016	0.000	0.000	0.000	0.000	0.000



Sample	201	201	201	201	201	201	201	201	201	201	703	703	* 703	703	703	703	703	703	703
Code	C.R	C.R	C.R	C.I	C.I	C.I	C.I	C.I	C.I	C.I	SAO	SAO	SAO	SAO	SAO	SAO	SAO	SAO	SAO
Spot	101	201	211	221	231	232	233	234	241	11	12	13	14	15	16	21	22	23	24
S102	0.26	n.d.	1.25	0.60	n.d.	n.d.	0.92	1.19	n.d.	0.19	0.50	0.67	1.15	1.14	n.d.	0.60	0.64	0.72	0.91
T102	n.d.	n.d.	0.24	n.d.	n.d.	n.d.	n.d.	n.d.	n.d.	n.d.	n.d.	n.d.	n.d.	n.d.	n.d.	n.d.	n.d.	n.d.	n.d.
AL203	n.d.	n.d.	0.83	0.35	n.d.	n.d.	0.45	0.53	n.d.	n.d.	0.39	0.50	0.69	0.72	n.d.	0.34	0.30	0.50	0.60
FE2	1.45	1.50	1.35	1.16	1.05	1.00	1.11	2.66	0.89	62.22	62.16	61.59	60.71	57.58	61.81	60.96	61.09	61.37	60.16
MG2	0.52	0.52	0.32	0.45	0.63	0.56	0.37	0.28	0.43	0.56	0.55	0.41	0.55	1.12	0.71	0.68	0.49	0.35	0.32
MAG	n.d.	n.d.	0.34	n.d.	n.d.	0.27	0.31	n.d.	n.d.	0.54	0.25	0.54	0.55	0.78	0.63	0.50	0.40	0.55	0.91
CA2	55.54	54.60	51.85	51.98	54.19	55.47	53.18	50.35	53.44	0.23	0.54	0.58	0.47	1.33	0.34	0.31	0.45	0.55	0.54
MA20	n.d.	n.d.	n.d.	n.d.	n.d.	n.d.	n.d.	n.d.	n.d.	n.d.	n.d.	n.d.	n.d.	n.d.	n.d.	n.d.	n.d.	n.d.	n.d.
K2O	n.d.	n.d.	n.d.	n.d.	n.d.	n.d.	n.d.	n.d.	n.d.	n.d.	n.d.	n.d.	n.d.	n.d.	n.d.	n.d.	n.d.	n.d.	n.d.
CO2	46.18	44.34	42.08	42.00	43.86	44.92	43.01	41.45	42.95	39.24	39.26	38.97	38.50	36.02	39.30	38.64	38.56	38.75	36.20
TOTAL	109.95	100.96	98.27	96.54	99.73	102.22	99.35	96.46	97.71	102.98	103.65	103.26	102.62	106.69	102.79	102.03	101.93	102.79	101.65

Recalculated carbonate composition

CA	95.976	96.647	95.703	97.138	95.925	96.903	97.033	95.331	97.636	0.460	1.080	1.168	0.958	2.745	0.679	0.630	0.916	1.114	1.116
FE2	1.843	2.672	1.965	1.692	1.467	1.364	1.581	3.931	1.269	97.128	96.996	96.823	96.596	92.766	96.354	96.646	97.053	97.019	96.514
MG	1.178	1.286	0.830	1.170	1.566	1.361	0.939	0.738	1.093	1.558	1.530	1.149	1.560	3.216	1.973	1.921	1.387	0.986	0.915
Mn	0.000	0.000	0.501	0.000	0.000	0.373	0.447	0.000	0.000	0.854	0.395	0.860	0.886	1.273	0.995	0.803	0.644	0.861	1.462

Sample 703 Spheruliths																			
Sample	703	703	703	703	* 703	703	703	703	A	A	A *	A	A	A	A	A	B	B *	B
Code	SAO	SAO	SAO	SAO	SAO	SAO	SAO	SAO	S	S	S	S	S	S	S	S	S	S	S
Spot	25	26	31	32	33	34	35	36	1	2	3	4	5	6	7	8	1	2	3
S102	2.91	1.01	1.00	0.61	0.26	1.07	1.29	1.67	0.22	0.32	1.61	0.44	0.23	0.97	0.69	0.67	0.62	1.03	1.06
T102	n.d.	n.d.	n.d.	n.d.	n.d.	n.d.	n.d.	n.d.	0.09	0.09	n.d.	n.d.	0.01	n.d.	0.22	n.d.	0.07	0.02	0.15
AL203	1.53	0.86	0.50	0.37	0.22	0.76	0.48	1.04	0.09	0.23	1.13	0.18	0.56	0.55	0.33	0.45	0.35	0.57	0.58
FE2	56.70	59.75	59.57	60.96	61.64	60.21	58.32	58.91	61.79	61.11	59.32	62.27	60.91	58.61	56.42	58.20	60.91	60.21	56.25
MG2	0.88	0.82	0.60	0.34	0.48	0.56	0.47	0.94	0.73	0.57	0.47	0.49	0.48	1.05	0.89	1.39	0.65	0.49	0.56
MAG	0.38	0.26	0.75	0.69	0.65	0.46	0.54	0.27	0.46	0.51	0.90	0.55	0.58	1.19	0.25	0.20	0.77	0.40	0.73
CA2	1.10	0.97	0.56	0.25	0.50	0.59	0.58	0.76	0.31	0.29	0.51	0.12	0.55	1.31	1.22	1.47	0.48	0.43	0.77
MA20	n.d.	0.50	n.d.	n.d.	n.d.	n.d.	0.60	0.36	0.09	0.15	0.25	0.01	0.30	0.46	0.26	0.13	0.32	0.41	0.36
K2O	n.d.	n.d.	n.d.	n.d.	n.d.	n.d.	n.d.	n.d.	n.d.	n.d.	0.23	0.01	n.d.	0.07	0.01	n.d.	0.04	n.d.	0.06
CO2	36.62	36.47	36.05	36.35	39.20	38.24	37.03	37.88	39.18	36.59	37.81	39.12	38.62	38.81	37.87	38.45	38.88	38.00	37.85
TOTAL	103.52	102.70	101.03	101.79	103.15	101.91	99.31	101.83	102.96	101.86	102.23	103.19	102.24	103.02	100.16	106.96	103.09	101.56	101.37

Recalculated carbonate composition

CA	2.269	1.979	1.155	0.512	1.001	1.211	1.229	1.575	0.619	0.586	1.069	0.249	1.122	2.641	2.530	2.997	0.975	0.880	1.597
FE2	94.564	95.130	95.901	97.404	96.633	96.444	96.460	95.274	96.611	96.999	96.096	97.517	96.604	92.501	94.491	92.723	95.968	97.059	95.780
MG	2.527	2.440	1.722	0.968	1.337	1.599	1.386	2.710	2.040	1.598	1.357	1.359	1.343	2.953	2.574	3.956	1.822	1.405	1.426
Mn	0.620	0.452	1.223	1.116	1.029	0.746	0.905	0.442	0.730	0.817	1.478	0.875	0.932	1.905	0.405	0.324	1.235	0.656	1.197

Sample	B	B	C	* C	C	C	C	D	D	D	D
Code	S	S	S	S	S	S	S	S	S	S	S
Spot	4	5	1	2	3	4	5	1	2	3	4
S102	0.20	0.18	0.11	0.15	0.59	1.42	2.28	0.50	0.09	0.22	0.75
T102	n.d.	n.d.	n.d.	0.02	n.d.	0.23	0.17	0.02	n.d.	0.02	0.06
AL203	0.06	0.06	0.06	0.02	0.37	0.67	1.29	0.11	0.13	0.15	0.36
FE2	60.61	60.42	61.90	62.74	61.29	57.24	57.66	62.65	63.15	61.19	60.47
MG2	0.72	0.89	0.76	0.59	0.20	0.93	1.62	0.56	0.57	0.24	0.56
MAG	0.45	0.27	0.66	0.68	0.73	0.96	0.32	0.23	0.20	0.72	0.12
CA2	0.39	0.78	0.23	0.33	0.36	1.17	0.67	0.33	0.21	0.24	0.37
MA20	0.58	0.22	0.10	0.46	0.19	0.09	0.20	0.31	0.15	0.16	0.50
K2O	0.05	0.02	n.d.	n.d.	0.08	0.12	0.25	n.d.	n.d.	0.02	0.05
CO2	36.50	38.76	39.34	39.76	38.50	37.60	37.93	39.36	39.59	38.38	38.01
TOTAL	101.56	101.60	103.16	104.75	102.31	100.46	102.59	104.09	104.09	101.34	101.25

Recalculated carbonate composition

CA	0.799	1.581	0.463	0.655	0.738	2.442	1.376	0.646	0.416	0.499	0.768
FE2	96.425	95.466	96.385	96.665	97.523	93.252	93.449	97.440	97.713	97.669	97.443
MG	2.056	2.496	1.623	0.556	2.715	4.666	1.550	1.561	0.671	1.597	
Mn	0.720	0.432	1.035	1.056	1.183	1.591	0.515	0.362	0.310	1.161	0.193

In sequential series of siderite analyses an asterisk marks the analysis closest to the ring of pyrite within the spherulith

BERTHIERINES

Sample Code Spot	681 B6F 21	681 B6F 22	681 B6P 31	681 B6P 32	681 B6P 33	681 B6P 34	681 B6P 41	681 B6P 42	681 B6P 43	681 B6P 44	681 B6P 51	681 B6P 52	683 B6P 11	683 B6P 12	683 B6P 21	683 B6P 22	683 B6P 31	683 B6P 32
S102	22.50	22.96	24.24	26.67	23.98	23.30	25.45	25.90	26.08	25.11	22.68	23.58	22.28	30.64	26.50	23.56	27.74	25.29
T102	n.d.	0.30	n.d.	n.d.	n.d.	n.d.	n.d.	n.d.	n.d.	n.d.	n.d.	n.d.	n.d.	n.d.	n.d.	n.d.	n.d.	n.d.
AL203	20.16	20.59	19.92	21.61	20.96	20.50	22.96	22.69	21.80	20.77	20.90	20.75	19.79	26.30	19.52	19.91	24.49	20.76
FE0	31.60	33.08	28.42	29.26	31.49	30.91	31.54	31.39	29.87	29.71	33.15	32.06	29.65	19.71	16.15	26.97	19.08	27.79
MG0	4.18	4.08	2.57	2.80	3.02	3.45	3.99	4.00	2.95	2.94	3.97	3.78	3.77	2.26	2.10	3.47	2.07	3.27
MND	n.d.	n.d.	n.d.	n.d.	n.d.	n.d.	n.d.	n.d.	n.d.	n.d.	n.d.	n.d.	n.d.	n.d.	n.d.	n.d.	n.d.	n.d.
CA0	n.d.	0.18	n.d.	n.d.	0.15	0.20	n.d.	n.d.	0.19	0.20	0.25	0.30	0.16	0.26	0.38	0.15	0.30	0.16
NA20	n.d.	0.23	n.d.	n.d.	n.d.	n.d.	n.d.	n.d.	n.d.	n.d.	n.d.	n.d.	n.d.	n.d.	n.d.	n.d.	n.d.	n.d.
K20	0.12	n.d.	1.14	1.37	0.81	0.41	n.d.	n.d.	1.11	0.96	n.d.	0.24	0.18	0.58	1.77	0.79	0.21	0.93
TOTAL	78.56	81.41	76.30	81.71	80.35	78.76	83.95	83.97	82.00	79.70	80.96	80.72	75.82	79.75	66.42	74.85	73.89	76.20

Recalculated formula on the basis of 28 oxygens

S1	5.558	5.498	6.056	5.169	5.766	5.708	5.755	5.844	6.036	6.009	5.465	5.655	5.658	6.688	7.022	5.960	6.568	6.096
ALIV	2.442	2.532	1.942	1.831	2.234	2.292	2.245	2.156	1.964	1.991	2.535	2.345	2.342	1.312	0.978	2.040	1.432	1.904
ALV1	3.426	3.309	3.926	4.060	3.691	3.626	3.874	3.876	3.983	3.868	3.399	3.518	3.583	5.453	5.116	3.893	5.401	3.995
FE2	6.525	6.624	5.941	5.659	6.334	6.332	5.965	5.921	5.781	5.947	6.680	6.430	6.299	3.598	3.578	5.705	3.777	5.603
MG	1.537	1.456	0.958	0.965	1.083	1.259	1.346	1.343	1.617	1.050	1.424	1.351	1.426	0.736	0.829	1.307	0.729	1.172
NA	0.000	0.000	0.000	0.000	0.000	0.000	0.000	0.000	0.000	0.000	0.000	0.000	0.000	0.000	0.000	0.000	0.000	0.000
CA	0.000	0.045	0.000	0.000	0.039	0.052	0.000	0.000	0.046	0.051	0.066	0.078	0.043	0.061	0.109	0.042	0.076	0.042
NA	0.000	0.106	0.000	0.000	0.000	0.000	0.000	0.000	0.000	0.000	0.000	0.000	0.000	0.000	0.000	0.000	0.000	0.000
K	0.038	0.000	0.364	0.403	0.248	0.127	0.000	0.000	0.327	0.292	0.000	0.075	0.057	0.161	0.599	0.254	0.065	0.285

Total aluminum

AL	5.869	5.811	5.866	5.891	5.925	5.918	6.120	6.032	5.947	5.858	5.934	5.863	5.925	6.765	6.094	5.934	6.833	5.899
----	-------	-------	-------	-------	-------	-------	-------	-------	-------	-------	-------	-------	-------	-------	-------	-------	-------	-------

Sample Code Spot	683 B6F 41	683 B6F 51	683 B6P 52	683 B6P 54	683 B6P 55	683 B6F 91	605 B6F 16	605 B6F 17	677 B6F 10	677 B6F 11	652 B6S 2	652 B6S 3	652 B6S 4	652 B6S 5	652 B6S 6	652 B6S 7	654 B6S 5	613 B6F 201	613 B6F 202
S102	23.63	23.03	22.46	17.22	19.55	25.74	11.26	35.34	31.83	32.13	21.90	23.44	22.42	12.83	15.69	42.32	25.47	39.02	15.82
T102	n.d.	n.d.	n.d.	n.d.	n.d.	0.28	n.d.	0.26	0.44	0.30	n.d.	n.d.	n.d.	n.d.	n.d.	n.d.	n.d.	n.d.	n.d.
AL203	20.91	18.17	20.72	15.15	15.49	20.66	6.36	20.98	22.18	22.53	15.64	16.16	15.89	13.89	10.81	25.93	18.01	27.84	10.79
FE0	30.61	21.50	31.75	29.89	18.01	24.82	4.17	12.74	21.06	18.45	21.46	19.53	21.35	16.24	8.97	8.78	24.88	12.11	4.66
MG0	3.73	2.78	3.60	2.14	2.14	3.59	0.71	1.70	2.21	1.98	2.01	2.10	2.03	1.31	1.15	1.37	2.15	0.72	0.27
MND	n.d.	n.d.	n.d.	n.d.	n.d.	n.d.	0.20	n.d.	0.25	n.d.	n.d.	n.d.	n.d.	n.d.	n.d.	n.d.	n.d.	n.d.	n.d.
CA0	0.15	0.37	0.32	0.43	0.36	0.21	0.19	n.d.	0.71	0.57	0.74	0.73	0.55	1.13	0.31	0.62	0.76	0.16	0.14
NA20	0.35	0.38	n.d.	n.d.	n.d.	n.d.	n.d.	0.37	n.d.	n.d.	0.21	n.d.	0.35	n.d.	n.d.	0.55	n.d.	n.d.	n.d.
K20	0.42	1.18	0.13	0.32	0.63	1.15	0.84	2.62	1.30	1.48	0.96	1.00	0.86	0.30	0.50	3.62	0.59	3.63	1.29
TOTAL	79.80	67.42	79.01	65.15	56.18	75.66	23.75	74.02	79.96	77.44	62.91	62.97	63.44	45.69	37.42	82.66	72.40	83.48	32.31

Recalculated formula on the basis of 26 oxygens

S1	5.696	6.333	5.523	5.353	6.402	6.298	8.035	8.020	7.061	7.227	6.524	6.812	6.589	5.352	7.279	8.295	6.573	7.752	7.991
ALIV	2.304	1.667	2.477	2.647	1.596	1.702	0.660	0.000	0.939	0.773	1.476	1.186	1.411	2.648	0.721	0.000	1.427	0.248	0.009
ALV1	3.637	4.222	3.526	2.903	4.378	4.083	5.361	5.611	4.858	5.201	4.014	4.349	4.091	4.176	5.189	5.991	4.050	6.270	6.414
FE2	5.171	4.944	6.525	7.767	4.932	5.076	2.489	2.418	3.907	3.472	5.345	4.747	5.247	5.662	3.461	1.440	5.369	2.012	1.690
MG	1.339	1.139	1.320	0.993	1.044	1.311	0.755	0.575	0.730	0.663	0.892	0.910	0.890	0.812	0.797	0.401	0.826	0.213	0.203
NA	0.000	0.000	0.000	0.000	0.000	0.000	0.120	0.000	0.047	0.000	0.000	0.000	0.000	0.000	0.000	0.000	0.000	0.000	0.000
CA	0.039	0.106	0.084	0.142	0.126	0.055	0.142	0.000	0.169	0.138	0.236	0.229	0.172	0.507	0.152	0.131	0.210	0.034	0.076
NA	0.165	0.295	0.000	0.000	0.000	0.000	0.000	0.161	0.000	0.000	0.122	0.000	0.198	0.000	0.000	0.000	0.275	0.000	0.000
K	0.129	0.413	0.041	0.128	0.262	0.358	0.763	0.756	0.366	0.423	0.364	0.369	0.321	0.157	0.294	0.906	0.194	0.920	0.831

Total aluminum

AL	5.941	5.889	6.062	5.550	5.976	5.784	5.361	5.611	5.798	5.974	5.490	5.536	5.502	6.825	5.910	5.991	5.476	6.518	6.423
----	-------	-------	-------	-------	-------	-------	-------	-------	-------	-------	-------	-------	-------	-------	-------	-------	-------	-------	-------

Sample Code	613 BFC	608 BFC	600 BFC	600 BFC	603 BFC	605 BFC	606 BFC	606 BFC	608 BFC	608 BFC	652 665	652 665	652 665	652 665	652 665	652 665	654 665		
Spot	203	11	12	13	14	15	16	17	16	18	665 8	665 9	665 10	665 11	665 12	665 13	665 15	665 2	
SIC1	23.52	18.78	21.11	18.36	21.00	24.40	18.75	21.07	22.39	22.15	36.44	28.15	22.67	43.84	42.30	21.45	10.95	17.45	26.49
TIO2	n.d.	n.d.	n.d.	n.d.	0.27	n.d.	n.d.	n.d.	n.d.	n.d.	0.46	n.d.	n.d.	n.d.	n.d.	n.d.	n.d.	n.d.	n.d.
AL2O3	15.92	14.50	15.85	14.08	15.60	17.30	14.68	15.22	16.29	16.39	23.11	17.87	13.20	26.06	24.53	13.49	8.40	9.50	18.12
FE3	16.02	22.50	24.97	22.52	23.26	19.06	25.75	18.37	23.00	20.26	12.26	17.88	12.62	6.08	7.97	18.92	15.38	10.83	20.60
NEO	0.52	2.02	2.05	1.96	2.00	1.87	1.93	1.65	2.13	1.81	2.00	2.54	1.79	1.16	1.02	1.57	1.08	1.31	2.05
NA2	n.d.	n.d.	n.d.	n.d.	n.d.	n.d.	n.d.	n.d.	n.d.	n.d.	n.d.	n.d.	n.d.	n.d.	n.d.	n.d.	n.d.	n.d.	n.d.
CAO	0.15	0.31	0.37	0.32	0.20	0.22	0.36	0.78	0.37	0.18	0.57	0.93	0.61	0.64	0.73	0.51	0.39	0.57	0.57
NA2O	n.d.	n.d.	0.39	n.d.	n.d.	n.d.	n.d.	n.d.	n.d.	n.d.	n.d.	n.d.	n.d.	n.d.	n.d.	0.98	n.d.	0.36	0.38
K2O	2.00	1.54	1.70	1.38	2.00	2.37	1.88	2.09	2.17	2.31	2.66	1.22	1.03	4.51	4.39	0.38	0.49	0.46	0.85
TOTAL	58.13	59.65	60.44	58.62	64.33	65.22	63.35	59.18	66.35	63.10	77.50	68.59	51.91	82.28	80.94	57.31	36.70	40.49	65.34

Recalculated formula on the basis of 26 oxygens

SI	7.253	6.091	6.155	6.077	6.261	6.842	5.869	6.626	6.412	6.557	7.851	7.271	7.629	8.517	8.476	6.932	5.902	7.639	6.944
ALIV	0.747	1.909	1.845	1.923	1.739	1.158	2.131	1.374	1.588	1.443	0.149	0.729	0.371	0.000	0.000	1.068	2.098	0.361	1.056
ALV1	5.040	3.633	3.601	3.570	3.743	4.559	3.285	4.267	3.911	4.276	5.719	4.712	4.864	5.967	5.794	4.069	3.236	4.540	4.543
FE2	4.132	6.103	6.088	6.234	5.800	4.470	6.741	4.831	5.509	5.016	2.208	3.862	3.551	0.988	1.335	5.111	6.931	3.964	4.516
NE	0.239	0.976	0.891	0.967	0.889	0.782	0.901	0.773	0.909	0.799	0.642	0.976	0.896	0.337	0.304	0.758	0.870	0.857	0.799
NA	0.000	0.000	0.000	0.000	0.000	0.000	0.000	0.000	0.000	0.000	0.000	0.000	0.000	0.000	0.000	0.000	0.000	0.000	0.000
CA	0.050	0.108	0.116	0.113	0.064	0.066	0.121	0.263	0.114	0.057	0.131	0.258	0.220	0.133	0.157	0.178	0.228	0.268	0.160
NA	0.000	0.000	0.220	0.000	0.000	0.000	0.000	0.000	0.000	0.000	0.000	0.000	0.000	0.000	0.000	0.616	0.000	0.306	0.193
K	0.767	0.635	0.632	0.583	0.761	0.848	0.750	0.838	0.793	0.872	0.731	0.402	0.443	1.117	1.123	0.155	0.337	0.259	0.284

Total aluminium

AL	5.766	5.542	5.446	5.493	5.482	5.717	5.416	5.641	5.498	5.718	5.869	5.441	5.235	5.967	5.794	5.137	5.334	4.901	5.590
----	-------	-------	-------	-------	-------	-------	-------	-------	-------	-------	-------	-------	-------	-------	-------	-------	-------	-------	-------

Sample Code	Spot	654 665	654 665	654 665	654 665	654 665	654 665	654 665	654 665	654 665	654 665	654 665	JENK 86.	JENK 86.	JENK 86.	JENK 86.	JENK 86.	JENK 86.	JENK 86.	JENK 86.
Spot		3	4	6	8	9	10	11	12	14	15	16	11	21	13	21	22	23	31	31
SIO2		25.11	27.47	22.12	23.61	25.09	14.09	35.66	27.07	14.45	25.82	16.61	19.97	19.52	19.09	20.27	19.60	23.04	21.91	22.58
TIO2		n.d.	0.21	n.d.	n.d.	n.d.	0.21	n.d.	n.d.	n.d.	0.19	n.d.	0.26	n.d.	n.d.	n.d.	n.d.	n.d.	n.d.	n.d.
AL2O3		17.97	18.65	14.63	16.48	17.39	11.28	19.23	18.55	12.51	16.90	9.47	17.28	16.58	16.64	17.57	17.00	19.65	16.46	19.46
FE3		20.49	22.89	15.93	21.04	22.40	26.15	21.93	22.27	36.53	17.75	10.37	39.00	37.53	38.00	40.8	45.78	44.05	41.11	42.67
NEO		2.28	2.32	1.81	2.13	2.18	1.24	2.57	2.46	1.47	1.98	1.16	2.28	2.08	2.21	2.25	2.28	2.46	2.24	2.54
NAO		n.d.	n.d.	n.d.	n.d.	n.d.	3.12	n.d.	n.d.	n.d.	n.d.	n.d.	n.d.	n.d.	n.d.	n.d.	n.d.	n.d.	n.d.	n.d.
CAO		0.57	0.70	0.66	0.46	0.45	0.62	0.35	0.48	0.40	0.33	2.50	0.21	n.d.	n.d.	n.d.	0.14	0.18	0.28	0.25
NA2O		0.74	0.69	0.67	0.68	0.85	1.09	0.69	0.97	0.50	0.80	1.16	n.d.	n.d.	n.d.	n.d.	n.d.	n.d.	n.d.	n.d.
K2O		0.52	0.46	0.37	0.73	0.48	0.62	0.97	0.59	0.82	0.74	0.57	n.d.	n.d.	n.d.	n.d.	n.d.	n.d.	n.d.	n.d.
TOTAL		67.69	73.61	56.40	65.32	68.83	52.41	81.40	72.39	66.69	64.53	41.83	79.00	75.71	75.94	86.89	84.80	89.38	84.12	85.54

Recalculated formula on the basis of 28 oxygens

SI	6.746	6.812	7.032	6.725	6.722	5.468	7.731	6.826	4.749	7.144	7.208	5.210	5.115	5.208	5.203	4.940	5.309	5.358	5.261
ALIV	1.252	1.168	0.968	1.275	1.278	2.512	0.269	1.174	3.251	0.856	0.792	2.780	2.685	2.794	2.797	3.060	2.691	2.642	2.739
ALV1	4.440	4.321	4.587	4.211	4.212	2.667	4.645	4.337	1.596	4.654	4.050	2.543	2.635	2.555	2.519	1.990	2.645	2.667	2.664
FE2	4.605	4.748	4.235	4.960	5.020	6.564	3.976	4.696	10.039	4.107	3.761	8.525	8.546	8.667	8.759	9.656	8.468	8.467	8.519
NE	0.914	0.859	0.857	0.895	0.872	0.719	0.831	0.924	0.722	0.817	0.752	0.885	0.644	0.696	0.661	0.857	0.845	0.616	0.662
NA	0.000	0.000	0.000	0.000	0.000	1.030	0.000	0.000	0.000	0.000	0.000	0.000	0.000	0.000	0.000	0.000	0.000	0.000	0.000
CA	0.164	0.186	0.231	0.146	0.128	0.259	0.082	0.129	0.140	0.098	1.161	0.159	0.000	0.000	0.000	0.000	0.644	0.673	0.071
NA	0.388	0.333	0.413	0.371	0.440	0.819	0.292	0.475	0.315	0.431	0.978	0.660	0.660	0.660	0.660	0.660	0.660	0.660	0.660
K	0.178	0.151	0.150	0.264	0.163	0.306	0.269	0.191	0.345	0.261	0.313	0.000	0.000	0.000	0.000	0.000	0.000	0.000	0.000

Total aluminium

AL	5.692	5.569	5.555	5.466	5.490	5.179	4.914	5.511	4.847	5.510	4.843	5.323	5.321	5.346	5.316	5.051	5.336	5.326	5.343
----	-------	-------	-------	-------	-------	-------	-------	-------	-------	-------	-------	-------	-------	-------	-------	-------	-------	-------	-------





Sample Code Spot	59J F00 12	59C F00 13	59I F00 14	59U F00 15	59V F00 51	54B F0M 11	54B F0M 12	54B F0M 13	54E F0M 21	54B F0M 31	54B F0M 41	54B F0M 51	54B F0M B1	54B F0M 101	54E F0M 121	54E F0M 122	20C FE1 11	20C FE1 21	20C FE1 55
S102	68.65	67.84	69.17	68.90	65.78	64.33	63.97	63.71	63.41	63.31	63.16	64.14	65.46	64.82	65.69	65.85	64.02	66.74	64.44
T102	n.d.	n.d.	n.d.	n.d.	n.d.	n.d.	n.d.	n.d.	n.d.	n.d.	n.d.	n.d.	n.d.	n.d.	n.d.	n.d.	n.d.	n.d.	n.d.
AL2O3	19.22	19.75	19.53	19.73	18.56	19.17	18.46	17.72	18.09	17.96	18.06	18.38	18.44	18.09	18.82	18.83	18.58	19.87	18.17
FeO	n.d.	n.d.	n.d.	n.d.	n.d.	n.d.	n.d.	n.d.	n.d.	n.d.	n.d.	n.d.	n.d.	n.d.	n.d.	n.d.	n.d.	n.d.	n.d.
MgO	n.d.	n.d.	n.d.	n.d.	n.d.	n.d.	n.d.	n.d.	n.d.	n.d.	n.d.	n.d.	n.d.	n.d.	n.d.	n.d.	n.d.	n.d.	n.d.
MnO	n.d.	n.d.	n.d.	n.d.	n.d.	n.d.	n.d.	n.d.	n.d.	n.d.	n.d.	n.d.	n.d.	n.d.	n.d.	n.d.	n.d.	n.d.	n.d.
CaO	n.d.	0.25	n.d.	0.21	n.d.	n.d.	n.d.	n.d.	n.d.	n.d.	n.d.	n.d.	n.d.	n.d.	n.d.	n.d.	n.d.	0.60	n.d.
Na2O	11.27	11.41	11.55	10.87	11.15	n.d.	n.d.	n.d.	0.67	1.07	0.72	0.88	1.28	n.d.	0.59	0.58	0.49	10.24	0.52
K2O	n.d.	n.d.	0.10	n.d.	n.d.	16.77	17.11	16.47	15.64	15.69	15.49	15.91	16.14	17.09	16.67	16.59	16.43	n.d.	16.43
TOTAL	99.14	99.25	100.35	99.71	95.49	99.27	99.54	97.90	97.81	98.03	97.43	99.31	101.32	100.00	101.77	101.85	99.52	97.45	99.56

Elemental composition on the basis of 8 oxygens

Si	3.014	2.983	3.005	3.005	3.004	3.001	2.984	3.011	2.994	2.990	2.993	2.987	2.992	3.006	2.988	2.991	2.980	2.980	2.997
Al	0.995	1.024	1.000	1.014	0.999	0.999	1.015	0.987	1.007	1.000	1.009	1.009	0.993	0.989	1.009	1.008	1.019	1.040	0.995
Fe	0.000	0.000	0.000	0.000	0.000	0.000	0.000	0.000	0.000	0.000	0.000	0.000	0.000	0.000	0.000	0.000	0.000	0.000	0.000
Mg	0.000	0.000	0.000	0.000	0.000	0.000	0.000	0.000	0.000	0.000	0.000	0.000	0.000	0.000	0.000	0.000	0.000	0.000	0.000
Ca	0.000	0.012	0.000	0.010	0.000	0.000	0.000	0.000	0.000	0.000	0.000	0.000	0.000	0.000	0.000	0.000	0.000	0.029	0.000
Na	0.959	0.973	0.973	0.919	0.987	0.000	0.000	0.000	0.061	0.098	0.066	0.079	0.113	0.000	0.052	0.051	0.044	0.885	0.047
K	0.050	0.000	0.000	0.000	0.000	0.998	1.018	0.993	0.942	0.945	0.936	0.945	0.941	1.011	0.967	0.961	0.976	0.000	0.975

Mineralogical composition

AS	100.0	98.8	99.4	98.9	100.0	0.0	0.0	0.0	6.1	9.4	6.6	7.8	10.8	0.0	5.1	5.0	4.3	96.9	4.6
OR	0.0	0.0	0.6	0.0	0.0	100.0	100.0	100.0	93.9	90.6	93.4	92.2	89.2	100.0	94.9	95.0	95.7	0.0	95.4
AN	0.0	1.2	0.0	1.1	0.0	0.0	0.0	0.0	0.0	0.0	0.0	0.0	0.0	0.0	0.0	0.0	0.0	3.1	0.0

Sample Code Spot	65I F00 11	65C F00 121	65I F00 122	65U F00 151	65V F00 152	65B F00 153	65B F00 154	65B F00 155	65B F00 156	65B F00 157	65B F00 158	65B F00 159	65B F00 160	65B F00 161	65B F00 162	65B F00 163	65B F00 164	65B F00 165	65B F00 166
S102	68.23	67.41	68.13	67.17	67.78	68.14	68.00	67.03	67.75	68.86	67.34	68.92	65.10	65.02	67.63	68.64	68.02	67.80	68.00
T102	n.d.	n.d.	n.d.	n.d.	n.d.	n.d.	n.d.	n.d.	n.d.	n.d.	n.d.	n.d.	n.d.	n.d.	n.d.	n.d.	n.d.	n.d.	n.d.
AL2O3	19.36	19.26	19.80	18.48	19.26	19.86	18.52	19.55	19.76	19.04	20.67	20.76	20.94	20.46	19.00	19.44	19.34	19.25	19.56
FeO	n.d.	n.d.	n.d.	7.96	n.d.	n.d.	n.d.	n.d.	n.d.	n.d.	n.d.	1.59	n.d.	n.d.	n.d.	n.d.	n.d.	n.d.	n.d.
MgO	n.d.	n.d.	n.d.	2.13	n.d.	n.d.	n.d.	n.d.	n.d.	n.d.	n.d.	1.55	n.d.	n.d.	n.d.	n.d.	n.d.	n.d.	n.d.
MnO	n.d.	n.d.	n.d.	n.d.	n.d.	n.d.	n.d.	n.d.	n.d.	n.d.	n.d.	n.d.	n.d.	n.d.	n.d.	n.d.	n.d.	n.d.	n.d.
CaO	0.15	0.32	n.d.	n.d.	0.18	0.36	0.19	n.d.	0.43	0.84	0.70	0.43	2.01	1.89	n.d.	n.d.	n.d.	n.d.	n.d.
Na2O	11.25	10.16	11.42	6.36	10.79	10.39	10.64	9.89	10.57	n.d.	11.15	0.31	10.58	10.11	11.26	10.10	11.84	11.31	11.05
K2O	n.d.	n.d.	n.d.	0.15	0.14	n.d.	n.d.	n.d.	n.d.	11.37	n.d.	10.77	0.24	0.14	n.d.	n.d.	n.d.	0.13	n.d.
TOTAL	98.60	97.14	99.35	92.75	98.15	98.76	95.35	96.46	96.78	98.52	99.91	92.33	98.67	97.63	97.65	98.18	99.20	98.56	98.29

Elemental composition on the basis of 8 oxygens

Si	3.006	2.912	2.989	2.252	3.007	2.997	2.913	3.031	2.960	3.033	2.947	2.354	2.897	2.920	3.016	3.027	2.995	3.012	3.061
Al	1.006	1.014	1.024	1.751	1.007	1.000	0.990	1.012	1.037	1.050	1.066	1.818	1.078	1.083	0.997	1.010	1.004	1.004	1.018
Fe	0.000	0.000	0.000	0.248	0.000	0.000	0.000	0.000	0.000	0.000	0.000	0.000	0.000	0.000	0.000	0.000	0.000	0.000	0.000
Mg	0.000	0.000	0.000	0.100	0.000	0.000	0.000	0.000	0.000	0.000	0.000	0.116	0.000	0.000	0.000	0.000	0.000	0.000	0.000
Ca	0.007	0.015	0.000	0.000	0.005	0.018	0.009	0.006	0.020	0.031	0.035	0.023	0.076	0.091	0.000	0.000	0.000	0.000	0.000
Na	0.944	0.860	0.972	0.000	0.988	0.942	0.842	0.903	0.900	0.946	0.630	0.913	0.860	0.972	0.863	1.010	0.970	0.944	0.944
K	0.000	0.000	0.000	0.000	0.000	0.000	0.000	0.000	0.000	0.000	0.000	0.000	0.000	0.000	0.000	0.000	0.000	0.000	0.000

Mineralogical composition

AS	99.2	98.3	100.0	5.1	98.2	98.0	98.0	100.0	97.6	0.0	98.4	4.0	89.3	89.9	100.0	100.0	100.0	99.2	100.0
OR	0.0	0.0	0.0	94.9	0.0	0.0	0.0	0.0	0.0	95.5	0.0	52.9	1.4	0.8	0.0	0.0	0.0	0.8	0.0
AN	0.7	1.7	0.0	0.0	0.9	1.0	1.0	0.0	2.2	4.5	3.6	3.1	5.4	9.3	0.0	0.0	0.0	0.0	0.0

Sample Code Spot	677 FFC 19	677 FFC 20	677 FFC 22	355 FFC 1	355 FFC 2	355 FFC 3	355 FFC 4	355 FFC 5	355 FFC 6	355 FFC 9	355 FFC 12	652 FES 1	654 FES 1	306 FFC 1	306 FFC 2	306 FFC 4	306 FFC 6	306 FFC 7	332 FFC 11
SiO2	67.52	67.74	65.74	67.45	66.84	68.49	63.34	68.25	66.61	68.61	68.35	68.60	68.36	67.42	68.29	55.99	67.20	64.34	65.68
TiO2	n.d.	n.d.	n.d.	n.d.	n.d.	n.d.	n.d.	n.d.	n.d.	n.d.	n.d.	n.d.	n.d.	n.d.	n.d.	n.d.	n.d.	n.d.	0.23
AL2O3	18.89	19.06	20.75	19.39	18.81	19.45	19.27	19.50	18.92	19.50	19.75	19.99	19.58	19.33	19.93	16.12	20.31	19.80	20.04
FeO	n.d.	n.d.	n.d.	n.d.	n.d.	0.27	n.d.	n.d.	n.d.	0.23	n.d.	0.27	n.d.	n.d.	n.d.	n.d.	n.d.	n.d.	n.d.
MgO	n.d.	n.d.	n.d.	n.d.	n.d.	n.d.	n.d.	n.d.	n.d.	n.d.	n.d.	n.d.	n.d.	n.d.	n.d.	n.d.	n.d.	n.d.	n.d.
MnO	n.d.	n.d.	n.d.	n.d.	n.d.	n.d.	n.d.	n.d.	n.d.	n.d.	n.d.	n.d.	n.d.	n.d.	n.d.	n.d.	n.d.	n.d.	n.d.
CaO	n.d.	n.d.	1.84	n.d.	n.d.	n.d.	n.d.	n.d.	n.d.	n.d.	n.d.	n.d.	0.18	n.d.	n.d.	0.39	0.47	1.93	1.16
Na2O	11.18	11.22	10.61	11.72	11.56	11.92	11.42	11.86	11.89	11.77	11.87	11.38	11.52	11.59	11.67	8.90	11.12	10.17	10.44
K2O	n.d.	n.d.	n.d.	0.18	0.14	0.19	n.d.	n.d.	n.d.	n.d.	0.11	0.20	0.14	n.d.	n.d.	0.14	n.d.	0.16	n.d.
TOTAL	97.59	98.02	98.94	98.74	97.28	100.31	94.03	99.61	97.42	100.11	100.08	100.44	99.79	98.34	99.89	81.54	99.11	98.42	97.55

Elemental composition on the basis of 8 oxygens

Si	3.013	3.010	2.915	2.987	3.001	2.990	2.949	2.992	2.991	2.994	2.985	2.984	2.992	2.992	2.983	2.994	2.961	2.929	2.949
Al	0.993	0.998	1.084	1.012	0.995	1.000	1.057	1.008	1.001	1.003	1.016	1.025	1.010	1.011	1.026	1.016	1.055	1.062	1.061
Fe2	0.000	0.000	0.000	0.000	0.000	0.010	0.000	0.000	0.000	0.008	0.000	0.010	0.000	0.000	0.000	0.000	0.000	0.000	0.000
Mg	0.000	0.000	0.000	0.000	0.000	0.000	0.000	0.000	0.000	0.000	0.000	0.000	0.000	0.000	0.000	0.000	0.000	0.000	0.000
Ca	0.000	0.000	0.087	0.000	0.000	0.000	0.000	0.000	0.000	0.000	0.000	0.000	0.009	0.000	0.000	0.022	0.022	0.094	0.056
Na	0.968	0.967	0.912	1.006	1.001	1.009	1.031	1.008	1.035	0.996	1.005	0.959	0.978	0.997	0.988	0.923	0.950	0.898	0.909
K	0.066	0.066	0.060	0.010	0.008	0.010	0.000	0.000	0.000	0.000	0.006	0.011	0.008	0.000	0.000	0.009	0.000	0.010	0.000

Mineralogical composition

Ab	100.0	100.0	91.3	99.0	99.2	99.0	100.0	100.0	100.0	100.0	99.4	98.9	96.3	100.0	100.0	96.7	97.7	89.6	94.2
Or	0.0	0.0	0.0	1.0	0.8	1.0	0.0	0.0	0.0	0.0	0.6	1.1	0.8	0.0	0.0	1.0	0.0	1.0	0.0
An	0.0	0.0	8.7	0.0	0.0	0.0	0.0	0.0	0.0	0.0	0.0	0.0	0.9	0.0	0.0	2.3	2.3	9.4	5.8

Sample Code Spot	332 FFC 12	332 FFC 13	332 FFC 14	470 FBO 41	470 FBO 42	470 FBO 71	470 FBO 72	470 FBO 73	470 FBO 81	470 FBO 91	470 FBO 92	470 FBO 101	470 FBO 102	470 FBO 103	470 FBO 104	470 FBO 131	470 FBO 141	470 FBO 151	470 FBO 152
SiO2	67.21	68.57	67.77	67.06	67.29	62.49	63.58	62.80	67.45	63.87	63.26	43.10	62.10	64.96	69.93	63.24	66.52	63.44	37.80
TiO2	n.d.	n.d.	n.d.	n.d.	n.d.	n.d.	n.d.	n.d.	n.d.	n.d.	n.d.	n.d.	n.d.	n.d.	n.d.	n.d.	n.d.	n.d.	n.d.
AL2O3	20.12	20.96	20.30	19.17	19.67	17.77	17.93	18.16	19.29	18.23	18.48	11.68	22.51	18.51	16.38	17.97	18.84	18.01	10.38
FeO	n.d.	n.d.	n.d.	n.d.	n.d.	n.d.	n.d.	n.d.	n.d.	n.d.	n.d.	n.d.	n.d.	n.d.	n.d.	n.d.	n.d.	n.d.	n.d.
MgO	n.d.	n.d.	n.d.	n.d.	n.d.	n.d.	n.d.	n.d.	n.d.	n.d.	n.d.	n.d.	n.d.	n.d.	n.d.	n.d.	n.d.	n.d.	n.d.
MnO	n.d.	n.d.	n.d.	n.d.	n.d.	n.d.	n.d.	n.d.	n.d.	n.d.	n.d.	n.d.	n.d.	n.d.	n.d.	n.d.	n.d.	n.d.	n.d.
CaO	1.00	1.22	1.10	0.20	0.40	n.d.	n.d.	n.d.	n.d.	n.d.	n.d.	n.d.	4.20	0.44	n.d.	n.d.	n.d.	n.d.	n.d.
Na2O	10.56	10.95	11.18	10.94	10.33	n.d.	n.d.	0.36	10.60	0.43	1.98	6.60	9.20	10.66	9.71	0.48	11.34	0.48	0.46
K2O	n.d.	n.d.	n.d.	0.24	0.12	10.93	16.60	16.12	n.d.	16.29	13.62	n.d.	n.d.	n.d.	n.d.	15.96	n.d.	16.20	9.56
TOTAL	98.89	101.70	100.35	97.61	97.81	97.19	98.11	97.44	97.34	98.82	97.34	61.38	98.01	94.57	96.02	97.65	96.70	98.13	58.20

Elemental composition on the basis of 8 oxygens

Si	2.966	2.947	2.955	2.997	2.993	2.990	3.002	2.985	3.010	2.992	2.981	3.045	2.800	2.996	3.139	2.996	3.001	2.994	3.009
Al	1.046	1.062	1.043	1.010	1.031	1.002	0.998	1.017	1.014	1.006	1.026	0.972	1.196	1.006	0.867	1.003	1.002	1.002	0.974
Fe2	0.000	0.000	0.000	0.000	0.000	0.000	0.000	0.000	0.000	0.000	0.000	0.000	0.000	0.000	0.000	0.000	0.000	0.000	0.000
Mg	0.000	0.000	0.000	0.000	0.000	0.000	0.000	0.000	0.000	0.000	0.000	0.000	0.000	0.000	0.000	0.000	0.000	0.000	0.000
Ca	0.047	0.056	0.051	0.010	0.019	0.006	0.000	0.000	0.000	0.000	0.000	0.000	0.203	0.022	0.000	0.000	0.000	0.006	0.000
Na	0.903	0.913	0.945	0.948	0.891	0.000	0.000	0.033	0.917	0.039	0.181	0.904	0.804	0.953	0.845	0.044	0.992	0.044	0.071
K	0.000	0.000	0.000	0.014	0.007	1.033	1.000	0.977	0.000	0.973	0.819	0.000	0.000	0.000	0.000	0.984	0.000	0.975	0.971

Mineralogical composition

Ab	95.0	94.2	94.8	97.6	97.2	0.0	0.0	3.3	100.0	3.9	18.1	100.0	79.9	97.8	100.0	4.4	100.0	4.3	6.8
Or	0.0	0.0	0.0	1.4	0.7	100.0	100.0	96.7	0.0	96.1	81.9	0.0	0.0	0.0	0.0	95.6	0.0	95.7	93.2
An	5.0	5.8	5.2	1.0	2.1	0.0	0.0	0.0	0.0	0.0	0.0	0.0	20.1	2.2	0.0	0.0	0.0	0.0	0.0

Sample Code Spot	470 F60 171	470 F60 172	613 FFC 11	612 FFC 31	613 FFC 51	613 FFC 61	613 FFC 62	619 FFC 63	613 FFC 64	613 FFC 81	613 FFC 82	613 FFC 101	613 FFC 121	613 FFC 122	613 FFC 181	431 FAC 11	431 FAC 12	431 FAC 41	421 FAC 42
S102	66.76	67.15	67.62	68.00	67.32	68.14	67.51	67.32	68.17	68.53	68.10	62.82	55.50	67.88	68.23	63.48	63.14	63.16	62.76
T102	n.d.	n.d.	n.d.	n.d.	n.d.	n.d.	n.d.	n.d.	n.d.	n.d.	n.d.	n.d.	n.d.	n.d.	n.d.	n.d.	n.d.	n.d.	n.d.
AL203	18.60	19.13	19.59	17.87	19.41	20.14	19.46	19.65	19.93	19.64	19.74	17.50	15.86	19.27	19.58	18.34	17.87	18.26	17.92
FE2	n.d.	n.d.	n.d.	n.d.	n.d.	n.d.	n.d.	n.d.	n.d.	n.d.	n.d.	n.d.	n.d.	n.d.	n.d.	n.d.	n.d.	n.d.	n.d.
MG	n.d.	n.d.	n.d.	n.d.	n.d.	n.d.	n.d.	n.d.	n.d.	n.d.	n.d.	n.d.	n.d.	n.d.	n.d.	n.d.	n.d.	n.d.	n.d.
MND	n.d.	n.d.	n.d.	n.d.	n.d.	n.d.	n.d.	n.d.	n.d.	n.d.	n.d.	n.d.	n.d.	n.d.	n.d.	n.d.	n.d.	n.d.	n.d.
CAO	n.d.	n.d.	n.d.	n.d.	0.33	0.24	0.22	0.31	n.d.	n.d.	n.d.	n.d.	n.d.	n.d.	0.19	n.d.	n.d.	n.d.	n.d.
MA20	11.57	11.28	11.76	10.18	11.53	11.49	11.41	11.77	11.56	11.87	11.70	10.89	9.34	11.56	11.52	0.56	0.77	0.46	0.34
K2O	n.d.	n.d.	n.d.	n.d.	n.d.	n.d.	n.d.	n.d.	n.d.	n.d.	n.d.	n.d.	n.d.	n.d.	n.d.	16.24	16.45	16.27	16.35
TOTAL	97.07	97.56	99.11	86.65	98.59	100.01	98.87	99.05	99.66	100.04	99.54	91.21	86.70	98.71	99.52	98.62	98.23	98.15	97.37
Elemental composition on the basis of 8 oxygens																			
Si	3.000	3.000	2.987	2.980	2.984	2.974	2.965	2.973	2.984	2.991	2.986	3.007	2.998	3.000	2.992	2.982	2.987	2.962	2.969
Al	0.997	1.007	1.017	1.036	1.014	1.036	1.014	1.023	1.026	1.010	1.020	0.987	1.010	1.004	1.012	1.015	0.996	1.016	1.006
FE2	0.000	0.000	0.000	0.000	0.000	0.000	0.010	0.000	0.000	0.000	0.000	0.000	0.000	0.000	0.000	0.000	0.000	0.000	0.000
MG	0.000	0.000	0.000	0.000	0.000	0.000	0.000	0.000	0.000	0.000	0.000	0.000	0.000	0.000	0.000	0.000	0.000	0.000	0.000
CA	0.000	0.000	0.000	0.000	0.016	0.011	0.010	0.015	0.000	0.000	0.000	0.000	0.000	0.000	0.000	0.000	0.000	0.000	0.000
MA	1.009	0.977	0.999	0.971	0.991	0.972	0.978	1.008	0.981	1.004	0.995	1.011	0.978	0.990	0.979	0.051	0.071	0.042	0.031
K	0.000	0.000	0.000	0.000	0.000	0.000	0.000	0.000	0.000	0.000	0.000	0.000	0.000	0.000	0.000	0.973	0.993	0.986	0.993
Mineralogical composition																			
AB	100.0	100.0	100.0	100.0	98.4	98.9	98.9	98.6	100.0	100.0	100.0	100.0	100.0	100.0	99.1	5.0	6.6	4.1	3.1
OR	0.0	0.0	0.0	0.0	0.0	0.0	0.0	0.0	0.0	0.0	0.0	0.0	0.0	0.0	0.0	95.0	93.4	95.9	96.9
AM	0.0	0.0	0.0	0.0	1.6	1.1	1.1	1.4	0.0	0.0	0.0	0.0	0.0	0.0	0.9	0.0	0.0	0.1	0.0

Sample Code Spot	431 FAC 51	431 FAC 52	431 FAC 91	431 FAC 92	254 FBM 51	254 FBM 52	254 FBM 91	254 FBM 92	254 FBM 123	254 FBM 131	254 FBM 132	254 FBM 141	254 FBM 161	254 FBM 162
S102	66.57	67.17	63.51	62.97	69.55	67.92	63.85	64.07	63.94	61.35	63.43	65.19	67.32	66.13
T102	n.d.	n.d.	n.d.	n.d.	n.d.	n.d.	n.d.	n.d.	n.d.	n.d.	n.d.	n.d.	n.d.	n.d.
AL203	18.98	18.87	18.19	18.07	19.93	19.39	18.15	18.14	18.23	17.71	18.62	18.88	19.54	20.04
FE2	n.d.	n.d.	n.d.	n.d.	n.d.	n.d.	0.29	0.20	n.d.	0.98	n.d.	n.d.	n.d.	n.d.
MG	n.d.	n.d.	n.d.	n.d.	n.d.	n.d.	n.d.	n.d.	n.d.	n.d.	n.d.	n.d.	n.d.	n.d.
MND	n.d.	n.d.	n.d.	n.d.	n.d.	n.d.	n.d.	n.d.	n.d.	n.d.	n.d.	n.d.	n.d.	n.d.
CAO	0.37	n.d.	n.d.	n.d.	0.26	0.27	n.d.	n.d.	n.d.	n.d.	n.d.	n.d.	0.52	8.00
MA20	10.84	10.16	0.54	0.49	10.69	10.22	0.32	0.57	0.83	0.47	0.44	0.52	11.74	11.04
K2O	0.15	n.d.	16.32	16.30	n.d.	n.d.	16.59	16.36	16.02	15.83	16.35	16.86	n.d.	n.d.
TOTAL	96.91	96.26	98.56	97.83	100.37	97.80	99.20	98.80	99.02	96.34	98.84	101.45	99.12	105.21
Elemental composition on the basis of 8 oxygens														
Si	2.997	3.027	2.967	2.965	3.009	3.013	2.989	0.000	2.989	2.968	2.974	2.980	2.973	2.836
Al	1.007	1.002	1.008	1.010	1.016	1.014	1.001	3.957	1.004	1.010	1.029	1.017	1.017	1.011
FE2	0.000	0.000	0.000	0.000	0.000	0.000	0.011	0.031	0.000	0.040	0.000	0.000	0.000	0.000
MG	0.000	0.000	0.000	0.000	0.000	0.000	0.000	0.000	0.000	0.000	0.000	0.000	0.000	0.000
CA	0.016	0.000	0.000	0.000	0.009	0.013	0.000	0.000	0.000	0.000	0.000	0.000	0.025	0.367
MA	0.946	0.888	0.049	0.045	0.697	0.879	0.029	0.205	0.075	0.044	0.040	0.046	1.005	0.916
K	0.009	0.000	0.979	0.986	0.000	0.000	0.991	3.863	0.955	0.977	0.978	0.983	0.000	0.000
Mineralogical composition														
AB	97.3	100.0	4.8	4.4	99.0	98.6	2.8	5.0	7.3	4.3	3.9	4.5	97.6	71.4
OR	0.9	0.0	95.2	95.6	0.0	0.0	97.2	95.0	92.7	95.7	96.1	95.5	0.0	0.0
AM	1.8	0.0	0.0	0.0	1.6	1.4	6.0	0.0	0.0	0.0	0.0	0.0	2.4	28.6

# PYRITE

Sample	206	206	206	206
Code	PEI	PEI	PEI	PEI
Spot	201	202	203	204
FE	46.23	46.96	46.18	45.99
S	52.37	52.55	52.23	52.77
FeO	-	-	-	-
MgO	-	-	-	-
CaO	-	-	-	-
Na2O	-	-	-	-
P2O5	-	-	-	-

# APATITE

Sample	JEHR	JEHR	JEHR	JEHR	JEHR	JEHR	JEHR
Code	AG.	AG.	AG.	AG.	AG.	AG.	AG.
Spot	101	102	103	104	105	106	107
Fe	-	-	-	-	-	-	-
S	-	-	-	-	-	-	-
FeO	0.81	0.61	0.85	1.37	-	0.87	0.60
MgO	-	-	-	-	-	-	-
CaO	54.19	53.86	50.11	49.93	53.27	53.38	53.46
Na2O5	-	-	1.11	0.60	-	0.44	-
P2O5	41.05	40.82	38.18	37.49	40.85	40.93	40.25

## APPENDIX E: COMPILATION OF XRD RESULTS FROM YORKSHIRE SAMPLES.

Sample number	Size fraction	Mica, with upto 10% smectite interstratification	Chlorites	Kandites	Vermiculite	Smectites	Interstratified mica:smectite 80:20
207	2 $\mu$ m	20	5	75			
210	"	20		60			20
224	"	25	5	70			
228	"	10		85			5
230	"	30		50			20
231	"			100			
232	"	35		65			
234	"	10		90			
240	"	50		50			
247	"	15	5	75			5
248	"	30		60			10
249	"	30	10	60			
250	"			100			
251	"			100			
252	"	25		75			
253	"			100			
254	"	60		40			
261	"			100			
262	"	45		55			
269	"			100			
270	"			100			
271	"	55		45			
302	"	15		85			
303	"	30		70			
303	5 $\mu$ m	10		90			
303	10 $\mu$ m	10		90			
306	2 $\mu$ m	30		70			
310	"	65		20			15
310	5 $\mu$ m	25		70			5
310	10 $\mu$ m	15		80			5
314	2 $\mu$ m			100			
314	5 $\mu$ m	5		95			
314	10 $\mu$ m	5		95			
317	2 $\mu$ m	35		55			10
318	5 $\mu$ m	15		85			
318	10 $\mu$ m	15		85			
319	5 $\mu$ m	20		80			
319	10 $\mu$ m	20		80			
321	2 $\mu$ m	70		30			
322	"	20		80			

Sample number	Size fraction	Mica, with upto 10% smectite interstratification	Chlorites	Kandites	Vermiculite	Smectites	Interstratified mica:smectite 80:20
322	1 $\mu\text{m}$	25		75			
322	0.5 $\mu\text{m}$	65		35			
325	2 $\mu\text{m}$	30	5	50			15
328	"	10	5	85			
330	"	35		65			
332	"	30		60			10
333	"	50		50			
345	"	18	2	80			
349	"	20		80			
356	0.5 $\mu\text{m}$	55		35			10
356	1 $\mu\text{m}$	40		55			10
356	2 $\mu\text{m}$	25		70			5
356	5 $\mu\text{m}$	15		85			
356	10 $\mu\text{m}$	10		90			
358	2 $\mu\text{m}$	20	5	70			5
359	"	35		35			30
360	"	45		35			20
374	"	10		75	5		10
380	"	15		65			20
390	"	5		95			
393	"	25		65			10
396	"	20		70	10		
404	"	10	5	75			10
405	"	60		30			10
406	"	50		40			10
410	"	10		90			
410	5 $\mu\text{m}$			100			
410	10 $\mu\text{m}$			100			
415	2 $\mu\text{m}$		10	90			
415	0.5 $\mu\text{m}$			100			
422	2 $\mu\text{m}$	25		40		30	5
425	"	50		50			
430	"	50		50			
430	1 $\mu\text{m}$	60		40			
430	0.5 $\mu\text{m}$	65		35			
433	2 $\mu\text{m}$	15		80			5
437	"	40	5	55			
440	"	35		50	15		
444	"	40		45	15		
444	1 $\mu\text{m}$	40		45	15		

Sample number	Size fraction	Mica, with upto 10% smectite interstratification	Chlorites	Kandites	Vermiculite	Smectites	Interstratified mica:smectite 80:20
444	0.5 $\mu\text{m}$	70		30			
448	2 $\mu\text{m}$	55		45			
448	1 $\mu\text{m}$	55		40			5
448	0.5 $\mu\text{m}$	70		30			
450	2 $\mu\text{m}$	25		75			
454	"	35	5	60		25	
461	"	15		60			
470	"	20		70			10
480	"	5		95			
481	"	45		55			
483	"	70		20			10
484	"	80		20			
485	"	10	10	80			
485	1 $\mu\text{m}$	10	10	80			
485	0.5 $\mu\text{m}$	20	15	65			
496	2 $\mu\text{m}$	15	5	75			5
502	"			100			
526	"	45		15			40
528	"	45		55			
529	"	10		90			
540	"	10	15	70			5
542	"	5	20	75			
542	1 $\mu\text{m}$	5	20	75			
542	0.5 $\mu\text{m}$	20	20	60			
544	2 $\mu\text{m}$		20	80			
548	"	70		15	15		
550	"	15		75			10
553	"	50	5	35			10
556	"	15		85			
557	"	70		30			
558	"	15	15	70			
560	"	20		75			5
563	"	15		80			5
570	"	55		45			
572	"	25	15	50			10
577	"	95		5			
577	1 $\mu\text{m}$	75		25			
577	0.5 $\mu\text{m}$	80		20			
578	2 $\mu\text{m}$	80		5	15		
579	"	100					



Sample number	Size fraction	Mica, with upto 10% smectite interstratification	Chlorites	Kandites	Vermiculite	Smectites	Interstratified mica:smectite 80:20
590	2 $\mu$ m	15		65			20
592	"	40		45			15
600	"	30		60	10		
606	"	50		40			10
608	"	25		60	15		
613	"	70		20	10		
622	"	55		45			
624	"	20		60	20		
630	"	10		85			5
634	"	30		70			
638	"			100			
642	"	75	10	15			
655	"				100		
657	"	55		30	15		
662	"	30	5	60			5
667	"	25		50	25		
671	"	30		50			20
687	"	30		60			10
689	"	55		40			5
703	"	65		35			

## APPENDIX F: ANALYTICAL DATA FOR SAMPLES FROM THE NINIAN FIELD

Sample details			3/3-3 Beach ?			Shoreface/Foreshore					Micaceous sandstone									
Sample number			10632	10637	10640	10645	10616	10624	10628		10570	10575	10580	10594	10599	10608	10610			
Quartz - simple		48	59	50	62	60	64	69			67	66	61	49	55	42	60			
Quartz - polycrystalline		15	8	7	10	7	3	-			-	-	-	-	-	-	-			
Rock Fragments																				
Feldspars		1	1	2	3	3	3	2			2	2	1	1	3	-	2			
Mica					-	1	3	-			20	15	20	33	33	38	14			
Clay matrix																				
Opaque and heavy minerals																				
Fossils (plant debris)																				
Chlorites				-	3															
Illite		5	3	3	3	2	1	2			1		1				2			
Kandites		10	8	11	8	8	11	11			3	4	4	4	4	8	6			
Vermiculite																				
Quartz overgrowths		-	-	-	-	5	3	2			1	6	4	2	1	-	6			
Feldspar overgrowths						-	-													
Calcite			14	21				2			1	2	1	1						
Siderite (goethite)		10	3	-	2	1	2	2			3	1	1	2	4	11	8			
Ankerite		3	2	-	-	3	3							2						
Pyrite																				
Intergranular porosity		8	2	6	8	10	6	10			2	5	8	5	1	1	1			
Grain dissolution porosity		-	-	-	-	-	-	-												
Total detritus		64	68	59	75	71	73	71			89	83	82	83	91	80	76			
Total authigenics		28	30	35	16	19	20	19			9	13	11	11	9	19	22			
Total porosity		8	2	6	8	10	6	10			2	5	8	5	1	1	1			

Sample details		Distributary channels														3/3-3 Interdistributary bay filling sands. 3/3-2:													
Sample number		10525	10529	10538	10547	10552	10563		10464	10474	10495	10497	10502	10510	10438	10452													
Quartz - simple		70	70	50	60	70	65		70	68	68	70	30	49	57	74													
Quartz - polycrystalline		8	12	9	10	9	8		3																				
Rock Fragments									-		2			1		1													
Feldspars		2	1	-	6	4	4		5	5	6	2	3	5	2	4													
Mica		-	-	-	-	-	1		1	1	2	3	2	6	1	3													
Clay matrix									1																				
Opaque and heavy minerals		-	-	-	-	-	-		-	-	-	-	-	-	-	-													
Fossils (plant debris)													-	1		-													
Chlorites																													
Illite							2		1	-	1	2				1													
Kandites		5	2	7	7	5	7		5	3	3	6		-	1	3													
Vermiculite																													
Quartz overgrowths		3	3	-	-	2	2		7	11	5	8	-	23	4	5													
Feldspar overgrowths		-							-	-	-	-	-	-	-	-													
Calcite										-		1			17														
Siderite (goethite)		1		1					1	1	5	1	15	7	1	4													
Ankerite		-	-	23	-	-	-						50																
Pyrite		-							1	-	-	-	-	1	10	-													
Intergranular porosity		11	12	10	15	10	12		6	11	8	7		1	7	5													
Grain dissolution porosity		-	-		2	-	-								-	-													
Total detritus		80	83	59	76	83	78		80	74	78	75	35	62	60	82													
Total authigenics		9	5	31	7	7	11		14	15	14	17	65	37	33	15													
Total porosity		11	12	10	17	10	12		6	11	8	.7		1	7	5													

Sample details		Crevasse splay sandstones										Channel sandstones				
Sample number		10456	10465		9895	9916	10342	10420	10447	10454		9902	9906	10310	10319	10323
Quartz - simple		41	62		73	68	70	63	61	73		72	58	76	71	70
Quartz - polycrystalline	1								2				-	1	1	-
Rock Fragments			-						-				1	2	6	4
Feldspars	3	2	2		3	7	7	5	2	4		2	1	2	-	1
Mica	2	6			3	1	1	1	1	1						-
Clay matrix					10		2	15		1						
Opaque and heavy minerals	-	-	-									-	-	-	-	-
Fossils (plant debris)	-	-	-		7			1		1						
Chlorites																
Illite			2							2						-
Kandites			3				1	6	7	3		1		1	1	1
Vermiculite																
Quartz overgrowths	-	7			-	2	16	5	17	4		7	1	5	7	3
Feldspar overgrowths	-	-	-		-		-									
Calcite					-					-				-	-	1
Siderite (goethite)	10	14			-				1			1			-	-
Ankerite	39					24							38			
Pyrite	-	-	-		4			2	-	1						
Intergranular porosity			5		-		4	1	8	10		14		10	11	16
Grain dissolution porosity			-		-				-	-		3		3	2	
Total detritus	50	70			96	76	80	85	66	80		75	61	81	78	75
Total authigenics	49	25			4	26	17	13	25	10		9	39	6	9	6
Total porosity		5					4	1	8	10		17		13	13	16

Sample details		Channel sandstones, 3/3-2														3/3-3:			
Sample number		10365	10369	10380	10385	10400	10405	10295	10325	10350	10365	10385	10406	10425	10434				
Quartz - simple		72	70	71	72	60	77	69	72	67	70	76	70	65	55				
Quartz - polycrystalline				1	1	5			3	2	3				28				
Rock Fragments		3	6	-	1	2		2	3	2	-			-					
Feldspars		3	2	4	1	6	2		1	2	-	-	2	2	-				
Mica		-	-	-	-	-	-		-	-	-								
Clay matrix														7					
Opaque and heavy minerals		-	-	-	-	-	-	-	-	-	-	-	-	-	-				
Fossils (plant debris)																			
Chlorites																			
Illite							1			-									
Kandites		3	1	1	-	3	2	2	1	2	1	1	2	2	3				
Vermiculite																			
Quartz overgrowths		7	7	7	6	4	6	8	8	4	10	7	13	12	-				
Feldspar overgrowths													1						
Calcite			1				1	-		-			-	-	1				
Siderite (goethite)		-	-	1	1	-	-	1		-	-	-	-	2					
Ankerite																			
Pyrite		-								-	-		-		-				
Intergranular porosity		10	10	13	16	20	9	14	12	17	15	12	9	6	11				
Grain dissolution porosity		2	3	3	2		1		2	3	1	1	3	2					
Total detritus		78	78	76	75	73	79	71	76	74	72	79	73	75	83				
Total authigenics		10	9	9	8	7	11	11	9	7	11	8	15	16	5				
Total porosity		12	13	16	18	20	10	14	14	20	16	13	12	8	11				

### Microprobe analyses

Code. Column A: C Carbonates  
P Pyrite  
M Mica  
N Neomorphosing mica ( N01, N02, etc)  
F Feldspar  
K Kandites  
I Illitic clays

Spot. Sequential spot numbers refer to series of analyses on single grains, on single flakes of mica, or in the case of siderite on single spheruliths. Random or irregular spot numbers refer to analyses on different grains, flakes or pore-filling minerals.

Sample Code Spot	NEOMORPHOSING MICAS																	
	3/3-3 10480			3/3-3 10454					3/3-2 10452					3/3-2 10452				
	M04	M04	M04	M04	M05	M05	M05	M05	M05	M01	M01	M01	M01	M01	M01	M02	M02	M02
	1	2	3	4	1	2	3	4	5	1	2	3	4	5	6	1	2	3
SiO <sub>2</sub>	41.58	45.28	46.01	45.53	39.33	45.17	39.20	45.06	45.39	45.76	45.67	43.49	45.83	46.47	46.73	45.00	45.32	45.84
TiO <sub>2</sub>	1.99	n.d.	n.d.	n.d.	0.35	0.79	0.42	n.d.	0.37	0.33	1.04	1.40	36.69	0.77	n.d.	0.21	0.19	n.d.
Al <sub>2</sub> O <sub>3</sub>	28.78	35.99	36.02	37.09	30.65	35.63	30.29	37.30	36.34	35.77	33.80	31.47	0.34	36.21	36.92	35.21	36.06	37.69
FeO	4.78	0.82	0.88	0.42	0.74	1.07	0.60	n.d.	0.64	0.47	1.00	1.21	0.39	0.75	n.d.	1.20	1.02	n.d.
MgO	0.76	0.43	0.40	n.d.	0.21	0.29	0.40	n.d.	0.26	0.25	0.78	0.94	n.d.	0.49	n.d.	0.40	0.52	n.d.
MnO	n.d.	n.d.	n.d.	n.d.	n.d.	n.d.	n.d.	n.d.	n.d.	n.d.	n.d.	n.d.	n.d.	n.d.	n.d.	n.d.	n.d.	n.d.
CaO	n.d.	n.d.	n.d.	n.d.	n.d.	n.d.	n.d.	n.d.	n.d.	0.20	n.d.	n.d.	n.d.	n.d.	n.d.	n.d.	n.d.	n.d.
Na <sub>2</sub> O	0.20	1.60	1.34	0.67	0.63	0.63	0.65	n.d.	0.64	0.27	0.83	0.97	0.39	0.34	n.d.	0.79	0.64	n.d.
K <sub>2</sub> O	5.60	6.44	5.67	2.89	8.14	8.96	6.58	0.20	4.86	3.59	8.63	9.41	2.41	5.48	0.65	9.88	10.03	1.47
TOTAL	83.69	90.56	90.32	86.60	80.05	92.54	78.14	82.56	88.50	86.64	91.75	88.89	86.05	90.51	84.30	92.69	93.78	85.00

Recalculated formula on the basis of 22 oxygens

Si	6.269	6.181	6.250	6.281	6.176	6.128	6.227	6.347	6.232	6.340	6.242	6.210	6.736	6.261	6.460	6.140	6.105	6.333
Al <sup>IV</sup>	1.731	1.819	1.750	1.719	1.824	1.872	1.773	1.653	1.768	1.660	1.758	1.790	0.059	1.739	1.540	1.860	1.875	1.667
Al <sup>VI</sup>	3.382	3.971	4.017	4.311	3.848	3.824	3.897	4.539	4.113	4.181	3.686	3.506	0.000	4.010	4.475	3.803	3.830	4.469
Fe <sup>2</sup>	0.603	0.094	0.100	0.048	0.098	0.121	0.080	0.000	0.073	0.054	0.114	0.144	0.048	0.085	0.000	0.137	0.115	0.000
Mg	0.171	0.087	0.081	0.000	0.049	0.059	0.095	0.000	0.053	0.052	0.159	0.200	0.000	0.098	0.000	0.081	0.104	0.000
Mn	0.000	0.000	0.000	0.000	0.000	0.000	0.000	0.000	0.000	0.000	0.000	0.000	0.000	0.000	0.000	0.000	0.000	0.000
Ca	0.000	0.000	0.000	0.000	0.000	0.000	0.000	0.000	0.000	0.030	0.000	0.000	0.000	0.000	0.000	0.000	0.000	0.000
Na	0.058	0.423	0.353	0.179	0.192	0.166	0.200	0.000	0.170	0.073	0.220	0.269	0.111	0.089	0.000	0.209	0.167	0.000
K	1.077	1.121	0.983	0.509	1.630	1.551	1.333	0.036	0.851	0.635	1.505	1.714	0.452	0.942	0.115	1.720	1.723	0.259

Total aluminium

Total aluminium

Al	5.114	5.790	5.767	6.030	5.672	5.697	5.670	6.192	5.881	5.841	5.445	5.296	0.059	5.750	6.015	5.662	5.725	6.137
----	-------	-------	-------	-------	-------	-------	-------	-------	-------	-------	-------	-------	-------	-------	-------	-------	-------	-------

#### FELDSPARS

3/3-2

				3/3-3			3/3-2										
				10480			10454			10447			10452			→ 10470	
Sample	3/3-2			Sample	F.1	F.1	F.0	F.0	F.0	F.1	F.1	F.1	F.1	F.1	F.1	F.1	
Code	10470...			Code	Spot	3	4	1	1	2	1	2	8	0	10	1	
Spot	M03	M03	M03	Spot													
	1	2	3														
SiO <sub>2</sub>	45.78	45.93	44.77	SiO <sub>2</sub>	63.86	64.29	63.92	62.93	63.37	67.13	66.06	64.63	62.89	63.72	59.74		
TiO <sub>2</sub>	0.78	0.52	n.d.	TiO <sub>2</sub>	n.d.	n.d.	n.d.	n.d.	n.d.	n.d.	n.d.	n.d.	n.d.	n.d.	n.d.		
Al <sub>2</sub> O <sub>3</sub>	34.62	35.20	36.90	AL2O3	18.59	18.56	18.44	17.67	17.95	19.80	20.18	18.60	17.97	18.34	17.44		
FeO	1.17	0.62	n.d.	FeO	n.d.	n.d.	n.d.	n.d.	n.d.	n.d.	n.d.	n.d.	n.d.	n.d.	n.d.		
MgO	0.88	0.37	n.d.	MgO	n.d.	n.d.	n.d.	n.d.	n.d.	n.d.	n.d.	n.d.	n.d.	n.d.	n.d.		
MnO	n.d.	n.d.	n.d.	MNO	n.d.	n.d.	n.d.	n.d.	n.d.	n.d.	n.d.	n.d.	n.d.	n.d.	n.d.		
CaO	n.d.	n.d.	n.d.	CaO	n.d.	n.d.	n.d.	n.d.	n.d.	n.d.	n.d.	n.d.	n.d.	n.d.	n.d.		
Na <sub>2</sub> O	0.48	0.45	n.d.	Na2O	0.74	0.69	1.16	0.48	0.48	10.40	10.76	0.69	0.53	0.47	0.47		
K <sub>2</sub> O	7.29	5.18	0.42	K2O	16.25	16.29	16.13	16.80	16.88	0.26	0.24	16.35	16.42	16.53	15.25		
Total	91.00	88.27	82.09	TOTAL	99.44	99.83	99.65	97.88	98.68	96.92	98.90	100.27	97.80	95.06	92.90		
Total	91.00	88.27	82.09														

Elemental composition on the basis of 8 oxygens

Si	2.976	2.982	2.976	2.992	2.987	2.965	2.974	2.985	2.985	2.984	2.978	2.978	2.978	2.978	2.978
Al	1.021	1.015	1.012	0.990	0.997	1.032	1.039	1.012	1.005	1.012	1.025	1.025	1.025	1.025	1.025
Fe <sup>2</sup>	0.000	0.000	0.000	0.000	0.000	0.000	0.000	0.000	0.000	0.000	0.000	0.000	0.000	0.000	0.000
Mg	0.000	0.000	0.000	0.000	0.000	0.000	0.000	0.000	0.000	0.000	0.000	0.000	0.000	0.000	0.000
Ca	0.000	0.000	0.000	0.000	0.000	0.039	0.031	0.000	0.000	0.000	0.000	0.000	0.000	0.000	0.000
Na	0.067	0.062	0.105	0.044	0.044	0.935	0.912	0.062	0.051	0.043	0.045	0.045	0.045	0.045	0.045
K	0.966	0.964	0.958	1.019	1.015	0.015	0.013	0.963	0.984	0.967	0.970	0.970	0.970	0.970	0.970

Mineralogical composition

AB	6.5	6.0	9.9	4.2	4.1	94.5	95.4	6.0	4.8	4.1	4.5
OP	93.5	94.0	90.1	95.8	95.9	1.5	1.4	94.0	95.2	95.9	95.5
AN	0.0	0.0	0.0	0.0	0.0	4.0	3.2	0.0	0.0	0.0	0.0

Al.	5.564	5.716	6.171
-----	-------	-------	-------



MICAS

Sample Code Spot	3/3-3																10637 N..
	10624	10624	10624	10624	10624	10624	10624	10624	10624	10624	10613	10613	10613	10613	10613	10613	
	N..	N..	N..	N..	N..	N..	N..	N..	N..	N..	N..	N..	N..	N..	N..	N..	
Spot	11	12	13	21	22	23	41	42	43	44	31	51	52	53	71	72	41
SiO <sub>2</sub>	45.18	44.85	45.24	43.97	45.05	45.63	47.60	45.83	45.62	45.68	43.79	44.56	41.57	33.69	46.65	44.83	36.40
TiO <sub>2</sub>	0.27	0.42	n.d.	n.d.	n.d.	n.d.	0.40	0.45	n.d.	0.25	0.32	1.06	0.72	n.d.	0.56	0.63	n.d.
Al <sub>2</sub> O <sub>3</sub>	35.37	35.98	34.75	33.04	34.85	34.82	27.45	33.08	36.37	34.63	28.56	27.72	26.46	23.86	29.47	29.21	22.09
FeO	1.66	1.23	0.86	2.06	1.99	1.99	4.22	2.13	1.09	1.92	1.65	6.04	5.41	1.63	3.00	2.76	0.69
NaO	0.40	0.29	0.48	0.44	0.38	0.54	2.01	0.78	0.41	0.61	0.90	1.38	1.21	0.41	1.55	1.40	0.87
MnO	n.d.	n.d.	n.d.	n.d.	n.d.	n.d.	n.d.	n.d.	n.d.	n.d.	n.d.	n.d.	n.d.	n.d.	n.d.	n.d.	n.d.
CaO	n.d.	0.14	n.d.	n.d.	n.d.	n.d.	n.d.	n.d.	n.d.	n.d.	n.d.	n.d.	n.d.	0.16	n.d.	n.d.	0.49
Na <sub>2</sub> O	0.29	n.d.	n.d.	0.48	0.42	0.38	n.d.	n.d.	n.d.	n.d.	n.d.	0.39	n.d.	n.d.	0.30	0.24	n.d.
K <sub>2</sub> O	5.39	3.86	3.07	9.89	7.34	8.04	9.80	5.70	3.35	5.33	7.80	10.65	9.11	3.45	8.16	7.81	4.78
TOTAL	88.56	86.77	84.40	89.88	90.03	91.40	91.48	87.97	86.84	88.42	83.02	91.80	84.48	63.20	89.69	86.88	65.32

Recalculated formula on the basis of 22 oxygens

Si	6.251	6.244	6.409	6.221	6.232	6.244	6.666	6.406	6.304	6.326	6.587	6.366	6.389	6.507	6.556	6.495	6.827
Al <sub>IV</sub>	1.749	1.756	1.591	1.779	1.768	1.756	1.334	1.594	1.696	1.674	1.413	1.634	1.611	1.493	1.444	1.505	1.173
Al <sub>VI</sub>	4.019	4.146	4.210	3.730	3.914	3.859	3.196	3.855	4.228	3.977	3.651	3.033	3.182	3.938	3.436	3.482	3.710
Fe <sub>2</sub>	0.192	0.143	0.102	0.244	0.230	0.228	0.494	0.249	0.126	0.222	0.208	0.722	0.695	0.263	0.353	0.334	0.108
Na	0.082	0.060	0.101	0.093	0.078	0.110	0.420	0.163	0.084	0.126	0.202	0.294	0.277	0.118	0.325	0.302	0.243
Mn	0.000	0.000	0.000	0.000	0.000	0.000	0.000	0.000	0.000	0.000	0.000	0.000	0.000	0.000	0.000	0.000	0.000
Ca	0.000	0.021	0.000	0.000	0.000	0.000	0.000	0.000	0.000	0.000	0.000	0.000	0.000	0.000	0.000	0.000	0.000
Na	0.078	0.000	0.000	0.132	0.113	0.101	0.000	0.000	0.000	0.000	0.000	0.108	0.000	0.000	0.082	0.067	0.000
K	0.951	0.686	0.555	1.785	1.295	1.403	1.751	1.016	0.591	0.942	1.497	1.941	1.786	0.850	1.463	1.443	1.144

Total aluminium

Al	5.768	5.904	5.802	5.509	5.682	5.615	4.530	5.449	5.924	5.652	5.063	4.667	4.793	5.431	4.881	4.987	4.883
----	-------	-------	-------	-------	-------	-------	-------	-------	-------	-------	-------	-------	-------	-------	-------	-------	-------

ILLITIC CLAYS

Sample Code Spot	3/3-2 3/3-3							10454
	10470	10480						
	N.1	N.1	N.1	N.1	N.1	N.1	N.0	
Spot	2	1	2	5	6	7	2	
SiO <sub>2</sub>	43.28	46.19	45.83	45.56	41.54	46.94	46.62	
TiO <sub>2</sub>	0.53	0.26	0.27	n.d.	1.01	1.27	0.75	
Al <sub>2</sub> O <sub>3</sub>	27.02	34.69	35.56	35.94	26.73	25.78	28.26	
FeO	4.48	1.39	0.89	1.10	4.52	5.13	5.22	
H <sub>2</sub> O	1.39	0.89	0.56	n.d.	1.28	2.05	1.88	
MnO	n.d.	n.d.	n.d.	n.d.	n.d.	n.d.	0.27	
CaO	n.d.	n.d.	n.d.	n.d.	1.29	0.17	n.d.	
Na <sub>2</sub> O	0.45	0.96	1.10	1.23	0.65	0.57	0.39	
K <sub>2</sub> O	9.36	6.96	5.43	4.90	9.68	10.42	10.72	
Total	86.51	91.34	89.64	88.73	86.70	92.33	94.11	

Recalculated formula on the basis of 22 oxygens

Si	6.462	6.274	6.261	6.269	6.271	6.616	6.453
Al <sub>IV</sub>	1.538	1.726	1.739	1.731	1.729	1.384	1.547
Al <sub>VI</sub>	3.217	3.828	3.986	4.097	3.027	2.898	3.063
Fe <sub>2</sub>	0.559	0.158	0.102	0.127	0.571	0.605	0.604
Na	0.309	0.180	0.114	0.000	0.288	0.431	0.388
Mn	0.000	0.000	0.000	0.000	0.000	0.000	0.032
Ca	0.000	0.000	0.000	0.000	0.209	0.026	0.000
Na	0.130	0.253	0.291	0.328	0.190	0.156	0.105
K	1.783	1.206	0.946	0.860	1.864	1.873	1.893

Total aluminium

Al	4.755	5.554	5.725	5.828	4.756	4.282	4.610
----	-------	-------	-------	-------	-------	-------	-------

Sample Code Spot	3/3-2				3/3-3		3/3-3 10447
	10452				10454		
	I.1	I.1	I.1	I.1	I.0	I.0	
Spot	5	11	12	13	3	4	5
SiO <sub>2</sub>	44.48	45.69	48.07	45.56	29.53	43.85	46.94
TiO <sub>2</sub>	0.37	n.d.	n.d.	0.22	n.d.	n.d.	n.d.
Al <sub>2</sub> O <sub>3</sub>	34.30	28.05	29.40	35.97	14.91	30.17	29.35
FeO	1.53	0.90	2.70	0.59	2.00	1.15	2.75
H <sub>2</sub> O	0.44	0.90	2.01	n.d.	0.98	0.62	1.92
MnO	n.d.	n.d.	n.d.	n.d.	n.d.	n.d.	n.d.
CaO	n.d.	n.d.	n.d.	n.d.	0.21	n.d.	n.d.
Na <sub>2</sub> O	n.d.	n.d.	n.d.	0.45	0.28	n.d.	n.d.
K <sub>2</sub> O	3.19	9.44	10.41	5.19	3.87	5.85	6.58
Total	84.31	84.98	92.59	87.98	51.78	81.64	87.54

Si	6.349	6.742	6.609	6.293	7.099	6.578	6.657
Al <sub>IV</sub>	1.651	1.258	1.391	1.707	0.901	1.422	1.343
Al <sub>VI</sub>	4.120	3.621	3.373	4.148	3.323	3.912	3.563
Fe <sub>2</sub>	0.183	0.111	0.310	0.068	0.402	0.144	0.326
Na	0.094	0.198	0.412	0.000	0.351	0.139	0.406
Mn	0.000	0.000	0.000	0.000	0.000	0.000	0.000
Ca	0.000	0.000	0.000	0.000	0.054	0.000	0.000
Na	0.000	0.000	0.000	0.121	0.131	0.000	0.000
K	0.581	1.777	1.826	0.914	1.187	1.119	1.190

Al	5.770	4.878	4.764	5.855	4.224	5.334	4.906
----	-------	-------	-------	-------	-------	-------	-------

3/3-3								
10613	10613	10613	10613	10613	10637	10637	10637	
F..	F..	F..	F..	F..	F..	F..	F..	F..
11	12	13	61	62	11	12	13	
66.88	67.59	65.51	62.88	63.64	63.86	63.83	63.07	
n.d.	n.d.	n.d.	0.22	n.d.	n.d.	n.d.	0.26	
19.37	19.82	19.65	18.97	18.94	18.44	18.58	17.85	
n.d.	n.d.	n.d.	n.d.	n.d.	n.d.	n.d.	n.d.	
n.d.	n.d.	n.d.	n.d.	n.d.	n.d.	n.d.	n.d.	
n.d.	n.d.	n.d.	n.d.	n.d.	n.d.	n.d.	n.d.	
n.d.	0.32	0.22	0.39	n.d.	n.d.	n.d.	n.d.	
11.45	10.99	10.76	1.40	0.84	1.14	0.95	0.64	
n.d.	0.13	n.d.	14.67	15.68	16.34	15.91	15.85	
97.70	98.85	96.14	98.53	99.02	99.78	99.27	97.67	

Elemental composition on the basis of 8 oxygens

2.987	2.982	2.971	2.952	2.968	2.973	2.976	2.996
1.020	1.031	1.050	1.049	1.041	1.012	1.021	0.999
0.000	0.000	0.000	0.000	0.000	0.000	0.000	0.000
0.000	0.000	0.000	0.000	0.000	0.000	0.000	0.000
0.000	0.015	0.011	0.020	0.000	0.000	0.000	0.000
0.992	0.940	0.946	0.127	0.076	0.103	0.086	0.059
0.000	0.007	0.000	0.878	0.928	0.970	0.946	0.960

Mineralogical composition

100.0	97.7	98.9	12.4	7.6	9.6	8.3	5.8
0.0	0.8	0.0	85.7	92.4	90.4	91.7	94.2
0.0	1.6	1.1	1.9	0.0	0.0	0.0	0.0

# KANDITES

3/3-2				3/3-3		3/3-3	
Sample	10452			10454	10447		
Code	K.1	K.1	K.1	K.1	K.0	K.0	K.0
Spot	3	4	6	7	4	2	7
SiO <sub>2</sub>	44.16	37.70	45.84	45.34	46.23	45.54	42.20
TiO <sub>2</sub>	n.d.	n.d.	n.d.	n.d.	n.d.	n.d.	n.d.
Al <sub>2</sub> O <sub>3</sub>	36.17	22.61	37.76	36.84	37.72	37.23	34.56
FeO	n.d.	0.21	n.d.	n.d.	n.d.	n.d.	n.d.
MgO	n.d.	n.d.	n.d.	n.d.	n.d.	n.d.	n.d.
MnO	n.d.	n.d.	n.d.	n.d.	n.d.	n.d.	n.d.
CaO	n.d.	0.26	n.d.	n.d.	n.d.	n.d.	n.d.
Na <sub>2</sub> O	n.d.	0.35	n.d.	n.d.	n.d.	n.d.	n.d.
K <sub>2</sub> O	n.d.	0.67	0.13	0.23	0.16	n.d.	n.d.
Total	86.33	61.80	83.73	82.41	84.11	82.77	76.76

Si	4.060	4.527	4.048	4.070	4.064	4.064	4.061
Al	3.920	3.200	3.930	3.898	3.908	3.915	3.919
Fe <sub>2</sub>	0.000	0.021	0.000	0.000	0.000	0.000	0.000
Mg	0.000	0.000	0.000	0.000	0.000	0.000	0.000
Ca	0.000	0.033	0.000	0.000	0.000	0.000	0.000
Na	0.000	0.081	0.000	0.000	0.000	0.000	0.000
K	0.000	0.103	0.015	0.026	0.018	0.000	0.000

3/3-3							3/3-3											
Sample	10632	10632	10632	10637	10637	10637	10624	10624	10624	10624	10624	10613	10613	10613	10613	10613	10613	10632
Code	K..	K..	K..	K..	K..	K..	K..	K..	K..	K..	K..	K..	K..	K..	K..	K..	K..	K..
Spot	112	113	114	21	31	51	31	32	33	34	51	21	22	23	24	41	42	81
SiO <sub>2</sub>	45.08	45.75	41.61	42.52	45.08	27.65	45.45	44.59	46.46	45.53	46.00	35.20	37.66	34.75	46.03	44.89	46.42	44.69
TiO <sub>2</sub>	n.d.	n.d.	n.d.	n.d.	n.d.	n.d.	n.d.	0.20	n.d.	0.23	n.d.	n.d.	n.d.	n.d.	n.d.	n.d.	n.d.	n.d.
Al <sub>2</sub> O <sub>3</sub>	37.50	37.51	34.32	34.76	37.03	21.92	36.98	36.08	38.46	37.25	37.07	27.83	30.20	28.34	38.99	37.22	37.89	36.12
FeO	n.d.	n.d.	0.24	n.d.	n.d.	n.d.	n.d.	0.28	n.d.	n.d.	0.29	n.d.	n.d.	n.d.	n.d.	n.d.	n.d.	n.d.
MgO	n.d.	n.d.	n.d.	n.d.	n.d.	n.d.	n.d.	n.d.	0.22	n.d.	n.d.	n.d.	n.d.	n.d.	n.d.	n.d.	n.d.	n.d.
MnO	n.d.	n.d.	n.d.	n.d.	n.d.	n.d.	0.20	n.d.	n.d.	n.d.	n.d.	n.d.	n.d.	n.d.	n.d.	n.d.	n.d.	n.d.
CaO	n.d.	n.d.	n.d.	n.d.	n.d.	0.12	n.d.	0.16	0.14	n.d.	n.d.	n.d.	0.16	n.d.	0.13	n.d.	n.d.	n.d.
Na <sub>2</sub> O	n.d.	n.d.	n.d.	n.d.	n.d.	n.d.	n.d.	n.d.	n.d.	n.d.	n.d.	n.d.	n.d.	n.d.	n.d.	n.d.	n.d.	n.d.
K <sub>2</sub> O	n.d.	n.d.	0.16	n.d.	n.d.	n.d.	0.30	0.47	n.d.	1.35	0.87	n.d.	n.d.	0.13	n.d.	n.d.	0.12	0.28
TOTAL	82.58	83.26	76.33	77.28	82.11	49.69	82.93	81.78	85.28	84.36	84.23	63.03	68.02	63.22	84.25	82.11	84.43	81.09

Recalculated formula on the basis of 14 oxygens

Si	4.034	4.059	4.040	4.064	4.055	4.110	4.067	4.062	4.030	4.040	4.067	4.120	4.091	4.065	4.039	4.039	4.064	4.078
Al	3.955	3.922	3.927	3.915	3.926	3.840	3.900	3.874	3.932	3.896	3.863	3.839	3.866	3.907	3.939	3.947	3.910	3.885
Fe <sub>2</sub>	0.000	0.000	0.019	0.000	0.000	0.000	0.000	0.021	0.000	0.000	0.021	0.000	0.000	0.000	0.000	0.000	0.000	0.000
Mg	0.000	0.000	0.000	0.000	0.000	0.000	0.000	0.000	0.028	0.000	0.000	0.000	0.000	0.000	0.000	0.000	0.000	0.000
Ca	0.000	0.000	0.000	0.000	0.000	0.019	0.000	0.016	0.013	0.000	0.000	0.000	0.019	0.000	0.012	0.000	0.000	0.000
Na	0.000	0.000	0.000	0.000	0.000	0.000	0.000	0.000	0.000	0.000	0.000	0.000	0.000	0.000	0.000	0.000	0.000	0.000
K	0.000	0.000	0.020	0.000	0.000	0.000	0.034	0.055	0.000	0.153	0.098	0.000	0.000	0.019	0.000	0.000	0.013	0.033

## CARBONATES

Sample Code Spot	3/3-2 10470					10470		3/3-3 10480		3/3-3 10454		10454						
	C1	C1	C1	C1	C1	C1	C1	C1	C1	C1	C1	C1	C1	C1	C1	C1	C1	C1
	111	112	113	114	115	116	117	11	51	81	82	101	102	103	104	105	106	107
S102	0.56	2.29	n.d.	0.99	0.57	1.00	0.23	1.10	n.d.	2.49	0.45	0.24	3.98	0.83	0.36	2.36	n.d.	0.19
T102	n.d.	n.d.	n.d.	n.d.	n.d.	n.d.	n.d.	n.d.	n.d.	n.d.	n.d.	n.d.	n.d.	n.d.	n.d.	n.d.	n.d.	n.d.
AL203	n.d.	1.90	n.d.	0.44	n.d.	0.38	n.d.	0.73	n.d.	0.67	n.d.	n.d.	1.79	n.d.	n.d.	1.26	n.d.	n.d.
FE0	49.82	44.84	58.25	47.63	47.96	48.94	55.23	43.07	51.39	48.98	50.45	43.22	46.27	48.12	48.12	43.81	44.44	44.01
MgO	5.09	7.54	0.34	4.31	5.84	5.19	n.d.	8.81	5.74	6.93	7.11	7.49	6.31	7.45	7.45	6.82	7.71	7.40
MNO	1.06	1.42	1.03	1.02	1.36	1.17	1.75	1.08	0.89	0.68	0.93	1.88	1.58	0.86	0.86	2.14	2.14	2.06
CaO	1.98	1.89	0.63	1.66	1.99	1.77	1.49	1.82	2.17	2.25	1.62	5.66	2.40	2.74	2.74	3.97	5.89	5.84
Na2O	n.d.	n.d.	n.d.	n.d.	n.d.	n.d.	n.d.	0.44	n.d.	0.27	n.d.	n.d.	0.33	0.57	0.57	n.d.	n.d.	n.d.
K2O	n.d.	n.d.	n.d.	0.13	n.d.	n.d.	n.d.	n.d.	n.d.	n.d.	n.d.	0.43	n.d.	0.12	0.12	0.49	n.d.	n.d.
CO2	38.29	38.06	37.19	35.82	38.16	37.76	36.09	38.10	40.00	39.76	40.51	40.26	38.10	40.29	40.29	38.73	41.59	40.90
TOTAL	96.80	97.94	97.44	92.00	95.88	96.21	94.79	95.15	100.19	102.03	101.07	99.18	100.76	100.98	100.51	99.58	101.77	100.40

## Recalculated carbonate composition

CA	4.059	3.897	1.330	3.637	4.093	3.679	3.240	3.749	4.257	4.441	3.138	11.033	4.944	5.337	5.337	8.045	11.114	11.206
FE2	79.709	72.162	95.954	81.459	76.988	79.393	93.751	69.247	78.696	75.467	76.278	65.759	74.399	73.154	73.154	69.299	65.454	65.915
Mg	14.514	21.627	0.998	13.137	16.708	15.006	0.000	25.245	15.666	19.030	19.160	20.311	18.083	20.186	20.186	19.227	20.239	19.754
MN	1.718	2.315	1.718	1.767	2.211	1.922	3.009	1.759	1.380	1.061	1.424	2.897	2.573	1.324	1.324	3.428	3.192	3.125

Sample Code Spot	3/3-3 10480					3/3-3 10480							3/3-3 10454			3/3-3 10632		
	C1	C1	C1	C1	C1	C1	C1	C1	C1	C1	C1	C1	C1	C1	C1	C1	C1	C1
	52	53	54	55	61	62	63	71	72	73	81	82	83	131	132	133	11	12
S102	n.d.	0.29	n.d.	0.37	0.21	0.27	0.35	n.d.	n.d.	0.23	0.24	0.76	0.36	0.41	0.23	n.d.	4.03	2.67
T102	n.d.	n.d.	n.d.	n.d.	n.d.	n.d.	n.d.	n.d.	n.d.	n.d.	n.d.	n.d.	n.d.	n.d.	n.d.	n.d.	n.d.	n.d.
AL203	n.d.	n.d.	n.d.	n.d.	n.d.	n.d.	n.d.	n.d.	n.d.	n.d.	n.d.	0.49	n.d.	0.24	n.d.	n.d.	0.27	2.02
FE0	56.45	42.93	54.16	55.83	9.21	10.09	10.96	9.51	9.47	9.15	9.35	9.41	9.89	56.49	48.62	49.57	53.08	51.00
MgO	2.36	11.86	4.20	0.77	10.64	10.15	9.67	11.23	11.30	11.02	10.84	10.11	10.46	1.84	6.98	7.26	1.30	1.27
MNO	0.57	0.91	0.67	1.46	0.54	0.68	0.86	0.58	0.38	0.56	0.48	0.49	0.68	1.23	0.42	1.04	1.77	1.31
CaO	1.77	3.04	2.07	2.38	34.64	34.11	33.69	35.11	35.60	35.29	35.51	33.92	34.78	1.53	2.41	2.19	3.03	4.61
Na2O	n.d.	n.d.	n.d.	n.d.	n.d.	0.38	n.d.	0.37	0.29	n.d.	n.d.	n.d.	n.d.	n.d.	n.d.	n.d.	0.56	n.d.
K2O	n.d.	n.d.	n.d.	n.d.	n.d.	0.17	n.d.	0.14	n.d.	n.d.	n.d.	0.14	n.d.	n.d.	n.d.	n.d.	0.13	0.42
CO2	38.96	42.20	39.80	37.81	44.78	44.45	44.24	46.00	46.31	45.68	45.73	43.73	45.19	38.58	39.56	40.65	37.41	37.06
TOTAL	100.05	101.23	100.90	98.62	100.02	100.30	99.77	102.94	103.35	101.93	102.15	99.05	101.36	100.32	98.22	100.71	101.58	100.36

## Recalculated carbonate composition

CA	3.571	5.654	4.081	4.939	60.711	60.219	59.758	59.900	60.326	60.630	60.943	60.879	60.394	3.113	4.782	4.228	6.356	9.763
FE2	88.896	62.322	83.354	90.442	12.599	13.904	15.174	12.664	12.526	12.270	12.525	13.183	13.405	89.702	75.294	74.689	86.914	84.302
Mg	6.624	30.686	11.521	2.223	25.942	24.928	23.862	26.653	26.639	26.339	25.881	25.243	25.268	5.207	19.266	19.496	3.794	3.742
MN	0.909	1.338	1.044	2.395	0.748	0.949	1.206	0.782	0.509	0.761	0.651	0.695	0.933	1.978	0.659	1.587	2.935	2.193

Sample Code Spot	3/3-3 10632					3/3-3 10632							3/3-3 10632			3/3-3 10632		
	C1	C1	C1	C1	C1	C1	C1	C1	C1	C1	C1	C1	C1	C1	C1	C1	C1	C1
	14	15	21	22	23	24	31	32	33	41	42	51	52	53	54	55	56	71
S102	1.09	0.70	0.87	0.59	1.01	0.83	0.26	0.86	1.26	n.d.	0.27	n.d.	n.d.	0.27	0.32	0.25	n.d.	0.20
T102	n.d.	n.d.	n.d.	n.d.	n.d.	n.d.	0.00	n.d.	n.d.	n.d.	n.d.	n.d.	n.d.	n.d.	n.d.	n.d.	n.d.	n.d.
AL203	0.48	0.25	0.29	0.23	0.78	0.64	0.00	n.d.	0.45	n.d.	n.d.	n.d.	n.d.	n.d.	n.d.	n.d.	n.d.	n.d.
FE0	51.29	51.85	55.13	56.09	52.51	51.21	56.15	54.64	51.39	56.29	56.72	55.79	53.69	57.76	55.50	56.80	57.63	10.43
MgO	2.42	11.97	1.08	1.08	3.76	2.73	0.46	1.39	2.41	1.22	1.41	1.53	1.24	1.39	0.89	0.59	1.15	11.23
MNO	0.43	0.45	2.73	1.48	1.09	0.52	3.45	1.57	0.89	0.48	0.37	1.85	3.43	0.93	n.d.	0.36	n.d.	0.30
CaO	6.65	5.96	3.08	2.92	3.44	5.16	1.41	3.82	5.35	4.08	3.58	3.88	3.12	2.47	4.83	3.66	4.00	33.39
Na2O	0.46	n.d.	0.45	n.d.	n.d.	n.d.	n.d.	n.d.	0.47	n.d.	0.53	0.43	n.d.	n.d.	0.42	n.d.	0.46	n.d.
K2O	n.d.	n.d.	0.14	n.d.	n.d.	n.d.	n.d.	n.d.	n.d.	n.d.	n.d.	n.d.	n.d.	n.d.	n.d.	n.d.	n.d.	n.d.
CO2	39.55	49.79	39.06	38.75	39.65	38.72	38.14	38.96	38.86	39.31	39.32	40.04	38.82	39.41	38.76	38.53	39.70	45.04
TOTAL	102.37	120.97	102.83	101.14	102.24	99.81	99.87	101.24	101.08	101.38	102.20	103.52	100.30	102.23	100.72	100.19	102.94	100.59

## Recalculated carbonate composition

CA	13.197	9.395	6.188	5.914	6.809	10.458	2.901	7.695	10.804	8.145	7.145	7.605	6.308	4.918	9.780	7.454	7.908	58.180
FE2	79.448	63.795	86.457	88.673	81.131	81.012	90.171	85.910	81.004	87.710	88.357	85.356	84.723	89.768	87.713	90.295	88.929	14.185
Mg	6.681	26.249	3.019	3.043	10.354	7.697	1.317	3.895	6.771	3.388	3.915	4.172	3.487	3.850	2.507	1.672	3.163	27.222
MN	0.675	0.561	4.336	2.370	1.706	0.833	5.611	2.500	1.421	0.758	0.584	2.867	5.482	1.464	0.000	0.580	0.000	0.413



Sample number	Size fraction	Mica, with upto 10% smectite interstratification	Chlorites	Kandites	Vermiculite	Smectites	Interstratified mica:smectite 80:20
3/3-1 9911 9906	2 $\mu$ m "	50		50 100			
3/3-3 10290 10295 10323 10350 10406	" " " " "	30 25		60 75 100 100 85		10	
10454 10474 10495 10510 10519	" " " " "	15 15 30 45 12		85 85 60 55 85		10	3
10529 10538 10547 10562 10570	" " " " "	9 10 10 15	1	100 90 90 90 80			1
10580 10590 10599 10610 10620	" " " " "	20 15 16 15 10	1	80 80 75 80 90			4 5 9 4
10632 10640	" "	10 10		85 85			5 5

## APPENDIX G: ANALYTICAL DATA FOR SAMPLES FROM 210/15-2

Sample details      210/15-2																
Sample number	6781	6794	6804	6810	6818	6842	6849	6858	6865	6880	6888	6894	6900	6910	6918	
Quartz - simple	50	49	44	36	36	29	20	35	42	50	40	33	35	35	30	
Quartz - polycrystalline	3	3	14	14	7	5	7	14	20	4	7	23	13	13	5	
Rock Fragments																
Feldspars	18	13	16	18	12	8	3	12	9	12	11	14	11	9	8	
Mica	1	2	2	7	2	2	7			-	5	-	2	4	13	
Clay matrix								5								
Opaque and heavy minerals	-	-	-	-	-	-	-	-	-	-	-	-	-	-	-	
Fossils (plant debris)							-							-		
Chlorites																
Illite																
Kandites	2	3	-	10	20	7	5	17	2	5	11	4	15	11	15	
Vermiculite																
Quartz overgrowths	-	3	-	2	-	-	-	1	3	-	1	2	-	3	1	
Feldspar overgrowths	-	-	-	-	-	-	-	-	-	-	-	-	-	--	-	
Calcite	1			-	20	49	53			29			21			
Siderite (goethite)	1	3	1	4	2	-	4	4			2		1		7	
Ankerite																
Pyrite																
Intergranular porosity	18	20	18	10				13	20		20	20	1	20	18	
Grain dissolution porosity	4	4	5	-				-	5		3	3		4	3	
Total detritus	72	67	76	75	57	44	37	66	71	66	63	70	62	61	56	
Total authigenics	5	10	1	16	42	56	62	22	5	34	14	6	37	14	23	
Total porosity	22	24	23	10				13	25		23	23	1	24	21	

Microprobe analyses.

Codes. Column A: M Mica  
F Feldspar  
F.O Feldspar overgrowth  
K Kandites  
K.F Kandite replacement of feldspar  
C Carbonates

Spots. Generally refer to sequences of analyses on individual grains, for example, 11 to 19 refers to mica 1 analyses 1 to 9. Random or irregular numbers refer to analysis of different grains or pores of clays or carbonates.



## KANDITES

Sample Code Spot	6785 K.. 62	6785 K.. 81	6785 K.. 91	6818 K.. 21	6818 K.. 41	6818 K.. 62	6846 Kf. 11	6846 Kf. 12	6846 K.. 31	6846 K.. 32	6854 K.. 31	6854 K.. 32	6854 K.. 33	6854 K.. 41	6854 K.. 42	6854 K.. 61	6854 K.. 62	6854 K.. 81	6854 K.. 82	6785 K.. 61
S102	45.09	45.56	46.03	44.71	45.59	45.75	44.53	42.68	43.44	44.70	44.84	44.77	43.02	45.16	45.72	46.31	45.89	45.93	45.46	43.12
T102	n.d.	n.d.	n.d.	0.42	n.d.	n.d.	n.d.	n.d.	n.d.	n.d.	n.d.	n.d.	n.d.	n.d.	n.d.	n.d.	n.d.	n.d.	n.d.	n.d.
AL203	36.86	37.12	37.53	35.99	37.37	37.07	35.55	34.74	34.77	36.43	36.63	36.99	35.22	35.88	37.49	38.15	37.43	37.18	37.51	34.30
FE0	n.d.	n.d.	n.d.	1.07	n.d.	n.d.	0.90	0.80	n.d.	n.d.	0.55	n.d.	n.d.	0.66	n.d.	n.d.	0.24	n.d.	n.d.	n.d.
MGO	n.d.	n.d.	n.d.	0.22	n.d.	0.26	n.d.	0.18	n.d.	n.d.	n.d.	n.d.	n.d.	n.d.	0.29	n.d.	n.d.	n.d.	0.23	n.d.
MNO	n.d.	n.d.	n.d.	n.d.	n.d.	n.d.	n.d.	n.d.	n.d.	n.d.	n.d.	n.d.	n.d.	n.d.	n.d.	n.d.	n.d.	n.d.	n.d.	n.d.
CAO	n.d.	n.d.	n.d.	n.d.	n.d.	n.d.	n.d.	0.20	n.d.	n.d.	n.d.	n.d.	n.d.	n.d.	n.d.	n.d.	n.d.	n.d.	n.d.	n.d.
NA2O	n.d.	n.d.	n.d.	n.d.	n.d.	n.d.	n.d.	n.d.	n.d.	n.d.	0.30	n.d.	n.d.	n.d.	n.d.	n.d.	n.d.	n.d.	0.35	n.d.
K2O	n.d.	n.d.	0.22	0.12	0.47	0.21	0.17	n.d.	0.77	0.68	0.62	0.53	n.d.	1.60	0.12	n.d.	0.21	n.d.	0.11	0.17
TOTAL	81.95	82.68	83.78	82.53	83.43	83.29	81.15	78.60	78.98	81.81	82.94	82.29	78.24	83.30	83.62	84.46	83.77	83.11	83.66	77.59

Recalculated formula on the basis of 14 oxygens

Si	4.064	4.069	4.065	4.055	4.051	4.065	4.081	4.039	4.086	4.057	4.035	4.037	4.061	4.071	4.045	4.051	4.059	4.080	4.029	4.107
Al	3.915	3.908	3.906	3.847	3.914	3.882	3.840	3.875	3.854	3.897	3.885	3.931	3.918	3.812	3.909	3.933	3.902	3.893	3.918	3.850
Fe2	0.000	0.000	0.000	0.081	0.000	0.000	0.069	0.063	0.000	0.000	0.041	0.000	0.000	0.050	0.000	0.000	0.018	0.000	0.000	0.000
Mg	0.000	0.000	0.000	0.030	0.000	0.034	0.000	0.025	0.000	0.000	0.000	0.000	0.000	0.000	0.038	0.000	0.000	0.000	0.030	0.000
Ca	0.000	0.000	0.000	0.000	0.000	0.000	0.000	0.020	0.000	0.000	0.000	0.000	0.000	0.000	0.000	0.000	0.000	0.000	0.000	0.000
Na	0.000	0.000	0.000	0.000	0.000	0.000	0.000	0.000	0.000	0.000	0.052	0.000	0.000	0.000	0.000	0.000	0.000	0.000	0.060	0.000
K	0.000	0.000	0.025	0.014	0.053	0.024	0.020	0.000	0.092	0.079	0.071	0.061	0.000	0.184	0.014	0.000	0.024	0.000	0.012	0.021

## CARBONATES

Sample Code Spot	6818 C.. 1	6818 C.. 2	6818 C.. 3	6818 C.. 4	6818 C.. 5	6818 C.. 6	6818 C.. 6	6818 C.. 7	6818 C.. 8	6818 C.. 9	6818 C.. 10	6818 C.. 11	6818 C.. 12	6818 C 141	6854 C 41	6854 C 42	6854 C 43
S102	0.17	n.d.	n.d.	1.09	0.25	n.d.	n.d.	0.19	0.19	n.d.	n.d.	0.18	0.29	0.25	0.36	0.29	0.22
T102	n.d.	n.d.	n.d.	n.d.	n.d.	n.d.	n.d.	n.d.	n.d.	n.d.	n.d.	n.d.	n.d.	n.d.	1.15	n.d.	0.37
AL203	n.d.	n.d.	n.d.	n.d.	n.d.	n.d.	n.d.	n.d.	n.d.	n.d.	n.d.	n.d.	n.d.	n.d.	n.d.	n.d.	n.d.
FE0	1.25	1.26	1.16	1.02	1.40	1.05	1.05	1.27	1.12	0.71	0.87	1.21	0.38	52.52	50.92	62.05	48.75
MGO	n.d.	n.d.	n.d.	n.d.	0.26	n.d.	n.d.	n.d.	n.d.	n.d.	n.d.	n.d.	n.d.	3.29	3.98	n.d.	5.23
MNO	n.d.	0.26	n.d.	n.d.	n.d.	n.d.	n.d.	n.d.	n.d.	n.d.	n.d.	n.d.	n.d.	0.38	0.48	0.89	0.52
CAO	54.27	54.50	54.98	53.07	54.98	55.38	55.38	55.50	56.13	55.39	55.71	54.73	57.23	4.88	4.66	0.29	5.48
NA2O	n.d.	n.d.	n.d.	n.d.	n.d.	n.d.	n.d.	n.d.	n.d.	n.d.	n.d.	n.d.	n.d.	n.d.	n.d.	n.d.	n.d.
K2O	n.d.	n.d.	n.d.	n.d.	n.d.	n.d.	n.d.	n.d.	n.d.	n.d.	n.d.	n.d.	n.d.	n.d.	0.13	n.d.	n.d.
CO2	43.36	43.70	43.86	42.27	44.29	44.10	44.10	44.33	44.74	43.90	44.25	43.69	45.15	39.83	39.49	38.79	40.20
TOTAL	99.05	99.72	100.00	97.45	101.18	100.53	100.53	101.29	102.18	100.00	100.83	99.81	103.05	101.15	101.17	102.31	100.77

Recalculated carbonate composition

Ca	98.234	97.845	98.380	98.522	97.423	98.542	98.542	98.245	98.466	99.009	98.796	98.304	99.484	9.615	9.260	0.587	10.699
Fe2	1.766	1.766	1.620	1.478	1.936	1.458	1.458	1.755	1.534	0.991	1.204	1.696	0.516	80.774	78.983	97.990	74.293
Mg	0.000	0.000	0.000	0.000	0.641	0.000	0.000	0.000	0.000	0.000	0.000	0.000	0.000	9.018	11.063	0.000	14.205
Mn	0.000	0.369	0.000	0.000	0.000	0.000	0.000	0.000	0.000	0.000	0.000	0.000	0.000	0.592	0.754	1.424	0.803

Sample Code Spot	6785 C 91	6785 C 92	6846 C 11	6846 C 12	6846 C 13	6846 C 51	6846 C 52	6846 C 61	6846 C 62	6785 C 71	6785 C 72	6785 C 73	6818 C 91
S102	1.29	0.85	0.21	0.84	0.23	0.19	0.26	0.48	0.68	1.16	0.27	0.62	0.68
T102	n.d.	n.d.	n.d.	n.d.	n.d.	n.d.	n.d.	n.d.	n.d.	n.d.	n.d.	n.d.	n.d.
AL203	1.11	0.76	n.d.	0.49	n.d.	n.d.	n.d.	0.10	0.30	0.65	n.d.	0.56	0.45
FE0	46.93	48.47	51.16	51.48	49.32	44.83	48.46	50.14	49.64	44.25	46.79	46.11	52.59
MGO	6.11	3.89	3.44	3.97	6.24	5.65	4.36	4.87	3.92	6.60	4.43	8.45	1.98
MNO	0.40	0.52	0.28	0.32	0.42	0.45	0.47	0.46	0.46	0.38	0.38	0.46	0.72
CAO	4.79	5.53	5.84	3.61	3.39	7.43	6.84	4.49	5.07	6.86	7.12	3.95	4.94
NA2O	n.d.	n.d.	0.02	n.d.	n.d.	n.d.	n.d.	n.d.	n.d.	n.d.	0.58	0.47	n.d.
K2O	n.d.	n.d.	n.d.	0.16	n.d.	n.d.	n.d.	n.d.	n.d.	0.12	n.d.	n.d.	n.d.
CO2	39.43	38.60	39.85	38.90	39.95	39.74	40.10	39.84	38.95	39.93	39.32	40.86	38.70
TOTAL	100.06	98.62	100.80	99.77	99.55	98.29	100.49	100.38	99.02	99.95	98.89	101.48	100.06

Recalculated carbonate composition

Ca	9.535	11.243	11.501	7.283	6.660	14.673	13.385	8.845	10.215	13.482	14.210	7.587	10.018
Fe2	72.916	76.919	78.639	81.065	75.633	69.102	74.019	77.093	78.065	67.882	72.890	69.134	83.242
Mg	16.920	11.002	9.424	11.142	17.055	15.522	11.869	13.346	10.987	18.045	12.300	22.580	5.586
Mn	0.629	0.836	0.436	0.510	0.652	0.703	0.727	0.716	0.733	0.590	0.600	0.699	1.154

MICAS

Sample Code Spot	6854 M.. 21	6854 M.. 51	6854 M.. 52	6854 M.. 53	6854 M.. 54	6854 M.. 131	6854 M.. 132	6904 M.. 11	6904 M.. 12	6904 M.. 13	6904 M.. 14	6904 M.. 15	6904 M.. 16	6904 M.. 17	6904 M.. 18	6904 M.. 19	6904 M.. 31	6785 M.. 31	6785 M.. 32
SiO2	45.23	23.97	44.86	44.10	47.75	44.53	46.74	4.59	45.69	44.17	45.71	45.86	45.41	44.09	27.76	43.10	42.99	44.68	42.57
TiO2	0.20	0.64	0.27	0.48	0.90	0.68	1.48	0.97	0.81	0.98	1.23	0.87	n.d.	0.97	0.50	n.d.	n.d.	0.65	0.57
Al2O3	36.20	10.11	33.78	31.27	27.18	30.44	25.46	34.42	35.19	33.93	35.17	34.74	36.28	33.56	21.27	34.64	33.63	30.20	28.22
FeO	1.10	1.10	1.44	2.70	4.75	3.91	4.69	1.07	0.64	1.09	1.17	1.16	0.31	1.22	0.66	0.26	0.91	4.14	3.66
MgO	0.28	0.23	0.38	0.87	2.30	0.90	0.87	0.75	0.44	0.47	0.38	0.44	n.d.	0.58	0.31	0.27	0.58	1.08	1.10
MnO	n.d.	n.d.	n.d.	n.d.	n.d.	n.d.	n.d.	n.d.	n.d.	n.d.	n.d.	n.d.	n.d.	n.d.	n.d.	n.d.	n.d.	n.d.	n.d.
CaO	n.d.	n.d.	n.d.	n.d.	n.d.	n.d.	n.d.	n.d.	n.d.	n.d.	n.d.	n.d.	n.d.	n.d.	n.d.	n.d.	n.d.	n.d.	n.d.
Na2O	n.d.	0.18	n.d.	n.d.	n.d.	n.d.	n.d.	0.94	0.56	n.d.	0.44	n.d.	n.d.	n.d.	0.35	n.d.	1.09	0.47	0.59
K2O	2.84	4.80	3.29	5.20	10.06	7.84	9.54	9.95	6.67	9.99	9.59	9.96	2.98	9.58	5.12	3.07	6.39	10.22	9.39
TOTAL	85.85	41.03	84.02	84.62	92.94	88.30	88.78	52.69	90.00	90.63	93.69	93.03	84.98	90.00	55.97	81.34	85.59	91.45	86.04

Recalculated formula on the basis of 22 oxygens

Si	6.302	7.399	6.421	6.422	6.619	6.382	6.764	1.250	6.251	6.159	6.149	6.212	6.358	6.180	6.201	6.321	6.214	6.310	6.367
AlIV	1.698	0.601	1.579	1.578	1.381	1.618	1.236	6.750	1.749	1.841	1.851	1.788	1.642	1.820	1.799	1.679	1.786	1.690	1.633
AlVI	4.246	3.077	4.119	3.789	3.059	3.523	3.107	4.301	3.926	3.735	3.726	3.757	4.346	3.723	3.800	4.308	3.944	3.337	3.341
Fe2	0.128	0.284	0.172	0.329	0.551	0.469	0.568	0.244	0.073	0.127	0.132	0.131	0.036	0.143	0.123	0.032	0.110	0.489	0.450
Mg	0.058	0.106	0.081	0.189	0.475	0.192	0.188	0.305	0.090	0.098	0.076	0.089	0.000	0.121	0.103	0.059	0.125	0.227	0.245
Mn	0.000	0.000	0.000	0.000	0.000	0.000	0.000	0.000	0.000	0.000	0.000	0.000	0.000	0.000	0.000	0.000	0.000	0.000	0.000
Ca	0.000	0.000	0.000	0.000	0.000	0.000	0.000	0.000	0.000	0.000	0.000	0.000	0.000	0.000	0.000	0.000	0.000	0.000	0.000
Na	0.000	0.108	0.000	0.000	0.000	0.000	0.000	0.496	0.149	0.000	0.115	0.000	0.000	0.000	0.152	0.000	0.305	0.129	0.171
K	0.505	1.890	0.601	0.966	1.779	1.433	1.761	3.458	1.164	1.777	1.646	1.721	0.532	1.713	1.459	0.574	1.178	1.943	1.791

Total aluminium

Al	5.944	3.678	5.698	5.367	4.440	5.141	4.342	11.051	5.674	5.576	5.576	5.546	5.987	5.544	5.590	5.987	5.729	5.027	4.974
----	-------	-------	-------	-------	-------	-------	-------	--------	-------	-------	-------	-------	-------	-------	-------	-------	-------	-------	-------

Sample Code Spot	6785 M.. 33	6785 M.. 34	6785 M.. 35	6785 M.. 71	6818 M.. 31	6818 M.. 32	6818 M.. 33	6818 M.. 34	6818 M.. 35	6818 M.. 36	6818 M.. 41	6818 M.. 42	6818 M.. 43	6818 M.. 44	6818 M.. 51	6818 M.. 52	6818 M.. 53	6818 M.. 54	6818 M.. 55
SiO2	42.48	42.67	44.08	39.31	45.06	45.62	46.13	45.52	45.08	45.78	44.78	45.98	45.38	45.69	44.36	45.75	45.92	45.79	46.14
TiO2	0.69	0.55	0.46	0.89	0.54	0.80	0.64	0.57	0.44	0.28	0.62	0.68	0.47	0.45	0.73	0.95	0.79	0.78	0.68
Al2O3	32.50	28.93	34.72	24.54	32.75	34.55	34.97	34.94	35.60	36.46	34.54	35.32	35.17	37.32	32.87	33.68	33.42	33.12	33.75
FeO	4.80	3.54	3.01	4.72	4.10	0.88	0.87	0.90	0.47	0.45	1.03	1.06	0.86	0.54	1.86	1.99	2.08	1.92	1.92
MgO	1.10	0.93	0.58	1.29	1.00	0.78	0.92	0.56	0.32	0.48	0.40	0.85	0.65	0.42	0.65	0.86	0.85	0.78	0.46
MnO	n.d.	n.d.	n.d.	n.d.	n.d.	n.d.	n.d.	n.d.	n.d.	n.d.	n.d.	n.d.	n.d.	n.d.	n.d.	n.d.	n.d.	n.d.	n.d.
CaO	n.d.	n.d.	n.d.	n.d.	n.d.	n.d.	n.d.	n.d.	n.d.	n.d.	n.d.	n.d.	0.21	n.d.	n.d.	n.d.	n.d.	n.d.	0.17
Na2O	n.d.	0.48	n.d.	n.d.	0.39	1.06	1.09	0.82	0.25	0.60	1.07	1.16	1.09	0.42	0.78	0.95	0.73	0.71	0.89
K2O	1.08	8.79	0.60	8.28	10.96	9.02	8.64	7.28	3.38	3.60	6.79	8.27	5.92	2.97	5.67	6.69	7.22	7.48	5.65
TOTAL	82.65	85.89	83.45	79.03	94.80	92.71	93.26	90.59	85.54	87.65	89.23	93.32	89.75	87.81	86.92	90.87	91.01	90.58	97.69

Recalculated formula on the basis of 22 oxygens

Si	6.239	6.354	6.297	6.430	6.153	6.188	6.199	6.232	6.316	6.279	6.220	6.169	6.225	6.227	6.303	6.267	6.297	6.315	5.907
AlIV	1.761	1.646	1.703	1.570	1.847	1.812	1.801	1.768	1.684	1.721	1.780	1.831	1.775	1.773	1.697	1.732	1.703	1.685	2.093
AlVI	3.864	3.432	4.143	3.161	3.423	3.711	3.738	3.870	4.194	4.172	3.875	3.754	3.910	4.222	3.806	3.704	3.698	3.698	2.999
Fe2	0.590	0.441	0.360	0.646	0.468	0.100	0.098	0.103	0.055	0.052	0.120	0.119	0.099	0.062	0.221	0.228	0.239	0.221	0.206
Mg	0.241	0.206	0.124	0.315	0.204	0.158	0.184	0.114	0.067	0.098	0.083	0.170	0.133	0.095	0.138	0.176	0.174	0.160	1.614
Mn	0.000	0.000	0.000	0.000	0.000	0.000	0.000	0.000	0.000	0.000	0.000	0.000	0.000	0.000	0.000	0.000	0.000	0.000	0.000
Ca	0.000	0.000	0.000	0.000	0.000	0.000	0.000	0.000	0.000	0.000	0.000	0.000	0.031	0.000	0.000	0.000	0.000	0.000	0.023
Na	0.000	0.139	0.000	0.000	0.103	0.279	0.284	0.218	0.068	0.160	0.288	0.302	0.290	0.111	0.215	0.252	0.194	0.190	0.221
K	0.202	1.670	0.109	1.728	1.909	1.561	1.481	1.271	0.604	0.630	1.203	1.415	1.036	0.516	1.028	1.169	1.263	1.316	0.928

Total aluminium

Al	5.625	5.078	5.846	4.731	5.270	5.523	5.539	5.638	5.878	5.893	5.655	5.585	5.686	5.995	5.505	5.437	5.401	5.383	5.092
----	-------	-------	-------	-------	-------	-------	-------	-------	-------	-------	-------	-------	-------	-------	-------	-------	-------	-------	-------



Sample number	Size fraction	Mica, with upto 10% smectite interstratification	Chlorites	Kandites	Vermiculite	Smectites	Interstratified mica:smectite 80:20
6785	2 $\mu$ m			100			
6794	"			100			
6800	"	40		60			
6808	"			100			
6818	"	20		80			
6842	"			100			
6845	"			100			
6865	"			100			
6880	"			100			
6888	"			100			
6900	"			100			

## APPENDIX H: RAW ISOTOPE DATA FOR SIDERITE SAMPLES

Sample No.	Uncorrected $\delta^{18}\text{O}$ PDB	Sample No.	Uncorrected $\delta^{18}\text{O}$ PDB
10A (703)	5.80	3C	7.54
10B (703)	7.81	3M	1.67
5T	8.99	3S	1.88
5S	5.86	3B	3.42
5C	5.39	4T	9.61
7T	8.47	4C	7.53
7S	6.59	6T	6.21
7C	8.10	6S	5.71
9A	6.04	6C	5.97
9B	6.62	8C	6.95
1T	4.97	8S	7.11
1S	7.90	346	7.47
1C	7.24	348	5.19
2T	6.40	249	8.77
2S	8.54	370	2.44
2C	3.46	263	7.86
3T	7.38		
3U	4.63		
		3/3-2, 10456	-1.21
		10465	-10.33
		3/3-3, 10468	2.61
		10480	-3.74
		10502	-0.73